University of Strathclyde
Department of Pure and Applied Chemistry

An investigation into the ability of three analytical techniques to discriminate batches of methylamphetamine prepared by seven synthetic routes

by

Vanitha Kunalan

A thesis presented in fulfilment of the requirements for the degree of Doctor of Philosophy

2010

Acknowledgements

To my two supervisors, Dr Niamh Nic Daeid and Professor William John Kerr, thank you for giving me the opportunity to take on this PhD and for your continued support and advice.

To the Kerr Group, thank you for accepting me in the group and teaching me the organic chemistry and synthesis. I am really proud to be the member of this group. To WJK, BGA, HSB, SB, Marek, the Chief, Laura, LSB, ARC, TW, CF, MG and NM thanks for the great time together and for being there while I have been away from my family. HSB, you are my point of discussion and thanks for your sincere help. To all of you, your friendship and help have been indispensable.

Thanks to the research group and staff at the Centre for Forensic Science for your help and friendship. To NND, Kathy, Shane, Ainsley, Dzul, Wan, Kevin, Anika, Graham, Lucy, Ice, Four, Sara, Yuva, Bo, Alaia, Majid and Greg thanks for everything.

The Malaysian Government is gratefully acknowledged for the funding of this project. Thank you to the Department of Chemistry, Malaysia for giving me the time off from my job to pursue my study. To Jeff Comparin, Dr Tom Duncan and the staff at the DEA's Special Testing and Research Laboratory in Dulles, Virginia, thank you for sharing your time and expertise with me during the 3 months placement. Sincere thanks goes to David Morello and Byran Geer at DEA for the IRMS analyses. ICPMS analyses were made possible by Prof Andrew Hursthouse and David Stirling at University of West Scotland.

To mum and dad, thank you so much for the love, care and support you've given in my life. I would like to dedicate this thesis to my dad, my success would not have been possible without your continued support. To my family in Malaysia, thank you for the support and encouragement.

Posters, Presentations, and Publications

Poster presentation

(i) The characterisation of route specific impurities found in methylamphetamine synthesised by a number of preparative pathways
ISFE (International Symposium on Forensic Science and Environmental Health) Organised by Department of Chemistry, Malaysia 09 Nov-11 Nov 2009

(ii) Comparative analysis of methylamphetamine synthesized by five preparative pathways using ephedrine / *pseudo*ephedrine, using stable isotope ration mass spectrometry
ISFE (International Symposium on Forensic Science and Environmental Health) Organised by Department of Chemistry, Malaysia 09 Nov-11 Nov 2009

(iii) The characterisation of route specific impurities found in methylamphetamine synthesised by a number of preparative pathways
European Academy of Forensic Science (EAFS), Glasgow, Scotland, UK, Sept 8-11, 2009

(iv) Development of an analytical method for the organic impurity profiling of methylamphetamine
WestCHEM Research Day, University of Glasgow, Glasgow, Scotland, UK,May 30, 2008

Oral presentation

(i) An Investigation of various techniques to discriminate batches of methylamphetamine by synthetic route
ISFE (International Symposium on Forensic Science and Environmental Health) Organised by Department of Chemistry, Malaysia 09 Nov-11 Nov 2009

(ii) An Investigation of IRMS to discriminate batches of methylamphetamine by starting material and synthetic route
United States Drug Enforcement Agency (DEA), Special Testing Laboratories, Dulles, Virginia, USA, July 30, 2009

Papers published

Characterisation of route specific impurities found in methylamphetamine synthesised by the Leuckart and Reductive Amination methods
Analytical Chemistry, 2009, 81, 7342-7348

Table of Contents

Abstract

This project evaluates the abilities of gas chromatography mass spectrometry (GCMS), isotope ratio mass spectrometry (IRMS) and inductively coupled plasma mass spectrometry (ICPMS) to characterise methylamphetamine hydrochoride Repetitive batches of samples were prepared using seven synthetic routes commonly used by clandestine chemists (149 samples in total) and analysed by each technique to provide a robust sample set of known provenance for data interpretation.

Organic analysis of all samples was undertaken using a developed and partially validated GCMS impurity profiling method. Basic and acidic impurities were extracted separately and analysed using a DB-1 MS column. The GCMS method discriminated all routes based on a set of route specific target impurities determined through this project. This target set was compared with suggested literature impurities and better resolution was achieved. Furthermore, variations in impurity profiles reported in the literature were resolved through investigation of the respective synthetic processes. A comparison of the DB-1 MS with a DB-5 column and a single basic pH extraction method confirmed this as a viable alternative to many of the methods described in the literature.

Stable isotope ratios ($\delta^{13}C$, $\delta^{15}N$, $\delta^{2}H$) were measured by elemental analyzer/thermal conversion isotope ratio mass spectrometry (EA/TC-IRMS). This facilitated the differentiation of samples by starting material, with $\delta^{13}C$ providing the best results.

Inorganic impurities present in the samples were analysed by inductive couple plasma mass spectrometry (ICPMS). This facilitated some discrimination of the samples by synthetic pathway only.

Pattern recognition techniques were applied to the generated data (raw and processed) from each analytical technique both individually and together. Pearson's correlation coefficient, hierarchiral cluster analysis, principal component analysis and discriminate analysis were used to investigate the separation of the sample batches by starting material and synthetic route. These mathematical tools demonstrated that

methylamphetamine profiling linking samples by starting material and/or synthetic route was achievable.

Abbreviations

AIDIP	Australian Illicit Drug Intelligence Program
AIR	Atmospheric nitrogen
ATS	Amphetamine-Type Stimulants
AFP	Australian Federal Police
BMK	Benzyl methyl ketone
BSIA	bulk stable isotope analysis
CE	Capillary Electrophoresis
CF-IRMS	continuous flow isotope ratio mass spectrometry
CHAMP	Collaborative Harmonisation of Methods for Profiling of Amphetamine-Type-Stimulants
CI	Chemical Ionization
CMP	1-(1,4-cyclohexadienyl)-2-methylaminopropane
CSIA	compound specific isotope analysis
DEA	United State Drug Enforcement Administration
DWG	Drugs Working Group (part of ENFSI)
EA-IRMS	elemental analyzer isotope ratio mass spectrometry
EI	Electron Ionization
ENFSI	European Network of Forensic Science Institutes
FIRMS	Forensic Isotope Ratio Mass Spectrometry Network
FTIR	Fourier transform infrared spectroscopy
GCFID	Gas Chromatography Flame Ionization Detector
GC-IRMS	gas chromatography isotope ratio mass spectrometry
GCMS	Gas Chromatography Mass Spectrometry
GDPs	Gross Domestic Products

GHB	γ-Hydroxybutyrate
ICPMS	Inductively Coupled Plasma Mass Spectrometry
ICPOES	inductively coupled plasma optical emission spectroscopy
INCB	International Narcotics Control Board
IRMS	Isotope Ratio Mass Spectrometry
LSD	Lysergic Acid Diethylamide
MCA	Methylamphetamine Control Act
MDA 1971	Misuse of Drugs Act 1971
MDMA	3,4-methylenedioxymethylamphetamine
MDP-2-P	3,4-methylenedioxyphenyl-2-propanone *or* PMK
meth	methylamphetamine
MS	Mass spectrometry
m.t	metric tons
m/z	mass to charge ratio
NMR	Nuclear Magnetic Resonance
Opiates	opium, morphine and the final product heroin *(as defined in the UNODC's 2006 World Drug Report1)*
P-2-P	phenyl-2-propanone
PDB	Peedee Belemnite from *Belemnitella Americana*
PFTBA	Perfluorotributylamine
PMK	piperonylmethylketone *or* MDP-2-P
RSD	relative standard deviation
sum	signifies the data was normalized to the sum of the target impurities
TC/EA-IRMS	temperature conversion/ elemental analyzer isotope ratio mass spectrometry
TIC	total ion chromatogram

TMS	tetramethylsilane
UN	United Nations
UNODC	United Nations Office on Drugs and Crime
VPDB	Vienna PeeDee Belemnite, now replace PDB
VSMOW	Vienna Standard Mean Ocean Water

Glossary

Adulterants	bulking agents added to an illicit drug which have a pharmacological effect on the body, such as paracetamol
Aziridines	in this project refer to *cis*-1,2-dimethyl-3-phenylaziridine and *trans*-1,2-dimethyl-3-phenylaziridine
Diluents	bulking agents such as sucrose is added to an illicit drug
Ecstasy	MDMA and analogues such as MDEA and MDA (as defined in the UNODC world Drug Report)
Leuckart	synthesis of methylamphetamine with P-2-P via N-formylmethyamphetamine
Naphthalenes	in this project refer to 1,3-dimethyl-2-phenylnaphthalene and 1-benzyl-3-methyl-naphthalene
Precursor	in this project, a precursor is defined as a chemical required to synthesise an illicit drug
Profiling	the use of the methods to define the chemical and physical properties of a drug seizure for intelligence and evidential purposes
Provenance	the history of the methylamphetamine analysed in this project is known based on the reaction pathway used in the synthesis
Reductive Amination	synthesis of methylamphetamine with P-2-P and methylamine to form the corresponding imine, and then reduction to form the amine with Al/Hg amalgam
Route specific impurities	impurities present in an illicit substance which indicate the production pathway or method of synthesis used during the drug manufacture
Synthetic route	in this project, seven different synthetic routes (Leuckart , Reductive amination, Nagai, Rosenmund, Birch , Moscow and Emde) were used in methylamphetamine synthesis
Target impurities	impurities that are play important role in distinguish the synthetic pathyway in this project and also those take in count for the statistic study

List of Tables

List of Figures

List of Schemes

CHAPTER 1 : INTRODUCTION

1.0 Introduction

Illegal drugs are used by some 200 million people worldwide and represent a retail market of about $320 billion, making narcotic use a "monster" [1] of a problem to combat according to Antonio Maria Costa, Executive Director of the United Nations Office on Drugs and Crime (UNODC). He stated that the $320-billion retail market is "larger than the individual gross domestic products (GDPs) of nearly 90 percent of the countries of the world", and there were "few dimensions of human security that are not affected in some way by the illicit drug market".[1]

According to the 2009 World Drug Report (WDR), there were between 18 and 38 million problem drug users aged between 15-64 years in 2007.[2] There is evidence that the specific drug or drugs (such as cannabis, opiates, cocaine and amphetamines) used varies from country to country and from region to region [2-4] and in general, drug possession, sale, and use are illegal although individual countries have their own drug laws.[3] In the Guardian World news [5], Costa also suggested that individuals who take drugs need medical help, rather than criminal retribution. He said that treating this problem was one of the best ways of shrinking the market, since people with serious drug problems provided the bulk of drug demand.[5] He urged that international law enforcement should target traffickers rather than users.[5] This suggests that law enforcement should focus resources on the smaller number of high-profile, high-volume, and violent criminals instead of large numbers of smaller offenders and end users.

The ability to robustly identify specific synthetic routes and determine the potential of batch to batch linkages is therefore of consequence and is one of the objectives of this work in relation to the synthesis of methylamphetamine.

1.1 Law and Legislation

Legislation is one component of the solution to the world-wide drug problem. International drug control is one of the oldest forms of multilateralism, older than the United Nations and even predating its preceding organisation, the League of Nations. More than 50 years of effort have created the international system of control of narcotic substances.[6]

The first known legislative control was imposed by the International Opium Commission, Shanghai, 1909, and culminated in the Single Convention of 1961. The first multinational drug-control programme was the 1909 Shanghai Opium Commission.[6] As a commission, participants could only recommend actions necessary to prevent opium trafficking and abuse but could not make binding international agreements.[6] However, the participants passed resolutions urging national governments to enact measures to curb opium smoking in their respective countries, initiate regulation of opium use for nonmedical purposes, ban the export of opium to countries that prohibited importation, and control the manufacture and distribution of opium derivatives.[6]

The commission was the first effective step taken by the international community to combat drug abuse.[6] It served as a catalyst for countries to pass domestic legislation addressing drug problems within their borders.[6] Most importantly, the commission united countries in an international cooperative effort to address the problem of the opium trade.[6] The work of the commission led to the Hague Opium Conferences (1912-1914) and to the adoption of the 1912 International Opium Convention, sometimes called the Hague Opium Convention, and succeeding treaties that effectively restricted opium production and trade to legitimate purposes.[6]

The 1961 Single Convention on Narcotic Drugs was the first international treaty against illicit manufacture and trafficking of narcotic drugs that formed the bedrock of the current global drug control regime. Previous treaties had only controlled coca, opium and derivatives such as morphine and heroin.[7] The Single Convention, adopted in 1961, consolidated those treaties, broadening their scope to include cannabis and allow control

of any drugs with similar effects to those specified in the treaty. The Commission on Narcotic Drugs and the World Health Organization were empowered to add, remove, and transfer drugs among the treaty's four Schedules of controlled substances. The International Narcotics Control Board (INCB) was put in charge of administering controls on drug production, international trade, and dispensation. The United Nations Office on Drugs and Crime (UNODC) was delegated the Board's day-to-day work of monitoring the situation in each country and working with national authorities to ensure compliance with the Single Convention. This treaty has since been supplemented by the Convention on Psychotropic Substances, which controls LSD, Ecstasy, and other psychoactive pharmaceuticals, and the United Nations Convention Against Illicit Traffic in Narcotic Drugs and Psychotropic Substances, which strengthens provisions against money laundering and other drug-related offences.[7]

The Convention on Psychotropic Substances 1971 is a United Nations treaty designed to control psychoactive drugs such as amphetamines, barbiturates, and psychedelics.[8] During the 1960’s, drug use increased greatly around the world, especially in Western nations. Inspired by psychedelic advocates such as Aldous Huxley and Timothy Leary, [8] millions of people experimented with powerful hallucinogens, and drugs of all kinds became freely available. The Single Convention on Narcotic Drugs of 1961 could not ban the many newly discovered psychotropics, since its scope was limited to drugs with cannabis-, coca-, and opium-like effects.

The 1988 United Nations Convention Against Illicit Traffic in Narcotic Drugs and Psychotropic Substances was developed to include the newly discovered drug compounds and is one of three major drug control treaties currently in force.[9] It provides additional legal mechanisms for enforcing the 1961 Single Convention on Narcotic Drugs and the 1971 Convention on Psychotropic Substances.

From these origins began a process that has evolved into a multilateral drug control system. The scope of control of drugs has broadened and deepened over the years, from opium to cocaine to cannabis to psychotropic substances, and from the regulation of production and trade of medical drugs. International cooperation against the multi-faceted

problems associated with illicit drugs is now a reality and the legal framework for this whole multilateral control system is now provided by these three international drug conventions (1961, 1971 and 1988).

1.1.1 UK Legislation

In the United Kingdom, the principle legislative document for drug control is the Misuse of Drugs Act, 1971. This has been the subject of a number of modification orders and is accompanied by the Misuse of Drugs Act (Regulations), 1985, which was superceded by the Misuse of Drugs Act (Regulations), 2001.[10]

1.1.1.1 The Misuse of Drugs Act 1971

The Misuse of Drugs Act 1971 as amended, is the main piece of legislation regulating the availability and use of certain drugs in the UK; some other substances are regulated through the Medicines Acts.[11] The Misuse of Drugs Act created three categories: Class A, Class B and Class C, with different levels of penalties for possession and dealing. Drugs are divided between classes based on (i) whether the drug is being misused; (ii) whether it is likely to be misused and (iii) whether the misuse in either case is having or could have harmful effects sufficient to constitute a social problem.[11]

Historically, in the United Kingdom the Dangerous Drugs Act, 1951 simply controlled vegetable narcotics, such as Cannabis sativa (cannabis) and opium, and a few chemically related synthetic substances. This was superseded by the Dangerous Drugs Act, 1964, which organised the controlled drugs into three schedules based on internationally accepted principles.[12] The Misuse of Drugs Act 1971 also included drug analogues which were defined as: ‘structurally derived by substitution in the side-chain or by ring closure therein’.[12]

Since 1997 the UK Government has altered the classification of certain drugs, notably cannabis from Class B to Class C in January 2004 and reclassified to Class B in January 2009. Hallucinogenic mushrooms in all forms were classified as Class A drugs in 2005 (previously only dried mushrooms were included in Class A). Also, since 1996, several

drugs have become regulated under the Misuse of Drugs Act, including Ketamine (a veterinary tranquiliser classified in Class C in 2006), Gamma Hydroxybutyrate (GHB Class C 2003) and steroids from the Medicines Act 1968 into Class C. Some of the most common drugs controlled by the Misuse of Drugs Act and the Medicines Act are shown in Table 1.[11]

Classification	**Drugs**
Class A	heroin, LSD, ecstasy, amphetamine (prepared for injection), cocaine, crack, magic mushrooms, crystal meth
Class B	Amphetamine, cannabis, barbiturates
Class C	Temazepam, anabolic steroids, Valium, Ketamine, methylphenidate (Ritalin), Pholcodeine, GHB, mild amphetamine (such as slimming tablets)
Medical Act	Poppers (Amy nitrate)

Table 1: UK classification of drugs, 2005.[11]

Amphetamine, methylamphetamine, and their salts and stereoisomers are controlled by the Misuse of Drugs Act, 1971, as Class B drugs and as Class A drugs when in the form of a preparation designed for administration by injection. In most cases it is not necessary for the forensic scientist to identify the particular salt or stereoisomer. Purity is not normally required in cases of possession.

1.1.1.2 Misuse of Drugs Regulations 2001

The Misuse of Drugs Regulations 1985 controls the medicinal use of illegal drugs, which are placed in one of five Schedules. Schedule 1 drugs need a Home Office license in order to be used for research; Schedules 2-5 specify the circumstances in which drugs controlled by the 1971 Act may be used for medicinal purposes (for example, drugs in Schedule 2 may be prescribed by a doctor or dentist).

The Misuse of Drugs Regulations 2001 are concerned with the therapeutic use of drugs. They define the classes of persons who are authorised to supply and possess controlled drugs while acting in their professional capacities and lay down conditions under which these activities must be carried out. Under the Regulations, drugs are categorised in five

schedules which govern import, export, production, supply, possession, prescribing and record keeping. According to the Misuse of Drugs 1971:[13]

- Schedule 1 includes substances such as LSD and cannabis that are not available for medical purposes. Possession and supply are prohibited without specific Home Office approval.
- Schedule 2 includes prescription drugs such as morphine and diamorphine that, because of their potential to cause harm, are subject to special requirements relating to their safe custody, prescription, and the need to maintain registers relating to their acquisition and use.
- Schedule 3 drugs include barbiturates and are subject to special prescription, though not safe custody, requirements.
- Schedule 4 drugs include benzodiazepines and are subject neither to special prescribing arrangements, nor to safe custody requirements.
- Schedule 5 includes preparations that, because of their low strength, are exempt from most of the controlled drug requirements.

1.1.1.3 Legislation Relating to Precursors

Chemicals are essential to the manufacture of illicit drugs. Chemicals used in drug manufacture are divided into two categories, precursor and essential chemicals, although the term "precursors" is often used to identify both. Precursor chemicals are chemicals that are essential to the production of a controlled substance and for which no substitution can be made. Essential chemicals are used in the refining of coca and opium into cocaine and heroin. Although some remain in the final product, the basic raw material is the coca or opium. Many essential chemicals required for illicit drug manufacture have extensive commercial applications, are widely traded, and are available from numerous source countries.[14]

In the UK, the manufacture and the placing on the market of these precursor chemicals is regulated by the Controlled Drugs (Substances Useful for Manufacture) (Intra-Community Trade) Regulations 1993. The importation and exportation of these

precursors within the European Union is regulated by the Controlled Drugs (Substances Useful for Manufacture) Regulations 1991 and Amendment 1992.[15] The legislation relates to the regulation of drugs precursor chemicals in the United Kingdom and export of these compounds outside the EU.

Category 1	Category 2	Category 3
• Benzyl methyl ketone (BMK) • Acetylanthranilic Acid • Isosafrole • Piperonyl methyl ketone (PMK) • Piperonal • Safrole • Ephedrine • *Pseudo*ephedrine • Norephedrine • Ergometrine • Ergotamine • Lysergic acid	• Potassium Permanganate • Acetic anhydride • Phenylacetic acid • Anthranilic acid • Piperidine	• Acetone • Ethyl ether • Methyl ethyl ketone (MEK) • Toluene • Sulphuric acid • Hydrochloric acid

Table 2: Chemicals and categories [12]

Category 1 contains ‘true precursors’ which form the core structure of a controlled substance. Category 2 includes ‘secondary precursors’ which can be altered into Category 1 precursors or are essential reagents for the synthesis of the controlled substance (Table 2). Category 3 precursors are generally acids and solvents required for the manufacturing process.[16] Most of the methods for producing methylamphetamine use either phenyl-2-propanone, *l*-ephedrine or *d-pseudo*ephedrine as precursors which are listed as Category 1 precursors. Phenyl-2-propanone (P2P) is also known as phenylpropanone, phenylacetone and benzylmethylketone (BMK).

1.2 The Global Amphetamine Situation

Amphetamine-type stimulants (ATS), including amphetamines, methylamphetamine and ecstasy, remain the second most widely consumed group of illicit substances (Table 3).[2] UNODC [2] estimates that in 2007 (latest data available), amphetamine-group manufacture amounted to between 230 and 640 metric tons. Ecstasy-group manufacture was estimated at between 72 and 137 metric tons.[2]

	Cannabis	ATS		Cocaine	Opiates
		Amphetamine	Ecstasy		
Number of Abusers (in millions)	143-190	16-51	12-24	16-21	15-21
% of population (15-64 years olds)	3.3-4.4	0.4-1.2	0.3-0.5	0.4-0.5	0.3-0.5

Table 3: Illicit drug use at global level.[2]

The amphetamine-group dominates ATS seizures, but there was also a marked increase in ecstasy group seizures in 2007 (see Figure 1). It should be noted that the UNODC statistics combine methylamphetamine, amphetamine and non-specified amphetamine into the single category 'amphetamine'.

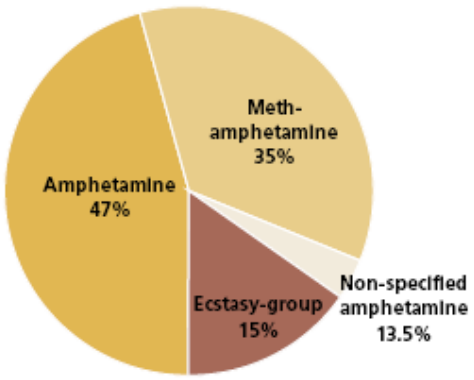

Figure 1: ATS seized, by substance type, 2007.[2]

The latest data available is for 2007 where 16% fewer ATS-related laboratories were reported to UNODC (6,990).[2] Most laboratory incidents (91%) were small methylamphetamine operations due mainly to the ease of manufacture and availability of inexpensive precursor chemicals.[2] These were concentrated in North America (particularly the USA), and to a lesser extent Oceania, and Central and Eastern Europe. Methylamphetamine laboratories are also increasingly found in large industrial-sized operations run by criminal organisations, particularly in East and South-East Asia and North America, although significant operations recently emerged in South Asia.[2]

In Europe, methylamphetamine manufacture was largely limited to a number of countries in Central Europe and East Europe (405 cases in 2007).[2] Compared to 2006, a 15% decline was noted in the total number of laboratories reported to the UNODC.[2] The majority of operations are small scale and the main producing country is the Czech Republic (96%). In 2007, Poland and Portugal also reported methylamphetamine manufacture.

Amphetamine-group laboratory seizures in Oceania have remained at high levels for the past several years. However, in 2007, there were signs of a moderate decrease. Australia reported a total of 328 (an 8% decline from the previous year) amphetamine-group operations and New Zealand reported 190 amphetamine-group laboratories (a 10% decrease), each predominantly methylamphetamine-related.[2]

According to the World Drug Report (2009) evidence points [2] to an increased frequency in the manufacturing of methylamphetamine using uncontrolled precursors, most notably tableted pharmaceutical preparations containing *pseudo*/ephedrine and P-2-P based processes in the manufacture of methylamphetamine. This is because regulation of tableted pharmaceutical preparations containing *pseudo*/ephedrine do not fall under the same international controls as bulk chemicals containing the identical chemicals, and therefore are more easily accessible.[2]

The report also noted that a growing number of other emerging substitute precursor chemicals have been recently identified related to methylamphetamine synthesis including: α-phenylacetoacetonitrile (converts easily into P-2-P), and methyl phenylacetate, ethyl phenylacetate, amyl phenylacetate and isobutyl phenylacetate (which can all be converted into phenylacetic acid).[2]

Due to the awareness, restrictions and enforcement against ATS production, manufacture has expanded into vulnerable nearby countries. For instance, from the USA, manufacture has moved south to Mexico. As Mexico responded with strong counter methylamphetamine initiatives, manufacturing activities moved south to Latin America, including Argentina, Guatemala, Honduras, and Peru. Similar shifts may also be occurring in South Asia where India and Sri Lanka reported their first operational methylamphetamine laboratories in 2008, and reported seized manufacturing equipment and chemicals in 2007.[2] As a consequence on the movement of production, trafficking routes are increasingly shifting into places that lack the stability, enforcement and forensic science infrastructure to detect movement of both precursor chemicals and finished products.[2] Four sub-regions were identified as the main producers of the majority of ATS worldwide based on seizure.[2]:

- Near and Middle East (29%)–primarily fake Captagon tablets likely containing amphetamine;
- East and South-East Asia (23%)–primarily methylamphetamine;
- West and Central Europe (22%)–primarily amphetamine and ecstasy; and
- North America (18%)–primarily methylamphetamine and ecstasy.

Seizures of amphetamine-group substances have increased considerably since the mid-1990s, and again since 2002. Seizures of methylamphetamine, until recently the main ATS seized in East and South-East Asia and North America, have declined since 2005, and remained at approximately 18 metric tons per annum until 2007 where a decline of about 2.5 metric tons was observed.[2] In 2007, the Near and Middle East accounted for about a third of global seizures of methylamphetamine (43.2 metric tons in total),

followed by East and South East Asia, West and Central Europe, and North America (see Figure 2).[2]

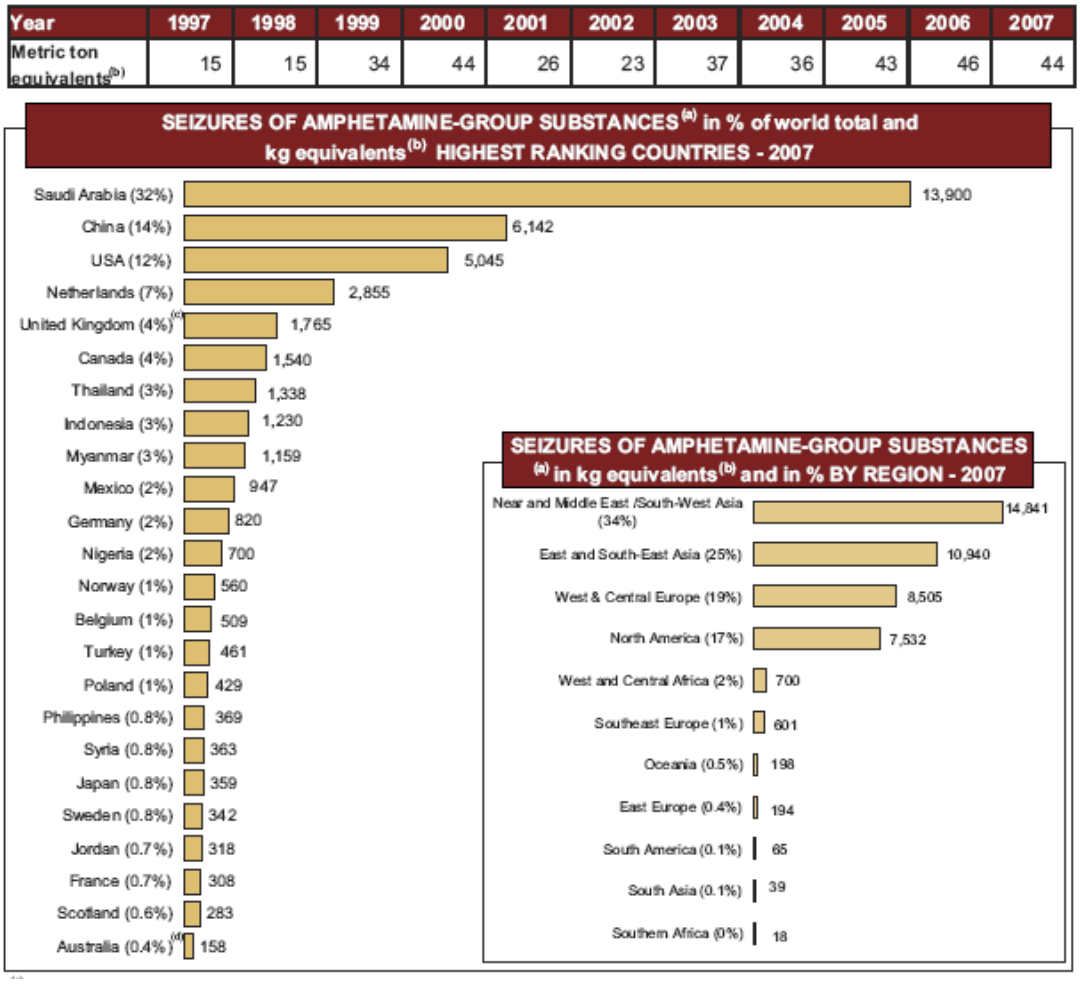

Figure 2: Global seizures of amphetamine group substances, 1997-2007.[2]

The UNODC in 2009 [2] reported that the total amount of methylamphetamine seized in 2007 had decreased in comparison with previous years but there had been an increase in the number of countries reporting seizures. This suggests that the market was expanding geographically (see Figure 3).[2] The sub-regions of East and South-East Asia (56%) and the North America marked (40%) continued to account for most of the world's seized methylamphetamine, with relatively low seizures reported elsewhere.[2]

Figure 3: Global amphetamine group substances trafficking routes, 2007.[2]

1.3 Drug Profiling

The drug supply chain consists of a producer/manufacturer, trafficker, distributor, supplier and user.[17] The analysis and comparison of illicit drug samples in order to obtain information relating to the compounds produced and distributed is called 'drug profiling'. Various definitions for drug profiling have been used in publications and discussions leading to a certain ambiguity with the terminology. According to the Scientific Section of the United Nations International Drug Control Programme, drug profiling is a:

"Systematic characterization of seized drug samples by physical and chemical means, which are valuable scientific tools used to support intelligence-gathering and operational work by law enforcement authorities".[18]

In 2006 at the Drugs Working Group (DWG) meeting of the European Network of Forensic Science Institutes (ENFSI) in Poland, a definition for drug profiling was agreed to be:

"The use of the methods to define the chemical and/or physical properties of a drug seizure for comparing seizures for intelligence and evidential purposes".[19]

For synthetic drugs such as methylamphetamine, practical experience has shown that the impurity profiles of the products from a given illicit laboratory can be characteristic.[20] Provided that there is no change in the method or the conditions of drug synthesis, variations in the impurity content of drugs synthesised at different times by the same chemist in a clandestine laboratory are believed to be relatively small and as such the potential of route identification and batch to batch linkage may be possible.[18]

Drug profiling of methylamphetamine can be used by law enforcement authorities for intelligence purposes to investigate synthetic route specification of samples. It has also been suggested that it may be possible to categorise within and between synthetic batch variations depending on the similarities between profiles.[18]

Methylamphetamine profiling databases can contain variables such as physical characteristics of the samples (appearance, colour, packaging, etc) and chemical characteristics of the samples (purity, adulterants, diluents, concentration of organic impurities, concentration of inorganic impurities, isotope ratios, chirality, etc). The majority of such databases are populated by analysed case samples rather than known provenance samples and as such the expected synthetic variation within the data of samples prepared under the same and under different conditions is uncertain.

Impurities in illicit methylamphetamine have been investigated and/or profiled by researchers around the world, based on seized street samples. Detailed impurity information has been reported on samples seized in countries such as Norway, Japan, Thailand, the Philippines and China, where methylamphetamine abuse is one with the most serious potential for harm.[21] Currently gas chromatograph mass spectrometry (GCMS) is widely been used for profiling organic methylamphetamine impurities.

The UNODC have developed a GCMS profiling method for impurity profiling of methylamphetamine samples [18] and various GCMS profiling methods have been used in Thailand [22], Japan [20, 23, 24], Australia [21], the United States [25, 26] and the Philippines.[27]

Since 2005, a collaboration between seven laboratories in Europe funded through the European Union (SMT – CT98 – 2277) resulted in a 'harmonised' GCMS amphetamine impurity profiling method [28] and the resultant published literature suggested that harmonised methods would allow the exchange of data and intelligence information.[28] This project was extended into the ''Collaborative Harmonisation of Methods for Profiling of Amphetamine Type Stimulants'' (CHAMP) and funded by the sixth framework programme of the European Commission in 2008.[29] The aim was to create a 'harmonised' GCMS impurity profiling methodology, which would facilitate the international comparison of samples.

The CHAMP project suggested the adoption of the GCMS amphetamine impurity profiling method from their previous project for the impurity analysis of methylamphetamine samples and claimed that the method produced excellent results without the necessity for modification.[30]

A number of publications have also suggested several drawbacks to GCMS impurity profiling techniques, which will be discussed in the next section. Besides GCMS profiling, isotope ratio mass spectrometry (IRMS) and inductively coupled plasma mass spectrometry (ICPMS) both offer potential as additional techniques for methylamphetamine profiling. Developments in this area are discussed in detail in Section 1.3.2 and 1.3.3.

1.3.1 Drug Profiling with Gas Chromatography Mass Spectroscopy (GCMS)

When performing impurity profiling work, the analyst's ultimate goal is to obtain profiles of the major and minor components in formats that allow him/her to use the data as a comparative tool for the purpose of locating other samples having similar profiles.[31] Such linkage information may then be used for both intelligence and perhaps evidential purposes.

The reasons for the presence of trace impurities in clandestinely manufactured drugs are varied; impurities may be generated as by-products during drug manufacture; they may already be present in the starting materials, reagents and/or solvents and may be carried over unchanged to the final product; or they may arise from reactions of original impurities present in starting materials. The relative amounts of the impurities in illicit methylamphetamine may show large variations, attributed to the exact nature of starting materials, the synthetic route, actual manufacturing conditions employed by the illicit laboratory 'chemist', cutting agents added, storage conditions and methods of distribution.[32] Research on impurity profiling has been directed at major synthetic drugs such as amphetamine and MDMA and researchers have used GCMS in order to identify 'route specific' impurities. Route specific impurities are those which, when present in an illicit substance, indicate the use of a specific synthetic pathway. A number

of potential difficulties have been suggested relating to GCMS impurity profiling. For instance, in some cases, during the clandestine manufacturing of high purity methylamphetamine which involves the purification and recrystallisation of raw products, very few impurities may remain and the derived information from GCMS analysis may be insufficient to indicate any specific clandestine manufacturing routes.[21]

A second problem highlighted by some researchers is the possibility that methylamphetamine base originating from ephedrine based synthetic route could also have been mixed with methylamphetamine base produced via a P-2-P based synthetic route thus resulting in a combination of impurities from both routes being present in the same drug profile.[33]

Additionally, the impurity extraction method may affect the nature and quantity of impurities present in the sample to be analysed. Extraction procedures usually involve the dissolution of methylamphetamine in a volume of buffer at acidic or basic pH, and then the extraction of impurities into an organic solvent containing an internal standard. The extraction of impurities is pH dependent and affects how efficiently acidic or basic impurities are extracted. Unfortunately, studies on methylamphetamine impurities have utilised different extraction methods, such as buffer at pH 6, pH 8.1 [30] and pH 10.5 making direct comparison of the results very difficult. The GCMS method and analytical parameters chosen will also affect the final chromatographic profile obtained and again a variety of methods are reported in the literature making direct comparison of published data difficult.

1.3.1.1 Route specific impurities

Methylamphetamine impurity profiling studies began appearing in the literature in the 1970s. Barron et al.[34] and Bailey et al.[35] suggested *N*-formylmethylamphetamine as a route specific impurity for Leuckart synthesized methylamphetamine. However, a study by Qi et al. [21] cast doubt on the "route specific" status of this impurity; the authors reported *N*-formylmethylamphetamine in seized methylamphetamine samples which were believed to have been synthesised from ephedrine (i.e., not from the Leuckart or Reductive Amination routes, which have P-2-P as the starting material).

Kram and Kreugal [36] identified several impurities present in methylamphetamine hydrochloride known to have been synthesised via the Leuckart method: dibenzylketone, α-benzyl-*N*-methylphenethylamine, and *N*-methyldiphenethylamine. The authors recognized that, while these impurities were associated with the Leuckart synthesis, it was not possible to determine if they were route specific. Barron et al.[34] and Kram and Kreugal [36], also found that α,α′-dimethyldiphenethylamine and *N*, α,α′-trimethyldiphenethylamine were two impurities associated with the Leuckart method and again it was not possible at that time to preclude them from being formed by other synthetic methods.

Verweij [37] published a review of the literature (up to 1989) relating to impurities found in methylamphetamine. From this review, impurities such as benzyl methyl ketone, amphetamine, 1-phenyl-2-propanol, *N*-*N*-dimethylamphetamine and dibenzylketone were found in methylamphetamine synthesised using the Reductive Amination method and reported that, based on work published in German, 1-phenyl-2-propanol was indicative of methylamphetamine synthesis by Reductive Amination.

Skinner [38] analysed samples from a clandestine laboratory known to use the Nagai route and found aziridine(s) and naphthalene(s) present. In 1992, Tanaka et al.[23] published a study and found the presence of a methylamphetamine dimer and ephedrine in street samples of unknown provenance. Tanaka et al.[23] proposed, and confirmed, that methylamphetamine dimer could result from the condensation of aziridine with

methylamphetamine. Since aziridine was previously identified in methylamphetamine synthesised by the Nagai route, Tanaka et al.[23] suggested that the street samples containing the dimer were synthesised by ephedrine method.

In 1994, Inoue et al.[39] analysed street samples seized in Japan and found some with both the methylamphetamine dimer and ephedrine present. Based on Tanaka's work, the presence of the dimer suggested that synthesis of the samples occurred from the ephedrine method. They also noted that naphthalene(s) and aziridine(s), which were found in methylamphetamine synthesised from ephedrine via Nagai route [38, 40] were not present in the profiles obtained. Inoue et al.[39] investigated impurity profiling analysis of methylamphetamine seized in Japan and the resultant profiles were compared and statistically analysed using Euclidian distances for evaluating similarity and/ or dissimilarity among exhibits.

In 1995, Windahl et al.[41] reported a study involving a series of experiments which varied the length of time over which the Nagai reaction proceeded (1/2 hour, 2 hour, 4 hour). Windahl et al.[41] analysed the product in oil form (i.e. basic or acidic impurities were not extracted; instead, the oil was diluted and analysed) and the authors found two unreported impurities: *N*-methyl-*N*-(α-methylphenethyl)amino-1-phenyl-2-propanone and (*Z*)-*N*-methyl-*N*-(α- methylphenethyl)-3-phenylpropenamide. They also concluded that the reaction time had an effect on the level of aziridines and naphthalenes present in the final product: as the reaction time increased, the aziridines decreased and the naphthalenes increased. This observations fitted with the claim of Tanaka et al.[23] that the dimer is formed from the condensation of methylamphetamine and aziridine: as the reaction time increased, the quantity of aziridine decreased and, consequently the dimer cannot be formed as readily. Importantly, the dimer was deemed to be not route specific since (1) it was not in all of the Nagai reaction products since it was dependent on the reaction times, and (2) it was also found in methylamphetamine synthesised via the Emde route. A summary of the impurities found by Windahl are presented in Table 4.

Impurities	Windahl
cis-1,2-dimethyl-3-phenylaziridine	√
trans-1,2-dimethyl-3-phenylaziridine	√
methylamphetamine dimer	
1,3-dimethyl-2-phenylnaphthalene	√
1-benzyl-3-methyl-naphthalene	√
isomers of N-methyl-N-(α -methylphenylethyl)amino-1-phenyl-2-propanone	√
(Z)-N-methyl-N-(α -methylphenethyl)-3-phenyl propenamide	√

Table 4: Impurities found by Windahl et al.[41] in their synthesis of methylamphetamine by the Nagai route.

In 2006, Lee et al.[42] published a study in which sixteen methylamphetamine samples were synthesised from ephedrine and *pseudo*ephedrine by the Nagai, Emde, and Moscow routes. Impurities which were claimed as those which "may be utilized as indicators of synthetic conditions" are presented in Table 5.

Impurities	Nagai (?h)	Emde	Moscow
cis-1,2-dimethyl-3-phenylaziridine		√	
trans-1,2-dimethyl-3-phenylaziridine		√	
1,3-dimethyl-2-phenylnaphthalene	√		
1-benzyl-3-methyl-naphthalene	√		
methylamphetamine dimer		√	√

Table 5:Impurities found by Lee et al.[42] in their synthesised methylamphetamine batches via Nagai, Emde and Moscow routes.

The authors identified the naphthalenes in the Nagai batches (they do not state the exact time used for their Nagai synthesis). They did not observe the aziridines or the dimer for the Nagai route (in contrast to Windahl), although these three impurities were found in the Emde batches, and the dimer was found in the Moscow route.

In 2007, Ko et al.[43] also synthesised methylamphetamine by the Nagai (5h reaction) and Emde methods and the impurities they identified are presented in Table 6.

Impurities	Nagai (5h)	Emde
cis-1,2-dimethyl-3-phenylaziridine		√
trans-1,2-dimethyl-3-phenylaziridine		√
chloroephedrine		√
unknown		√
methylamphetamine dimer		√
1,3-dimethyl-2-phenylnaphthalene	√	
1-benzyl-3-methyl-naphthalene	√	
isomers of N-methyl-N-(a-methylphenylethyl)amino-1-phenyl-2-propanone	√	
(Z)-N-methyl-N-(α-methylphenethyl)-3-phenyl propenamide	√	

Table 6: Impurities found by Ko et al.[43] in their synthesised methylamphetamine batches via Nagai and Emde routes.

Ko et al.[43] confirmed the findings of Lee et al.[42] of naphthalenes in the Nagai route, but they also suggested two additional impurities. Lee et al.[42] found the aziridines and the methylamphetamine dimer in their synthesised Emde batches, and Ko et al.[43] confirmed these three impurities and also identified chloroephedrine and another 'unknown' impurity. Unfortunately the work of both of these authors were undertaken using different methods of sample preparation, analytical column and GCMS conditions which may account for some of the differences reported. A summary of the results of Lee, Ko and Windhal are presented in Table 7 below illustrating the differences in impurity profiles obtained.

Impurities	Windahl (Nagai)	Lee (Nagai)	Ko (Nagai)	Lee (Emde)	Ko (Emde)	Lee (Moscow)
cis-1,2-dimethyl-3-phenylaziridine	√			√	√	
trans-1,2-dimethyl-3-phenylaziridine	√			√	√	
methylamphetamine dimer				√	√	√
1,3-dimethyl-2-phenylnaphthalene	√	√	√			
1-benzyl-3-methyl-naphthalene	√	√	√			
isomers of N-methyl-N-(α -methylphenylethyl)amino-1-phenyl-2-propanone	√		√			
(Z)-N-methyl-N-(α -methylphenethyl)-3-phenyl propenamide	√		√			
chloroephedrine					√	
unknown					√	

Table 7: Impurities found by Windahl et al.[41], Ko et al.[43] and by Lee et al.[42] in their synthesised methylamphetamine batches via Nagai, Emde and Moscow routes.

Inoue et al.[24] performed a comparative study between two chromatographic columns, DB-1 and DB-5. These authors suggested that the DB-5 column offered superior separation of impurities mainly between aziridine and methylamphetamine extracted with a phosphate buffer. 24 characteristic and diagnostic peaks were selected for the classification and comparison of chromatograms. The Euclidean distance of 24 relative peak areas after logarithmic transformation was effective for the evaluation of similarity and/or dissimilarity of impurity profiles.

Ely et al.[44] synthesised samples from a reaction scheme associated with a clandestine laboratory which followed the Birch reduction and found the method to be viable for the production of methylamphetamine; however, no impurities were reported. Person et al.[45] also synthesised methylamphetamine by this route, with ephedrine salt as the starting material. Person et al.[45] reported one impurity 1-(1,4-cyclohexadienyl)-2-methylaminopropane (CMP).

In 2006 Qi et al.[21] analysed nineteen crystalline methylamphetamine ('ice') seizures captured by the Australian Federal Police (AFP) at the Australian border between 1998 and 2004. Major impurities detected included 1,2-dimethyl-3-phenylaziridine, dimethylamphetamine, N-formylmethylamphetamine, N-acetylmethylamphetamine, 1,3-dimethyl-2-phenylnaphthalene, 1-benzyl-3-methylnaphthalene and methylamphetamine dimer. In 2007 they also identified and reported route specific marker compounds normally associated with two different synthetic routes in the 'ice' samples.[33] Using GCMS profiling and Inoue et al.'s sample preparation method [24], more than 30 impurities related to methylamphetamine and/or its synthetic routes were identified (typically purities of 75–80%). The impurities identified were suggested as being associated with the Leuckart synthesis, Reductive Amination, Emde and Nagai routes.[33]

An investigation of tablets seized in Thailand by Puthaviriyakorn in 2002 suggested that the tablets consisted of methylamphetamine hydrochloride (20-30%), caffeine (60-70%) and other compounds (starch, pigments and flavoring compounds). It was suggested that the presence of these diluents and adulterants could make it difficult to directly compare the impurity profiles of methylamphetamine itself.[22]

The samples were extracted with small amounts of ethyl acetate under alkaline conditions and the extracts were analysed. Nine compounds (1,2-dimethyl-3-phenylaziridine, ephedrine, methylephedrine, *N*-formylmethylamphetamine, N-acetylmethylamphetamine, *N*-formylephedrine, *N*-acetylephedrine, *N*,*O*-diacetylephedrie and methylamphetamine dimer) were identified as impurities in the tablets. Caffeine, ethyl vanillin, acetylcodeine monoacetylmorphine and diacetylmorphine were also observed in many of the samples.[22]

In 2004, Dayrit et al [27] described the application of cluster analysis of trace impurities in the profiling of methylamphetamine drug samples seized in the Philippines. Thirty milligrams of a homogenized drug sample were dissolved in 1 mL of pH 10.5 buffer solution and extracted with ethyl acetate containing three internal standards. The trace

impurities were identified using GCMS and quantified by gas chromatography with a flame ionization detector (GCFID). Thirty impurity peaks were selected from the GCFID chromatograms. The peak areas and retention times were referenced to the internal standards. The peak areas of the selected peaks were then grouped for cluster analysis. In order to check for consistency of clustering, two further cluster analyses were performed using 40 and 50 impurity peaks. For the seized drug samples used in this study [27], cluster analysis using at least 40 impurity peaks showed better consistency of clustering as compared to analysis using 30 peaks only.

In 2008 the CHAMP project introduced a harmonised GCMS profiling method for methylamphetamine and instigated the creation of a common database for amphetamines drug profiling in Europe.[30] Fourty three impurity peaks were selected based on the reproducibility of the target compounds within the samples. One hundred and fifty one methylamphetamine street samples, obtained from Finland, Estonia, Norway, Denmark and the Czech Republic were profiled using the CHAMP method without modification.

The initial target compounds were reduced to a set of 19 impurities based on correlation (*R* of Spearman), stability and integration criteria. A final list of 24 target compounds was proposed including five additional compounds included because of their presence and specificity in the chromatogram.[30] Several sample pre-treatment methods were assessed during the analysis of the resultant data including normalization, square root and fourth root processing. The CHAMP method was initially developed for amphetamine impurity profiling and different extraction and GCMS conditions may be needed in order to effectively extract the maximum number of impurities from methylamphetamine samples.

The best discrimination was obtained with the pre-treatment combination of $N+2R$ (normalization followed by the square root) and the application of squared cosine on the pre-treated data in order to calculate the similarity values between linked samples and between unlinked samples.[30]. Further to this multivariate analysis was used to evaluate the possibility of separating samples from the two main synthetic routes, via phenyl-2-

propanone (P-2-P) and ephedrine/*pseudo*ephedrine.[30] Partial least square-discriminant analysis (PLS-DA) was performed to visualize the data and separated the samples between the two synthetic routes. The loading plot produced also graphically illustrated which impurities were important and correlated to each other. From this plot impurities related to a specific route was deduced. Finally cluster analysis was performed on 90 street samples (Czech Republic, Finland), which were produced via the ephedrine route. Using Euclidean distance as the dissimilarity parameter and the Ward method as the clustering method, a dendogram of cluster analysis containing six clusters were obtained.[30]

1.3.2 Drug Profiling with Isotope Ratio Mass Spectroscopy (IRMS)

The analysis of isotope ratios has been found to be a powerful tool to trace the origin of organic compounds. The distribution of stable isotopes within the atomic species of an organic molecule is not random, but depends on the way in which the molecule was formed during synthesis (in the case of methylamphetamine compounds). The measurement of stable isotope ratios of carbon and other elements, using IRMS, is a more recent profiling technique in terms of its application to illicit drug samples. It has been successfully employed to complement conventional chemical profiling in determining the geographical origin of cultivated drugs such as cocaine and heroin, and synthetic route for drugs such as methylamphetamine and 'ecstasy'.[46]

This section will provide an overview of the application of IRMS to drug profiling as it's development has been recorded in the literature. A discussion of the theory, instrumentation, and δ notation of IRMS can be found in Section 2.7.

The application of IRMS in determining the geographic origin and/or discriminating between batches of various types of drug compounds has had been applied over 30 years. In 1991, Desage et al.[47] quoted that Bommer et al., effectively differentiated between production batches of diazepam using IRMS analysis. Desage et al.[47] performed gas chromatography isotope ratio mass spectrometry (GC-IRMS) analysis with samples from various geographical regions in order to determine the geographic origin. Heroin samples

are usually a mixture of diamorphine and diluents/adulterants. The authors were able to distinguished Turkish heroin from all other samples by analysing the $\delta^{13}C$ enrichment of the diamorphine molecule. However, they were unable to discriminate between heroin samples from Pakistan, Niger and Thailand due to similarities in the $\delta^{13}C$.

In 1995, Mas, et al.[48] used GC-IRMS to analyse 16 randomly chosen MDMA tablets seized between 1989-1992. The tablets were separated into four groups based on $\delta^{13}C$ values. Further discrimination was possible with $\delta^{15}N$ values as some of the samples with very similar $\delta^{13}C$ values could be separated on the basic of their $\delta^{15}N$ values.

In 1997 Besacier et al.[49] analysed diamorphine samples using isotopic analysis to determine the isotopic fractionation due to morphine acetylation. They observed differences in $\delta^{13}C$ enrichments between diamorphine and morphine within 17 seized heroin samples and suggested that the differences could be linked to the acetylating agent used in production of the samples. In the same year Besacier et al.[50] recommended a three step procedure for profiling heroin. The first step involved the identification and quantification of the major and minor constituents of heroin, including diluents/adulterants. The second step concerned the charaterisation of manufacturing impurities and reaction by-products and the authors suggested analysis by IRMS as a third step. Besacier et al.[50] reported a case study in which the three steps method was applied to heroin seized from two separate residences of a drug smuggler and analysed these together with an unrelated heroin sample. It was reported that carbon isotope measurements could distinguish the samples into three separate groups while the GC profiles of the samples could not.

In 2000, Ehleringer et al. [51] published a study in *Nature* which correctly identified the origin of cocaine (in 96% of cases) on the basis of $\delta^{13}C$ and $\delta^{15}N$ values together with the content of trace alkaloids of truxilline and trimethoxycocaine. The authors performed their analysis on 200 coca leaf samples collected from five regions in South America.

In 2002, Carter et al. [52] analysed 50 tablets containing MDMA, 10 from each of five different seizures. Isotopic analysis was undertaken to determine whether IRMS could separate the 50 tablets into five batches since the 10 tablets from a single seizure were assumed to be from the same batch. Carter et al. confirmed the previous study of Mas et al.[48] and demonstrated that the N isotope analysis revealed a greater discriminating power than C isotope analysis alone. H isotope analysis was also included in the analysis and the availability of isotopic data for all three elements demonstrated that graphical plots of two and three elements values produced five different sample groupings corresponding to the five sets of samples which was not possible using carbon isotopic values alone.

Carter et al.[53] also investigated isotopic fractionation of amphetamines during synthesis. The authors performed an investigation into the synthesis of methylamphetamine and MDMA. They sythesised various samples of methylamphetamine via the Reductive Amination method using phenylacetone as starting material and two different batches of methylamine. The measured $\delta^{13}C$ values of methylamphetamine which they obtained were consistent with theoretical calculations and indicated no observable kinetic isotopic effects (KIE) with respect to carbon. $\delta^{15}N$ values for the two batches of methylamine reagent showed them to be isotopically distinct by *ca* 1.4‰. However, the isotopic differences between the methylamine and product methylamphetamine, had $\delta^{15}N$ values between +9.2 to -0.3‰ and the authors concluded that since methylamine was the only source of nitrogen in the product, these differences were clearly due to KIE's more than differences between the reagents. The relative reaction rates of $\delta^{14}N$ and $\delta^{15}N$ within the methylamine must, therefore, be highly dependent upon changes in the reaction conditions such as the rate of reagent addition and resulting reaction temperature.

In the second part of this study, Carter et al.[53] explored IRMS analysis of chemically degraded samples of MDMA. The MDMA was isolated and purified from four illicit ecstasy tablets and was oxidised to give the corresponding ketone and aldehyde. Differences (ranging from 1.2 to 5.4‰) were observed between the $\delta^{13}C$ of the MDMA

and its oxidation products were observed in one sample synthesized from piperonal while the remaining samples (synthesized from safrole or isosafrole) exhibited no significant differences between the $\delta^{13}C$ values of the corresponding ketone and aldehyde. Carter et al.[53] concluded that the isotopic content appeared to be characteristic of a specific synthesis.

In 2004, Palhol et al.[54] investigated the discriminating power of $^{15}N/^{14}N$ isotopic ratios in 106 samples of MDMA extracted from Ecstasy tablets. A combination of principal component analysis (PCA) and hierarchical cluster analysis (HCA) allowed the authors to group the tablets into five groups. (Figure 4), and the authors suggested potential links between the samples based upon these results.

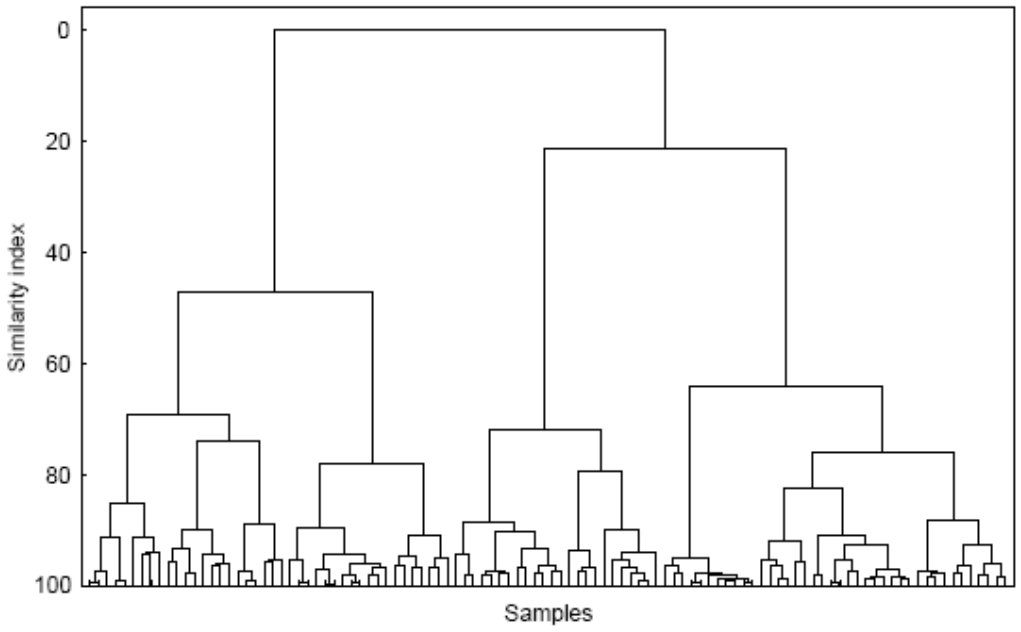

Figure 4: Resulting dendrogram from HCA analysis showing linkages of MDMA samples against similarity index.

Kurashima et al.[55] investigated the possibility of determining the geographic origin of ephedrine on the basis of $\delta^{13}C$ and $\delta^{15}N$ values. Ephedrine is one of the precursors of methylamphetamine, and it can be produced by three routes (Scheme 1): (a) full chemical synthesis; (b) semi-synthesis from sugar; and (c) extraction from the ephedra plant,

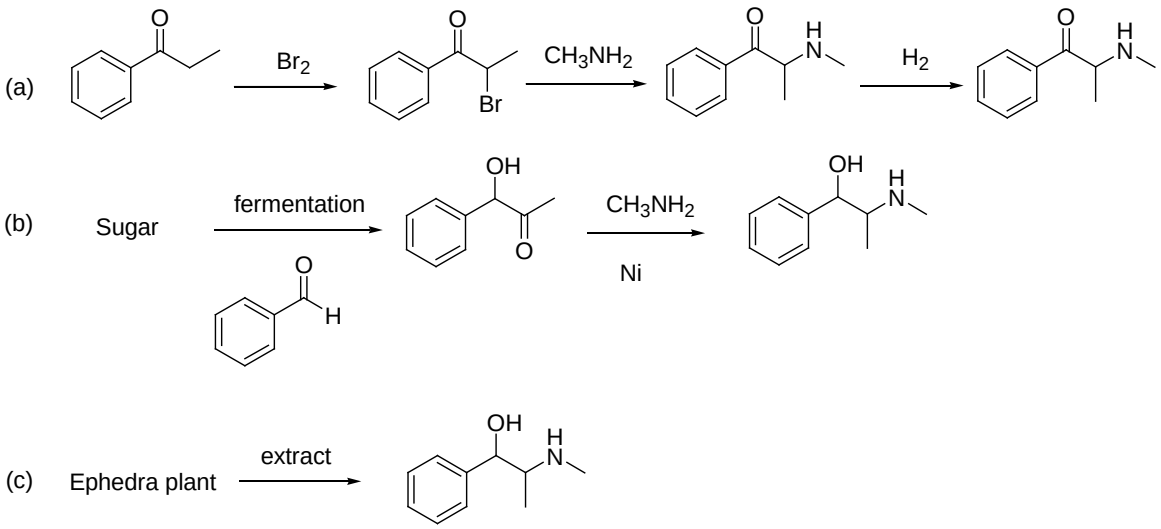

Scheme 1: Three synthesis routes for ephedrine: synthetic, semi-synthetic and natural.[55]

Kurashima et al.[55] reported that combining $\delta^{13}C$ and $\delta^{15}N$ values obtained allowed discrimination of all three forms of ephedrine (Figure 5), thus confirming the importance of the nitrogen isotope abundances in facilitating greater sample discriminating than carbon alone.

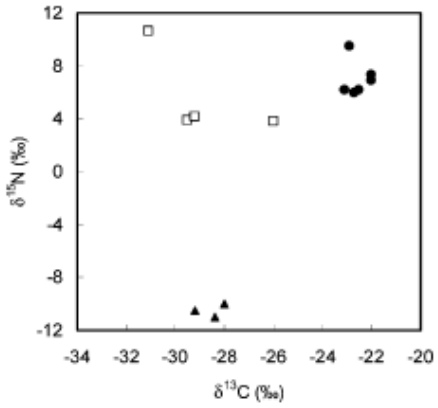

Figure 5: Graphical plot of carbon and nitrogen isotope ratios of ephedrine samples: natural (□), synthesized (▲), and semisynthetic (●).[55]

The authors noted that the $\delta^{15}N$ values of synthetic ephedrine were lower (more negative) than those of ephedrine from other sources. During the ephedrine synthetic process, nitrogen contributed by methylamine. The authors suggested that the drop in $\delta^{15}N$ values was due to the distillation process used to increase the purity of the compound. In the second part of their study, Kurashima et al.[55] undertook a number of methylamine distillations and monitored any changes in the nitrogen isotopic ratios. They reported that

the $\delta^{15}N$ values of methylamine were more negative as the distillation number increased (Figure 6). However the authors did not address why the affect was not observed in semi-synthetic ephedrine as the nitrogen source is also methylamine.

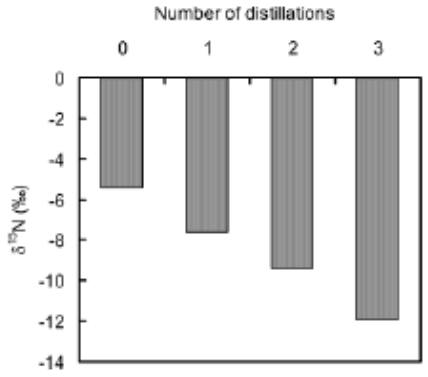

Figure 6 : The variation of $\delta^{15}N$ values of methylamine with increasing number of distillations.[55]

Kurashima et al.[55] also synthesised methylamphetamine samples using ephedrine via three different routes (see Scheme 2). The authors reported that the $\delta^{13}C$ and $\delta^{15}N$ values of methylamphetamine were well correlated with the ephedrine that was used in the synthesis, and concluded that it was possible to link the precursor by measuring the values of $\delta^{13}C$ and $\delta^{15}N$ of the final methylamphetamine product.

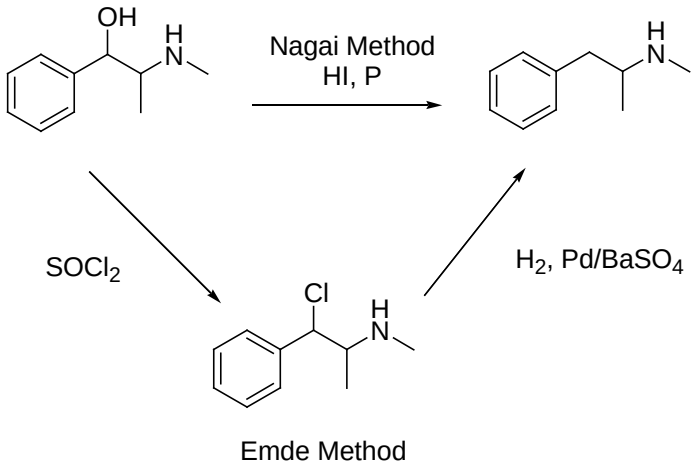

Scheme 2: Two synthesis routes from ephedrine to methylamphetamine.[55]

In 2005, Makino et al.[56] confirmed the work of Kurashima et al.[55] and suggested that there was potential for IRMS to reveal the geographic origin of the ephedrine that had been used as a precursor. The authors investigated the isotopic ratios for carbon and nitrogen for ephedrine samples produced from three synthesis methods (natural, semi-synthetic and synthetic) together with *pseudo*ephedrine of known origin obtained from six different manufacturers. Manufacture A used the ephedrine semi synthetic route and converted the product to *pseudo*ephderine via an isomerization process. Manufacture B used ephedrine produced via the natural route and Manufacture C, D, E used European semi synthetic ephedrine manufactured from sugar beets instead of sugar cane and converted to *pseudo*ephderine via an isomerization process and finally Manufacture F used ephedrine produced via the synthetic method.

The results of Makino et al.[56] agreed with those of Kurashima et al.[55] and demonstrated that the $\delta^{15}N$ values of synthetic ephedrine were lower (more negative) than those obtained for ephedrine obtained from either of the other two methods.. Makino et al.[56] also observed lower $\delta^{15}N$ vales of *d-pseudo*ephedrine (illustrated in Figure 7) and suggested that it was a result of nitrogen isotope fractionation during the manufacturing (isomerization) process, similar to the impact of successive distillations on $\delta^{15}N$ values in methylamine.

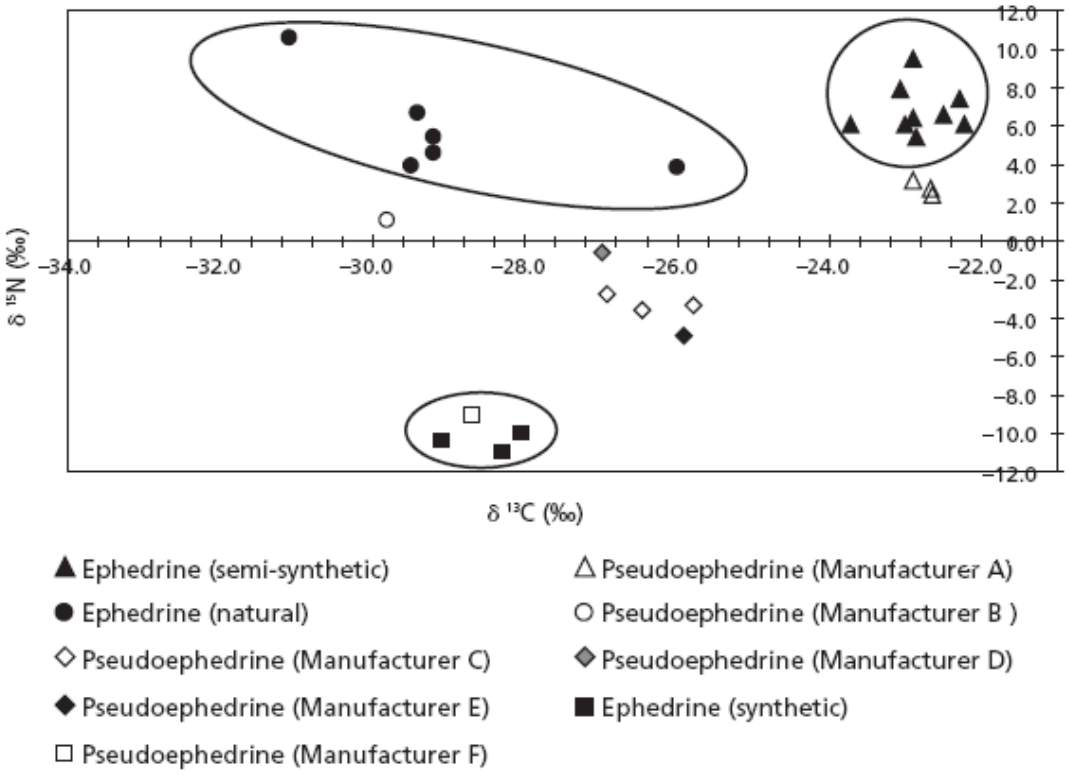

Figure 7: Graphical two dimensional plot of carbon and nitrogen isotope ratios of ephedrine and *pseudo*ephedrine samples.[56]

Makino et al.[56] also investigated whether the carbon and nitrogen stable isotope ratios of ephedrine were carried through to the methylamphetamine end product. They synthesised methylamphetamine from the ephedrine produced via the three different methods using the Nagai route. The results indicated that the $\delta^{13}C$ and $\delta^{15}N$ values for the type of ephedrine were well correlated with those for the corresponding end product. As a consequence the authors suggested that IRMS may be a useful analytical tool to link precursor and end product.

As a application for this study, Makino et al.[56] analysed a total of 15 samples of crystalline methylamphetamine seized in Japan with law enforcement information as to the presumed source countries. IRMS results obtained suggested that the precursor of all seized methylamphetamine samples investigated was natural or semi-synthetic rather

than synthetic (Figure 8). Sample 16 is methylamphetamine synthesized from synthetic ephedrine (shown for reference purposes).

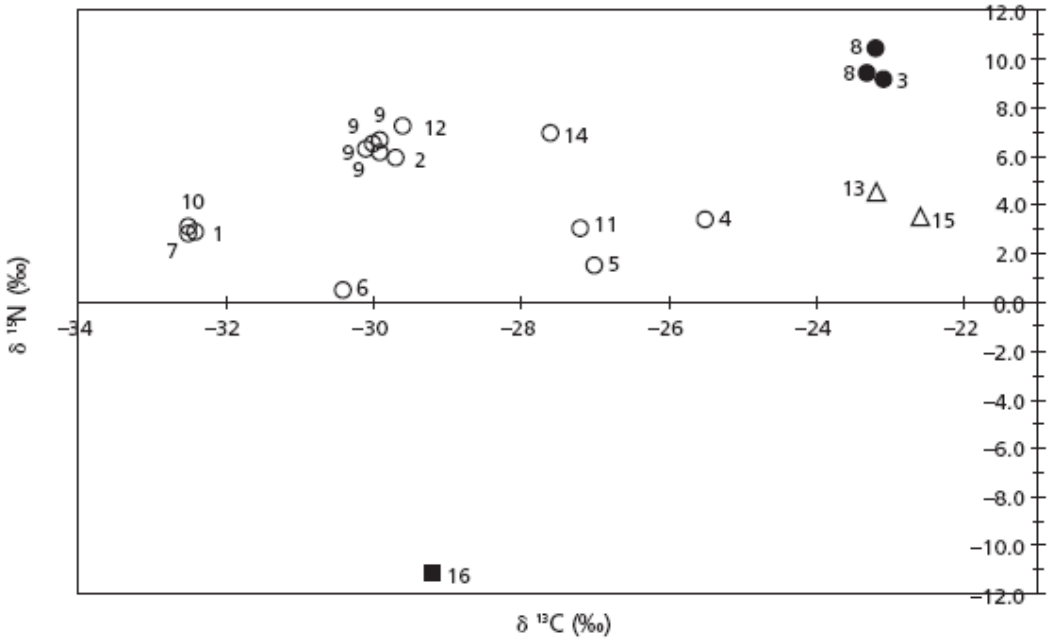

Figure 8: Graphical two dimensional plot of carbon and nitrogen isotope ratios of crystalline methylamphetamine seized in Japan.[56]

In 2006 Casale et al.[57] published a case study involving the analysis of heroin HCl seized from the Merchant Vessel Pong Su involving stable isotope analysis. Two independent national laboratories performed impurity profiling on the sample, but concluded the origin of the substance to be unknown. The authors examined samples from 20 different kilogram packages for isotopic content and compared the values with 200 authenticated specimens from Southeast Asian, Southwest Asia, South America and Mexico. In addition, the heroin samples were converted to morphine, without apparent isotopic fractionation, and analysed. The Pong Su samples were found to be isotopically and isotopically/alkaloidally distinct from the known origin/process classifications of Southwest Asian, Southeast Asian, South American, and Mexican heroin. The results are presented in Figure 9 and Figure 10; where the error bars illustrate one standard deviation of mean values.[57]

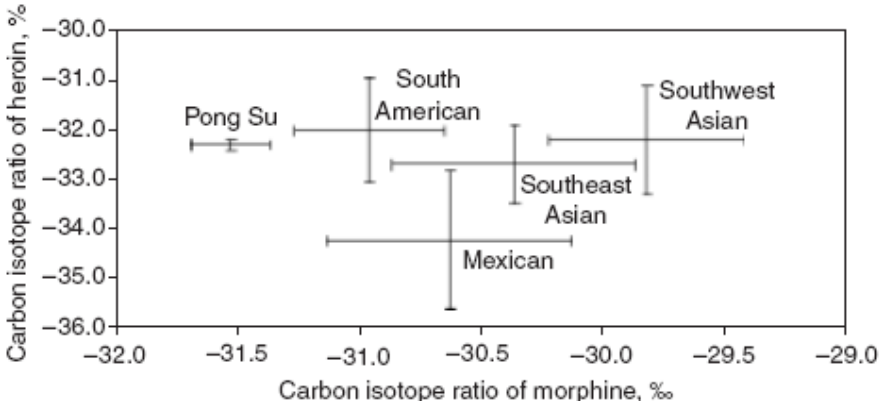

Figure 9: $\delta^{13}C$ values of heroin (diamorphine) and morphine.[57]

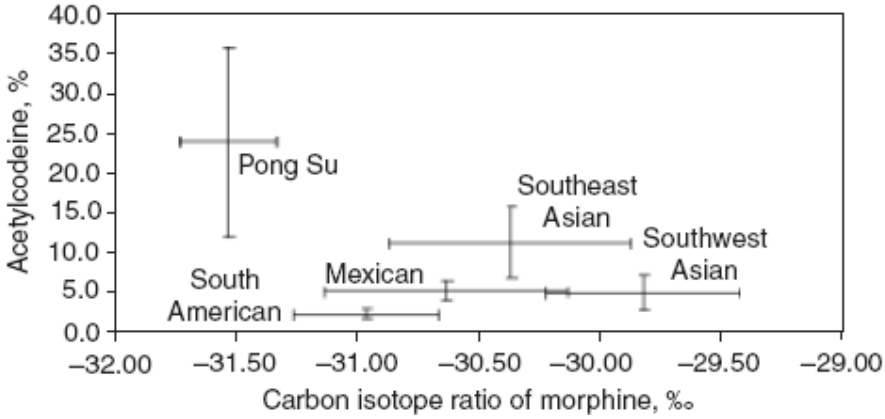

Figure 10: Combined alkaloid and isotope data. Acetylcodeine content (relative to heroin) and $\delta^{13}C$ values of morphine.[57]

In 2007, Billaut et al. [58] investigated $^{15}N/^{14}N$ and $^{13}C/^{12}C$ isotopic ratio values as a tool to distinguished MDMA synthesised by different routes and using different precursors. In order to validate this investigation, the authors synthesised 45 MDMA samples using five different synthetic routes: Reductive Amination (using Al/Hg amalgam, $NaBH_4$ and $NaCNBH_3$ as reducing agents), Leuckart, via N-formyl MDA, via the tosylate, and via nitrostyrene from safrole, isosafrole or piperonal and using a range of sources of nitrogen (aqueous methylamine, methylamine HCl, *N*-methylformamide, ammonium acetate, nitromethane and nitroethane). All the samples and precursors were analysed by elemental analyzer isotope ratio mass spectrometry (EA-IRMS) for $\delta^{13}C$ and $\delta^{15}N$.

The authors noted that the Reductive Amination and Leuckart routes (with 2 and 3 steps respectively) did not introduce ^{13}C fractionation but synthesis via the tosylate or via

nitrostyrene (with four steps) did lead to ^{13}C fractionation. Billaut et al.[58] reported that, it was not possible to discriminate among reducing agents used for Reductive Amination of MDMA batches based on $\delta^{13}C$ values alone.

The authors noted a strong within-pathway correlation between $\delta^{15}N$ values of the nitrogen source and the resultant MDMA, but were unable to discriminate the samples according to synthetic route. They reported that $\delta^{15}N$ values of MDMA were strongly influenced by $\delta^{15}N$ values of the source of nitrogen used, the synthetic route used and the experimental condition. The authors also reported that $\delta^{15}N$ values for individual batches of MDMA produced via the nitrostyrene route (four steps), were not reproducible. They concluded that that it could be unwise to try to link seized batches of ecstasy tablets on the basis of $\delta^{13}C$ and ^{15}N values only.

Ehleringer et al.[59] reported on the forensic applications of stable isotope ratio analysis and cited the work of Lott et al.[60] in the investigation of $\delta^{13}C$, ^{15}N , ^{2}H and ^{18}O values of *pseudo*ephedrine manufactured in different countries using different synthetic processes. The authors noted that *pseudo*ephedrine of different origins were noticed to cluster on some isotopic plots ($\delta^{18}O$ vs $\delta^{2}H$), while being successfully discriminated and identifiable using other isotopic plots ($\delta^{13}C$ vs $\delta^{2}H$).

In 2008, Buchanan et al.[61] analysed 18 MDMA samples which were synthesised from the same precursors, piperonyl methyl ketone (PMK) by three common Reductive Amination routes (Al/Hg amalgam, $NaBH_4$ and Pt/H_2) and determined the $\delta^{13}C$, $\delta^{15}N$ and $\delta^{2}H$ values. The authors converted safrole, to isosafrole and finally to PMK and reported route discrimination on the basis of the $\delta^{2}H$ isotopic abundance as demonstrated in Figure 11. The authors also reported that hierarchical cluster analysis (HCA) using $\delta^{2}H$ values on its own or combination with $\delta^{13}C$ and/or $\delta^{15}N$ provided a statistical means for accurate discrimination by the three Reductive Amination methods (Figure 12).

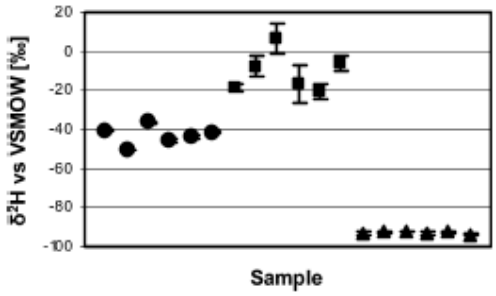

Figure 11: ^{2}H values of 18 synthesised MDMA batches: (●) Al/Hg amalgam, (■) $NaBH_4$, (▲)Pt/H_2.[61]

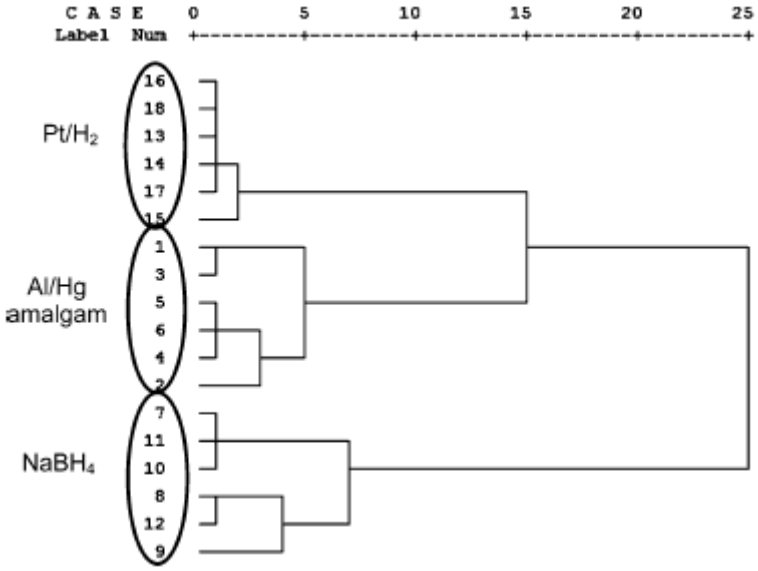

Figure 12: HCA results using δ^{13}C, ^{15}N and ^{2}H values of 18 synthesised MDMA batches.[61]

In 2009 Collins et al.[46] published a study investigating the potential for $\delta^{13}C$, $\delta^{15}N$ and $\delta^{2}H$ values to determine the origin of the methylamphetamine precursors, ephedrine and *pseudo*ephedrine. In this study 23 methylamphetamine samples were synthesised from five different sources of precursors using four common routes (Nagai, Emde, Moscow and Hypophosphorous acid methods). The authors reported that the isotopic measurement by elemental analyzer/thermal conversion isotope ratio mass spectrometry (EA/TC-IRMS) in high purity samples allowed the determination of the synthetic source of the ephedrine or *pseudo*ephedrine precursor as being either of a natural, semi-synthetic, or fully synthetic origin. It also should be noted that $\delta^{13}C$, $\delta^{15}N$ and $\delta^{2}H$ values of the

synthesised methylamphetamine samples clustered according to the precursors used and not the synthetic route that been used (Figure 13)

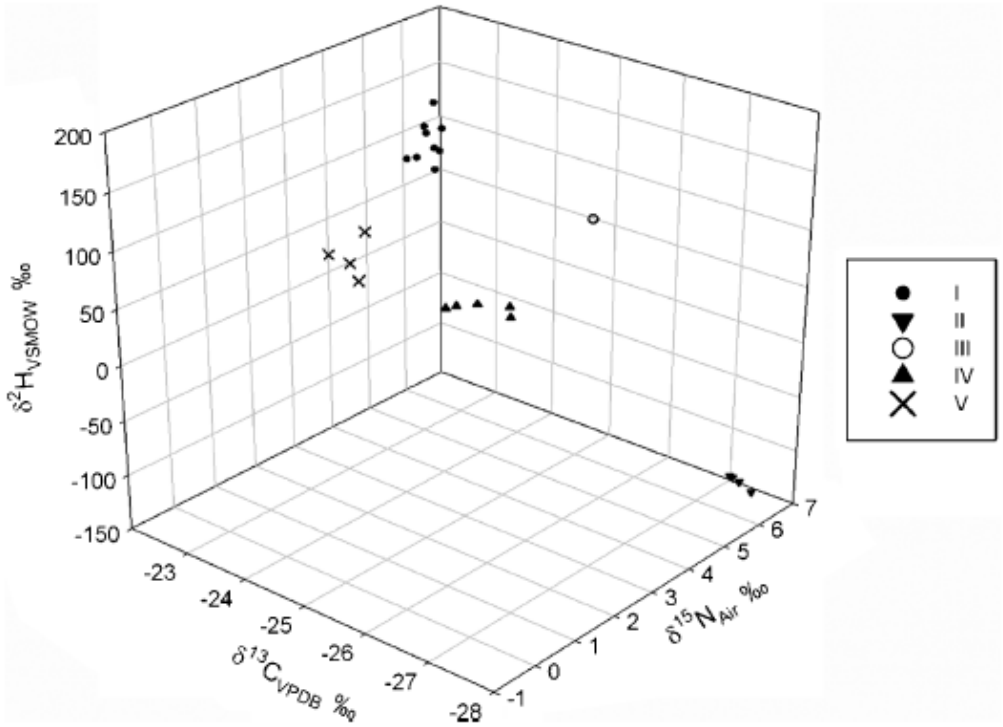

Figure 13: Graphical three dimensional plot of carbon, nitrogen and hydrogen isotope ratios of methylamphetamine synthesised from five different sources of precursors.[46]

Collins et al.[46] citing the work of Butzenlechner et al.[62] and Culp et al.[63] investigating benzaldehyde as an adulterant in flavors suggested that δ^2H values could discriminate synthetic materials from botanically derived materials. The authors also analysed a number of seized high purity methylamphetamine and concluded that ephedrine produced from synthetic benzaldehyde and *pseudo*ephedrine derived from the ephedrine both revealed positive δ^2H values suggesting that the positive ^2H values precursors are maintained in the resultant methylamphetamine.

In 2009, Kurashima et al.[64] further investigated the origin of ephedrine and *pseudo*ephedrine using IRMS. The authors analysed 27 precursor samples originating from various manufacturing methods (natural, synthetic and semi-synthetic; derived from

molasses and pyruvic acid). The authors noted that, based on $\delta^{13}C$ and $\delta^{15}N$ values, the semi-synthetic ephedrines derived from pyruvic acid could not be discriminated from natural ephedrines and synthetic ephedrines (Figure 14) but could be discriminated based on $\delta^{2}H$ values (Figure 15).

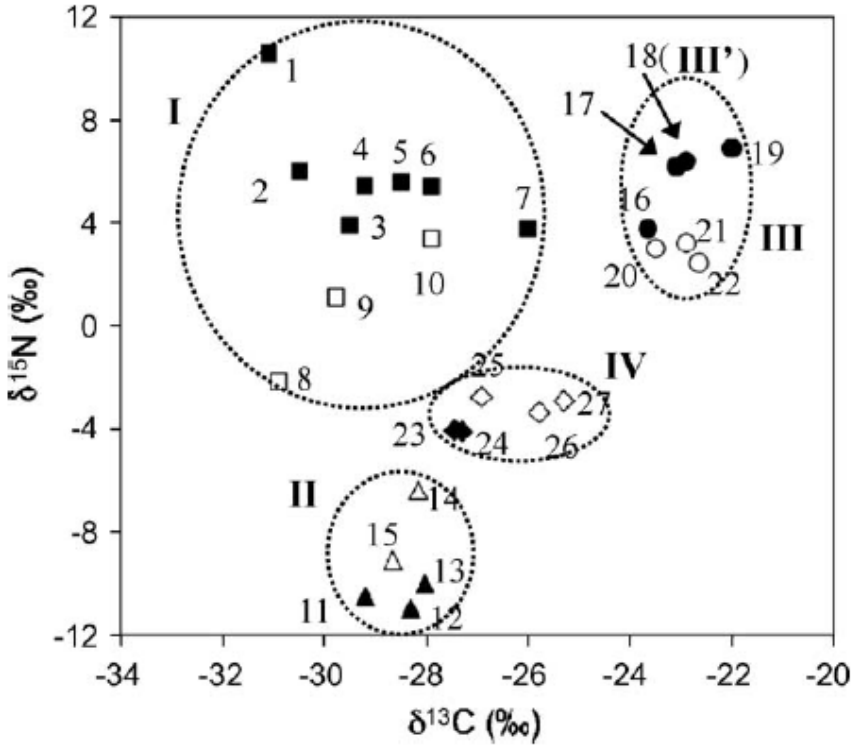

Figure 14: Graphical two dimensional plot of carbon and nitrogen isotope ratios of *l*-ephedrine and *d-pseudo*ephedrine samples: biosynthetic (■), synthetic (▲), semi-synthetic from molasses (●), and semi-synthetic from pyruvic acid (♦). Open symbols indicate *d-pseudo*ephedrine samples. The biosynthetic group is indicated as 'I', the synthetic group as 'II', the semisynthetic group from molasses as 'III', and the semisynthetic group from pyruvic acid as 'IV. [64]

Kurashima et al.[64] reported that $\delta^{2}H$ values of naturally derived ephedrines (^{2}H: -193 to -151%) allows a clear distinction from synthetic ephedrines (^{2}H: -73 to -30%), semi-synthetic ephedrines derived from pyruvic acid (^{2}H: +75 to +148%) and semi-synthetic ephedrines derived from molasses (^{2}H: -74 to +243%) (Figure 15).

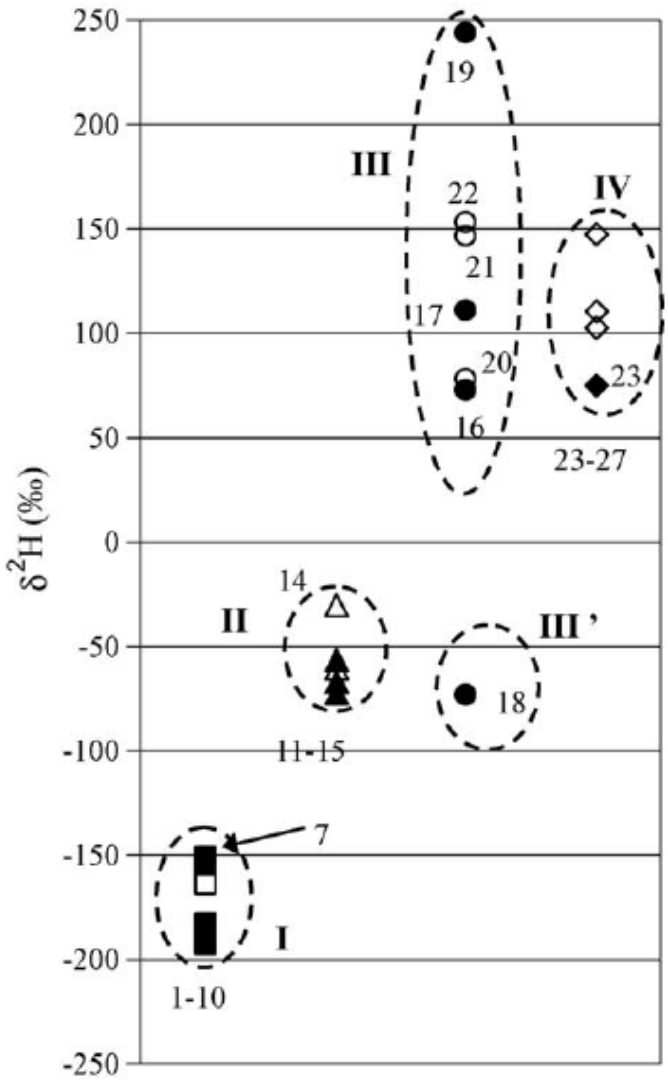

Figure 15: ^{2}H values of of *l*-ephedrine and *d-pseudo*ephedrine samples: biosynthetic (■), synthetic (▲), semi-synthetic from molasses (●), and semisynthetic from pyruvic acid (♦). Open symbols indicate *d-pseudo*ephedrine samples. I–IV are the same as in Fig. 14.[64]

Kurashima et al.[64] also synthesised seven methylamphetamine samples by either the Nagai or Emde routes and observed a substitution of exchangeable hydrogen atoms during the synthesis. In order to study this substitution, samples were synthesised with untreated (treated with water) and treated with Milli-Q water. The authors suggested the δ^2H values of ephedrine and methylamphetamine may be affected by various experimental conditions during the synthesis. Exchangeable hydrogen atoms were substituted in order to eliminate the influence of these atoms on the measured δ^2H values.

The authors concluded that the change in the results observed due to substitution of exchangeable hydrogens would not have a great influence on the inference as to the origin of the samples.

In 2009, Schneiders et al.[65] investigated the isotopic ratios of 1-phenyl-2-propanone (P-2-P, benzylmethylketone), a common precursor in amphetamine and methylamphetamine synthesis. The authors determined the variation of the isotopic ratios within precursor samples produced by one manufacturer and compared these to similar values obtained from the analysis of seized samples of unknown origin. The authors noted considerable differences between the precursor values and those obtained from the seized samples. They also noted that most of the batches of seized samples were not isotopically homogenous based on the intra variability of $\delta^{13}C$, $\delta^{2}H$ and $\delta^{18}O$ values.

1.3.3 Drug Profiling with Inductively Coupled Plasma Mass Spectrometry (ICPMS)

In the 1980's inductively coupled plasma mass spectrometry (ICPMS) methods were developed for qualitative or quantitative trace level multi elemental analysis. Recent interest has been focused on the nature and level of inorganic trace impurities present in the final product of the synthesis of illicit drugs. Inorganic impurities are the elemental synthetic impurities in illicit drugs (synthetic and semi synthetic) that have the potential to indicate the synthetic pathway used for manufacture. A discussion of the theory and instrumentation of ICPMS can be found in Section 2.8.

In 1988, Suzuki et al.[66] determined inorganic impurities in seized crystalline methylamphetamine by ICPMS and ion chromatography (IC). The authors observed large variations of the target elements within the same crystal and concluded that several parts of the crystal should be analysed.

In 1994 Marumo et al.[67] investigated the validity of inorganic impurity profiling in discriminating seized methylamphetamine samples using ICPMS and atomic absorption spectrometry (AAS). Triplicate analysis was carried out on 17 methylamphetamine

samples seized in Japan. Ba, Sb, Pd, Sr, Br ,Zn and Cu were determined by ICP-MS, and Na was determined by AAS. The authors observed that most cations exhibited good heterogeneity in their content and they classified the seized methylamphetamine samples into five groups based on the elemental composition.

Suh et al.[68] carried out inorganic impurity analysis on 51 samples of illicit methylamphetamine using ICPMS. In their work, iodine was detected in most of the samples produced via the Nagai method and palladium or barium was detected in two thirds of the Emde samples. The authors reported that they detected bromine in 29 samples (Nagai, Emde, and other undetermined route) and suggested further studies on this element was necessary. They concluded that analysis of inorganic impurities in illicit methylamphetamine could be considered complementary to organic impurity analysis.[68]

In 2007, Koper et al.[69] investigated the elemental composition of MDMA powders (57 samples from known origin) and tablets (97 samples) obtained from illicit production in the Netherlands. The authors used a microwave digestion method for sample preparation and quantitative performed qualitative analysis of the samples using ICPMS and ICPAES. They suggested the synthetic route for 48 MDMA of the 57 powder samples analysed on the basis of Pt, B or Hg content and suggested a possible discrimination between the various Reductive Amination processes. They also suggested the synthetic method for 88 of the MDMA tablets analysed. Data analysis using the Pearson correlation process further identified 13 links within the 97 MDMA tablets and suggested that elemental analysis was a valuable additional tool for drug profiling.

1.4 Objectives of This Work

The development of the CHAMP and various other GCMS profiling methods, have successfully demonstrated the potential of organic impurity profiling in facilitating the comparison of seized methylamphetamine, however this was based only on some of the synthetic routes used in its manufacture. Moreover, the available literature predominantly reports on analysis performed on single examples of seized samples or small samples of synthesised products rather than multiple samples of known provenance. Where synthetic samples have been produced and analysed, they have been done so with limited repetition of the synthesis, synthetic variation between researchers and using various GCMS methods thus rendering cross study comparisons difficult and providing limited, if any, interpretation of between batch variation within a single synthetic method. Similar criticisms exist in relation to IRMS and ICPMS analysis. The literature reports data derived from both seized methylamphetamine samples and synthesised samples using only a limited number of the possible routes and without the robustness of repetitive carefully controlled synthesis.

The main aim and focus of this work was to address these deficiencies. In total this project involved the synthesis of 149 samples of methylamphetamine using seven different synthetic routes where 20-25 samples were produced for each route using identical reaction conditions.

Two different precursors were used in the synthesis depending on the synthetic route used as follows;

(a) starting from phenyl-2-propanone (P-2-P); the Leuckart route and Reductive Amination

(b) starting from *l*-ephedrine or *d-pseudo*ephedrine; the Nagai route, Rosenmund hydrogenation, Birch reduction, Emde route with chloro-ephedrine as intermediate and Moscow route.

Following the synthesis of the methylamphetamine samples the objectives of this work were as follows:

- The development of a GCMS profiling method which incorporated the extraction of both acidic and basic impurities and the generation of a list of target impurities. This would allow a full exploration of the range of route specific impurities produced in the synthesis of methylamphetamine and clarify the existing literature in this area.

- The comparison of known provenance methylamphetamine samples using IRMS analysis to investigate linkage abilities to precursors and to synthetic route across all seven synthetic methods. The samples set produced would allow the inter-synthesis variation (batch to batch variation) to also be assessed. Isotopic variations between methylamphetamine and crystalline methylamphetamine formed from the same reaction products would also be assessed.

- Elemental analysis of known provenance methylamphetamine samples by ICPMS to comprehensively investigate the efficacy of ICPMS as a profiling tool for this drug.

- The final objective of this work was to assess the ability of three data analysis techniques to provide meaningful discrimination of the methylamphetamine data sets generated by the analytical techniques employed. Hierarchical cluster analysis, principal component analysis, and discriminant analysis were applied to the GCMS data on its own, the IRMS data on its own, ICPMS data on its own, combinations of data from two techniques and combinations data from all of the techniques data to assess which technique and which data interpretation methods would provide the best chance of accurate methylamphetamine profiling. Various data pretreatment methods were also investigated.

1.5 Thesis Overview

In Chapter 2, the analytical techniques and instrumentation used in this project are discussed. Nuclear magnetic resonance (NMR), Fourier transform infra red spectroscopy (FTIR), melting point and capillary electrophoresis (CE), which were used for confirmation of the identity of compounds during the synthesis of methylamphetamine, are addressed briefly. GCMS, IRMS and ICPMS are discussed in greater detail as they were the main analytical techniques used in the project.

The synthesis of methylamphetamine by seven synthetic routes is described in Chapter 3. A discussion of the mechanism and chemistry which contributes to the final methylamphetamine molecule is undertaken in this chapter.

Chapter 4 and 5 outlines in detail the GCMS profiling work. Chapter 4 details the preliminary work used to test column performance to ensure repeatability of the chromatography and method validation for the extraction procedure and GCMS conditions. The results of the analysis of the synthesised methylamphetamine are discussed and a list of 'target' organic impurities proposed are presented in Chapter 5. The results were analysed using the Pearson correlation matrix to evaluate the degree of similarity between samples based on the types and quantity of impurities present in each batch.

The results of the IRMS analysis of the 149 synthesised methylamphetamine samples are presented and discussed in Chapter 6, and the discrimination by precursors and/or synthetic route afforded by one, two and three-dimensional plots of the isotope data (i.e. the δ values) is addressed.

In Chapter 7, the results of the ICPMS analysis of the synthesised methylamphetamine samples is presented. The concentration of each inorganic element is assessed and evaluated within the context of the synthetic route used.

Multivariate analysis of the analytical data sets produced from the various techniques employed is discussed in Chapter 8. The data sets incorporated 429 separate items of data (143 samples x 3 techniques). Data from GCMS, IRMS and ICPMS was subjected to HCA, PCA and DA in order to assess which data analysis techniques including preprocessing techniques afford meaningful discrimination of the samples. The overall conclusions of this work are outlined in Chapter 9, together with suggestions for future research in order to advance the field of methylamphetamine profiling.

1.6 References

1. United Nations Office on Drugs and Crime, *World Drug Report*; 2005.

2. United Nations Office on Drugs and Crime, *World Drug Report*; 2009.

3. Drug Use Around the World. Available at http://www.gale.cengage.com/pdf/samples/sp65756X pdf. Last accessed on 04/01/10.

4. Singer, M., Drugs and development: The global impact of drug use and trafficking on social and economic development. *International Journal of Drug Policy* 2008, 19, 467–478.

5. Guardian News. Available at http://www.guardian.co.uk/world/2009/jun/24/united-nations-world-drug-report. Last accessed 27/12/09.

6. Carson, R.; Macmillan, D.; Gale, T., Shanghai Opium Conference -Encyclopedia of Drugs, Alcohol, and Addictive Behavior, 2001 Available at http://www.enotes.com/drugs-alcohol-encyclopedia/shanghai-opium-conference. Last accessed on 04/12/09.

7. United Nations, Single Convention on Narcotic Drugs, 1961. Available at http://www.incb.org/pdf/e/conv/convention_1961_en.pdf. Last accessed on 12/12/09.

8. United Nations, Convention on Psychotropic Substances, 1971. Available at http://www.incb.org/pdf/e/conv/convention_1971_en.pdf. Last accessed on 14/12/2009

9. United Nations, Convention Against the Illicit Traffic in Narcotic Drugs and Psychotropic Substances, 1988. Available at http://www.incb.org/pdf/e/conv/convention_1988_en.pdf. Last accessed on 16/12/09.

10. Introduction to Drug Trends, Control, Legislation and Analysis. Available at http://www.drugscope.org/druginfo/drugreport.asp. Last accessed on 19/12/09.

11. The Evidence Base for the Classification of Drugs, 2006. Available at http://www.rand.org. Last accessed on 10/12/09.

12. King, L., Forensic Chemistry of Substance Misuse: *A Guide to Drug Control*. RCS: Cambridge, 2009.

13. King, L., The Misuse of Drugs Act - *A Guide for Forensic Scientists*. RCS: Cambridge, 2003.

14. Affairs, B.f.I.N.a.L.E., International Narcotics Control Strategy Report 2006. Available at http://www.state.gov/p/inl/rls/nrcrpt/2006/vol1/html/62105.htm. Last accessed on 20/12/09.

15. Controlled Drugs (Substances Useful for Manufacture) (Intra-Community Trade) Regulations 1993. Available at http://www.uk-legislation.hmso.gov.uk/si/si1993/Uksi_19932166_en_1.htm. Last accessed on 10/11/08.

16. Home Office, Drug Laws & Licensing. Available at http://drugs.homeoffice.gov.uk/drugs-laws/misuse-of-drugs-act/. Last accessed on 10/12/08.

17. United Nations International Drug Control Programme, *Drug Characterization/Impurity Profiling : Background and Concepts*; Vienna 2001.

18. Remberg, B. and A.H. Stead. Drug characterization/impurity profiling, with special focus on methamphetamine: recent work of the United Nations International Drug Control Programme. *Bulletin on Narcotics 1999 (Volume LI Nos. 1 and 2),* Available at http://www.unodc.org/unodc/en/data-and-analysis/bulletin/bulletin_1999-01-01_1_page008.html. Last accessed on 12/12/09.

19. Buchanan, H.A.S., *An evaluation of isotope ratio mass spectrometry for the profiling of 3,4-methylenedioxymethamphetamine*, PhD Thesis in Department of Pure and Applied Chemistry, University of Strathclyde: Glasgow, 2009, 15.

20. Tanaka, K.; Ohmort, T.; Inonue, T.; Seta, S., Impurity Profiling Analysis of Illicit Methamphetamine by Capillary Gas Chromatography. *Journal of Forensic Sciences* 1994, 39(2), 500-511.

21. Qi, Y.; Evans, I.D.; McCluskey, A., Australian Federal Police seizures of illicit crystalline methamphetamine ('ice') 1998–2002: Impurity analysis. *Forensic Science International* 2006, 164(2-3), 201-210.

22. Puthaviriyakorn, V.; Siriviriyasomboon, N.; Phorachata, J.; Pan, W.; Sasaki, T.; Tanaka, K., Identification of impurities and statistical classification of methamphetamine tablets (Ya-Ba) seized in Thailand. *Forensic Science International* 2002, 126, 105-113.

23. Tanaka, K.; Ohmori, T.; Inoue, T., Analysis of impurities in illicit methamphetamine. *Forensic Science International* 1992, 56 (2), 157 - 165.

24. Inoue, H.; Kanamori, T.; Iwata, Y.T.; Ohmae, Y.; Tsujikawa, K.; Saitoh, S.; Kishi, T., Methamphetamine impurity profiling using a 0.32 mm i.d. nonpolar capillary column. *Forensic Science International* 2003, 135(1), 42-47.

25. Lurie, I.S.; Bailey, C.G.; Anex, D.S.; Bethea, M.J.; McKibben, T.D.; Casale, J.F., Profiling of impurities in illicit methamphetamine by high-performance liquid chromatography and capillary electrochromatography. *Journal of Chromatography A* 2000, 870, 53-68.

26. Koester, C.J.; Andresen, B.D.; Grant, P.M., Optimum Methamphetamine Profiling with Sample Prepearation by Solid-Phase Microextraction. *Journal of Forensic Sciences* 2002, 47(5).

27. Dayrit, F.M.; Dumlao, M.C., Impurity profiling of methamphetamine hydrochloride drugs seized in the Philippines. *Forensic Science International* 2004, 144, 29-36.

28. Ballany, J.; Caddy, B.; Cole, M.; Finnon, Y.; Aalberg, L.; Janhunen, K.; Sippola, E.; Andersson, K.; Bertler, C.; Dahle´n, J.; Kopp, I.; Dujourdy, L.; Lock, E.; Margot, P.; Huizer, H.; Poortman, A.; Kaa, E.; Lopes, A., Development of a harmonised pan-European method for the profiling of amphetamines. *Science and Justice*, 2001, 41(3),193-196.

29. Andersson, K.; Lock, E.; Jalava, K.; Huizer, H.; Jonson, S.; Kaa, E.; Lopes, A.; Poortman, A.; Sippola, E.; Dujourdy, L.; Dahle´n, J., Development of a harmonised method for the profiling of amphetamines VI Evaluation of methods for comparison of amphetamine. *Forensic Science International* 2007, 169**,** 86–99.

30. Dujourdy, L.; Dufey, V.; Besacier, F.; Miano, N.; Marquis, R.; Lock, E.; Aalberg, L.; Dieckmann, S.; Zrcek, F.; Bozenko, J.S., Drug intelligence based on organic impurities in illicit MA samples. *Forensic Science International* 2008, 177, 153-161.

31. United Nations Office on Drugs and Crime, *Methods For Impurity Profiling of Heroin and Cocaine*.

32. Forensic Science Service, *Methylamphetamine : Chemistry, Seizure Statistics, Analysis, Synthetic Routes And History Of Illicit Manufacture In UK And USA*, 2004.

33. Qi, Y.; Evans, I.; McCluskey, A., New impurity profiles of recent Australian imported ‘ice’: Methamphetamine impurity profiling and the identification of (pseudo)ephedrine and Leuckart specific marker compounds. *Forensic Science International*, 2007, 169, 173–180.

34. Barron, R.P.; Kruegel, A.V.; Moore, J.M.; Kram, T.C., Identification of Impurities in Illicit Methamphetamine Samples. *Journal of the Association of Official Analytical Chemists*, 1974, 57(5), 1147-1158.

35. Bailey, K.; Boulanger, J.G.; Legault, D.; Taillefer, S.L., Identification and Synthesis of Di-(1-phenylisopropyl)methylamine, an Impurity in Illicit Methamphetamine. *Journal of Pharmaceutical Sciences*, 1974, 63(10),1575-1578.

36. Kram, T.C.; Kruegel, A.V., The Identification of Impurities in Illicit Methamphetamine Exhibits by Gas Chromatography/Mass Spectrometry and Nuclear Magnetic Resonance Spectroscopy. *Journal of Forensic Sciences* 1977, 22(1), 40-52.

37. Verweij, A.M.A., Impurities in Illicit Drug Preparations: Amphetamine and Methamphetamine. *Journal of Forensic Sciences* 1989, 1(1), 1-11.

38. Skinner, H.F., Methamphetamine Synthesis via HI/Red Phosphorus Reduction of Ephedrine. *Forensic Sciences International* 1990, 48, 123-134.

39. Inoue, T.; Tanaka, K.; Ohmori, T.; Togawa, Y.; Seta, S., Impurity profiling analysis of methamphetamine seized in Japan. *Forensic Science International* 1994, 69(1), 97-102.

40. Cantrell, T.S.; John, B.; Johnson, L.; Allen, A.C., A Study of Impurities Found in Methamphetamine Synthesized From Ephedrine. *Forensic Science International* 1988, 39, 39-53.

41. Windahl, K.L.; McTigue, M.J.; Pearson, J.R.; Pratt, S.J.; Rowe, J.E.; Sear, E.M., Investigation of the impurities found in methamphetamine synthesised from pseudoephedrine by reduction with hydriodic acid and red phosphorus. *Forensic Science International* 1995, 76, 97-114.

42. Lee, J.S.; Han, E. Y.; Lee, S. Y.; Kim, E. M.; Park, Y. H.; Lim, M. A.; Chung, H. S.; Park, J. H., Analysis of the impurities in the methamphetamine synthesized by three different methods from ephedrine and pseudoephedrine. *Forensic Science International* 2006, 161(2-3), 209-215.

43. Ko, B.J.; Suh, S.; Suh, Y.J.; In, M.K.; Kim, S.H., The impurity characteristics of methamphetamine synthesized by Emde and Nagai method. *Forensic Science International* 2007, 170(1), 142-147.

44. Ely, R.A.; McGrath, D.C., Lithium-Ammonia Reduction of Ephedrine to Methamphetamine: An Unusual Clandestine Synthesis. *Journal of Forensic Sciences* 1990, 35(3), 720-723.

45. Person, E.C.; Meyer, J.A.; Vyvyan, J.R., Structural Determination of the Principal Byproduct of the Lithium-Ammonia Reduction Method of Methamphetamine Manufacture. *Journal of Forensic Sciences* 2005, 50(1), 1-9.

46. Collins, M.; Cawley, A.T.; Heagney, A.C.; Kissane, L.; Robertson, J.; Salouros, H., $\delta^{13}C$, $\delta^{15}N$ and $\delta^{2}H$ isotope ratio mass spectrometry of ephedrine and pseudoephedrine: application to methylamphetamine profiling. *Rapid Communications in Mass Spectrometry* 2009, 23, 2003-2010.

47. Desage, M.; Guilluy, R.; Brazier, J.L.; Chaudron, H.; Girard, J.; Cherpin, H.; Jumeau, J., Gas chromatography with mass spectrometry or isotope-ratio mass spectrometry in studying the geographical origin of heroin. *Analytica Chimica Acta* 1991, 247, 249-254.

48. Mas, F.; Beemsterboera, B.; Veltkamp, A.C.; Verweij, A.M.A., Determination of 'common-batch' members in a set of confiscated 3,4-(methylendioxy)-methylamphetamine samples by measuring the natural isotope abundances: a preliminary study. *Forensic Science International* 1995, 71, 225-231.

49. Besacier, F.; Guilluy, R.; Brazier, J.L.; Thozet, H.C.; Girard, J.; Lamotte, A., Isotopic Analysis of 13C as a Tool for Comparison and Origin Assignment of Seized Heroin Samples. *Journal of Forensic Science* 1997, 42(3), 429-433.

50. Besacier, F.; Thozet, H. C.; Tsangaris, M.R.; Girard, J.; Lamotte, A., Comparative chemical analysis of drug samples: general apporach and application to heroin. *Forensic Science International* 1997, 85, 113-125.

51. Ehleringer, J. R.; Casale, J.F.; Lott, M. J.; Ford, V. L., Tracing the geographical origin of cocaine. *Nature* 2000, 408.

52. Carter, J.F.; Titterton, E.L.; Murray, M.; Sleeman, R., Isotopic characterisation of 3,4-methylenedioxyamphetamine and 3,4-methylenedioxymethylamphetamine (ecstasy). *Analyst* 2002, 127, 830-833.

53. Carter, J. F.; Titterton, E. L.; Grantc, H.; Sleeman, R., Isotopic changes during the synthesis of amphetamines. *Chemical Communication*s 2002, (21) 2590–2591.

54. Palhol, F.; Lamoureux, C.; Chabrillat, M.; Naulet, N., $^{15}N/^{14}N$ isotopic ratio and statistical analysis: an efficient way of linking seized Ecstasy tablets. *Analytica Chimica Acta* 2004, 510, 1–8.

55. Kurashima, N.; Makino, Y.; Sekita, S.; Uranob, Y.; Nagano, T., Determination of Origin of Ephedrine Used as Precursor for Illicit Methamphetamine by Carbon and Nitrogen Stable Isotope Ratio Analysis. *Journal of Analytical Chemistry* 2004, 76(14), 4233-4236.

56. Makino, Y.; Urano, Y.; Nagano, T., Investigation of the origin of ephedrine and methamphetamine by stable isotope ratio mass spectrometry: a Japanese experience. *Bulletin on Narcotics* 2005, 57, 63-68.

57. Casale, J.; Casale, E.; Collins, M.; Morello, D.; Cathapermal, S.; Panicker, S., Stable Isotope Analyses of Heroin Seized from the Merchant Vessel Pong Su. *Journal of Forensic Science* 2006, 51(3), 603-606.

58. Billault, I.; Courant, F.; Pasquereau, L.; Derrien, S.; Robins, R. J.; Naulet, N., Correlation between the synthetic origin of methamphetamine samples and their ^{15}N and ^{13}C stable isotope ratios. *Analytica Chimica Acta* 2007, 593, 20-29.

59. Ehleringer, J.R.; Cerling, T.E.; West, J.B., Forensic Science Applications of Stable Isotope Ratio Analysis, in *Forensic Analysis on the Cutting Edge: New Methods for Trace Evidence Analysis*. John Wiley & Sons, Inc: 2007, 398-417.

60. Lott, M.J.; Howa, J.; Ehleringer, J.R.; Jauregui, J.F.; Douthitt, C., Detecting the manufacturing origin of pseudoephedrines through stable isotope ratio analysis. 2002, Poster, *Forensics Isotope Ratio Mass Spectrometry Conference*, 17 September. http://www.forensic-isotopes.rdg.ac.uk/conf/conf.htm.

61. Buchanan, H.A.S.; Dae´ id, N. N.; Augenstein, W. M.; Kemp, H. F.; Kerr, W. J.; Middleditch, M., Emerging Use of Isotope Ratio Mass Spectrometry as a Tool for Discrimination of 3,4-Methylenedioxymethamphetamine by Synthetic Route. *Analytical Chemistry* 2008, 80(9), 3350-3356.

62. Butzenlechner, M.; Rossmann, A.; Schmidt, H.L., *Journal of Agricultural and Food Chemistry* 1989, 37, 410.

63. Culp, R.A.; Noakes, J.E., *Journal of Agricultural and Food Chemistry* 1992 1992(40), 1892.

64. Kurashima, N.; Makino, Y.; Urano, Y.; Sanuki, K.; Ikehara, Y.; Nagano, T., Use of stable isotope ratios for profiling of industrial ephedrine samples: Application of hydrogen isotope ratios in combination with carbon and nitrogen. *Forensic Science International* 2009, 189, 14-18.

65. Schneiders, S.; Holdermann, T.; Dahlenburg, R., Comparative analysis of 1-phenyl-2-propanone (P2P), an amphetamine-type stimulant precursor, using stable isotope ratio mass spectrometry Presented in part as a poster at the 2nd meeting of the Joint European Stable Isotope User Meeting (JESIUM), Giens, France, September 2008. *Science and Justice* 2009, 1-8.

66. Suzuki, H.I.; Tsuchihashi, H.; Nakajima, K.; Matsushita, A.; Nagao, T., Analyses of impurities in methamphetamine by ICPMS and ion chromatography. *Journal of Chromatography* 1988, 437, 322–327.

67. Marumo, Y.; Inoue, T.; Seta, S., Analysis of inorganic impurities in seized methamphetamine samples. *Forensic Science International* 1994, 69(1) 89-95.

68. Suh, S.; Ko, B. J.; Suh, Y. J.; In, M. K.; Kim, S. H., Analysis of inorganic impurities in illicit methamphetamine using Inductively Coupled Plasma Mass Spectrometry (ICP-MS). Poster, *The International Association of Forensic Toxicologists (TIAFT)*, 2006.

69. Koper, C. ; Boom, C.V.D.; Wiarda, W.; Schrader, M. Joode, P.D.; Peijl, G. V.D.; Bolck, A., Elemental analysis of 3,4-methylenedioxymethamphetamine (MDMA): A tool to determine the synthesis method and trace links. *Forensic Science International* 2007, 171, 171–179.

CHAPTER 2 : ANALYTICAL TECHNIQUES

2.0 Introduction

The identity of the compounds synthesised for this project was confirmed by a variety of analytical techniques and comparison of the results obtained with literature values. Fourier transform infrared spectroscopy (FTIR) and nuclear magnetic resonance spectroscopy (NMR) together with melting point determination were used to confirm the synthetic products. Capillary electrophoresis (CE) was used to distinguish the *d,l* and racemic forms of methylamphetamine produced in some of the synthesis.

GCMS was used to analyse the synthesised samples with a view to identify organic 'target' impurities which could link the samples to a specific synthetic route.

All of the synthesised samples were subjected to IRMS analysis at the Drug Enforcement Agency (DEA), Special Testing Laboratories, Virginia, USA.

Inorganic impurities were analysed using ICPMS facilitated by the University of West Scotland, Paisley, Scotland.

All of these instrumental techniques will be briefly described here, with particular attention being paid to GCMS, IRMS and ICPMS as they are the main analytical techniques used in the project.

2.1 Fourier Transform Infrared Spectrometry (FTIR)

Infrared spectrometry (IR) is an invaluable tool in organic structural determination and is used widely by synthetic organic chemists. A molecule absorbs infrared radiation when the vibration of the atoms in the molecule produces an oscillating electric field with the same frequency as the frequency of incident IR "light". This absorption of light causes an energy transition in the form of vibrational excitation of bonds within the molecule. There are two types of molecular vibrations which result in the stretching and bending of bonds.[1, 2] After the light has passed through the sample, the frequencies which have been absorbed are detected due to their absence, and the intensities are recorded as troughs in the resultant spectrum. Light of wavelength λ will only be absorbed if there is an energy transition ($\triangle$E) according to the following equation:

$$(\triangle E) = hc/\lambda \qquad \ldots\ldots\ldots\ldots\ldots\ldots \quad \text{Equation 2.1}$$

where h is Planck's constant (6.6×10^{-34} Js), c is the speed of light (3.0×10^{8} m/s) and λ is the wavelength of light in metres.[1, 2]

Different types of bonds have different vibrational frequencies, so the presence or absence of characteristic frequencies in the spectrum can provide information about the functional groups present in an organic molecule; most useful for functional group identification are absorptions above 1400 cm^{-1} and below 900 cm^{-1}. For instance, carbonyl compounds generally absorb IR at 1670-1780 cm^{-1}, alkenes (non-terminal) at 1640-1680 cm^{-1} and amines at 3300-3500 cm^{-1} (for N-H) and 1030-1250 cm^{-1} (for C-N) (see Table 8).[1, 3]

Functional Group	Characteristic Absorption(s) (cm^{-1})
Alkyl C-H Stretch	2950 - 2850 (m or s)
Alkenyl C-H Stretch Alkenyl C=C Stretch	3100 - 3010 (m) 1680 - 1620 (v)
Alkynyl C-H Stretch Alkynyl C≡C Stretch	~3300 (s) 2260 - 2100 (v)
Aromatic C-H Stretch Aromatic C-H Bending Aromatic C=C Bending	~3030 (v) 860 - 680 (s) 1700 - 1500 (m,m)
Alcohol/Phenol O-H Stretch	3550 - 3200 (broad, s)
Carboxylic Acid O-H Stretch	3000 - 2500 (broad, v)
Amine N-H Stretch	3500 - 3300 (m)
Nitrile C≡N Stretch	2260 - 2220 (m)
Aldehyde C=O Stretch Ketone C=O Stretch Ester C=O Stretch Carboxylic Acid C=O Stretch Amide C=O Stretch	1740 - 1690 (s) 1750 - 1680 (s) 1750 - 1735 (s) 1780 - 1710 (s) 1690 - 1630 (s)
Amide N-H Stretch	3700 - 3500 (m)

Table 8: The characteristic region for infrared.[1, 3]

The complexity of infrared spectra in the 1400 to 900 cm^{-1} region makes it difficult to assign all the absorption bands, and because of the unique patterns found there, it is often called the fingerprint region. Absorption bands in the 4000 to 1400 cm^{-1} region are usually due to stretching vibrations of diatomic units, and this is sometimes called the functional group region.[1, 3]

Fourier transform is the mathematical operation of converting signal data from an interferogram to an easily understandable spectrum, thus giving rise to the name ‘Fourier transform infrared spectrometry, (FTIR).[1, 3]

2.2 Nuclear Magnetic Resonance Spectroscopy (NMR)

Nuclear magnetic resonance (NMR) spectroscopy uses radio frequency radiation to induce transitions between different nuclear spin states of samples in a magnetic field. NMR spectroscopy can be used for quantitative measurements, but it is most useful for determining the structure of molecules. The utility of NMR spectroscopy for structural characterization arises because different atoms in a molecule experience slightly different magnetic fields and therefore transitions at slightly different resonance frequencies in an NMR spectrum. Furthermore, splittings of the spectra lines arise due to interactions between different nuclei, providing information about the proximity of different atoms in a molecule.[4, 5]

Nuclei (such as ^{1}H or ^{13}C) with an odd number of protons, neutrons, or both, will have an intrinsic nuclear angular momentum or "nuclear spin". When a nucleus with a non-zero spin is placed in a magnetic field, the nuclear spin can align in either the same direction or in the opposite direction to the external magnetic field. A nucleus that has its spin aligned with the external field will have a lower energy than when it’s spin is aligned in the opposite direction to the field. Therefore, these two nuclear spin alignments have different energies and application of a magnetic field results in an energy level.[4][5]

The local environment around a given nucleus in a molecule disturbs the local magnetic field that is exerted on that nucleus. Since the resonance frequency of the transition, nuclei in different environments have slightly different transition energies. This dependence of the transition energy on the position of a particular atom in a molecule gives NMR spectroscopy it's utility for structural characterization. Nuclei which are deshielded resonate at higher frequencies, and nuclei which are shielded resonate at lower frequencies.[5]

The resonance frequencies of different nuclei in an atom are described by a relative shift compared to the frequency of a standard. This relative shift is called the chemical shift, δ, and is given by:

$$\delta = \left(\frac{\nu_{sample} - \nu_{ref}}{\nu_{ref}} \right) 1x10^{6}$$

……Equation 2.2

where has δ units of ppm. For ^{1}H and ^{13}C NMR spectroscopy the reference compound is tetramethylsilane, $Si(CH_3)_4$, or TMS.[4, 5]

Both ^{1}H and ^{13}C NMR are routinely used for the identification of organic compounds. ^{1}H is more powerful than ^{13}C NMR because it has greater sensitivity. This is due to the fact that ^{13}C has only about 1.1% natural abundance (of carbon atoms) and because of low abundance, ^{13}C-^{13}C coupling is not usually observed. Overlap of peaks for ^{13}C NMR is much less common than for ^{1}H -NMR which makes it easier to determine how many types of carbon are present.[6]

2.3 Capillary electrophoresis (CE)

Electrophoresis can been defined as the differential migration of charged species (ions) in an electric field.[7] In its simplest form, capillary electrophoresis involves the separation of charged analytes, based on the difference in their electrophoretic mobilities, resulting in different migration velocities. These separations are carried out in fused silica capillaries, typically 25–75 μm i.d. and 50–100 cm in length, filled with a background electrolyte.[8]

Electroosmotic flow can ensure that both negatively and positively charged species migrate towards the same end of the capillary, which under typical conditions, is towards the cathode end, with neutral species not being separated and migrating with the electro-osmotic flow. The output of the detector is sent to a data output and handling device such as an integrator or computer. The data is displayed as an electropherogram, which reports detector response as a function of time. Separated chemical compounds appear as peaks with different retention times in the electropherogram.[8]

Most amphetamine type stimulants (ATS) have one asymmetric carbon atom resulting in a pair of enantiomers. Depending on the source of precursors, therefore, different enantiomeric forms of amphetamine, methylmphetamine or other ATS may be encountered in seized samples submitted for analysis. Under the 1971 UN Convention on Psychotropic Substances, each optical isomer (*d*- and *l*-) as well as the racemic mixture (*dl*) of amphetamine and methylamphetamine are controlled.[9]

Enantiomers do not differ in their electrophoretic mobility in free solution. This means that they are unresolved in an ideal free solution.[10] However, many chiral separations have been described in buffer solutions containing chiral selectors, or in capillaries which are coated with a chiral selector or alternatively in capillaries which are packed with microparticulate silica, containing an adsorbed or covalently bonded chiral selector.[10]

Thus, to obtain chiral separations in CE one needs a chiral selector (such as phenyl-b-cyclodextrin) which can recognize both enantiomers steroselectively i.e. with different binding constants. Additionally, a migration mechanism should be used through the capillary, which enables the differentiation between the mobilities of free and bonded analytes effectively. In addition, the exchange between free and bonded forms of the analyte must be rapid. If one of these requirements is not fulfilled, enantioseparation in CE will not occur.[10]

2.4 Melting point

Pure, crystalline solids have a characteristic melting point**,** the temperature at which the solid melts to become a liquid. The transition between the solid and the liquid is so sharp for small samples of a pure substance that melting points can be measured to 0.1^{o}C.[11]

2.5 Optical rotation

Optical rotation is the turning of the plane of linearly polarized light about the direction of motion as the light travels through certain materials. It occurs in solutions of chiral molecules such as sucrose (sugar), solids with rotated crystal planes such as quartz, and spin-polarized gases of atoms or molecules. It is used in chemistry to characterize substances in solution. [12]

2.6 Gas Chromatography Mass Spectrometry (GCMS)

2.6.1 Introduction

Gas chromatography mass spectrometry (GCMS) is an instrumental technique, comprising a gas chromatograph (GC) coupled to a mass spectrometer (MS), by which complex mixtures of chemicals may be separated, identified and quantified.[13, 14] This makes it ideal for the analysis of relatively low molecular weight compounds. In order for a compound to be analysed by GCMS it must be sufficiently volatile and thermally stable.[14]

Samples are usually analysed as organic solutions, consequently materials of interest (e.g. soils, sediments, tissues etc.) need to be solvent extracted and the extract subjected to various 'wet chemical' techniques before GCMS analysis is possible.[14] Functionalised compounds may require chemical modification (derivatization), prior to analysis, to eliminate undesirable adsorption effects that would otherwise affect the quality of the data obtained.[14]

GCMS cannot differentiate between certain types of stereoisomers such as enantiomers and diastereomers. Those compounds have essentially the same GC retention times and mass spectra. *d*-metylamphetamine and *l*-methylamphetamine are examples of compounds which form an enantiomeric pair. *l*-ephedrine and *d-pseudo*ephderine are examples of compounds which form a diastereomer pair. In order to differentiate those stereoisomers, a chiral column would be required.[15] Derivatization is an alternative method which can be used to perform such analysis.[16, 17] Li et al.[18] however did

report the successful separation of ephedrine and *pseudo*ephedrine using a HP-5 column without any tedious pre-treatment methods such as derivatization.

Mass spectroscopy (MS) uses the pattern of molecular fragments (ions) produced when a molecule breaks apart after it is exposed to a beam of electrons (in the case of electron impact (EI) ionisation) or collides with reagent gas molecules (such as methane) in the case of chemical impact (CI) ionisation.[14] These fragments are then used as a means of identification and these ionisation methods are discussed in more detail in Section 2.6.3. The mass spectrometer exposes the compound under analysis to a beam of high-energy electrons that shatters the molecules. The mass spectrometer then sorts and counts the resulting fragments (ions) and produces a pattern, the mass spectrum. When the energy of the electron beam remains constant, the molecule will produce the same mass spectrum, which is considered one of the compound's chemical fingerprints.

MS has its limitations. It cannot differentiate between certain types of isomers. Stereoisomers and geometric isomers may produce mass spectra that are essentially identical. Stereoisomers (molecules that are mirror images of each other) have identical mass spectra. For example, when ephedrine and *pseudo*ephedrine are fragmented, the patterns are identical.[19] Geometric or positional isomers will also produce similar, if not the same mass spectra. In some cases the compounds can be differentiated by their chromatographic retention times. In other cases, there may be one or two clusters of ions that have ratios specific to a particular isomer. Methylamphetamine and phentermine are two geometric isomers that can be differentiated through the use of MS.[20]

The mass spectrometer generally cannot distinguish between the salt and freebase form of a drug. The salt portion of the compound is generally outside the detection range of the MS and the detector only detects the freebase portion of the compound. There are a number of mass spectra libraries available to assist in the identification of unknowns. The spectra in these libraries can provide insight into the identity of numerous components that can potentially be within these mixtures.

2.6.2 Gas Chromatography (GC) Instrumentation

The sample solution containing, in some cases, a complex mixture of components is injected into a heated inlet where it is vaporized and swept onto a chromatographic column by the carrier gas (usually helium).[14, 21] The sample travels through the column and the compounds in the mixture are separated by virtue of their relative interaction with the coating of the column (stationary phase) and the carrier gas (mobile phase).[14] The level of interaction is dependant upon the polarity of the component and the retention can also be manipulated by altering the temperature of the column (temperature programme). This latter method utilises difference in component boiling points to facililate a separation. The latter part of the column passes through a heated transfer line and ends at the entrance to the detector.[14, 21] The general layout of a GC is displayed in Figure 16.[22]

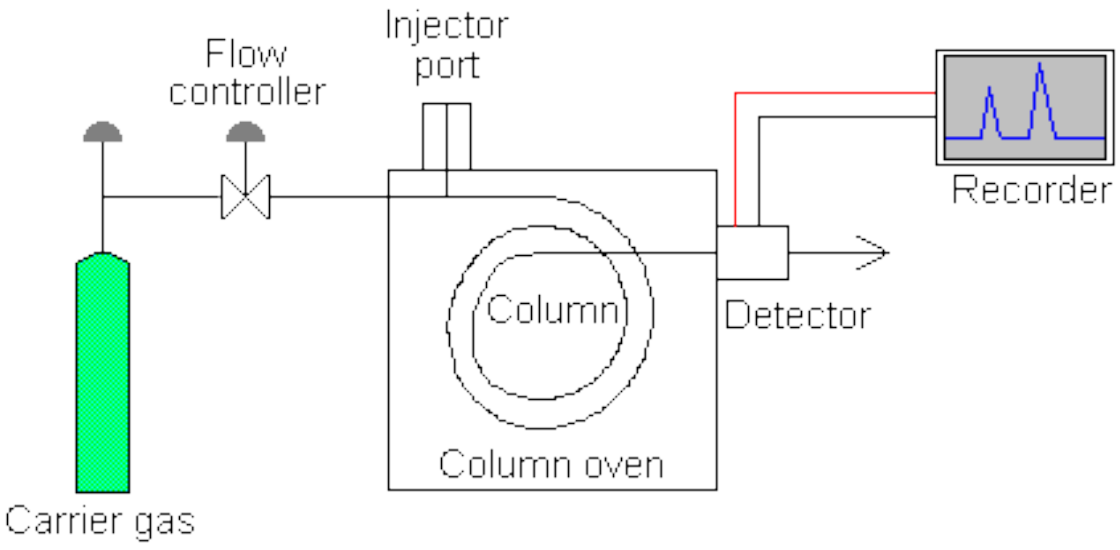

Figure 16 : **Schematic of a gas chromatograph.[22]**

The sample (usually 1-2 μL) is injected through a rubber septum into a flash vapouriser port at the head of the column. The temperature of the injection port is usually set higher than the boiling point of the least volatile component of the sample.[23]

The injection port can be used in one of two modes; split or splitless.[23] The injection port consists of a heated chamber containing a glass liner into which the sample is injected through the septum. Effectively, the split inlet can be used to take an 'on-column' aliquot of the sample, whereas in the splitless mode the entire sample is transferred to the column.[23] The splitless injector can produce high-sensitivity analysis and this mode was chosen in the GC analysis technique in this project.

There are two general types of column, packed and capillary (open tubular columns).[23] Packed columns contain a finely divided, inert, solid support material. Most packed columns are 1.5 - 10m in length and have an internal diameter of 2 - 4mm. Capillary columns have an internal diameter of a few tenths of a millimetre. The interior of the column is coated with a thin layer of stationary phase.[23] Capillary columns are most commonly used in GC due to the best separation factor for a particular mixture.[23] The use of a temperature programme rather than isothermal separation allows control of the elution rate of peaks based on differences in component boiling points.

2.6.3 Mass Spectrometer (MS)

There are many detectors which can be used in gas chromatography, but only the mass spectrometer will be discussed as it was the detection system used in this project.

Two potential methods exist for ion production within the mass spectrometer. The most frequently used method is electron ionization (EI) with chemical ionization (CI) being used less often.[13, 14] For EI, a beam of electrons ionize the sample molecules resulting in the loss of one electron. A molecule with one electron missing is called the molecular ion and is represented by $M^{+\cdot}$ (a radical cation). When the resulting peak from this ion is seen in a mass spectrum, it gives the molecular weight of the compound.[13, 14] Due to the large amount of energy imparted to the molecular ion it usually fragments producing further smaller 'daughter' ions with characteristic relative abundances that provide a 'fingerprint' for that molecular structure. This information may be then used to identify compounds of interest and help elucidate the structure of unknown components of mixtures.[14]

CI begins with the ionization of methane (or another suitable gas), creating a radical which in turn will ionize the sample molecule to produce $(M+H)^+$ molecular ions.[13, 14] CI is a less energetic way of ionizing a molecule hence less fragmentation occurs with CI than with EI, hence CI yields less information about the detailed structure of the molecule, but does yield the molecular ion; sometimes the molecular ion cannot be detected using EI, and as such the two methods complement one another. Once ionized a small positive charge is used to repel the ions out of the ionization chamber.[14] Diagrams of the ion source is given in Figures 17.[14]

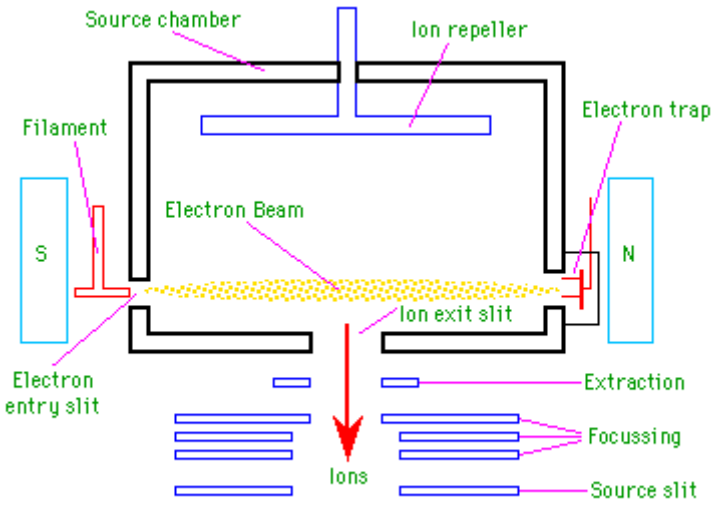

Figure 17: **A schematic of an ion source.[14]**

The next component is a mass analyser (filter), which separates the positively charged ions according to various mass related properties depending upon the analyser used.[14] Several types of analyser exist: quadrupoles, ion traps, magnetic sector, time-of-flight, radio frequency, cyclotron resonance and focusing to name a few.[14]

Once the ions enter the mass spectrometer, they are separated by their mass-to-charge ratio. The most commonly used type of mass analyser is the quadrupole mass filter**.** In

this type, 4 rods (approximately 1 cm in diameter and 15-20 cm long) are arranged (see Figure 18).[14]

In a quadrupole mass filter, alternating AC and DC voltages are applied to opposite pairs of the rods. These voltages are then rapidly switched along with an RF-field.[24, 25] The result is that an electrostatic filter is established that only allows ions of a single mass-to-charge ratio (m/z) pass through the rods to the detector at a given instant in time.[24, 25] So, the quadrupole mass filter is really a sequential filter, with the settings being change for each specific m/z at a time.[24, 25] The voltages on the rods can be switched at a very rapid rate.[24, 25] The result is that the quadrupole mass filter can separate up to 2400 amu (atomic mass units) per second.[24, 25]

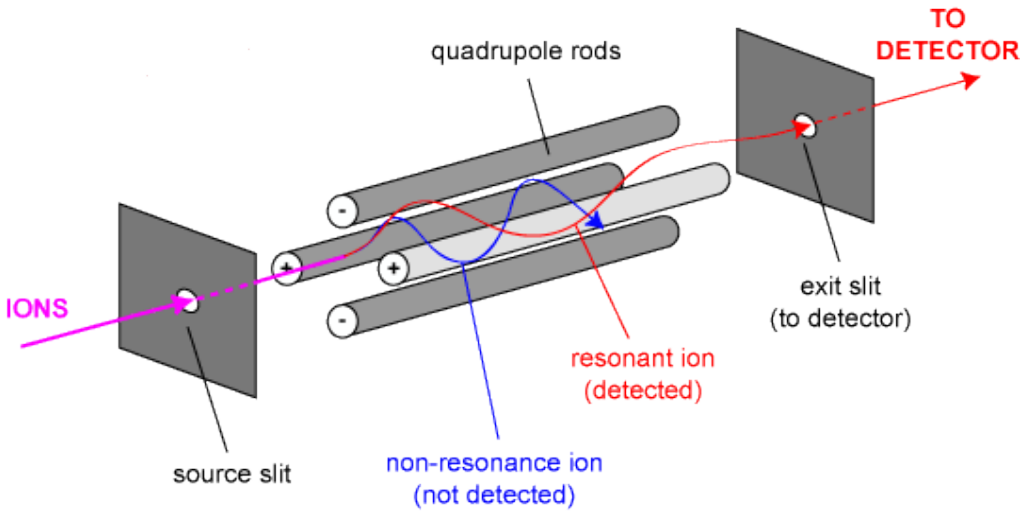

Figure 18: **A schematic of a quadrupole analyser. [14]**

The mass analyzer sorts the ions according to the mass to charge ratio (m/z) of the fragment and the detector records the abundance of each m/z. The detector output is amplified to boost the signal. The detector sends information to a computer that records all of the data produced, converts the electrical impulses into visual displays and hard copy displays.[22] In addition, the computer can also be used to control the operation of the mass spectrometer.

2.7 Isotope Ratio Mass Spectrometry (IRMS)

2.7.1 Introduction

The isotope ratio mass spectrometer (IRMS) allows the precise measurement of mixtures of certain stable isotopes. This technique has two different applications in the Earth and environmental sciences.[26] The analysis of 'stable isotopes' is normally concerned with measuring isotopic variations arising from mass-dependent isotopic fractionation in natural systems.[26] On the other hand, radiogenic isotope analysis involves measuring the abundances of decay-products of natural radioactivity, and is used in most long-lived radiometric dating methods.[26]

Isotopes are defined as atoms of the same element that differ in the number of neutrons present in their nuclei, i.e. have different mass numbers. All but 12 elements exist as mixtures of isotopes.[26] Each element has a dominant light isotope (e.g. ^{12}C (carbon), ^{14}N (nitrogen), ^{16}O (oxygen), ^{32}S (sulfur), and ^{1}H (hydrogen)), and one or two heavy isotopes (e.g. ^{13}C, ^{15}N, ^{17}O, ^{18}O, ^{33}S, ^{34}S, ^{36}S and ^{2}H) with a natural abundance of a few percent or less.[26] Table 9 displays relative abundances of naturally occurring isotopes of elements commonly analysed by IRMS.[26]

Element	Isotope	Relative abundance (%)
Hydrogen (H)	^{1}H	99.984
	^{2}H	0.0156
Carbon (C)	^{12}C	98.892
	^{13}C	1.108
Nitrogen (N)	^{14}N	99.635
	^{15}N	0.365
Oxygen (O)	^{16}O	99.759
	^{17}O	0.037
	^{18}O	0.204
Sulphur (S)	^{32}S	95.02
	^{33}S	0.76
	^{34}S	4.22
	^{36}S	0.014

Table 9: Natural abundances of H, C, N, O and S isotopes.[26]

2.7.2 Fractionation effects

Isotopic fractionation refers to any process that changes the relative abundances of stable isotopes of an element. Isotopic fractionation can occur during chemical, physical and biological processes. The two main mechanisms that cause isotopic fractionation are the kinetic isotope effect, which is produced by differences in reaction rates, and the thermodynamic isotope effect, which relates to the energy state of a system.[26]

Kinetic isotope effects are a result of differences in bond strength (i.e. vibration energy levels of bonds) between heavier isotopes and lighter isotopes.[26] When different isotopes of the same element are involved in a reaction/process, this difference in bond strength can result in different reaction rates for the bond.[26] Kinetic isotope effects represent changes in bonding between the ground state and the transition state of a reaction.[26] Statistical models predict that the lighter (lower atomic mass) of two isotopes of an element will form the weaker bond during kinetic isotope processes. The lighter isotope is more reactive, hence is concentrated in reaction products and reactants are enriched with the heavier isotope.[26]

The thermodynamic isotope effect is the second common isotope effect, and relates to the free energy change brought about when one atom in a compound is replaced by its isotope.[26] A compound that has a heavier isotope in its composition has a smaller reserve of free energy, compared to the same compound containing the lighter isotope. The thermodynamic isotope effect is associated with differences in the physico-chemical properties of the samples being analysed.[26] This includes properties such as infrared absorption, molar volume, vapour pressure, boiling point, and melting point, which are all related to vibration energy levels.[26] These effects are evident in processes where chemical bonds are not formed or broken, e.g. infrared spectroscopy, distillation, and any two-phase partitioning process.[26]

2.7.3 Delta Notation

Stable isotope abundances are presented in "delta" notation (δ), with stable isotope abundance expressed relative to a standard,

$$\delta = \left(\frac{R_{sample}}{R_{standard}} - 1 \right) 1000 \quad \text{…… Equation 2.3}$$

These are reported in units of per mil (''mil'' = 1000), written ‰. R_{sample} is the ratio of the heavy to the light isotope measured for the sample, and $R_{standard}$ is the equivalent ratio for the standard.[26] Generally, δ values are quoted relative to an internationally recognised standard that is arbitrarily set at 0‰ to serve as a benchmark. The use of universal standards is necessary to facilitate the comparison of IRMS measurements across laboratories. Table 10 lists some international standards and their absolute isotope ratios.

International standard	Isotope ratio of reference material
PeeDee Belemnite (PDB)	$^{13}C/^{12}C = 0.0112372$
	$^{18}O/^{16}O = 0.0020671$
Atmospheric nitrogen (AIR)	$^{15}N/^{14}N = 0.0036765$
Vienna standard mean ocean water (V-SMOW)	D/H ($^{2}H/^{1}H$) = 0.00015576
	$^{18}O/^{16}O = 0.0020052$
Canyon Diablo meteorite troilite (CDT)	$^{34}S/^{32}S = 0.0450045$
Standard mean ocean chloride (SMOC)	$^{37}Cl/^{35}Cl = 0.324$

Table 10: International standards for some common elements analysed by IRMS.[26]

2.7.4 Isotope Ratio Mass Spectrometers

Isotope ratio mass spectrometers (IRMS) are specialized mass spectrometers that produce precise and accurate measurements of variations in the natural isotopic abundance of light stable isotopes (such as hydrogen, carbon, nitrogen, and oxygen). IRMS instruments are different from conventional mass spectrometers, in that they do not scan a mass range for characteristic fragment ions in order to provide structural information on the sample being analysed.[26] The mass spectrometers used for isotopic analysis generally comprise three main sections: an ion source, a mass analyser, and an ion collection assembly (see Figure 19).

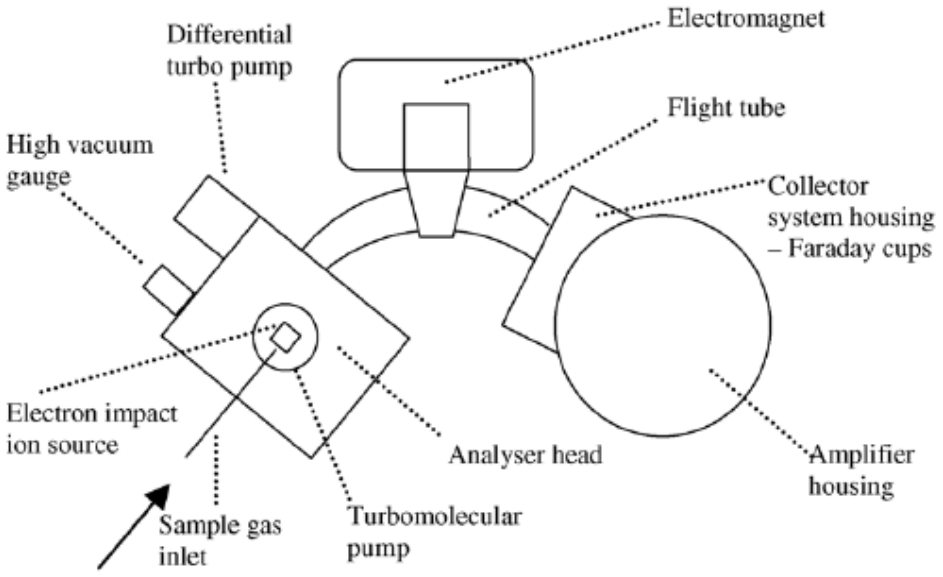

Figure 19: Diagram showing the main sections of an IRMS instrument.[26]

Relatively light elements are typically measured using a gas isotope ratio mass spectrometer.[26] The mass spectrometer consists of a source to ionize the gas, a flight tube with a magnet to deflect the path of the ionized gas, and a detector system at the end of the flight tube to measure the different isotopic species.[26] First, the element of interest must be converted to a gaseous form for introduction into the mass spectrometer. The most commonly used approaches involve introducing H as H_2, C as CO_2, N as N_2, and O as CO.[26]

As the gas is introduced into the mass spectrometer, it is ionized by removal of an electron as the gas is bombarded by high energy electrons.[26] Then, as the ionized gas travels down the flight tube (under vacuum), the paths of light and heavy isotopic species are deflected differently by the magnet.[26] Detectors are positioned at the end of the flight tube to measure the abundance ratios of the heavy and light isotopic species.[26] There are two common sample introduction techniques for IRMS analysis. Both of these techniques require solid, liquid, and gaseous samples to be converted into pure gases. The techniques are ‘dual inlet’ or ‘continuous flow (CF-IRMS)’.[26]

With a dual inlet system, the samples for analysis are prepared (i.e. converted into simple gases) off-line. The offline sample preparation procedure utilises a specially designed apparatus involving vacuum lines, compression pumps, concentrators, reaction furnaces, and micro-distillation equipment. This technique is time consuming, usually requires larger samples, and contamination and isotopic fractionation can occur at each of the steps.[26]

The continuous flow sample introduction technique consists of a helium carrier gas that carries the analyte gas into the ion source of the IRMS. This technique is used to connect an IRMS to a range of automated sample preparation devices. Two of the preparation techniques are bulk stable isotope analysis (BSIA) and compound specific isotope analysis (CSIA).[26]

While dual inlet is generally the most precise method for stable isotope ratio measurements, continuous flow mass spectrometry offers on-line sample preparation, smaller sample size, faster and simpler analysis, increased cost effectiveness, and the possibility of interfacing with other preparation techniques, including elemental analysis, gas chromatography (GC), and more recently, liquid chromatography (LC). Because of that, CF-IRMS is the method used in the majority of research currently being conducted in the field of forensic science.[26]

2.7.4.1 Bulk Stable Isotope Analysis (BSIA)

The isotopic values obtained from bulk stable isotope analyses represent the isotopic composition of all the components in the mixture as a whole.[26] The instrument for BSIA consists of an elemental analyser coupled with an isotope ratio mass spectrometer (EA/IRMS). There are two common instrument peripherals/techniques for the preparation of samples for bulk stable isotope analysis: Quantitative High Temperature Combustion and Quantitative High Temperature Conversion.[26]

Combustion elemental analysers are used for the analysis of nitrogen, carbon, and sulfur isotope ratios of bulk samples.[26] The sample for analysis, sealed in a tin capsule, automatically falls from the carousel into a combustion tube containing an oxidation catalyst and other materials. A pulse of oxygen temporarily replaces the helium carrier gas. A flash combustion of the solid sample to N_2, NO_x, CO_2, O_2, and water (H_2O) raises the temperature from approximately 1000 to 1700 °C.[26] The combustion products are swept into a reduction tube (approximately 600 °C) to reduce NO_x to N_2 and remove excess O_2. The samples then pass through a trap to remove the H_2O. The analyte gases (e.g. N_2 and CO_2) are then separated from each other and also impurities on a packed GC column and a fraction of each gas enters the IRMS as discussed in Section 2.7.4 (see Figure 20) [26]

High Temperature Conversion Elemental Analysers (TC/EA) are used for the analysis of hydrogen and oxygen isotope ratios of bulk samples. The sample for analysis is sealed in a silver capsule. The sample is dropped from the autosampler into the reaction tube, where the high temperature pyrolytic conversion commences.[26] The sample is converted to H_2 and CO gases. Reaction temperatures range from 1100 °C, to temperatures greater than 1450 °C. The analyte gases, H_2 and CO, are then separated on a packed GC column. The gases then enter the IRMS for analysis via an open split interface.[26]

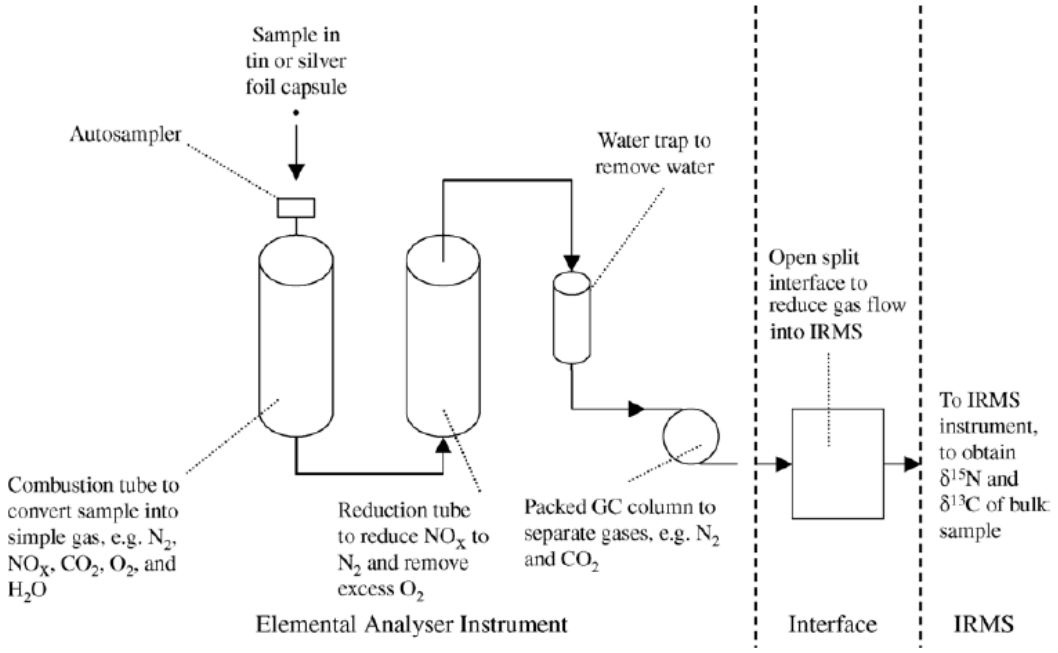

Figure 20: Schematic showing a flash combustion elemental analyser in series with an interface and IRMS for the analysis of nitrogen and carbon isotope ratios of bulk samples.[26]

2.7.4.2 Compound Specific Isotope Analysis (CSIA)

In CSIA, the isotopic compositions of individual compounds within the sample are measured. The substance to be analysed is dissolved in an organic solvent and automatically injected onto the GC.[26] Complex organic mixtures are separated on the capillary GC column.[26] Baseline separated peaks are the basis for high precision CSIA as isotope ratios cannot be accurately determined from the partial examination of a GC peak. A splitter at the end of the GC column sends >95% of the sample to a combustion or pyrolysis tube (see Figure 21). The remainder is sent to an optional FID, ion trap MS, or is vented to the atmosphere.[26]

Like BSIA, two sample conversion systems are required for the preparation of samples into simple gas form for analysis by the IRMS instrument. Nitrogen and carbon isotope ratio values cannot be measured in the same sample. When nitrogen isotope ratios are being measured, the CO_2 must be removed from the source as the ions formed from the

CO_2 interfere with the measurement of the nitrogen isotope ratios. Removal of CO_2 is achieved by cryogenic trapping. Similarly, the hydrogen and oxygen isotope ratios cannot be measured in the same sample.

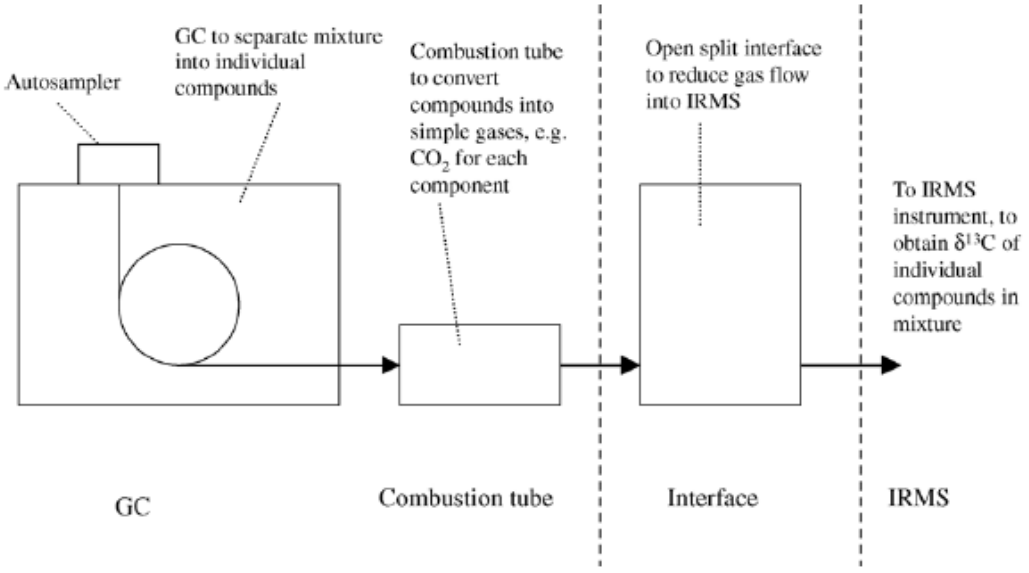

Figure 21: Schematic showing the basic set-up of a GC/IRMS instrument for the analysis of carbon isotope ratios [26]

2.8 Inductively Coupled Plasma Mass Spectrometry (ICPMS)

2.8.1 Introduction

The analysis of inorganic ions by ICPMS offers better sensitivity than graphite furnace atomic absorption (GFAAS) with the multi-element speed of inductively coupled plasma optical emission spectroscopy (ICPOES). An ICPMS combines a high-temperature ICP (Inductively Coupled Plasma) source with a mass spectrometer. The ICP source converts the atoms of the elements in the sample to ions. These ions are then separated and detected by the mass spectrometer.[24, 25] By acquiring the mass spectrum of the plasma, data can be obtained for almost the entire periodic table in just minutes with detection limits below 0.1 ug/L for most elements.[24, 25]

In a typical application, metals are placed in solution by acid digestion. The solution is sprayed into a flow of flowing argon and passed into a torch which is inductively heated to approximately 10,000^{o}C.[24, 25] At this temperature, the gas and almost everything in it is atomized and ionized, forming a plasma which provides a rich source of both excited and ionized atoms. In ICPMS, positive ions in the plasma are focused down a quadrapole mass spectrometer.[24, 25]

2.8.2 Inductively Coupled Plasma Mass Spectrometers

Argon gas flows inside the concentric channels of the ICP torch. The RF load coil is connected to a radio-frequency (RF) generator and as power is supplied to the load coil from the generator, oscillating electric and magnetic fields are established at the end of the torch.[24, 25] When a spark is applied to the argon flowing through the ICP torch, electrons are stripped off of the argon atoms, forming argon ions. These ions are caught in the oscillating fields and collide with other argon atoms, forming an argon discharge or plasma.[24, 25]

The sample is typically introduced into the ICP plasma as an aerosol, either by aspirating a liquid or dissolved solid sample into a nebulizer or using a laser to directly convert solid samples into an aerosol.[24, 25] Once the sample aerosol is introduced into the ICP torch,

it is completely desolvated and the elements in the aerosol are converted first into gaseous atoms and then ionized towards the end of the plasma.[24, 25]

Once the elements in the sample are converted into ions, they are then brought into the mass spectrometer via the interface cones. The interface region in the ICPMS transmits the ions traveling in the argon sample stream at atmospheric pressure (1-2 torr) into the low pressure region of the mass spectrometer ($<1 \times 10^{-5}$ torr). This is done through the intermediate vacuum region created by the two interface cones, the sampler and the skimmer.[24, 25] The sampler and skimmer cones are metal disks with a small hole (~1mm) in the center. The purpose of these cones is to sample the center portion of the ion beam coming from the ICP torch.[24, 25] A shadow stop or similar device blocks the photons coming from the ICP torch, which is also an intense light source.[24, 25] Due to the small diameters of the orifices in the sampler and skimmer cones, ICPMS has some limitations as to the amount of total dissolved solids in the samples. Generally, it is recommended that samples have no more than 0.2% total dissolved solids (TDS) for best instrument performance and stability.[24, 25] If samples with very high TDS levels are run, the orifices in the cones will eventually become blocked, causing decreased sensitivity and detection capability and requiring the system to be shut down for maintenance. This is why many sample types, including digested soil and rock samples must be diluted before running on the ICPMS.[24, 25]

The ions from the ICP source are focused by the electrostatic lenses in the system. The ions coming from the system are positively charged, so the electrostatic lens, which also has a positive charge, serves to focus the ion beam into the entrance aperture or slit of the mass spectrometer.[24, 25] Different types of ICPMS systems have different types of lens systems. The simplest employs a single lens, while more complex systems may contain as many as 12 ion lenses. Each ion optic system is specifically designed to work with the interface and mass spectrometer design of the instrument.[24, 25]

The most common mass spectometer used with ICPMS are quadrupoles and ion traps. In the case of this research a quadrapole mass analyser was used and its operation is as described in section 2.6.3.

Once the ions enter the mass spectrometer, they are separated by their mass-to-charge ratio (see Figure 22). This speed of the quadrupole mass filter to separate the atomic mass units per second is why the quadrupole ICP-MS is often considered to have simultaneous multi-elemental analysis properties. The ability to filter ions on their mass-to-charge ratio allows ICP-MS to supply isotopic information, since different isotopes of the same element have different masses.[24, 25]

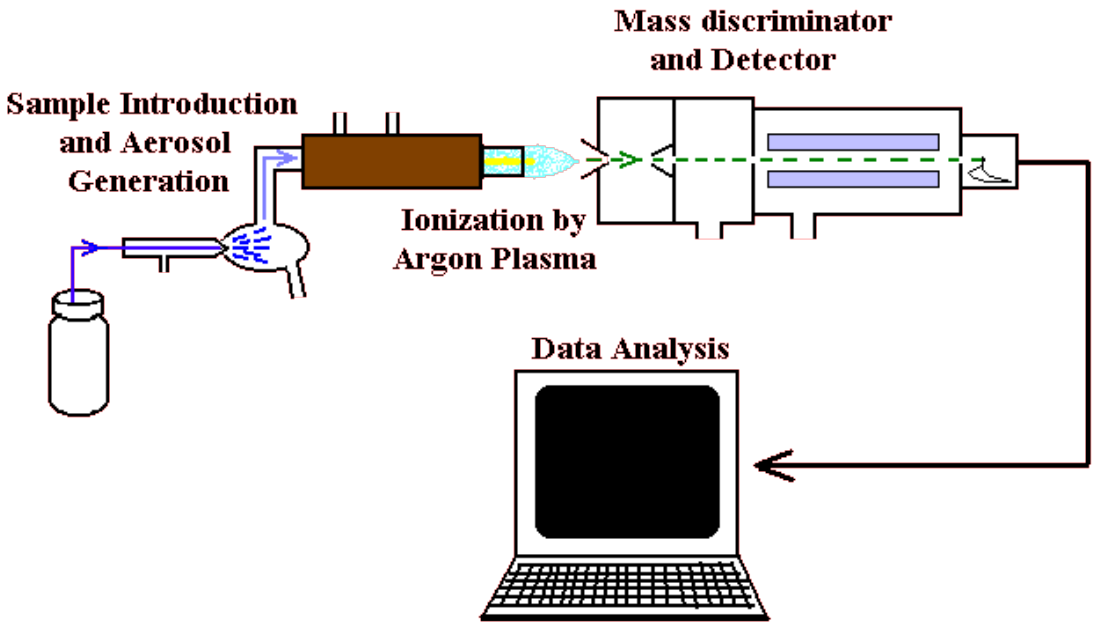

Figure 22: Schematic of ICPMS main processes. [27]

2.9 References

1. Griffiths, P.R.; Haseth, J.A., *Fourier Transform Infrared Spectrometry*. John Wiley & Sons, Inc: New Jersey, 2007.

2. Infrared Spectroscopy: Theory. Available at http://wwww.orgchem.colorado.edu/hndbksupport/irtutor/IRtheory.pdf. Last accessed on 12/02/10.

3. Infrared Spectroscopy. Available at http://www.cem.msu.edu/~reusch/VirtualText/Spectrpy/InfraRed/infrared.html. Last accessed on 10/01/10.

4. Claridge, T.D.W., *High-Resolution NMR Techniques in Organic Chemistry*. 2nd ed.; Elsevier: Boston, 2009.

5. Nuclear Magnetic Resonance (NMR) Spectroscopy. Available at http://www.files.chem.vt.edu/chem-ed/spec/spin/nmr.html. Last accessed on 02/01/10.

6. Spectroscopy. Available at http://www.chem.ucalgary.ca/courses/351/Carey/Ch13/ch13-nmr-1.html. Last accessed on 04/01/10.

7. Background Theory and Principles of Capillary Electrophoresis. Available at http://www.bris.ac.uk/nerclsmsf/techniques/gcms.html. Last accessed on 30/03/10.

8. Anastos, N.; Barnett, N.W.; Lewis, S.W.; Capillary electrophoresis for forensic drug analysis : A review. *Talanta* 2005, 67, 269-279.

9. United Nations, Convention on Psychotropic Substances, 1971. Available at http://www.incb.org/pdf/e/conv/convention_1971_en.pdf. Last accessed on 14/01/10.

10. Chankvetadze, B., *Capillary electrophoresis in chiral analysis*. John Wiley & Sons Ltd : England, 1997.

11. What is the Difference Between Melting Point and Freezing Point? Available at http://www.dillpickletheater.com/REMSL/index.htm. Last accessed on 02/03/10

12. Optical rotation. Available at http://www.chemistry.adelaide.edu.au/external/soc-rel/content/polarim.html. Last accessed on 04/03/10.

13. Grob, R.L.; Barry, E.F., *Modern Practice of Gas Chromatography*. John Wiley & Sons Inc: New Jersey, 2004.

14. Gas Chromatography Mass Spectrometry (GC/MS). Available at http://www.bris.ac.uk/nerclsmsf/techniques/gcms.html.
Last accessed on 12/03/10.

15. United Nations Office on Drugs and Crime, Recommended methods for the identification and analysis of Amphetamine, Methamphetamine and their Ring-Substituted Analogues in seized materials; 2006.

16. Ranieri, T.L.; Ciolino, L.A., Rapid Selective Screening and Determination of Ephedrine Alkaloids Using GC-MS footnote mark. *Phytochemical Analysis* 2008, 19, 127-135.

17. Liau, A.S.; Liu, J.T.; Lin, L.C.; Chiu, Y.C.; Shu, Y.R.; Tsai, C.C.; Lin, C.H., Optimization of a simple method for the chiral separation of methamphetamine and related compounds in clandestine tablets and urine samples by β-cyclodextrine modified capillary electrophoresis: a complementary method to GC–MS. *Forensic Science International* 2003, 134, 17-24.

18. Li, H.X.; Ding, M.Y.; Lv, K.; Yu, J.Y., Separation and Determination of Ephedrine Alkaloids and Tetramethylpyrazine in Ephedra sinica Stapf by Gas Chromatography–Mass Spectrometry. *Journal of Chromatographic Science* 2001, 39, 370-374.

19. Distinguishing the Good and the Bad from the Ugly with GC and FT-IR. Available at http://www.forensicmag.com/articles.asp?pid=47.
Last accessed on 29/03/10.

20. Awad, T.; Belal, T.; DeRuiter, J.; Kramer, K.; Clark, C. R., Comparison of GC–MS and GC–IRD methods for the differentiation of methamphetamine and regioisomeric substances. *Forensic Science International* 2009, 185**,** 67-77.

21. Braithwaite, A. and Smith, F.J., *Chromatographic methods*. 5th ed.; Blackie Academic & Professional : Glasgow, 1996.

22. Gas Chromatography. Available at
http://www.teaching.shu.ac.uk/hwb/chemistry/tutorials/chrom/gaschrm.html.
Last accessed on 20/03/10.

23. Handley, A.J. and Adlard, E.R., *Gas Chromatographic Techniques and Applications*. Sheffield Academic Press Ltd: England, 2001.

24. Thomas, R., *Pratical Guide to ICP-MS*. Taylor & Francis Ltd: New York, 2005.

25. What is ICP-MS?... and more importantly, what can it do? Available at http://minerals.cr.usgs.gov/icpms/intro.html. Last accessed on 29/03/10.

26. Benson, S.; Lennarda, C.; Maynard, P.; Roux, C., Forensic applications of isotope ratio mass spectrometry—A review. *Forensic Science International* 2006, 157**,** 1–22.

27. ICPMS. Available at http://www.cee.vt.edu/ewr/environmental/teach/smprimer/icpms/icpms.htm. Last accessed on 09/03/10.

CHAPTER 3 : METHYLAMPHETAMINE AND ITS SYNTHESIS

3.0 Introduction

There are a number of well documented synthetic routes used for the clandestine manufacture of methylamphetamine. The ephedrine/*pseudo*ephedrine reduction method is the most widely employed and accounted for 89 percent of all methylamphetamine laboratory seizures reported to the DEA in 1995. This method is also common among traffickers from Mexico and Asia. The phenyl-2-propanone method was used in 6 percent of the methylamphetamine laboratories seized by DEA during 1995. However it is the most commonly used synthetic route in Europe and yields a racemic mixture of *dl*-methylamphetamine. The ephedrine/*pseudo*ephedrine reduction method is generally preferred over the P-2-P method for several reasons. First, it is a simpler method of synthesis. Second, ephedrine/*pseudo*ephedrine is less strictly controlled than P-2-P, and is more readily available to clandestine laboratory operators. It can also be extracted from natural resources such as *Ephedrae* herba. Finally, it produces the more potent *d* isomer of methylamphetamine.[1] These synthetic routes are illustrated in Scheme 3.[2]

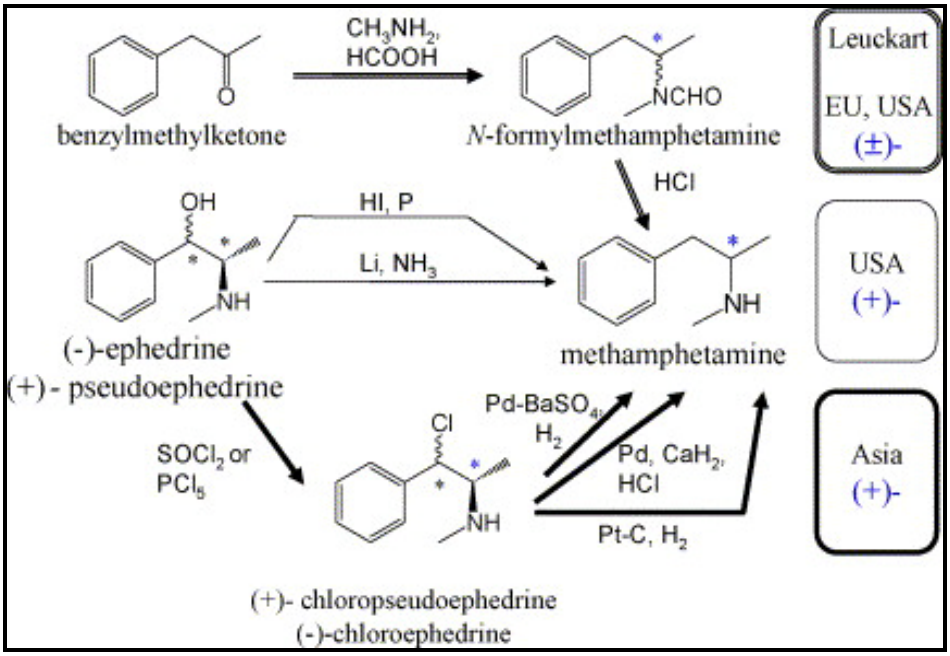

Scheme 3: Synthetic routes of methylamphetamine. *Asymmetric carbon and the *l* isomer is indicated as (-), the *d* isomer as (+) and the racemic mixture (*dl*) as (±).[2]

3.1 Methylamphetamine Synthesis

In order to know the exact history of the samples to be analysed in this project, the illicit substances must be manufactured in house. This will afford knowledge of the pathway, reagents and reaction conditions used during the synthesis so that conclusions drawn from the analysis can be validated.

Various methods for the production of methylamphetamine are readily available from the scientific literature, patents, published books [3] and the Internet.[4] Many of the methods are analogous to those used for the production of amphetamine and ring substituted phenethylamines (e.g. 'ecstasy' drugs). The choice of method depends on many factors, however from an investigative point of view the main factors are availability of precursors and other chemicals, complexity of the process, availability of equipment and chemical hazards associated with the synthesis.

The illicit manufacture of methylamphetamine can be accomplished in a variety of ways, but it is produced most commonly by using either of two primary synthesis methods. The fundamental difference between the two methods is in the use of precursor chemicals. The first method requires the use of phenyl-2-propanone (P-2-P) as the precursor, while the second method uses ephedrine or *pseudo*ephedrine (known as the ephedrine/*pseudo*ephedrine reduction method).

Scheme 4 and 5 show the seven most frequently encountered routes used in the clandestine manufacture of methylamphetamine. The seven routes can be separated into general groups. The first of these groups utilised P-2-P as the starting compound yielding racemic methylamphetamine and includes the Leuckart method and the reductive amination method (Scheme 4).

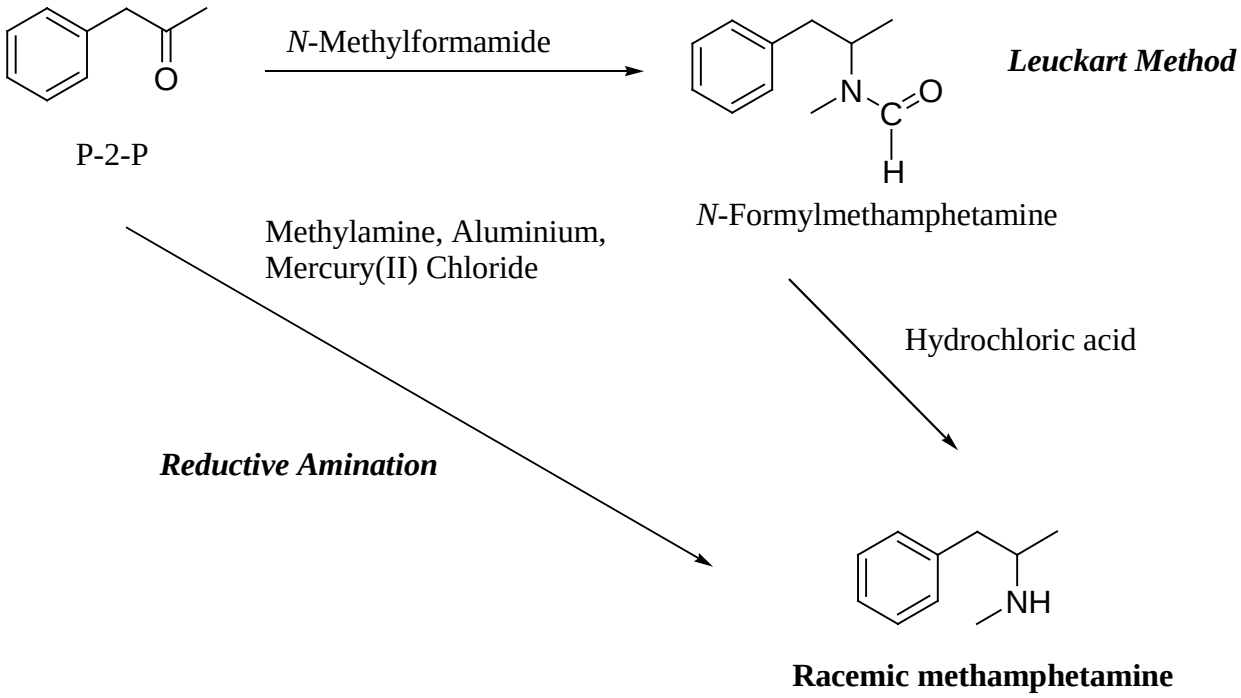

Scheme 4: Summary of synthetic pathways via P-2-P towards methylamphetamine that will be used in this project. [39]

The second group involves the use of (*l*) ephedrine and *(d*) *pseudo*ephedrine as starting reagents yielding only (*d*) methylamphetamine, the more potent isomer and includes the Nagai method, Rosenmund hydrogenation, Birch reduction, Moscow method and the Emde method with chloro-ephedrine as an intermediate (Scheme 5).[5]

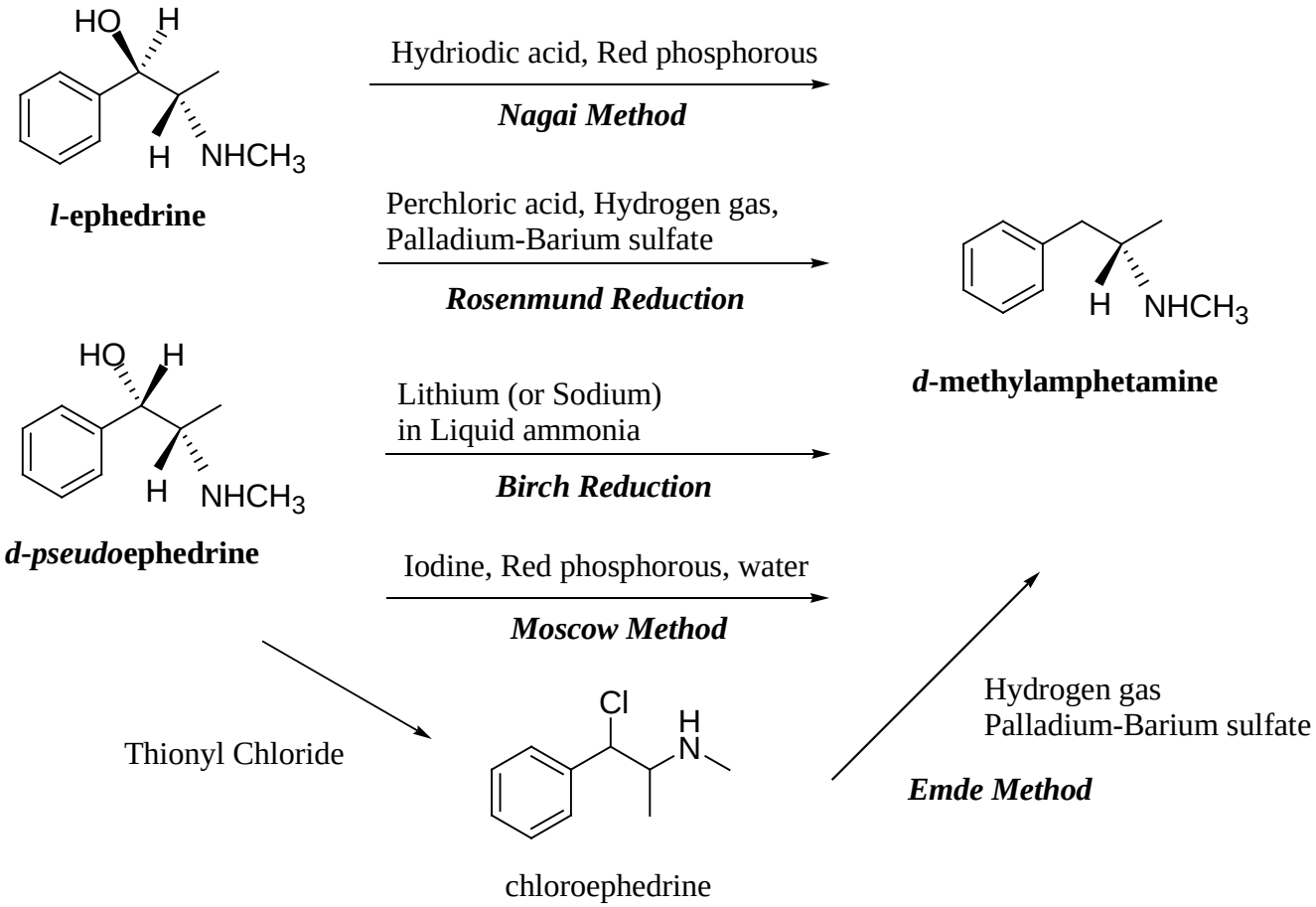

Scheme 5: Summary of synthetic pathways via ephedrine or *pseudo*ephedrine towards methylamphetamine that will be used in this project. [39]

In this project, methylamphetamine was synthesised using each of these 7 synthetic routes. The exact reaction conditions of each synthesis were modified from the methods presented in a commonly available book used by clandestine chemists, Uncle Fester's "Secrets of Methylamphetamine Manufacture" 5th Edition.[6]

For this project 20-25 repetitive batches of methylamphetamine were synthesised by each of the seven chosen routes providing a total of 149 batches of the final product in total.

3.2 Materials and Methods

Reagents and materials were purchased from commercial suppliers. Toluene, diethyl ether and chloroform were purchased from Fisher Scientific. Mercuric chloride (≥ 99.5%) was purchased from BDH (Poole, England). Aluminium (kitchen) foil was purchased from Tesco. Hydrochloric acid (37%), glacial acetic acid, methanol (≥ 99.7%) and sulfuric acid (95-97%) were purchased from Riedel de Haën (Germany). Sodium chloride, Celite, sodium hydroxide pellets (≥ 97.5%), sodium sulfate and magnesium sulfate were purchased from GPR (Poole, England). Phenyl-2-propanone (P-2-P), *N*-methylformamide, methylamine hydrochloride, *l*-ephedrine hydrochloride, *d*-*pseudo*ephedrine hydrochloride, *l*-ephedrine base, red phosphorus, hydriodic acid (50%), perchloric acid (70%), thionyl chloride and iodine were purchased from Sigma Aldrich. Palladium on barium sulfate (5% unreduced) was purchased from Sigma Aldrich and Alfa Aesar.

^{1}H and ^{13}C spectra were recorded on a Bruker DPX 400 spectrometer at 400 MHz and 100 MHz respectively. Chemical shifts are reported in parts per million (ppm). Infrared spectra were obtained with a Perkin Elmer Spectrum 1. Exemplar spectra of each substance can be found in Appendix A.

3.3 The phenyl-2-propanone reactions

3.3.1 The Leuckart Method

The Leuckart reaction can be initiated with phenyl-2-propanone (P-2-P) and either methylamine and formic acid or *N*-methylformamide, producing *N*-formylmethylamphetamine as an intermediate. Hydrolysis of the intermediate with a strong acid such as hydrochloric acid produces methylamphetamine as a racemic mixture (typical yield, 43%).[7] This is illustrated in Scheme 6.[7]

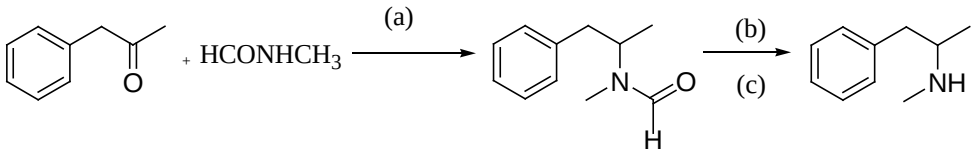

in which (a): 170-190°C; (b): H_2SO_4 or HCl; (c): 120-170°C.[7]

Scheme 6: Leuckart Reaction.

3.3.1.1 The Leuckart Reaction- specific synthesis

Phenyl-2-propanone (5.4 mL, 40.2 mmol) was added *N*-methylformamide (13.4 mL, 229 mmol, 5.7 equiv) with stirring. The temperature was gradually increased to 165-170 °C and held for 2 days (Scheme 7).

Scheme 7: Leuckart Reaction –Formation of intermediate.

After cooling to room temperature, a 10 M NaOH solution (24 mL, 0.24 mmol) was added, and the reaction mixture refluxed for 2 h.

After cooling to room temperature, the aqueous layer was discarded, and 37% HCl (10.7 mL, 0.004 mmol) was added to the red organic layer. The mixture was refluxed for 2 h (Scheme 8).

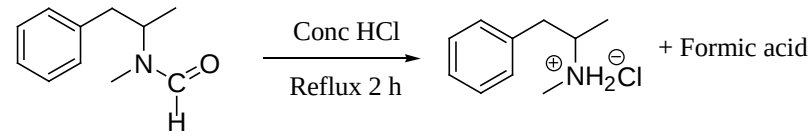

N-formylmethamphetamine methylamphetamine HCl

Scheme 8: Leuckart Reaction – Hydrolysis of intermediate.

After cooling to room temperature, an 8.3 M NaOH solution (16.0 mL, 0.13 mmol) was slowly added, and the crude methylamphetamine base extracted with toluene (3 × 20 mL). The combined organic layers were dried over $MgSO_4$, and the volatiles removed *in vacuo* to reveal the crude methylamphetamine base as a brown oil. The crude methylamphetamine base was distilled under vacuum (2 mbar, 60-100°C) using Kugelrohr distillation to yield methylamphetamine as a clear to pale yellow oil (2.5 g, 42%).

Analysis was in agreement with published data for IR,[8] ^{1}H NMR and ^{13}C NMR.[9] IR ν_{max} (film)/cm^{-1}: 1605 (N-C), 1454, 1373, 1155, 741, 697. ^{1}H NMR (400 MHz, $CDCl_3$): δH 1.08 (d, 3H, *J* = 8.0 Hz, CH_3), 2.42 (s, 3H, CH_3), 2.62 (dd, 1H, *J* = 20.0, 8.0 Hz, CH), 2.65 (dd, 1H, *J* = 20.0, 4.0 Hz, CH), 2.71-2.83 (m, 1H, CH), 7.17-7.37 ppm (m, 5H, C_6H_5). ^{13}C NMR (100 MHz, $CDCl_3$): δ 19.8, 34.0, 43.5, 56.4, 126.2, 128.4, 129.3, 139.5 ppm.

The reaction mechanism for the formation of *N*-methylformamide is shown in Scheme 9. Scheme 10 shows the reaction mechanism for the formation of methylamphetamine hydrochloride from *N*-methylformamide.

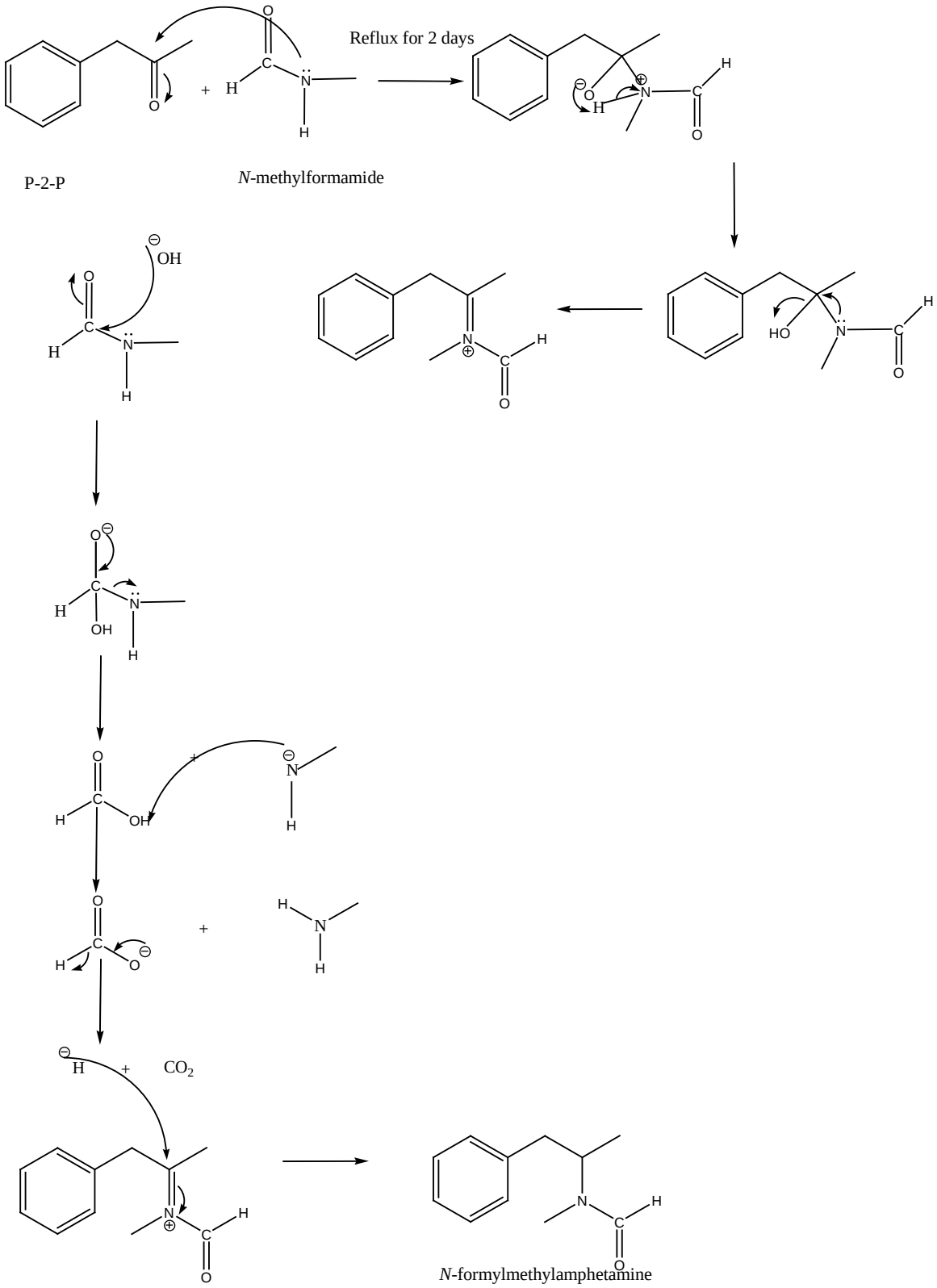

Scheme 9: Reaction mechanism for the formation of *N*-formylmethylamphetamine.

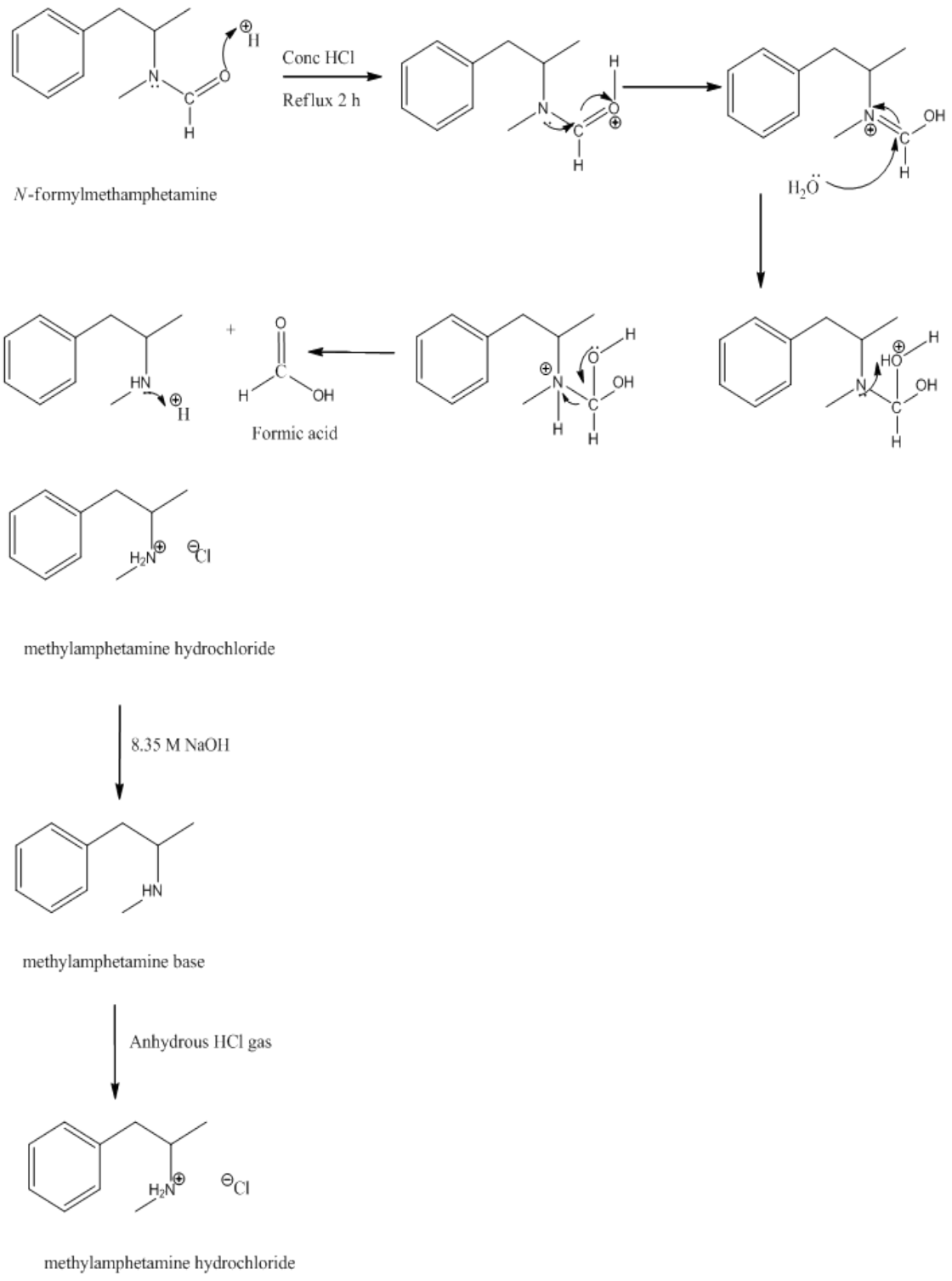

Scheme 10: Reaction mechanism from *N*-formylmethylamphetamine to methylamphetamine via the Leuckart route.

The hydrochloride salt of the previously prepared methylamphetamine was obtained according to the method suggested by Uncle Fester.[6] The source of anhydrous hydrogen chloride was obtained from the reaction between the mixture of sodium chloride and concentrated hydrochloric acid (in paste form) with concentrated sulfuric acid. The methylamphetamine base was dissolved in toluene and anhydrous hydrogen chloride gas was bubbled through the solution. White crystals were filtered off and washed with toluene and then dried under high vacuum. In total, 24 repetitive batches of methylamphetamine were synthesised via the Leuckart route. The typical yield for this route was 17-26%.

Analysis was in agreement with published data for IR,[10] ^{1}H NMR,[11] and ^{13}C NMR.[12] IR ν_{max} (KBr)/cm^{-1}: 3419 (N-H), 2971, 2731, 2461 (C-C), 1603 (N-C). ^{1}H NMR (400 MHz, D_2O): δH 1.22 (d, 3H, J = 8.0 Hz, CH_3), 2.64 (s, 3H, CH_3), 2.87 (dd, 1H, J = 24.0, 8.0 Hz, CH), 3.03 (dd, 1H, J = 20.0, 8.0 Hz, CH), 3.44-3.50 (m, 1H, CH), 7.25-7.38 (m, 5H, C_6H_5). ^{13}C NMR (100 MHz, D_2O): δ 14.8, 29.9, 38.8, 56.4, 127.5, 129.1, 129.5, 135.8 ppm.).

3.3.2 The Reductive Amination Method

Dissolving metal reductions are the popular synthetic route to produce methylamphetamine in clandestine laboratories in United States.[13] The simplest of these is the aluminium amalgam method. Phenyl-2-propanone (P-2-P) and methylamine in alcohol are combined to produce an intermediate Schiff's base, which reacts with a reducing agent to produce methylamphetamine.[14] Activated aluminium (aluminium amalgam) is a readily available reducing agent obtained from aluminium foil or turnings and a small amount of mercuric chloride (Scheme 11). Cooling is required if the reaction becomes too violent (typical yield is 70%).[14]

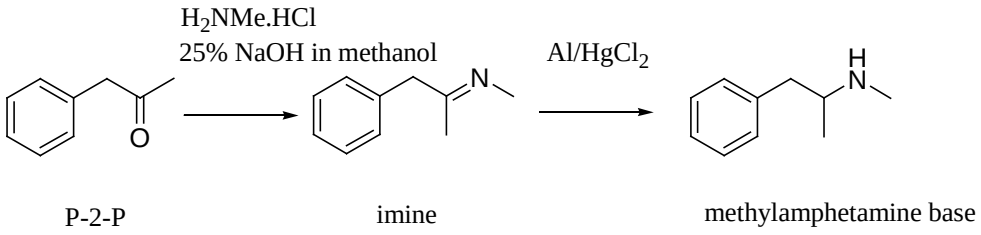

Scheme 11: Reductive Amination reaction.

3.4.2.1 The Reductive Amination Method- specific synthesis

To aluminum foil (2.9 g) cut into 2 cm squares was added distilled water (100 mL) containing mercuric chloride (0.067 g, 0.247 mmol). The amalgamation was allowed to proceed for 15 min. The water was then decanted, and the aluminium amalgam mixture was rinsed with distilled water (2 × 300 mL). In a separate flask, NaOH (4.4 g, 109 mmol, 2.7 equiv) was dissolved in methanol (20 mL). Methylamine hydrochloride (7.2 g, 107 mmol, 2.7 equiv) was added, and the mixture cooled to -10°C. P-2-P (5.4 mL, 40.2 mmol) was then added to the methylamine solution.

The P-2-P and methylamine solution was poured onto the activated aluminium with swirling. During this addition process, the flask was immersed in an ice bath as it is necessary to keep the temperature at around 0°C. After the addition process, the reaction

mixture was heated to around 50-60°C. After 90 min the reaction was complete (as determined by NMR of preliminary reaction runs). Celite (2 g) was added to the alcohol solution containing the product. The resultant mixture was then filtered and rinsed with methanol. The combined organic layers were dried over magnesium sulfate and the volatiles removed *in vacuo* to reveal the crude methylamphetamine base as a pale yellow oil. The crude product was distilled according to the procedure detailed in Section 3.3.1.1. to reveal a clear to pale yellow coloured oil (4.09 g, 69%). The methylamphetamine base was then converted to the hydrochloride salt, again, according to the procedure detailed above. Analyses to confirm the identity of the base were as reported in Section 3.3.1.1.

In total, 20 repetitive batches of methylamphetamine were synthesised by the Reductive Amination route. Typical yield for this route was 40-60%. Analyses to confirm the identity of the salt were as reported in Section 3.3.1.1. Scheme 12 shows the complete reaction mechanism.

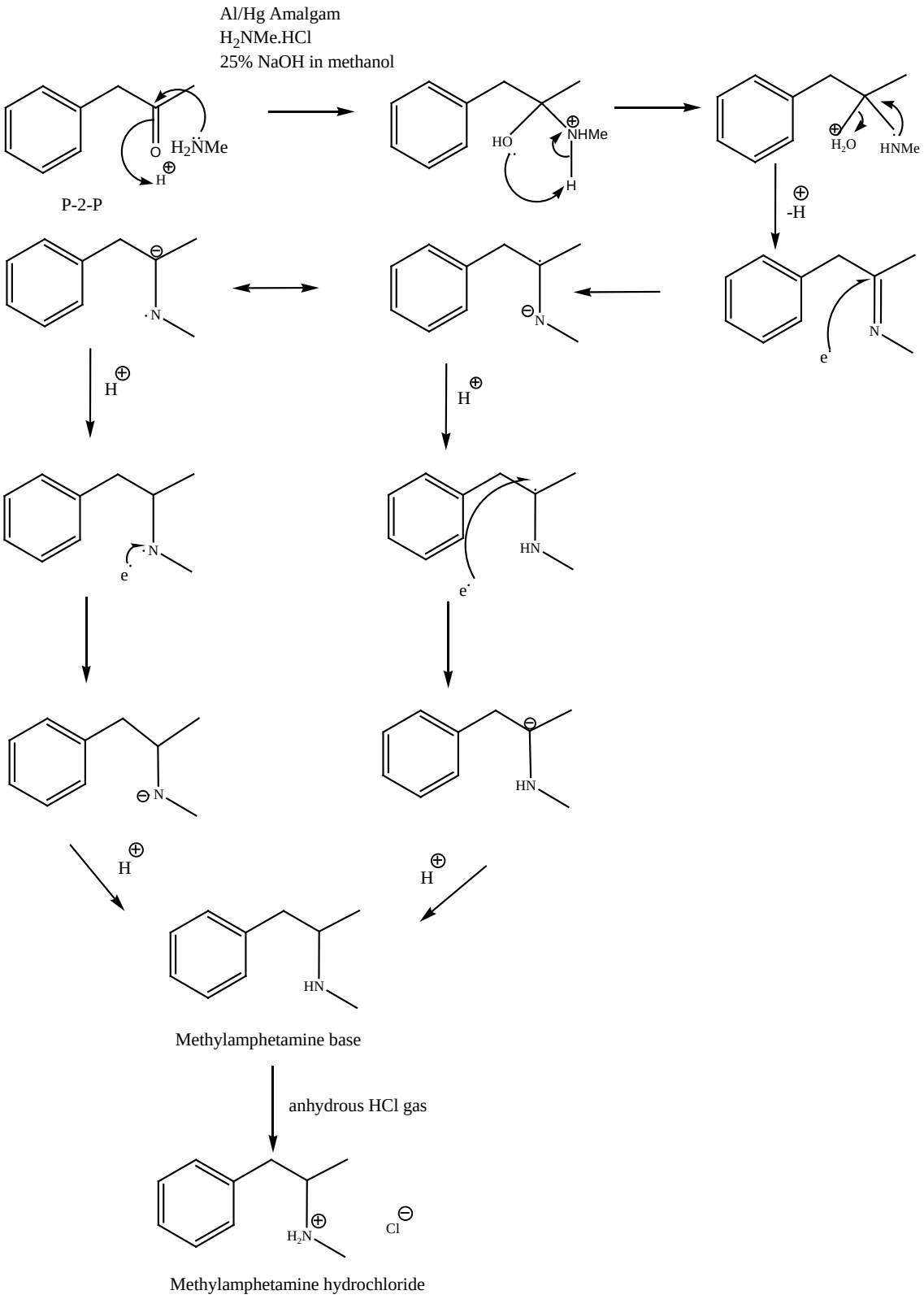

Scheme 12: Reaction mechanism from phenylacetone to methylamphetamine via the 'Al/Hg amalgam' route.

3.4 The ephedrine/*pseudo*ephedrine reactions

3.4.1 The Nagai Method

The Nagai method for reducing a benzyl alcohol group has been known for many years and the application of the method to produce methylamphetamine has been described by Skinner in 1990 (typical yield 50-75%).[15] Typically, ephedrine or *pseudo*ephedrine is heated with red phosphorus and hydriodic acid to produce methylamphetamine. The method is very simple and can be used for large-scale production (Scheme 13).

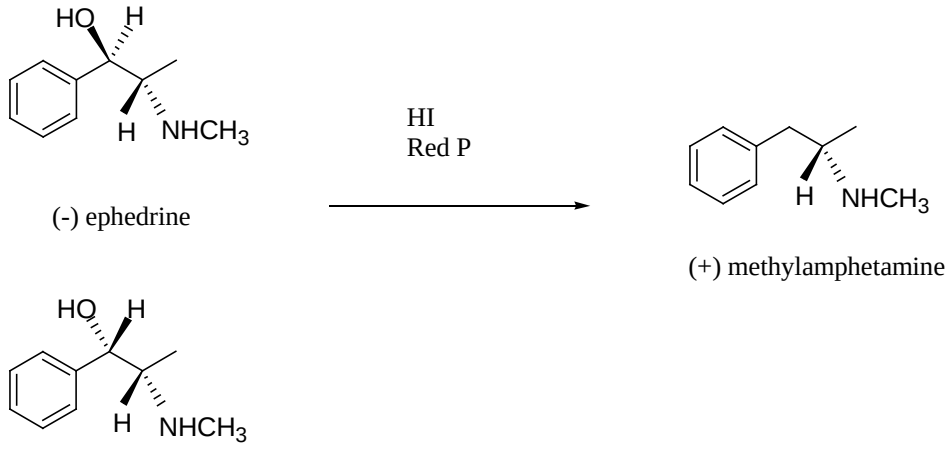

(-) ephedrine

(+) methylamphetamine

(+) *pseudo*ephedrine

Scheme 13: Nagai reaction.

According to the clandestine method, a mixture of ephedrine, red phosphorus, and hydriodic acid is heated, filtered, made basified, extracted, and the product is crystallised as the hydrochloride salt from ether/acetone with hydrochloric acid or hydrogen chloride gas or from trichloromonofluoromethane (i.e. “Freon – 11”) and hydrogen chloride gas. The salt is filtered and dried.[15]

Hydriodic acid can be made *in situ* from red phosphorus, iodine and water, but phosphorous acid is produced as a by-product.[16, 17] If the reaction mixture is over heated, phosphorous acid breaks down to produce phosphine gas, which is extremely toxic and can ignite spontaneously.[16, 17]

Hydriodic acid can also be produced *in situ* from hypophosphorous acid and iodine.[18] Reduction of ephedrine or *pseudo*ephedrine with iodine and hypophosphorous acid does not require the use of red phosphorus, as hypophosphorous acid acts as a reducing agent in the same way as red phosphorus. Hypophosphorous acid is more prone than red phosphorus to cause a fire and can produce deadly phosphine gas.[18] Production of methylamphetamine using the iodine/hypophosphorous acid method (known as the 'Hypo' method) is therefore even more dangerous than the iodine/red phosphorus method.[18]

3.4.1.1 The Nagai Method- specific synthesis

A 100 mL round bottom flask was filled with either ephedrine hydrochloride or *pseudo*ephedrine hydrochloride (6.05 g, 30 mmol, 1 equiv). Also added to the flask were red phosphorus (1.61 g, 52 mmol, 1.74 equiv) and 50% hydriodic acid (14.00 mL, 180 mmol, 6 equiv). With the ingredients mixed together in the flask, a condenser was attached to the flask, and the mixture was refluxed or 24 hours. After this time the flask was allowed to cool and the contents diluted with an equal volume of water. Any remaining red phosphorus was removed by filtration.

25% NaOH solution (24.0 mL, 100.8 mmol) was slowly added and the crude methylamphetamine base extracted with toluene (3 x 20 mL). The combined organic layers were dried over magnesium sulfate and the volatiles removed *in vacuo* to reveal the methylamphetamine base as a clear to pale yellow coloured oil. The product was very clean with no distillation necessary. Analyses to confirm the identity of the base were as reported in Section 3.3.1.1.

The methylamphetamine base was converted to the hydrochloride salt according to the procedure detailed previously. In total 20 repetitive batches of methylamphetamine were synthesised (10 batches from ephedrine hydrochloride and 10 batches from *pseudo*ephedrine hydrochloride) by Nagai route. Typical yield for this route was 55-82%.

Analyses to confirm the identity of the salt were as reported in Section 3.3.1.1. Scheme 14 shows the complete reaction mechanism.

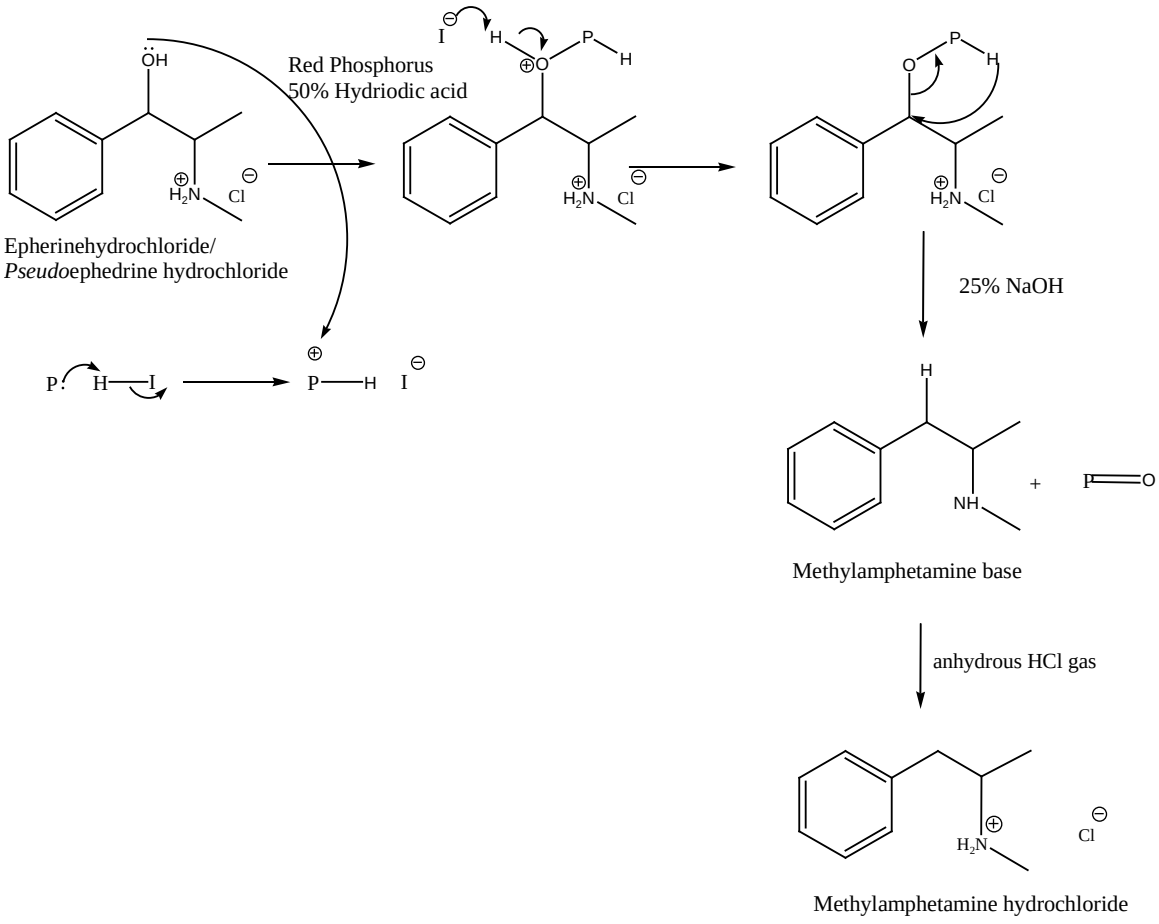

Scheme 14: Reaction mechanism from ephedrine HCl/*pseudo*ephedrine HCl to methylamphetamine via the Nagai route.

Ephedrine and *pseudo*ephedrine are isomers of 1-phenyl-1-hydroxy-2-methylamino-propane; each contain two chiral centers at the No.1 and No. 2 carbons of the propane chain. Reduction to methylamphetamine eliminates the chiral center at the No.1 carbon.

The reduction of ephedrine to methylamphetamine with hydriodic acid/red phosphorous, involves a cyclic oxidation of the iodide anion to iodine and reduction of iodine back to the anion by red phosphorus, the latter being converted to phosphorous or phosphoric acid.[15]

3.4.2 The Rosenmund Reduction

A benzyl alcohol group ArCH(OH) can be easily reduced catalytically to $ArCH_2$ in acetic acid or propionic acid in the presence of $HClO_4$ (perchloric acid).[19] Methylamphetamine can, thus, be synthesised from ephedrine hydrochloride or *pseudo*ephedrine hydrochloride via hydrogenation with glacial acetic acid, perchloric acid and palladium on barium sulfate according to a method known as the Rosenmund reaction (Scheme 15).

The reaction was unsuccessful at low (18°C) or high (100°C) temperature, low (2 bar) or high (70 bar) pressure and with $Pd/BaSO_4$ (reduced and unreduced) purchased from Sigma Aldrich. It returned only ephedrine and acetic ester. The reaction was successful with Pd/C catalyst hydrogenated at 70 bar for 3 hours and heated to 100°C. In order to mimic the clandestine synthesis, $Pd/BaSO_4$ was purchased from a different supplier and the reaction undertaken again. Unreduced $Pd/BaSO_4$ from Alfa Aesar gave the desire product. In order to fully explore the reason behind the varation between the reacitivity of the catalysts available from different suppliers further work in this area should undertaken

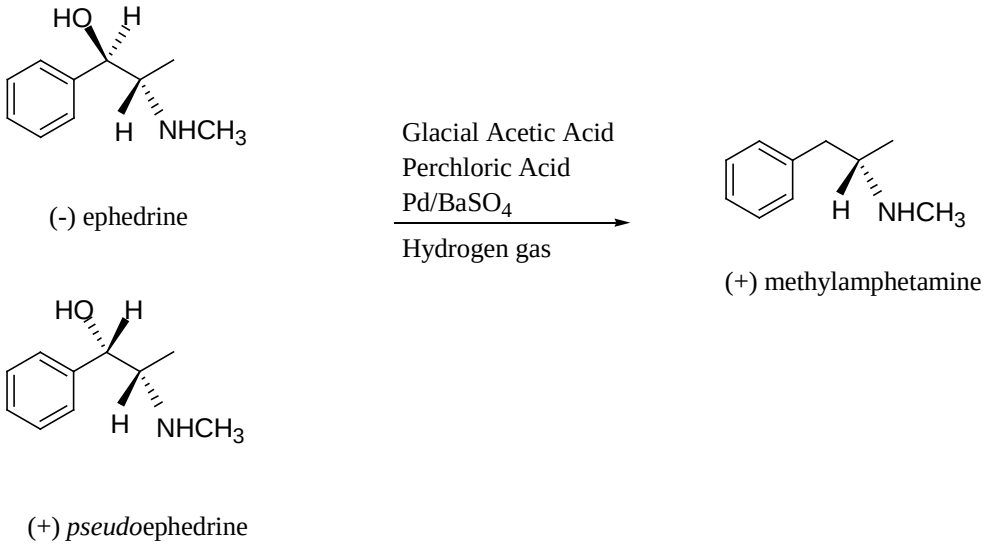

Scheme 15: Rosenmund reaction.

3.4.2.1 The Rosenmund Method – specific synthesis

To an autoclave hydrogenation vessel was added ephedrine hydrochloride (4.0 g, 19.8 mmol), 90 mL of glacial acetic acid (4.7 g, 47.2 mmol, 2.36 equiv) of 70% perchloric acid and (1 g, 2.97 mmol, 0.14 equiv) of palladium on barium sulfate. The vessel was attached to an autoclave hydrogenation apparatus. Air was removed and the flask flushed with hydrogen three times, charged to a pressure of 70 bar with hydrogen and heated at 100°C with mechanical shaking for 4 hours. The catalyst was filtered and acetic acid was removed *in vacuo*. 20% sodium hydroxide solution was slowly added until the mixture was strongly alkaline and the crude methylamphetamine base extracted with toluene (3 x 20 mL).

The combined organic layers were dried over magnesium sulfate and the volatiles removed *in vacuo* to reveal the methylamphetamine base as a clear to pale yellow coloured oil.

Analyses to confirm the identity of the base were as reported in Section 3.3.1.1.

The methylamphetamine base was converted to the hydrochloride salt according to the procedure detailed previously. In total 20 repetitive batches of methylamphetamine were synthesised (12 batches from ephedrine hydrochloride and 8 batches from *pseudo*ephedrine hydrochloride) by Rosenmund route. Typical yield for this route was 27-54%.

Analyses to confirm the identity of the salt were as reported in Section 3.3.1.1. Scheme 16 shows the complete reaction mechanism.

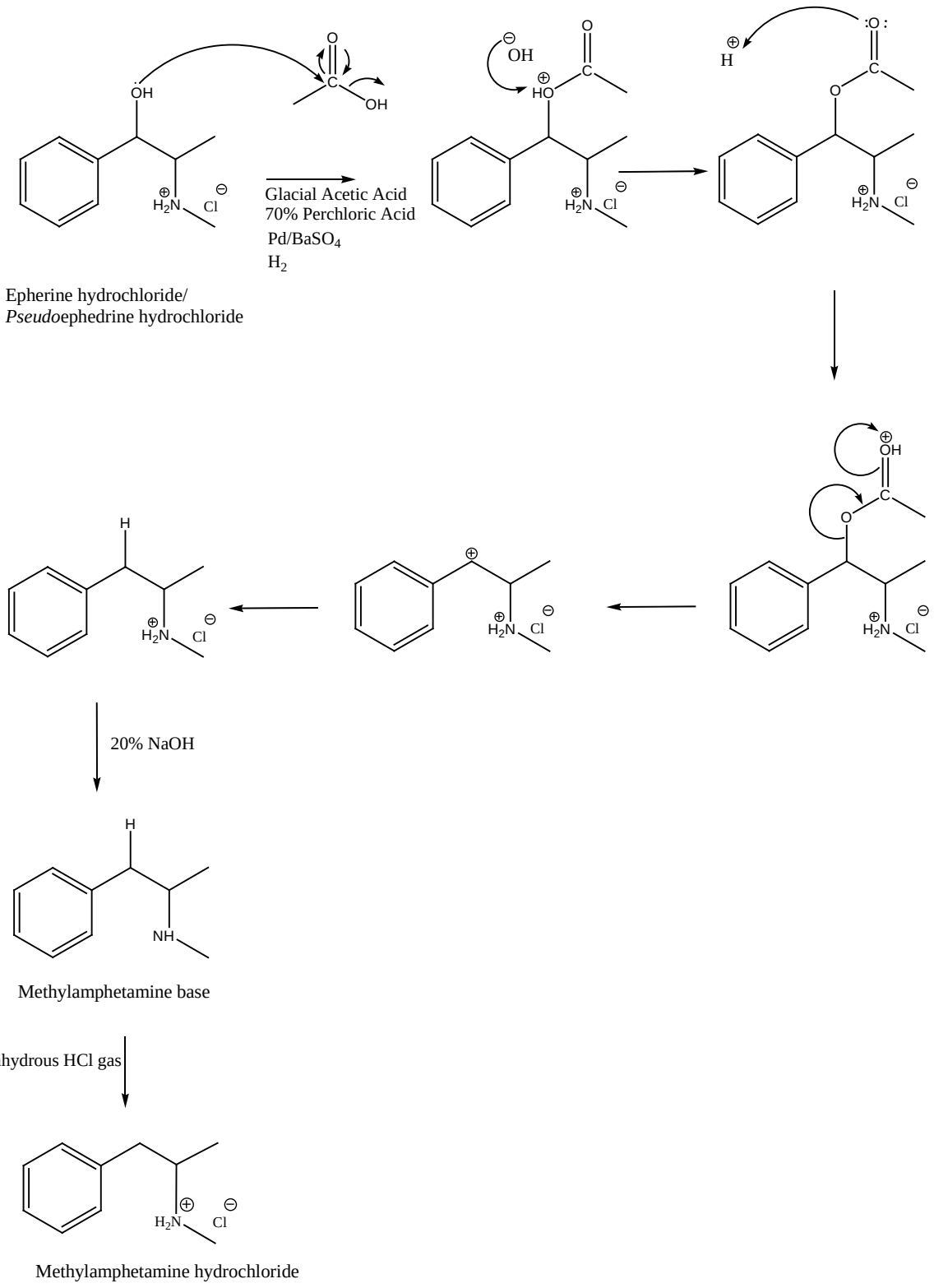

Scheme 16: Reaction mechanism from ephedrine HCl/pseudoephedrine HCl to methylamphetamine via the Rosenmund route.

3.4.3 The Birch Reduction

In 1990, a suspected clandestine methylamphetamine laboratory was seized in Vacaville, California.[20] Examination of the suspect's notes showed documentation for several different common synthesis routes to methylamphetamine and a novel route utilising a lithium/ammonia/ammonium chloride reduction. The reduction of ephedrine to methylamphetamine using this procedure had not been reported in the literature. The authors reproduced the suspect's reaction scheme and found the lithium/ammonia/ammonium chloride reduction of ephedrine to be a viable synthesis for methylamphetamine.[20]

The lithium-ammonia reduction method is now one of the most common methods of illicit methylamphetamine manufacture in the United States.[21] It is a dissolving metal reduction reaction where an alkali metal, typically lithium, serves as an electron source with ammonia as a solvent that allows the electrons to chemically reduce the hydroxyl group of ephedrine to form methylamphetamine.[21]

The hydroxyl group of ephedrine is preferentially reduced by an alkali metal in the presence of a proton source, such as water absorbed from the atmosphere, an excess of the alkali metal under these reaction conditions can lead to a further partial reduction of the aromatic ring of methylamphetamine (Scheme 17).[21]

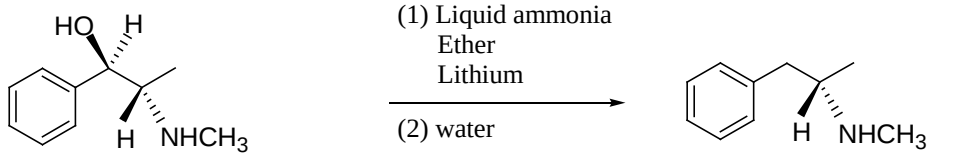

(-) ephedrine base (+) methylamphetamine

Scheme 17: Birch Reduction.

These conditions are similar to a classical Birch reduction where sodium, ammonia, and an alcohol are used to reduce aromatic rings to form cyclohexadienes.[21] This similarity results in the use of the term Birch reduction in describing this method. It has also been

referred to as the Birch-Benkeser reduction and the “Nazi” method within the forensic community.[21]

3.4.3.1 The Birch Method - specific synthesis

Ammonia gas was condensed using a dry-ice condenser into a 250 mL flask until the flask was about ½ full. The liquid ammonia then allowed to partially evaporate until the volume was approximately 90 mL. *l*-ephedrine base (3.30 g, 20 mmol) in ether (30 mL) was added dropwise to the ammonia solution over a period of approximately 10 min with stirring. Small pieces of lithium metal (0.42 g, 60.6 mmol, 3 equiv) were rinsed in petroleum ether, patted dry with a paper towel, and added to flask. After 10 min, water was added to the solution to quench any unreacted lithium metal.

The ammonia mixture was allowed to warm to room temperature and evaporate from the flask through the side necks. When the ammonia had evaporated, the remaining solution was transferred from the flask to a separating funnel. 30-50 mL of ether was added and shaken to extract methylamphetamine into the organic layer. The aqueous layer was discarded. The ether layer was dried with magnesium sulfate and the solid was removed by filtration. Anhydrous hydrogen chloride gas was bubbled through the ether solution to reveal a white precipitate. The precipitate was filtered and washed with ether. The solid was dried under high vacuum. In total 20 repetitive batches of methylamphetamine were synthesised by Birch route. Typical yield for this route was 60-80%.

Analyses to confirm the identity of the salt were as reported in Section 3.3.1.1.Scheme 18 illustrates the complete reaction mechanism.

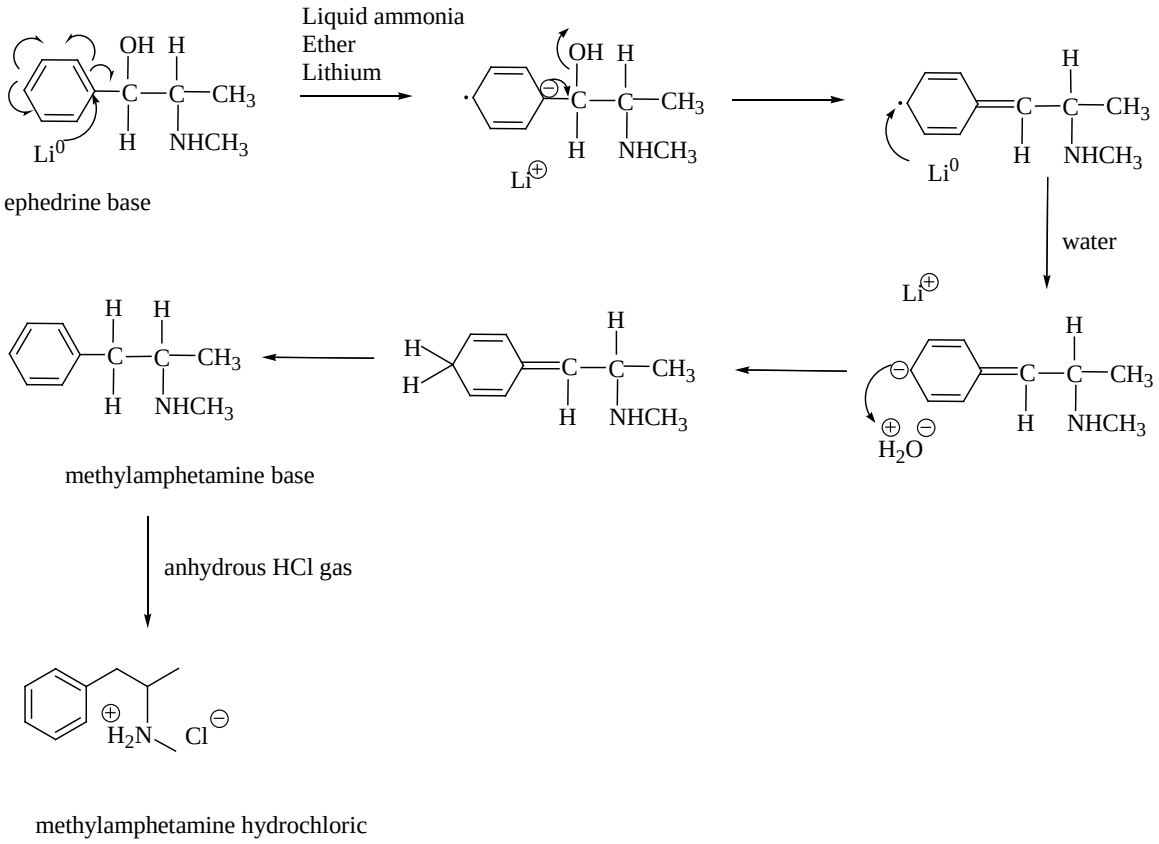

Scheme 18: Reaction mechanism from ephedrine base to methylamphetamine via the Birch route.[20]

The dissolved lithium metal gives up an electron to the phenyl ring and forms a radical anion.[20] The hydroxyl group is eliminated, forming a double bond between the ring and the alpha carbon.[20] A second atom of lithium gives up an electron to the radical, and the resulting carbanion is protonated by the water.[20] Through keto-enol tautomerism, methylamphetamine is formed as the more stable species.[20]

3.4.4 Reduction of Chloroephedrine

Prior to the adoption of the Birch Reduction method, the most commonly applied clandestine laboratory conversions of ephedrine to methylamphetamine involved first converting the ephedrine to its chloro analog by reaction with $SOCl_2$, PCl_5, $POCl_3$, or PCl_3. Secondly, the chloro analog was reduced by catalytic hydrogenation (Scheme 19). The reaction of ephedrine or *pseudo*ephedrine with $SOCl_2$ yields the chloro analog with complete inversion of configuration around the carbon alpha to the benzene ring, yielding chloropseudoephedrine in 90% and 60% respectively. [22]

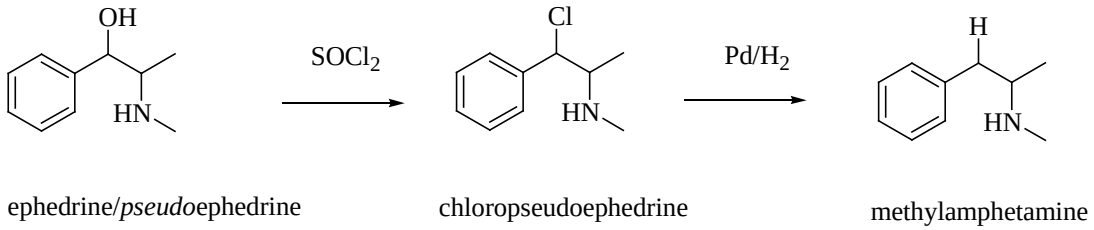

Scheme 19: Reduction of Chloroephedrine.[22]

A solution of ephedrine hydrochloride or *pseudo*ephedrine hydrochloride (8.5 g, 51.5 mmol) and thionyl chloride (17 mL) in chloroform (17 mL) was stirred in ice bath for 3 hours. Addition of anhydrous ether (200 mL) resulted in crystallisation of the 1-phenyl-1-chloro-2-(methylamino) propane hyrdrochlorides (Scheme 20).

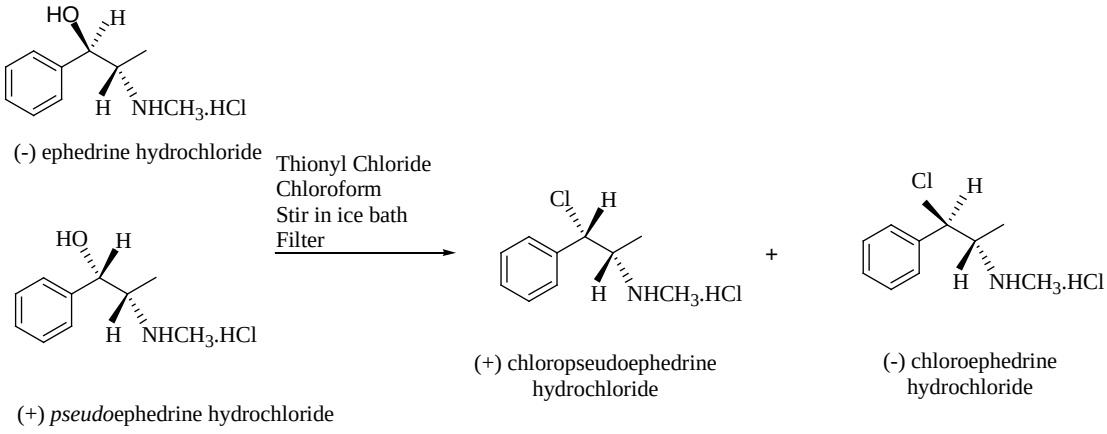

Scheme 20: Formation of chloro analog.

NMR was used to the identity of the chloro analog and an exemplar of the spectra can be found in Appendix A. Analysis was in agreement with published data for ^{1}H NMR.[22]

Scheme 21 illustrates the possible reaction mechanism.

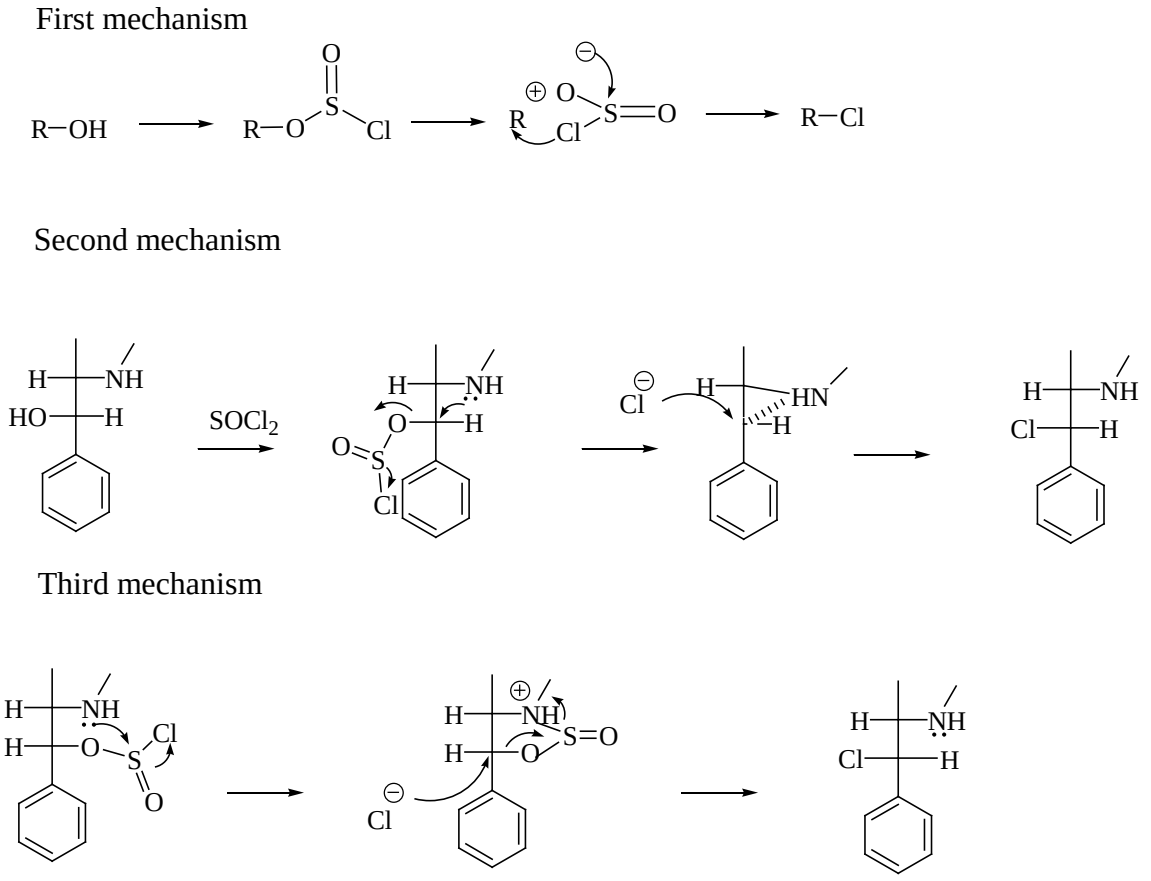

Scheme 21: Reaction mechanism from ephedrine HCl/*pseudo*ephedrine HCl to chloro analog. [22]

3.4.4.1 Reduction of Chloroephedrine (Emde route)

In a hydrogenation vessel, sodium acetate trihydrate (4.88 g, 35.86 mmol, 3.89 equiv) was dissolved in 20 mL of water. Glacial acetic acid (190 mL, 3319 mmol, 360.8 equiv) and unreduced palladium on barium sulfate (2.0 g, 5.88 mmol, 0.64 equiv) were then added to the solution. Finally a mixture of the 1-phenyl-1-chloro-2-(methylamino)-propane hydrochloride (2.0 g, 9.2 mmol, 1 equiv) was added. This solution was hydrogenated at 43 psi for 3 hours.

After the uptake of hydrogen ceased, the catalyst was removed by filtration and washed with water (200 mL). The combined filtrate and water washings were concentrated *in vacuo* and the resulting oil was dissolved in water (200 mL) and acidified with 5 mL of concentrated HCl (pH 1). The acidic aqueous solution was extracted with chloroform (2 x 50 mL), then made basic (pH 12) with 40 mL of 10% NaOH. The basic aqueous solution was extracted with chloroform (3 x 75 mL), and the combined chloroform extracts were washed with water (100 mL) and dried over magnesium sulfate. The volatiles removed *in vacuo* to reveal the methylamphetamine base. Analyses to confirm the identity of the base were as reported in Section 3.3.1.1.

The product was dissolved in ether and anhydrous hydrogen chloride gas was bubbled through to reveal a white precipitate, which was washed again with ether. The solid was dried under high vacuum. In total 20 repetitive batches of methylamphetamine were synthesised (11 batches from ephedrine hydrochloride and 9 batches from *pseudo*ephedrine hydrochloride) by Emde route. Typical yield for this route was 70-80%.

Analyses to confirm the identity of the salt were as reported in Section 3.3.1.1.

3.4.5 The Moscow Method

As mentioned in relation to the Nagai synthesis (Section 3.4.1.1), hydriodic acid can be made *in situ* from red phosphorus, iodine and water.[23] The synthesis of methylamphetamine using this means of production of hydriodic acid is called the Moscow route and is detailed in Scheme 22.

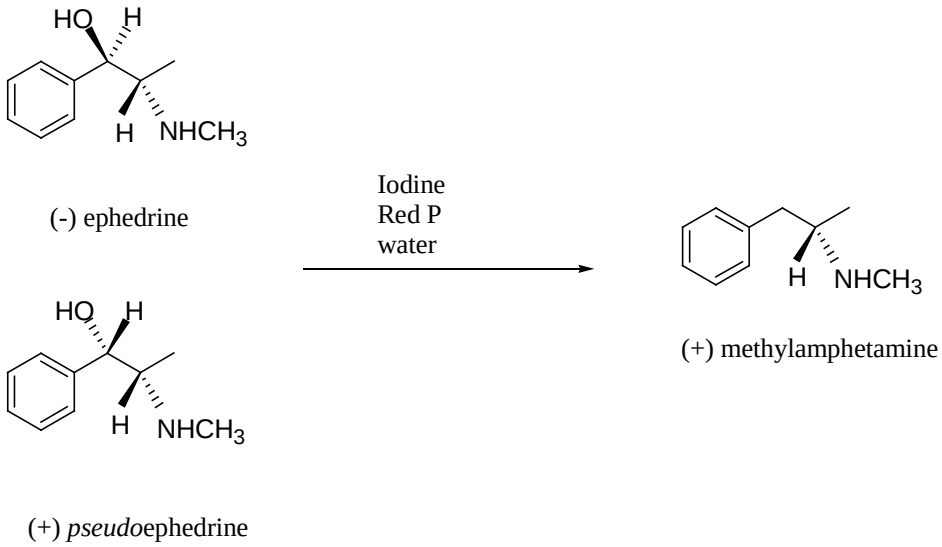

Scheme 22: Moscow reaction.

3.4.5.1 The Moscow route- specific synthesis

A 100 mL round bottom flask was filled with of either ephedrine hydrochloride or pseudoephedrine hydrochloride (3.0 g, 15 mmol, 1 equiv). Also added to the flask were red phosphorus (1.0 g, 32.5 mmol, 2.2 equiv), iodine (6.0 g, 47.7 mmol, 3.2 equiv) and 6 mL of water. The reagents were mixed together and a condenser was attached to the flask, and the mixture was refluxed for 24 hours. After this time the flask was allowed to cool, and the contents diluted with an equal volume of water. Any remaining red phosphorus was removed by filtration.

25% NaOH solution (12.0 mL, 75.6 mmol) was slowly added and the crude methylamphetamine base extracted with toluene (3 x 20 mL). The combined organic layers were dried over magnesium sulfate and the volatiles removed *in vacuo* to reveal the methylamphetamine base as a clear to pale yellow coloured oil. Analyses to confirm the identity of the base were as reported in that Section 3.3.1.1.

The methylamphetamine base was converted to the hydrochloride salt as described previously. In total 25 repetitive batches of methylamphetamine were synthesised (21 batches from ephedrine hydrochloride and 4 batches from *pseudo*ephedrine hydrochloride) by Moscow route. Typical yield for this route was 46-77%.

Analyses to confirm the identity of the salt were as reported in Section 3.3.1.1. Scheme 23 shows the complete reaction mechanism.

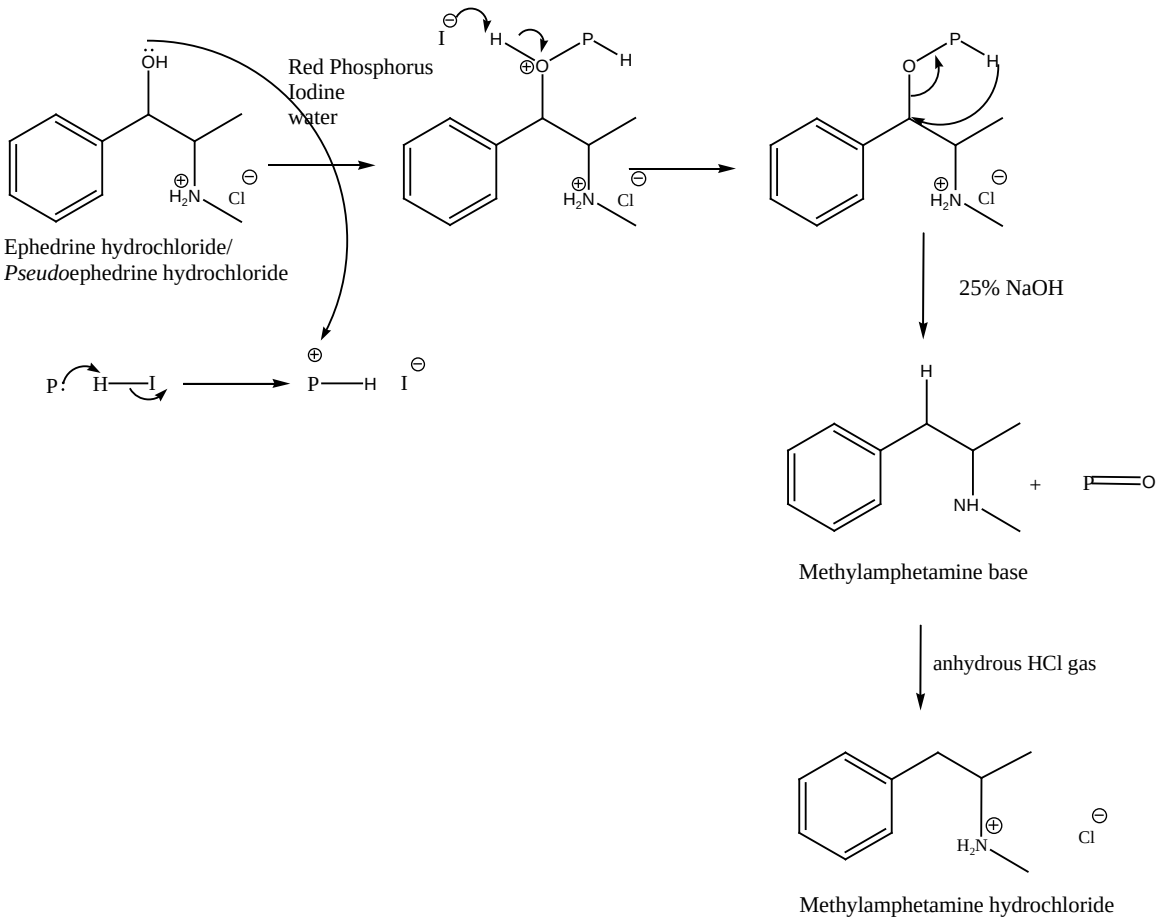

Scheme 23: Reaction mechanism from ephedrine HCl/pseudoephedrine HCl to methylamphetamine via the Moscow route.

3.5 Summary of synthesised methylamphetamine samples

In total 149 methylamphetmaine samples were produced using seven methods. The various quantites of samples and their starting materials are summarised in Table 11.

Synthetic route	P-2-P	Ephedrine HCl	*Pseudo*ephedrine HCl	Ephedrine base
Leuckart	24			
Reductive Amination	20			
Nagai		10	10	
Rosenmund		12	8	
Birch				20
Emde		11	9	
Moscow		21	4	

Table 11: Summary of the samples synthesised in this study.

3.6 Other confirmation analysis for the synthesised samples

Optical isomers differ to some extent in pharmacological activity and are subject to different regulatory measures in certain countries. In some countries, national legislation requires that the specific optical isomer present be identified. Melting point and optical rotation may also be used as a preliminary technique for methylamphetamine identification. These tests have been shown to distinguish the *d,l* and racemic forms of methylamphetamine.[24] Capillary electrophoresis (CE) shows chromatograph separation to distinguish the *d,l* and racemic forms of methylamphetamine.

3.6.1 Melting point

Table 12 shows the melting point results obtained for selected samples prepared in this study. Methylamphetamine synthesised from phenyl-2-propanone (P-2-P) could be differentiated from ephedrine or *pseudo*ephedrine.

Route	Precursors	Melting point of methylamphetamine product
Leuckart	phenyl-2-propanone	130-131ºC (*dl*-methylamphetamine)
Reductive Amination	phenyl-2-propanone	130-131ºC (*dl*-methylamphetamine)
Nagai	*l*-ephedrine HCl and *d*-*pseudo*ephedrine HCl	170-173ºC (*d*-methylamphetamine)
Rosenmund	*l*-ephedrine HCl and *d*-*pseudo*ephedrine HCl	170-172ºC (*d*-methylamphetamine)
Birch	*l*-ephedrine base	170-173ºC (*d*-methylamphetamine)
Emde	*l*-ephedrine HCl and *d*-*pseudo*ephedrine HCl	170-173ºC (*d*-methylamphetamine)
Moscow	*l*-ephedrine HCl and *d*-*pseudo*ephedrine HCl	170-173ºC (*d*-methylamphetamine)

Table 12: Melting point results from this study.

3.6.2 Optical Rotation

Optical rotation was used to distinguish the *d,l* and racemic forms of methylamphetamine and, thus elucidate which methylamphetamine samples were synthesised from the P-2-P routes - Leuckart and Reductive Amination routes ($[\alpha_D]^{20} = 0^o$) and which were via the ephedrine / *pseudo*ephedrine routes - Nagai, Rosenmund, Birch Reduction, Emde and Moscow routes ($[\alpha_D]^{20} = +17.7$). $[\alpha_D]^{20}$ is the observed angel of optical rotation of methylamphetamine at 20ºC

3.6.3 Capillary electrophoresis (CE)

CE analysis was used to distinguish the *d,l* and racemic forms of methylamphetamine via chromatographic separation using a phenyl-β-cyclodextrin (CD) capillary as chiral selector to a capillary electrophoresis phosphate buffer. N-ba (n-butylamphetamine) was used as the internal standard and the concentration of the internal standard is 0.1 mg/ml of n-butylamphetmaine HCl. N-ba(1) is *l*-n-butylamphetamine and

N-ba(2) is *d*-n-butylamphetamine. Figure 23-25 illustrates the racemic forms of methylamphetamine, which were obtained using P-2-P as starting material in the Leuckart and Reductive Amination routes.

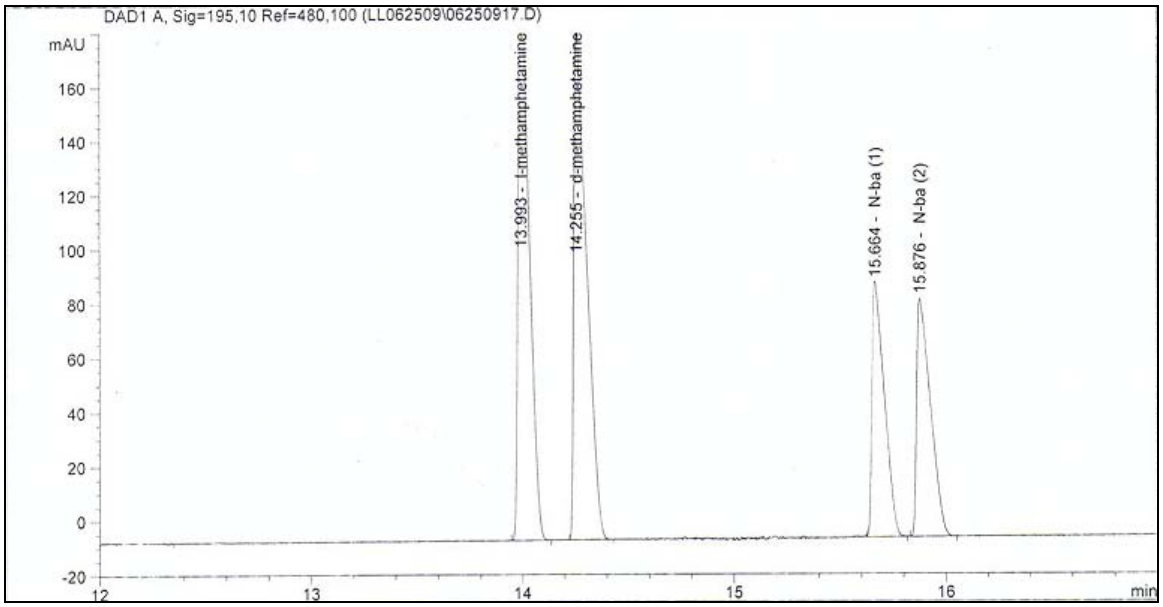

Figure 23: Chiral chromatogram of methylamphetamine synthesised from the Leuckart route.

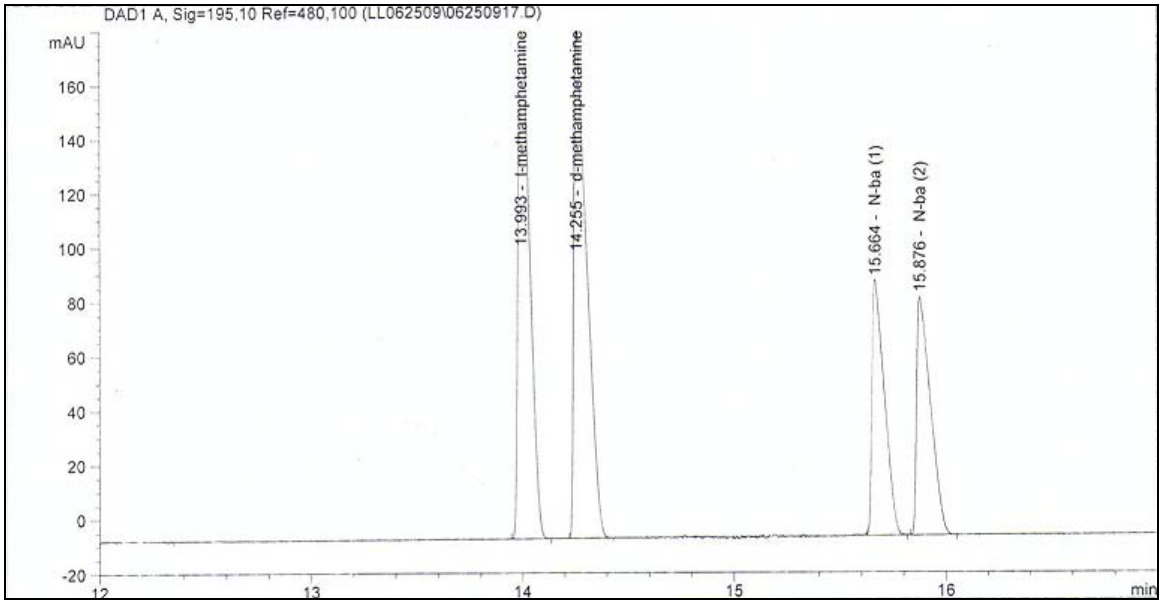

Figure 24: Chiral chromatogram of methylamphetamine synthesised from the Reductive amination route.

Figure 25-29 shows *d*-methylamphetamine, which was obtained, using *l*-ephedrine or *d*-*pseudo*ephedrine as starting material in Nagai, Rosenmund, Birch Reduction, Emde and Moscow routes.

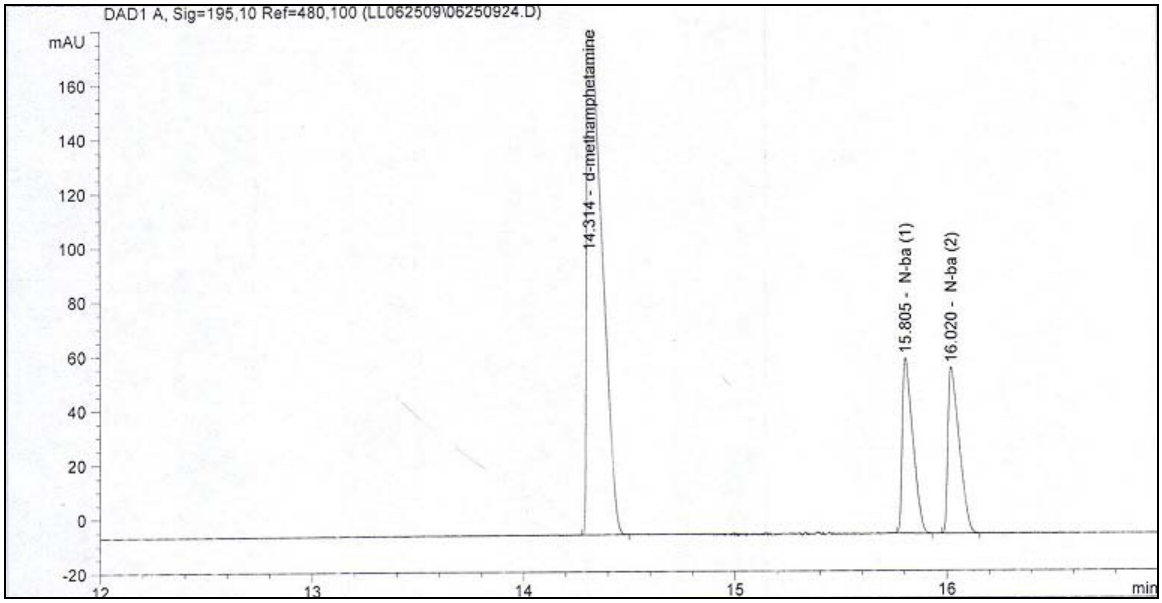

Figure 25: Chiral chromatogram of methylamphetamine synthesised from the Nagai route

In Figure 26, CE analysis was also able to identify *l*-ephedrine (peak 2) as a precursor that was used in the Rosemund route. In the chromatogram, *l-pseudo*ephedrine (peak 1), *l*-methylamphetamine (peak 3) and *d-pseudo*ephedrine (peak 5) were also observed. But the UV spectra did not relate to these compounds but to some other impurities which eluted at the same retention time and were misidentified by the software package used.

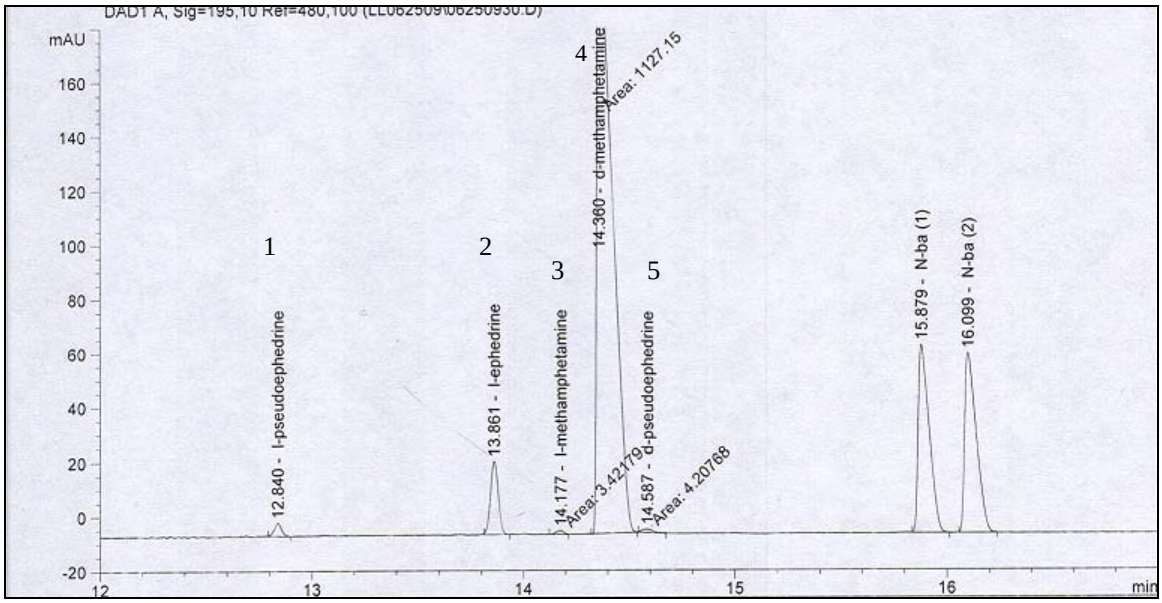

Figure 26: Chiral chromatogram of methylamphetamine synthesised from the Rosemund route.

In Figure 27, CE analysis again was able to identify *l*-ephedrine as a precursor that was used in the Birch route.

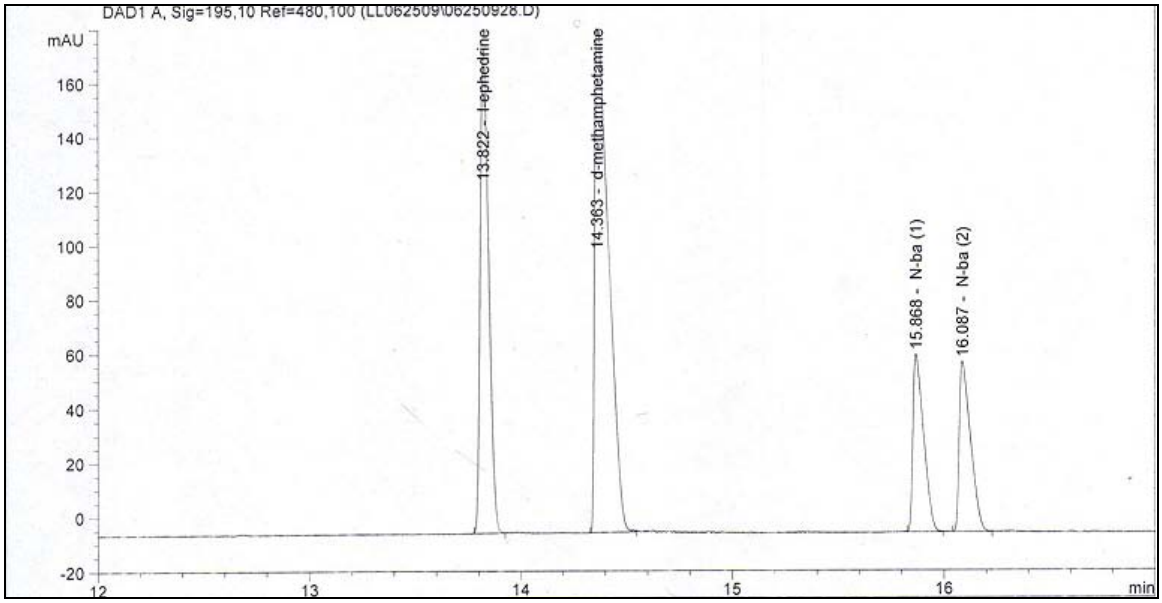

Figure 27: Chiral chromatogram of methylamphetamine synthesised from the Birch route.

Figure 28: Chiral chromatogram of methylamphetamine synthesised from the Emde route.

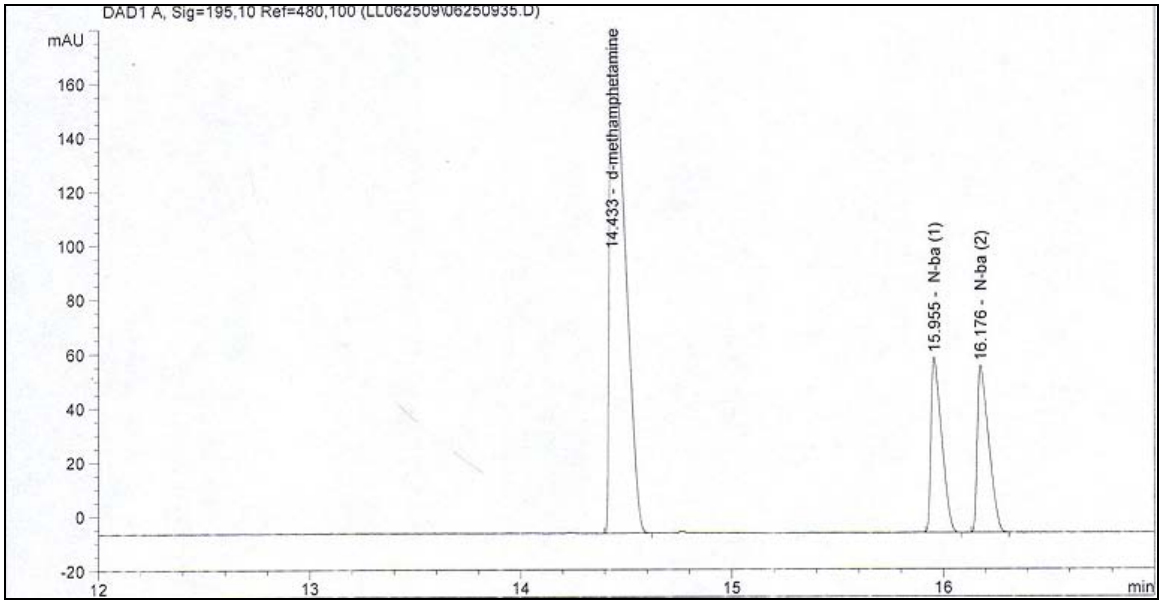

Figure 29: Chiral chromatogram of methylamphetamine synthesised from the Moscow route.

3.7 References

1. Drug Enforcement Administration, Methamphetamine: A Growing Domestic Threat, 1996 Available at http://www.fas.org/irp/agency/doj/dea/product/meth/toc.htm. Last accessed on 02/03/10.

2. Iwata, Y.T.; Inoue, H.; Kuwayamaa, K.; Kanamoria, T.; Tsujikawaa, K.; Miyaguchia , H.; Kishi, T., Forensic application of chiral separation of amphetamine-type stimulants to impurity analysis of seized methamphetamine by capillary electrophoresis. *Forensic Science International* 2006, 161(2-3), 92-96.

3. Uncle Fester, *Secrets of Methamphetamine Manufacture*. 2nd ed. Loompanics Unlimited Port Townsend: Washington, 1989.

4. Labtop, *Racemic Methylamphtamine (ICE) synthesis with $NaBH_4$.* Available at http://www.erowid.org/archive/rhodium/chemistry/meth-nabh4.html. Last accessed on 12/03/10.

5. Remberg, B. and A.H. Stead. Drug characterization/impurity profiling, with special focus on methamphetamine: recent work of the United Nations International Drug Control Programme. *Bulletin on Narcotics 1999 (Volume LI Nos. 1 and 2),* Available at http://www.unodc.org/unodc/en/data-and-analysis/bulletin/bulletin_1999-01-01_1_page008.html. Last accessed on 12/12/09.

6. Uncle Fester, *Secrets of Methamphetamine Manufacture*. 5th ed. Loompanics Unlimited, Port Townsend, Washington, 1999.

7. Crossley, F.S.; Moore, M.L., Studies on the Leuckart Reaction. *Journal of Organic Chemistry*, 1944, 9, 529-536.

8. United Nations, *Recommended Methods for Testing Amphetamine and Methamphetamine: Manual for Use by National Narcotics Laboratories*. 2004. 27-29.

9. Almena, J.; Foubelo, F.; Yus, M., N,2-Dilithioalkylamines from Aziridines by Naphthalene-Catalyzed Reductive Opening- Synthetic Applications. *Journal of Organic Chemistry*, 1993, 59, 3210-3215.

10. Chappell, J.S., Infrared Discrimination of Enantiomerically Enriched and Racemic Samples of Methamphetamine Salts. *Analyst*, 1997, 122, 755-760.

11. Kram, T.C.; Kruegel, A.V., The Identification of Impurities in Illicit Methamphetamine Exhibits by Gas Chromatography/Mass Spectrometry and Nuclear Magnetic Resonance Spectroscopy. *Journal of Forensic Sciences* 1977, 22(1), 40-52.

12. Lee, G.S.H.; Taylor, R.C.; Dawson, M.; Kannangara, G.S.K.; Wilson, M.A.L., High-resolution solid state 13C nuclear magnetic resonance spectra of 3,4-methylenedioxyamphetamine hydrochloride and related compounds and their mixtures with lactose. *Solid State Nuclear Magnetic Resonance* 2000, 16, 225-237.

13. Allen, A.C.; Cantrell, T.S., Synthetic Reductions in Clandestine Amphetamine and Methamphetamine Laboratories - A Review. *Forensic Science International* 1989, 42, 183-199.

14. Station., Reductive Alkylation Review. Available at http://www.erowid.org/archive/rhodium/chemistry/reductive.alkylation.html. Last accessed on 17/03/10.

15. Skinner, H.F., Methamphetamine Synthesis via HI/Red Phosphorus Reduction of Ephedrine. *Forensic Sciences International* 1990, 48, 123-134.

16. Cantrell, T.S., A Study of Impurities Found in Methamphetamine Synthesized From Ephedrine. *Forensic Science International* 1988, 39, 39-53.

17. Forensic Science Service, *Methylamphetamine : Chemistry, Seizure Statistics, Analysis, Synthetic Routes And History Of Illicit Manufacture In UK And USA*, 2004.

18. Assessment, N.D.I.C.W.V.D.T. Methamphetamine. 2003. Available at http://www.justice.gov/ndic/pubs5/5266/meth.html. Last accessed on 17/03/10.

19. Rosenmund, K.W.; Karg, E.; Marcus, F.K., Concerning the Preparation of beta-Aryl-Alkylamines. *Berichte* 75B(1942), 1850-1859, *C.A.*, 1944, 38, 1219.

20. Ely, R.A.; McGrath, D.C., Lithium-Ammonia Reduction of Ephedrine to Methamphetamine: An Unusual Clandestine Synthesis. *Journal of Forensic Sciences* 1990, 35(3), 720-723.

21. Person, E.C.; Meyer, J.A.; Vyvyan, J.R., Structural Determination of the Principal Byproduct of the Lithium-Ammonia Reduction Method of Methamphetamine Manufacture. *Journal of Forensic Sciences* 2005, 50(1), 1-9.

22. Allen, A.C., Methamphetamine From Ephedrine: I. Chloroephedrines and Aziridines. *Journal of Forensic Sciences* 1987, 32, 953-962.

23. Lee, J.S.; Han, E. Y.; Lee, S. Y.; Kim, E. M.; Park, Y. H.; Lim, M. A.; Chung, H. S.; Park, J. H., Analysis of the impurities in the methamphetamine synthesized by three different methods from ephedrine and pseudoephedrine. *Forensic Science International* 2006, 161(2-3), 209-215.

24. United Nations Office on Drugs and Crime, Recommended methods for the identification and analysis of Amphetamine, Methamphetamine and their Ring-Substituted Analogues in seized materials; 2006.

CHAPTER 4: ESTABLISHMENT OF THE GAS CHROMATOGRAPHIC CONDITIONS AND SAMPLE EXTRACTION

4.0 Introduction

Before chromatographic analysis of any methylamphetamine route specific impurities could be undertaken, an appropriate impurity extraction method and GCMS conditions needed to be devised. The ideal extraction procedure should efficiently extract the maximum number of impurities and the optimum GCMS conditions should produce reproducible chromatograms with well-resolved peaks.

The development of the analytical method for organic impurity profiling was divided into four phases, which, on completion established the most suitable method of analysis of the methylamphetamine samples for the purpose of chemical characterisation.

The phases were as follows:

1. Partial validation of literature derived GCMS conditions
2. Selection of GCMS and extraction conditions for methylamphetamine impurity profiling
3. Study into the effect of sample homogeneity on impurity profile reproducibility
4. Determination of the extract stability

4.1 Partial validation of literatured derived GCMS conditions

In order to evaluate the performance of instrument, partial validation of an existing GCMS protocol was undertaken. Partial validation was undertaken as the samples under study were not quantified and hence some aspects of a normal validation process such as limit of quantification were omitted. The following parameters were investigated: column performance, instrumental precision, repeatability of chromatography and linearity of detector response and are discussed in the following sections.

4.1.1 Experimental Methods

Chemicals used for this project were reagent grade unless stated otherwise. Manufactures were as follows: ethyl acetate and toluene from Fisher Scientific; hexane by Rathburn; methyl decanoate ester, 1-octanol, potassium phosphate monobasic (KH_2PO_4), sodium phosphate dibasic dihydrate ($Na_2HPO_4.2H_2O$) and sodium acetate (CH_3CO_2Na) from Fluka; dicyclohexylamine, 2,6-dimethylaniline, 2,6-dimethylphenol, dodecanoate, eicosane, methyl undecanoate ester, tetracosane and tridecanoate from Sigma Aldrich; glacial acetic acid from Riedel de Haën. Tridecane was decanted from stock within the university and the manufacturer was not available.

Other apparatus used were a Philips PW9421 pH meter, a Fisons Whirlimixer vortex, an American Beauty S/70 sonicatior, an Edmund Buhler Swip KS-10 rotative shaker, and a Jouan centrifuge. Distilled water was obtained from an in house water purification system.

Glassware was washed with Teepol and then rinsed with acetone and dried. Samples prepared for GCMS analysis were transferred to 250 μL silanised microvial inserts (Agilent part no. 5181-8872) inside non-deactivated amber vials (Agilent part no. 5182-0716) with PTFE/silicone septa screw caps (Agilent part no. 5182-0720).

4.1.2 Instrumental Parameters

A GCMS method reported in the literature for quality test of column was selected.[1, 2] Analysis was performed using a Hewlett Packard 6890 gas chromatograph (GC) coupled to a 5973 mass selective detector. The column was a DB-1MS J & W column (25 m length × 0.2 mm inner diameter, 0.33 μm film thickness). The oven temperature was programmed as follows: 60°C for 1 min, 10°C/min to 300°C, and then a hold at 300°C for 1 min. The injector and detector temperatures were set at 260 and 250°C, respectively. Helium was used as the carrier gas at a constant column flow-rate of 0.5 ml/min. Injection of 1 μL of the extract was made in the splitless mode (purge on time; 1.0 min). Hewlett-Packard HP3365 Chemstation software was used for controlling the

GCMS system, data acquisition and integration of the gas chromatograms. Data were acquired at a rate of 20 Hz and a peak width of 0.05 min.

The MS was tuned weekly using the tuning compound heptacosa (PFTBA) and an air and water check was performed daily, column performance was monitored using a Grob mixture in approximately six weekly cycles, and solvent blanks were run between sample injections (unless indicated otherwise). Peaks were integrated using the total ion chromatogram.

4.1.3 Assessment of Column Performance

Two tasks were undertaken to evaluate the column performance: analysis of a suitable analyte mixture and evaluation of peak symmetry within that mixture. A mixture of acids, bases, alcohols, hydrocarbons and neutral compounds was suggested by Grob, et al.[1] as a single test mixture for the evaluation of capillary columns. The purpose of any capillary column test mix is to determine its quality and/ or monitor the performance and deterioration of a column during use. Column efficiency, activity and film thickness are easily evaluated using an appropriately designed test mixture. A comprehensive test was developed by the Grobs, published in 1978.[2]A modified Grob test mixture was prepared for this work using the following components:

1. 1-octanol
2. 2,6-dimethylphenol
3. 2,6-dimethylaniline
4. dodecane, C12
5. tridecane, C13
6. methyl decanoate ester
7. methyl undecanoate ester
8. dicyclohexylamine
9. eicosane, C20
10. tetracosane, C24.

Each compound was weighed (40 mg) into clean 5 mL volumetric flasks and filled to the mark with hexane to give a stock solution concentration of 8 mg/mL. A volume of each stock solution (5 µL) was removed and combined in one 5 mL volumetric flask which was filled to the mark with hexane. This resulted in a Grob mixture of all ten components, each at a concentration of 8 µg/mL as shown in Figure 30. This concentration was used so that, theoretically, a 1 µL injection would result in 8 ng of analyte on the column, as recommended by Grob.

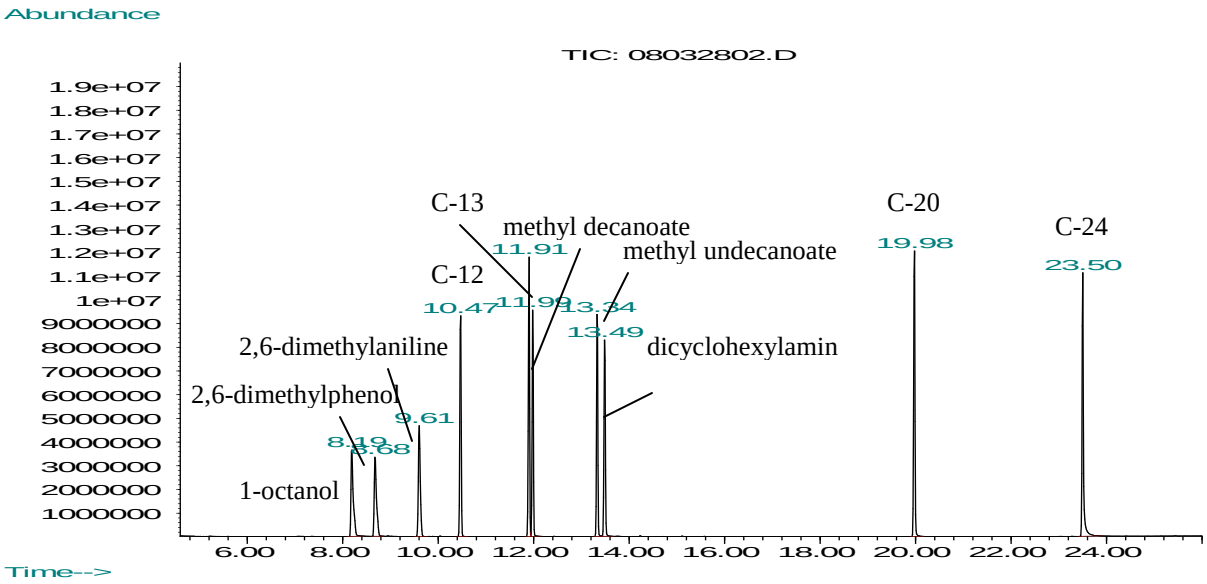

Figure 30: Grob mixture with 0.008 mg/mL.

The 10 peaks are well resolved, including the closely eluting C-13 and methyl decanoate ester, and the methyl undecanoate ester and dicyclohexylamine compounds. Future analysis of the Grob mixture could indicate degradation of the column's stationary phase if the peak heights, shapes or retention times change. Adsorption of acidic compounds could indicate the presence of active silanols in the stationary phase; reduced peak height or poor shape of basic compounds may indicate the presence of exposed silanols.

Peak symmetry can be used as an indication of column efficiency. The asymmetry factor, *A*, can be calculated according to the following equation:

$$A = b/a \qquad \ldots\ldots\ldots\ldots\ldots\ldots \quad \text{Equation 4.1}$$

where *a* and *b* are the left and right halves of the peak width at 10% peak height. Measurements were made by hand for peak symmetry of the Grob mixture components. Results are displayed in Table 13.

Peak	Compound	Asymmetry Factor
1	1-octanol	1.7
2	2,6-dimethylphenol	1.7
3	2,6-dimethylaniline	1.0
4	C-12	1.0
5	methyl decanoate	1.0
6	methyl undecanoate	1.5
7	C-13	0.7
8	dicyclohexylamine	0.6
9	C-20	1.0
10	C-24	1.0

Table 13: Asymmetry factors for the 10 peaks in the Grob mixture.

If *A* is greater than one, the peak is said to be 'tailing'; this occurs when components are strongly retained on the stationary phase and lag behind the main body of the component band. Alcohols are often adsorbed due to hydrogen bonding involving the hydroxyl group with the stationary phase of the column, and this is the most likely reason for the observed asymmetry factor of 1.7 for 1-octanol and 2,6-dimethylphenol. Peak fronting occurs when *A* is less than one, and this is observed when components are retained to a lesser extent and elute before the main body of the component band. Neutral compounds such as the long chain hydrocarbons (alkanes) should have sharp, symmetrical peak shapes. These results indicate that the hydrocarbon peaks are sharp, but the asymmetry factor for C-13 is perhaps due to the limitations of measuring (half widths at 10% peak height) by hand. These results were used as a baseline for comparison of column performance during the project. The Grob mixture was analysed in an approximate six weekly cycle.

4.1.4 Instrumental Precision and Repeatability of Chromatography

Instrumental precision was assessed based on the response for the internal standard eicosane, C20 peak of six injections of one extract (0.008mg/ml). The relative standard deviation of the peak across these six injections was calculated. The RSD value was calculated and found to be 3.96%, a level of instrumental precision acceptable for the intended purpose of the analysis.[3]

Similar to the assessment of instrumental precision, the repeatability of the chromatography was assessed by six replicate injections of one extract of the Grob mixture. Results are displayed in Table 14.

No	Components	RSD(peak area)
1	1-octanol	1.84%
2	2,6-dimethylphenol	1.95%
3	2,6-dimethylaniline	2.01%
4	dodecane, C12	1.88%
5	tridecane, C13	1.63%
6	methyl decanoate ester	1.59%
7	methyl undecanoate ester	1.85%
8	dicyclohexylamine	1.94%
9	eicosane, C20	1.28%
10	tetracosane, C24	0.70%

Table 14: Relative standard deviation of Grob mixture based on 6 separate injections.

4.1.5 Linearity of the Detection Response (by serial dilution)

The objective of this task was to study the linearity of response of the MS as a detector, with respect to an increase in concentration of each of the individual standards. If the MS demonstrated a linear range, this would allow quantification of compounds as well as identification based on both retention time and mass spectra. Table 15 illustrates the correlation coefficient for the calibration curve of each of the 10 compounds within the Grob mixture ranging in concentration from 0.002mg/mL to 0.010 mg/mL.

Serial dilutions of the Grob mixture (0.002 mg/mL, 0.004mg/mL, 0.006mg/mL, 0.008mg/mL, 0.010mg/mL) were prepared from a 0.040 mg/mL stock solution. Each standard was injected 6 times. Graphs of concentration versus average of peak area were plotted for each compound. Table 13 shows the value of correlation coefficients of each of the10 compounds.

	1	2	3	4	5	6	7	8	9	10
R^2	0.9892	0.9994	0.9993	0.9996	0.9996	0.9996	0.9993	0.9995	0.9962	0.9932

Table 15: Correlation coefficient of 10 components in Grob mixture from serial dilution.

4.2 Selection of GCMS and extraction conditions for methylamphetamine impurity profiling

Four aspects were studied. There were:

(i) The examination and comparison of two published GCMS methods for methylamphetamine. In order to determine which of these methods provided the best results for the samples synthesised in this study.

(ii) Optimisation of the impurity extraction method with different pH buffers - For this study, both basic (phosphate buffer, pH 10.5) and acidic (acetate buffer pH 6.0) extractions were used in order to see the full spectrum of impurities. Reproducibility of the extraction method was also investigated.

(iii) Investigation into the effect of varying the mass of methylamphetamine - In this study, 50, 100, and 200 mg of methylamphetamine hydrochloride were used for the extraction of impurities.

(iv) Study of the extraction solvent - Different types of solvent was used in the extraction method, in order to determine the most suitable solvent to facilitate the identification of all the impurities. The solvents investigated for this study were chosen based on those in operational use in forensic science laboratories. These were ethyl acetate, hexane and toluene.

4.2.1 Selection of the GCMS conditions

There are many parameters within a GC system, which must be optimised to determine which the most effective overall method is. These parameters include, choice of injection type, injection volume, inlet temperature, sample preparation, injection speed, column type, temperature program and detection system.[4] In this study, the resolving power of two GCMS impurity profiling methods previously developed by Inoue et al.[5, 6] and Tanaka et al.[7] for methylamphetamine impurity profiling were compared.

The GC system must be optimised for a specific sample type since different analytes and different sample compositions may be more effectively analysed using different operating parameters. Therefore, in order to determine the best system for methylamphetamine profiling, the samples tested must be representative of the type of sample one would expect to see in a 'street' sample. To this end, the samples tested in this particular experimental section were prepared in such a way as to represent a typical methylamphetamine impurity extraction.

4.2.2 Optimisation of impurity extraction with different pH buffers

The extraction method plays a major role in the analysis of the impurities within each sample. Since the extraction of impurities is pH dependent, buffers are used to maintain a specific pH and aqueous buffers were used to dissolve the methylamphetamine sample before extraction into the organic solvent. The buffer is used to maintain a specific pH even when the sample (which may be basic, neutral or acidic) is added thus ensuring reproducible pH values for the extraction. The buffer is selected for its ability to 'push' the impurities of the methylamphetamine sample out of the aqueous phase and into the organic phase.

It is likely that different buffer types will be more suitable for particular sample matrices. That is to say, one buffer may prove better at dissolving the impurities present in a methylamphetamine synthesised via P-2-P than methylamphetamine synthesised via ephedrine or pseudoephedrine since these routes have different target impurities. Other buffers may have difficulty in dissolving bulking agents in samples. The buffer currently

suggested in some operational laboratories is a phosphate salt buffer.[8] However, to determine if this is suitable for the majority of methylamphetamine samples and matrix types, two buffers, a phosphate and an acetate buffer were assessed in this work.

Seized methylamphetamine samples may be slightly acidic, basic or neutral depending on the methods used for production, the amount of active drug present and what impurities and diluents have been introduced. The pH of batches of drug made by the same method may also vary depending on the concentrations of certain impurities present. Therefore, when the sample is dissolved in the buffer, it must be checked and readjusted to the default pH value of the buffer to ensure a reproducible extraction. However, this pH adjustment procedure may not be practical in a busy operational laboratory due to time-constraints.

In addition, the optimum volume of buffer required to dissolve the methylamphetamine must be assessed. Here, a compromise must be reached since while a larger buffer volume would be likely to give a more reproducibly dissolved solution it will also prove more difficult to bring the smaller extraction solvent volume into contact with a larger buffer volume. It is also technically more difficult to remove a smaller extraction solvent volume from a larger surface area of the buffer.

Clandestine laboratories producing methylamphetamine may be using sophisticated methods and purification techniques and clean methylamphetamine samples containing few impurities at very low concentrations are now commonly found. Therefore, any extraction technique developed must be sensitive and selective for impurities in preference to the active drug and matrix diluents.

4.2.2.1 Preparation of buffer solutions

For this study, both basic (phosphate buffer, pH 10.5) and acidic (acetate buffer pH 6.0) extractions were used in order to see the full spectrum of impurities.

The phosphate buffer solution was initially at pH 7 and 0.1 M was prepared by combining 1.360 g of KH_2PO_4 and 1.779 g of $Na_2HPO_4.2H_2O$ in a 100 mL volumetric flask and filling to the mark with distilled water. This solution was made to pH 10.5 by adding 10 % sodium carbonate. [6]

The acetate buffer solution was initially at pH 8 and 0.1 M was prepared by combining 0.820 g of CH_3CO_2Na in a 100 mL volumetric flask and filling to the mark with distilled water. This solution was made to pH 6 by adding few drops of acetic acid. [7]

4.2.3 Investigation into the effect of varying the mass of methylamphetamine

Ideally, the buffer should dissolve a relatively large sample mass in a relatively small volume. This should enable the use of a quantity of methylamphetamine sufficient to allow detection sensitivity for trace level concentrations of impurities. A partially dissolved sample will inevitably have a different profile to that of a completely dissolved sample since selected components in the mixture may preferentially dissolve, leading to a larger relative peak area in a chromatogram when compared to an internal standard.

4.2.3.1 Sample preparation

Varying amounts of homogenised methylamphetamine hydrochloride (50 mg, 100 mg, 200 mg) were placed in a centrifugation tube and dissolved in 2.0 mL of buffer. The mixture was sonicated for 5 minutes and vortexed for 1 minute. 400 μL of extraction solvent containing eicosane, C20 an internal standard (0.05 mg/mL) was added and centrifuged for 5 minutes, and the organic layer transferred to a GC vial insert for analysis.

4.2.4 Study of the extraction solvent

Possibilities for the solvent type and the factors influencing the choice of the solvent type are many and varied. The solvent should be compatible with GCMS analysis and must not cause the sample to degrade. The extraction solvent must not be too volatile since the small extraction volume could evaporate quickly in the mixing process. The solvent must also be completely immiscible with the buffer solution to enable the extract to be removed from the surface of the buffer without taking in any of the aqueous phase.

Perhaps the most important consideration in choosing a suitable extraction solvent is the ability to extract all of the target impurities in as high a concentration as possible. This should be achieved without also extracting high levels of methylamphetamine or diluents ie. the solvent must be selective in extraction. The solvents investigated for this study (ethyl acetate, hexane and toluene), were chosen based on those in operational use in forensic science laboratories.[7]

4.3 Study into the effect of sample homogeneity on impurity profile reproducibility

It was thought that if the sample was sufficiently homogenised, the methylamphetamine and impurities content taken from different areas of the sample would be significantly different and therefore any dissimilarity in profiles would not necessarily be attributable to the extraction method.

Homogenised and unhomogensied batches of methylamphetamine were profiled and the reproducibility of the chromatograms assessed. A batch of methylamphetamine was homogenised with mortar and pestle. Six homogensied and six unhomogenised samples from a single production batch of methylamphetamine were impurity profiled using the established optimum conditions. The RSDs of a number of peaks areas (relative to the internal standard) were calculated.

4.4 Determination of the extract stability

The stability of the impurities in solution is also an important consideration in choosing the most suitable solvent for extraction and profiling. These experiments set out to explore the premise that the concentration of each impurity may alter if the sample is left for a lengthy period in the solvent. Since the impurities are by-products or intermediates in the same reaction, the possibility that species may react together or degrade cannot be overlooked.

Because forensic laboratories often have a high volume of drug cases, several hours or days may elapse between extract preparation and analysis. Therefore, the stability of the impurities in solution is an important consideration. This study investigated the period of time (0, 1, 2, 3 days) and storage temperature (8° C and room temperature) at which the extract remained stable and the impurities were still detectable without any degradation.

4.5 Results and Discussion of Method Validation

4.5.1 GCMS Conditions - System 1

The extraction solvent, mass of methylamphetamine, and pH of the buffer were varied for both GCMS conditions under evaluation. System 1 conditions are as follows: an Agilent 6890 GC and 5973 mass selective detector (MSD) fitted with a non-polar column (DB-1MS); the oven temperature programme started at 50 ºC for 1 min and then increased at 10 ºC/min until 300 ºC, and held for 10 min; the injector and detector (transfer line) temperatures were set at 250 and 300 ºC, respectively; helium was used as a carrier gas at a constant flow rate of 1 mL/min; 1µL of extract was injected in the splitless mode. [5, 6]

Figures 31-33 show the impurity profiles produced at pH 10.5 with the three solvents studied and three different amounts of (50 mg, 100 mg and 200 mg) of methylamphetamine. Ethyl acetate extracted a greater number of impurities than the other two solvents. The main peak at 10 mins is methylamphetamine and the peak at 19.7 mins is the internal standard, eicosane.

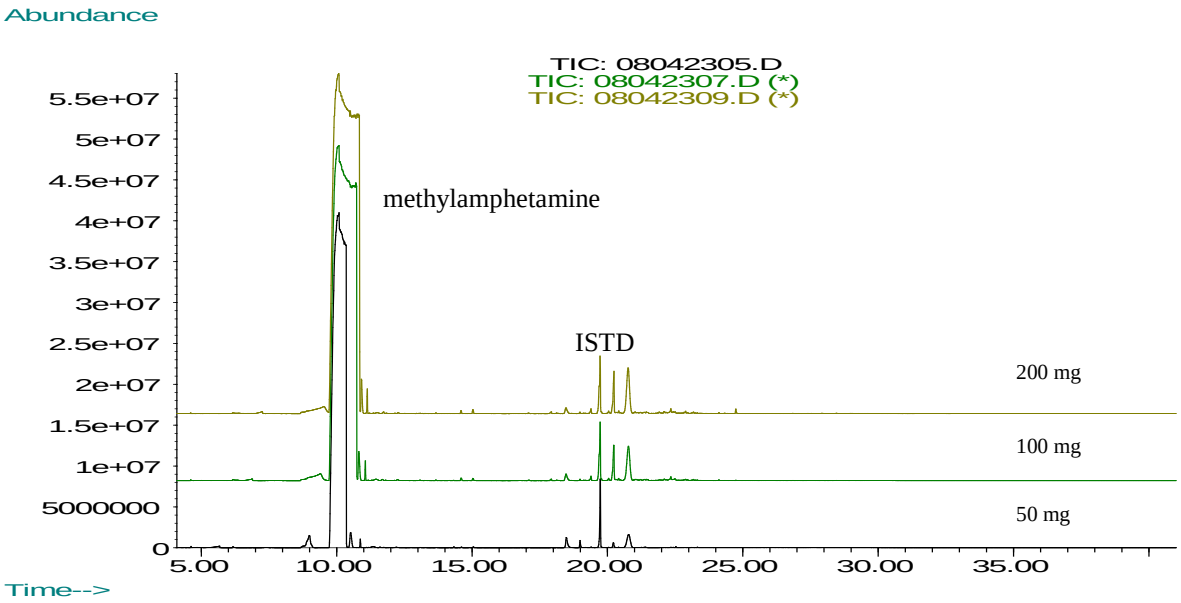

Figure 31: Overlay of profiles from different amounts of methylamphetamine at pH 10.5 with ethyl acetate.

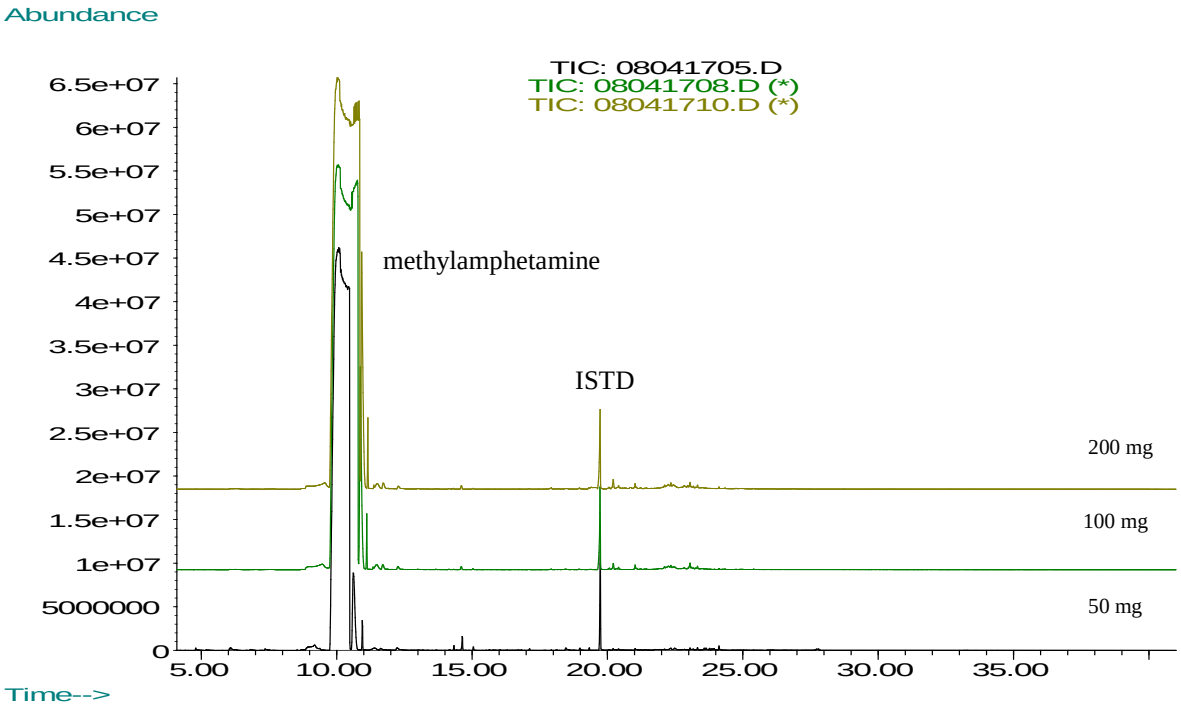

Figure 32: Overlay of profiles from different amounts of methylamphetamine at pH 10.5 with hexane.

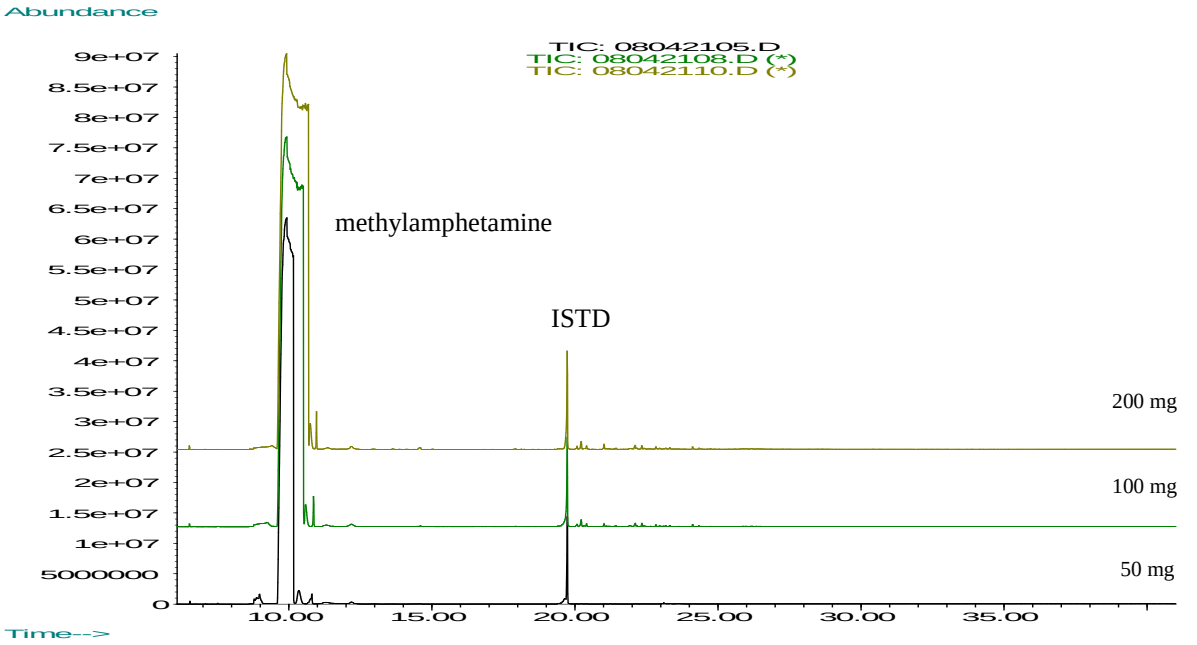

Figure 33: Overlay of profiles from different amounts of methylamphetamine at pH 10.5 with toluene.

Figures 34-36 show the impurity profiles produced at pH 6.0 with of the three solvents and three different amounts of methylamphetamine (50 mg, 100 mg and 200 mg). Acidic extracts of methylamphetamine exhibited peaks at retention times between 8 - 9 minutes.

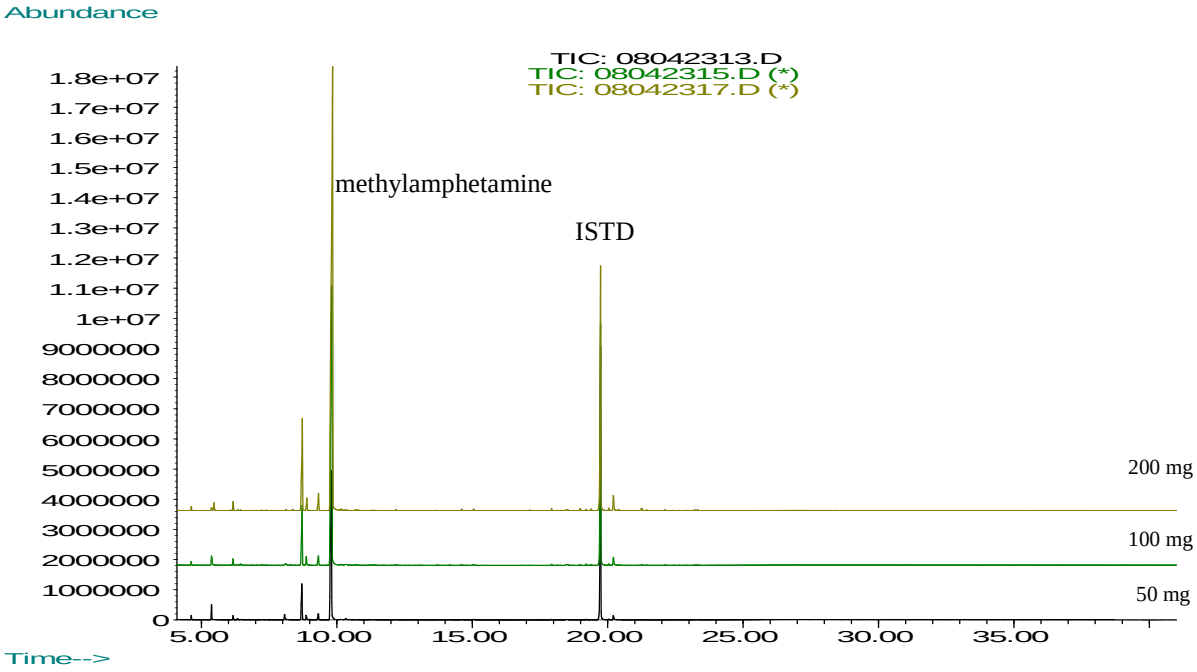

Figure 34: Overlay of profiles from different amounts of methylamphetamine at pH 6 with ethyl acetate.

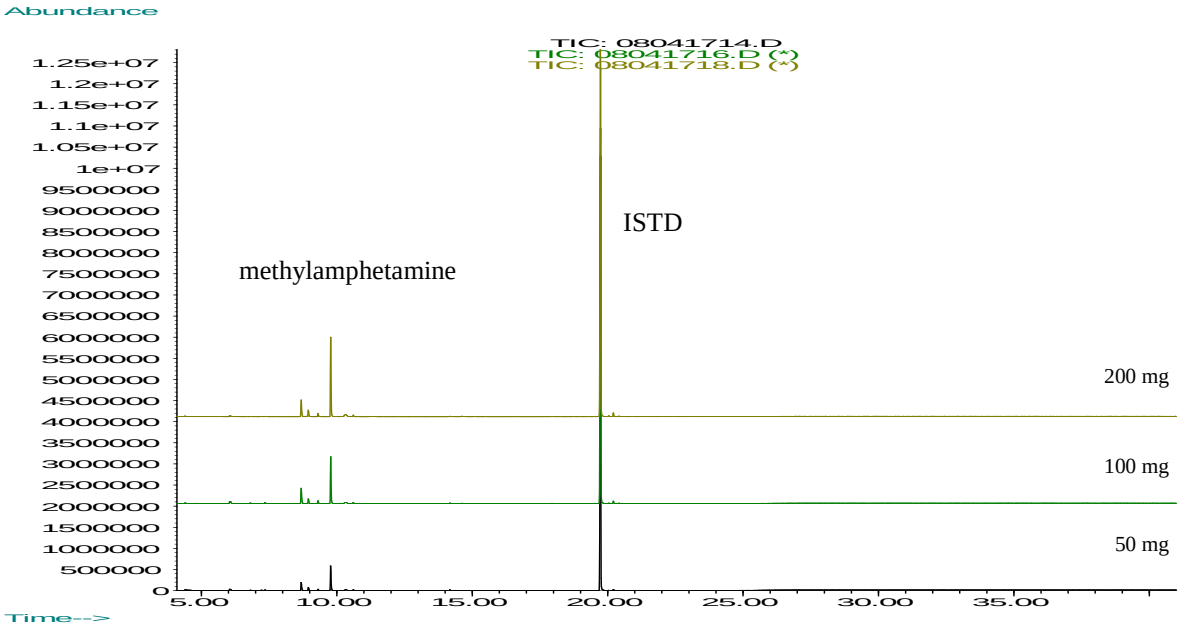

Figure 35: Overlay of profiles from different amounts of methylamphetamine at pH 6 with hexane.

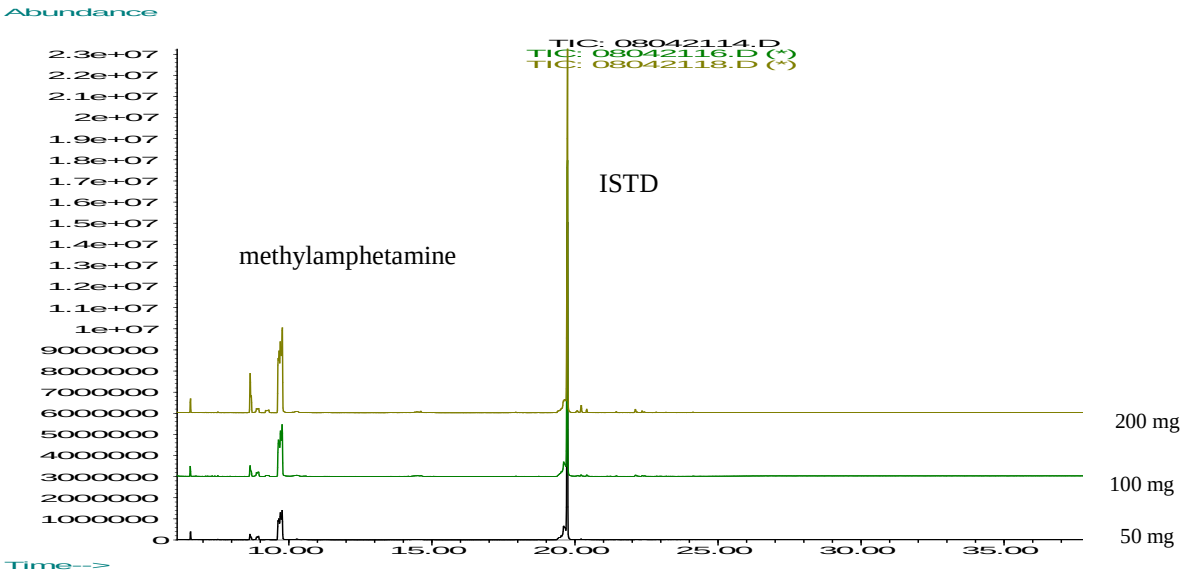

Figure 36: Overlay of profiles from different amounts of methylamphetamine at pH 6 with toluene.

Again these impurities were extracted most efficiently with ethyl acetate where; furthermore, the resolution of these peaks was also better than with hexane and toluene.

The 100 mg methylamphetamine sample was found to produce the best peak shape and the greatest number of detectable impurites with reasonable reproducibility at both pH's (based on the relative standard deviations of a number of peak areas normalised to the

internal standard). The result is displayed in Table 16 and 17. The peaks in tables 16 and 17 below are based on impurities present in the basic and acidic extracts and are different from each other for each extract. The total number of detectable peaks is given in each table.

pH 10.5					
50 mg		100 mg		200 mg	
Peak	RSD Area	Peak	RSD Area	Peak	RSD Area
1	50.49	1	5.30	1	21.57
2	27.90	2	50.64	2	74.75
3	6.40	3	11.28	3	88.63
4	16.83	4	36.00	4	92.13
5	3.65	5	15.63	5	46.04
6	5.98	6	12.89	6	19.94
7	20.13	7	64.05	7	63.11
8	59.63	8	19.17	8	37.45
9	6.34	9	6.43	9	37.44
10	12.84	10	36.17	10	49.13
Avg	21.02	Avg	25.76	Avg	53.02
Total peak number	40	Total peak number	70	Total peak number	75

Table 16: Results used to assess the mass of methylamphetamine for the analysis in ethyl acetate pH 10.5 extract.

pH 6					
50 mg		100 mg		200 mg	
Peak	RSD Area	Peak	RSD Area	Peak	RSD Area
1	22.90	1	37.01	1	18.18
2	14.41	2	9.58	2	11.44
3	35.83	3	41.46	3	20.67
4	34.92	4	14.49	4	4.97
5	13.08	5	18.09	5	16.50
6	27.84	6	30.66	6	4.13
7	0.83	7	10.01	7	2.08
8	8.94	8	7.05	8	5.69
9	33.49	9	38.42	9	27.32
10	16.00	10	29.70	10	38.40
Avg	20.82	Avg	23.65	Avg	14.94
Total peak number	30	Total peak number	50	Total peak number	55

Table 17: Results used to assess the mass of methylamphetamine for the analysis in ethyl acetate pH 6 extract.

In order obtain the full spectrum of impurities in one pH extract from the methylamphetamine samples, a number of further extractions at different pH buffers (pH 7, 8 and 9) were performed. The profiles from different pH extracts are as shown in Figure 37.

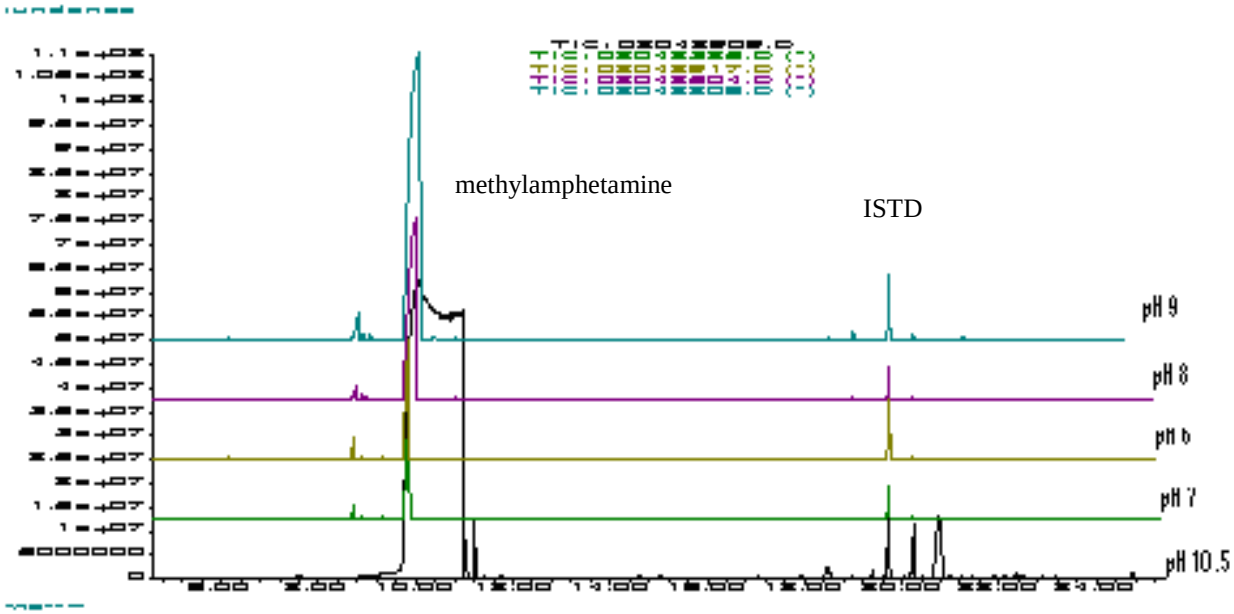

Figure 37: Overlay of profiles from different pH extracts.

It is evident from these profiles that different impurities are extracted depending on the buffer's pH. Therefore, in order to identify route specific impurities in future work, both acidic (pH 6.0) and basic (pH 10.5) extractions were carried out.

4.5.2 GCMS Conditions - System 2

The System 2 conditions differed from System 1 as follows: the oven temperature programme started at 100 ºC for 1 min, increased to 200 ºC at 15 ºC/min, increased to 208 ºC at 2 ºC/min, then increased to 300 ºC at 10 ºC/min and held for 18 min; the injector and detector (transfer line) temperatures were set at 270 and 250 ºC, respectively.[7] The main peak at 4-5 mins is methylamphetamine and the peak at 13.5 mins is the internal standard, eicosane.

Figures 38-40 show the impurity profiles produced at pH 10.5 with of the three solvents investigated and three different amounts of (50 mg, 100 mg and 200 mg) of methylamphetamine.

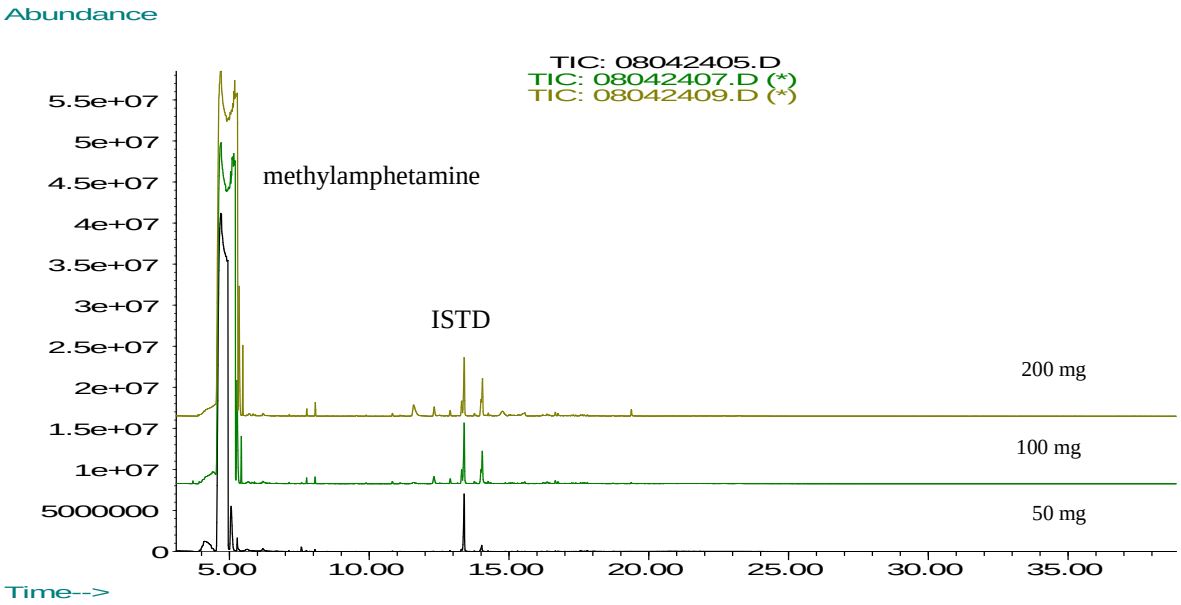

Figure 38: Overlay of profiles from different amounts of methylamphetamine at pH 10.5 with ethyl acetate.

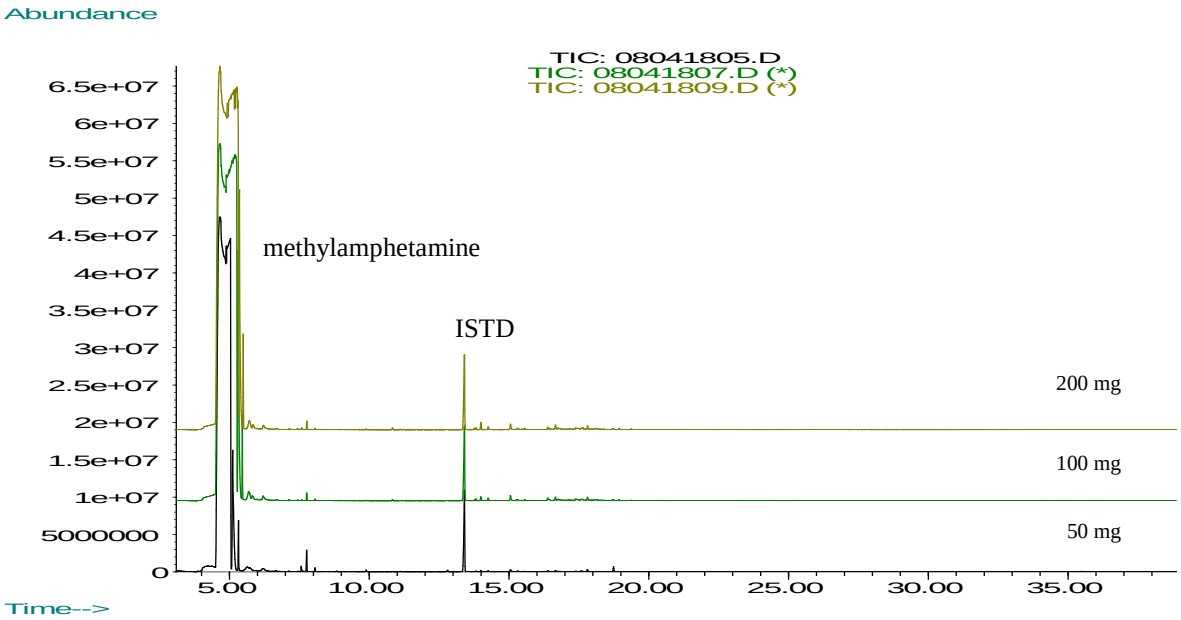

Figure 39: Overlay of profiles from different amounts of methylamphetamine at pH 10.5 with hexane.

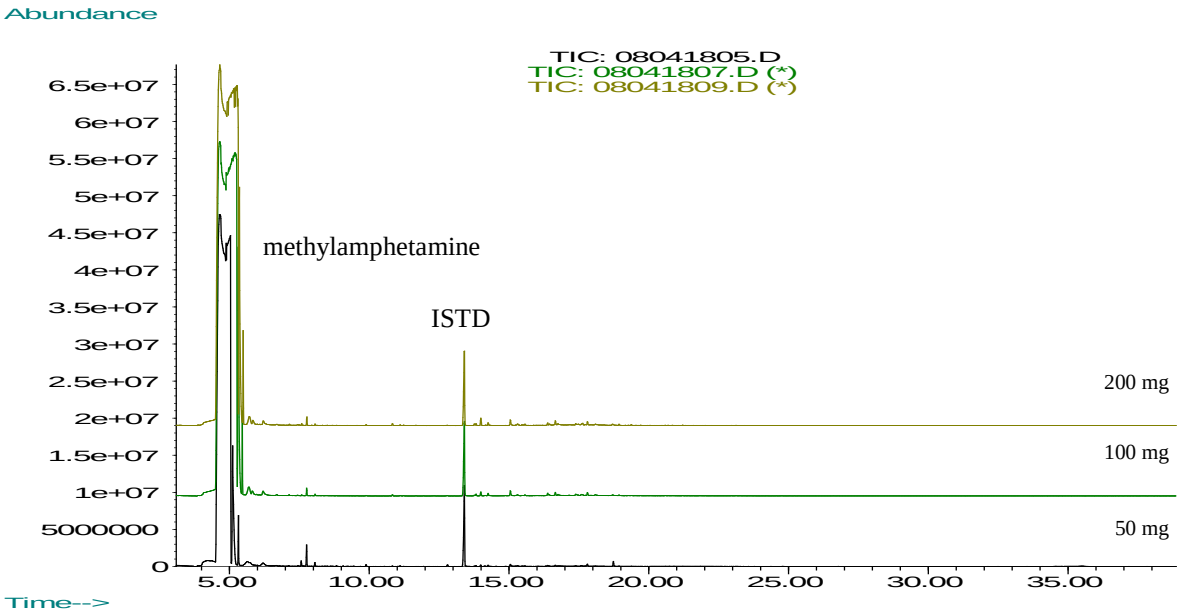

Figure 40: Overlay of profiles from different amounts of methylamphetamine at pH 10.5 with toluene.

Ethyl acetate extracted more impurities at retention time 11 – 14 minutes than the other two solvents. The 200 mg sample provided the best reproducibility, although this was not as effective as that achieved with the System 1 conditions (100 mg, ethyl acetate).

Figures 41-43 show the impurity profiles produced at pH 6.0 with the three solvents and different amounts of (50 mg, 100 mg and 200 mg) of methylamphetamine.

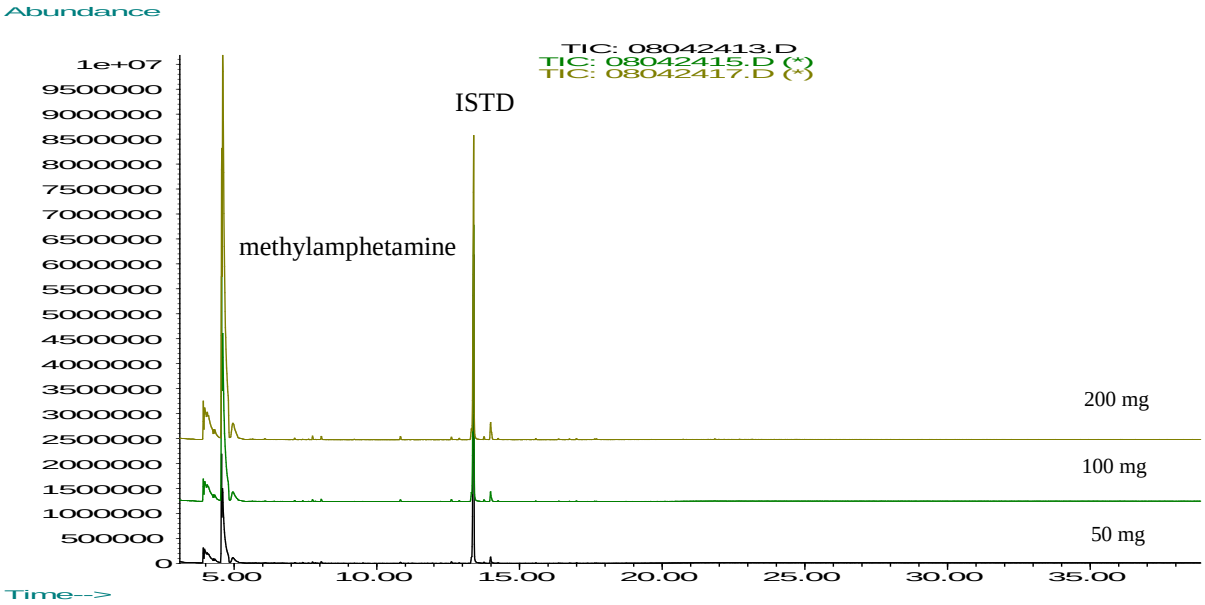

Figure 41: Overlay of profiles from different amounts of methylamphetamine at pH 6 with ethyl acetate.

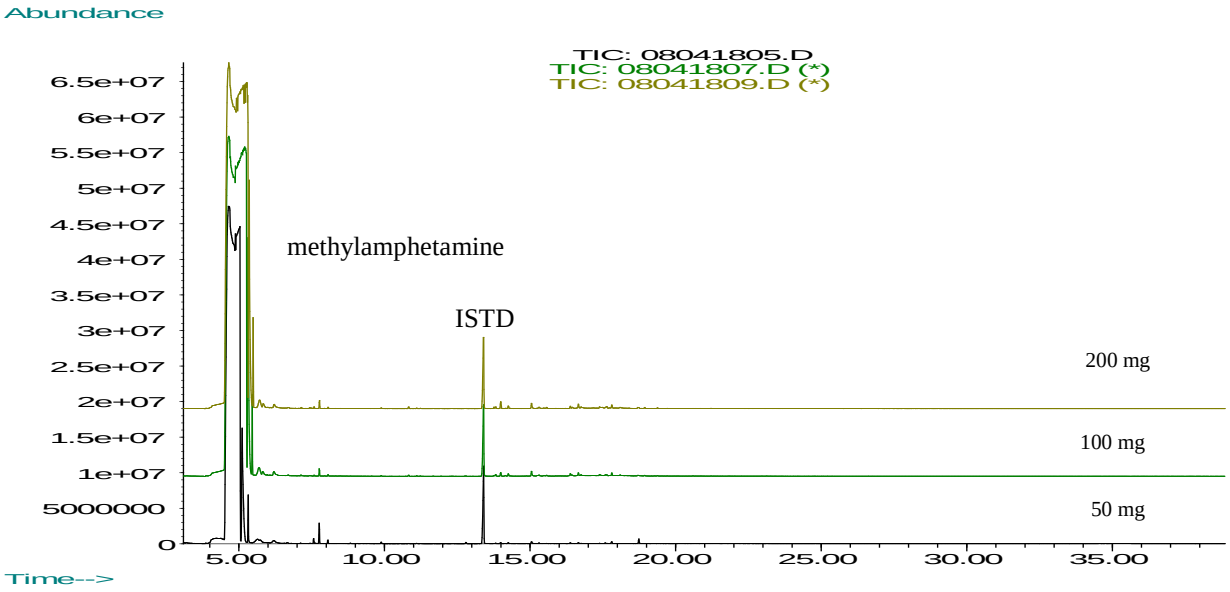

Figure 42: Overlay of profiles from different amounts of methylamphetamine at pH 6 with hexane.

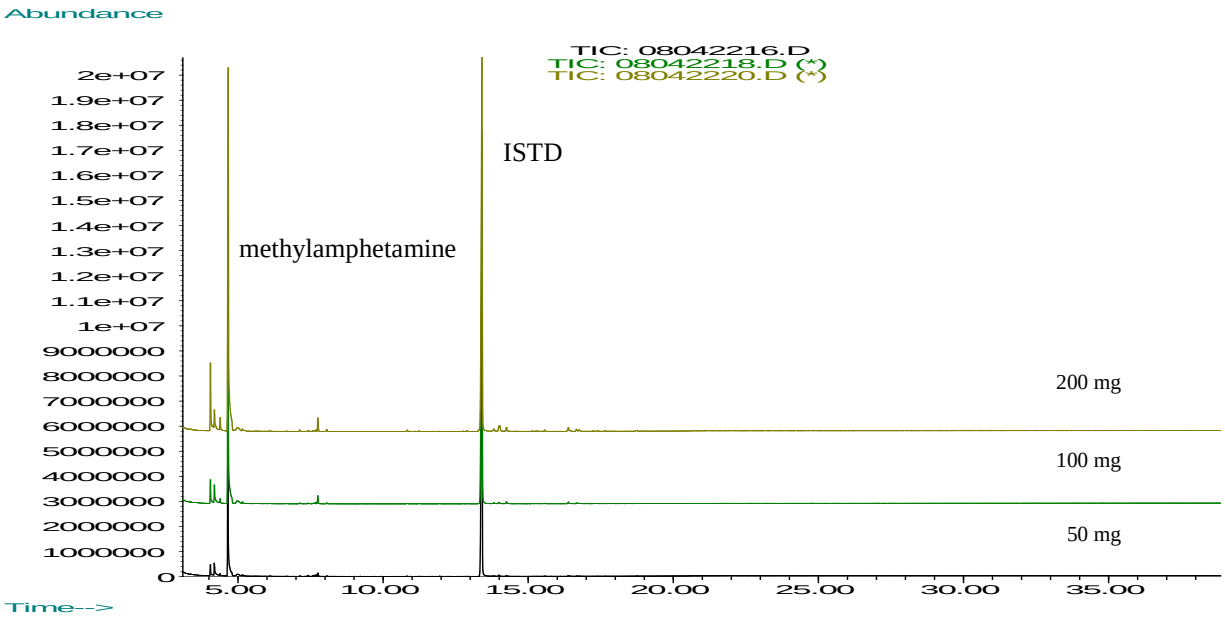

Figure 43: Overlay of profiles from different amounts of methylamphetamine at pH 6 with toluene.

With the pH 6.0 buffer the early eluting peaks (retention time 4 – 5 minutes) were not well resolved with any solvent due to the initial high oven temperature.

100 mg was chosen as a sample size despite having RSDs which were slightly worse than those of the 50 mg sample because it produced impurity profiles of greater intensity and good well resolved peaks. The RSD values obtained were in line with previously published data for similar extractions of ATS.[9]

Overall, System 1 GCMS conditions used with ethyl acetate and 100 mg of sample provided the optimum profiling conditions. Consequently, these conditions were used for the homogeneity and stability studies.

4.6 Reproducibility of the Extraction Analytical Method

4.6.1 Within Day Reproducibility

The within day reproducibility of the analysis was assessed by preparing in parallel six extractions of a homogenised batch of methylamphetamine hydrochloride. Six separate extractions were prepared from six different sub samples of 100 mg each. Extractions and analysis were undertaken on the same day. This study was performed using 10 normalised impurity peaks in a homogenised batch of methylamphetamine. The result is displayed in Table 18.

pH 10.5		pH 6.0	
Peak	RSD Area	Peak	RSD Area
1	17.9	1	6.0
2	26.4	2	3.7
3	28.7	3	11.0
4	44.4	4	13.2
5	24.4	5	18.1
6	14.0	6	8.7
7	74.1	7	5.8
8	17.6	8	8.2
9	6.9	9	17.9
10	11.0	10	9.1
Avg	26.5	Avg	10.2

Table 18: Results of the within day reproducibility of the analysis study.

The within day reproducibility of the analysis takes into account both the instrumental precision and the variability in the extraction process. It is noted that RSDs for peaks 1-8 and 10 decreases in the pH 6 extract. It may be that certain impurities are so strongly basic or acidic that they are not efficiently and consistently extracted; thus, inconsistent levels of these impurities may be observed from extract to extract in both buffers. However the RSDs determined are in line with the published literature for similar samples.[10]

4.6.2 Reproducibility of the Analysis Over Time

Because environmental conditions such as temperature and humidity can affect the extraction process, a study was carried out to assess the reproducibility of the analysis over time or 'between days'. For this study, one extract from one homogenised batch of methylamphetamine was prepared and analysed on four consecutive days. Peak area RSDs were calculated for normalised impurity peaks across the four days. The results are given in Table 19. A decrease in the average peak area RSD for pH 10.5 and slight increase in the average peak area for RSD for pH 6 when compared to the within day study .

pH 10.5		pH 6.0	
Peak	RSD Area	Peak	RSD Area
1	11.2	1	6.0
2	16.7	2	5.7
3	10.9	3	3.3
4	26.5	4	30.8
5	6.0	5	14.5
6	24.3	6	23.4
7	23.5	7	9.6
8	28.5	8	8.0
9	2.2	9	3.2
10	13.1	10	16.5
Avg	16.3	Avg	12.1

Table 19: Results used to assess the reproducibility of the analysis over time.

4.6.3 Extract stability

The stability of the extract over four days was assessed by preparing one extract from one homogenised batch of methylamphetamine which was analysed at day 0, day 1, day 2 and day 3 (day 0 indicates the day in which the sample was prepared).

This extract was stored at room temperature in the dark. Peak areas for selected components were plotted against time. The results are displayed in Figure 44.

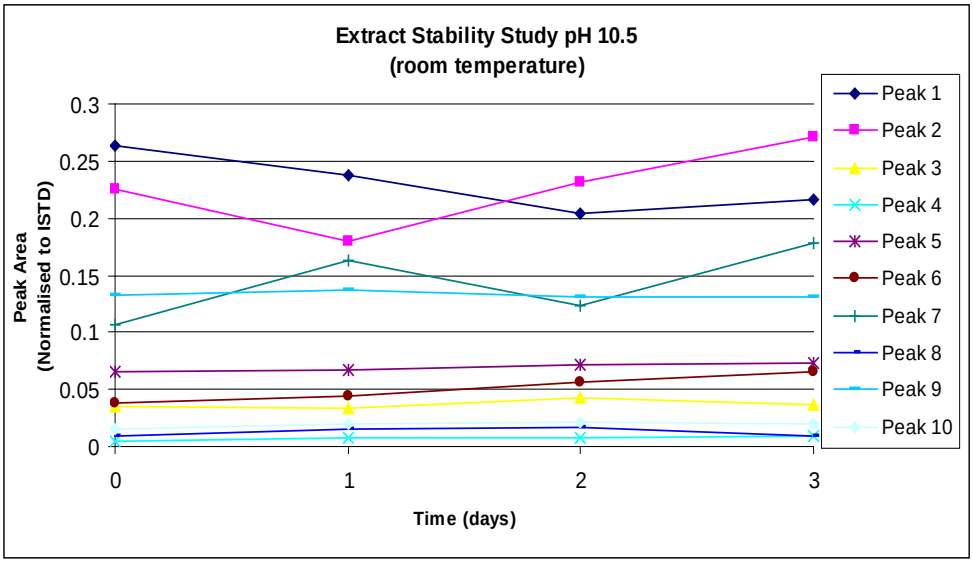

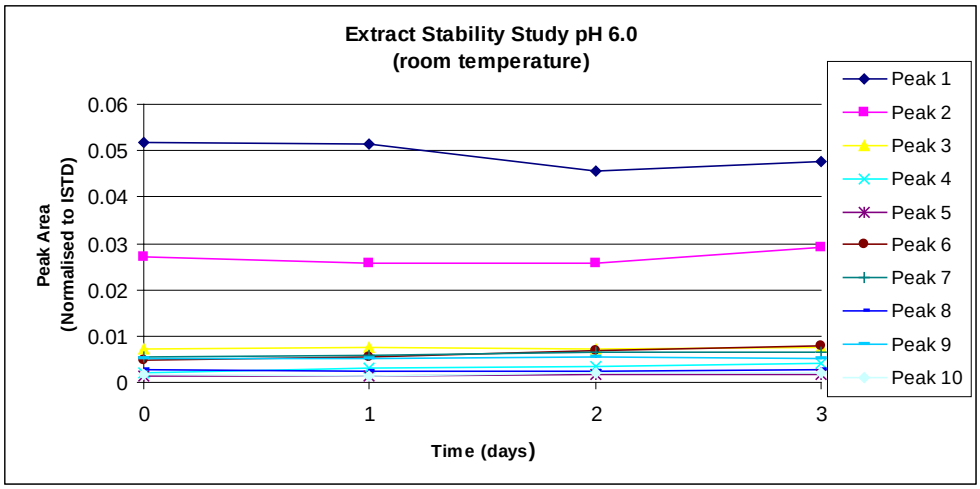

Figure 44: Methylamphetamine extract stability (pH 10.5 and pH 6) over three days at room temperature.

It can be seen from examination of the graphs in Figure 46 that the concentrations of the selected components change relative to each other even after one day. For example, peaks 1, 2 and 7 in the pH 10.5 extract changes dramatically between days. Similar changes in concentration can be observed for peaks 1 and 2 in the pH 6 extract.

This study was repeated where the extract was stored at 8°C rather than room temperature. The results are displayed in Figure 45. These graphs illustrate that, like the

room temperature results, components change in concentration relative to one another after one day in both pH 10.5 and pH 6 extracts. This indicates that storage at 8°C does not increase extract stability over one day. As a result of these studies, it was decided that extracts would be freshly prepared and analysed within one day.

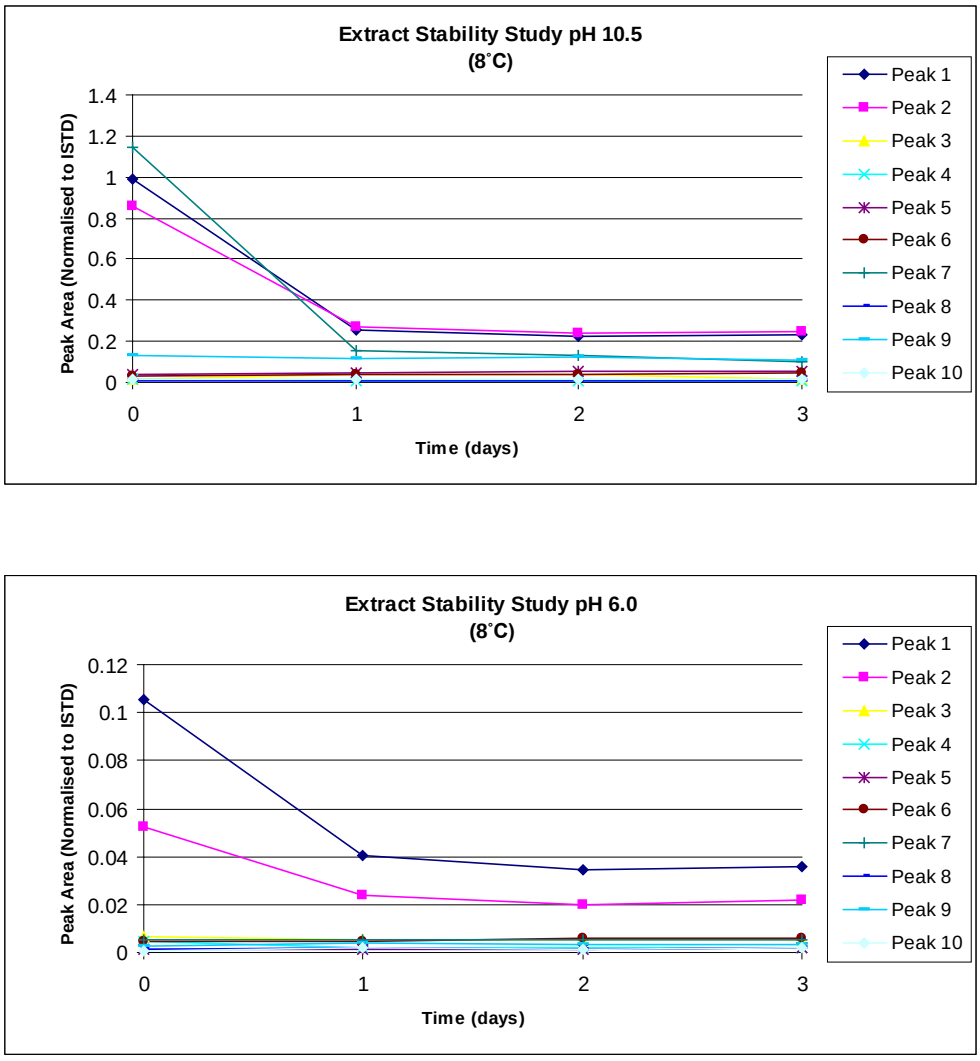

Figure 45: Methylamphetamine extract stability (pH 10.5 and pH 6) over three days when stored at 8˚C.

4.6.4 Homogeneity of Samples

Evaluation of the RSDs of the normalised peak areas indicated that the homogenised methylamphetamine gave more reproducible results across a wider range of impurities than unhomogenised samples as illustrated in Table 20.

The peak area RSDs for the extracts from the unhomogenised methylamphetamine average 57.0% and 26.4% respectively, while the average RSDs for the extracts from the homogenised methylamphetamine average 26.5% and 10.2%. The lower value is, of course, more acceptable, and as such all synthesised methylamphetamine was homogenised before extraction in order to obtain better precision. It is noted that the RSDs for peaks 7, 8 and 10 increased for the pH 10.5 extraction when the sample was homogenised, and this cannot be explained.

unhomogenised methylamphetamine				homogenised methylamphetamine			
pH 10.5		pH 6.0		pH 10.5		pH 6.0	
Peak	RSD Area	Peak	RSD Area	Peak	RSD Area	Peak	RSD Area
1	68.5	1	37.2	1	17.9	1	6.0
2	76.6	2	21.5	2	26.4	2	3.7
3	140.3	3	14.1	3	28.7	3	11.0
4	138.1	4	30.2	4	44.4	4	13.2
5	59.5	5	19.5	5	24.4	5	18.1
6	20.9	6	15.2	6	14.0	6	8.7
7	34.3	7	16.0	7	74.1	7	5.8
8	15.6	8	43.5	8	17.6	8	8.2
9	9.8	9	37.0	9	6.9	9	17.9
10	6.0	10	29.7	10	11.0	10	9.1
Avg	57.0	Avg	26.4	Avg	26.5	Avg	10.2

Table 20: Results of homogeneity study comparing RSDs of extracts from unhomogenised and homogenised synthesised methylamphetamine.

4.7 Conclusions

The GCMS system 1 was chosen as the most suitable analytical system for the analysis of methylamphetamine hydrochloride extracts. The following conditions were used with a non-polar column (DB-1MS); the oven temperature programme started at 50 ºC for 1 min and then increased at 10 ºC/min until 300 ºC, where it held for 10 min; the injector and detector (transfer line) temperatures were set at 250 and 300 ºC, respectively; helium was used as a carrier gas at a constant flow rate of 1 mL/min; 1µL of extract was injected in the splitless mode.

In order to obtain the full spectrum of impurities from the samples, both basic and acidic buffers was used in the identification of these route specific impurities. Ethyl acetate as a extraction solvent and 100 mg of sample provided the optimum profiling conditions.

All samples required homogenisation before analysis, and the extracts required to be analysed within 24 hours of extraction.

4.8 References

1. Grob Jr, K.; Grob, K., Evalluation of Capillary Columns by Separation Number of Plate Number. *Journal of Chromatography A* 1981, 207, 291-297.

2. Grob Jr, K.; Grob, G.; Grob, K., Comprehensive, Standardized Quality Test for Glass Capillary Columns. *Journal of Chromatography A* 1978, 156, 1-20.

3. Gonza´lez, A.G.; Herrador, M.A., A practical guide to analytical method validation, including measurement uncertainty and accuracy profiles. *Trends in Analytical Chemistry* 2007, 26(3), 227-238.

4. Ballany, J.; Caddy, B.; Cole, M.; Finnon, Y.; Aalberg, L.; Janhunen, K.; Sippola, E.; Andersson, K.; Bertler, C.; Dahle´n, J.; Kopp, I.; Dujourdy, L.; Lock, E.; Margot, P.; Huizer, H.; Poortman, A.; Kaa, E.; Lopes, A., Development of a harmonised pan-European method for the profiling of amphetamines. *Science and Justice* 2001, 41(3),193-196.

5. Inoue, T.; Tanaka, K.; Ohmori, T.; Togawa, Y.; Seta, S., Impurity profiling analysis of methamphetamine seized in Japan. *Forensic Science International* 1994, 69(1), 97-102.

6. Inoue, H.; Kanamori, T.; Iwata, Y.T.; Ohmae, Y.; Tsujikawa, K.; Saitoh, S.; Kishi, T., Methamphetamine impurity profiling using a 0.32 mm i.d. nonpolar capillary column. *Forensic Science International* 2003, 135(1), 42-47.

7. Tanaka, K.; Ohmort, T.; Inonue, T.; Seta, S., Impurity Profiling Analysis of Illicit Methamphetamine by Capillary Gas Chromatography. *Journal of Forensic Sciences* 1994, 39(2), 500-511.

8. Remberg, B. and A.H. Stead. Drug characterization/impurity profiling, with special focus on methamphetamine: recent work of the United Nations International Drug Control Programme. *Bulletin on Narcotics 1999 (Volume LI Nos. 1 and 2),* Available at http://www.unodc.org/unodc/en/data-and-analysis/bulletin/bulletin_1999-01-01_1_page008.html.
   Last accessed on 12/12/09.

9. Aalberg, L.; Andersson, K.; Bertler, C.; Cole, M.D.; Finnon, Y.; Huizer, H.; Jalava, K.; Kaa, E.; Lock, E.; Lopes, A.; Poortman, A.; Sippola, E.; Dahle´n, J.Aalberg, L., Development of a harmonised method for the profiling of amphetamines II. Stability of impurities in organic solvents. *Forensic Science International* 2005, 149**,** 231–241.

10. Lock, E.; Aalberg, L.; Andersson, K.; Dahle'n, J.; Cole, M.D.; Finnon, Y.; Huizer, H.; Jalava, K.; Kaa, E.; Lopes, A.; Poortman, A.; Sippola, Erkki L., Development of a harmonised method for the profiling of amphetamines V : Determination of the variability of the optimised method. *Forensic Science International* 2007, 169, 77–85.

CHAPTER 5: ANALYSIS AND IMPURITY PROFILING OF THE SYNTHESISED METHYLAMPHETAMINE SAMPLES USING GCMS

5.0 Introduction

The samples synthesised during the course of this work were extracted and analysed by GCMS using the methods developed and detailed in Chapter 4 in order to generate impurity profiles for subsequent data analysis. The final extraction and analytical methods used are described in Sections 4.2.2.1 and 4.7 respectively.

5.1 Batch Variations

When a drug is manufactured, separate and discrete "batches" of materials are usually prepared at any one time. Because production conditions may not be reproduced exactly each time, variations will occur in the impurity content of the final products from the same source, i.e., different batches from the same clandestine operator or "laboratory" will have different chemical characteristics (so-called inter-batch variation). In addition, because illicit products are usually non-homogenous, differences in impurity content may also be seen across a single batch of drug (so-called intra-batch variation). Under normal circumstances, it is reasonable to assume that inter-batch variations will be greater than intra-batch variations.

Successful classification of samples is thus only possible if sufficient information is generated by the analytical methods employed and if the variation in chemical composition observed between different batches is greater than that within the same batch. This study used gas chromatography to give a representation of the 'chemical signature' of each sample to determine the extent of inter and intra batch variation in the resultant chemical profile. Experiments were designed to determine how the method of production (seven routes) affected the 'chemical signature'.

The statistical analysis of the resultant data is also of importance. While the resultant chromatograms can be visually examined, the use of statistical analysis (in this case using the Pearson correlation coefficient matrix) can facilitate the robust categorisation of the samples on the basis of their chromatographic profiles.

5.1.1 Intra-batch variation

The clandestine preparation of methylamphetamine tends to be small scale. In such cases the production batches themselves together with the inherent intra-batch variations are relatively small, such that in most cases there is little difference in impurity content across a single batch of drug.[1] Samples from a single synthetic batch may theoretically be linked relatively easily.

5.1.2 Inter-batch variation

Inter-batch variations may occur, as each synthetic run may be slightly different from the next. Differences in reaction time and temperature, reactant quality etc can all cause slight variations in the impurity profiles of the final product. If the same synthetic route is used in each batch production, it would be expected that different batches of the drug may still be linked by their impurity profiles. Practical experience has confirmed that samples produced by an established method, though in different batches, in the same illicit laboratory may be linked by their impurity profiles.[1, 2]

5.2 Experimental methods

Intra-batch variation

One batch from each synthetic route (Leuckart method, Reductive Amination method, Nagai method, Rosenmund method, Birch method, Emde method and Moscow method) was separated into 6 sub batches. Each of these was extracted and analysed to examine both the extraction variation and the intra batch variation associated with each route according to the procedure previously described in Chapter 4. For GCMS analysis, 146 out of 149 batches of synthesised samples were analysed.

To assess the variation of the selected target impurities within a synthetic batch, the RSD of each impurity was calculated using the 6 sub batches. The peak areas were first normalised to the internal standard before the RSDs were calculated. The peak area RSDs for the target impurities present in each synthetic routes are reported in the next section.

Inter-batch variation

Forty-one batches of methylamphetamine hydrochloride were synthesised by the Leuckart (21 batches) and Reductive Amination (20 batches) methods using the same starting material, 1-phenyl-2-propanone (P-2-P). One hundred and five batches of methylamphetamine hydrochloride were synthesised by the Nagai (20 batches), Rosenmund (20 batches), Birch (20 batches), Emde (20 batches) and Moscow (25 batches) methods using either ephedrine or *pseuod*ephedrine as starting material. Each sample was extracted and analysed to examine both the extraction variation and the inter batch variation associated with each synthetic route according to the procedure previously described in Chapter 4.

To assess the variation of the selected target impurities for each synthetic route, the RSD of each impurity was calculated from each batch. The peak areas were first normalised to the to the sum of the targets impurities before the RSDs were calculated.

5.3 Results and Discussion

For this study, both basic (phosphate buffer, pH 10.5) and acidic (acetate buffer, pH 6.0) extractions were used in order to see the full spectrum of impurities. Both basic and acidic impurities were extracted separately and analysed by GCMS as detailed previously. Due to the satisfactory RSDs for the instrumental repeatability (as detailed in Chapter 4), each impurity extract was injected once, and a solvent blank was analysed before every sample. The impurity profiles for each synthetic route are displayed in following section. The major ions for impurities present in both extracts for all seven synthetic routes are tabulated with the peak m/z ions (bold m/z is the base peak of the compound). The identity of the compounds was confirmed based on matches identified by the NIST library and published literature for the same compound. The main peak at 10 mins is methylamphetamine and peak at 19.7 mins is the internal standard, eicosane in each chromatogram presented. A table of the molecular weight for each compound is presented in Appendix B.

5.3.1 Intra batch variation

Six sub samples of one single batch from each synthetic route were extracted at each pH. The extracts were analysed on GCMS and the resultant chromatographic profiles examined. An example of the chromatographic profiles are given for the Leuckart synthesis in Figure 46 and Figure 47.

In each case (i.e for each synthetic route) very little difference was observed between the chromatographic responses for each batch of six sub samples. A full set of the relevant chromatograms (Reductive Amination, Nagai, Rosenmund, Birch, Emde and Moscow) is presented in Appendix C.

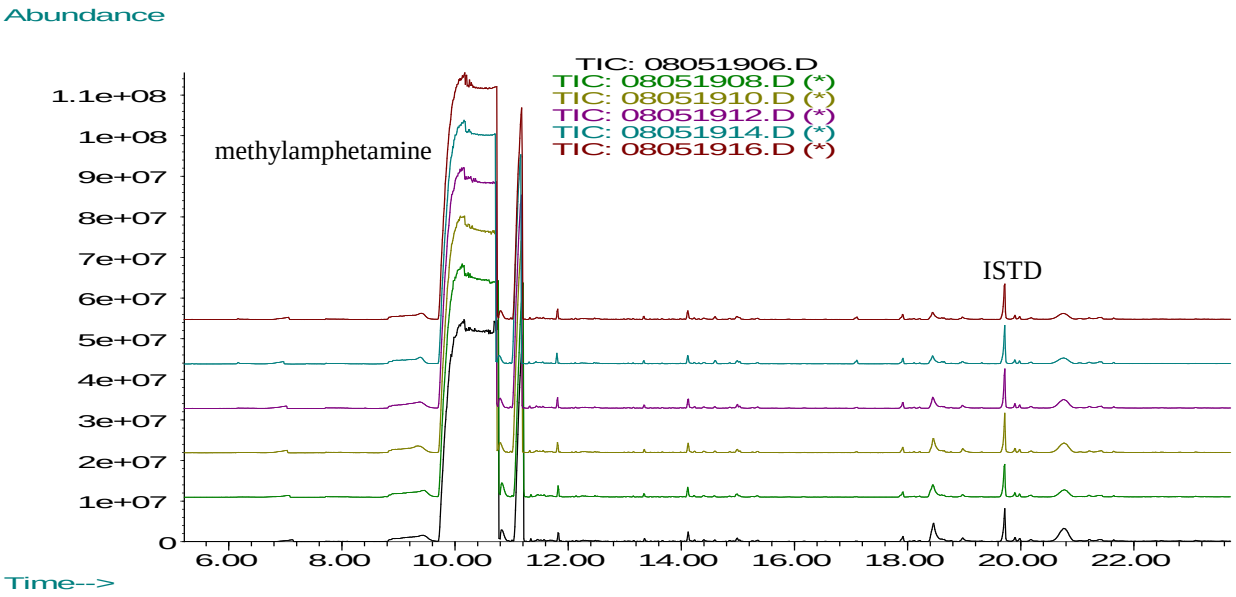

Figure 46: Overlay of the impurity profiles from the six extracts of a Leuckart synthesised sample at pH 10.5.

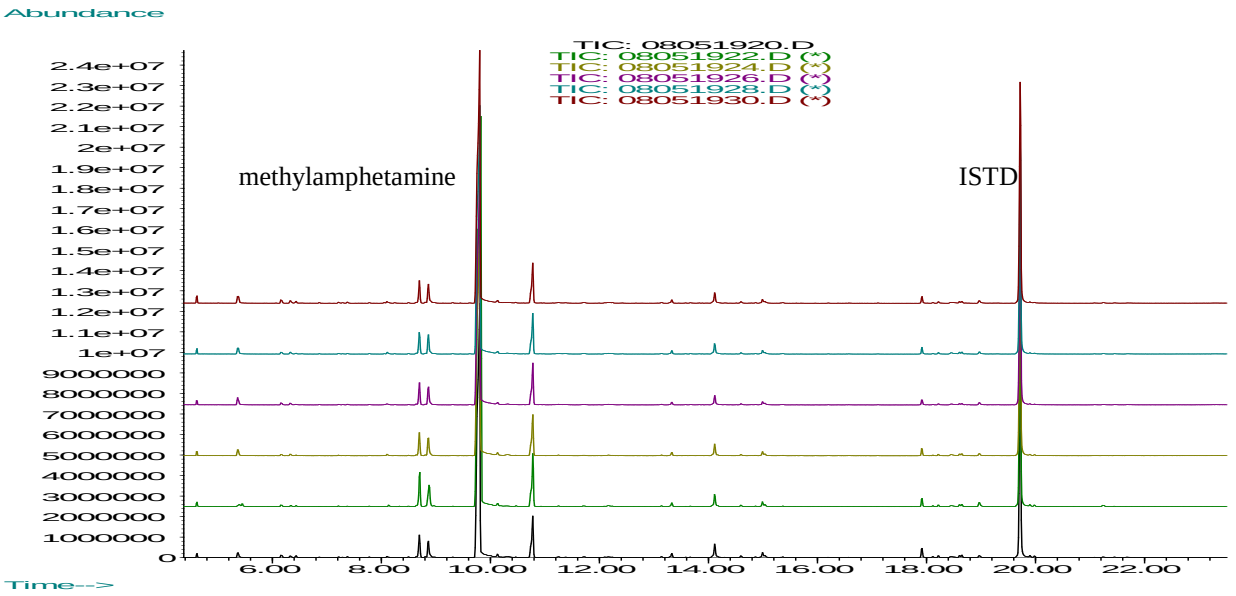

Figure 47: Overlay of the impurity profiles from the six extracts from a Leuckart synthesised sample at pH 6.

5.3.2 Inter-batch variation

5.3.2.1 Leuckart Method

In total, 21 independent samples of methylamphetamine hydrochloride were synthesised using the Leuckart method as previously described in Chapter 3. Each of these samples were extracted using both acidic and basic buffers and analysed.

Table 21 shows impurities from the phosphate buffer extract (basic).

No	RT	Compound	Peak m/z
1	6.949	Acetic acid	**43**, 60, 91, 134
2	9.187	Amphetamine	**44**, 91, 65, 134
3	10.797	*N*-(1-Methyl-2-phenylethylidene) methenamine	**56**, 91, 65, 39, 77
4	11.048	Dimethylamphetamine (DMA)	**72**, 91, 56, 42
5	13.663	*N*-formylamphetamine	**118**, 72, 44, 91
6	14.321	Bibenzyl	**91**, 182
7	14.593	*N*-formylmethylamphetamine	**86**, 58, 118
8	15.032	*N*-acetylmethylamphetamine	**58**, 100
9	16.286	Dibenzylketone	**91**, 65, 119, 39, 51, 210
10	17.920	*cis* 3,4-Diphenyl-3-buten-2-one	**179**, 178, 222, 221
11	18.05	α-benzyl-N-methylphenethylamine	**134,** 91, 42, 119, 65, 135, 58, 86, 77, 105
12	18.127	Benzylmethylamphetamine	**91**, 148, 65, 105
13	18.569	*N*-β-(phenylisopropyl) benzyl methyl ketimine	**91**, 160, 119, 65, 77, 207
14	18.224	*trans* 3,4-Diphenyl-3-buten-2-one	**179**, 178, 222, 221
15	18.608, 18.650	α,α-dimethyldiphenethylamine	**91**, 162, 119, 65, 44
16	18.827	*N*-methyldiphenethylamine	**148**, 91, 65, 119, 105, 44, 77
17	19.897, 19.981	*N*,α,α-trimethyldiphenethylamine	**176**, 91, 58, 119
18	20.19	*N*-benzoylamphetamine	**105**, 77, 148, 91, 118
19	20.417	*N*-benzoylmethylamphetamine	**105**, 162, 77, 91
20	21.075	2,6-Dimethyl-3,5-diphenylpyridine	**259**, 258, 91, 188, 186
21	21.212	Pyridine 7 and 14	**258**, 186, 91, 259
22	22.331	*N*,*N*-di-(β-phenylisopropyl) formamide	**190**, 91,58, 119, 77, 105
23	23.252	*N*-methyl-*N*-(1-methyl-2-phenylethyl)-2-phenylacetamide	**58**, 91, 219, 176

Table 21: List of impurities found in pH 10.5 extract.

Table 22 shows impurities from the acetate buffer extract (acidic)

No	RT	Compound	Peak m/z
1	8.705	1-phenyl-2-propanone	**43**, 91, 134
2	8.872	Amphetamine	**44**, 91, 134
3	9.312	1-phenyl-1,2-propanedione	**105**, 77, 51, 43
4	10.274	*N*-*N*-Dimethylbenzylamine	**58**, 135, 107,79
5	10.786	Dimethylamphetamine (DMA)	**72**, 91, 56,42
6	13.672	*N*-formylamphetamine	**118**, 72, 44, 91
7	14.603	*N*-formylmethylamphetamine	**86**, 58, 97, 118
8	15.052	*N*-acetylmethylamphetamine	**58**, 100
9	18.608, 18.66	α,α-dimethyldiphenethylamine	**91**, 162, 119, 65, 44

Table 22: List of impurities found in pH 6.0 extract.

Using both basic and acidic extracts, it was possible to identify two Leuckart route specific impurities in the samples (Figure 48). These were *α, α* -dimethyldiphenethylamine and *N*- *α, α* -trimethyldiphenethylamine and both isomers of each were present in the pH 10.5 extract.

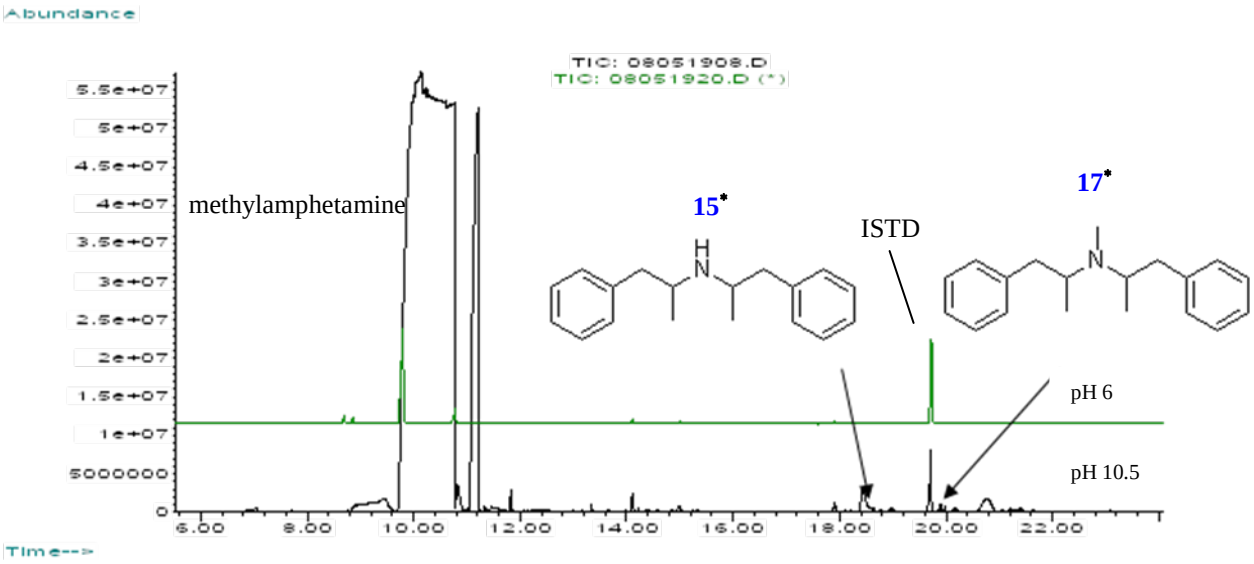

Figure 48: Overlay of the impurity profiles for both extracts. * refer to Table 21

The chromatographic results for each of the 21 batches synthesised via the Leuckart method are presented in Figure 49 - Figure 52. Visual comparison of the impurity profiles show some obvious variation between the 21 profiles, particularly within the 18-21 minute range in pH 10.5 extraction (Figure 50). In all cases the route specific impurities were identified.

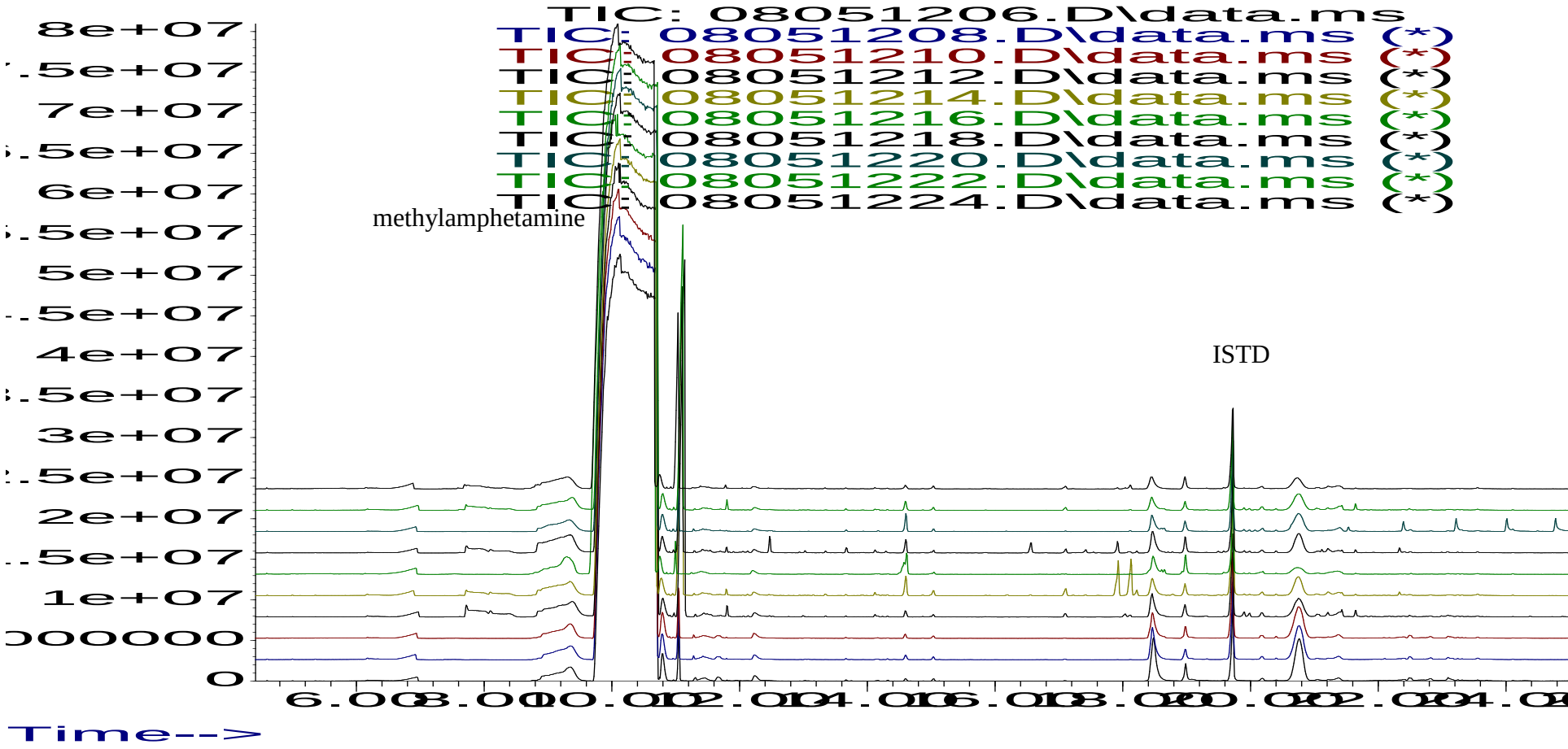

Figure 49: Overlay of the impurity profiles from the first ten batches extract at pH 10.5.

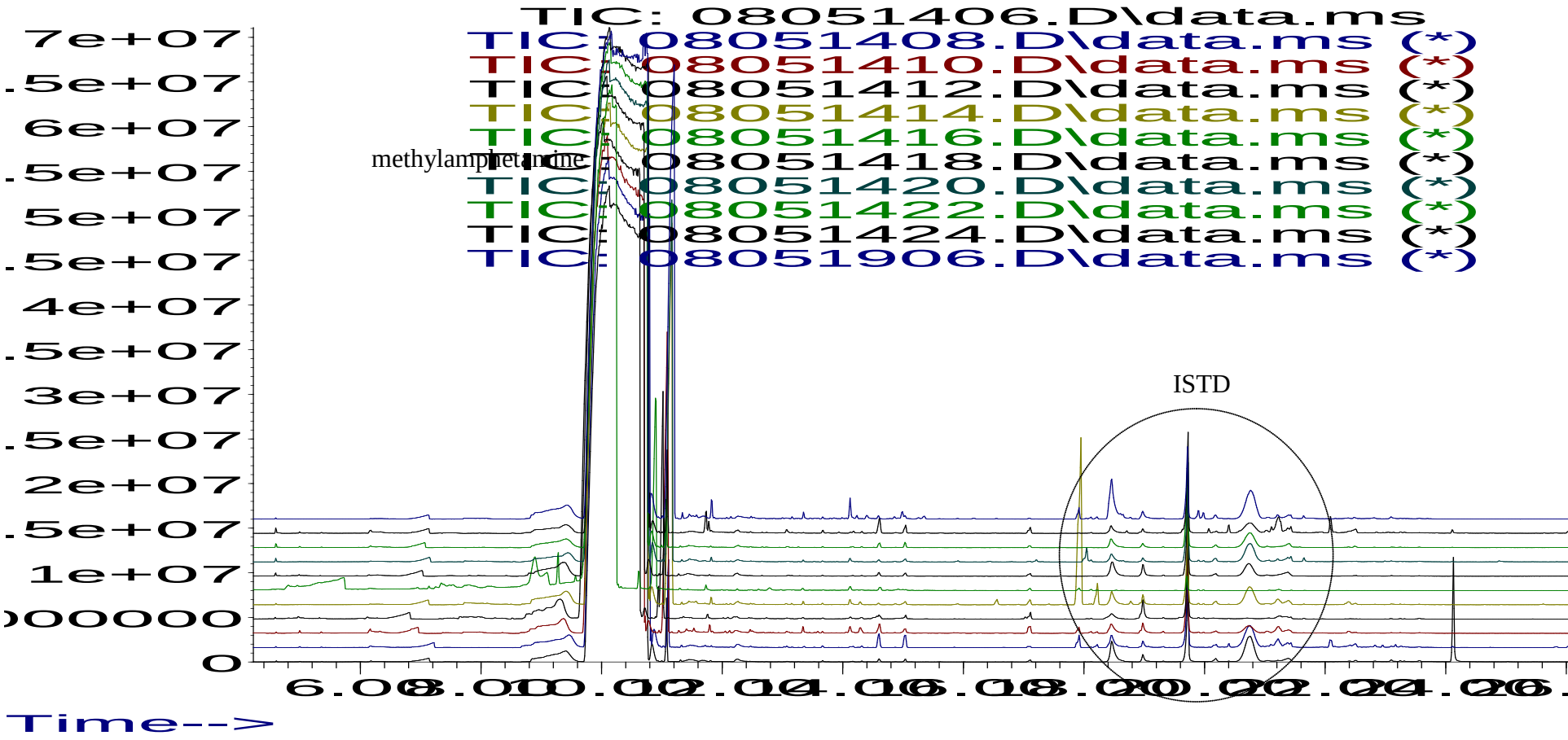

Figure 50: Overlay of the impurity profiles from the remaining eleven batches extract at pH 10.5.

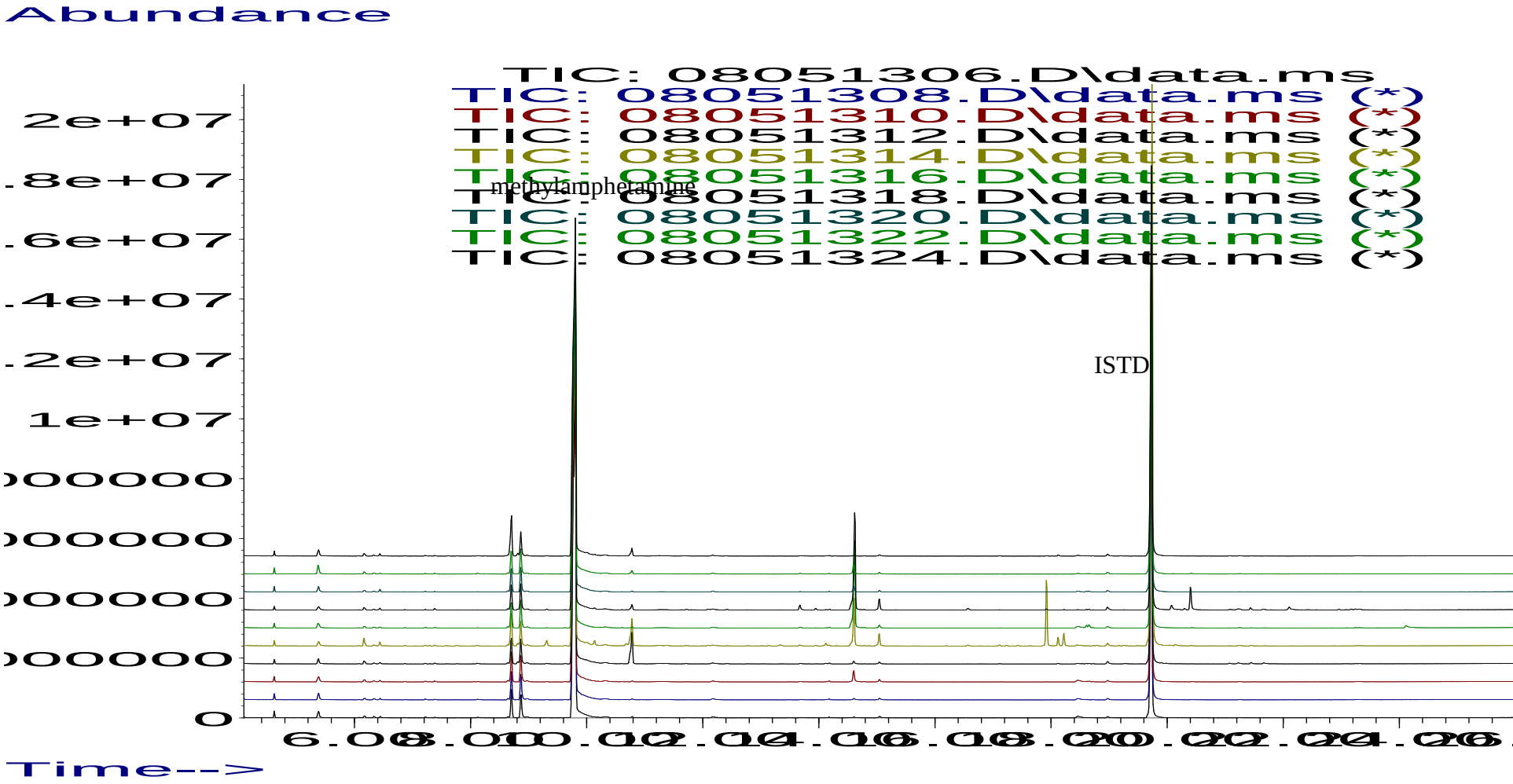

Figure 51: Overlay of the impurity profiles from the first ten batches extract at pH 6.

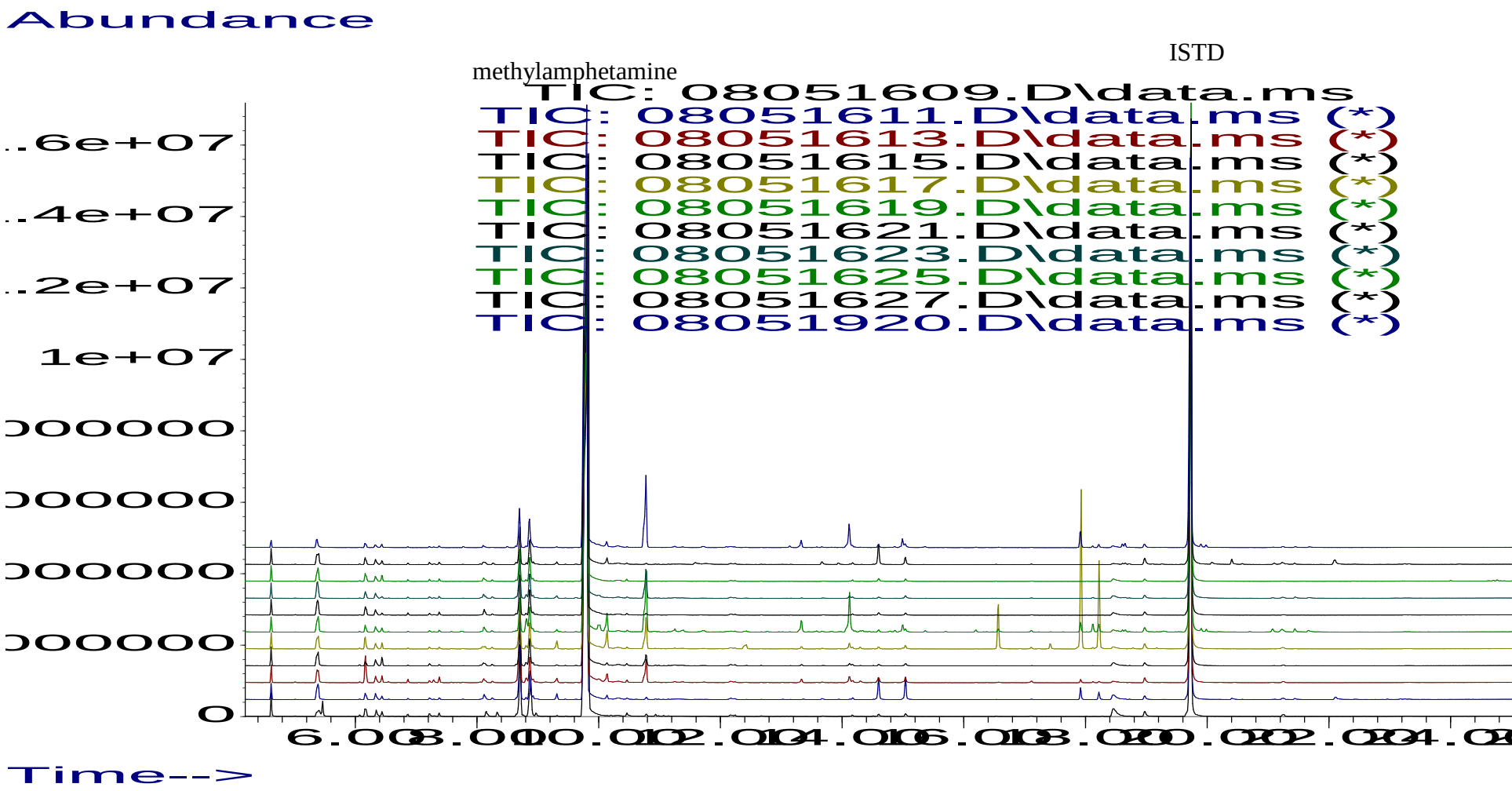

Figure 52: Overlay of the impurity profiles from the remaining eleven batches extract at pH 6.

5.3.2.2 Reductive Amination

Twenty batches of methylamphetamine hydrochloride were synthesised using the Reductive Amination method as previously described in Chapter 3. Each of these samples were extracted using both acidic and basic buffers and analysed.

Table 23 details the impurities from the phosphate buffer extract (basic).

No	RT	Compound	Peak m/z
1	6.949	Acetic acid	**43**, 60, 91, 134
2	9.187	Amphetamine	**44**, 91, 65, 134
3	10.797	*N*-(1-Methyl-2-phenylethylidene) methenamine	**56**, 91, 65, 39, 77
4	11.019	Dimethylamphetamine (DMA)	**72**, 91, 56, 42
5	13.654	*N*-formylamphetamine	**118**, 72, 44, 91
6	14.321	Bibenzyl	**91**, 182
7	14.593	*N*-formylmethylamphetamine	**86**, 58, 118
8	15.035	*N*-acetylmethylamphetamine	**58**, 100
9	16.279	Dibenzylketone	**91**, 65, 119, 39, 51, 210
10	17.909	*cis* 3,4-Diphenyl-3-buten-2-one	**179**, 178, 222, 221
11	18.064	α-benzyl-N-methylphenethylamine	**134**, 91, 65, 77, 58, 225
12	18.127	Benzylmethylamphetamine	**91**, 148, 65, 105
13	18.212	*trans* 3,4-Diphenyl-3-buten-2-one	**179**, 178, 222, 221
14	18.485	*N*-β-(phenylisopropyl) benzyl methyl ketimine	**91**, 160, 119, 65, 77, 207
15	18.817	*N*-methyldiphenethylamine	**148**, 91, 65, 77, 105, 239
16	20.19	*N*-benzoylamphetamine	**105**, 77, 148, 91, 118
17	20.417	*N*-benzoylmethylamphetamine	**105**, 162, 77, 91
18	21.077	2,6-Dimethyl-3,5-diphenylpyridine	**259**, 258, 91, 188, 186
19	21.204	Pyridine 7 and 14	**258**, 186, 91, 259
20	22.331	*N*,*N*-di-(β-phenylisopropyl) formamide	**190**, 91,58, 119, 77, 105
21	23.241	*N*-methyl-*N*-(1-methyl-2-phenylethyl)-2-phenylacetamide	**58**, 91, 219, 176

Table 23: List of impurities found in pH 10.5 extract

Table 24 details the impurities from the acetate buffer extract (acidic).

No	RT	Compound	Peak m/z
1	8.69	1-phenyl-2-propanone	**43**, 91, 134
2	8.87	Amphetamine	**44**, 91, 134
3	8.89	1-phenyl-2-propanol	**92**, 91, 65, 45, 77
4	10.274	*N*-*N*-Dimethylbenzylamine	**58**, 135, 107,79
5	10.776	Dimethylamphetamine (DMA)	**72**, 91, 42

Table 24: List of impurities found in pH 6 extract

Only one route specific impurity for the Reductive Amination method (Figure 53) was identified: 1-phenyl-2-propanol, and this was found only in the acidic extract of all samples. P-2-P which was used as the starting material for both of the Leuckart and Reductive Amination routes was also present in the acidic extract.

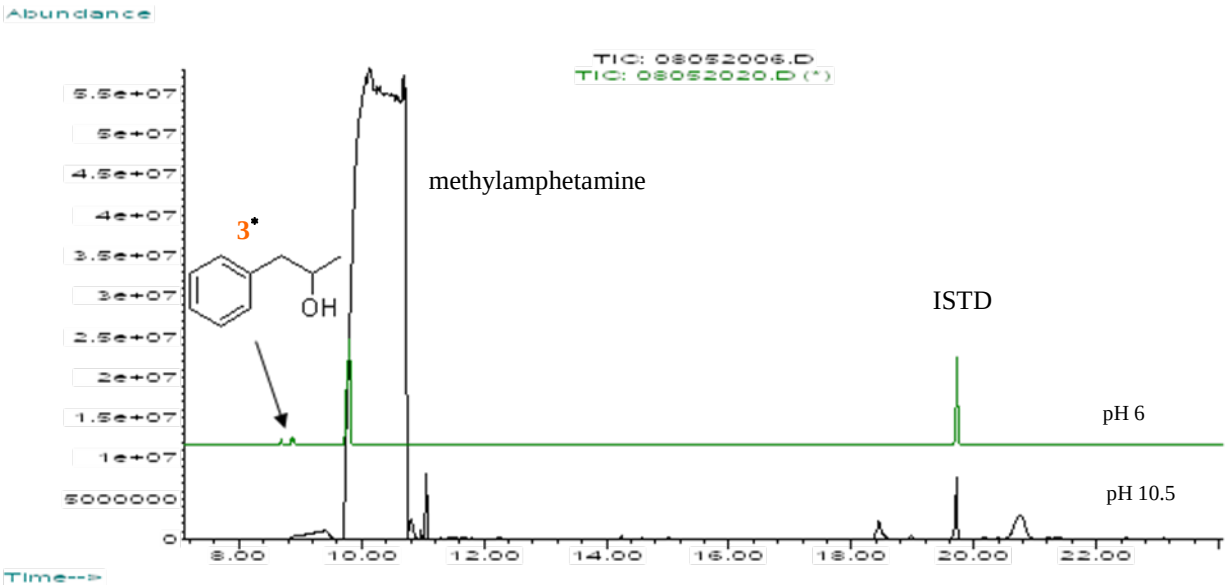

Figure 53: Overlay of the impurity profiles for both extracts. * refer to Table 24

The chromatographic results for each of the 20 batches synthesised via the Reductive Amination method are presented in Figure 54 - Figure 57. Visual comparison of the impurity profiles show some obvious variation between the 20 profiles, particularly within the 18 - 21 minute range in pH 10.5 extraction (Figure 55), and in the 8 – 9 minute range in pH 6.0 extraction (Figure 56).

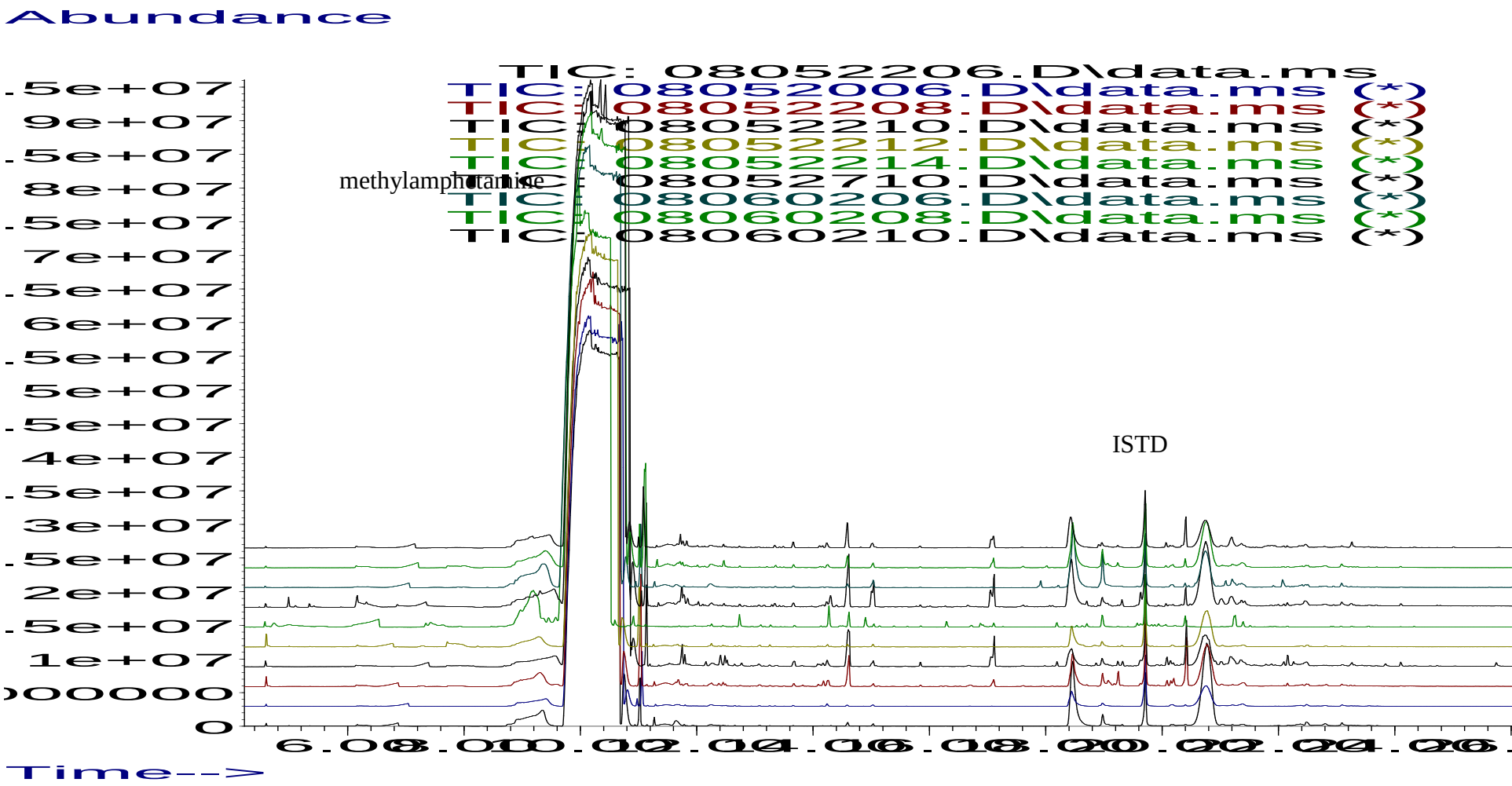

Figure 54: Overlay of the impurity profiles from the first ten batches extract at pH 10.5.

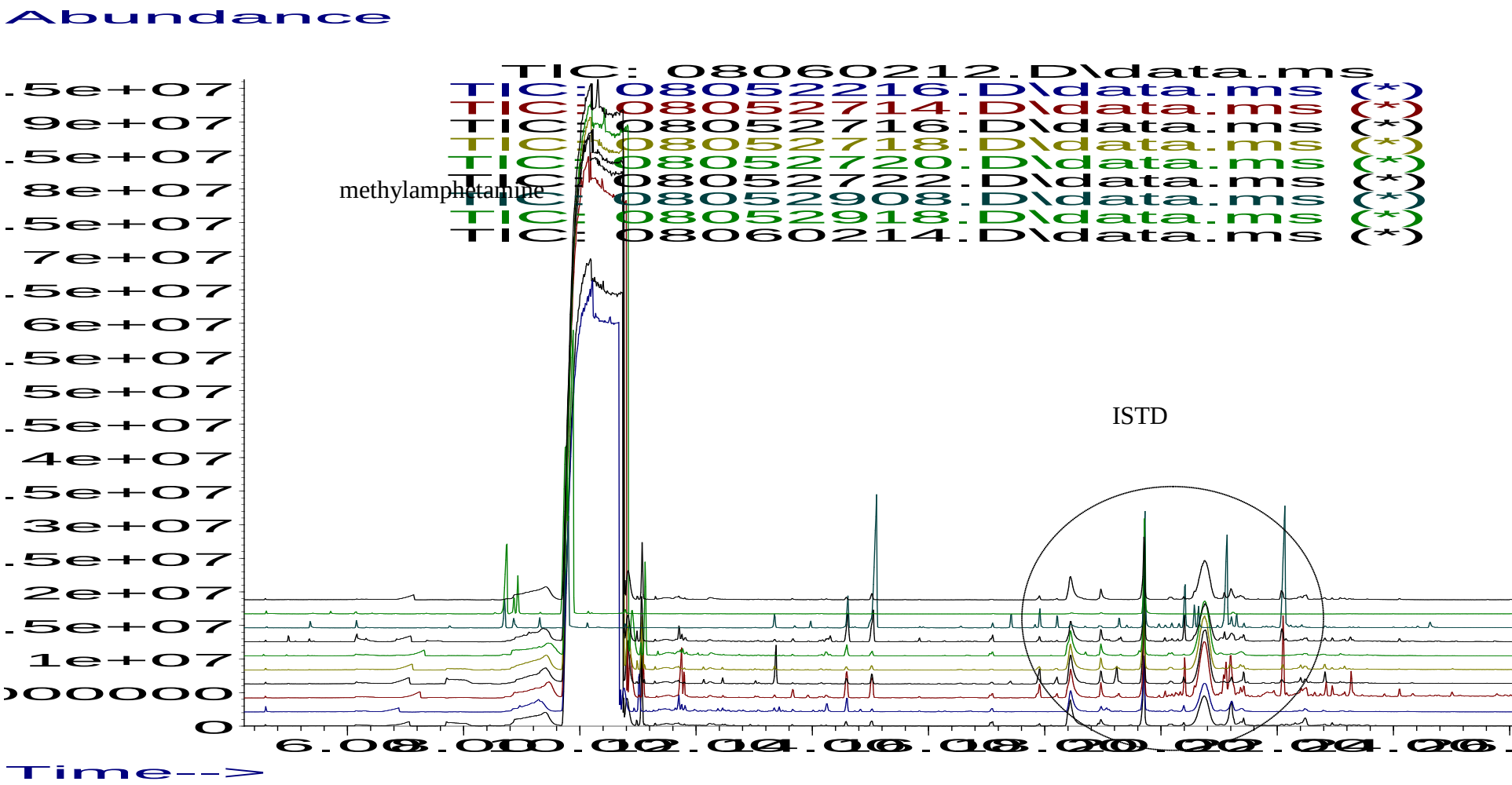

Figure 55: Overlay of the impurity profiles from the remaining ten batches extract at pH 10.5.

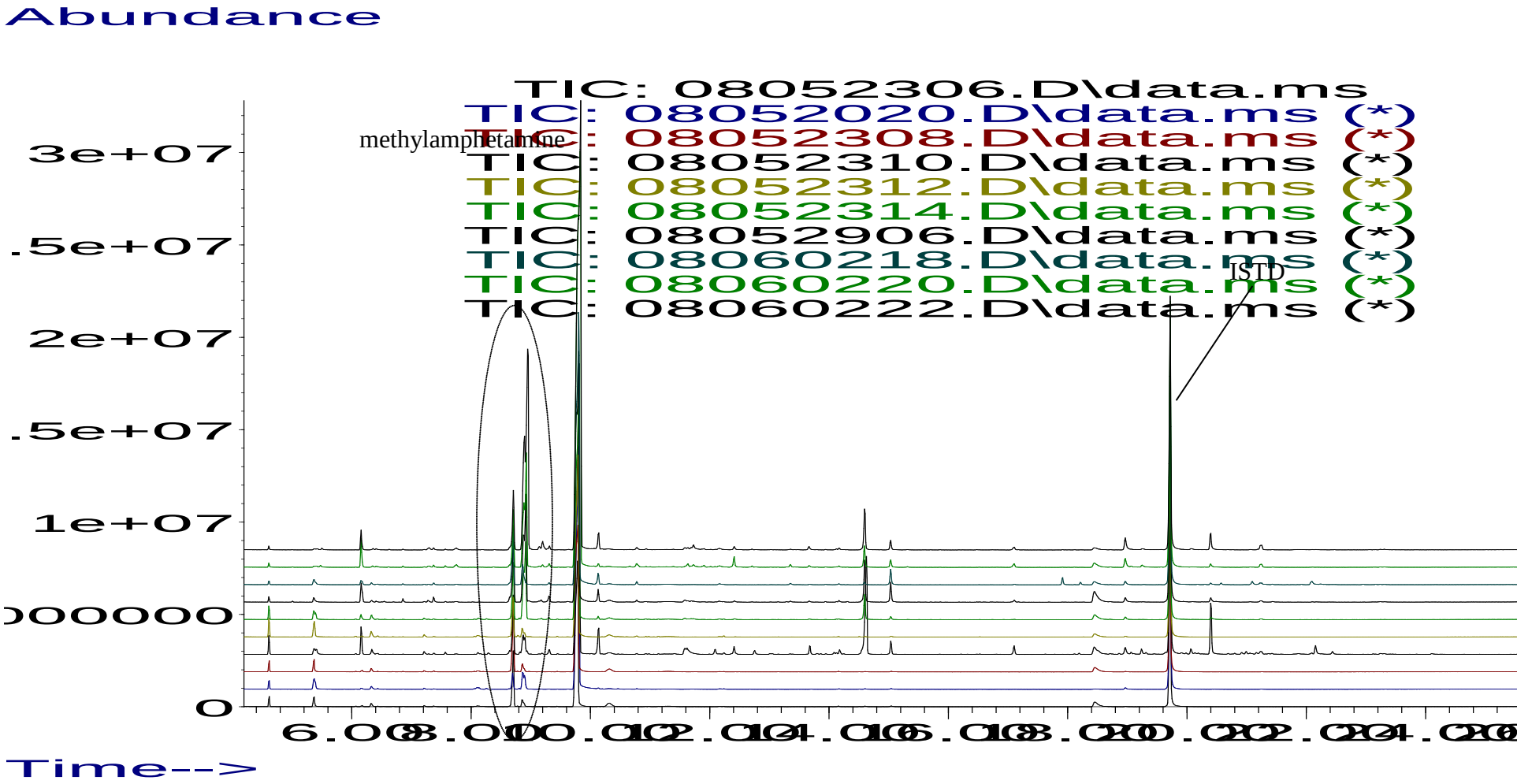

Figure 56: Overlay of the impurity profiles from the first ten batches extract at pH 6.0.

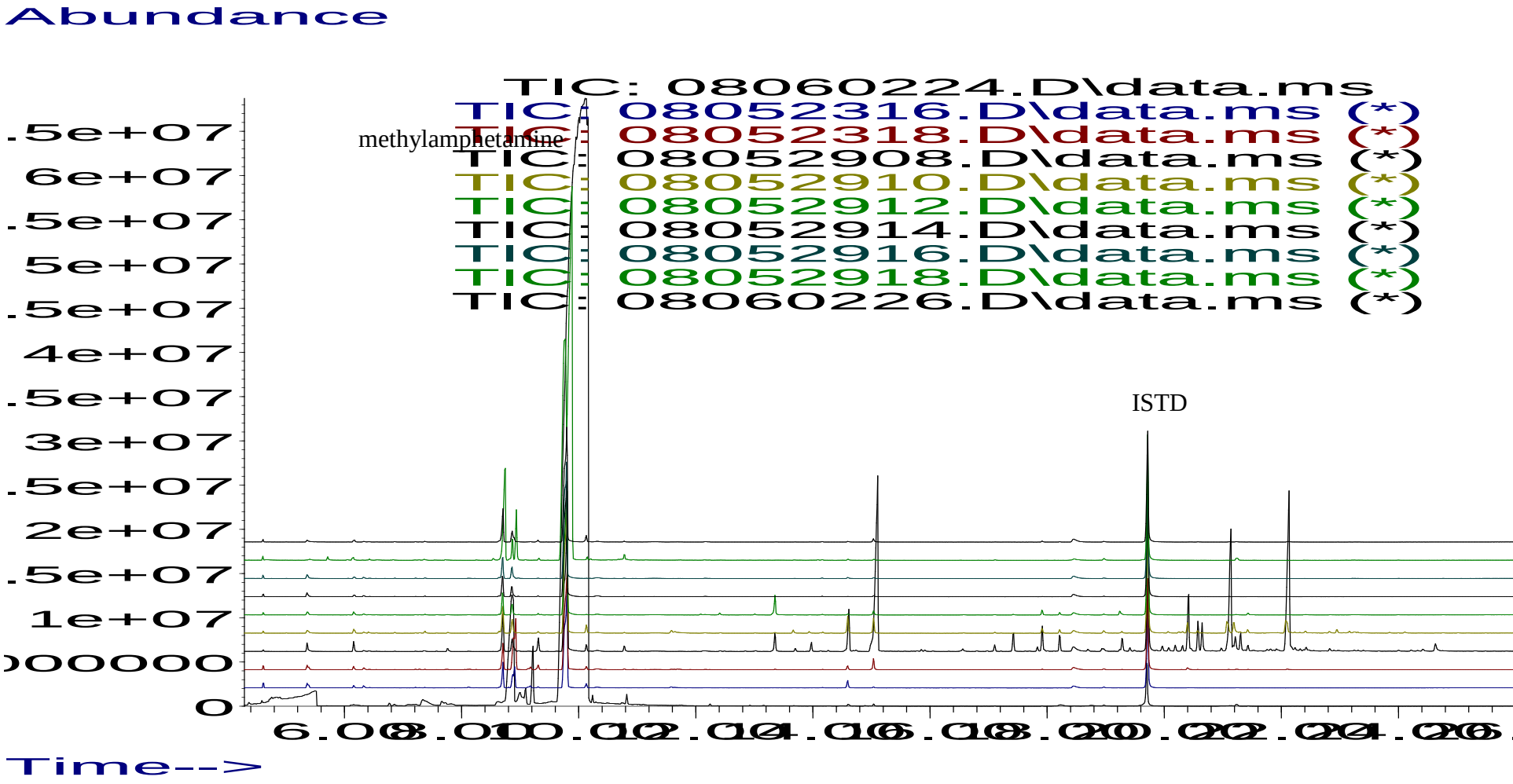

Figure 57: Overlay of the impurity profiles from the remaining ten batches extract at pH 6.0.

5.3.2.3 Conclusions of the synthetic methods utilising P-2-P as starting material

N-formylmethamphetamine was found in *all* batches of methylamphetamine, regardless of whether the Leuckart or Reductive Amination routes were used, thus confirming that *N*-formylmethylamphetamine is not route specific for the Leuckart method of methylamphetamine synthesis.

This study confirmed the finding of Kram et al.[3] where five impurities were identified from the Leuckart method; however, this study could also identify three of these five impurities in the Reductive Amination batches (i.e. three of the impurities reported by Kram et al.[3] indicate synthesis by *either* the Leuckart *or* Reductive Amination). This present work is the first study comparing the impurities present in methylamphetamine synthesised by the Leuckart and the Reductive Amination methods where two extracts (acidic and basic) were utilised. It was determined that an impurity extract at pH 10.5 only is not sufficient to detect the route specific impurity for the Reductive Amination which appears only in the acidic extract.

5.3.2.4 Nagai Method

20 batches of methylamphetamine hydrochloride were synthesised using the Nagai method as previously described in Chapter 3. Each of these samples were extracted using both acidic and basic buffers and analysed.

Table 25 shows impurities from the phosphate buffer extract (basic).

No	RT	Compound	Peak m/z
1	7.252	Acetic acid	**43**, 60, 91, 134
2	9.521	Amphetamine	**44**, 91, 65, 134
3	10.912	*N*-(1-Methyl-2-phenylethylidene) methenamine	**56**, 91, 65, 39, 77
4	11.131	Dimethylamphetamine (DMA)	**72**, 91, 56, 42
5	11.738	*Z* (1-phenylpropan-2-one oxime)	**91**, 149, 116, 131
6	11.780	*E* (1-phenylpropan-2-one oxime)	**91**, 131, 116, 149
7	12.47	3,4-Dimethyl-5-phenyloxazolidine	**71**, 56, 91
8	12.51	3,4-Dimethyl-5-phenyloxazolidine	**71**, 56, 91
9	13.662	*N*-formylamphetamine	**118**, 72, 44, 91
10	14.321	Bibenzyl	**91**, 182
11	14.593	*N*-formylmethylamphetamine	**86**, 58, 118
12	15.032	*N*-acetylmethylamphetamine	**58**, 100
13	18.127	Benzylmethamphetmine	**91**, 148, 65, 105
14	17.911	*cis* 3,4-Diphenyl-3-buten-2-one	**179**, 178, 222, 221
15	18.21	*trans* 3,4-Diphenyl-3-buten-2-one	**179**, 178, 222, 221
16	18.440	*N*-β-(phenylisopropyl) benzyl methyl ketimine	**91**, 160, 119, 65, 77, 207
17	20.051	Dimethylphenylnaphthalene	**232**, 217, 202, 77
18	20.117	*N*-benzoylamphetamine	**105**, 77, 148, 91, 118
19	20.208	Benzylmethnaphthalene	**232**, 217, 202, 58
20	20.344	*N*-methyl-N-(α-methylphenethyl) amino-1-phenyl-2-propanone	**238**, 91, 105, 190, 120
21	20.417	*N*-benzoylmethylamphetamine	**105,** 162, 77, 91
22	22.361	*N,N*-di-(β-phenylisopropyl) formamide	**190**, 91, 58, 119, 77, 105
23	22.425	(*Z*)-*N*-methyl-*N*-(α-methylphenethyl)-3-phenylpropenamide	**131**, 91, 58, 103, 188, 77
24	23.425	(*E*)-*N*-methyl-*N*-(α-methylphenethyl)-3-phenylpropenamide	**131**, 91, 58, 103, 188, 77

Table 25: List of impurities found in pH 10.5 extract.

Table 26 shows impurities from the acetate buffer extract (acidic).

No	RT	Compound	Peak m/z
1	8.716	1-phenyl-2-propanone	**43**, 91, 134
2	8.894	Amphetamine	**44**, 91, 134
3	9.323	1-phenyl-1,2-propanedione	**105**, 77, 51, 43
4	10.138	3-phenyl-3-buten-2-one	**103, 146, 91**
5	10.211	*N*-*N*-Dimethylbenzylamine	**58**, 135, 107,79
6	13.673	*N*-formylamphetamine	**118**, 72, 44, 91
7	14.603	*N*-formylmethylamphetamine	**86**, 58, 97, 118
8	15.053	*N*-acetylmethylamphetamine	**58**, 100
9	20.041	Dimethylphenylnaphthalene	**232**, 217, 202, 58
10	20.208	Benzylmethnaphthalene	**232**, 217, 202, 58
11	20.355	*N*-methyl-N-(α-methylphenethyl) amino-1-phenyl-2-propanone	**238**, 91, 105, 190, 120
12	20.407	*N*-benzoylmethylamphetamine	**105**, 162, 77, 91

Table 26: List of impurities found in pH 6 extract.

Four specific impurities were detected in methylamphetamine synthesised by the Nagai method (Figure 58), however these impurities were also detected in samples synthesised via the Moscow route. These impurities are 1,3-dimethyl-2-phenylnaphthalene, 1-benzyl-3-methylnaphthalene, *N*-methyl-*N*-(α-methylphenethyl)amino-1-phenyl-2-propane and *N*-methyl-*N*-(α-methylphenethyl)-3-phenylpropenamide.

This study also confirms that the naphthalenes are target impurities for the Nagai method, but the aziridines (*cis*-1,2-dimethyl-3-phenylaziridine and *trans*-1,2-dimethyl-3-phenylaziridine) and methylamphetamine dimer may or may not always be present, depending on the time allowed for the reaction to proceed. For the 24 hour reaction time, aziridines and methylamphetamine dimer were not observed. This is further discussed in Section 5.4.

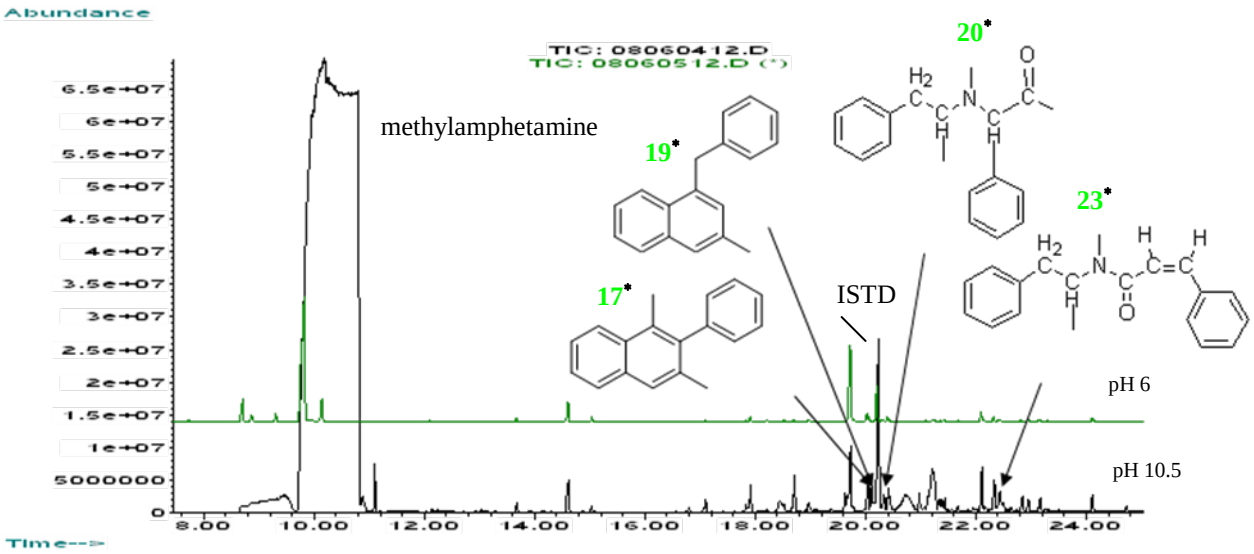

Figure 58: Overlay of the impurity profiles for both extracts. * refer to Table 25

The chromatographic results for each of the 20 batches synthesised via the Nagai method are presented in Figure 59 - Figure 62. Visual comparison of the impurity profiles show some obvious variation between the 20 profiles, particularly within the 18 - 21 minute range in pH 10.5 extraction (Figure 60).

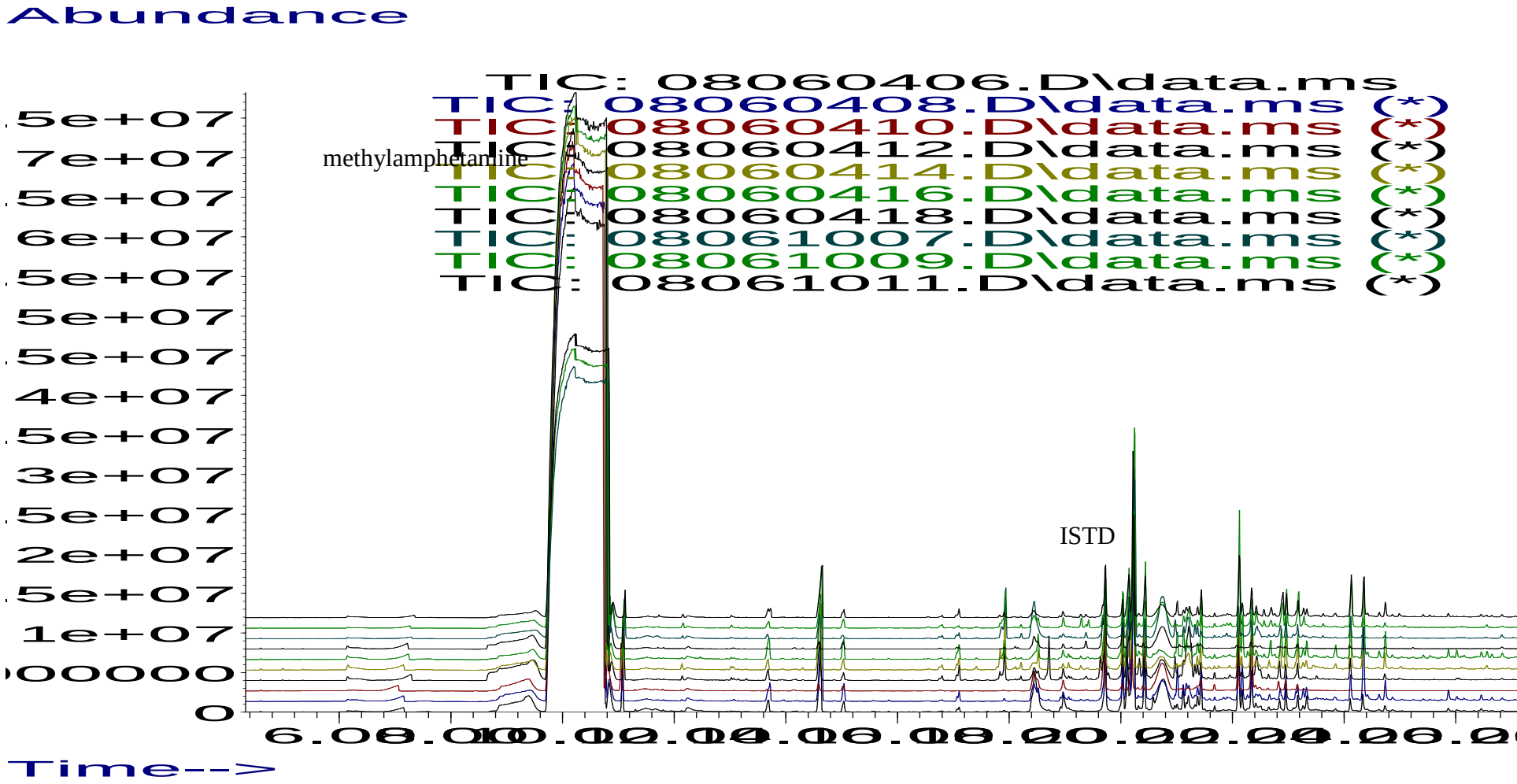

Figure 59: Overlay of the impurity profiles from the first ten batches extract at pH 10.5

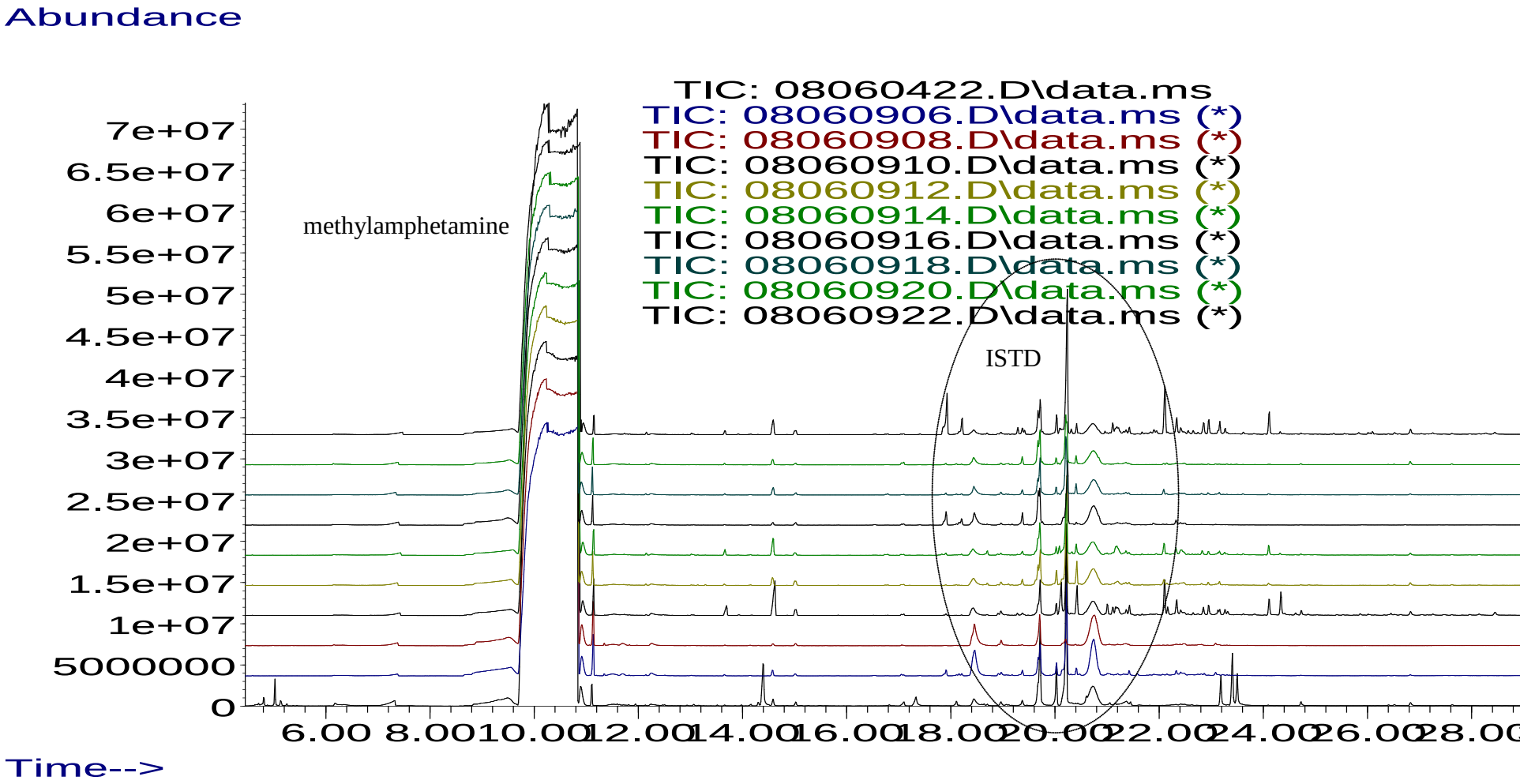

Figure 60: Overlay of the impurity profiles from the remaining ten batches extract at pH 10.5.

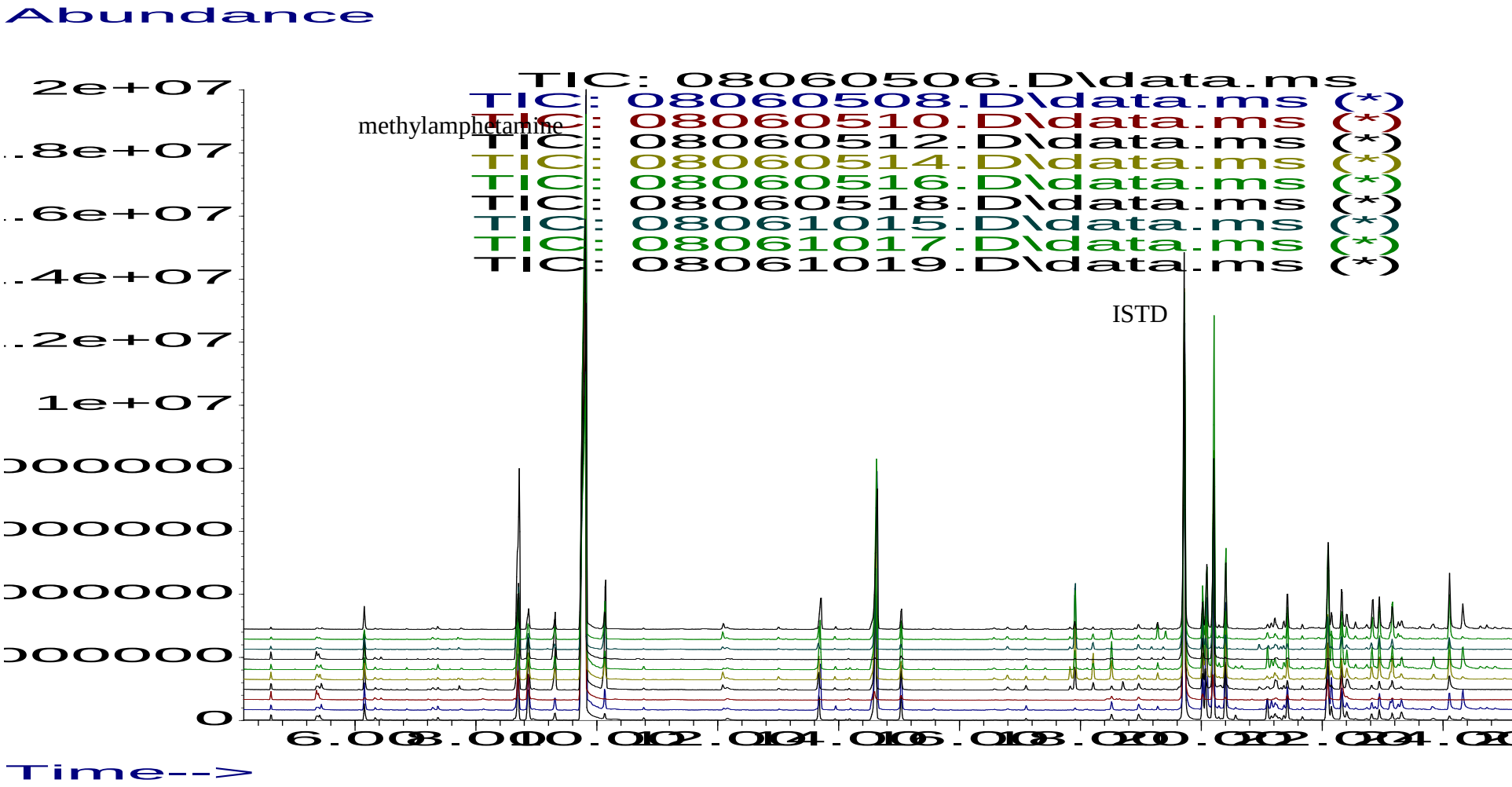

Figure 61: Overlay of the impurity profiles from the first ten batches extract at pH 6.0.

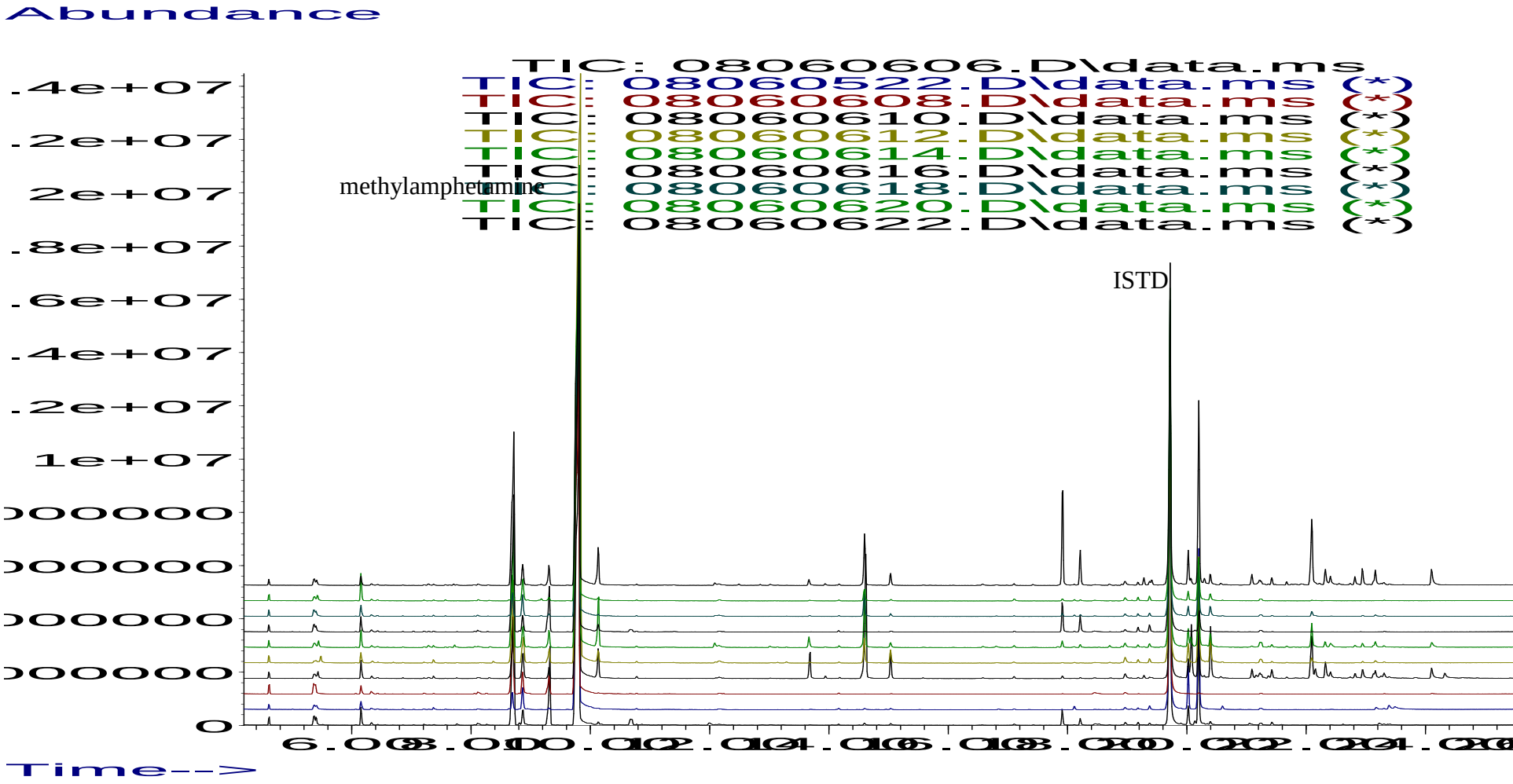

Figure 62: Overlay of the impurity profiles from the remaining ten batches extract at pH 6.0

5.3.2.5 Rosenmund Method

20 batches of methylamphetamine hydrochloride were synthesised using the Rosenmund method as previously described in Chapter 3. Each of these samples were extracted using both acidic and basic buffers and analysed.

Table 27 shows impurities from the phosphate buffer extract (basic).

No	RT	Compound	Peak m/z
1	6.136	Benzaldehyde	**106**, 105, 77, 51
2	6.899	Acetic acid	**43**, 60, 91, 134
3	8.917	Amphetamine	**44**, 91, 65, 134
4	11.009	Dimethylamphetamine (DMA)	**72**, 91, 56, 42
5	11.863	Ephedrone	**58**, 77, 105
6	12.388	Ephedrine	**58**, 77, 117, 132, 148
7	13.913	Ethylamphetamine	**72**, 44, 58, 91
8	14.258	*N*-formylamphetamine	**44**, 118, 72, 91, 58
9	14.498	*N*-acetylamphetamine	**44**, 86, 118, 91, 65
10	14.657	*N*-formylmethylamphetamine	**86**, 58, 118
11	15.075	*N*-acetylmethylamphetamine	**58**, 100
12	17.919	*cis* 3,4-Diphenyl-3-buten-2-one	**179**, 178, 222, 221
13	18.222	*trans* 3,4-Diphenyl-3-buten-2-one	**179**, 178, 222, 221
14	20.038	Unknown 1	**58**, 91, 118, 239
15	20.458	Unknown 2	**58**, 263, 248

Table 27: List of impurities found in pH 10.5 extract.

Table 28 shows impurities from phosphate buffer extracts.

No	RT	Compound	Peak m/z
1	6.104	Benzaldehyde	**106**, 105, 77, 51
2	8.729	1-phenyl-2-propanone	**43**, 91, 134
3	8.865	Amphetamine	**44**, 91, 65, 134
4	10.778	Dimethylamphetamine (DMA)	**72**, 91, 56, 42
5	13.778	*N*-formylamphetamine	**44**, 118, 72, 91, 58
6	14.039	*N*-acetylamphetamine	**44**, 86, 118, 91, 65
7	14.658	*N*-formylmethylamphetamine	**86**, 58, 118
8	14.919	*N*-acetylmethylamphetamine	**58**, 100

Table 28: List of impurities found in pH 6 extract.

No impurity profiling work has been published for the Rosenmund method. This study has found 3 route specific impurities (Ethylamphetamine and 2 unknown compounds) at pH 10.5 which were present in all of the samples synthesised by this route. *N*-acetylmethamphetamine was also found as an impurity in all six synthetic routes but in greater quantities in the samples synthesised by the Rosenmund method. These are illustrated in Figure 63.

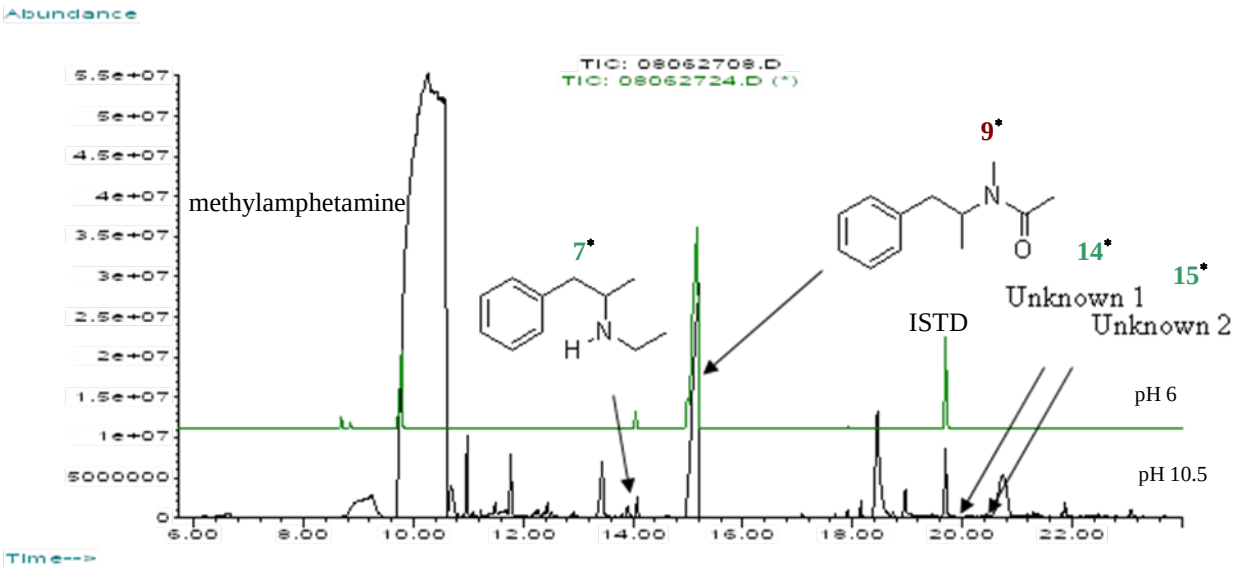

Figure 63: Overlay of the impurity profiles for both extracts. * refer to Table 27

The chromatographic results for each of the 20 batches synthesised via the Rosenmund method are presented in Figure 64 - Figure 67. Visual comparison of the impurity profiles show obvious variation between the 20 profiles, particularly within the 11 - 21 minute range in pH 10.5 extraction.

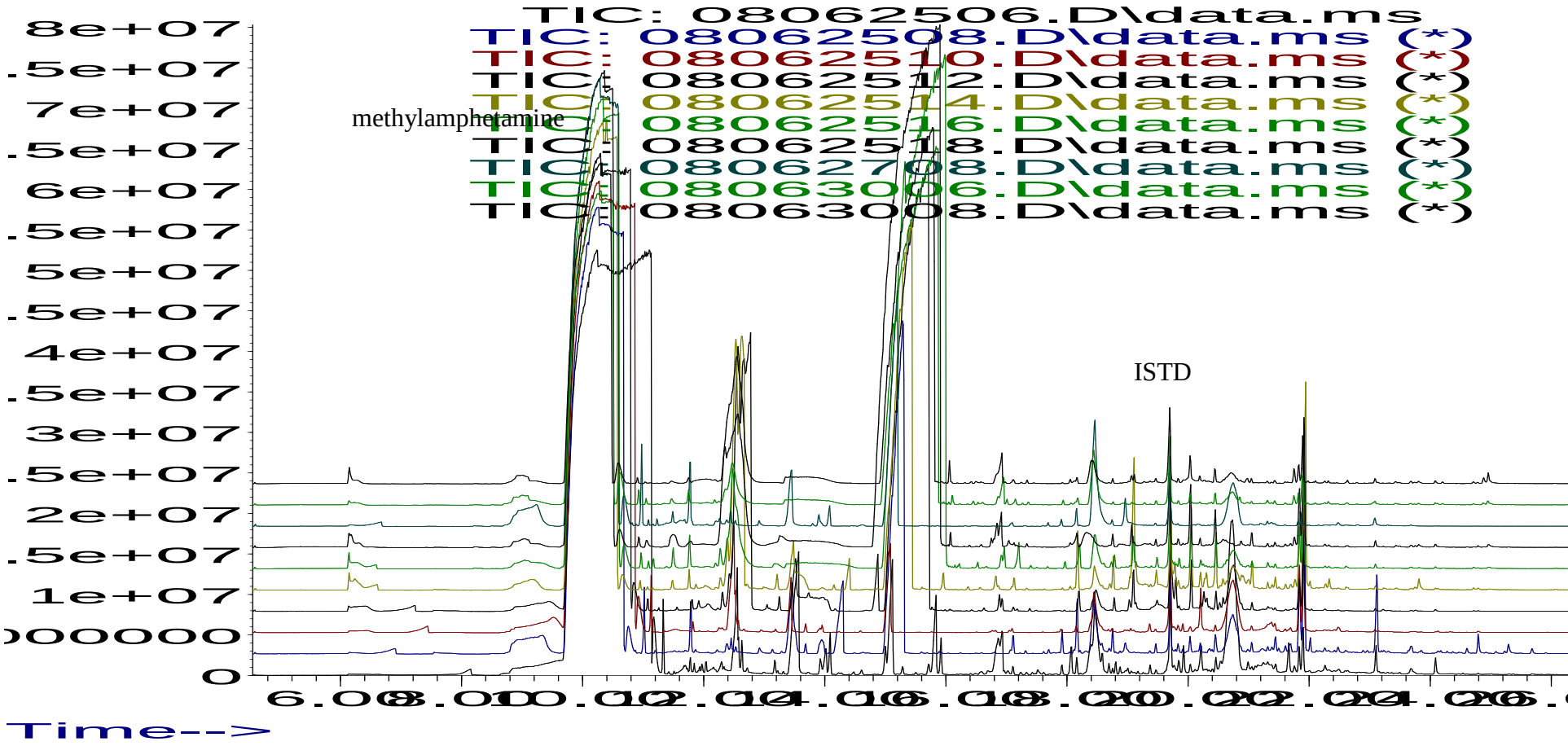

Figure 64: Overlay of the impurity profiles from the first ten batches extract at pH 10.5.

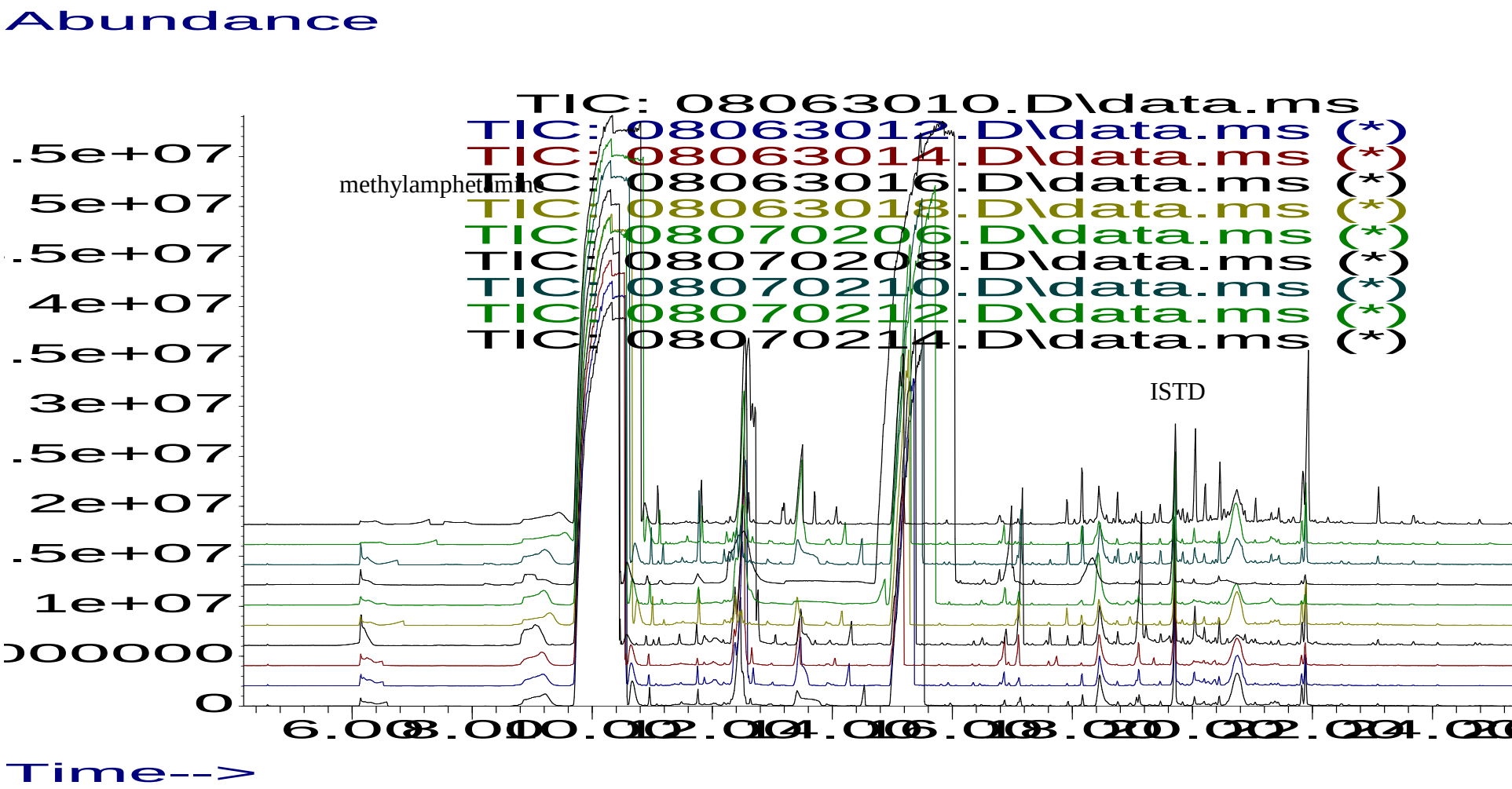

Figure 65: Overlay of the impurity profiles from the remaining ten batches extract at pH 10.5.

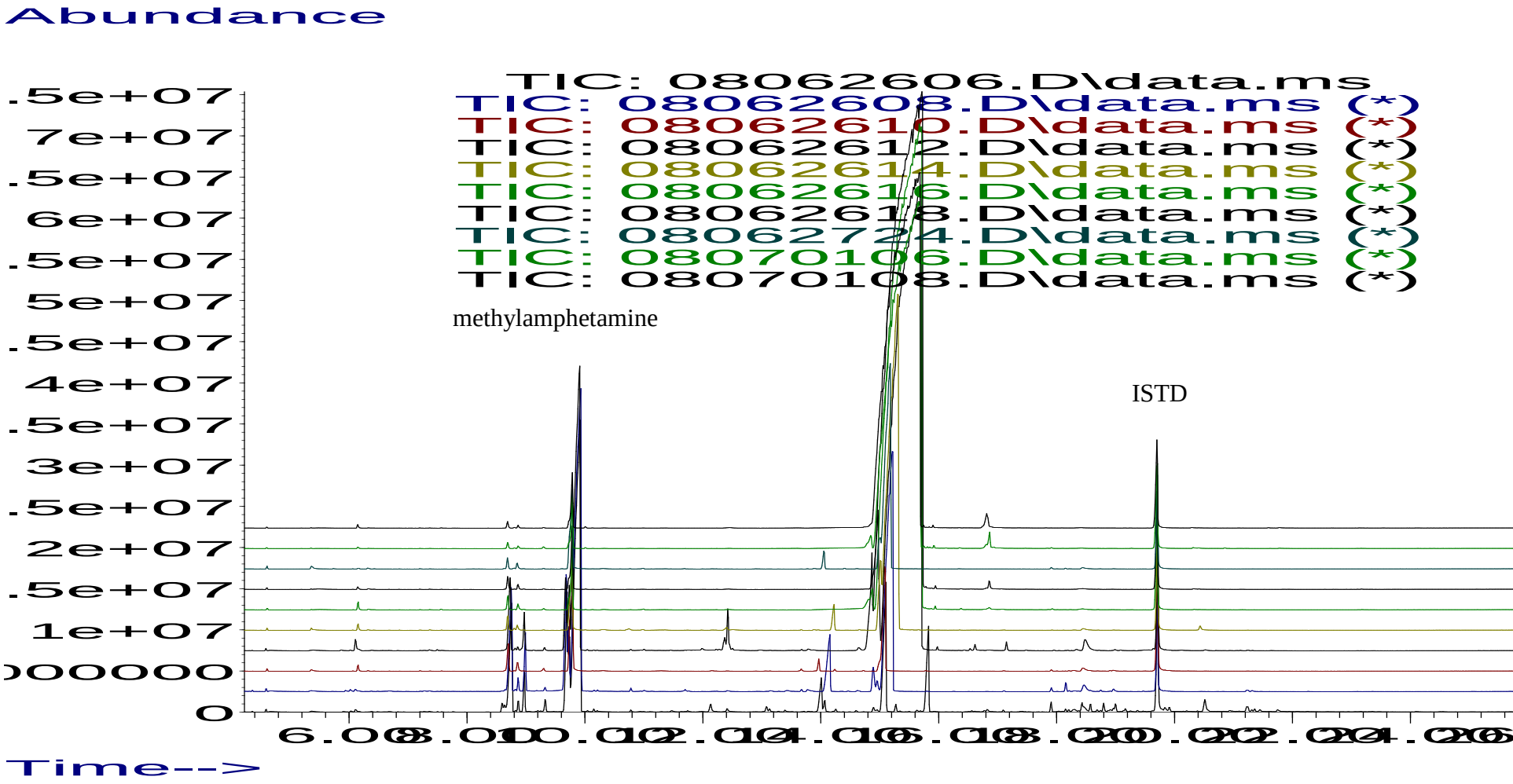

Figure 66: Overlay of the impurity profiles from the first ten batches extract at pH 6.0.

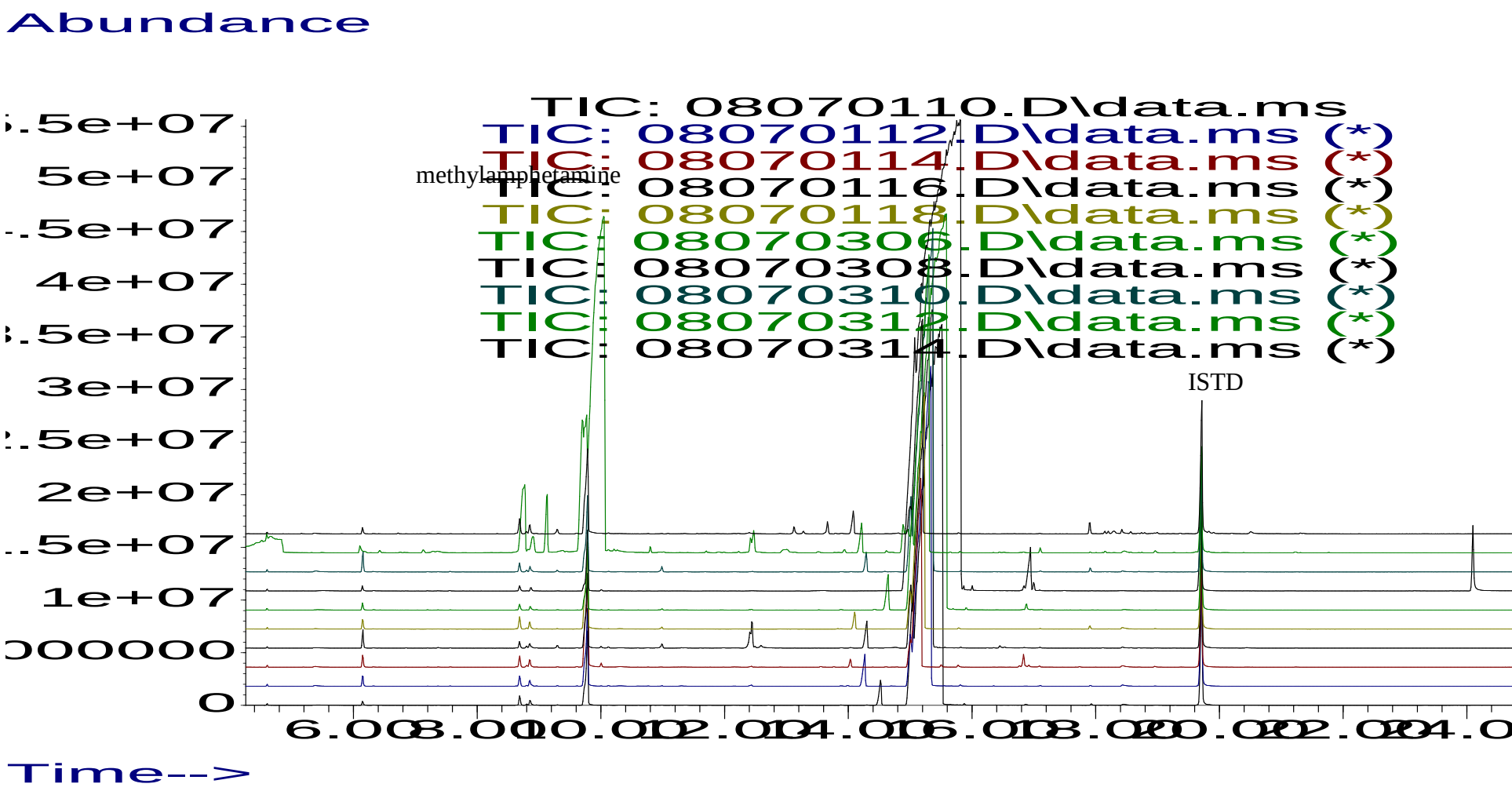

Figure 67: Overlay of the impurity profiles from the remaining ten batches extract at pH 6.0.

5.3.2.6 Birch Method

20 batches of methylamphetamine hydrochloride were synthesised using the Birch method as previously described in Chapter 3. Each of these samples were extracted using both acidic and basic buffers and analysed.

Table 29 shows impurities from phosphate buffer extracts.

No	RT	Compound	Peak m/z
1	6.176	Benzaldehyde	**105**, 106, 77, 51
2	6.866	Acetic acid	**43**, 60, 91, 134
3	8.979	Amphetamine	**44**, 91, 65, 134
4	10.537	*N*-(1-Methyl-2-phenylethylidene) methenamine	**56**, 91, 65, 39, 77
5	10.882	Dimethylamphetamine (DMA)	**72**, 91, 56, 42
6	11.907	Ephedrone	**58**, 77, 105
7	12.388	Ephedrine	**58**, 77, 117, 132, 148
8	13.101	Unknown 3	**58**, 77
9	14.657	*N*-formylmethylamphetamine	**86**, 58, 118
10	15.075	*N*-acetylmethylamphetamine	**58**, 100
11	18.118	Benzylmethylamphetamine	**91**, 148, 65, 105
12	18.463	*N*-β-(phenylisopropyl) benzyl methyl ketimine	**91**, 160, 119, 65, 77, 207
13	19.132	3,4-Dimethyl-2,5-diphenyl-oxazolidine	**146**, 147, 105, 132

Table 29: List of impurities found in pH 10.5 extract.

Table 30 shows impurities from acetate buffer extracts.

No	RT	Compound	Peak m/z
1	8.694	1-phenyl-2-propanone	**43**, 91, 134
2	8.809	*cis*-1,2-dimethyl-3-phenylaziridine	**146**, 105,132, 32
3	8.851	Amphetamine	**44**, 91, 134
4	9.311	1-phenyl-1,2-propanedione	**105**, 77, 51, 43
5	10.015	*trans*-1,2-dimethyl-3-phenylaziridine	**146**, 105,132, 32
6	12.437	3,4-Dimethyl-5-phenyloxazolidine	**71**, 56, 91, 105

Table 30: List of impurities found in pH 6 extract.

For the Birch reduction, this study has identified an unreported route specific impurity, unknown 3 at (pH 10.5) which was present in all samples. Person et al.[4] also synthesised methylamphetamine by this route and reported one impurity 1-(1,4-cyclohexadienyl)-2-methylaminopropane (CMP) which was absent in the samples prepared in this study. However Person used ephedrine salt as the starting material rather

than the free base which may account for the differences. An example of the chromatograms obtained are illustrated in Figure 68.

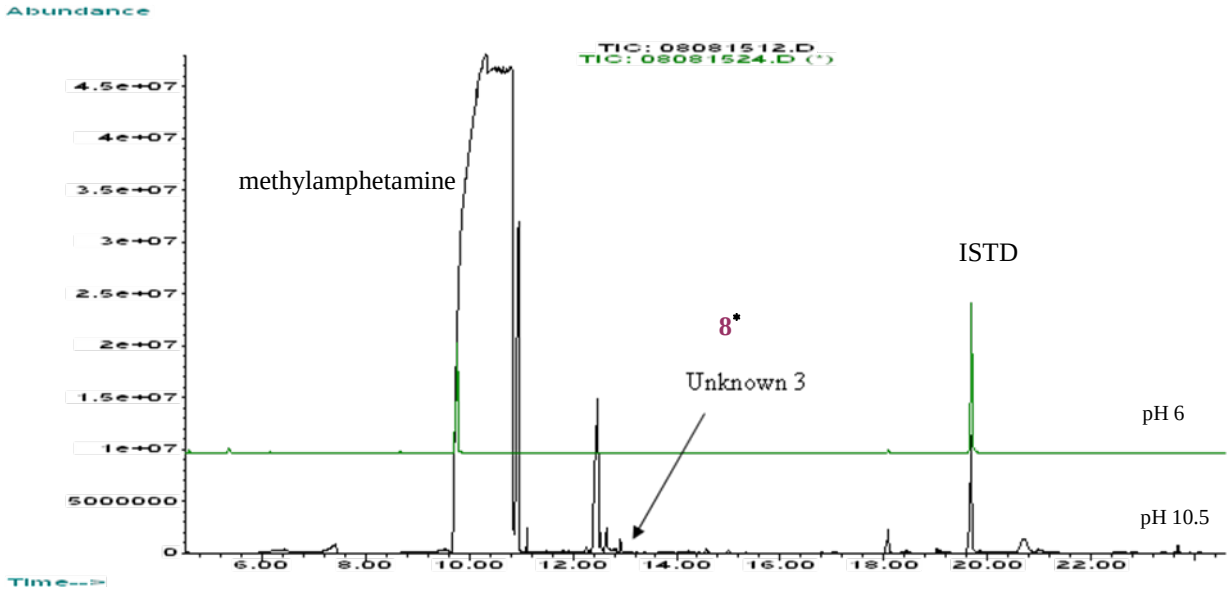

Figure 68: Overlay of the impurity profiles for both extracts. * refer to Table 29

The results of an additional study into the effect of the Birch reaction substrate on the impurity profile of methylamphetamine are presented in Section 5.5

The chromatographic results for each of the 20 batches synthesised via the Birch method are presented in Figure 69 - Figure 72. Visual comparison of the impurity profiles show small variation between the 20 profiles in the pH 10.5 extract with a greater variation between samples in the acidic extract.

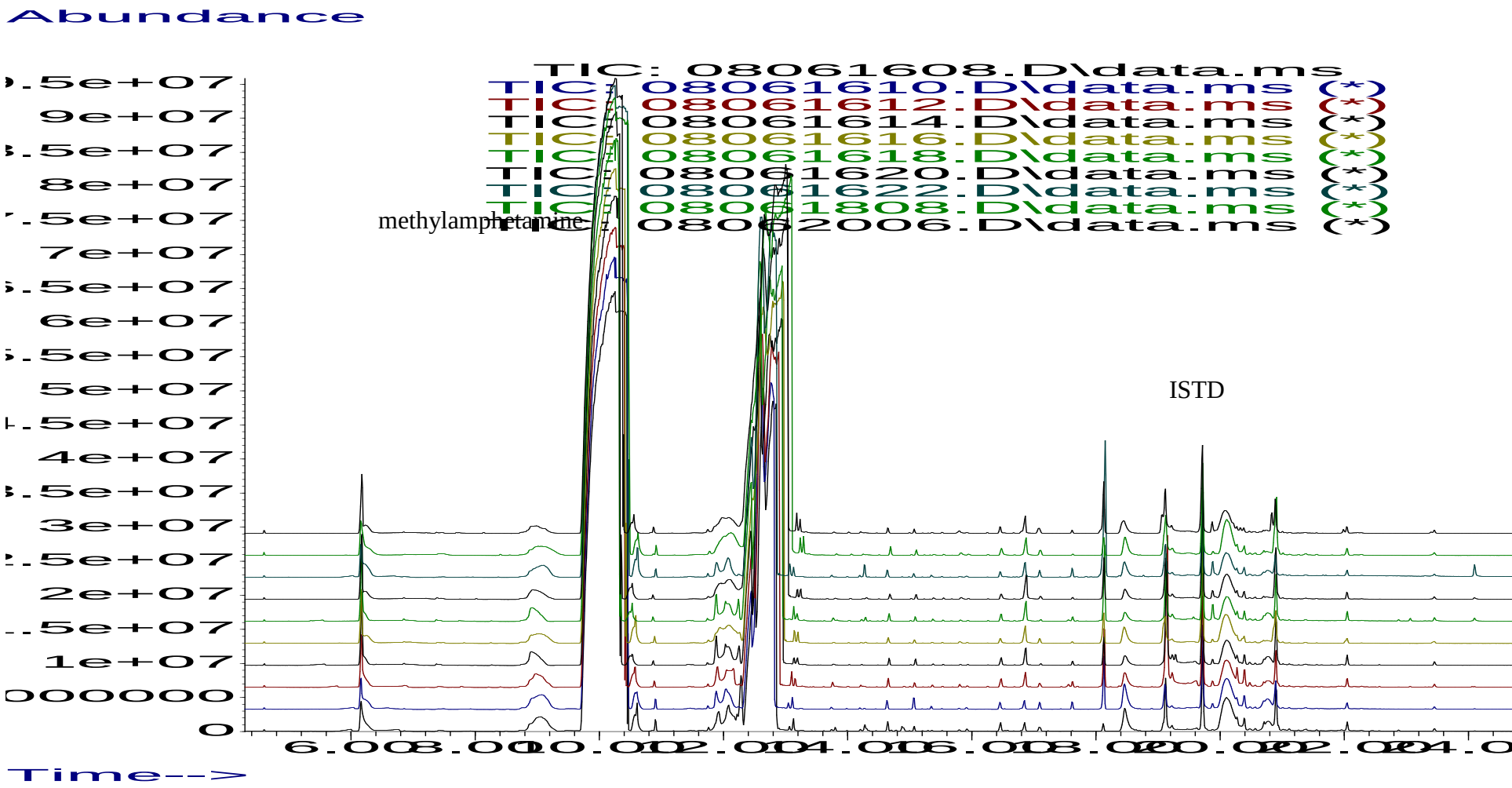

Figure 69: Overlay of the impurity profiles from the first ten batches extract at pH 10.5.

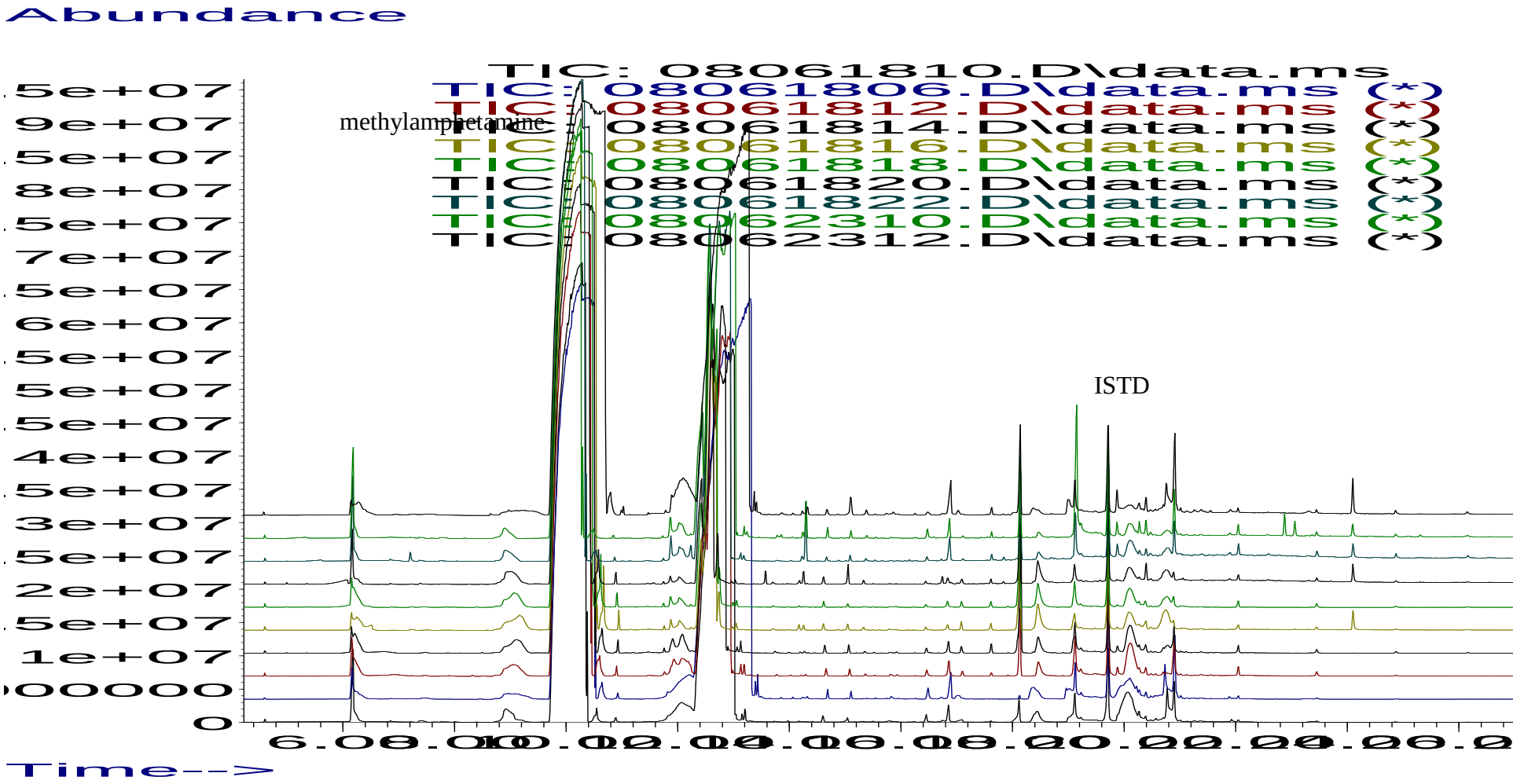

Figure 70: Overlay of the impurity profiles from the remaining ten batches extract at pH 10.5.

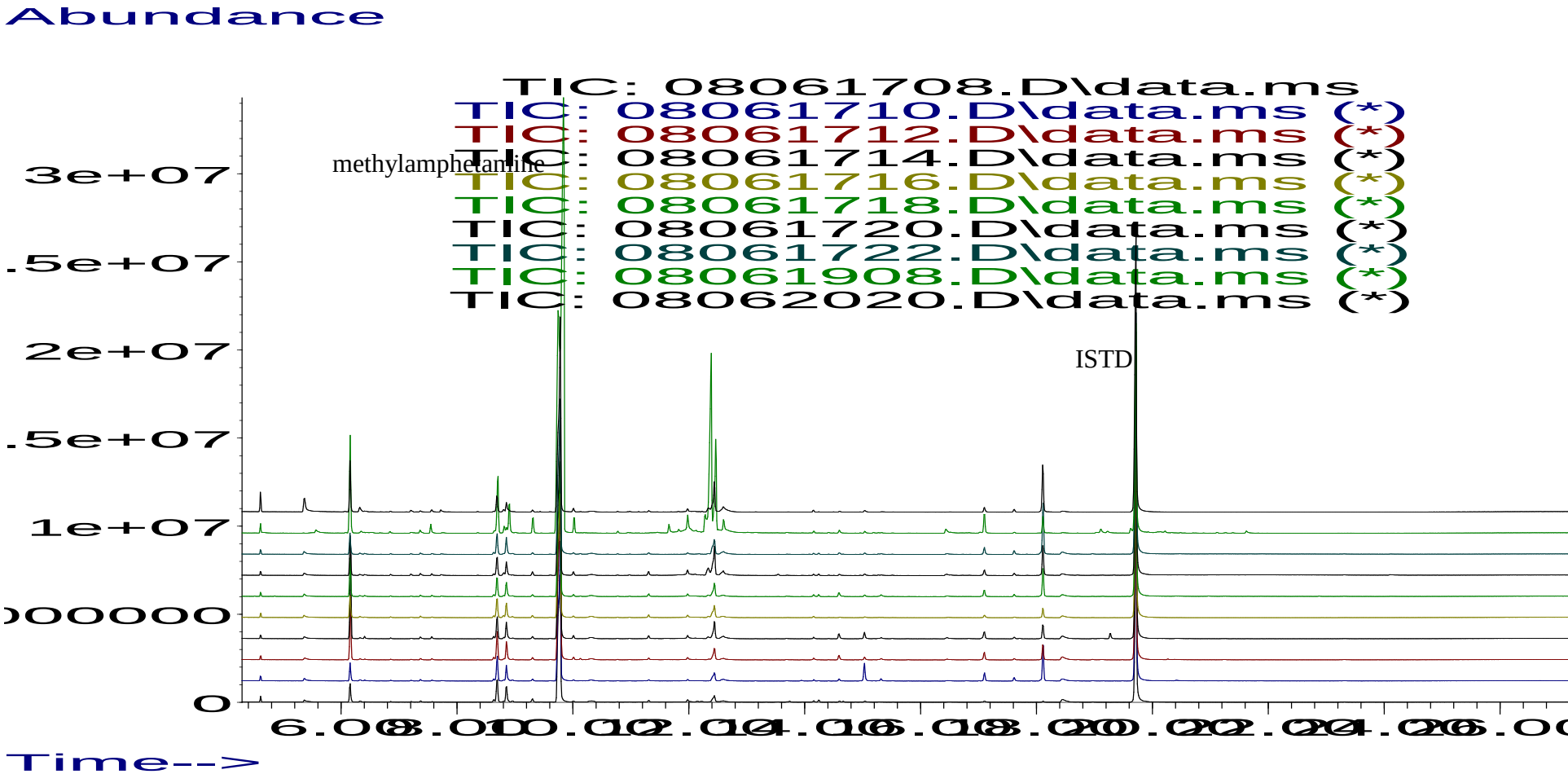

Figure 71: Overlay of the impurity profiles from the first ten batches extract at pH 6.0.

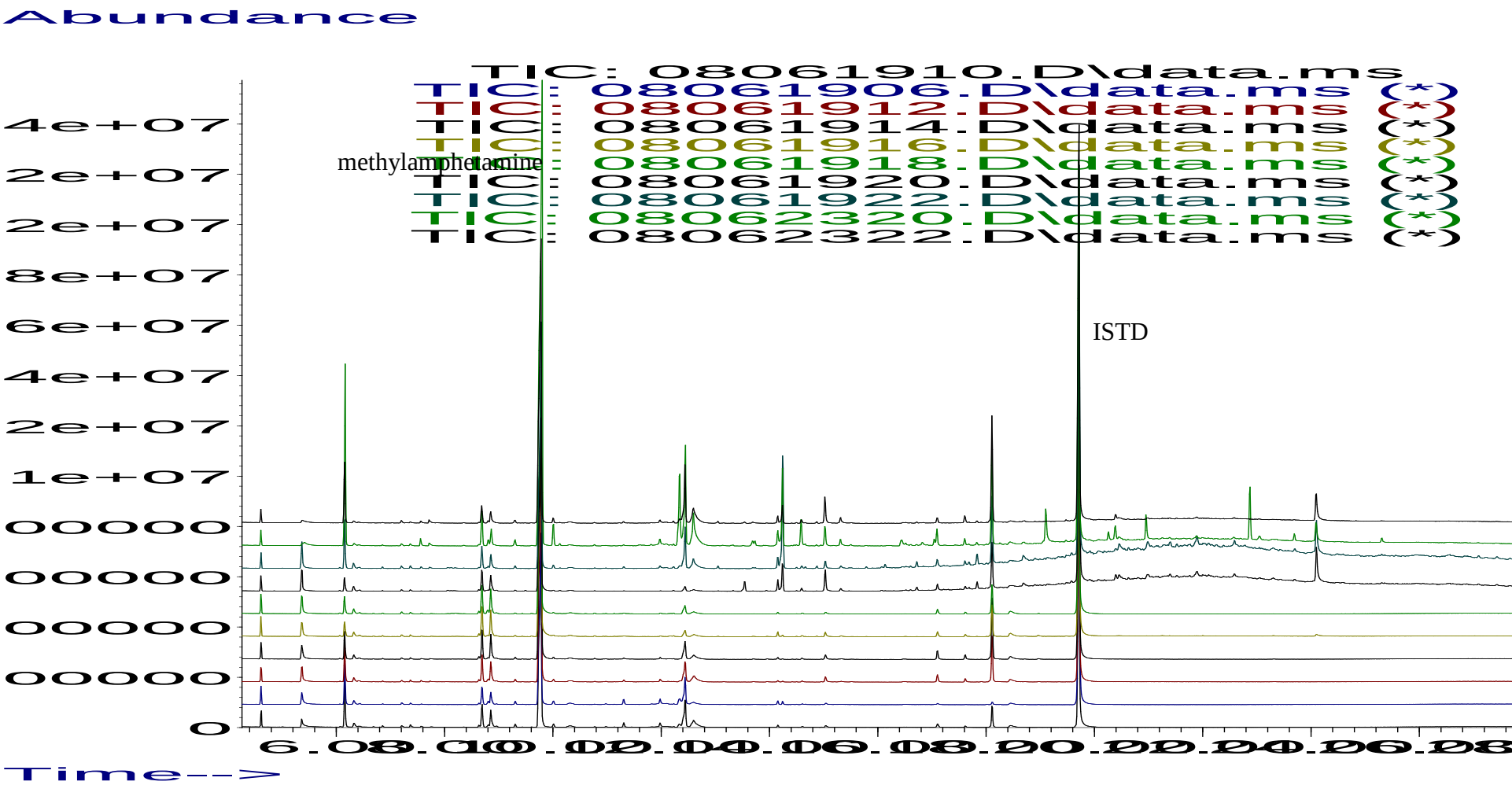

Figure 72: Overlay of the impurity profiles from the remaining ten batches extract at pH 6.0.

5.3.2.7 Emde Method

20 batches of methylamphetamine hydrochloride were synthesised using the Emde method as previously described in Chapter 3. Each of these samples were extracted using both acidic and basic buffers and analysed.

Table 31 shows impurities from the phosphate buffer extract (basic).

No	RT	Compound	Peak m/z
1	5.968	Acetic acid	**43**, 60, 91, 134
2	6.083	Benzaldehyde	**105**, 106, 77, 51
3	8.890	*cis*-1,2-dimethyl-3-phenylaziridine	**146**, 105,132, 91
4	10.496	*N*-(1-Methyl-2-phenylethylidene) methenamine	**56**, 91, 65, 39, 77
5	10.799	Dimethylamphetamine (DMA)	**72**, 91, 56, 42
6	11.363	Unknown 4	**120**, 42, 77, 91, 104, 158
7	11.769	Ephedrone	**58**, 77, 105
8	12.074	Chloroephedrine	**58**, 77, 91, 146, 166
9	12.273	Ephedrine	**58**, 77, 117, 132, 146
10	12.357	3,4-Dimethyl-5-phenyloxazolidine	**71**, 56, 91
11	12.430	unknown	**85**, 148, 70, 57, 117, 176
12	14.511	*N*-formylmethamphetamine	**86**, 58, 118
13	14.950	*N*-acetylmethamphetamine	**58**, 100
14	18.02	Benzylmethamphetamine	**91**, 148, 65, 105
15	18.38	*N*-β-(phenylisopropyl) benzyl methyl ketimine	**91**, 160, 119, 65, 77, 207
16	18.98	3,4-Dimethyl-2,5-diphenyl-oxazolidine	**146**, 147, 105, 132
17	20.294, 20.911	Methylamphetamine dimer	**238**, 91, 120,148
18	20.299	*N*-benzoylmethamphetamine	**105**, 162, 77, 91

Table 31: List of impurities found in pH 10.5 extract.

Table 32 shows impurities from the acetate buffer extract (acidic).

No	RT	Compound	Peak m/z
1	8.613	1-phenyl-2-propanone	**43**, 91, 134
2	8.728	*cis*-1,2-dimethyl-3-phenylaziridine	**146**, 105,132, 91
3	8.801	Amphetamine	**44**, 91, 134
4	9.240	1-phenyl-1,2-propanedione	**105**, 77, 51, 43
5	9.930	*trans*-1,2-dimethyl-3-phenylaziridine	**146**, 105,132, 91
6	11.290	Unknown 4	**120**, 42, 77, 91
7	12.179	Chloroephedrine	**58**, 77, 91, 146, 166
8	12.356	3,4-Dimethyl-5-phenyloxazolidine	**71**, 56, 91
9	12.524	unknown	**85**, 148, 70
10	14.51	*N*-formylmethamphetamine	**86**, 58, 118
11	14.96	*N*-acetylmethamphetamine	**58**, 100
12	18.98	3,4-Dimethyl-2,5-diphenyl-oxazolidine	**146**, 147, 105, 132
13	20.304	*N*-benzoylmethamphetamine	**105**, 162, 77, 91

Table 32: List of impurities found in pH 6 extract.

For the Emde route, previous work and this study indicate that chloroephedrine and unknown 4 are the route specific impurities and were present in all synthesised samples. Chloroephedrine is the intermediate that is used in the synthesis of methylamphetamine by the Emde route. The aziridines and the methylamphetamine dimer are also present, although they may be present in the Nagai and Moscow routes as well. These are illustrated in Figure 73.

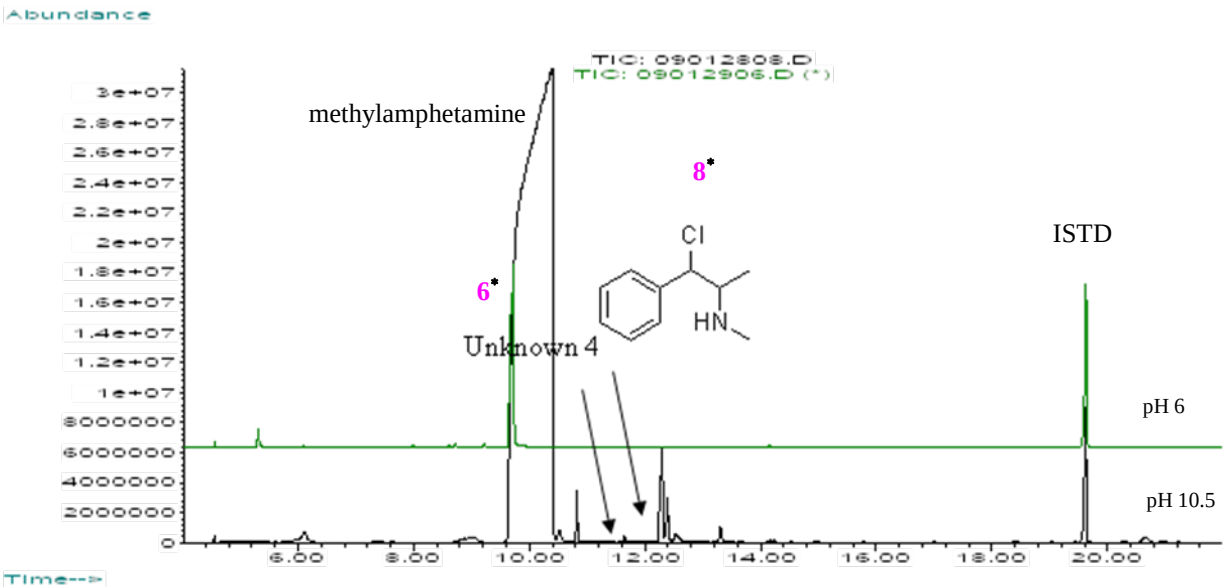

Figure 73: Overlay of the impurity profiles for both extracts. * refer to Table 31

The chromatographic results for each of the 20 batches synthesised via the Emde method are presented in Figure 74 - Figure 79. Visual comparison of the impurity profiles show obvious variation between the 20 profiles, particularly within the 12 - 19 minute range, and in the range 20 – 22 minute range in pH 10.5 extraction (Figure 75).

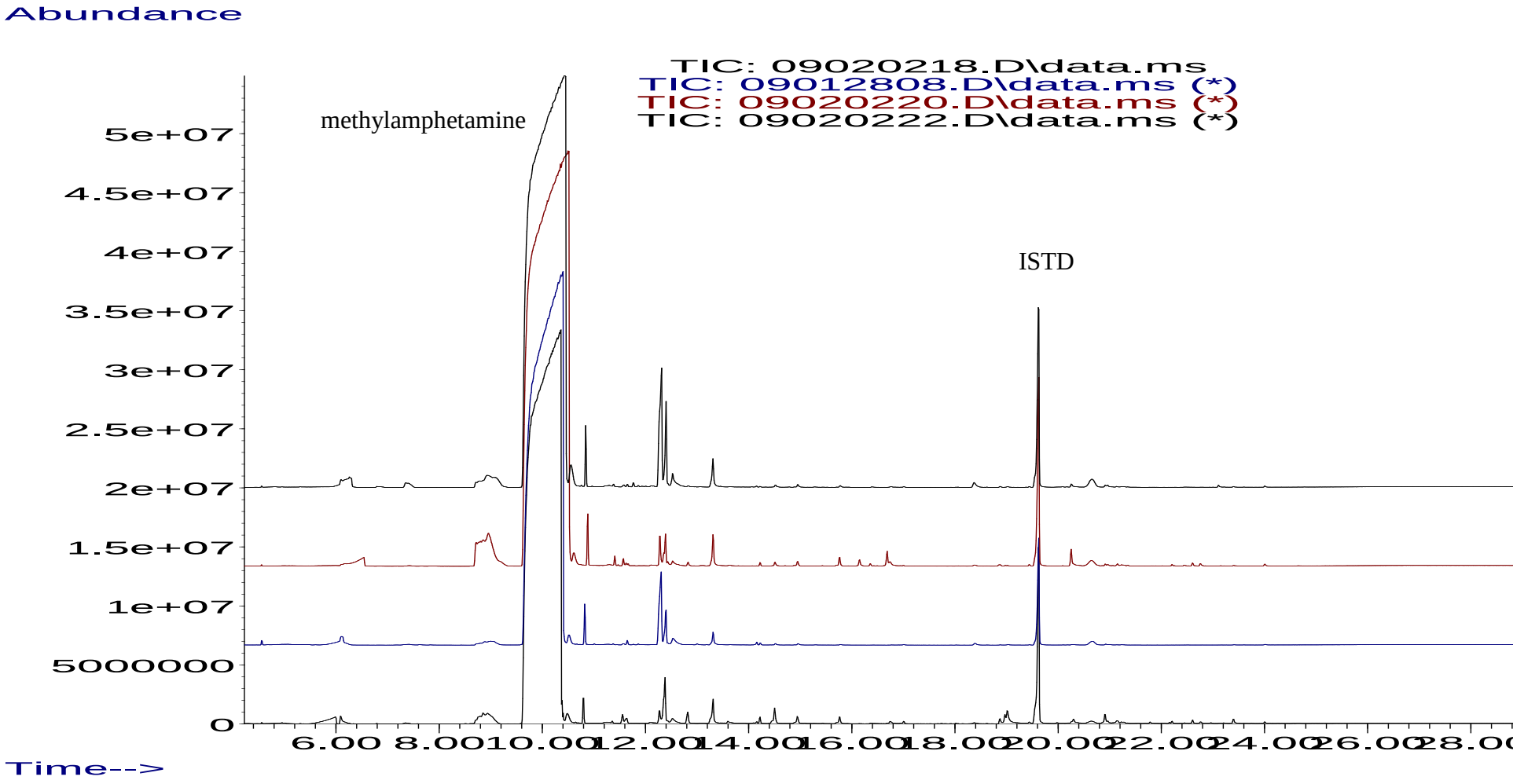

Figure 74: Overlay of the impurity profiles from the first four batches extract at pH 10.5.

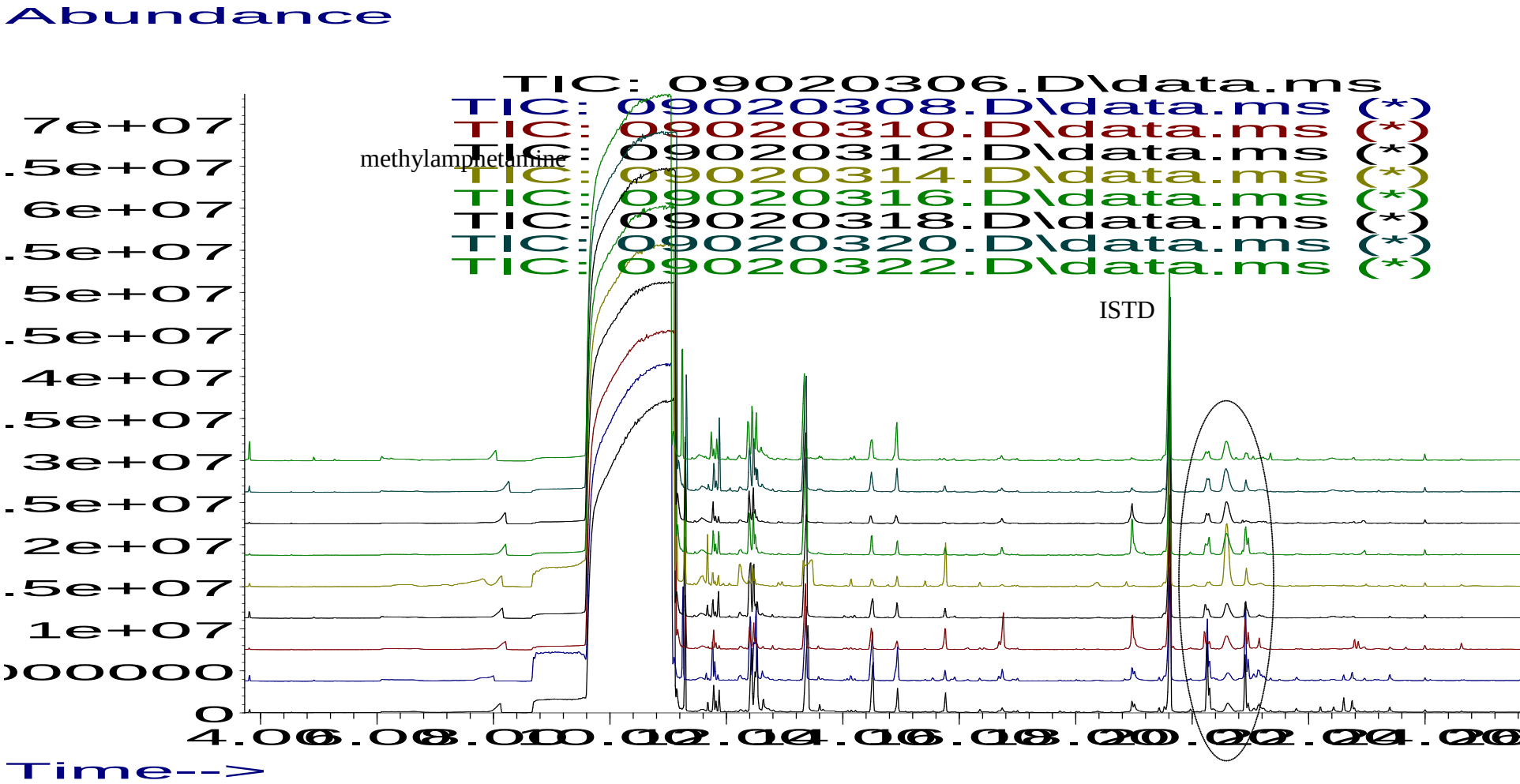

Figure 75: Overlay of the impurity profiles from the next nine batches extract at pH 10.5.

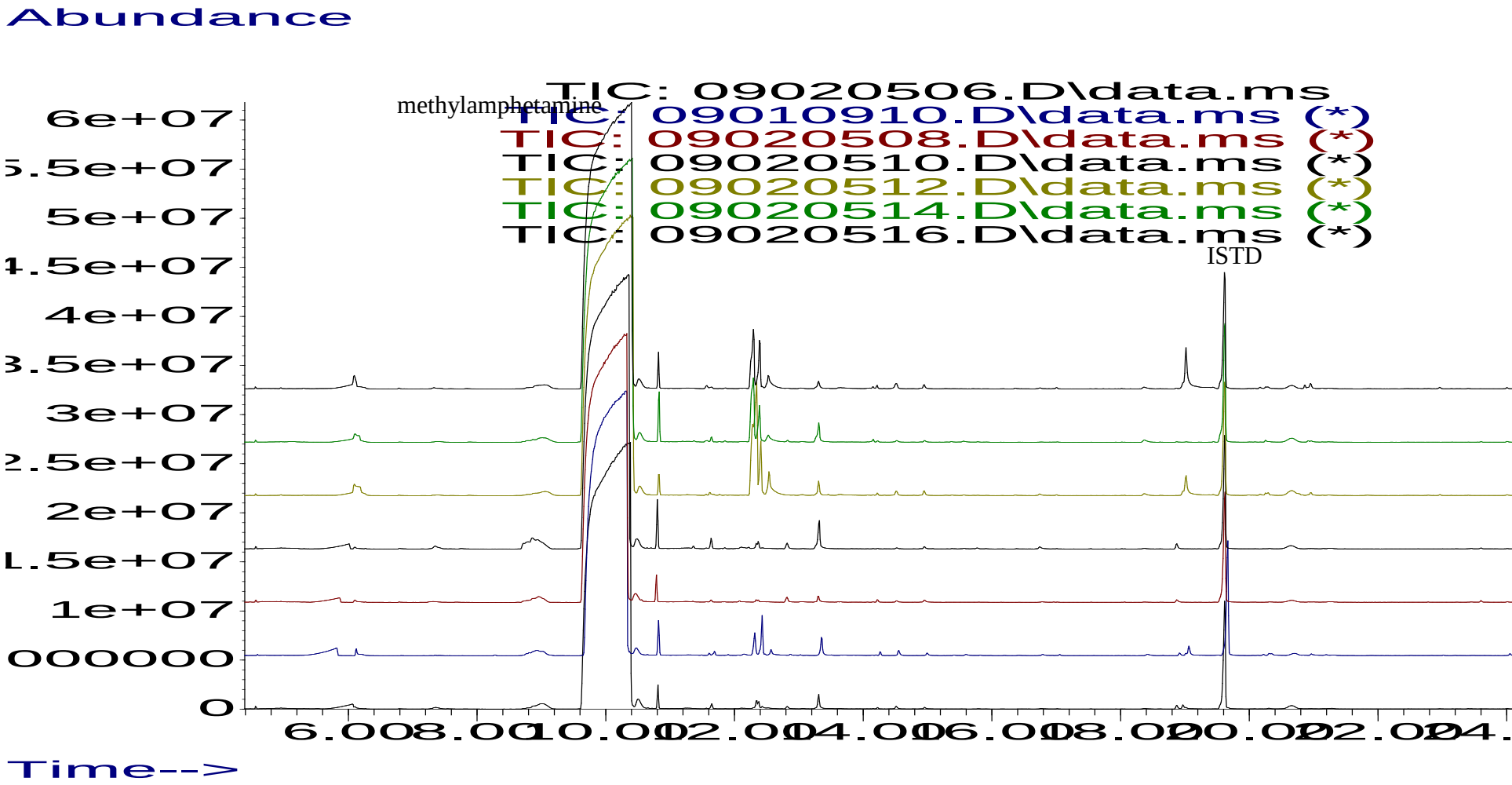

Figure 76: Overlay of the impurity profiles from the remaining seven batches extract at pH 10.5

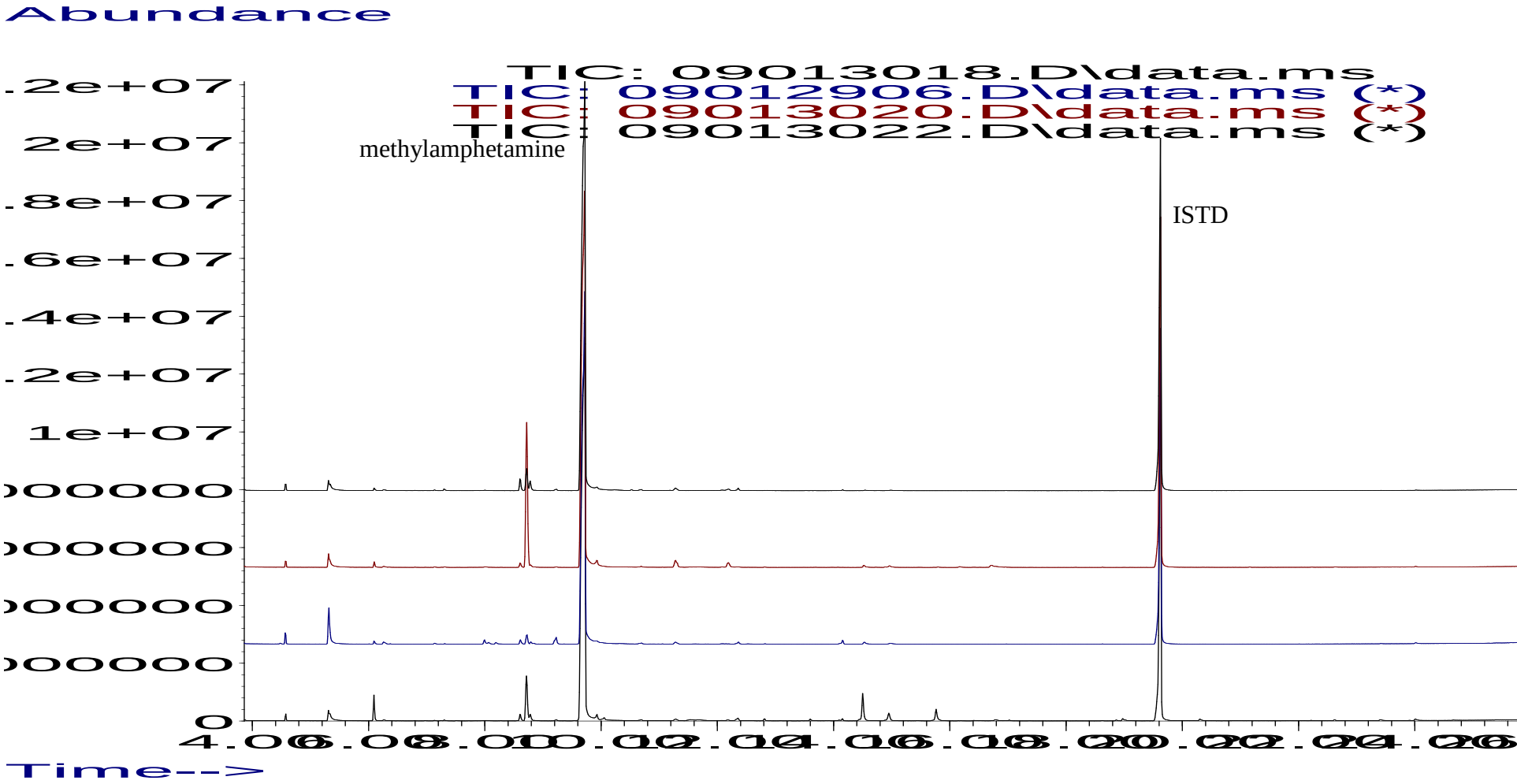

Figure 77: Overlay of the impurity profiles from the first four batches extract at pH 6.0.

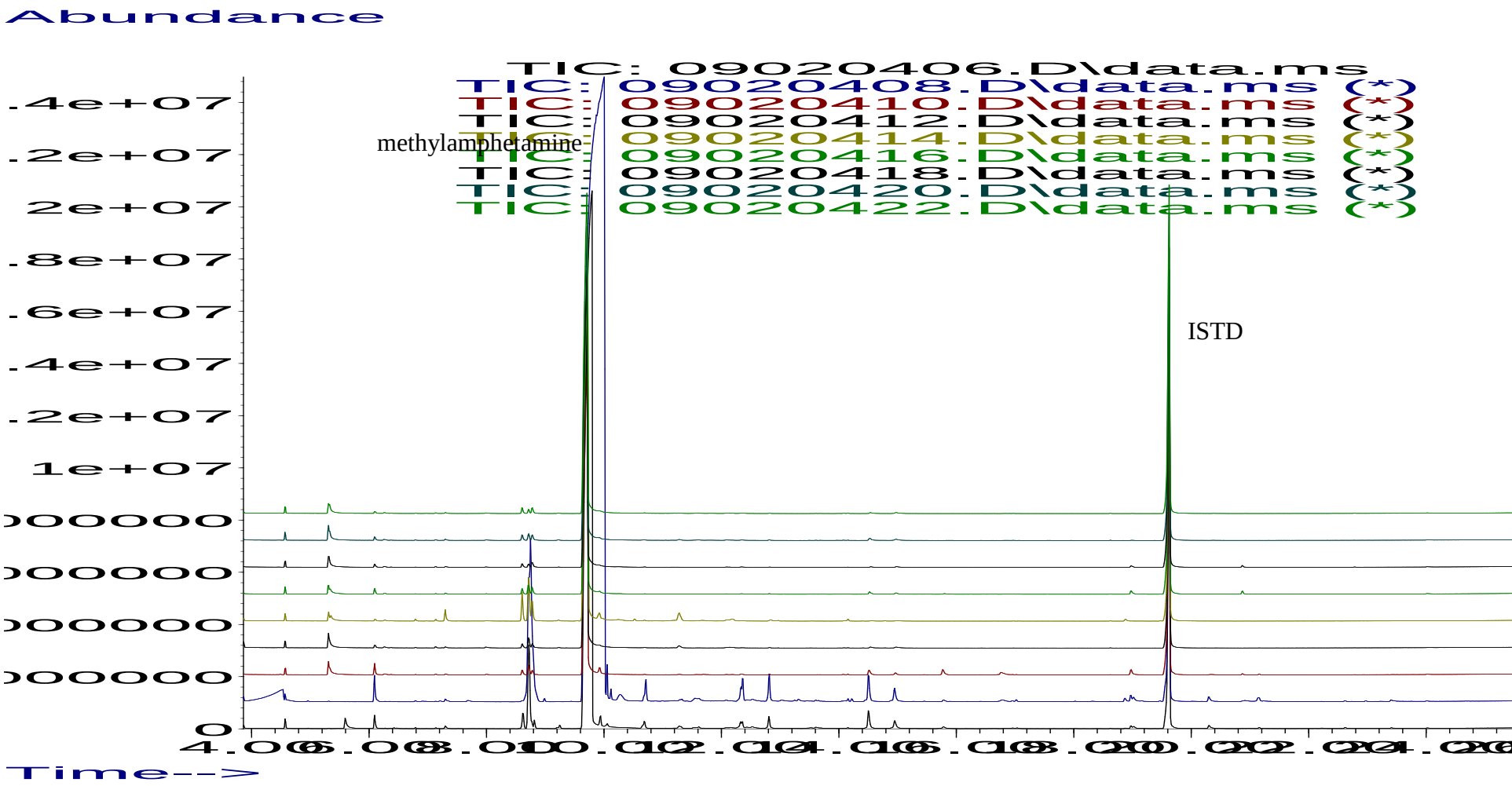

Figure 78: Overlay of the impurity profiles from the next nine batches extract at pH 6.0.

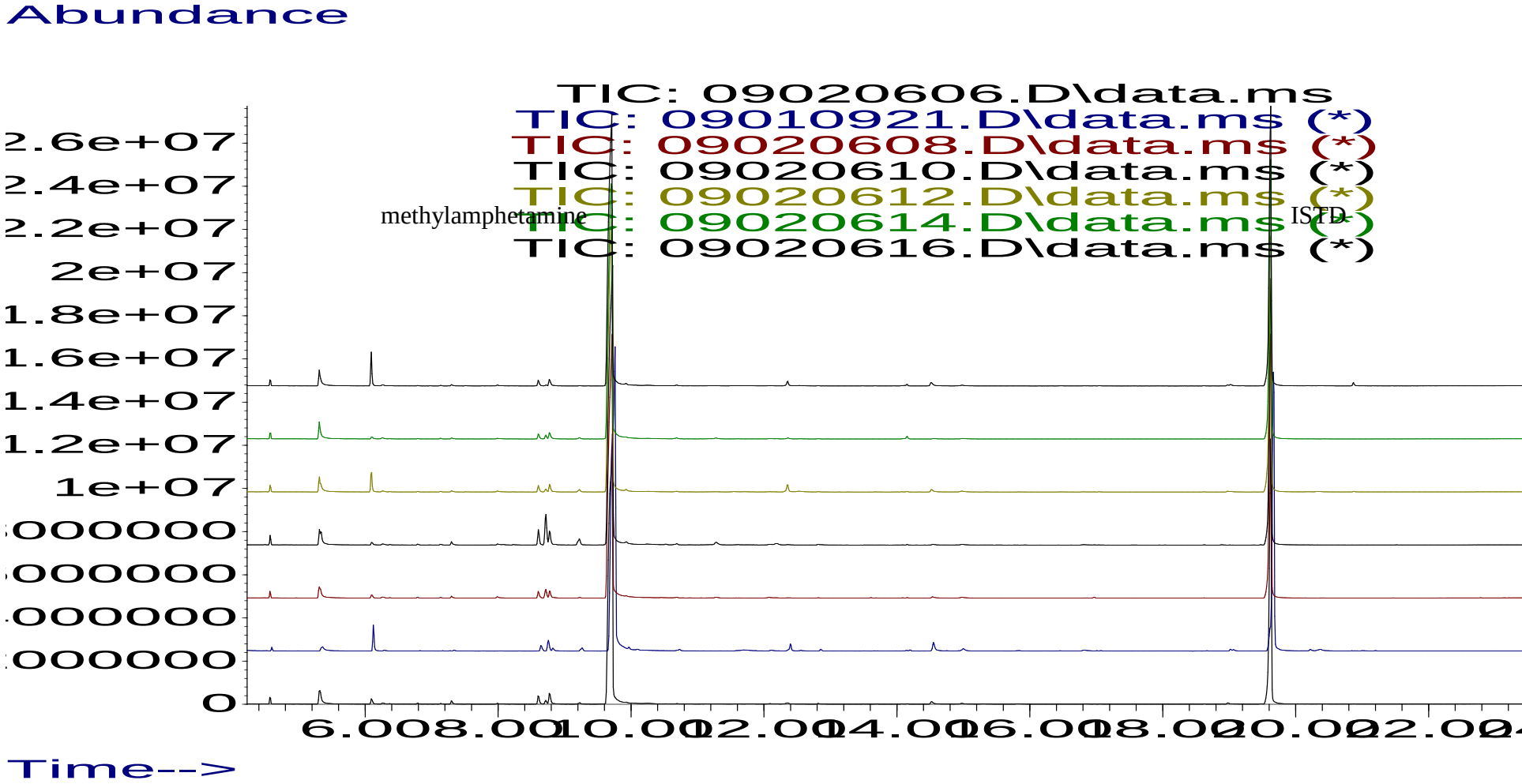

Figure 79: Overlay of the impurity profiles from the remaining seven batches extract at pH 6.0.

5.3.2.8 Moscow Method

25 batches of methylamphetamine hydrochloride were synthesised using the Moscow method as previously described in Chapter 3. Each of these samples were extracted using both acidic and basic buffers and analysed.

Table 33 shows impurities from the phosphate buffer extract (basic).

No	RT	Compound	Peak m/z
1	7.252	Acetic acid	**43**, 60, 91, 134
2	9.521	Amphetamine	**44**, 91, 65, 134
3	10.801	Unknown 5	**43**, 125, 89, 168, 105, 91, 63
4	10.912	*N*-(1-Methyl-2-phenylethylidene) methenamine	**56**, 91, 65, 39, 77
5	11.131	Dimethylamphetamine (DMA)	**72**, 91, 56, 42
6	11.738	*Z* (1-phenylpropan-2-one oxime)	**91**, 149, 116, 131
7	11.780	*E* (1-phenylpropan-2-one oxime)	**91**, 131, 116, 149
8	12.47	3,4-Dimethyl-5-phenyloxazolidine	**71**, 56, 91
9	12.51	3,4-Dimethyl-5-phenyloxazolidine	**71**, 56, 91
10	13.662	*N*-formylamphetamine	**118**, 72, 44, 91
11	14.321	Bibenzyl	**91**, 182
12	14.593	*N*-formylmethylamphetamine	**86**, 58, 118
13	15.032	*N*-acetylmethylamphetamine	**58**, 100
14	17.818	*cis* 3,4-Diphenyl-3-buten-2-one	**179**, 178, 222, 221
15	18.111	*trans* 3,4-Diphenyl-3-buten-2-one	**179**, 178, 222, 221
16	18.127	Benzylmethamphetmine	**91**, 148, 65, 105
17	18.440	*N*-β-(phenylisopropyl) benzyl methyl ketimine	**91**, 160, 119, 65, 77, 207
18	18.801	Unknown 6	**91**, 145, 262
19	20.051	Dimethylphenylnaphthalene	**232**, 217, 202, 77
20	20.117	*N*-benzoylamphetamine	**105**, 77, 148, 91, 118
21	20.208	Benzylmethnaphthalene	**232**, 217, 202, 58
22	20.344	*N*-methyl-N-(α-methylphenethyl) amino-1-phenyl-2-propanone	**238**, 91, 105, 190, 120
23	20.417	*N*-benzoylmethylamphetamine	**105,** 162, 77, 91
24	22.361	*N,N*-di-(β-phenylisopropyl) formamide	**190**, 91, 58, 119, 77, 105
25	22.425	(*Z*)-*N*-methyl-*N*-(α-methylphenethyl)-3-phenylpropenamide	**131**, 91, 58, 103, 188, 77

Table 33: List of impurities found in pH 10.5 extract.

Table 34 shows impurities from the acetate buffer extract (acidic).

No	RT	Compound	Peak m/z
1	8.716	1-phenyl-2-propanone	**43**, 91, 134
2	10.801	Unknown 5	**43**, 125, 89, 168, 105, 91, 63
3	8.894	Amphetamine	**44**, 91, 134
4	9.323	1-phenyl-1,2-propanedione	**105**, 77, 51, 43
5	10.138	3-phenyl-3-buten-2-one	**103, 146, 91**
6	10.211	*N*-*N*-Dimethylbenzylamine	**58**, 135, 107,79
7	13.673	*N*-formylamphetamine	**118**, 72, 44, 91
8	14.603	*N*-formylmethylamphetamine	**86**, 58, 97, 118
9	15.053	*N*-acetylmethylamphetamine	**58**, 100
10	20.041	Dimethylphenylnaphthalene	**232**, 217, 202, 58
11	20.208	Benzylmethnaphthalene	**232**, 217, 202, 58
12	20.355	*N*-methyl-N-(α-methylphenethyl) amino-1-phenyl-2-propanone	**238**, 91, 105, 190, 120
13	20.407	*N*-benzoylmethylamphetamine	**105**, 162, 77, 91

Table 34: List of impurities found in pH 6 extract.

All the four specific impurities which were identified in the Nagai method samples were also observed in the samples synthesised via the Moscow route. Two route specific unknown impurities however were detected in methylamphetamine synthesised by the Moscow method allowing differentiation from Nagai route samples. Samples synthesised by the Moscow route also exhibit a relatively large P-2-P peak. These are illustrated in Figure 80.

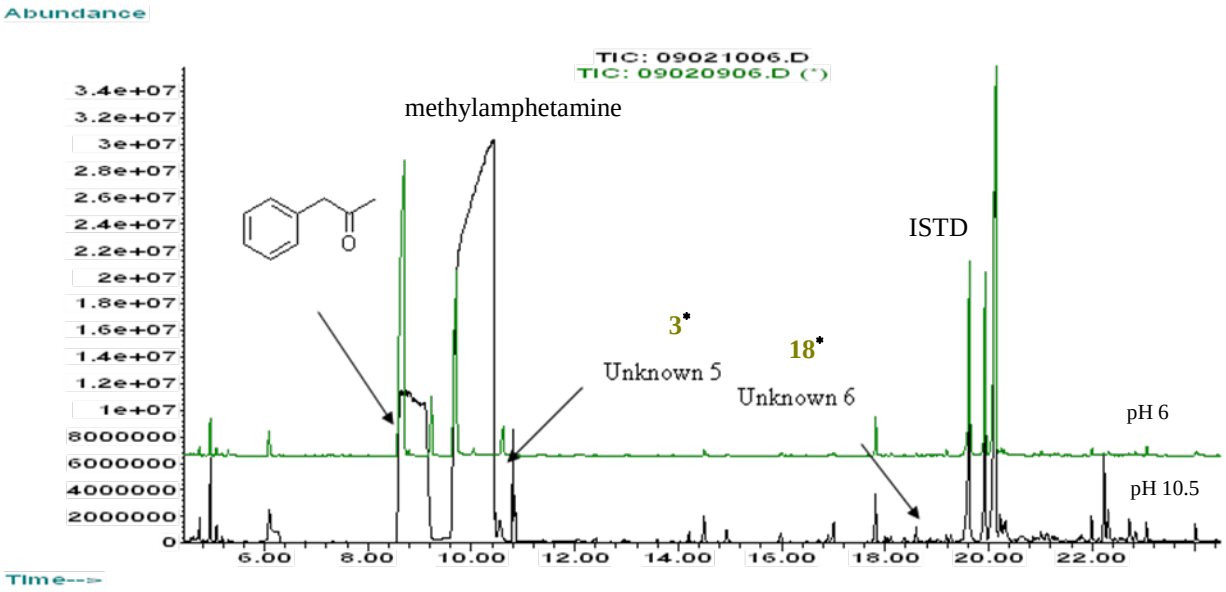

Figure 80: Overlay of the impurity profiles for both extracts. * refer to Table 33

The chromatographic results for each of the 25 batches synthesised via the Moscow method are presented in Figure 81- Figure 84. Visual comparison of the impurity profiles show obvious variation between the 25 profiles, particularly within the 8 - 9 minute range, and in the range 14 – 24 minute range in pH 10.5 extraction (Figure 81).

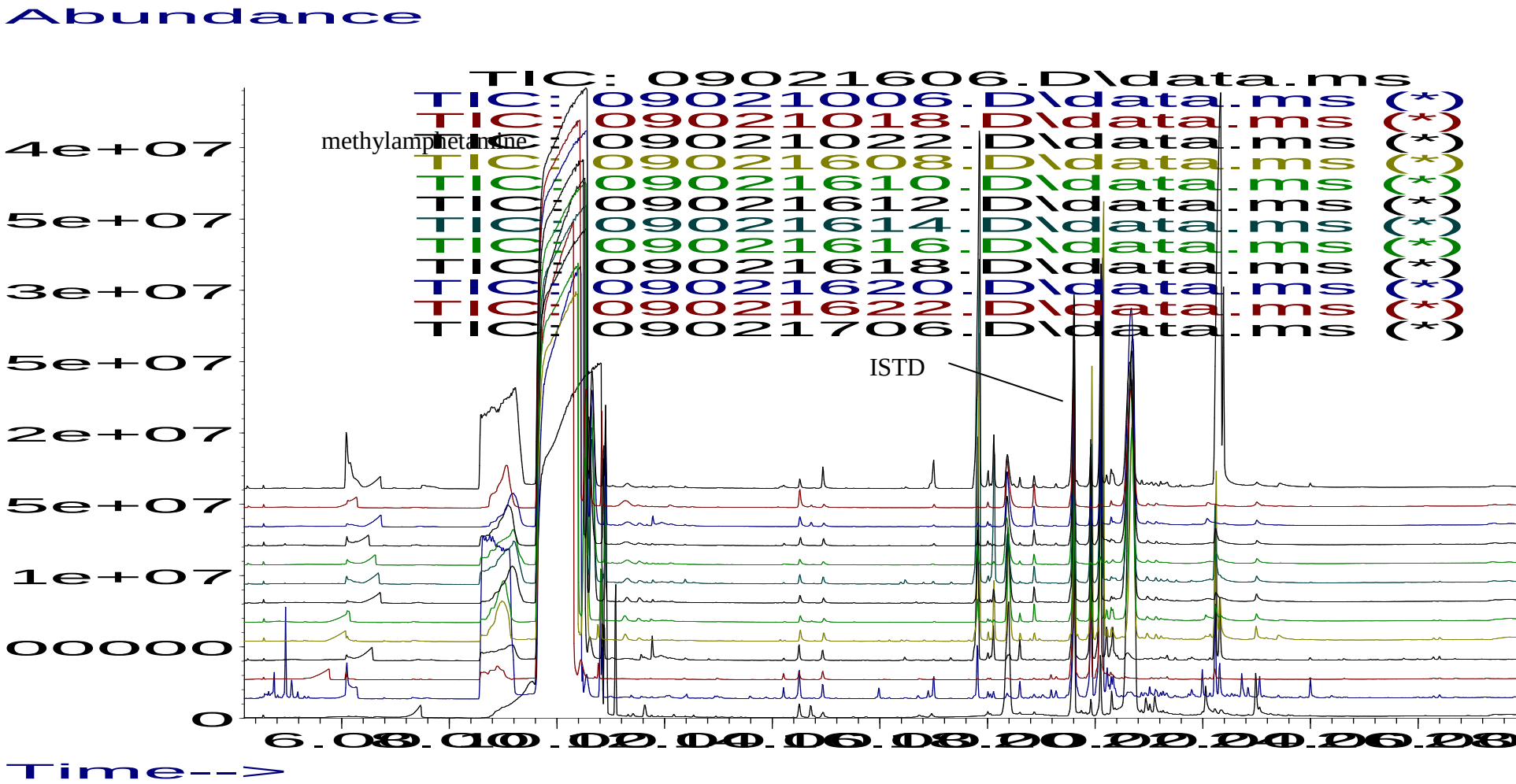

Figure 81: Overlay of the impurity profiles from the first thirteen batches extract at pH 10.5.

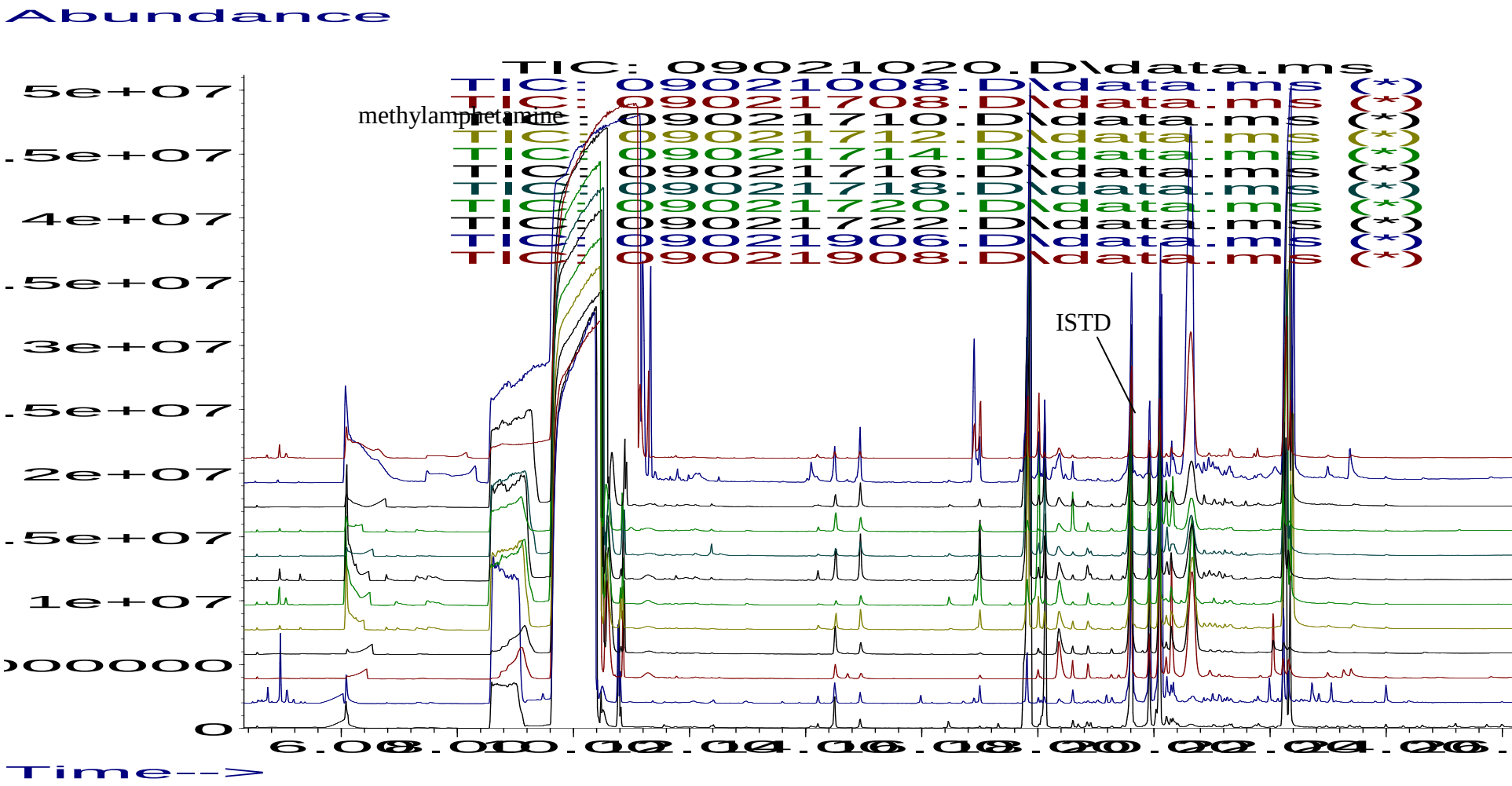

Figure 82: Overlay of the impurity profiles from the remaining twelve batches extract at pH 10.5.

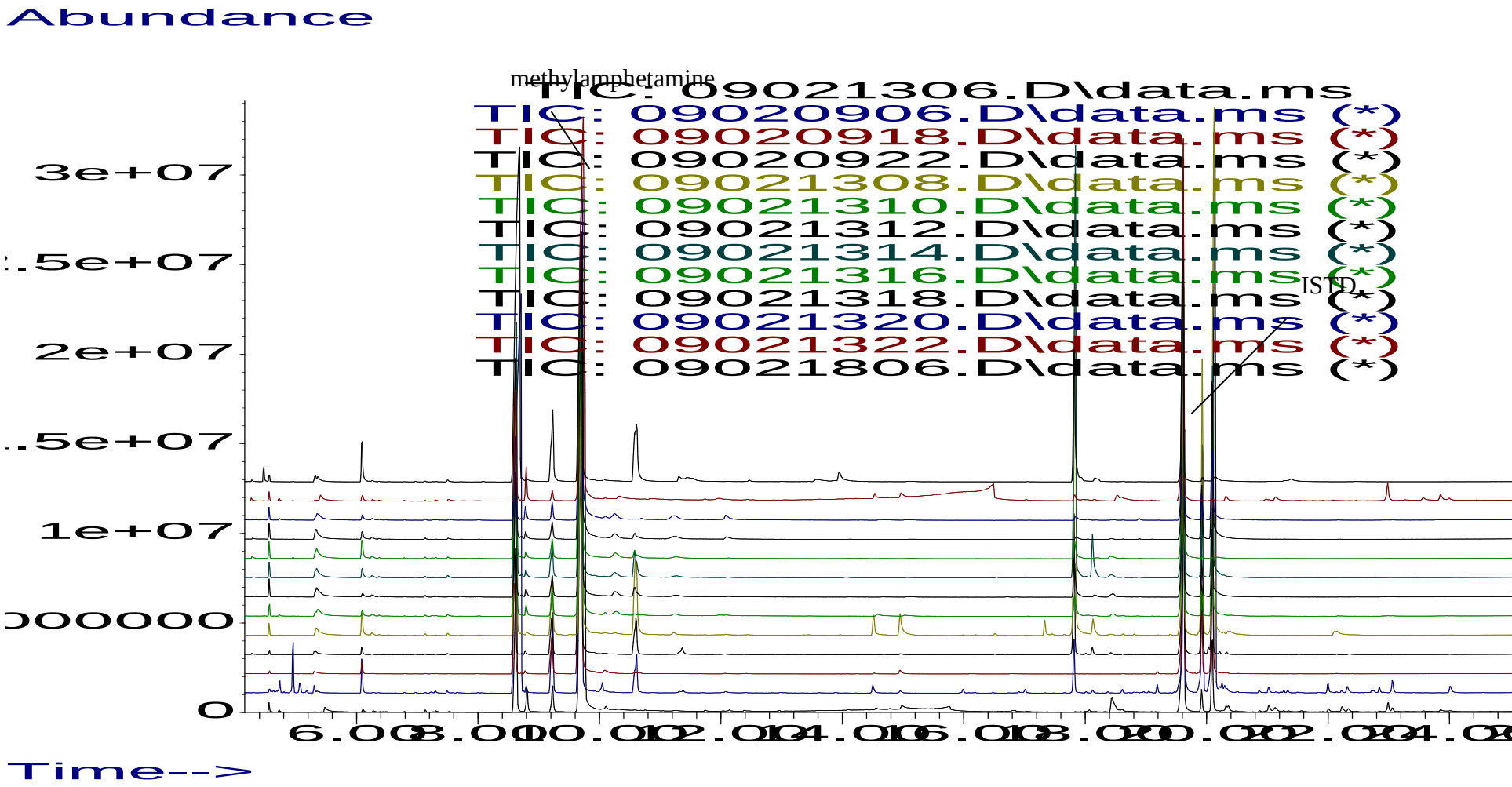

Figure 83: Overlay of the impurity profiles from the first thirteen batches extract at pH 6.0

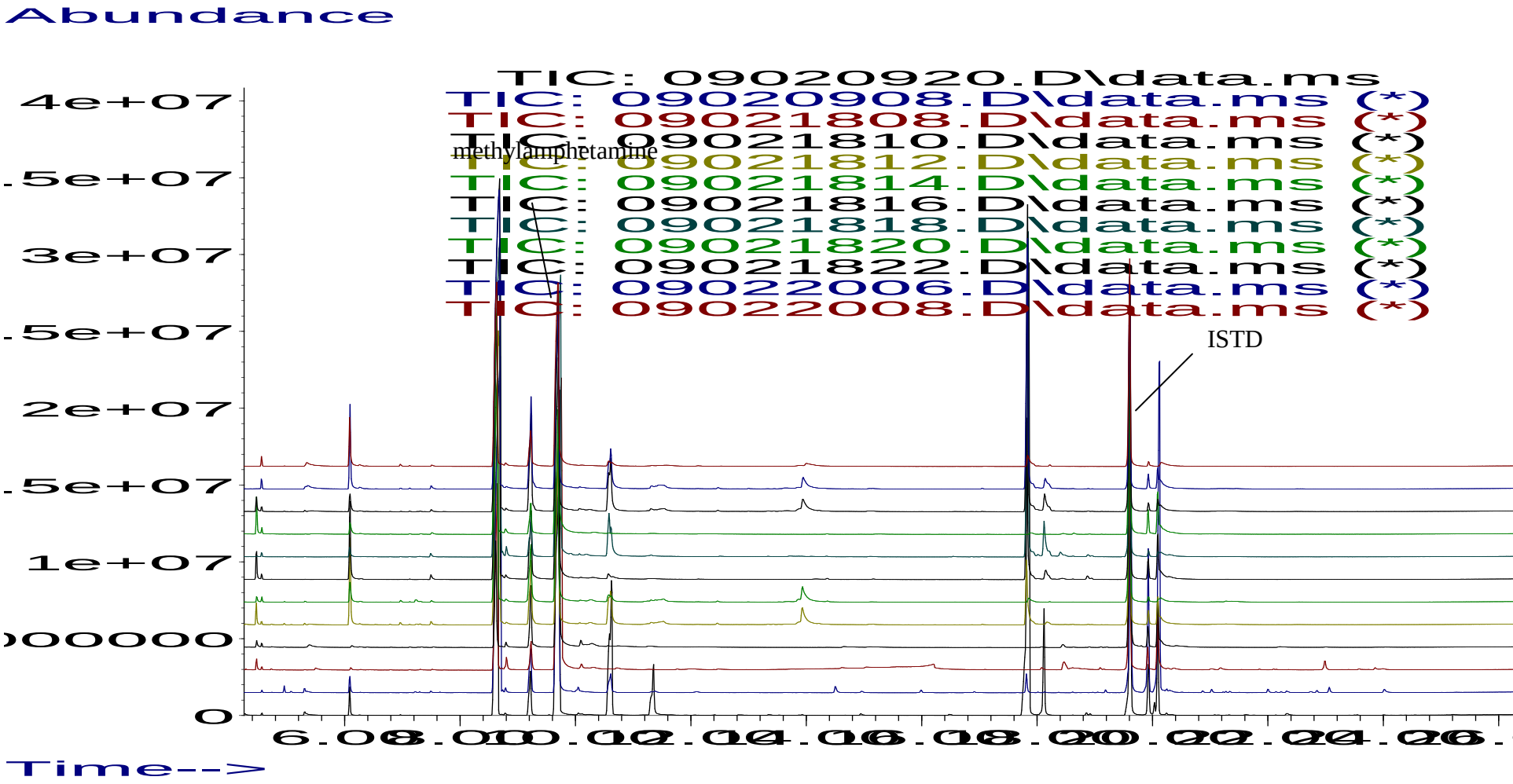

Figure 84: Overlay of the impurity profiles from the remaining twelve batches extract at pH 6.0.

5.3.2.9 Conclusions of the synthetic methods utilising ephedrine or *pseudo*ephedrine as starting materials

Separation of methylamptetamine produced by the Nagai and Emde methods seems to be the most complicated in terms of previously published studies. Previous studies have focused mainly on the naphthalenes, aziridines and methylamphetamine dimer. This study confirmed the work of Ko et al.[5] in the determination of the Emde route specific impurities as two aziridines, methylamphetamine dimer, chloroephedrine, and the unknown 4.

Inoue et al.[6] used a DB-5 column to separate the aziridine and methylamphetamine extracted with a phosphate buffer at pH 10.5. It was not possible to achieve this separation using a DB-1MS column with the same pH 10.5 extraction as the broad methylamphetamine peak masked the small aziridine peak. However, using an acidic extraction (pH 6), both components could be resolved using a DB-1MS column because the methylamphetamine is not extracted in such a great quantity. While this is important to report, an acidic extract may not be necessary since the aziridines are not required for (or capable of) discriminating the Nagai and Emde samples. A further comparison of the performance of the DB-5 column using a pH 10.5 extraction for selected batches of the samples synthesised in this study is reported in Section 5.6.

5.3.3 Comparison of the chromatographic profiles of all synthesised samples using the Pearson Correlation matrix approach

The impurity profiles were compared with each other using a Pearson correlation coefficient matrix where the linkage threshold defined the goodness of fit for samples within their synthetic group. The chromatographic profiles revealed for the synthesised samples were interrogated for two different sets of impurities. The first were obtained from the GCMS and extraction conditions reported by Andersson et al.[7] where a list of suggested methylamphetamine impurities were presented [8] and have been designated as CHAMP (''Collaborative Harmonisation of Methods for Profiling of Amphetamine Type Stimulants'') impurities in this work. The second was a set of target impurities revealed through the GCMS analysis within this study and selected as the route specific impurities previously identified. A full set of the relevant impurities from CHAMP study [8] and this study are presented in Appendix D.

In total, nine data pre treatment refinements of the various GCMS data sets were investigated in an effort to gain the most accurate mathematical discrimination of the samples using the Pearson correlation matrix. The data pre-treatment methods were selected based on those suggested by the CHAMP authors[8] (i.e. normalisation, square root and fourth root). In this study a further pretreatment method, the sixteen root was also incorporated. The nine refinements were as follows:

1. CHAMP impurities normalised to the sum of the targets and pre-treated with square root method;
2. CHAMP impurities normalised to the sum of the targets and pre-treated with fourth root method;
3. CHAMP impurities normalised to the sum of the targets and pre-treated with sixteen roots method;
4. Target impurities from this study normalised to the sum of the targets and pre-treated with square root method;
5. Target impurities from this study normalised to the sum of the targets and pre-treated with fourth root method;

6. Target impurities from this study normalised to the sum of the targets and pre-treated with sixteen roots method;
7. CHAMP impurities plus target impurities from this study normalised to the sum of the targets and pre-treated with square root method;
8. CHAMP impurities plus target impurities from this study normalised to the sum of the targets and pre-treated with fourth root method; and
9. CHAMP impurities plus target impurities from this study normalised to the sum of the targets and pre-treated with sixteen roots method.

The success of the GCMS profiling method was assessed by its ability to produce Pearson correlation coefficients which would facilitate the correct allocation of individual drug batches to their synthetic route, while not permitting the batches between synthetic routes to be deemed similar. Before the results are presented, a discussion of the calculation of Pearson correlation coefficients and the effect of the data pre-treatment methods is undertaken in the following two sections.

5.3.3.1 Pearson Correlation Coefficient

Pearson correlation coefficient, r, is a measure of the correlation between two variables. The value usually ranges from –1 to +1 (with +1 indicating a positive linear relationship, -1 indicating a negative linear relationship, and 0 indicating no linear relationship between the two variables), although the coefficients may be scaled over a different range for ease of use if required. The coefficient can be calculated by the following equation:

$$r = \frac{\sum_{i=1}^{n} x_i y_i - \sum_{i=1}^{n} x_i \sum_{i=1}^{n} y_i}{\sqrt{\left[n\sum_{i=1}^{n} x_i^2 - (\sum_{i=1}^{n} x_i)^2\right]\left[n\sum_{i=1}^{n} y_i^2 - (\sum_{i=1}^{n} y_i)^2\right]}}$$ ……..Equation 5.1

where x and y represent the two samples under comparison and n is the number of variables per sample.[9]

An Excel macro, which allows convenient calculation of Pearson correlation coefficients for data input by the user, has been developed by the European Network of Forensic Institutes (ENFSI) drug working group and was used in this study.[10] The coefficients are scaled such that a maximum positive correlation corresponds to a value of +100, maximum negative correlation corresponds to a value of –100, and no correlation corresponds to a value of 0. For the purpose of comparing chromatograms, a value of +100 represents maximum similarity between profiles.[10]

While Pearson correlation coefficients conveniently qualify the relative similarity between impurity profiles in a data set, it is up the user to evaluate the meaning of the value of r. Application of this statistic to a data set of samples of which the origin (i.e. similarity) is known will allow the threshold value to be set such that all of the known samples within each synthetic route are grouped together.

5.3.3.2 Data Pre-Treatment Methods

In order to reduce the influence of larger peak areas in, for example, a chromatogram, data can be pre-treated, or transformed, before statistical analysis. Two pre-treatment methods investigated by the (CHAMP) authors[8] were the square root and fourth root methods. When pre-treating the data with the square root method, each data point is replaced by its square root. Similarly, the fourth root and sixteenth roots require replacing each data point by its fourth root and sixteenth roots respectively. These types of pre-treatment effectively reduce the range over which the data points are spread by reducing the magnitude of the larger data points (or increasing the magnitude of the smaller points for values between 0 and 1). This effect is highlighted in Table 35 in which a hypothetical set of 10 randomly generated data points is pre-treated using both methods.

Random Raw Data	After Square Root Pre-Treatment	After Fourth Root Pre-Treatment	After Sixteen Root Pre-Treatment
9.99	3.16	1.78	1.15
3.31	1.82	1.35	1.08
7.07	2.66	1.63	1.13
0.86	0.93	0.96	0.99
6.5	2.55	1.60	1.12
8.62	2.94	1.71	1.14
4.56	2.14	1.46	1.10
1.19	1.09	1.04	1.01
5.21	2.28	1.51	1.11
2.45	1.57	1.25	1.06

Table 35: The effects of square root, fourth root and sixteenth roots data pre-treatment techniques on a set of randomly generated data.

It is apparent that the spread of the raw data, which originally spanned 0.86 through 9.99, is reduced to a range of 0.93 to 3.16 after pre-treating with the square root technique, and further reduced to 0.96 to 1.78 and 0.99 to 1.15 after pre-treating with the fourth and sixteenth root technique respectively. These pre-treatment effects are illustrated graphically in Figure 85.

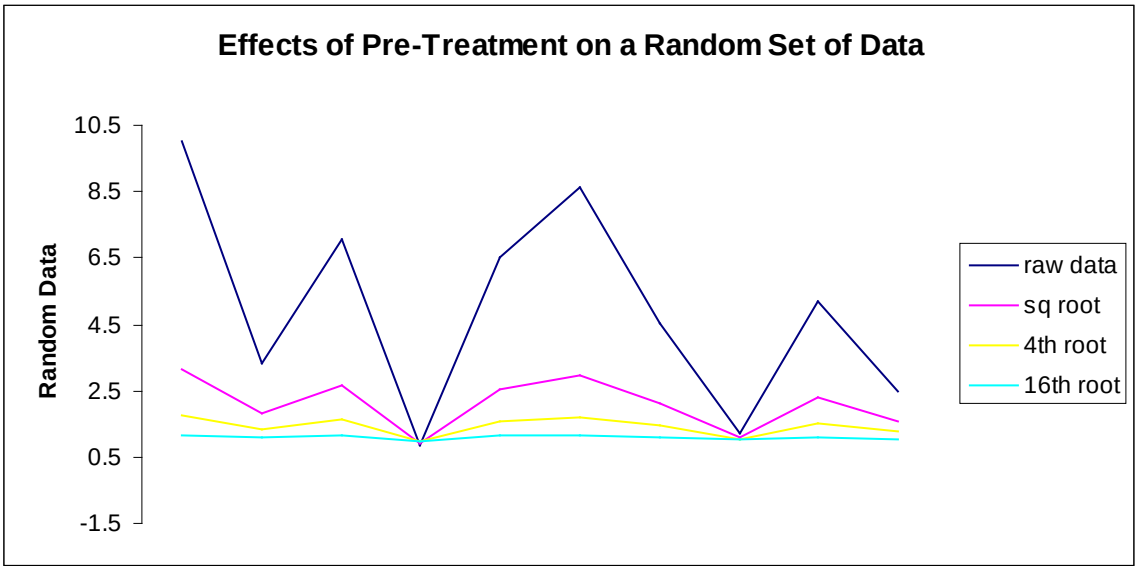

Figure 85: Graphical illustration of the effect of square, fourth and sixteen root pre-treatment on a random set of data.

The square root method and, to a lesser extend, the fourth and sixtenth root methods are accepted and used relatively widely as data transformation methods [11, 12] similar to the common log transformation.[11] The square, fourth and sixteenth roots methods are more suitable than the log transformation when the data set has many zeroes (as is the case with drug profiling data in which some of the target impurities are not present).

5.3.3.3 Results of Pearson Correlation Coefficient analysis

To compare the profiles as the CHAMP method recommend, Pearson correlation coefficients were calculated for every pair of samples in the nine data sets detailed in beginning of this section (i.e. both the CHAMP and this study target impurity lists, and the three data pre-treatment methods as outlined previously). After interrogation of each of the 146 methylamphetamine samples analysed for target impurities, 21 of the 24 CHAMP impurities were identified within the analytical results derived from the samples together with the additional 15 route specific impurities across the seven synthetic routes. The Pearson correlation coefficients were calculated for each pair of samples using the nine data sets discussed previously. Since the 'true' relationships of the samples were known, a threshold value for the calculated coefficients was sought such that values above the threshold indicated the related samples and values below the threshold indicated unrelated samples.

The correct synthetic route assignment at a threshold level of 95.00 (equivalent to 95%) was not facilitated by using the CHAMP impurities on their own, and/or in combination with the 15 route specific impurities identified in this study, where the peak areas were normalised to the sum of the targets and pre-treated with either the square root method or fourth root method.

Similarly, the CHAMP impurities on their own, normalised to the sum of the targets and pre-treated with the sixteenth root method did not completely resolve all of the sample batches into their respective synthetic routes and some overlap between Nagai and Moscow batches was observed. This demonstrated that 5.48% (500 pairing) of the samples were incorrectly linked together because their Person correlation coefficients are

below than the 95.00 threshold. CHAMP impurity list suggested for methylamphetamine samples did not incorporate sufficient route specific impurities to facilitate differentiation between the Nagai and Moscow route.

Accurate discrimination by synthetic route of the 146 batches was achieved using only the 15 target impurities identified in this study, normalised to the sum of the targets and pre-treated with the sixteen root method. The lowest coefficient calculated for a pair of samples from within a synthetic route was 79.60 and the maximum threshold that would allow the 146 samples within each route to be deemed similar was 97.37. With a 95.00 threshold value (equivalent to 95%), all sample batches were correctly classified into their respective synthetic routes. Combining the CHAMP impurities with the 15 target impurities identified in this study normalised to the sum of the targets and pre-treated with the sixteen root method revealed similar results. A summary of the results are tabulated in Tables 36 – Table 38.

An obvious explanation for the poor performance of the CHAMP method is that the target impurity lists does not adequately draw out the information from each sample which would facilitate accurate discrimination. An inclusion of route specific impurities such as those indicated in this study would therefore be advantageous.

CHAMP impurities normalised to the sum of the targets and pre-treated			
Square root			
Route	MIN	MAX	AVERAGE
Leuckart	1.84	100	72.56
Red Amination	-2.94	100	77.14
Nagai	48.68	100	90.99
Rosenmund	69.25	100	93.94
Birch	87.95	100	98.83
Emde	29.17	100	80.55
Moscow	34.71	100	76.73
4th Root			
Route	MIN	MAX	AVERAGE
Leuckart	49.81	100	88.02
Red Amination	79.18	100	91.99
Nagai	81.27	100	96.59
Rosenmund	84.57	100	96.32
Birch	88.29	100	98.69
Emde	71.86	100	92.90
Moscow	70.94	100	91.24
16th Root			
Route	MIN	MAX	AVERAGE
Leuckart	96.27	100	99.04
Red Amination	98.39	100	99.40
Nagai	98.71	100	99.75
Rosenmund	98.47	100	99.57
Birch	98.88	100	99.85
Emde	98.41	100	99.54
Moscow	97.35	100	99.34

Table 36: Summary of the Pearson correlation coefficients for 146 methylamphetamine batches synthesised by seven synthetic routes using CHAMP impurities normalised to the sum of the targets and pre-treated with square root, fourth root and sixteenth root method.

Target impurities from this study normalised to the sum of the targets and pre-treated			
Square root			
Route	MIN	MAX	AVERAGE
Leuckart	-5.44	100	60.21
Red Amination	73.28	100	90.36
Nagai	51.47	100	90.48
Rosenmund	51.67	100	88.34
Birch	98.22	100	99.68
Emde	31.85	100	82.74
Moscow	37.07	100	76.99
4th Root			
Route	MIN	MAX	AVERAGE
Leuckart	61.60	100	90.99
Red Amination	87.13	100	94.88
Nagai	81.43	100	95.88
Rosenmund	73.60	100	93.74
Birch	97.13	100	99.44
Emde	72.90	100	93.44
Moscow	73.27	100	91.45
16th Root			
Route	MIN	MAX	AVERAGE
Leuckart	97.22	100	99.33
Red Amination	98.88	100	99.53
Nagai	98.62	100	99.67
Rosenmund	97.64	100	99.48
Birch	99.67	100	99.92
Emde	98.53	100	99.59
Moscow	97.45	100	99.37

Table 37: Summary of the Pearson correlation coefficients for 146 methylamphetamine batches synthesised by seven synthetic routes using target impurities from this study normalised to the sum of the targets and pre-treated with square root, fourth root and sixteenth root method.

CHAMP impurities plus target impurities from this study normalised to the sum of the targets and pre-treated

Square root

Route	MIN	MAX	AVERAGE
Leuckart	15.43	100	78.53
Red Amination	75.46	100	90.16
Nagai	52.45	100	89.98
Rosenmund	68.86	100	93.21
Birch	87.86	100	98.78
Emde	32.96	100	81.84
Moscow	35.46	100	76.55

4^{th} Root

Route	MIN	MAX	AVERAGE
Leuckart	62.68	100	91.53
Red Amination	87.53	100	94.69
Nagai	82.92	100	95.97
Rosenmund	83.02	100	95.44
Birch	89.36	100	98.74
Emde	75.68	100	93.78
Moscow	73.77	100	91.50

16^{th} Root

Route	MIN	MAX	AVERAGE
Leuckart	97.38	100	99.35
Red Amination	98.79	100	99.50
Nagai	98.71	100	99.68
Rosenmund	98.18	100	99.50
Birch	99.12	100	99.88
Emde	98.79	100	99.62
Moscow	97.58	100	99.39

Table 38: Summary of the Pearson correlation coefficients for 146 methylamphetamine batches synthesised by seven synthetic routes using CHAMP impurities plus target impurities from this study normalised to the sum of the targets and pre-treated with square root, fourth root and sixteenth roots method.

5.4 Time study for the Nagai route

When investigating the literature surrounding the synthesis of methylamphetamine using the Nagai route some confusion was evident in relation to the exact nature of the route specific impurity products for this synthetic method. According to Windahl et al.[13] the length of time over which the Nagai reaction proceeds (1/2 hour vs 2 hour vs 4 hour) had an effect on the level of aziridines and naphthalenes present in the final product. As the reaction time increases, the concentration of the aziridines decreased and the naphthalenes increased.

Tanaka et al.[14] also reported the presence of a methylamphetamine dimer formed from the condensation of methylamphetamine and aziridine. The presence of the methylamphetamine dimer was not reported by Windal et al.[13] The work of Ko et al.,[5], which involved a 5 hour reaction, corroborated the presence of naphthalenes, propanone and propenamide and the absence of the aziridines and methylamphetamine dimer.

In order to investigate the various impurities reported in the literature a time study was undertaken where the reaction time was varied from 1/2 hours, 2 hours and 4 hours. Eighteen batches of methylamphetamine hydrochloride were synthesised by the Nagai method with 6 batches from each of the 3 various reaction times. The results obtained were also compared to the previously synthesised Nagai samples where the reaction was allowed to proceed for 24 hours.

5.4.1 ½ hour reaction

Table 39 details the impurities from the phosphate buffer extracts of methylamphetamine synthesised at ½ hour reaction time. Highlighted are the presence of the aziridines as suggested by Windahl, and methylamphetamine dimers as suggested by Tanaka.

No	RT	Compound	Peak m/z
1	6.187	Benzaldehyde	**106**, 105, 77, 51
2	8.895	*cis*-1,2-dimethyl-3-phenylaziridine	**146**, 105,132, 91
3	10.422	*trans*-1,2-dimethyl-3-phenylaziridine	**146**, 105,132, 91
4	12.357	Ephedrine	**58**, 77, 44, 105,146
5	13.821	*N*-formylamphetamine	**118**, 72, 44, 91
6	14.688	*N*-formylmethylamphetamine	**86**, 58, 118
7	15.107	*N*-acetylmethylamphetamine	**58**, 100
8	16.592	*N*-formylephedrine	**86**, 87,58, 77, 100
9	16.895	*N*-acetylephedrine	**58**, 77, 100
10	20.764	Methylamphetamine dimer	**238**, 91, 120, 148, 58
11	21.025	Methylamphetamine dimer	**238**, 91, 120, 148, 58

Table 39: List of impurities found in pH 10.5 extract.

Table 40 details the impurities from the acetate buffer extracts of methylamphetamine synthesised at ½ hour reaction time. In this case the methylamphetamine dimers have not been extracted.

No	RT	Compound	Peak m/z
1	6.187	Benzaldehyde	**106**, 105, 77, 51
2	8.830	*cis*-1,2-dimethyl-3-phenylaziridine	**146**, 105,132, 91
3	10.022	*trans*-1,2-dimethyl-3-phenylaziridine	**146**, 105,132, 91
4	13.682	*N*-formylamphetamine	**118**, 72, 44, 91
5	14.582	*N*-formylmethylamphetamine	**86**, 58, 118
6	15.031	*N*-acetylmethylamphetamine	**58**, 100
7	16.422	*N*-formylephedrine	**86**, 87,58, 77, 100
8	16.757	*N*-acetylephedrine	**58**, 77, 100

Table 40: List of impurities found in pH 6 extract.

5.4.2 2 hour reaction

Table 41 details the impurities from the phosphate buffer extracts of methylamphetamine synthesised at 2 hour reaction time. The presence of the naphthalene compounds was observed in both extracts whereas the presence of the methylamphetamine dimer was only in evidence in the basic extract and the aziridines were only present in the acidic extract Also noted was the formation of the propanone and propenamide species as suggested by Windahl et al.[13]

No	RT	Compound	Peak m/z
1	6.144	Benzaldehyde	**106**, 105, 77, 51
2	12.439	Ephedrine	**58**, 77, 44, 105,146
3	13.924	*N*-formylamphetamine	**118**, 72, 44, 91
4	14.572	*N*-formylmethylamphetamine	**86**, 58, 118
5	15.001	*N*-acetylmethylamphetamine	**58**, 100
6	20.051	Dimethylphenylnaphthalene	**232**, 217, 202, 77
7	20.198	Benzylmethnaphthalene	**232**, 217, 202, 58
8	20.365	*N*-methyl-N-(α-methylphenethyl) amino-1-phenyl-2-propanone	**238**, 91, 105, 190, 120
9	20.491	*N*-methyl-N-(α-methylphenethyl) amino-1-phenyl-2-propanone	**238**, 91, 105, 190, 120
10	21.003	Methylamphetamine dimer	**238**, 91, 120, 148, 58
11	22.425	(*Z*)-*N*-methyl-*N*-(α-methylphenethyl)-3-phenylpropenamide	**131**, 91, 58, 103, 188, 77
12	23.425	(*E*)-*N*-methyl-*N*-(α-methylphenethyl)-3-phenylpropenamide	**131**, 91, 58, 103, 188, 77

Table 41: List of impurities found in pH 10.5 extract.

Table 42 shows the impurities from the acetate buffer extracts of methylamphetamine synthesised at 2 hour reaction time.

No	RT	Compound	Peak m/z
1	6.154	Benzaldehyde	**106**, 105, 77, 51
2	8.810	*cis*-1,2-dimethyl-3-phenylaziridine	**146**, 105,132, 91
3	10.002	*trans*-1,2-dimethyl-3-phenylaziridine	**146**, 105,132, 91
4	13.672	*N*-formylamphetamine	**118**, 72, 44, 91
5	14.593	*N*-formylmethylamphetamine	**86**, 58, 118
6	15.021	*N*-acetylmethylamphetamine	**58**, 100
7	19.999	Dimethylphenylnaphthalene	**232**, 217, 202, 77
8	20.176	Benzylmethnaphthalene	**232**, 217, 202, 58
9	20.312	*N*-methyl-N-(α-methylphenethyl) amino-1-phenyl-2-propanone	**238**, 91, 105, 190, 120
10	20.471	*N*-methyl-N-(α-methylphenethyl) amino-1-phenyl-2-propanone	**238**, 91, 105, 190, 120
11	22.425	(*Z*)-*N*-methyl-*N*-(α-methylphenethyl)-3-phenylpropenamide	**131**, 91, 58, 103, 188, 77
12	23.425	(*E*)-*N*-methyl-*N*-(α-methylphenethyl)-3-phenylpropenamide	**131**, 91, 58, 103, 188, 77

Table 42: List of impurities found in pH 6 extract.

5.4.3 4 hour reaction

Table 43 shows the impurities from the phosphate buffer extracts of methylamphetamine synthesised for a 4 hour reaction time where both naphthalene products are present. The methylamphetamine dimer is now absent from the profile in both extracts.

No	RT	Compound	Peak m/z
1	6.16	Benzaldehyde	**106**, 105, 77, 51
2	13.640	*N*-formylamphetamine	**118**, 72, 44, 91
3	14.571	*N*-formylmethylamphetamine	**86**, 58, 118
4	14.999	*N*-acetylmethylamphetamine	**58**, 100
5	20.008	Dimethylphenylnaphthalene	**232**, 217, 202, 77
6	20.249	Benzylmethnaphthalene	**232**, 217, 202, 58
7	20.301	*N*-methyl-N-(α-methylphenethyl) amino-1-phenyl-2-propanone	**238**, 91, 105, 190, 120
8	20.426	*N*-methyl-N-(α-methylphenethyl) amino-1-phenyl-2-propanone	**238**, 91, 105, 190, 120
9	22.425	(*Z*)-*N*-methyl-*N*-(α-methylphenethyl)-3-phenylpropenamide	**131**, 91, 58, 103, 188, 77
10	23.425	(*E*)-*N*-methyl-*N*-(α-methylphenethyl)-3-phenylpropenamide	**131**, 91, 58, 103, 188, 77

Table 43: List of impurities found in pH 10.5 extract.

Table 44 details the impurities from the acetate buffer extracts of methylamphetamine synthesised with a 4 hour reaction time indicating the presence of the aziridines as well as the naphthalene compounds.

No	RT	Compound	Peak m/z
1	6.142	Benzaldehyde	**106**, 105, 77, 51
2	8.798	*cis*-1,2-dimethyl-3-phenylaziridine	**146**, 105,132, 91
3	10.002	*trans*-1,2-dimethyl-3-phenylaziridine	**146**, 105,132, 91
5	14.591	*N*-formylmethylamphetamine	**86**, 58, 118
6	15.030	*N*-acetylmethylamphetamine	**58**, 100
7	20.018	Dimethylphenylnaphthalene	**232**, 217, 202, 77
8	20.186	Benzylmethnaphthalene	**232**, 217, 202, 58
9	20.301	*N*-methyl-N-(α-methylphenethyl) amino-1-phenyl-2-propanone	**238**, 91, 105, 190, 120
10	20.416	*N*-methyl-N-(α-methylphenethyl) amino-1-phenyl-2-propanone	**238**, 91, 105, 190, 120
11	22.45	(*Z*)-*N*-methyl-*N*-(α-methylphenethyl)-3-phenylpropenamide	**131**, 91, 58, 103, 188, 77
12	23.425	(*E*)-*N*-methyl-*N*-(α-methylphenethyl)-3-phenylpropenamide	**131**, 91, 58, 103, 188, 77

Table 44: List of impurities found in pH 6 extract.

Figure 86 and Figure 87 show profiles of methylamphetamine synthesised using the three different reaction times (½ hr, 2 hr, 4 hr) for the Nagai route. The change in impurity profiles over time for both pH extracts is quite obvious.

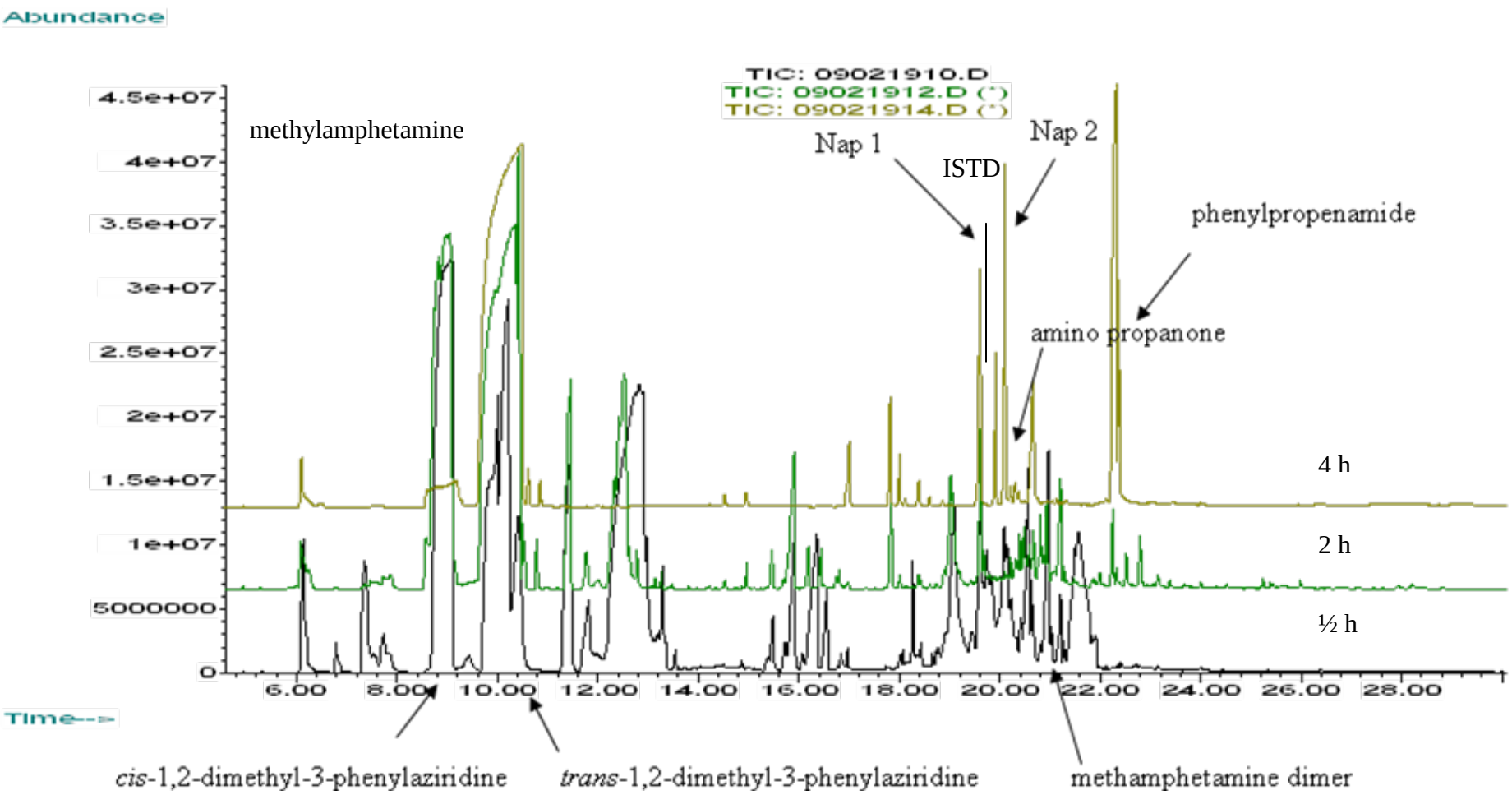

Figure 86: Overlay of the impurity profiles at pH 10.5 for the 3 reaction times

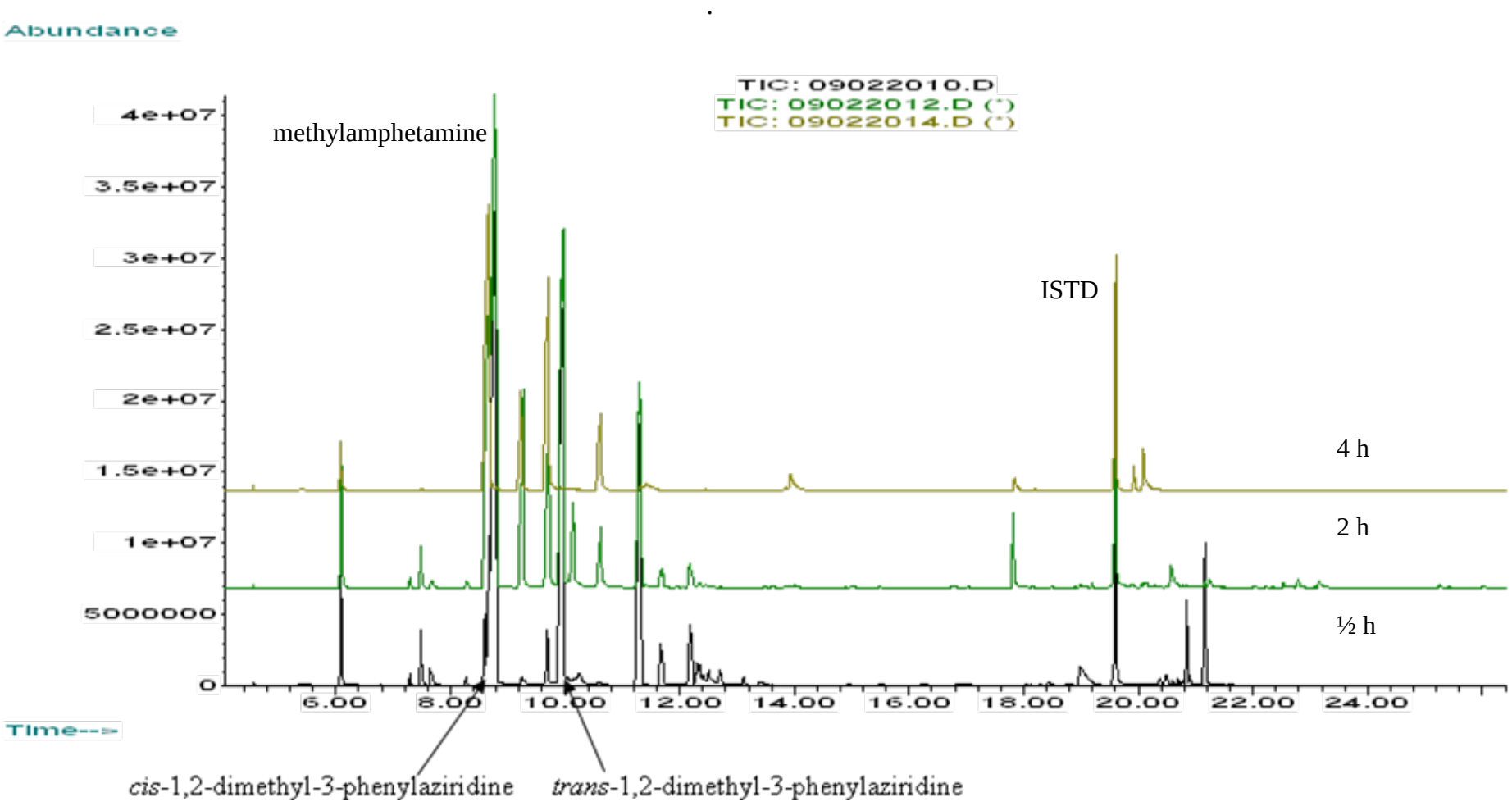

Figure 87: Overlay of the impurity profiles at pH 6 for the 3 reaction times.

Windahl et al.[13] suggested that as the reaction time increased, the quantity of the aziridines decreased, and the quantity of the two naphthalenes increased. This study confirmed these results.

While Windahl et al.[13] did not report the presence of the methylamphetamine dimer in any reaction batches, this study did find this compound present in both the ½ hour and 2 hour reaction batches, but not the 4 hour or 24 hour reaction batches thus confirming that the methylamphetamine dimer was formed but could not be considered as a route specific impurity. This observations fits with the claim by Tanaka et al.[14] that the methylamphetamine dimer is formed from the condensation of methylamphetamine and aziridine: as the reaction time increases, the quantity of aziridine decreases and, therefore, the methylamphetamine dimer cannot be formed as readily. It should be noted that, Tanaka et al.[14] did not perform any time study reactions for the Nagai route. A summary of the impurities found by Windahl and in this study are in the Table 45.

This study has clarified the previous literature in relation to impurities presented for the Nagai route

Impurities	Windahl[13]	Tanaka[14]	This work
cis-1,2-dimethyl-3-phenylaziridine	√		√
trans-1,2-dimethyl-3-phenylaziridine	√		√
methylamphetamine dimer		√	√
1,3-dimethyl-2-phenylnaphthalene	√		√
1-benzyl-3-methyl-naphthalene	√		√
isomers of N-methyl-N-(a-methylphenylethyl)amino-1-phenyl-2-propanone	√		√
(Z)-N-methyl-N-(a-methylphenethyl)-3-phenyl propenamide	√		√

Table 45: Impurities found by Windahl et al.[13], Tanaka et al.[14] and this study in their synthesis of methylamphetamine by the Nagai route.

5.5 Substrate study for the Birch route

Person et al.[4] published the only study on impurities found in methylamphetamine synthesised by the Birch route. The authors synthesised methylamphetamine by the Birch reduction and identified impurities in the final product. Notably, however, they used ephedrine hydrochloride rather than ephedrine base as the starting material. They found only one impurity 1-(1,4-cyclohexadienyl)-2-methylaminopropane (CMP).

This study synthesised methylamphetamine using both the salt and base forms of ephedrine. Twelve batches of methylamphetamine hydrochloride were synthesised by the Birch method with 6 batches from each of two starting materials.

Table 46 details the impurities from the phosphate buffer extracts of methylamphetamine synthesised from both the ephedrine HCl and ephedrine base.

No	RT	Compound	Peak m/z	Salt	Base
1	6.215	Benzaldehyde	**105**, 106, 77, 51	√	√
2	10.607	CMP	**58**, 56, 91, 77, 152	√	
3	10.910	Dimethylamphetamine (DMA)	**72**, 91, 56, 42	√	√
4	11.851	Ephedrone	**58**, 77, 105	√	√
5	12.353	Ephedrine	**58**, 77, 117, 132, 148	√	√
6	13.101	Unknown 3	**58**, 77	√	√
7	14.612	*N*-formylmethylamphetamine	**86**, 58, 118	√	√
8	15.030	*N*-acetylmethylamphetamine	**58**, 100	√	√
9	16.476	*N*-formylephedrine	**86**, 87,58, 77, 100	√	√
10	16.818	*N*-acetylephedrine	**58**, 77, 100	√	√
11	19.088	3,4-Dimethyl-2,5-diphenyl-oxazolidine	**146**, 147, 105, 132	√	√

Table 46: List of impurities found in pH 10.5 extract.

Table 47 details the impurities from the acetate buffer extracts of methylamphetamine synthesised from ephedrine HCl and ephedrine base.

No	RT	Compound	Peak m/z	Salt	Base
1	6.144	Benzaldehyde	**106**, 105, 77, 51	√	√
2	8.685	1-phenyl-2-propanone	**43**, 91, 134	√	√
3	8.851	Amphetamine	**44**, 91, 134	√	√
4	9.311	1-phenyl-1,2-propanedione	**105**, 77, 51, 43	√	√
5	10.015	*trans*-1,2-dimethyl-3-phenylaziridine	**146**, 105,132, 32	√	√
6	12.428	3,4-Dimethyl-5-phenyloxazolidine	**71**, 56, 91, 105	√	√

Table 47: List of impurities found in pH 6 extract.

When the base form of ephedrine was used, this study found one route specific impurity (Unknown 3), but CMP was not present and may have been masked by the larger methylamphetamine peak in the extract.

Figure 88 and Figure 89 show profiles of methylamphetamine synthesised from the 2 different starting materials (ephedrine HCl and ephedrine base) for the Birch route.

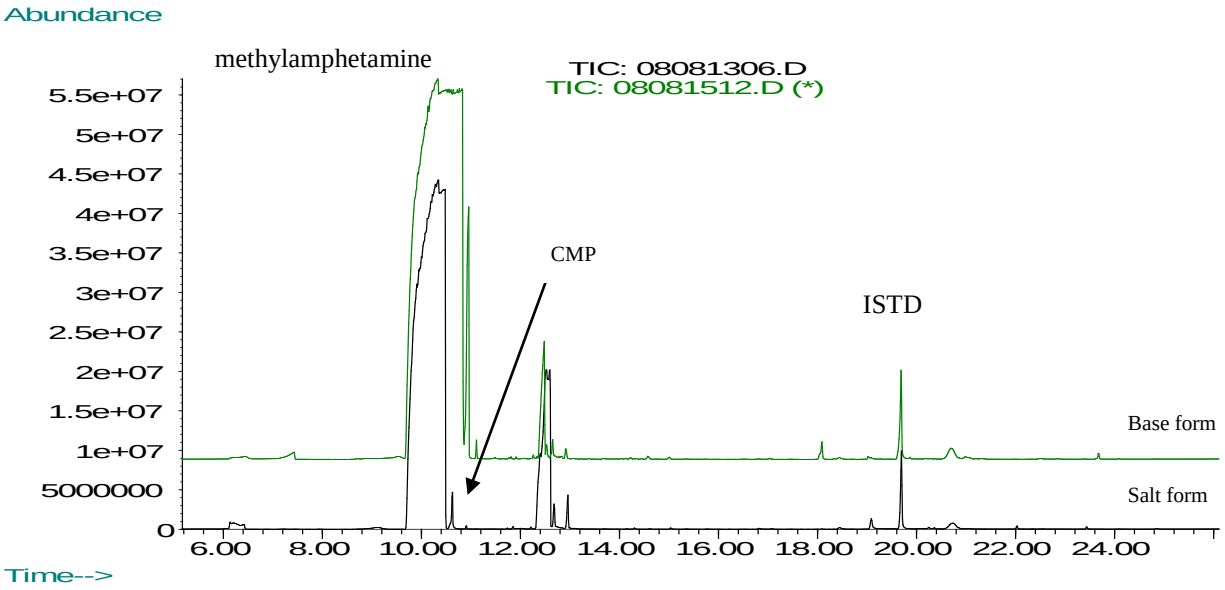

Figure 88: Overlay of the impurity profiles at pH 10.5 for 2 types of starting material.

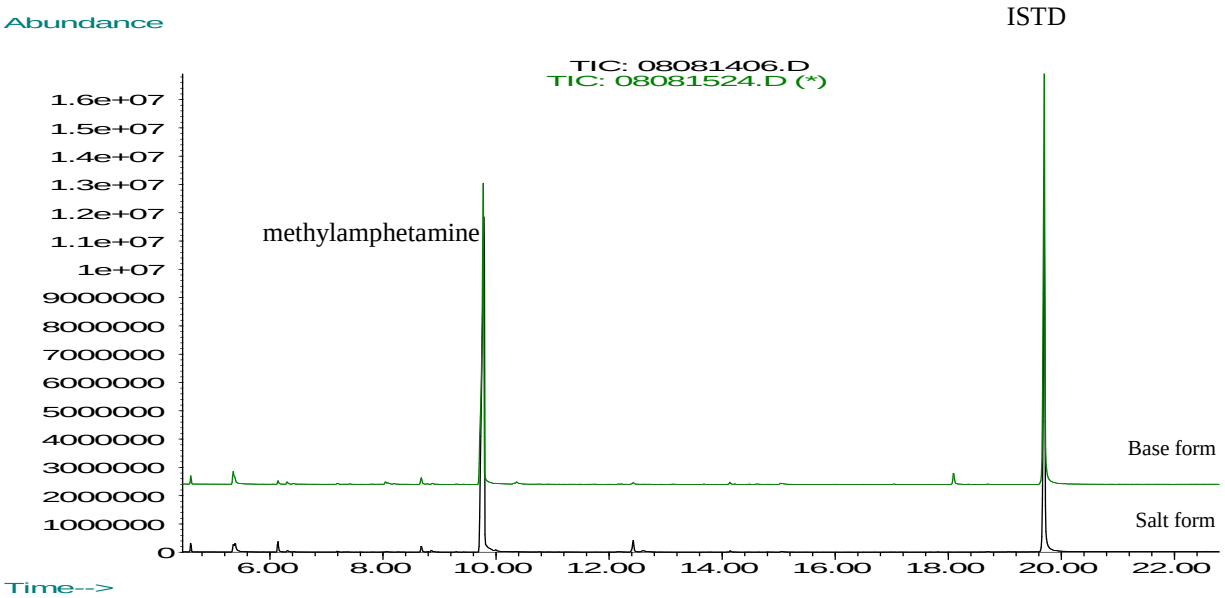

Figure 89: Overlay of the impurity profiles at pH 6 for 2 types of starting material.

5.6 Chromatographic column

Inoue et al.[6] reported the use of a DB-5 column rather than a DB-1MS column to separate the aziridines and methylamphetamine extracted from a street seized sample with a phosphate buffer at pH 10.5.

In order to examine the effectiveness of this single pH extraction method combined with analysis on the DB-5 column across the range of synthetic routes (as opposed to one synthetic route) a small study was undertaken where a selection of methylamphetamine samples from each of the seven routes was extracted and analysed.

5.6.1 Experimental methods

A DB-5 column (J & W column (30 m length × 0.32 mm inner diameter, 1.0 μm film thickness) was installed into the GCMS and the repeatability of the system established using a Grob mixture as previously outlined in Chapter 4. In order to evaluate the performance of instrument, the partial validation for DB-5 column was carried out according to the procedure previously described in Section 4.1 and the results are presented in Appendix E. For the methylamphetamine profiling, 10 batches of

synthesised samples randomly selected from each of the seven routes were analysed, giving 70 samples in total. The analysis was undertaken with the oven temperature was programmed as follows: 50°C for 1 min, 10°C/min to 300°C, and then a hold at 300°C for 10 min. The injector and detector temperatures were set at 250 and 300°C, respectively. Helium was used as the carrier gas at a constant column flow-rate of 2.0 ml/min.[6]

5.6.2 Results and Discussion

Both the aziridines and 1-phenyl-2-propanol were separated effectively using only the phosphate buffer at pH 10.5. Previously the aziridines impurities could only be elucidated with the DB-1MS column by using an acidic extraction.

This is a significant finding as it suggests that all route specific impurities across the seven synthetic routes could be elucidated through analysis using a DB-5 column with the basic extraction rather than a DB-1MS column as suggested in the literature [14-16] which requires both an acidic and basic extractions. A full set of the relevant chromatograms (Leuckart, Reductive Amination, Nagai, Rosenmund, Birch, Emde and Moscow) is presented in Figure 90 - Figure 103. All the route specific impurities which were observed using the DB-1MS column were also identified within the samples analysed DB-5 column using a single phosphate buffer at pH 10.5. The main peak at 11 mins is methylamphetamine and peak at 21.6 mins is the internal standard, eicosane.

Visual comparison of the impurity profiles for the Leuckart batches show obvious variation between the ten profiles, particularly within the 12 – 20 minute range (Figure 90).

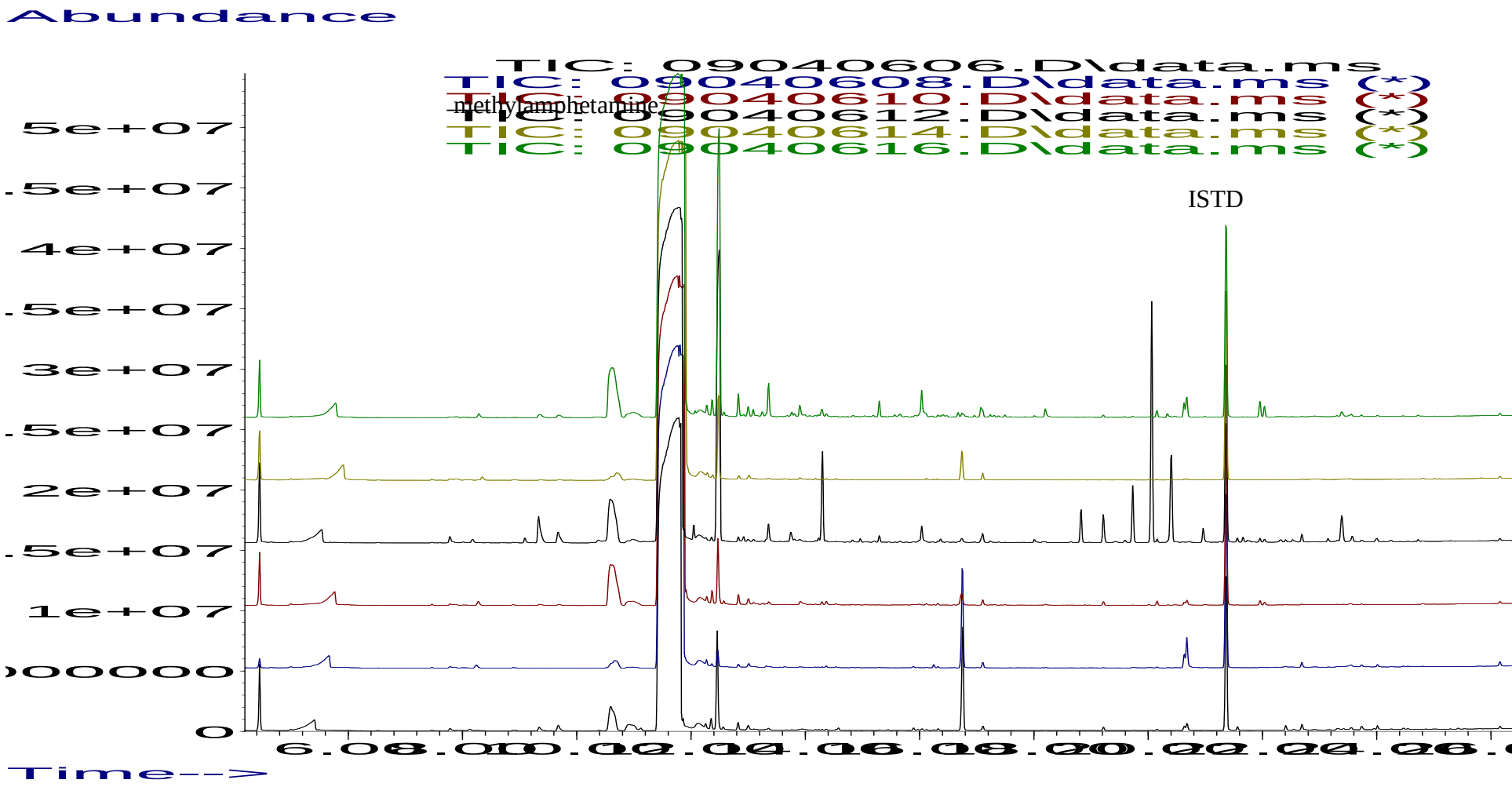

Figure 90: Overlay of the impurity profiles from the first six Leuckart batches.

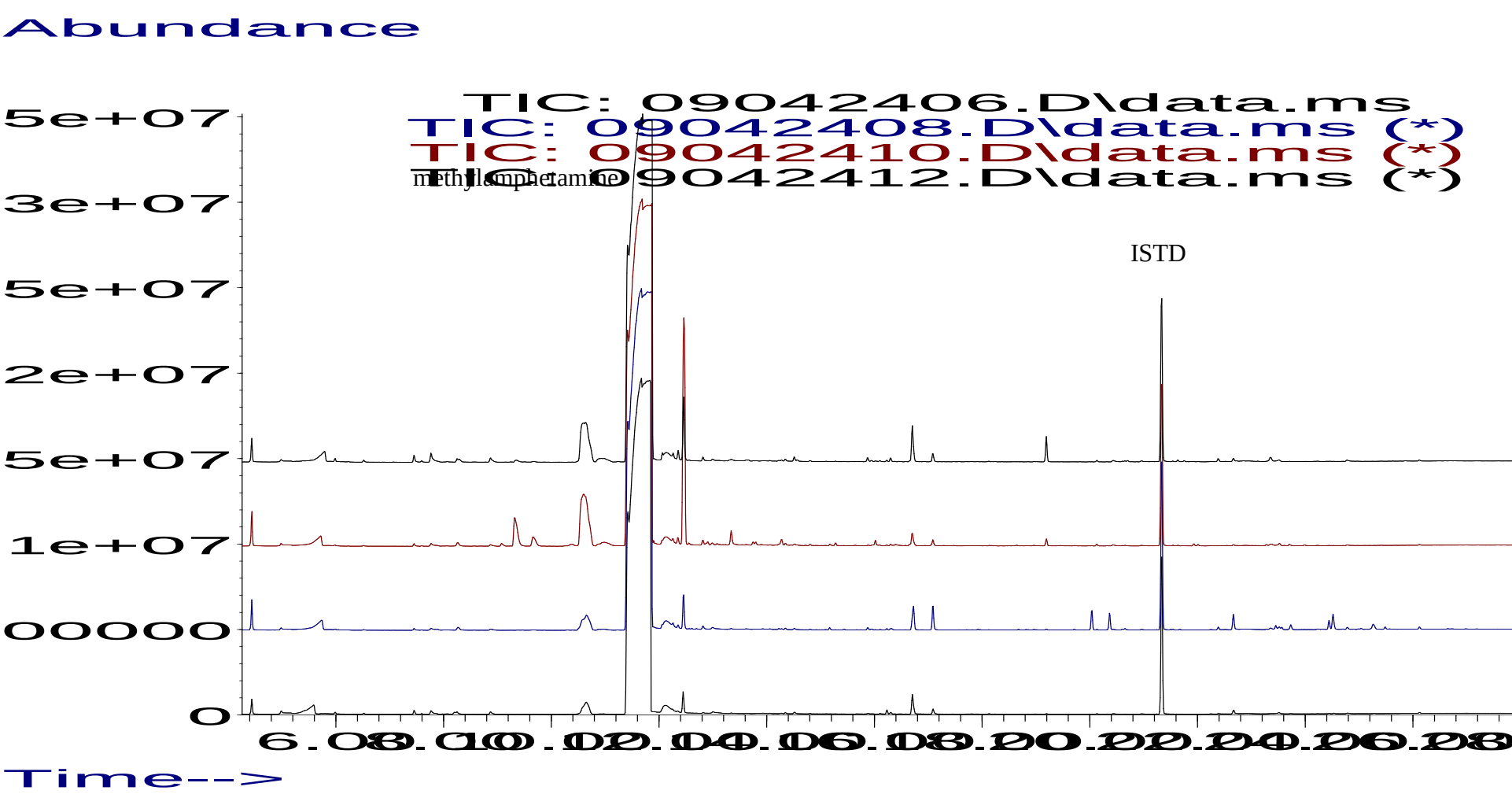

Figure 91: Overlay of the impurity profiles from the remaining four Leuckart batches.

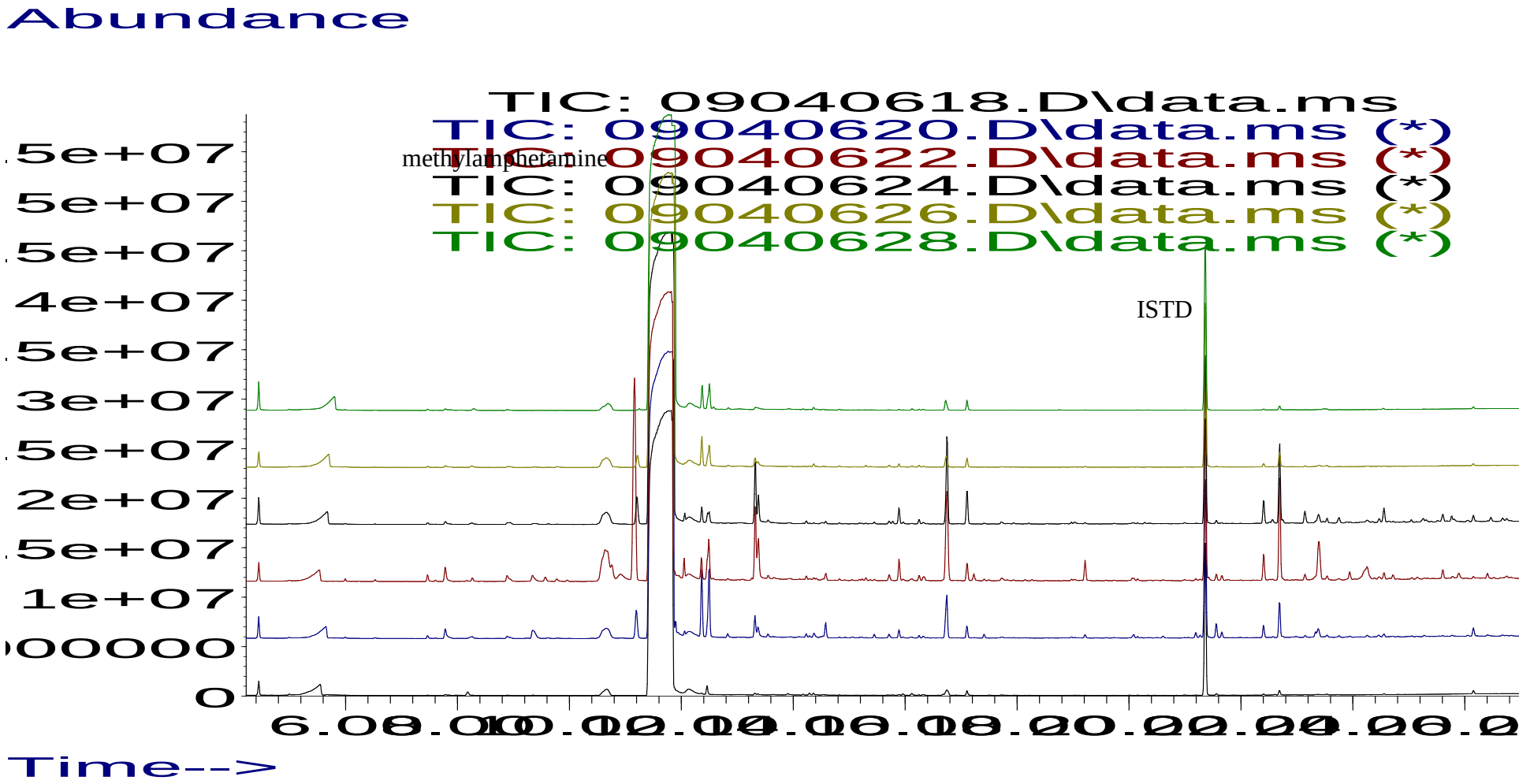

Figure 92: Overlay of the impurity profiles from the first six Reductive Amination batches.

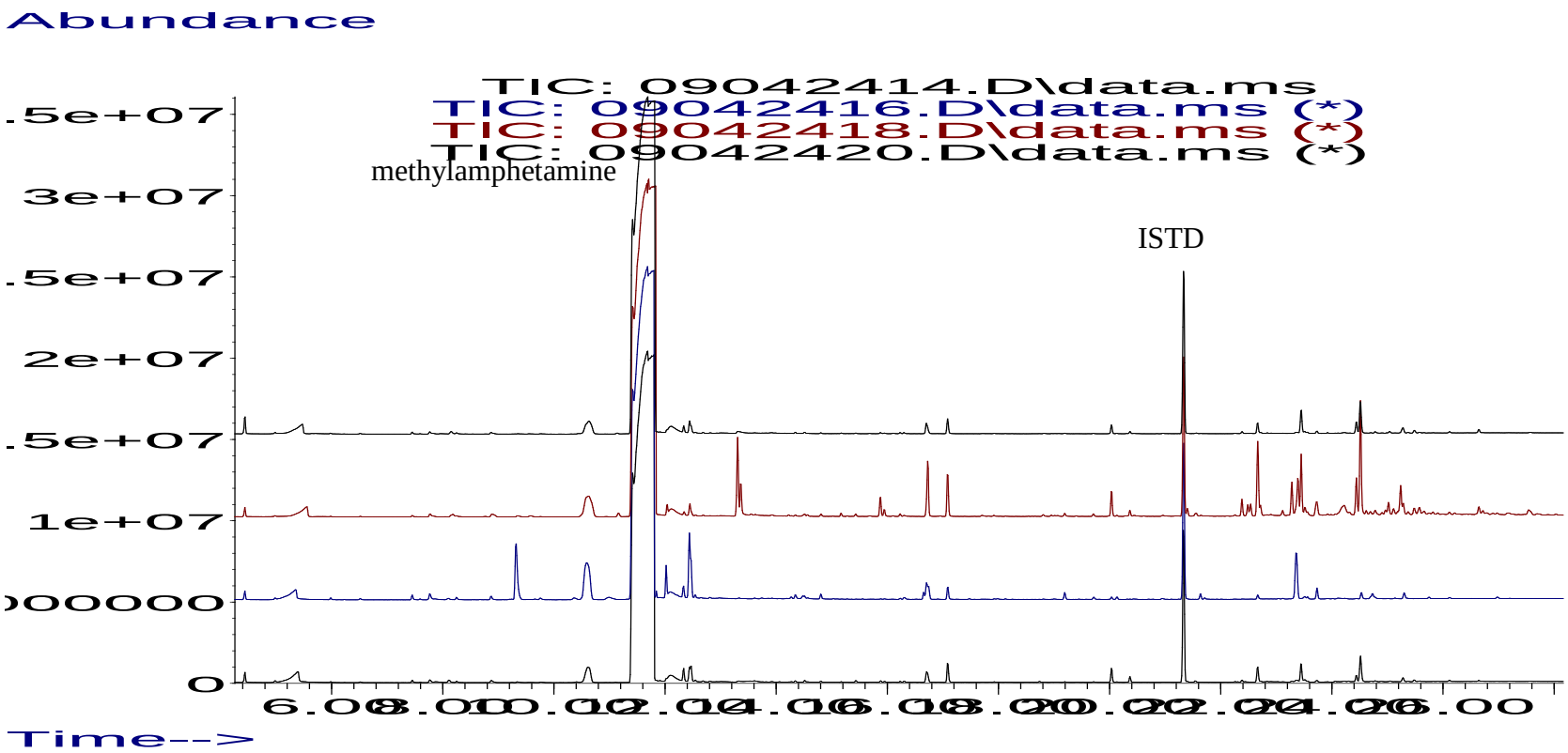

Figure 93: Overlay of the impurity profiles from the remaining four Reductive Amination batches.

Visual comparison of the impurity profiles for the Reductive Amination batches show obvious variation between the ten profiles, particularly within the 12 - 19 minute range, and in the range 22 – 24 minute range.

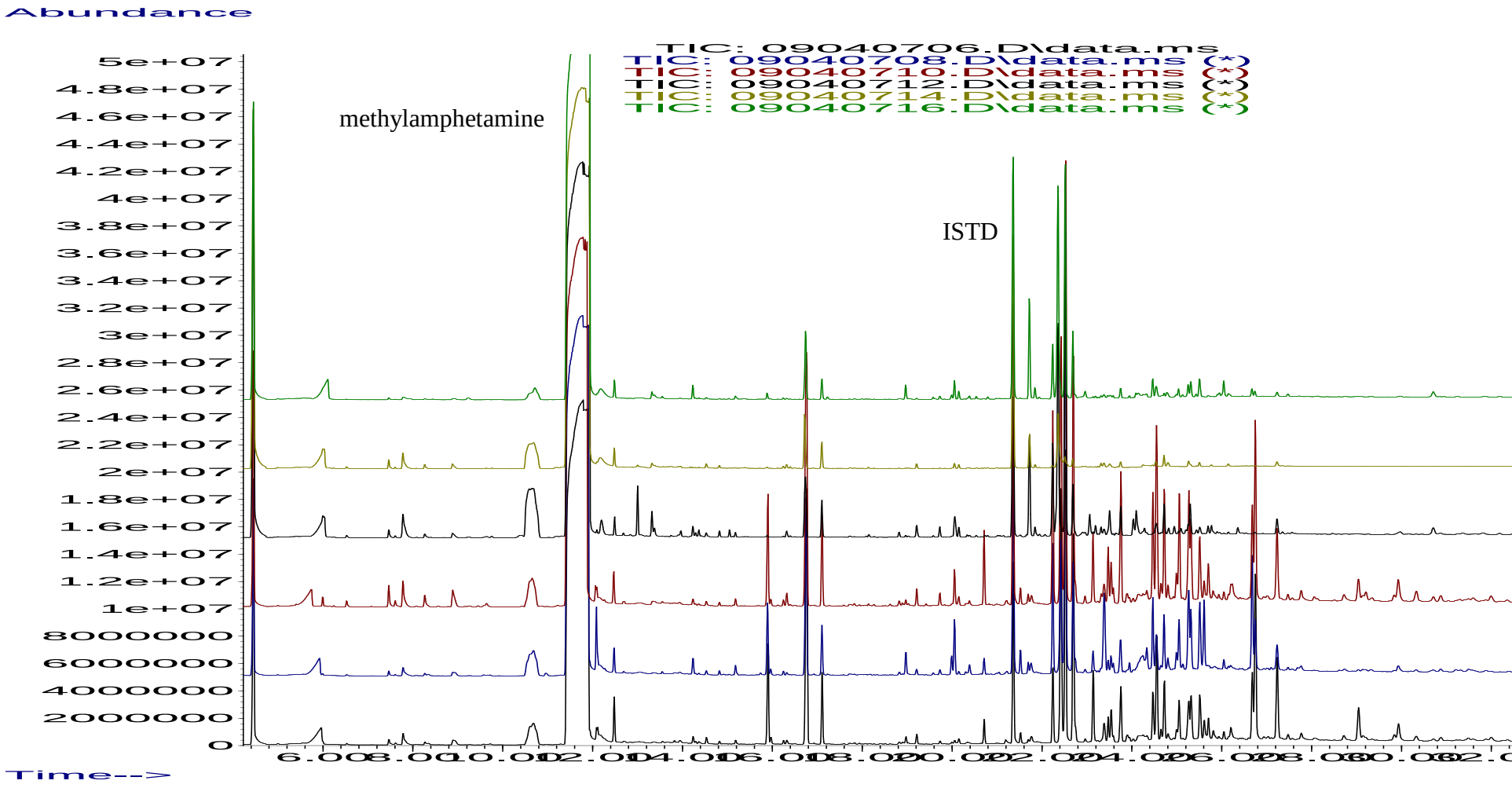

Figure 94: Overlay of the impurity profiles from the first six Nagai batches.

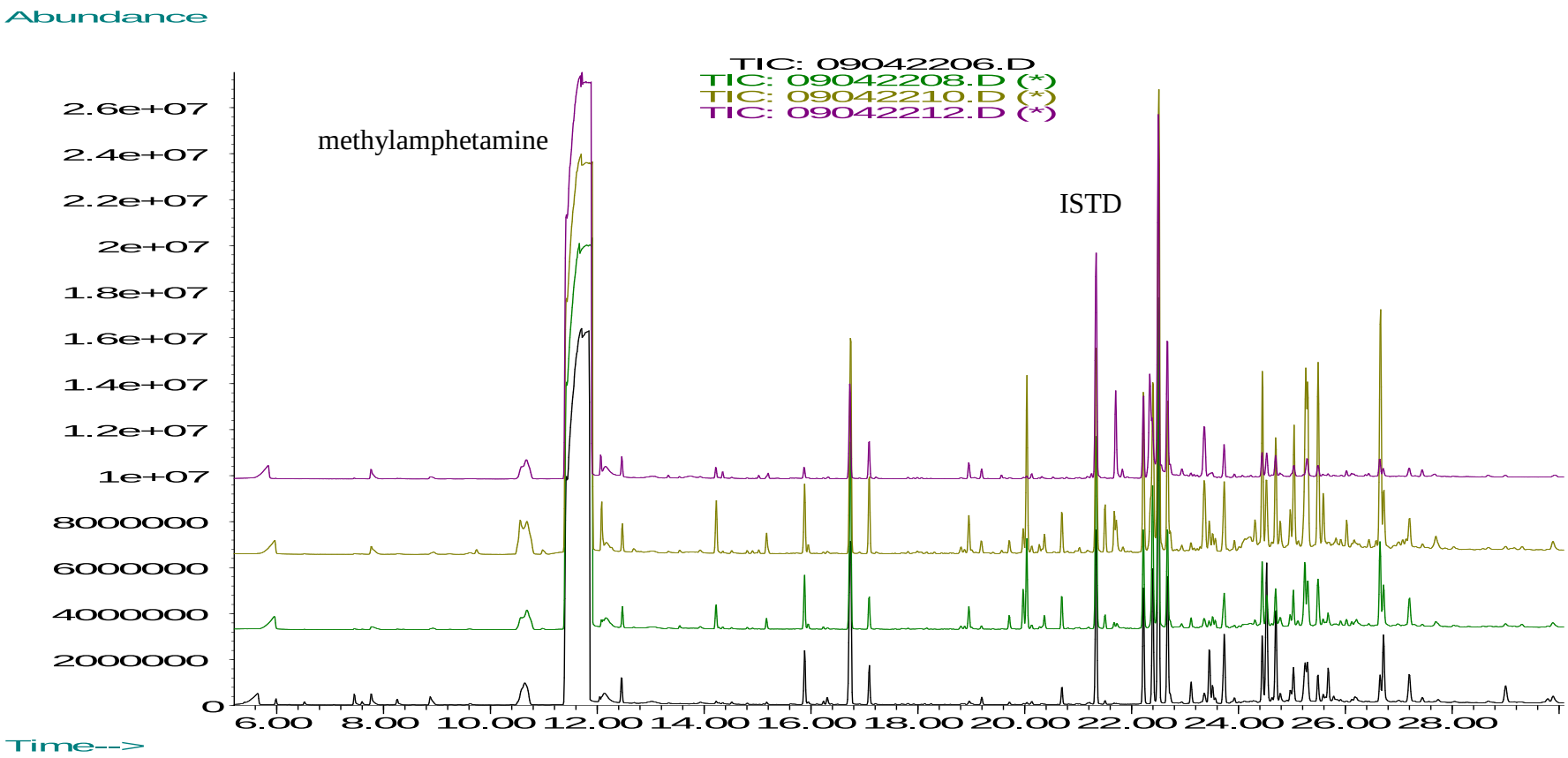

Figure 95: Overlay of the impurity profiles from the remaining four Nagai batches.

Visual comparison of the impurity profiles for the Nagai batches show obvious variation between the ten profiles, particularly within the 16 - 21 minute range, and in the range 24 – 28 minute range.

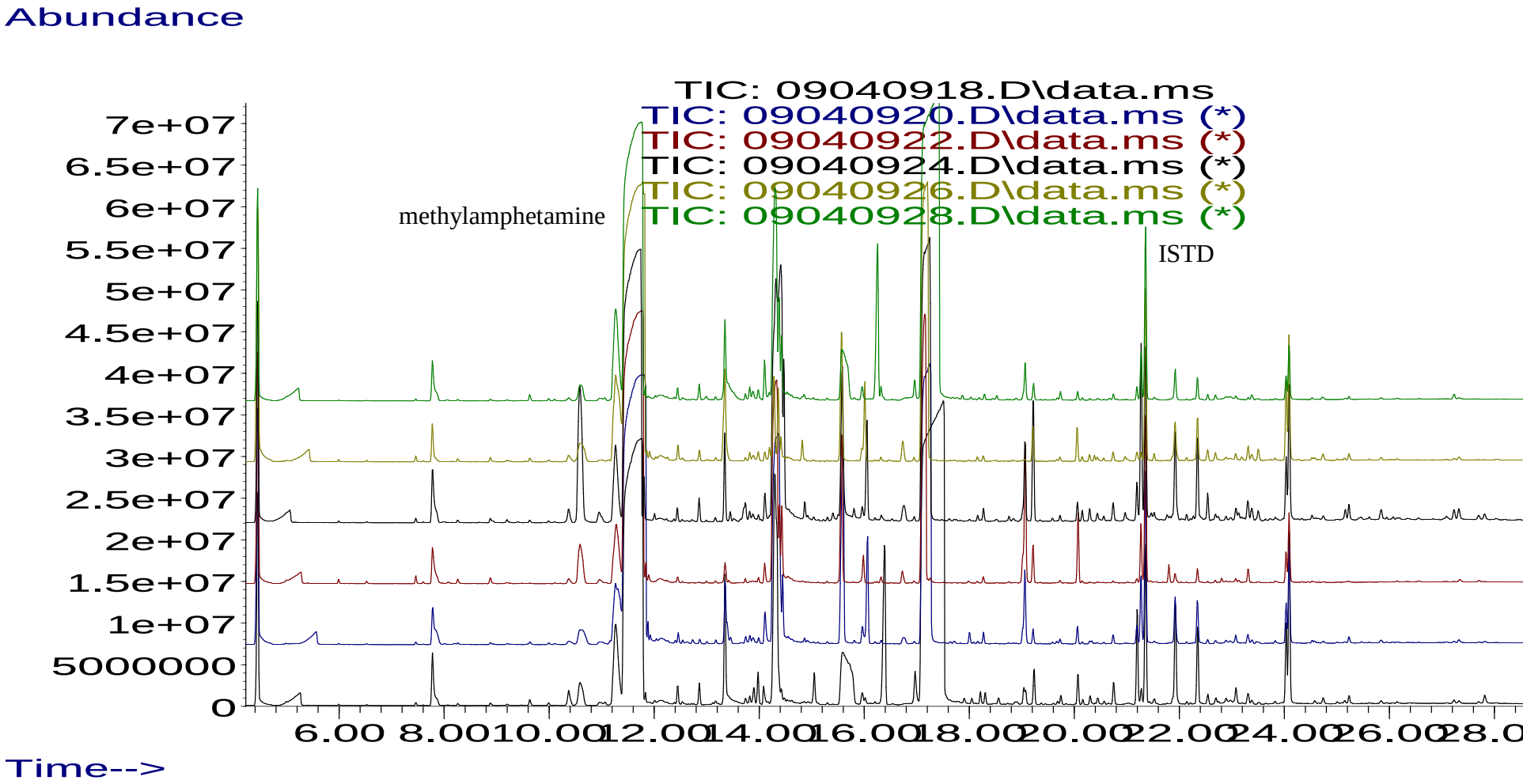

Figure 96: Overlay of the impurity profiles from the first six Rosenmund batches.

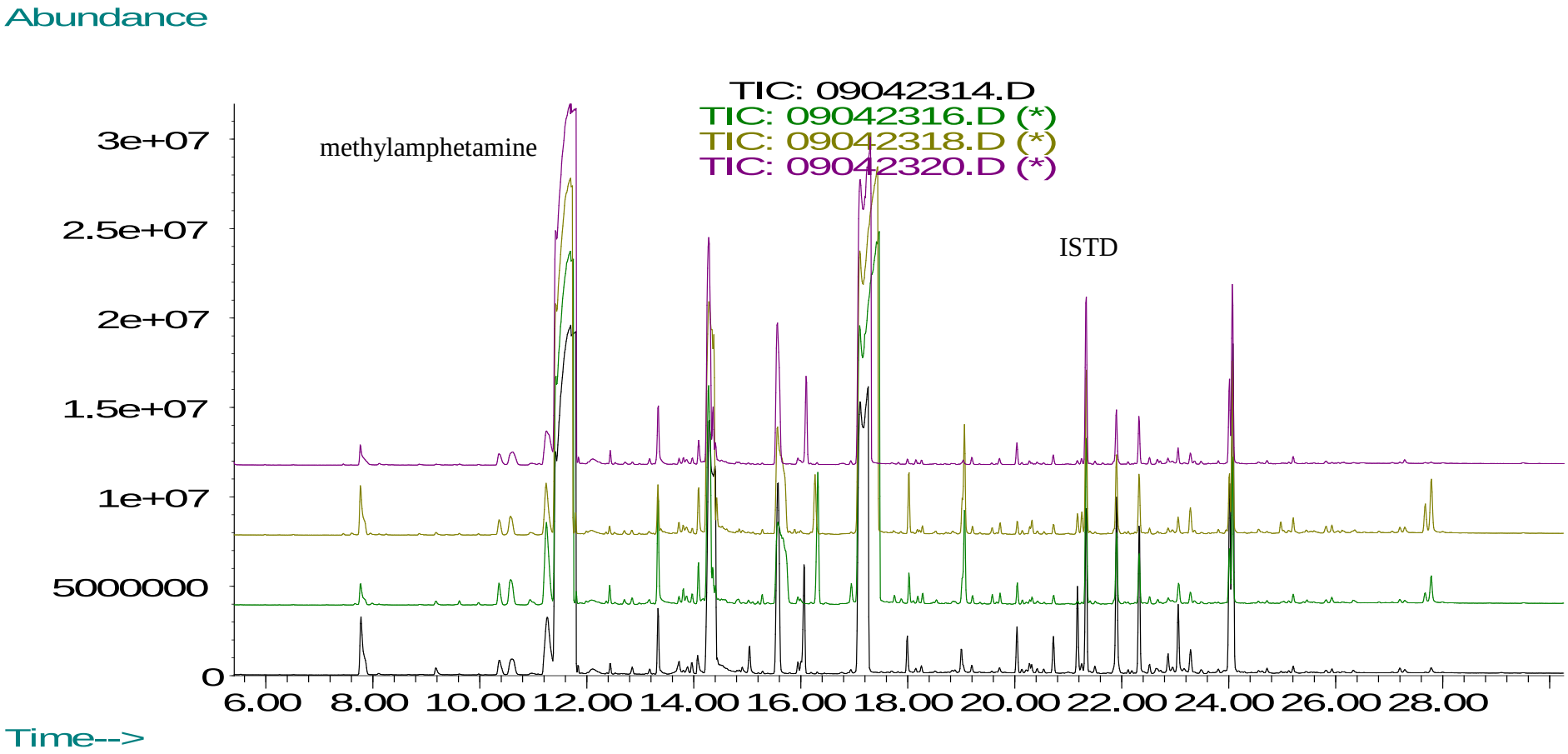

Figure 97: Overlay of the impurity profiles from the remaining four Rosenmund batches.

Visual comparison of the impurity profiles for the Rosenmund batches show little variation between the six profiles.

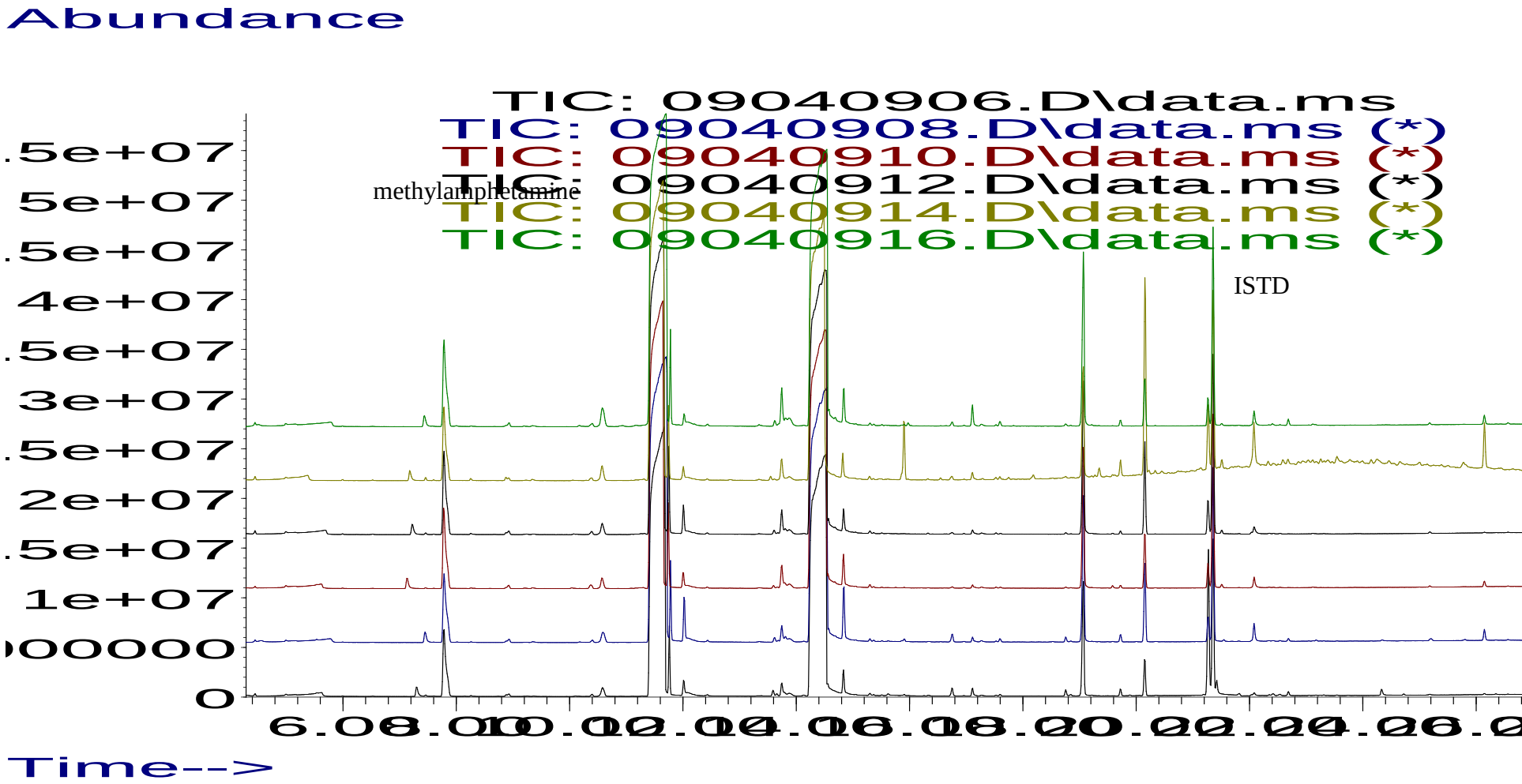

Figure 98: Overlay of the impurity profiles from the first six Birch batches.

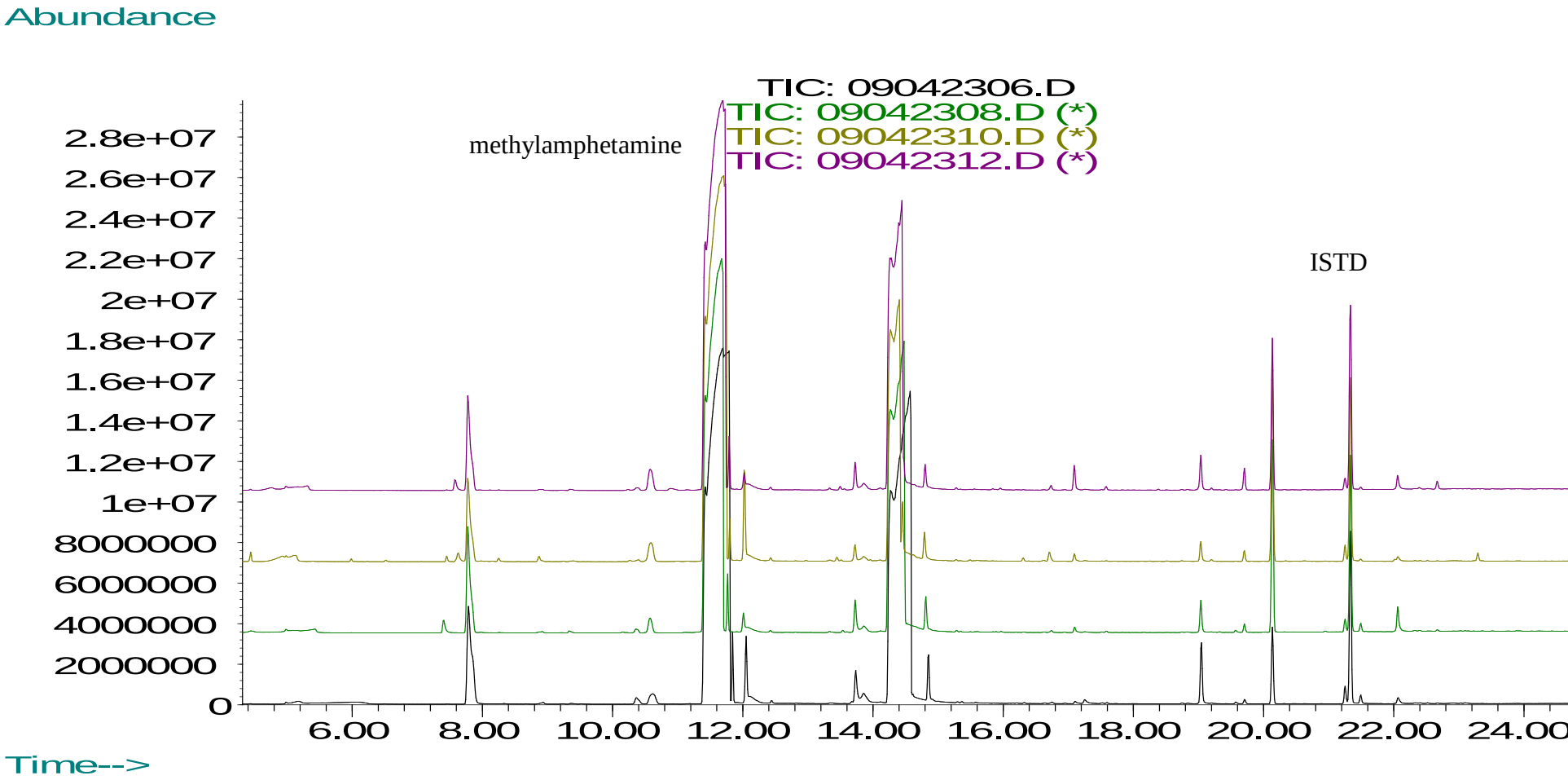

Figure 99: Overlay of the impurity profiles from the remaining four Birch batches.

Visual comparison of the impurity profiles for the Birch batches show little variation between the ten profiles.

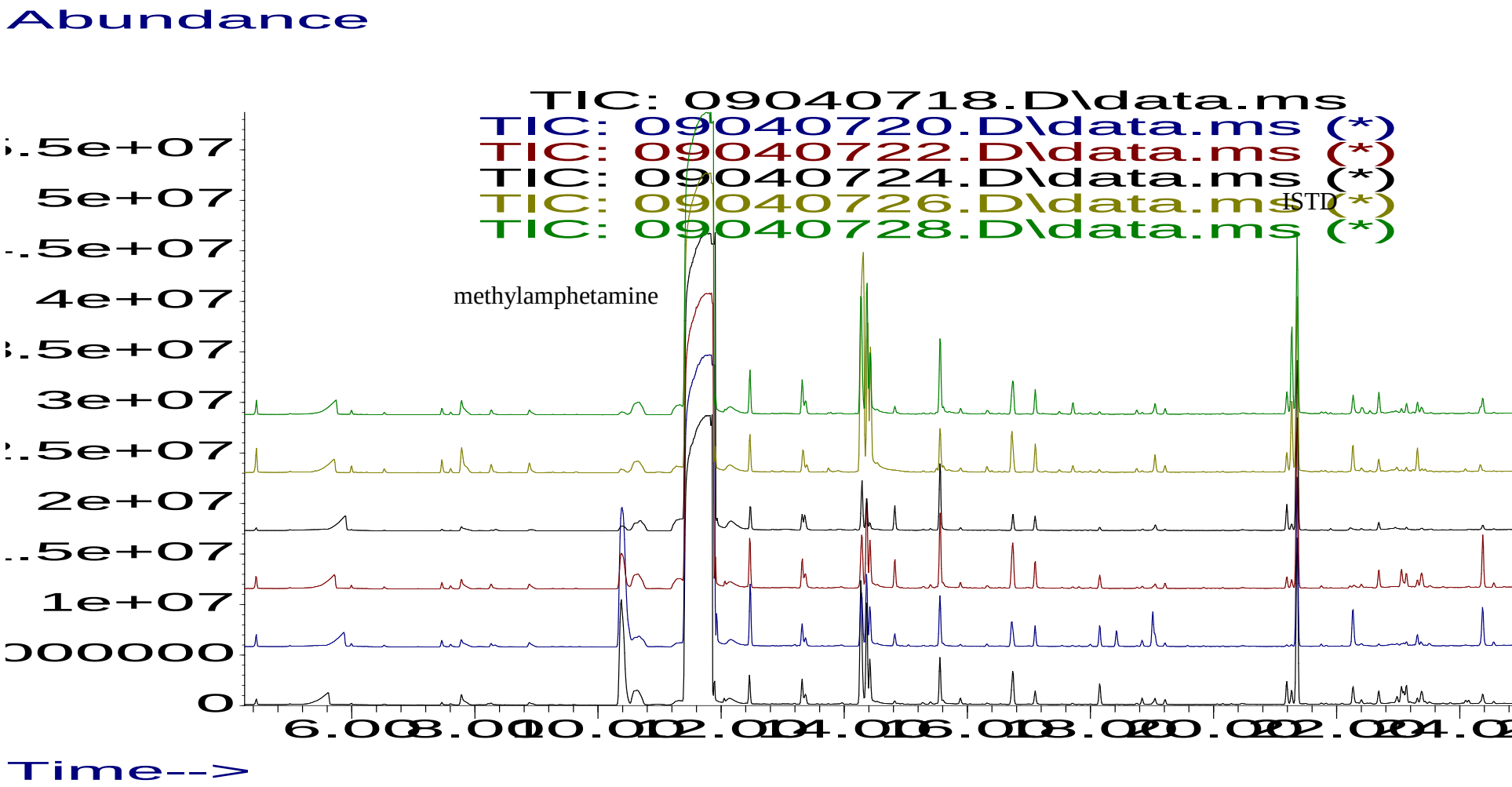

Figure 100: Overlay of the impurity profiles from the first six Emde batches.

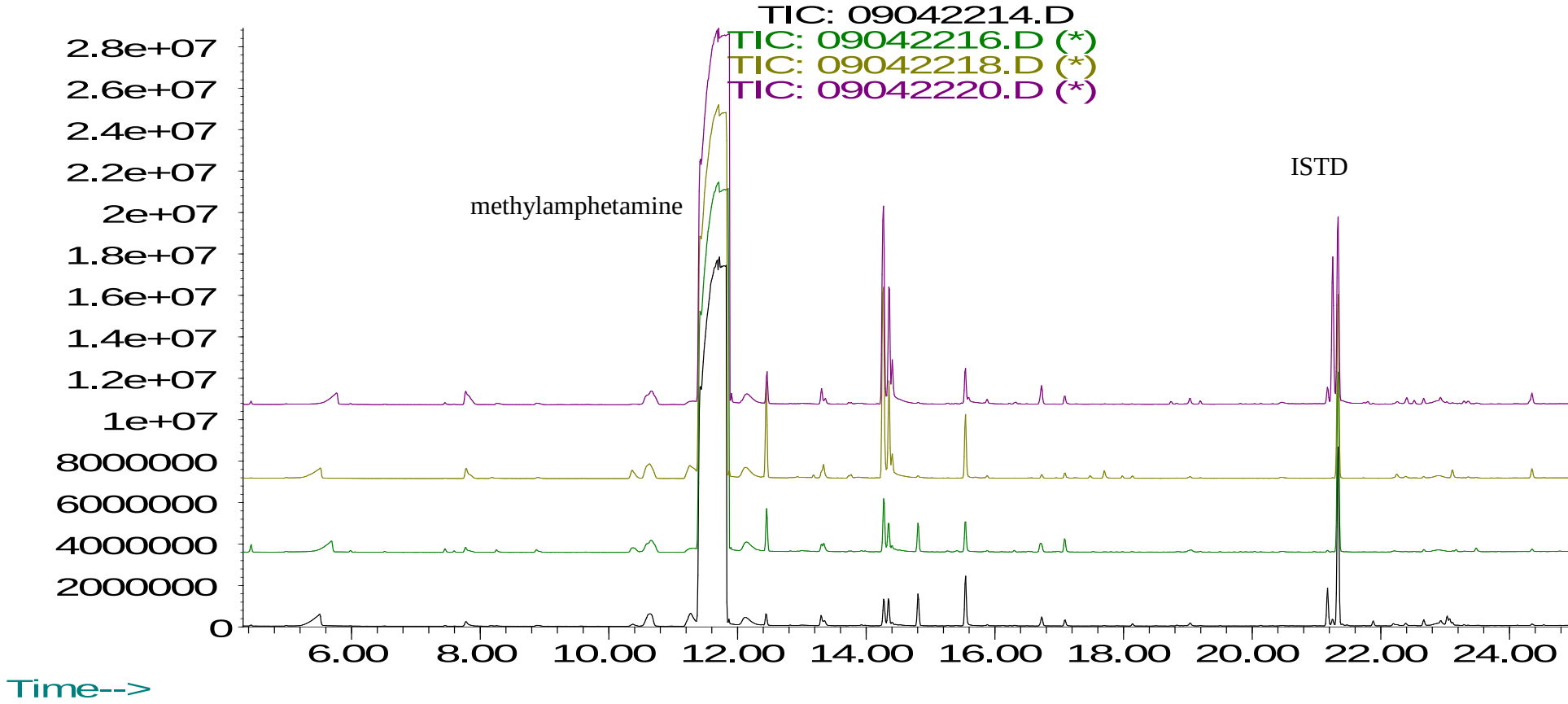

Figure 101: Overlay of the impurity profiles from the remaining four Emde batches.

Visual comparison of the impurity profiles for the Emde batches show little variation between the ten profiles.

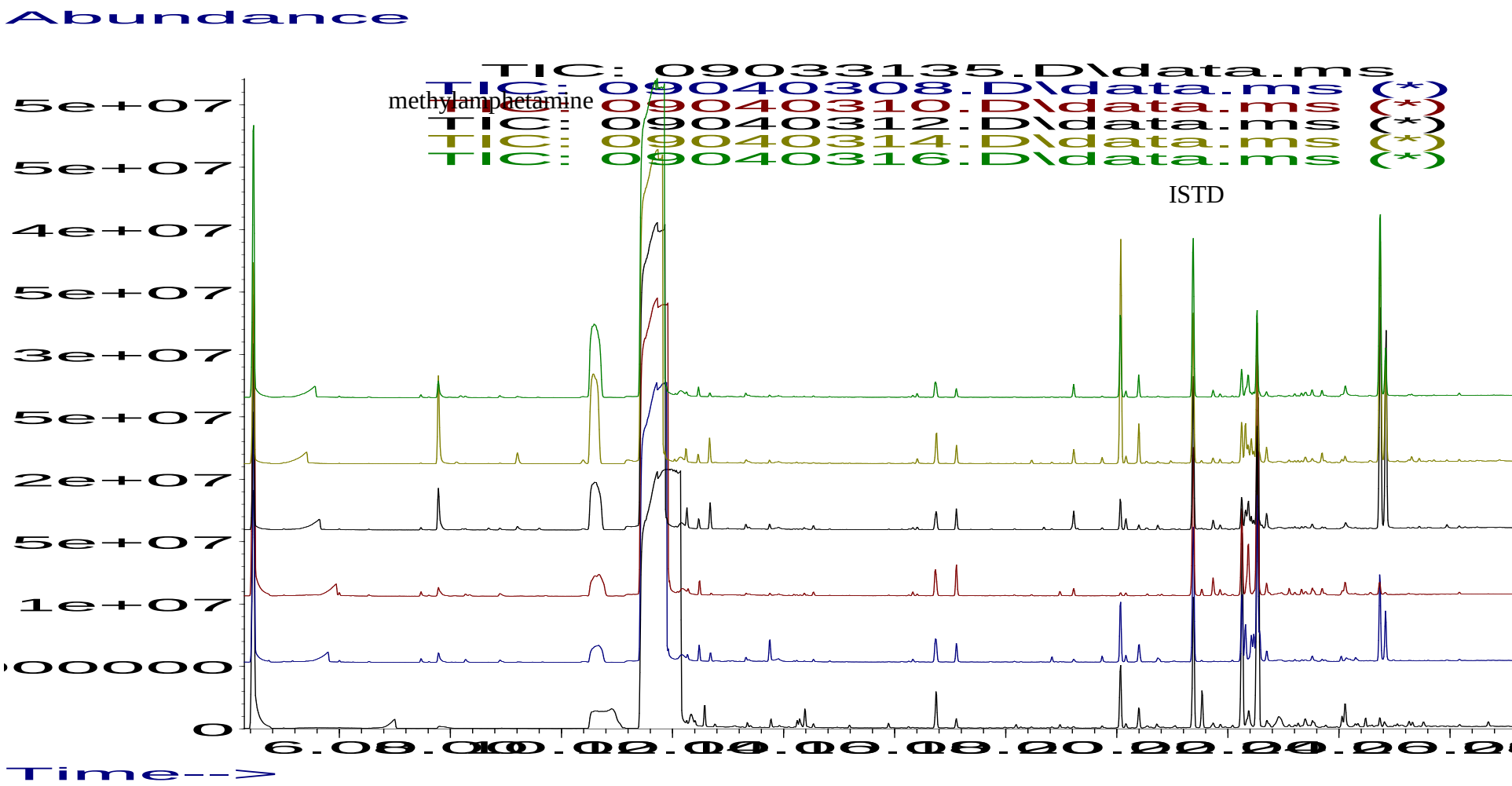

Figure 102: Overlay of the impurity profiles from the first six Moscow batches.

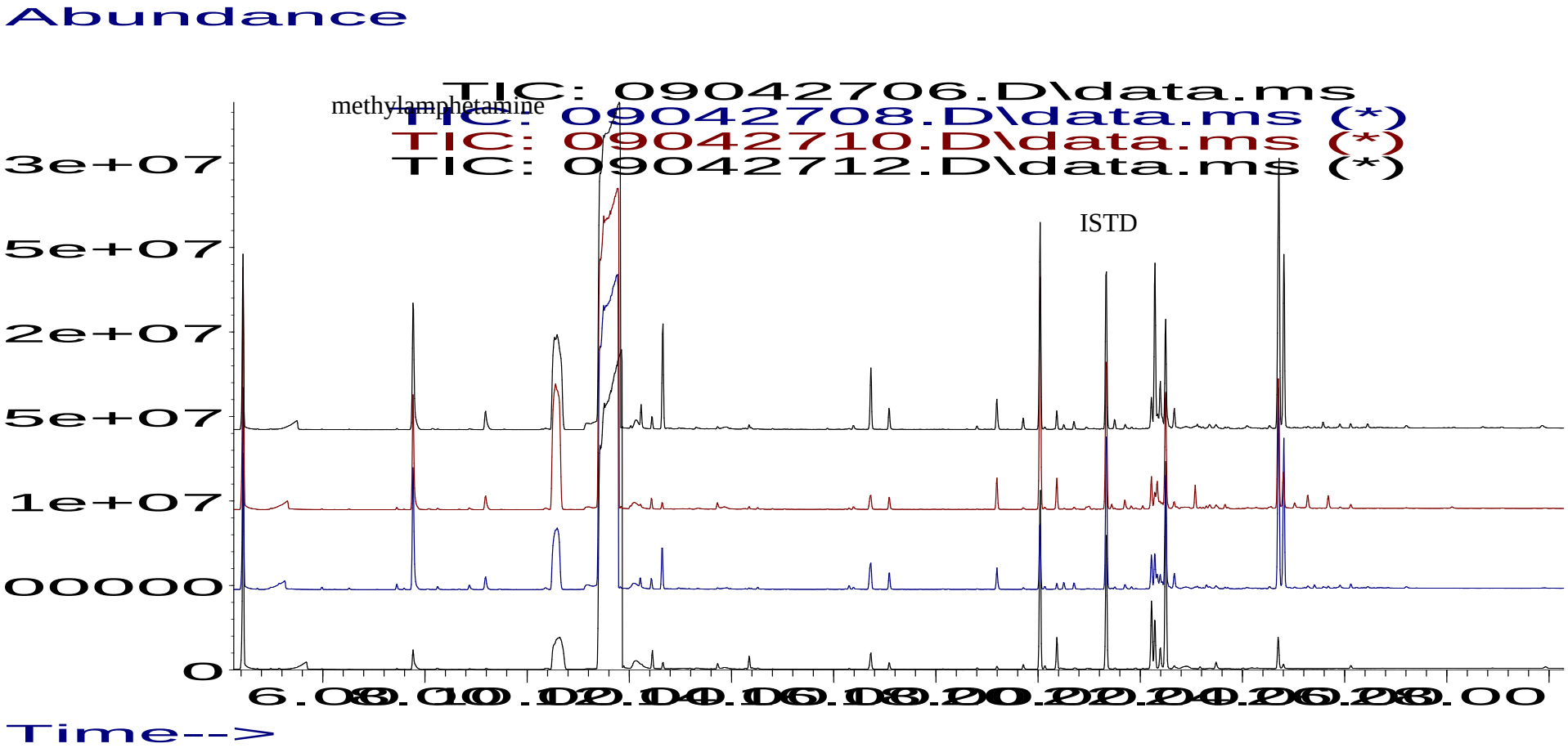

Figure 103: Overlay of the impurity profiles from the remaining four Moscow batches.

Visual comparison of the impurity profiles for the Moscow batches show obvious variation between the ten profiles, particularly within the 20 - 22 minute range, and in the range 24 – 26 minute range.

5.6.3 Data analysis of the single extracted samples

Section 5.3 demonstrated that for the 15 identified impurities normalised to the sum of the targets and pre-treated with either the square root method or fourth root method, a threshold of 95.00 did not facilitate linkage of all samples to their appropriate synthetic routes. Accurate discrimination by synthetic route of the 146 batches was achieved using the data set pre-treated via the sixteenth root method. The Pearson correlation coefficients were also calculated for the data derived from the sample analysis using the single extraction and DB-5 analytical column. It should be noted two additional target impurities (*trans*-aziridine and CMP) were included in the target impurity list as a result of the DB-5 column study. A full set of the relevant impurities from CHAMP study [8] and this study are presented in Appendix C.

The three refinements which were subjected to the data analysis were as follows:

1. CHAMP impurities normalised to the sum of the targets and pre-treated with sixteen roots method
2. Target impurities from this study normalised to the sum of the targets and pre-treated with sixteen roots method and
3. CHAMP impurities plus target impurities from this study normalised to the sum of the targets and pre-treated with sixteen roots method.

As a set point, the 95.00 threshold value was chosen across the three data sets. Again the most accurate discrimination by synthetic route of the 70 batches was achieved using the target impurities from this study normalised to the sum of the targets and pre-treated by the sixteenth root method. The lowest coefficient calculated for a pair of samples from within a synthetic route was 84.10 and the maximum threshold that would allow the 70 samples within each route to be deemed similar was 97.40.

Interrogation of the CHAMP impurities together with the target impurities from this study normalised to the sum of the targets and pre-treated by the sixteenth root method revealed similar results however, as before. Again CHAMP impurities normalised to the sum of the targets and pre-treated with sixteen roots method data sets reveals some

overlap between the Nagai and Moscow batches was in evidence and 4.76% (100 pairing) of the samples were incorrectly linked together.

A summary of the results are tabulated in Table 48 – Table 50.

CHAMP impurities normalised to the sum of the targets and pre-treated 16^{th} Root			
Route	MIN	MAX	AVERAGE
Leuckart	96.27	100	98.78
Red Amination	98.68	100	99.69
Nagai	99.48	100	99.81
Rosenmund	98.29	100	99.65
Birch	99.81	100	99.94
Emde	98.70	100	99.69
Moscow	99.01	100	99.71

Table 48: Summary of the Pearson correlation coefficients for 70 methylamphetamine batches synthesised by seven synthetic routes using CHAMP impurities normalised to the sum of the targets and pre-treated with square root, fourth root and sixteenth roots method.

Target impurities from this study normalised to the sum of the targets and pre-treated 16^{th} Root			
Route	MIN	MAX	AVERAGE
Leuckart	97.48	100	99.21
Red Amination	98.56	100	99.58
Nagai	99.17	100	99.71
Rosenmund	99.00	100	99.77
Birch	99.85	100	99.96
Emde	98.87	100	99.58
Moscow	98.89	100	99.66

Table 49: Summary of the Pearson correlation coefficients for 70 methylamphetamine batches synthesised by seven synthetic routes using target impurities from this study normalised to the sum of the targets and pre-treated with square root, fourth root and sixteenth roots method.

CHAMP impurities plus target impurities from this study normalised to the sum of the targets and pre-treated 16^{th} Root			
Route	MIN	MAX	AVERAGE
Leuckart	97.40	100	99.19
Red Amination	98.71	100	99.62
Nagai	99.27	100	99.74
Rosenmund	98.91	100	99.65
Birch	99.84	100	99.94
Emde	99.02	100	99.62
Moscow	98.93	100	99.68

Table 50: Summary of the Pearson correlation coefficients for 70 methylamphetamine batches synthesised by seven synthetic routes using CHAMP impurities plus target impurities from this study normalised to the sum of the targets and pre-treated with square root, fourth root and sixteenth roots method.

It is clear from this study that profiling with a DB-5 column was successful using only one extraction buffer as opposed to the two required for the DB-1MS system particulary for Reductive Amination route specific impurities. The DB-5 column also facilitated the identification of the CMP impurity which was only detected in methylamphetamine synthesised by ephedrine or pseudoephedrine salt using the DB-1MS column for the Birch synthesised samples.

5.7 Conclusions

The elucidation and investigation of a GCMS profiling system was one of the major objectives of this work. The literature investigating GCMS profiling methods for methylamphetamine samples, as opposed to MDMA or amphetamine, is more diverse with some variation in the results presented across different studies.

Through the analysis presented, it was determined that the variation within a single synthetic batch of material were relatively minor and the same impurities were identified in each case although at different concentrations.

The variation in the impurity profile between batches synthesised by the same chemist illustrated greater differences as would be expected. In some cases the number and type of impurities present from batch to batch varied, however the presence of the route specific impurities associated with a particular synthetic method, and identified in this work, always demonstrated a link between all samples produced via that method regardless of batch.

It could be suggested that the impurities defined by the CHAMP method (which was originally defined for amphetamine samples), may also be appropriate for chemical profiling of methylamphetamine samples, however, this work has demonstrated that reliance on the presence of CHAMP impurities is not sufficient for synthetic route discrimination of methylamphetamine samples. The CHAMP impurity list was capable of 100% accurate discrimination of 5 methylamphetamine synthetic routes (Leuckart, Reductive Amination, Rosenmund, Birch and Emde), but it did not cope well with

discriminating the Nagai and Moscow routes. The target impurities from this study normalised to the sum of the targets and pre-treated by a sixteenth root method provided accurate discrimination of all seven synthetic routes.

The timed synthetic study undertaken for the Nagai route has explained and clarified the differing results obtained in the previously published literature. The methylamphetamine dimer is formed from the condensation of methylamphetamine and aziridine: as the reaction time increases, the quantity of aziridine decreases and, therefore, the dimer cannot be formed as readily. Importantly, the dimer cannot be deemed route specific since (1) it is not in all of the Nagai reactions, and (2) it can be found in Emde batches.

The Birch substrate study again clarified previous literature and has demonstrated the differences observed in the impurity profiles obtained when the starting material is either ephedrine base or salt. The work presented has illustrated that when the base form of starting material was used, CMP was not observed due to masking by the large methylamphetamine peak extracted. This impurity was detected when salt form of starting material was used and analysis preformed on a DB-1MS column.

Analysis of samples from each synthetic route using a DB-5 column rather than the DB-1MS column suggested by Inoue et al.[15] and Tanaka et al.[14] revealed that all the target impurities listed in this study could be extracted and identified using a single phosphate buffer at pH 10.5 as opposed to the two buffer extraction required for successful discrimination using the DB-1MS column. In addition, CMP which is a route specific impurity for the Birch route was identified using the DB-5 column regardless of whether the starting material was ephedrine base or salt. This may have significant implications for laboratories which wish to undertake methylamphetamine impurity profiling.

5.8 References

1. United Nations International Drug Control Programme, *Drug Characterization/Impurity Profiling : Background and Concepts*; Vienna 2001.

2. Lee, J.S.; Han, E. Y.; Lee, S. Y.; Kim, E. M.; Park, Y. H.; Lim, M. A.; Chung, H. S.; Park, J. H., Analysis of the impurities in the methamphetamine synthesized by three different methods from ephedrine and pseudoephedrine. *Forensic Science International* 2006, 161(2-3), 209-215.

3. Kram, T.C.; Kruegel, A.V., The Identification of Impurities in Illicit Methamphetamine Exhibits by Gas Chromatography/Mass Spectrometry and Nuclear Magnetic Resonance Spectroscopy. *Journal of Forensic Sciences* 1977, 22(1), 40-52.

4. Person, E.C.; Meyer, J.A.; Vyvyan, J.R., Structural Determination of the Principal Byproduct of the Lithium-Ammonia Reduction Method of Methamphetamine Manufacture. *Journal of Forensic Sciences* 2005, 50(1), 1-9.

5. Ko, B.J.; Suh, S.; Suh, Y.J.; In, M.K.; Kim, S.H., The impurity characteristics of methamphetamine synthesized by Emde and Nagai method. *Forensic Science International* 2007, 170(1), 142-147.

6. Inoue, H.; Kanamori, T.; Iwata, Y.T.; Ohmae, Y.; Tsujikawa, K.; Saitoh, S.; Kishi, T., Methamphetamine impurity profiling using a 0.32 mm i.d. nonpolar capillary column. *Forensic Science International* 2003, 135(1), 42-47.

7. Andersson, K.; Lock, E.; Jalava, K.; Huizer, H.; Jonson, S.; Kaa, E.; Lopes, A.; Poortman, A.; Sippola, E.; Dujourdy, L.; Dahle´n, J., Development of a harmonised method for the profiling of amphetamines VI Evaluation of methods for comparison of amphetamine. *Forensic Science International* 2007, 169**,** 86–99.

8. Dujourdy, L.; Dufey, V.; Besacier, F.; Miano, N.; Marquis, R.; Lock, E.; Aalberg, L.; Dieckmann, S.; Zrcek, F.; Bozenko, J.S., Drug intelligence based on organic impurities in illicit MA samples. *Forensic Science International* 2008, 177, 153-161.

9. Pearson's Correlation Coefficient. Available at http://www.vias.org/tmdatanaleng/cc_corr_coeff.html. Last accessed on 10/04/10.

10. Buchanan, H.A.S., *An evaluation of isotope ratio mass spectrometry for the profiling of 3,4-methylenedioxymethamphetamine*, PhD Thesis in Department of Pure and Applied Chemistry, University of Strathclyde: Glasgow, 2009.

11. Altman, D.G., *Why Transform Data? In Practical Statistics for Medical Research*. Chapman & Hall/CRC: Boca Raton, Florida, 1999, 143-149.

12. Bland, M., *The Use of Transformations. In An Introduction to Medical Statistics*. 3rd ed.; Oxford University Press: New York, 2005, 164-167.

13. Windahl, K.L.; McTigue, M.J.; Pearson, J.R.; Pratt, S.J.; Rowe, J.E.; Sear, E.M., Investigation of the impurities found in methamphetamine synthesised from pseudoephedrine by reduction with hydriodic acid and red phosphorus. *Forensic Science International*, 1995, 76, 97-114.

14. Tanaka, K.; Ohmori, T.; Inoue, T., Analysis of impurities in illicit methamphetamine. *Forensic Science International*, 1992, 56 (2), 157 - 165.

15. Inoue, T.; Tanaka, K.; Ohmori, T.; Togawa, Y.; Seta, S., Impurity profiling analysis of methamphetamine seized in Japan. *Forensic Science International*, 1994, 69(1), 97-102.

16. Tanaka, K.; Ohmort, T.; Inonue, T.; Seta, S., Impurity Profiling Analysis of Illicit Methamphetamine by Capillary Gas Chromatography. *Journal of Forensic Sciences* 1994, 39(2), 500-511.

CHAPTER 6: IDENTIFYING THE SOURCES AND SYNTHETIC ROUTES OF METHYLAMPHETAMINE SAMPLES BY IRMS

6.0 Introduction

This part of the study investigated the carbon, nitrogen and hydrogen isotopic ratios present in each of the methylamphetamine samples synthesised by the various routes studied. The aim was to establish if there were any discernable links between the synthesis method and/or precursors used and the derived isotopic profiles. For IRMS analysis, all 149 batches of synthesised samples were analysed.

6.1 Experimental Methods

6.1.1 ^{13}C and ^{15}N Isotope Analysis by EA-IRMS

Carbon and nitrogen isotope ratio analyses were undertaken using an elemental analyzer (Costech Analytical Technologies Inc., Valencia, CA) coupled to an isotope ratio mass spectrometer (Thermo Fisher Scientific Inc., Bremen, Germany). Typically 0.9-1.2 mg of sample material was weighed into tin capsules (Costech Analytical Technologies Inc., Valencia, CA) and introduced via a solid Costech Zero-Blank autosampler (Costech Analytical Technologies Inc., Valencia, CA). The Elemental Analyzer (EA) reactor tubes were comprised of two quartz glass tubes filled with chromium(III) oxide / copper oxide and reduced copper, held at 1040 °C and 640 °C for combustion and reduction, respectively. A water trap filled with magnesium perchlorate was used to remove water from generated combustion gases, and a post reactor GC column was kept at 65 °C for separation of evolved N_2 and CO_2. Data were processed using proprietary ISODAT software (Thermo Fisher Scientific Inc., Bremen, Germany). Measured isotope ratios were expressed in the δ notation [‰] (equation as shown in Section 2.9) relative to the appropriate international isotope standard material anchoring the isotope scale (e.g., VPDB for ^{13}C and AIR for ^{15}N).

6.1.2 Isotopic Calibration and Quality Control of EA-IRMS Measurements

Each batch of samples contained blanks (empty tin capsules) and laboratory certified standards of known isotopic composition (St. Louis, MO). The within run standard was atropine ($\delta^{13}C$ VPDB -30.45‰, $\delta^{15}N$ AIR -14.22‰). The quality of the isotope

abundance measurement was monitored by participation in annual inter-laboratory exercises organized by the Forensic Isotope Ratio Mass Spectrometry Network (FIRMS).

6.1.3 ^{2}H Isotope Analysis by TC/EA-IRMS

A Delta V isotope ratio mass spectrometer (IRMS) coupled to a high-temperature conversion/ elemental analyzer (TC/EA; both Thermo Fisher Scientific Inc., Bremen, Germany) was used for $^{2}H/^{1}H$ isotope ratio measurement of synthesised methylamphetamine and precursor materials. Typically, 0.3-0.5 mg of solid sample was weighed into a silver capsule before the samples were introduced into the TC/EA by means of a solid Costech Zero-Blank solid autosampler (Costech Analytical Technologies Inc., Valencia, CA). The reactor tube was self-packed and comprised of a ceramic tube containing a glassy carbon tube filled with glassy carbon granulate, silver and quartz wool (Costech Analytical Technologies Inc., Valencia, CA). The reactor temperature was set to 1450 °C while the post reactor GC column was maintained at 90 °C. Data were processed using proprietary ISODAT software (Thermo Fisher Scientific Inc., Bremen, Germany). The run time per analysis was 400 s. Measured $^{2}H/^{1}H$ isotope ratios are expressed as δ values in ‰ relative to VSMOW (equation as shown in Section 2.7.3).

6.1.4 Isotopic Calibration and Quality Control of TC/EA-IRMS Measurements

The hydrogen working reference gas was research grade (Roberts Oxygen, Rockville, MD) and was calibrated against the international reference material (IRM), IAEACH-7 polyethylene (δ^{2}H VSMOW -100.3‰; IAEA, Vienna, Austria). The instrument was checked on a daily basis using method described by Sharp et al.[1] A typical batch analysis comprised of atropine and ephedrine HCl in-house standards, and IRM IAEA-CH-7 all analysed at the beginning and end of the set, with synthesised methylamphetamine and/or precursors samples in between. An atropine sample was analysed after every six samples to ensure no sample carry over occurred. The in-house standards atropine and ephedrine HCl had δ^{2}H VSMOW values of -187.8 and +175.2, respectively. Each batch was preceded and followed by a blank silver capsule. Precision of ^{2}H isotope analysis as monitored by the IRMS and lab standards was 2.2‰ or better. Measured δ^{2}H-values were normalized according to the method

described by Sharp et al.[1] with stretch factors typically being of the order of 1.029 to 1.060.

6.2 Results and Discussion

6.2.1 Methylamphetamine synthesised by P-2-P methods

Four different batches of P-2-P were used to synthesise methylamphetamine hydrochloride via two different reaction pathways as illustrated in reaction Scheme 4 in Chapter 3 and Section 3.1. In total 44 batches of methylamphetamine were prepared, 24 of these were via the Leuckart synthesis (using three different P-2-P batches) and the remaining 20 were prepared via the Reductive Amination method (using two different P-2-P batches, one of which was also used in the Leuckart synthesis).

The $\delta^{13}C$, $\delta^{15}N$ and $\delta^{2}H$ data of the 44 batches are given in Table 51 and are graphically represented in Figures 104 – Figure 106. These results are in line with published IRMS values of methylamphetamine.[2] The least variation was observed in the $\delta^{13}C$ data (3.6‰); and illustrated in Figure 81. The small variation in $\delta^{13}C$ values of the samples is not unexpected given that 9 of the 10 carbon atoms on the final methylamphetamine molecule are contributed by the P-2-P starting material. Even though all of the 24 samples for the Leuckart method were synthesised using 3 different batches of P-2-P the variation in carbon isotopic value was small.

Two different batches of P-2-P were used for the preparation of 20 samples synthesised via the Reductive Amination method, one of which was also the starting material for some of the Leuckart synthesised samples. $\delta^{13}C$ values for all 20 samples were very similar, however a clear difference was observed between the carbon isotope values between both routes (even though one batch of precursor was from the same source)

This is probably because of the *N*-methyl carbon on the molecule is contributed by *N*-methylformamide for the Leuckart method and methylamine hydrochloride for the Reductive Amination synthesised samples.

	Methylamphetamine			Phenyl-2-propanone		
Sample ID	$\delta^{15}N$	$\delta^{13}C$	$\delta^{2}H$	$\delta^{13}C$	$\delta^{2}H$	$\delta^{18}O$
L1	0.2	-32.5	-67.2	-28.7	-61.4	28.1
L2	3.6	-32.2	-68.2	-28.7	-61.4	28.1
L3	-0.3	-32.4	-59.2	-30.2	-48.0	19.5
L4	-6.5	-32.1	-73.3	-30.2	-48.0	19.5
L5	-6.1	-32.6	-74.9	-30.2	-48.0	19.5
L6	3.2	-32.5	-73.0	-30.2	-48.0	19.5
L7	1.6	-32.4	-76.1	-30.2	-48.0	19.5
L8	-1.4	-32.5	-69.8	-30.2	-48.0	19.5
L9	-3.1	-32.1	-77.1	-30.2	-48.0	19.5
L10	-6.5	-33.0	-79.2	-30.2	-48.0	19.5
L11	1.3	-32.6	-72.0	-30.2	-48.0	19.5
L12	-3.2	-33.0	-88.7	-30.2	-48.0	19.5
L13	-6.4	-33.1	-94.4	-30.2	-48.0	19.5
L14	-4.1	-32.8	-86.7	-30.2	-48.0	19.5
L15	-3.7	-32.7	-98.3	-30.2	-48.0	19.5
L16	-9.3	-32.3	-85.4	-30.2	-48.0	19.5
L17	1.5	-32.4	-79.2	-30.2	-48.0	19.5
L18	-7.6	-32.5	-90.5	-30.2	-48.0	19.5
L19	5.6	-32.5	-75.3	-30.2	-48.0	19.5
L20	6.4	-32.3	-79.0	-30.2	-48.0	19.5
L21	6.0	-32.4	-76.3	-30.3	-56.9	20.5
L22	2.4	-32.4	-78.8	-30.3	-56.9	20.5
L23	-2.1	-32.6	-85.0	-30.3	-56.9	20.5
L24	-2.6	-32.3	-77.6	-30.3	-56.9	20.5
RA31	8.5	-30.7	-74.0	-30.3	-56.9	20.5
RA32	3.7	-30.8	-77.2	-30.3	-56.9	20.5
RA33	0.4	-30.6	-90.6	-30.3	-56.9	20.5
RA34	6.2	-29.5	-102.6	-28.7	-77.4	21.5
RA35	1.4	-30.6	-92.4	-28.7	-77.4	21.5
RA36	-4.7	-29.7	-118.0	-28.7	-77.4	21.5
RA37	4.8	-29.5	-110.1	-28.7	-77.4	21.5
RA38	4.8	-29.4	-105.1	-28.7	-77.4	21.5
RA39	4.2	-29.5	-107.5	-28.7	-77.4	21.5
RA40	4.7	-30.2	-102.9	-28.7	-77.4	21.5
RA41	5.5	-30.4	-107.9	-28.7	-77.4	21.5
RA42	18.9	-29.4	-85.3	-28.7	-77.4	21.5
RA43	13.2	-30.2	-93.4	-28.7	-77.4	21.5
RA44	13.2	-30.2	-93.3	-28.7	-77.4	21.5
RA45	-4.8	-30.7	-108.1	-28.7	-77.4	21.5
RA46	17.1	-29.2	-89.1	-28.7	-77.4	21.5
RA47	-0.5	-30.3	-107.2	-28.7	-77.4	21.5
RA48	8.3	-30.0	-106.3	-28.7	-77.4	21.5
RA49	-2.1	-29.7	-124.9	-28.7	-77.4	21.5
RA50	-2.3	-29.7	-123.7	-28.7	-77.4	21.5

Table 51: $\delta^{13}C$, $\delta^{15}N$, and $\delta^{2}H$ values for the methylamphetamine samples synthesised using P-2-P as starting material and the four different batches of starting material.

In general when plotted, the $\delta^{13}C$ data points within a synthetic route clustered together as shown in Figure 104. This suggests that the fractionation induced within the synthetic process was reproduced from batch to batch.

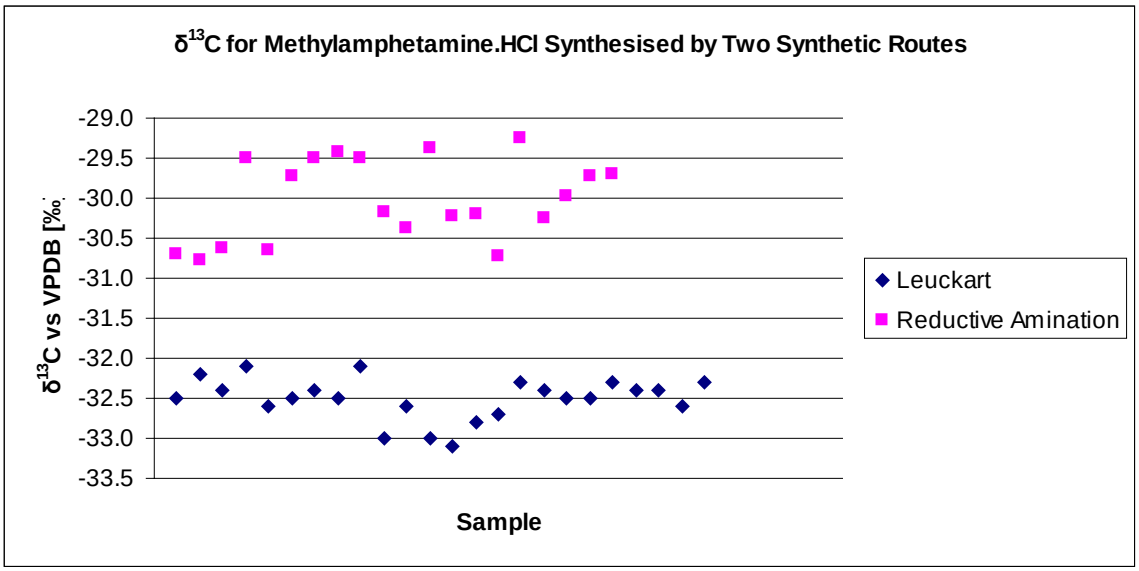

Figure 104: $\delta^{13}C$ results for the batches synthesised by two synthetic routes.

Examination of the $\delta^{15}N$ data reveals a variation of 28.2 ‰, for P-2-P samples (Figure 105). By $\delta^{15}N$ data, the values of the Leuckart and Reductive Amination routes overlap with no route discrimination possible. In general, methylamphetamine synthesed via the Reductive Amination method was difficult to replicate as the temperature of the exothermic reaction was difficult to control exactly, and a series of reagents were required to be added by hand in quick succession; thus, the temperature reached and rate of addition of reagents were likely to vary from batch to batch.

The $\delta^{15}N$ data appears to be the most sensitive to these inadvertent differences in preparative method, confirming the observations by Carter et al.[2] However, results published by Billault et al. in which a different Al/Hg amalgam method was used, produced MDMA with consistent $\delta^{15}N$ values.

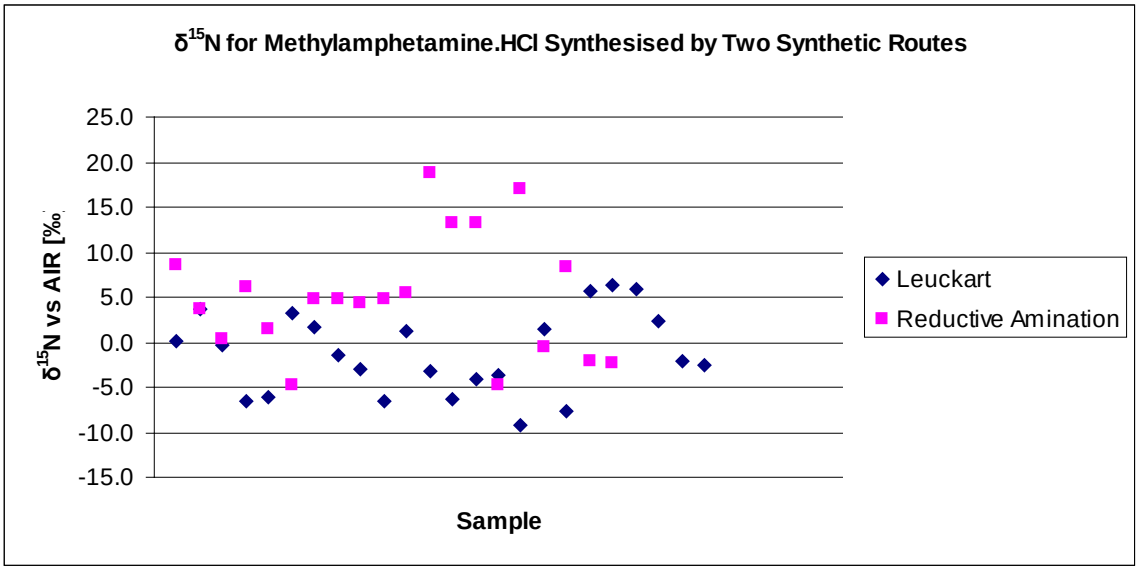

Figure 105: $\delta^{15}N$ results for the batches synthesised by two synthetic routes.

It is also interesting to examine the $\delta^{15}N$ data in relation to the nitrogen contributing precursor used. The nitrogen atom along with the *N*-methyl carbon on the methylamphetamine molecule is contributed by *N*-methylformamide (Leuckart) or methylamine hydrochloride (Reductive Amination). If the $\delta^{15}N$ of the nitrogen contributing reagent was solely responsible for the $\delta^{15}N$ of the methylamphetamine hydrochloride, then the $\delta^{15}N$ values would be expected to fall into two groups. Instead the Leuckart and Reductive Amination data points fall within the same range, indicating the synthetic process itself is responsible for fractionation of the nitrogen isotopes.

The $\delta^{2}H$ data show the greatest variation at 65.7‰, and is illustrated in Figure 106. This is perhaps unsurprising due to the number of potential proton contributors in both reactions. Furthermore, hydrogen atoms at select positions under certain conditions may be prone to exchange. For the synthetic routes in this study, a few of the possible hydrogen atom contributors are *N*-methylformamide, NaOH, MeOH, H_2SO_4, H_2O, CH_3NH_2 and HCl. Fractionation due to the synthetic process is also likely to contribute to the variation observed.

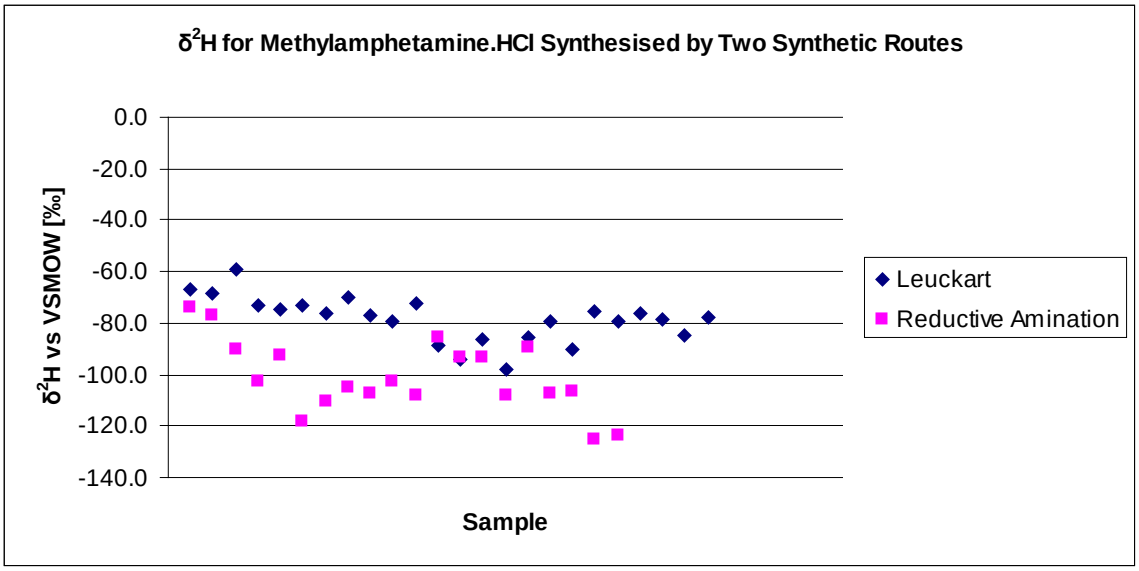

Figure 106: δ^2H results for the batches synthesised by two synthetic routes.

Two variable plots were then assessed to determine if two elements in combination might afford better visual discrimination than single variable plots.

Discrimination afforded by the combination of $\delta^{13}C$, $\delta^{15}N$ and δ^2H in two dimensional plots was investigated using Minitab (version 15.0). It is clear from a visual interpretation of Figures 107 – Figure 109 that the 44 samples cluster into two distinct groups according to the synthetic route. The ellipses drawn have no statistical significance and have been included for illustrative purpose only.

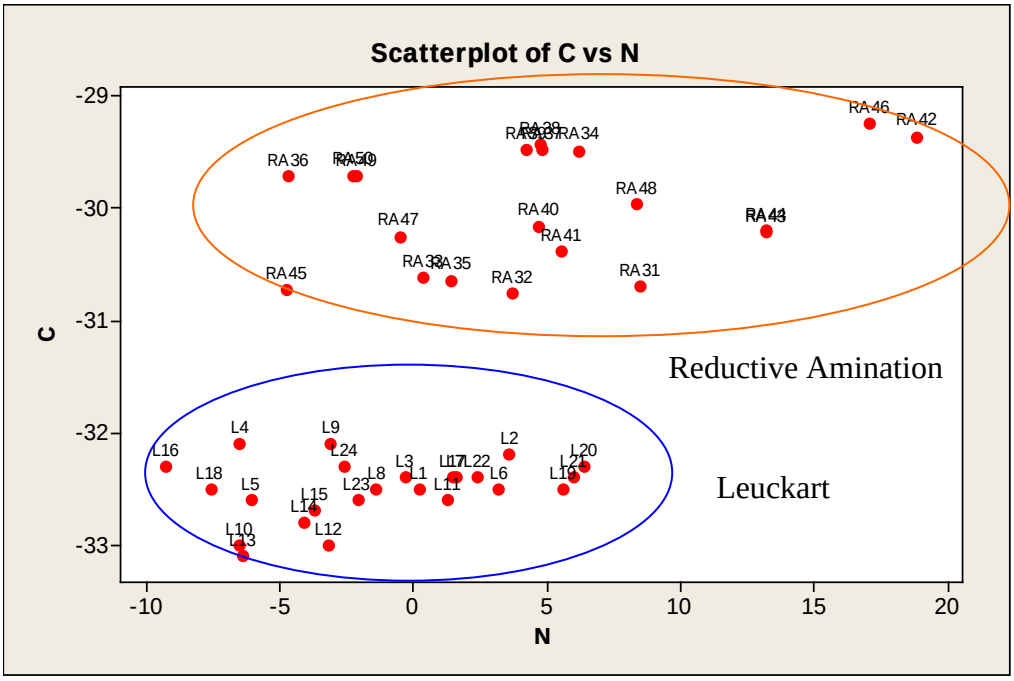

Figure 107: Two variable plot of the $\delta^{13}C$ and $\delta^{15}N$ data.

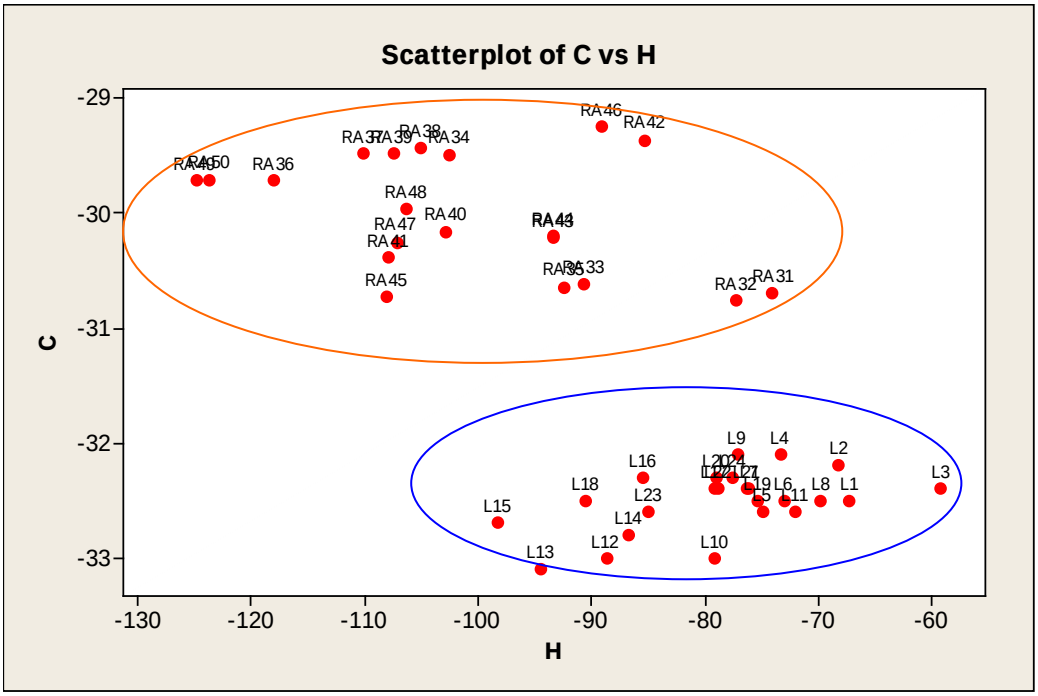

Figure 108: Two variable plot of the $\delta^{13}C$ and $\delta^{2}H$ data.

The single variable plot using $\delta^{13}C$ and two variable plots using $\delta^{13}C$ in combination with $\delta^{2}H$ or $\delta^{15}N$ data provide the best visual discrimination according to synthetic route while $\delta^{2}H$ or $\delta^{15}N$ either alone or in combination with each other provide a convoluted data set. Again this emphasizes the influence of the single transferred carbon atom from the reactants N-methylformamide or methylamine.

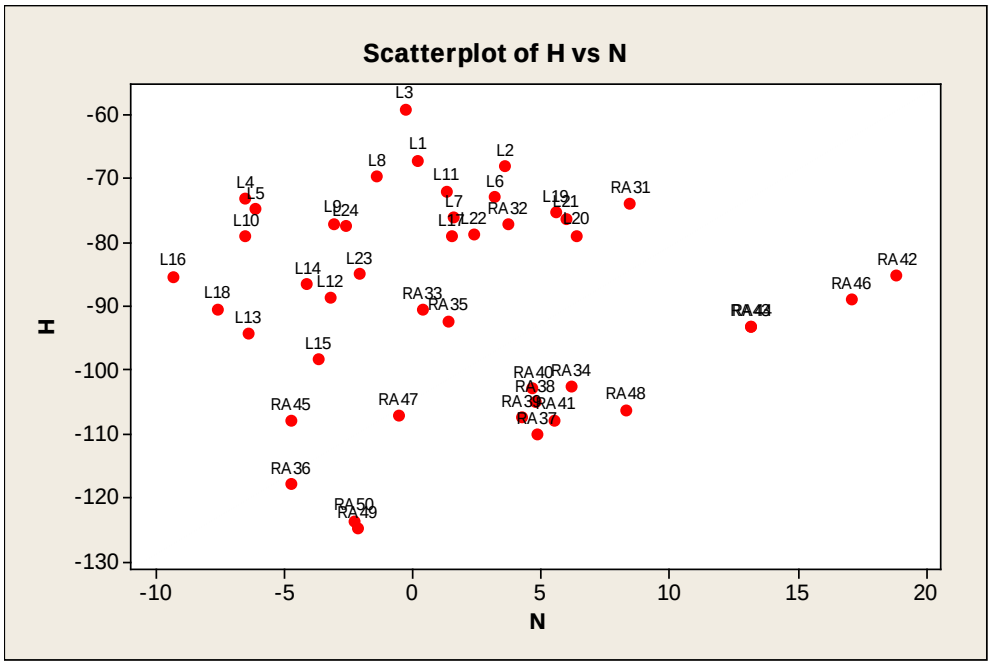

Figure 109: Two variable plot of the $\delta^{15}N$ and $\delta^{2}H$ data.

6.2.2 Methylamphetamine synthesised by ephedrine or *pseudo*ephedrine methods

Three different batches of ephedrine hydrochloride, one batch of *pseudo*ephedrine hydrochloride and one batch of ephedrine base were used to synthesise the methylamphetamine hydrochloride batches according to the five reaction pathways in Scheme 5 in Chapter 3 and Section 3.1. The $\delta^{13}C$, $\delta^{15}N$ and $\delta^{2}H$ data of the 105 batches are presented in Table 52 – Table 56.

	Methylamphetamine			*Pseudo*ephedrine and Ephedrine Hydrochloride			
Sample ID	$\delta^{15}N$	$\delta^{13}C$	$\delta^{2}H$	$\delta^{15}N$	$\delta^{13}C$	$\delta^{2}H$	$\delta^{18}O$
N51	18.6	-27.1	78.7	5.9	-27.0	108.1	27.0
N52	15.0	-27.1	76.2	5.9	-27.0	108.1	27.0
N53	12.5	-27.1	73.8	5.9	-27.0	108.1	27.0
N54	12.6	-27.1	64.4	5.9	-27.0	108.1	27.0
N55	12.2	-27.1	60.7	5.9	-27.0	108.1	27.0
N56	13.1	-27.1	79.5	5.9	-27.0	108.1	27.0
N57	2.1	-27.3	60.7	5.9	-27.0	108.1	27.0
N58	2.8	-27.2	59.6	5.9	-27.0	108.1	27.0
N59	8.6	-27.2	68.6	5.9	-27.0	108.1	27.0
N60	8.8	-27.2	64.5	5.9	-27.0	108.1	27.0
N61	-6.7	-26.1	62.2	0.7	-25.9	142.7	20.3
N62	3.4	-26.0	97.1	0.7	-25.9	142.7	20.3
N63	5.4	-25.9	109.1	0.7	-25.9	142.7	20.3
N64	4.6	-25.9	106.4	0.7	-25.9	142.7	20.3
N65	5.8	-25.9	93.5	0.7	-25.9	142.7	20.3
N65	-4.1	-26.0	81.2	0.7	-25.9	142.7	20.3
N67	4.5	-26.0	102.9	0.7	-25.9	142.7	20.3
N68	2.6	-26.0	98.1	0.7	-25.9	142.7	20.3
N69	-6.6	-26.0	70.8	0.7	-25.9	142.7	20.3
N70	-8.6	-26.1	69.1	0.7	-25.9	142.7	20.3

Table 52: $\delta^{13}C$, $\delta^{15}N$, and $\delta^{2}H$ values for the methylamphetamine samples synthesised via the Nagai reaction using *pseudo*ephedrine (orange) or ephedrine (blue) as starting material.

Table 52 shows significant variations in $\delta^{13}C$, $\delta^{15}N$ and $\delta^{2}H$ values between two different starting material, ephedrine and *pseudo*ephedrine. The $\delta^{13}C$ value for methylamphetamine shows that it depends on the starting material that was used during the synthesis.

	Methylamphetamine			*Pseudo*ephedrine and Ephedrine Hydrochloride			
Sample ID	$\delta^{15}N$	$\delta^{13}C$	$\delta^{2}H$	$\delta^{15}N$	$\delta^{13}C$	$\delta^{2}H$	$\delta^{18}O$
R71	7.3	-27.3	71.4	5.9	-27.0	108.1	27.0
R72	6.3	-27.6	77.6	5.9	-27.0	108.1	27.0
R73	3.3	-27.4	66.3	5.9	-27.0	108.1	27.0
R74	4.4	-27.5	65.6	5.9	-27.0	108.1	27.0
R75	6.6	-26.9	52.7	5.9	-27.0	108.1	27.0
R76	4.9	-27.2	43.7	5.9	-27.0	108.1	27.0
R77	5.6	-27.5	58.6	5.9	-27.0	108.1	27.0
R78	3.5	-27.6	78.7	5.9	-27.0	108.1	27.0
R79	-0.1	-26.1	61.9	0.7	-25.9	142.7	20.3
R80	-0.8	-26.3	73.2	0.7	-25.9	142.7	20.3
R81	-0.6	-26.2	76.4	0.7	-25.9	142.7	20.3
R82	-1.1	-26.3	87.5	0.7	-25.9	142.7	20.3
R83	-2.1	-26.5	55.2	0.7	-25.9	142.7	20.3
R84	-2.9	-26.3	78.5	0.7	-25.9	142.7	20.3
R85	2.9	-26.0	77.4	0.7	-25.9	142.7	20.3
R86	-1.6	-26.2	69.2	0.7	-25.9	142.7	20.3
R87	-4.0	-26.4	83.1	0.7	-25.9	142.7	20.3
R88	0.9	-25.5	63.4	0.7	-25.9	142.7	20.3
R89	-3.6	-25.8	68.6	0.7	-25.9	142.7	20.3
R90	0.5	-25.9	61.5	0.7	-25.9	142.7	20.3

Table 53: $\delta^{13}C$, $\delta^{15}N$, and $\delta^{2}H$ values for the methylamphetamine samples synthesised via the Rosenmund reaction using *pseudo*ephedrine (orange) or ephedrine (blue) as the starting material.

In Rosenmund reaction same batches of starting material from Nagai reaction was used during the synthesis. There are no significant variations in the $\delta^{13}C$, $\delta^{15}N$ and $\delta^{2}H$ values for methylamphetamine synthesised from these two routes (as shown in Table 52 and 53).

	Methylamphetamine			Ephedrine base			
Sample ID	$\delta^{15}N$	$\delta^{13}C$	$\delta^{2}H$	$\delta^{15}N$	$\delta^{13}C$	$\delta^{2}H$	$\delta^{18}O$
B91	7.6	-21.8	37.1	4.2	-23.2	36.8	26.9
B92	6.0	-22.8	23.7	4.2	-23.2	36.8	26.9
B93	4.7	-23.1	17.6	4.2	-23.2	36.8	26.9
B94	5.6	-22.5	22.6	4.2	-23.2	36.8	26.9
B95	4.4	-23.4	23.6	4.2	-23.2	36.8	26.9
B96	5.8	-22.7	10.5	4.2	-23.2	36.8	26.9
B97	5.2	-21.7	19.4	4.2	-23.2	36.8	26.9
B98	5.6	-22.9	30.1	4.2	-23.2	36.8	26.9
B99	6.1	-22.2	31.0	4.2	-23.2	36.8	26.9
B100	4.0	-22.7	28.1	4.2	-23.2	36.8	26.9
B101	4.4	-22.9	26.9	4.2	-23.2	36.8	26.9
B102	6.7	-23.3	19.0	4.2	-23.2	36.8	26.9
B103	5.4	-23.1	16.4	4.2	-23.2	36.8	26.9
B104	6.8	-23.3	16.0	4.2	-23.2	36.8	26.9
B105	5.0	-22.6	26.6	4.2	-23.2	36.8	26.9
B106	7.6	-21.8	25.5	4.2	-23.2	36.8	26.9
B107	5.7	-22.8	22.2	4.2	-23.2	36.8	26.9
B108	7.2	-22.4	29.1	4.2	-23.2	36.8	26.9
B109	5.8	-22.8	30.4	4.2	-23.2	36.8	26.9
B110	5.8	-22.7	31.4	4.2	-23.2	36.8	26.9

Table 54: $\delta^{13}C$, $\delta^{15}N$, and $\delta^{2}H$ values for the methylamphetamine samples synthesised via the Birch reaction using ephedrine base as starting material.

Ephedrine in base form was used in Birch reaction and the $\delta^{13}C$, $\delta^{15}N$ and $\delta^{2}H$ values for ephedrine and methylamphetamine are shown in Table 54

	Methylamphetamine			*Pseudo*ephedrine and Ephedrine Hydrochloride			
Sample ID	$\delta^{15}N$	$\delta^{13}C$	$\delta^{2}H$	$\delta^{15}N$	$\delta^{13}C$	$\delta^{2}H$	$\delta^{18}O$
E111	0.5	-25.9	111.4	0.2	-25.7	132.8	20.4
E112	0.7	-25.9	125.7	0.2	-25.7	132.8	20.4
E113	0.2	-25.9	120.5	0.2	-25.7	132.8	20.4
E114	1.5	-25.8	129.7	0.2	-25.7	132.8	20.4
E115	1.3	-25.8	123.4	0.2	-25.7	132.8	20.4
E116	5.7	-27.1	100.2	5.9	-27.0	108.1	27.0
E117	6.8	-27.1	96.8	5.9	-27.0	108.1	27.0
E118	6.0	-27.0	87.9	5.9	-27.0	108.1	27.0
E119	6.2	-27.0	88.2	5.9	-27.0	108.1	27.0
E120	7.0	-27.1	83.3	5.9	-27.0	108.1	27.0
E121	6.6	-27.1	82.0	5.9	-27.0	108.1	27.0
E122	5.9	-27.1	75.1	5.9	-27.0	108.1	27.0
E123	1.5	-27.3	78.9	5.9	-27.0	108.1	27.0
E124	1.6	-27.2	76.5	5.9	-27.0	108.1	27.0
E125	0.9	-25.8	118.4	0.2	-25.7	132.8	20.4
E126	0.2	-25.8	104.7	0.2	-25.7	132.8	20.4
E127	0.8	-25.8	113.3	0.2	-25.7	132.8	20.4
E128	0.2	-25.8	111.0	0.2	-25.7	132.8	20.4
E129	0.3	-25.9	103.0	0.2	-25.7	132.8	20.4
E130	-0.1	-25.9	100.5	0.2	-25.7	132.8	20.4

Table 55: $\delta^{13}C$, $\delta^{15}N$, and $\delta^{2}H$ values for the methylamphetamine samples synthesised via the Emde reaction using ephedrine (brown) or *pseudo*ephedrine (orange) as starting material.

Methylamphetamine synthesised by Emde route utilised different batch of ephedrine hydrochloride compare to Nagai and Rosenmund routes. However it doesn't show any significant variations in the $\delta^{13}C$, $\delta^{15}N$ and $\delta^{2}H$ values for methylamphetamine.

In Moscow reaction same batch of ephedrine hydrochloride from Emde reaction was used during the synthesis. Again there are no significant variations in the $\delta^{13}C$, $\delta^{15}N$ and $\delta^{2}H$ values for methylamphetamine synthesised from these two routes (as shown in Table 55 and 56).

It should be noted that same batch of *pseudo*ephedrine was used in all the four synthetic routes (Nagai, Rosenmund, Emde and Moscow).

	Methylamphetamine			*Pseudo*ephedrine and Ephedrine Hydrochloride			
Sample ID	$\delta^{15}N$	$\delta^{13}C$	$\delta^{2}H$	$\delta^{15}N$	$\delta^{13}C$	$\delta^{2}H$	$\delta^{18}O$
M131	3.2	-27.3	95.7	5.9	-27.0	108.1	27.0
M132	5.4	-27.5	78.6	5.9	-27.0	108.1	27.0
M133	6.5	-27.3	87.5	5.9	-27.0	108.1	27.0
M134	6.0	-27.3	81.1	5.9	-27.0	108.1	27.0
M135	-0.4	-26.2	95.6	-1.5	-25.4	143.2	19.5
M136	-0.2	-26.1	95.3	-1.5	-25.4	143.2	19.5
M137	-2.0	-25.8	113.2	-1.5	-25.4	143.2	19.5
M138	-1.8	-25.8	106.1	-1.5	-25.4	143.2	19.5
M139	-1.8	-26.1	95.3	-1.5	-25.4	143.2	19.5
M140	-1.8	-25.7	115.7	-1.5	-25.4	143.2	19.5
M141	-2.4	-25.8	108.6	-1.5	-25.4	143.2	19.5
M142	-2.3	-25.8	118.1	-1.5	-25.4	143.2	19.5
M143	-4.3	-26.0	103.9	-1.5	-25.4	143.2	19.5
M144	-1.4	-25.9	95.7	-1.5	-25.4	143.2	19.5
M145	-1.5	-25.7	106.7	-1.5	-25.4	143.2	19.5
M146	-9.8	-25.8	118.6	-1.5	-25.4	143.2	19.5
M147	-3.4	-25.8	113.4	-1.5	-25.4	143.2	19.5
M148	-1.6	-25.7	114.2	-1.5	-25.4	143.2	19.5
M149	-1.6	-25.7	115.1	-1.5	-25.4	143.2	19.5
M150	-1.5	-25.7	105.8	-1.5	-25.4	143.2	19.5
M151	-0.8	-25.7	112.3	-1.5	-25.4	143.2	19.5
M152	-1.8	-25.7	103.5	-1.5	-25.4	143.2	19.5
M153	-1.4	-25.7	103.7	-1.5	-25.4	143.2	19.5
M154	-1.7	-25.8	108.5	-1.5	-25.4	143.2	19.5
M155	-1.8	-25.8	105.0	-1.5	-25.4	143.2	19.5

Table 56: $\delta^{13}C$, $\delta^{15}N$, and $\delta^{2}H$ values for the methylamphetamine samples synthesised via the Moscow reaction using *pseudo*ephedrine (orange) or ephedrine (green) as starting material.

The $\delta^{13}C$, $\delta^{15}N$ and $\delta^{2}H$ data for the 105 methylamphetamine samples are graphically represented in Figures 110-112. These results are in line with published IRMS values of methylamphetamine.[2, 4-8] When examining first the $\delta^{13}C$ data, the least variation is shown by this element respectively for four of the five routes (Nagai, Rosenmund, Emde and Moscow) using ephedrine and *pseudo*ephedrine (1.0‰ and 0.7‰ respectively), as starting materials. In both cases the hydrochloride salt was utilised. Again this was not unexpected as 10 carbon atoms on the final methylamphetamine molecule are contributed by the either the ephedrine or *pseudo*ephedrine starting material.

One batch of ephedrine base was used to synthesis 20 batches of methylamphetamine hydrochloride via the Birch route. The $\delta^{13}C$ data for these samples when compared to the $\delta^{13}C$ data for the samples from the other four routes illustrated significant variations which can only be attributed to the starting material (Figure 110).

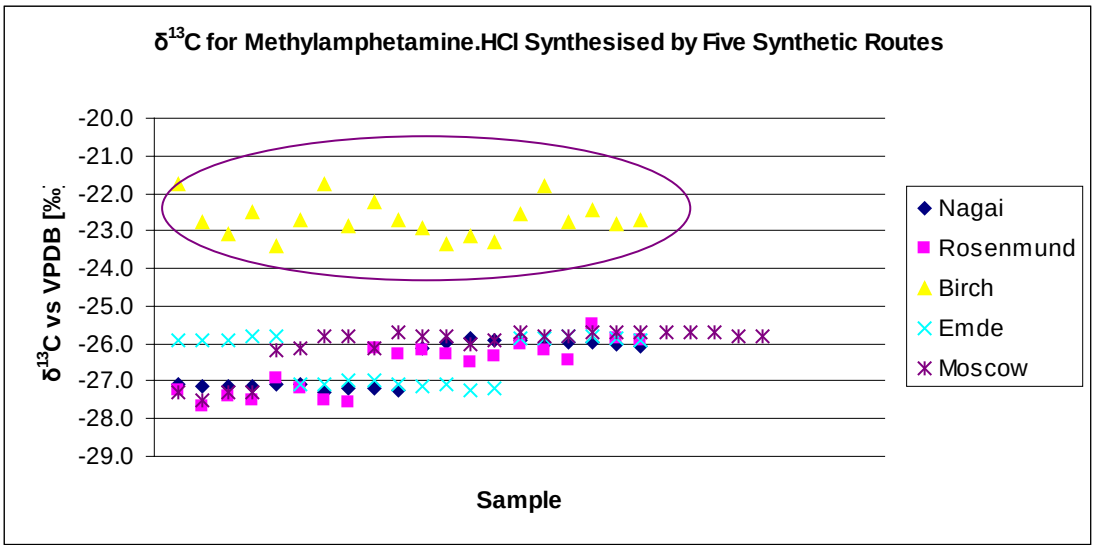

Figure 110: $\delta^{13}C$ results for the batches synthesised by five synthetic routes.

In general, the $\delta^{13}C$ data points within a synthetic route cluster together visually, indicating the fractionation induced within the synthetic process is reproducible by the same chemist using the same method and materials. By $\delta^{13}C$ data alone it is difficult to clearly separate the samples synthesised with ephedrine hydrochloride and *pseudo*ephedrine hydrochloride however the samples synthesised from ephedrine base were clearly separated. Clear separation of two groups within the Emde method and Rosenmund method were observed, however a T-test (two-tail at 95% confidence) demonstrated that the difference observed between the groups was not statistically significant at the level 95% level.

Examination of the $\delta^{15}N$ data points reveals a wide variation the Nagai batches exhibiting the widest batch to batch variation of the five synthetic routes (Figure 111). By $\delta^{15}N$ data, the values of the all the five routes are convoluted and overlap each other indicating that the $\delta^{15}N$ data appears to be the most sensitive to inadvertent differences in preparative method between batches synthesised by the same synthetic method. The nitrogen atom on the methylamphetamine molecule is contributed by the nitrogen from the ephedrine or *pseudo*ephedrine starting material.

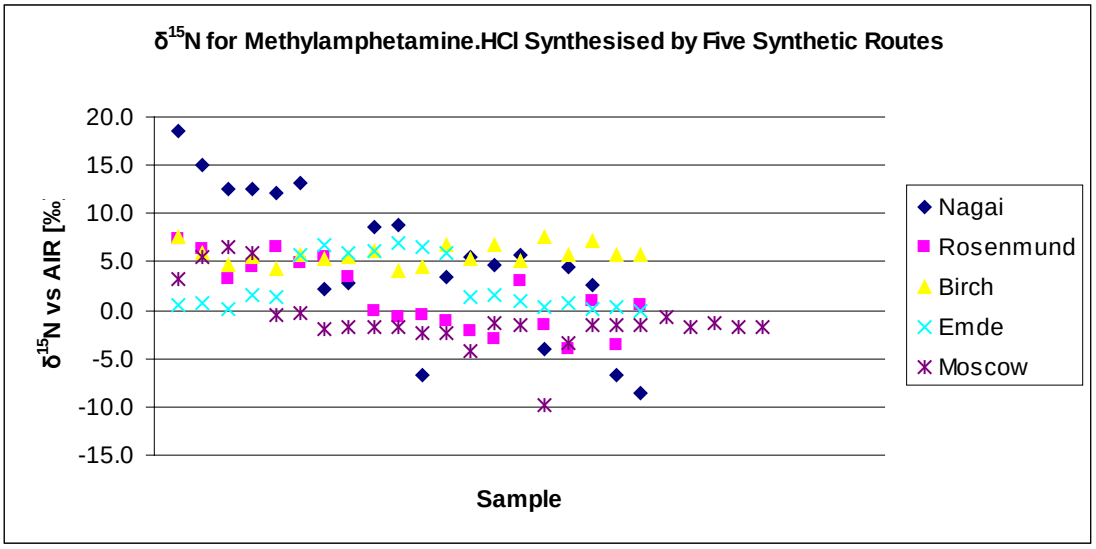

Figure 111: $\delta^{15}N$ results for the batches synthesised by five synthetic routes.

The $\delta^{15}N$ data points fall within the same range and this is unsurprising given that the same starting material was used either ephedrine or *pseudo*ephdrine for all the four routes. It should be noted that the $\delta^{15}N$ data points within the Birch route (from ephedrine base) also overlap with all the four routes. The $\delta^{15}N$ data varied more in the Nagai, Rosenmund and Moscow samples compared to those prepared by the Emde route. This may be due to the protonation of nitrogen and elimination process which will occur under acidic conditions. In the Emde route, chlorine is preferred for elimination and the $\delta^{15}N$ data points do not vary as much as in the other three routes. The data for Nagai and Moscow varied differently. The $\delta^{15}N$ variation for the Moscow route samples was smaller compared to Nagai route samples possibly because of a different source of iodine used for each of these routes.

The $\delta^{2}H$ data points show the most variation and are illustrated in Figure 112. This is perhaps unsurprising due to the number of potential proton contributors and hydrogen atoms at select positions under certain conditions may be prone to exchange. For the synthetic routes in this study, a few of the possible hydrogen atom contributors are, HI, CH_3COOH, H_2O, and CH_3COONa. The observed variation of the $\delta^{2}H$ values is therefore expected due to the large number of possible hydrogen contributors, but fractionation due to the synthetic process is also likely to contribute. The samples prepared via the Birch route can be distinguished from the other samples and have a batch to batch $\delta^{2}H$ data variation of within 26.6‰.

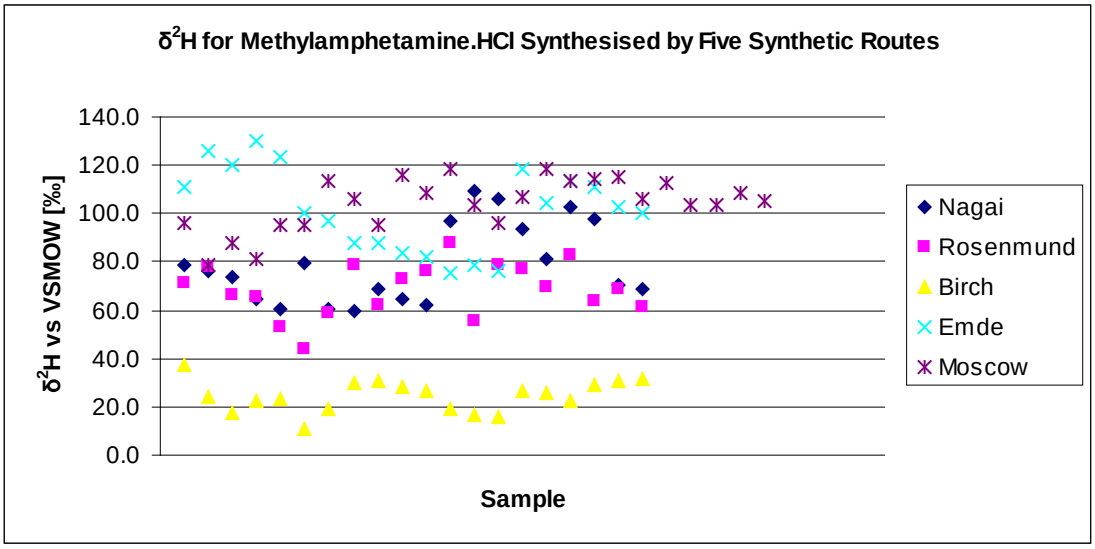

Figure 112: δ^2H results for the batches synthesised by five synthetic routes.

It is clear from visual interpretation of Figures 113 – Figure 115 that the 105 samples cluster into three groups according to starting material, with the best separations being illustrated by plots of carbon and hydrogen and carbon and nitrogen. It was not possible, however to separate the samples by specific synthetic route, only by precursor (salt and base form).

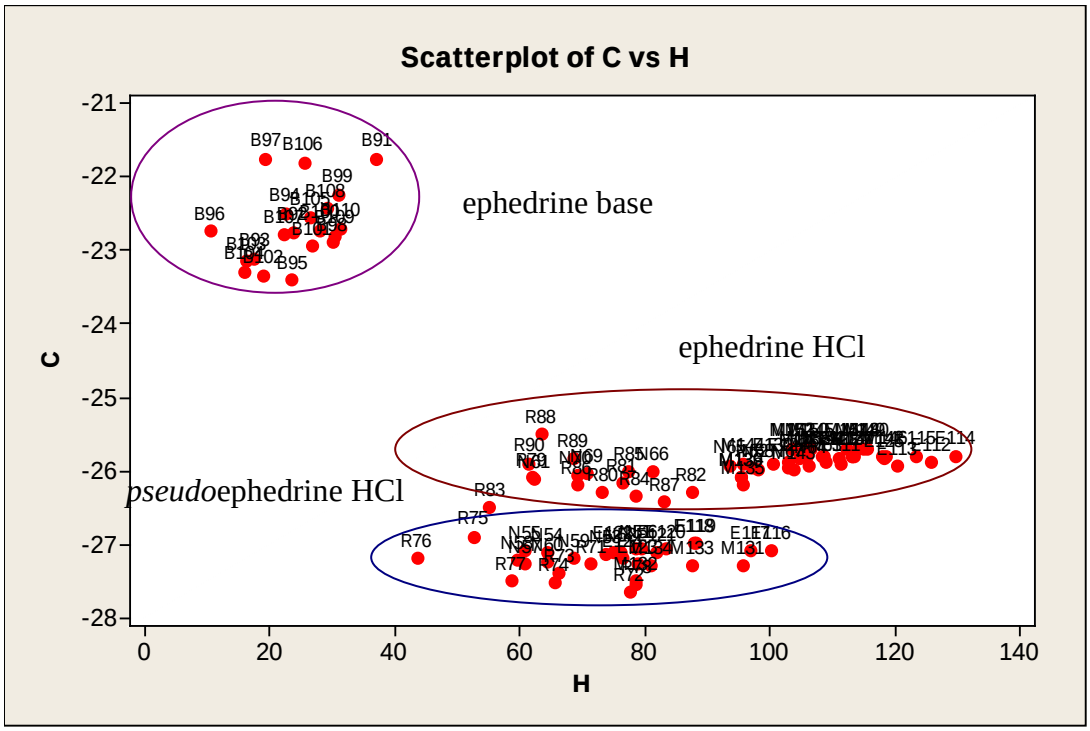

Figure 113: Two variable plot of the $\delta^{13}C$ and $\delta^{2}H$ data.

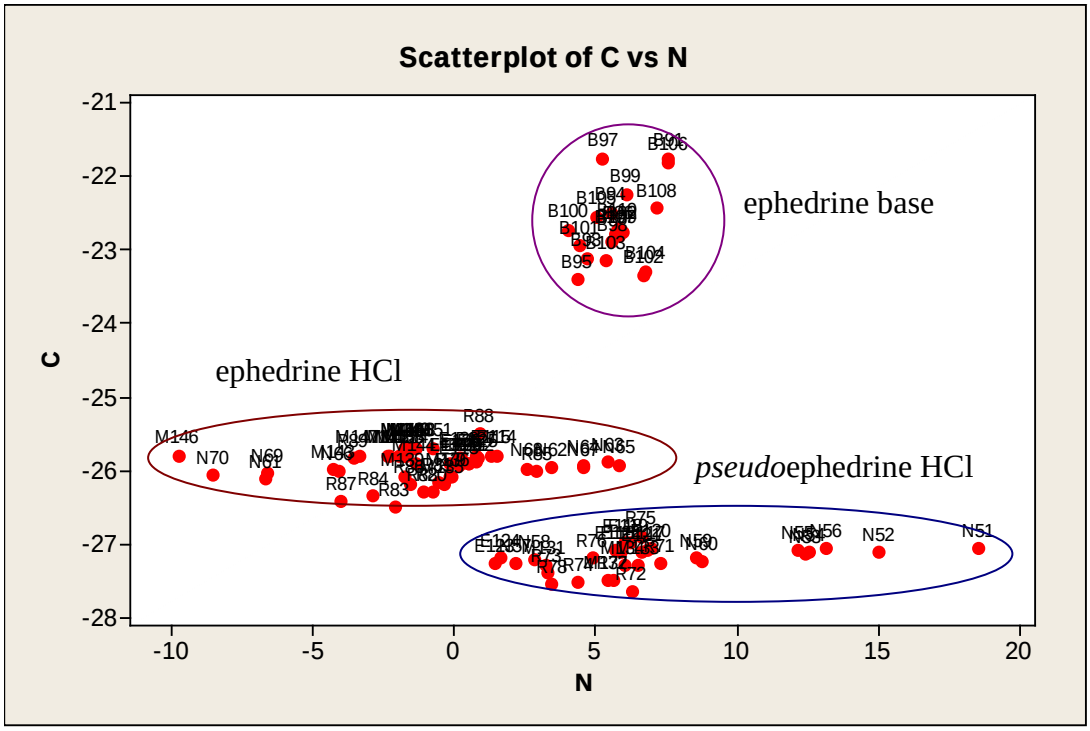

Figure 114: Two variable plot of the $\delta^{13}C$ and $\delta^{15}N$ data.

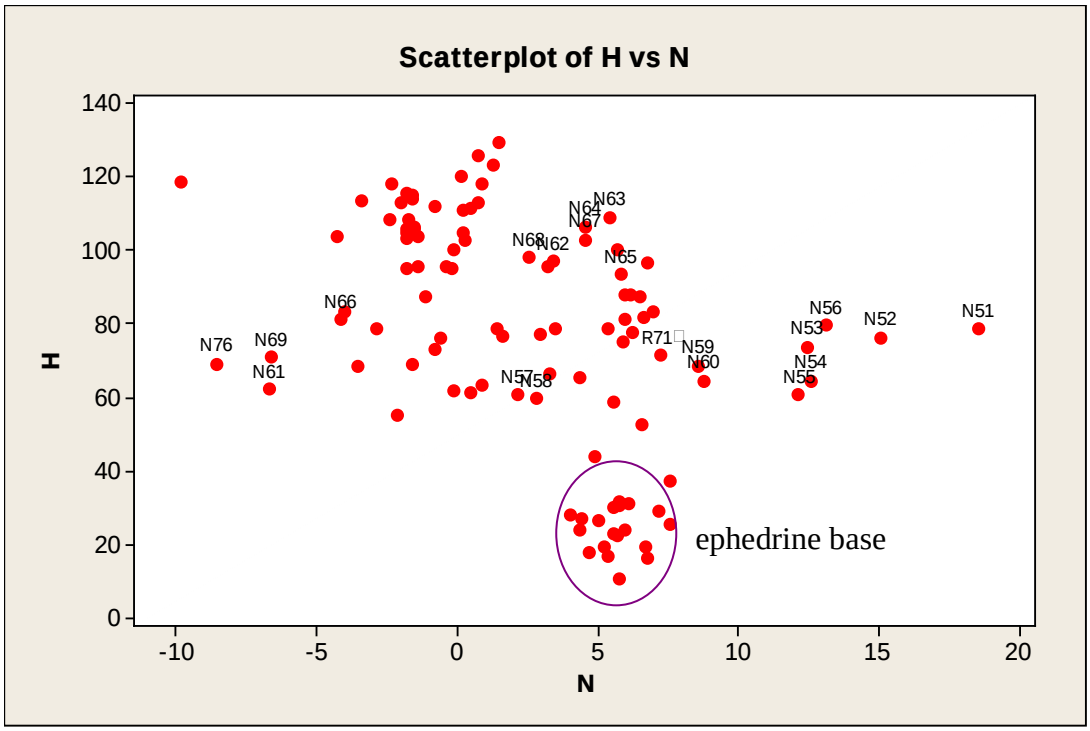

Figure 115: Two variable plot of the δ^{2}H and δ^{15}N data.

Figure 115 shows that nitrogen and hydrogen plot is difficult to clearly separate the samples by precursor (ephedrine base).

6.2.3 Methylamphetamine synthesised by all the 7 methods

All the 149 batches of methylamphetamine hydrchloride synthesised from the seven routes were combined in a data set and the $\delta^{13}C$, $\delta^{15}N$ and $\delta^{2}H$ data are graphically represented in Figures 116-119. Visual discrimination of the four different precursors (P-2-P, ephedrine HCl, *pseudo*ephedrine HCl and ephedrine base) are possible in carbon plot (Figure 116) with further discrimination within the P-2-P route for Leuckart and Reductive Amination routes.

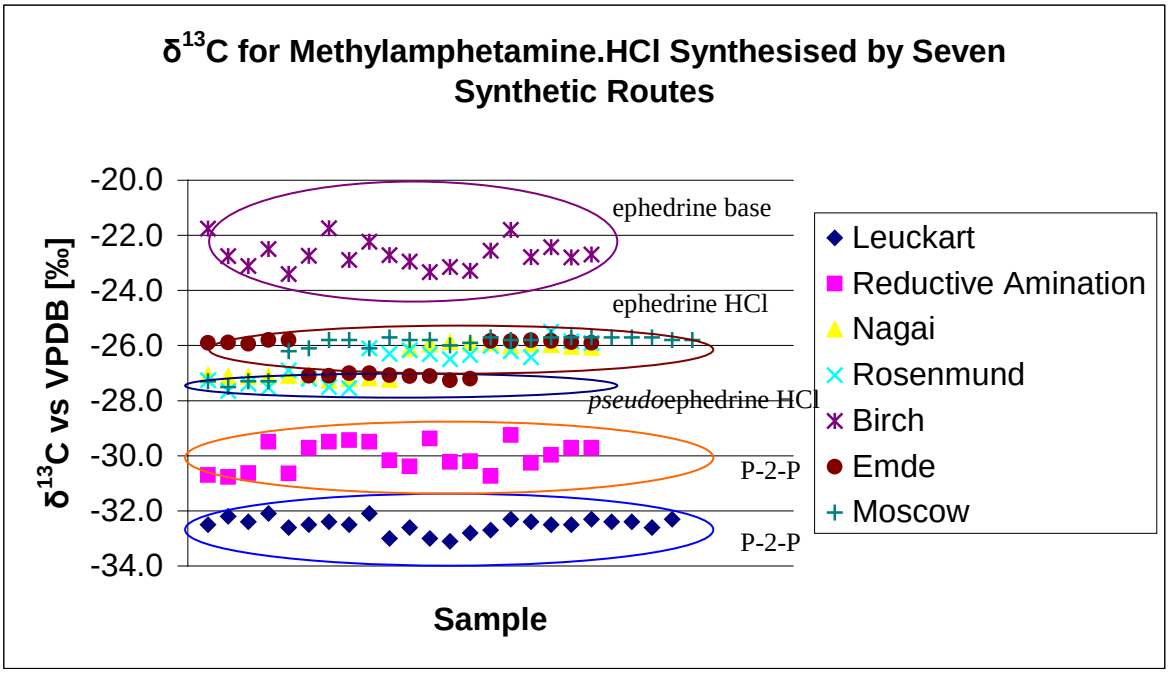

Figure 116: $\delta^{13}C$ results for the batches synthesised by seven synthetic routes.

Again nitrogen plot (Figure 117) failed to show any possible discrimination by starting material or synthetic route.

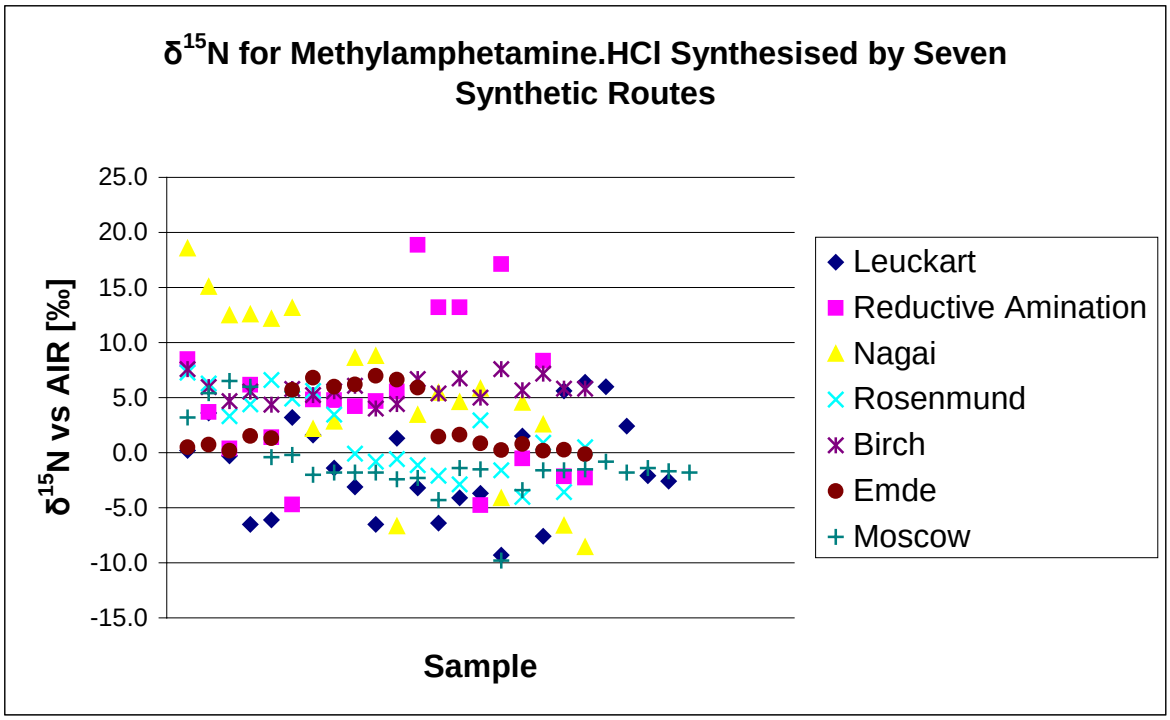

Figure 117: $\delta^{15}N$ results for the batches synthesised by seven synthetic routes.

Methylamphetamine synthesised from P-2-P precursors had $\delta^{2}H$ values that were negative while methylamphetamine synthesised from the ephedrine or *pseudo*ephedrine precursors had positive $\delta^{2}H$ values (Figure 118).

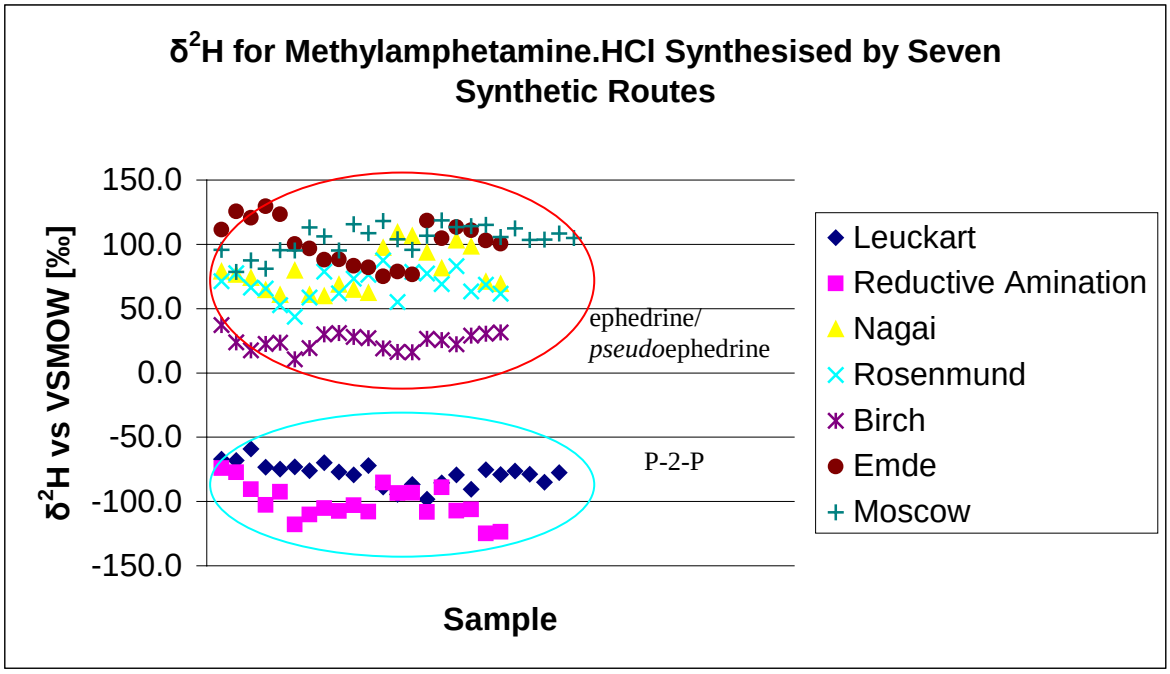

Figure 118: $\delta^{2}H$ results for the batches synthesised by seven synthetic routes.

When viewed as two dimensional plots using $\delta^{13}C$ and $\delta^{2}H$ or $\delta^{13}C$ and $\delta^{15}N$ data, Figures 119 – Figure 121, it is clear that the 149 samples cluster into four distinct groups according to the starting material used in two variable plots and the clearest discrimination was afforded by the carbon-nitrogen plot.

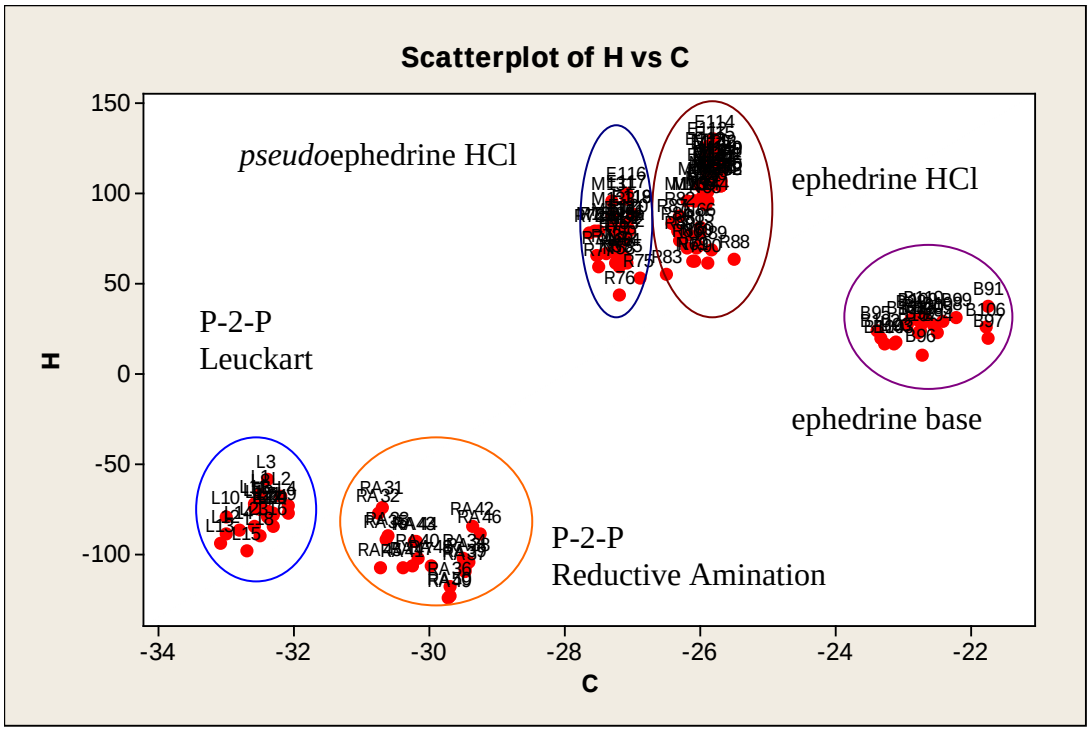

Figure 119: Two variable plot of the $\delta^{13}C$ and $\delta^{2}H$ data.

Further discrimination within the P-2-P route for Leuckart and Reductive Amination routes was achieved as shown in Figure 119 and 120. Figure 121 shows that samples cluster into two groups according to the starting material (P-2-P and ephedrine/*pseudo*ephedrine). It should be noted that samples synthesised with ephedrine base is difficult to clearly separate with nitrogen and hydrogen plot.

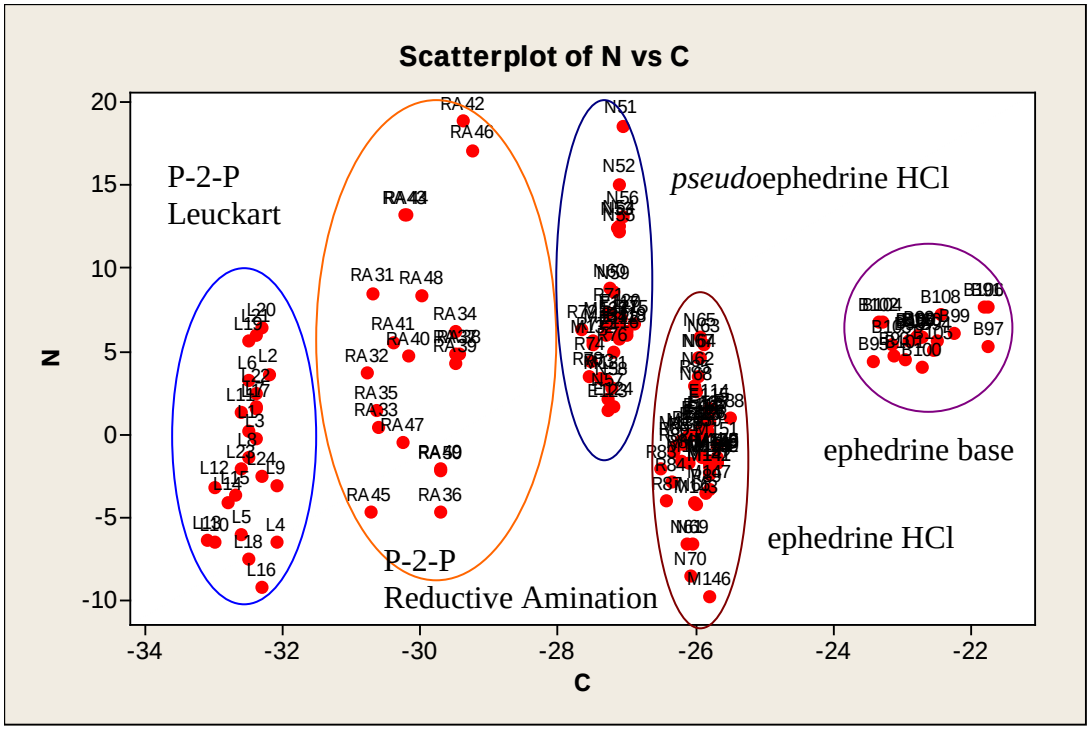

Figure 120: Two variable plot of the $\delta^{13}C$ and $\delta^{15}N$ data.

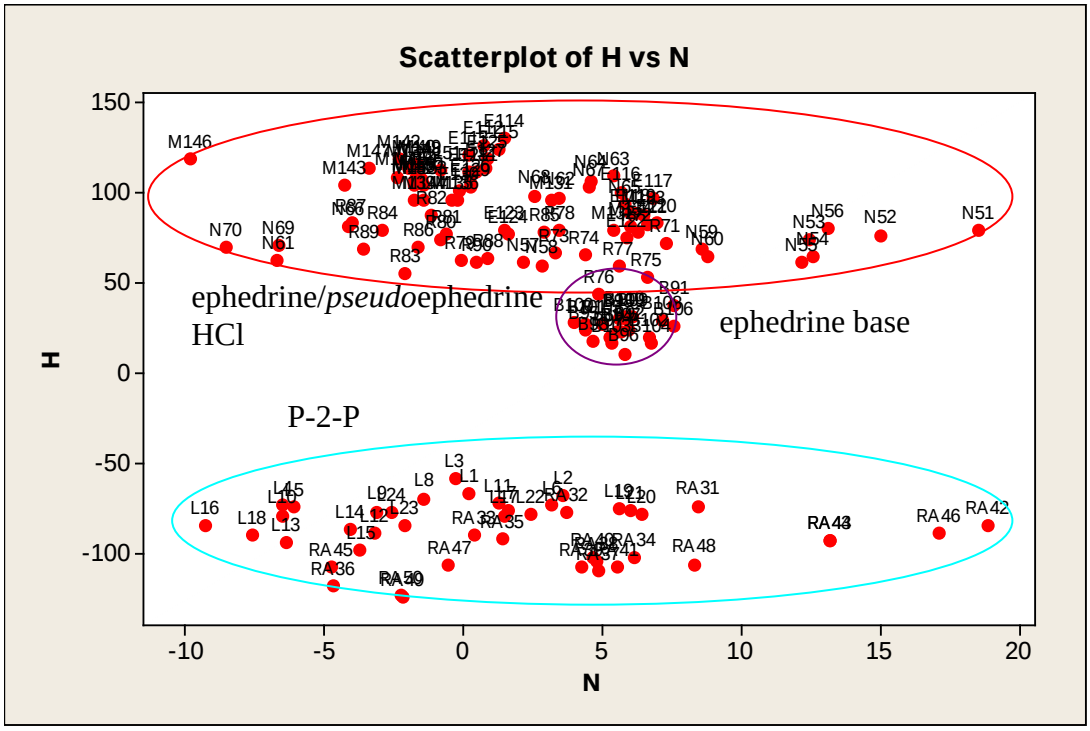

Figure 121: Two variable plot of the $\delta^{2}H$ and $\delta^{15}N$ data.

The combination of $\delta^{13}C$, $\delta^{15}N$ and $\delta^{2}H$ data in a three dimensional plot was also investigated. Figure 122 shows that, even with a combination of all three isotope ratios, separation of the samples by the different precursors (P-2-P, ephedrine HCl with *pseudo*ephedrine HCl and ephedrine base) was possible to some degree however samples prepared from ephedrine HCl and *pseudo*ephedrine HCl were clustered in one group. The discrimination between sample groups was less defined than that achieved by the carbon, nitrogen and hydrogen with 2 dimensional plots. With large data sets, as would be encountered in operational methylamphetamine profiling, 3-D plots can also often be too cluttered to be of use.

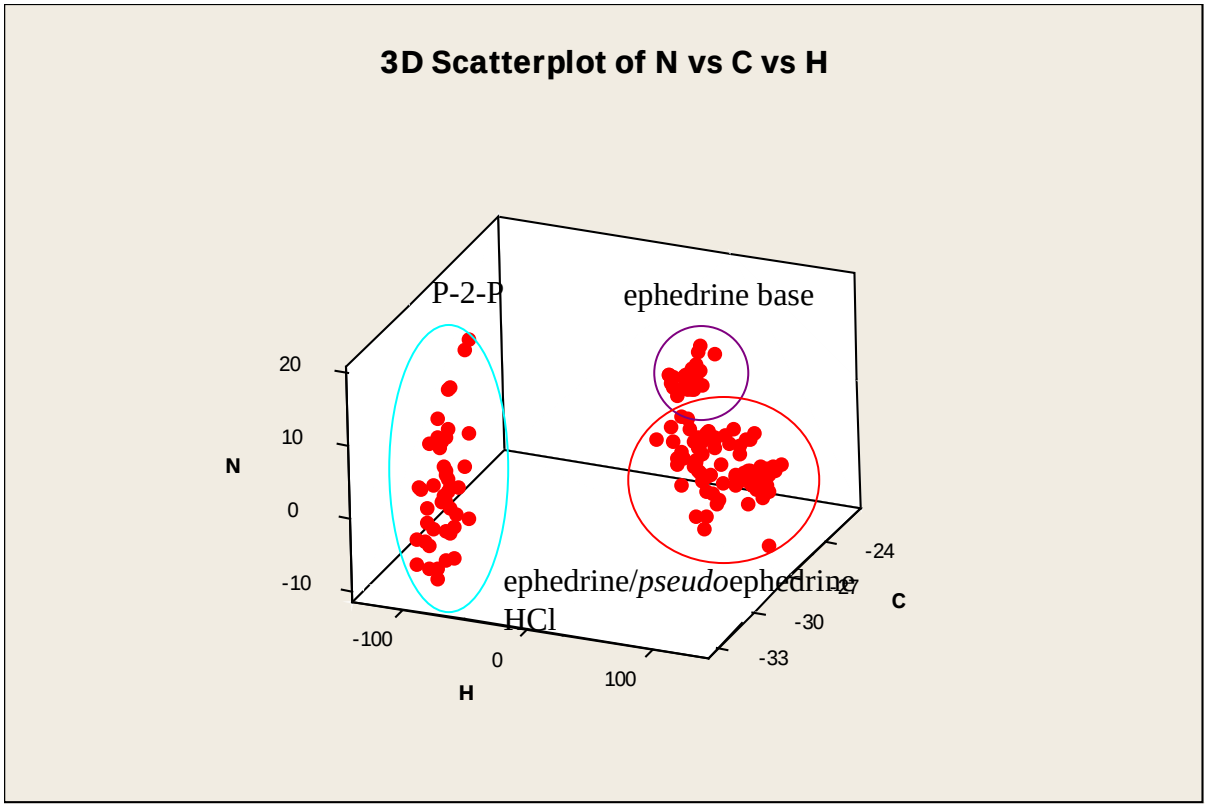

Figure 122: 3-D plot of methylamphetamine synthesised by seven synthetic routes.

6.3 Conclusions

IRMS analysis of the 149 methylamphetamine batches prepared via seven synthetic routes offered a method for the discrimination of samples by precursors. The P-2-P precursors had δ^2H values that were negative while the ephedrine or *pseudo*ephedrine precursors had positive δ^2H values. δ^{13}C data in combination with either hydrogen or nitrogen isotopic data facilitated the discrimination of the samples into four groups according to precursor where samples prepared via the hydrochloride salts of ephedrine or *pseudo*ephedrine and ephedrine base could clearly be resolved from each other while those prepared from P-2-P. Furthermore the P-2-P samples could also be discriminated by synthetic route using IRMS data.

It should be noted that although different batches of precursors were used within the synthetic route, there is no variation observed in δ^{13}C, δ^{15}N and δ^2H data.

If these methylamphetamine HCl samples had been seized samples and subjected to IRMS analysis, δ^{13}C and δ^2H or δ^{13}C and δ^{15}N data would have allowed tentative discrimination into groups corresponding to the precursors used for manufacture based on the IRMS preparation technique.

The work detailed in this chapter utilised BSIA (see Section 2.7.4.1), but since the synthesised methylamphetamine was pure, the results of the analysis should, in theory, be the same as using CSIA (see Section 2.7.4.2) and target the methylamphetamine component peak. With authentic methylamphetamine street powder, however, BSIA would return δ values which reflect the entire sample (i.e. methylamphetamine, diluents, adulterant, etc). If isotopic analysis of only the methylamphetamine component is desired, then CSIA is required to isolate and analyse the methylamphetamine components in powder sample, or the methylamphetamine must be extracted from the powder the street sample before isotope analysis using BSIA.

6.4 References

1. Sharp, Z.D.; Atudorei,; V.; Durakiewicz, T.; A rapid method for determination of hydrogen and oxygen isotope ratios from water and hydrous minerals. *Chemical Geology* 2001, 178, 197–210.

2. Carter, J. F.; Titterton, E. L.; Grantc, H.; Sleeman, R., Isotopic changes during the synthesis of amphetamines. *Chemical Communication*s 2002, (21) 2590–2591.

3. Billault, I.; Courant, F.; Pasquereau, L.; Derrien, S.; Robins, R. J.; Naulet, N., Correlation between the synthetic origin of methamphetamine samples and their ^{15}N and ^{13}C stable isotope ratios. *Analytica Chimica Acta* 2007, 593, 20-29.

4. Kurashima, N.; Makino, Y.; Sekita, S.; Uranob, Y.; Nagano, T., Determination of Origin of Ephedrine Used as Precursor for Illicit Methamphetamine by Carbon and Nitrogen Stable Isotope Ratio Analysis. *Journal of Analytical Chemistry* 2004, 76(14), 4233-4236.

5. Makino, Y.; Urano, Y.; Nagano, T., Investigation of the origin of ephedrine and methamphetamine by stable isotope ratio mass spectrometry: a Japanese experience. *Bulletin on Narcotics* 2005, 57, 63-68.

6. Ehleringer, J.R.; Cerling, T.E.; West, J.B., Forensic Science Applications of Stable Isotope Ratio Analysis, in *Forensic Analysis on the Cutting Edge: New Methods for Trace Evidence Analysis*. John Wiley & Sons, Inc: 2007, 398-417.

7. Cox, M.; Klass, G.; Koo, C.W.M., Manufacturing by-products from, and stereochemical outcomes of the biotransformation of benzaldehyde used in the synthesis of methamphetamine. *Forensic Science International* 2009, 189**,** 60-67.

8. Kurashima, N.; Makino, Y.; Urano, Y.; Sanuki, K.; Ikehara, Y.; Nagano, T., Use of stable isotope ratios for profiling of industrial ephedrine samples: Application of hydrogen isotope ratios in combination with carbon and nitrogen. *Forensic Science International* 2009, 189, 14-18.

CHAPTER 7: IDENTIFYING THE SOURCES AND SYNTHETIC ROUTES OF METHYLAMPHETAMINE SAMPLES BY ICPMS

7.0 Introduction

This part of the study investigated the inorganic impurities present in each of the methylamphetamine samples synthesised by the various routes studied. The aim was to establish if there were any discernable links between the synthesis method and the derived elemental profile revealed by ICPMS analysis. For IRMS analysis, 146 out of 149 batches of synthesised samples were analysed.

7.1 Experimental Methods

7.1.1 Reagents and standards

Trace metal grade nitric acid (65%, w/w) and laboratory reagent grade tetramethylammonium hydroxide (TMAH) (25%, v/v) were both obtained from Sigma Aldrich (UK). Potassium iodide was obtained from Fluka. Ultrapure water was used throughout. Regenerated cellulose syringe filters (brown code) were purchased from Spec and Burke Analytical (Scotland). Multi-element standards were obtained from Merck (Germany) and CPI International (USA). Calibration solutions were prepared from a Spex "CertiPrep" certified standard diluted as required with 2% Fisher Trace Metal grade nitric acid.

7.1.2 Sample Preparation

7.1.2.1 Multi element analysis

Approximately 100 mg of sample was weighed into a 10 mL polypropylene tube and 4 mL of 1% HNO_3 was added. The tubes were placed on an Edmund Buhler Swip KS-10 rotative shaker overnight. The solution was filtered with a regenerated cellulose syringe filter (25 mm and diameter 0.45μm pore size). The following elements were analysed in multi element analysis with ICP-MS (isotopic abundances): Na (23), Mg (24), Al (27), Li (7), P (31), Pd (105), Pd (106), Pd (108), Ba (137), Ba (138), Hg (200), Hg (202), Pb (208).

7.1.2.2 Iodine analysis

At low pH, iodide is easily oxidised to volatile molecular iodine via dissolved oxygen. Iodine is not a stable element in dilute nitric acid and carry over can result even after nitric acid washes between samples. To avoid losses due to iodine's volatility and complex redox chemistry, the sample was prepared in an alkaline media since at high pH, the oxidation of iodide to iodine is avoided.[1] Strong alkali conditions lead to the conservation of the iodine as iodide or iodate, which can then be determined by ICPMS. Approximately 100 mg of a sample was weighed into a 10 mL polypropylene tube; 4 mL of 1% TMAH was added and followed the procedure as in Section 7.1.2.1. A set of iodine calibration standards were prepared from potassium iodide.

7.1.3 ICPMS Instrument Parameters

X-Series II plus quadrupole ICP-MS instrument (Thermo Electron Corporation) was used with a Cetac ASX-520 autosampler. The instrument was operated with a Peltier cooled conical single-pass spray chamber with impact bead and has an integral peristaltic pump for sample uptake from the autosampler. A hexapole for CCT ED (Collision Cell Technology with Energy Discrimination) mode was used to remove polyatomic interferences.

Instrumental operating conditions used were 1400 W RF forward power; 13 L/min plasma flow; 1.0 L/min nebulizer flow and 0.8 L/min auxiliary flow, respectively. For the ICP-MS a sample flush time of 60 s, a wash time of 90 s and a peak hopping scan mode was used with a dwell time per isotope of 10 ms.

A solution 1% HNO_3 was used as the wash solution for Li, Pd, Ba and Hg analysis and 1% TMAH was used as the wash solution for iodine analysis as previously discussed.

7.2 Results and Discussion

Elemental analysis was performed on all 146 methylamphetamine batches prepared in the synthetic phase of the project. Elemental analysis was expected to reveal information on the catalyst or reducing agent that was use during the synthesis of methylamphetamine via the various routes chosen. In this study Na (23), Mg (24), Al (27), Li (7), P (31), Pd (105), Pd (106), Pd (108), Ba (137), Ba (138), Hg (200), Hg (202), Pb (208) and I^- (127) were identified and quantified. Among these, six elements; Li (7), P (31), Pd (105), Ba (138), Hg (202) and I^- (127) were chosen as target inorganic impurities because of their prevalence within the synthesis and the results obtained are discussed in this section.

The concentrations of each element were reported based on the preparation of the methylamphetamine after dilution. This is in line with the reporting method used in published literature. The concentrations of each element revealed within each route were plotted against the batch and are shown in the following section. Table 57 – Table 63 summarises the minimum, maximum, Q1 (quartile 1), Q3 (quartile 3) and average concentration of each element for each route. In each table the value of blank acid that was used to dissolve the samples was also presented. The blank acid value shows the level of those elements which can found as background.

7.2.1 Leuckart route

Figure 123 reveals that all the six elements were present in low concentrations (0 ppb to 159 ppb) within the 24 samples synthesised via the Leuckart route. This is unsurprising since no catalyst or reducing agent was introduced during synthesis of methylamphetamine by this route and gives an indication of the background levels of these elements expected within a given sample.

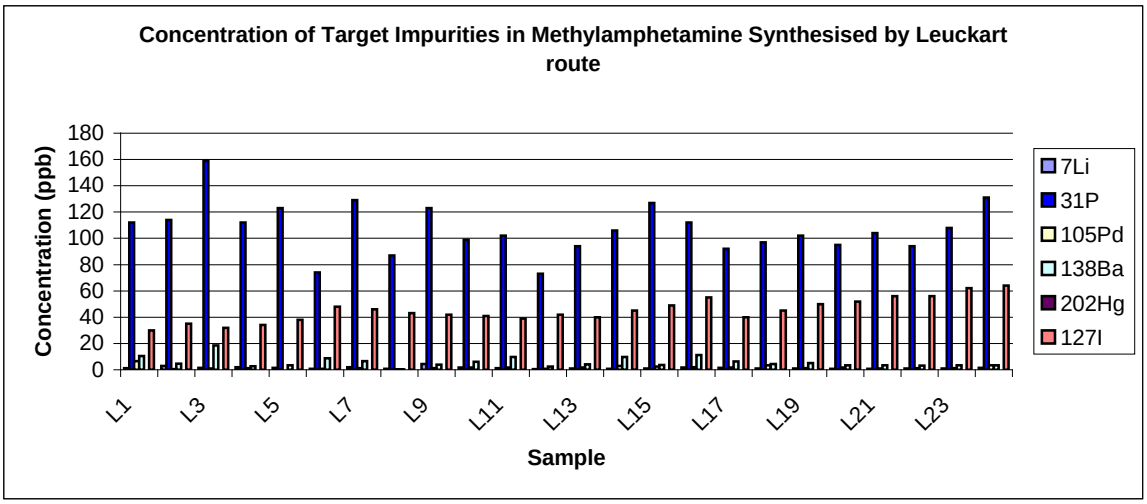

Figure 123: The concentration of the selected target impurities across the 24 batches synthesised via the Leuckart route.

	7Li	31P	105Pd	138Ba	202Hg	127I
MIN	0.57	73.00	0.08	0.29	0.00	30.00
MAX	4.37	159.00	6.61	18.61	0.04	64.00
AVERAGE	1.38	107.04	1.68	5.80	0.00	45.17
STDEV	0.82	19.08	1.37	3.93	0.01	9.04
RSD	59.57%	17.83%	81.52%	67.85%	284.46%	20.01%
Q1	0.87	94.75	1.03	3.49	0.00	39.75
Q3	1.59	116.25	1.82	7.03	0.00	50.50
MEDIAN	1.09	105.00	1.23	4.19	0.00	44.00
BLANK	0.08	4.00	0.00	0.00	0.16	1.00

Table 57: Summary of the concentration (ppb) in samples within the Leuckart route.

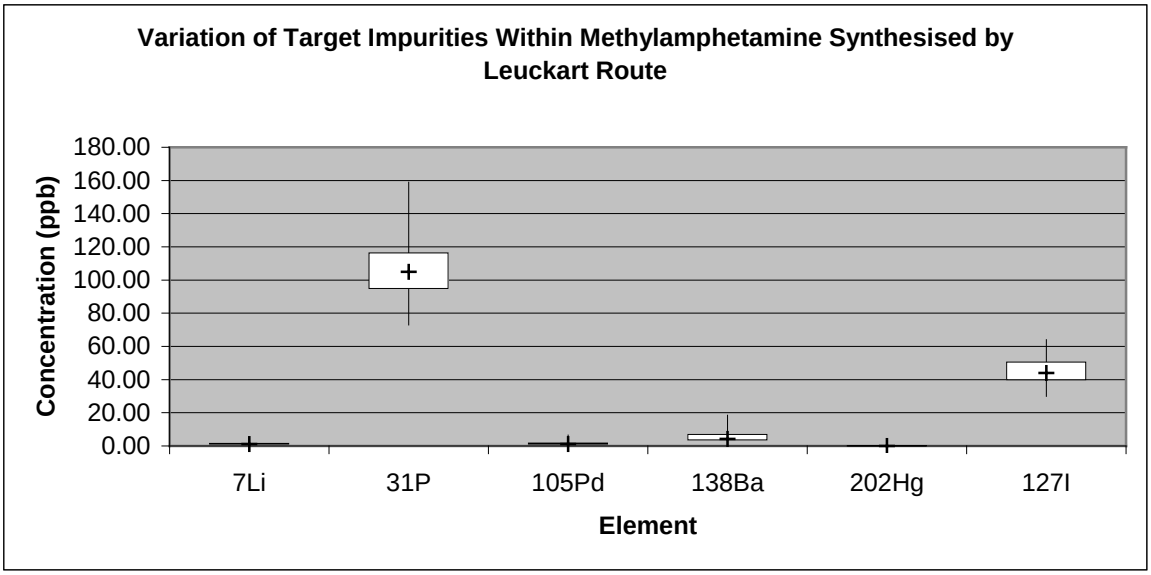

Figure 124: The variation of the selected target impurities across the 24 batches synthesised via the Leuckart route.

Figure 124 reveals that the variation of the concentrations of phosphorus and iodine are high (P: 94.75-116.25 ppb and I: 39.75-50.50 ppb). These elements were not introduced during the synthesis and the Leuckart synthesis samples were the first set of prepared in the study so that there was no possibility of carry over of these elements from the use of the same glassware as used in the other synthesis. It should be noted that these values were still low compared to the presence of these elements in for example the Nagai and Moscow samples.

7.2.2 Reductive Amination

Figure 125 reveals the presence of mercury in significant amounts throughout the 20 separate batches of methylamphetamine produced by this method. This can be attributed to the introduction of $HgCl_2$ as part of the formation of the aluminium amalgam introduced as a reducing agent during the synthesis. The variation between mercury levels from batch to batch were observed to vary considerably with one sample containing a much higher concentration than the others producing an overall high interbatch variation (RSD : 391.02%). The levels of the other elements of interest were comparable with those identified in the Leuckart synthesised samples.

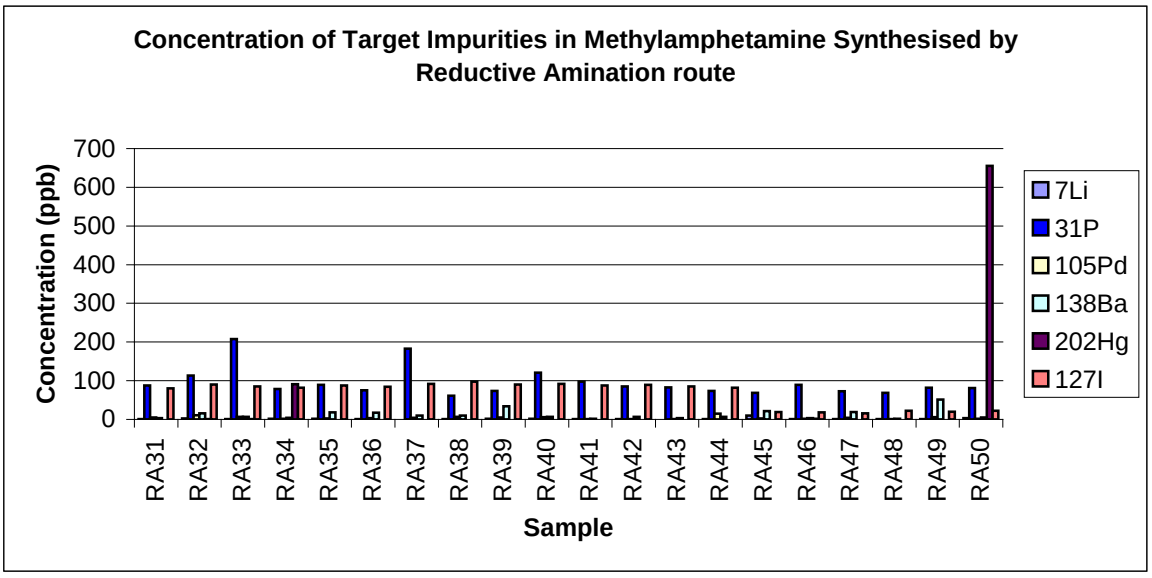

Figure 125: The concentration of the selected target impurities across the 20 batches synthesised via the Reductive Amination route.

	7Li	31P	105Pd	138Ba	202Hg	127I
MIN	0.35	61.00	0.62	1.79	0.01	16.00
MAX	9.76	208.00	15.09	51.23	655.40	98.00
AVERAGE	1.58	94.70	4.21	12.26	37.55	67.10
STDEV	2.08	37.54	3.67	12.45	146.82	32.25
RSD	132.06%	39.64%	87.07%	101.56%	391.02%	48.06%
Q1	0.65	74.00	1.33	3.86	0.04	22.00
Q3	1.51	91.25	5.78	17.57	0.44	89.25
MEDIAN	0.85	82.50	3.39	6.48	0.08	84.50
BLANK	0.00	0.00	0.00	0.02	0.00	0.00

Table 58: Summary of the concentration (ppb) in samples within the Reductive Amination route.

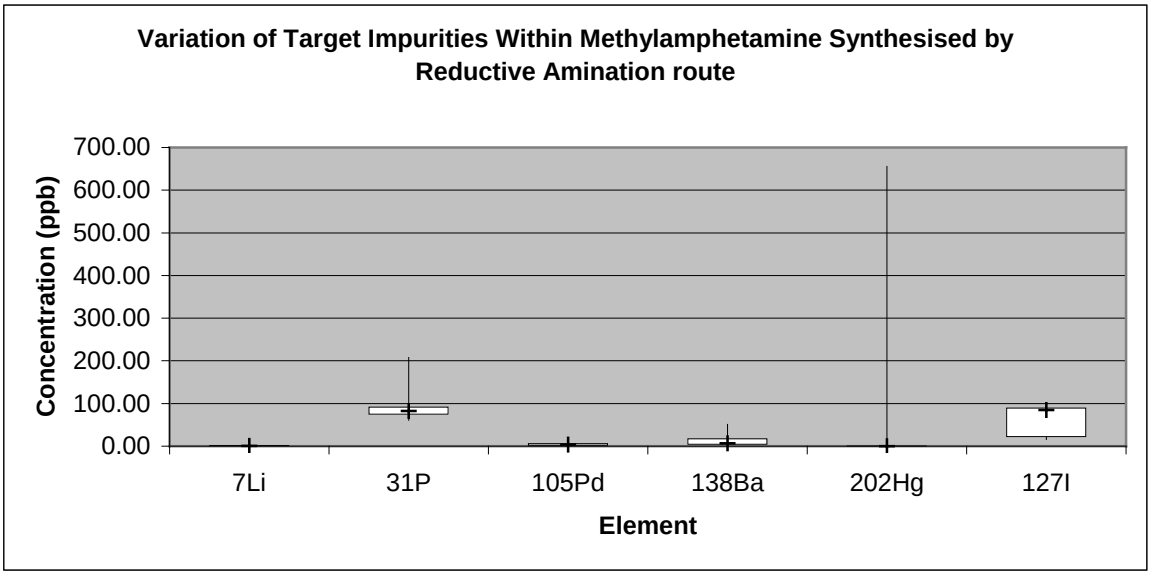

Figure 126: The variation of the selected target impurities across the 20 batches synthesised via the Reductive Amination route.

Figure 126 also shows that the variation of the concentrations of phosphorus and iodine are again high (P: 74.00-91.20 ppb and I: 22.00-89.25 ppb) even though those elements were not introduced during the synthesis.

There is a possibility that these element could be present in trace levels within P-2-P which was used as the starting material for both the Leuckart and Reductive Amination routes. P-2-P can be synthesised from phenylacetealdehyde and dimethylcadium.[2] Dimethylcadium is synthesised by using methyl iodide and cadmium chloride. [2] The literature indicates that both iodine and phosphorus are used in the preparation of methyl iodide and as such could be the source of these elements in the final methylampheetamine samples.[3]

7.2.3 Nagai route

Figure 127 reveals the presence of phosphorous and iodine in high concentrations throughout the 20 batches synthesised via the Nagai route. Hydriodic acid and red phosphorus were both introduced during the synthesis and their elevated concentrations reflect this (P: 131.80-3642.00 ppb and I: 836.00-11550.00 ppb). Again the inter batch variation observed for both elements was high (RSD P: 107.09% and I: 77.23%).

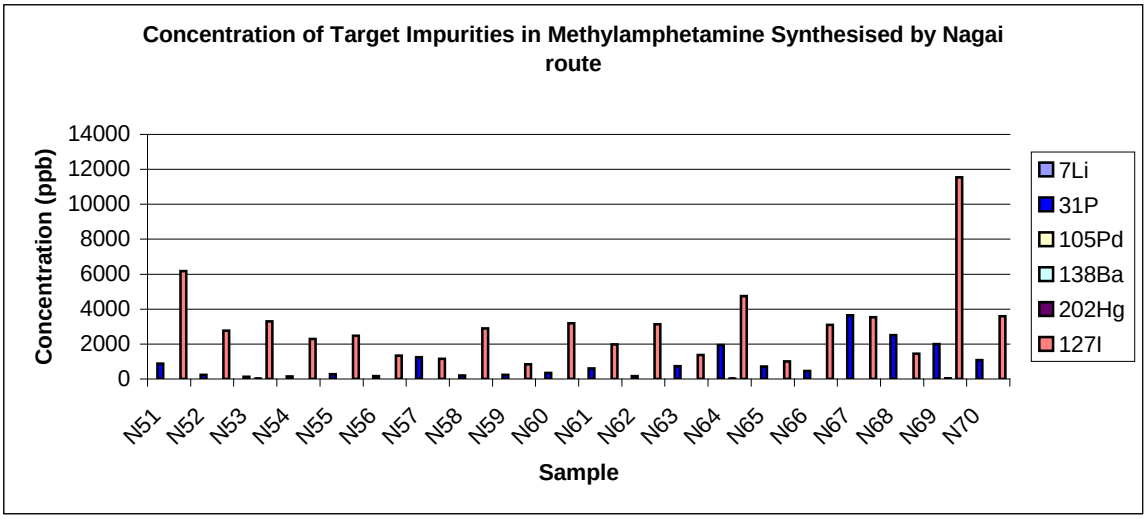

Figure 127: The concentration of the selected target impurities across the 20 batches synthesised via the Nagai route.

	7Li	31P	105Pd	138Ba	202Hg	127I
MIN	0.23	131.80	0.05	1.08	0.00	836.00
MAX	3.80	3642.00	2.56	44.38	0.69	11550.00
AVERAGE	0.87	886.59	0.48	6.22	0.06	3095.30
STDEV	1.05	949.44	0.60	10.22	0.17	2390.41
RSD	120.84%	107.09%	124.68%	164.36%	296.17%	77.23%
Q1	0.32	231.98	0.16	1.48	0.00	1429.50
Q3	0.90	1123.75	0.50	6.48	0.00	3359.00
MEDIAN	0.44	536.40	0.25	2.03	0.00	2831.00
BLANK	0.04	12.21	0.00	0.51	0.29	1.00

Table 59: Summary of the concentration (ppb) in samples within the Nagai route.

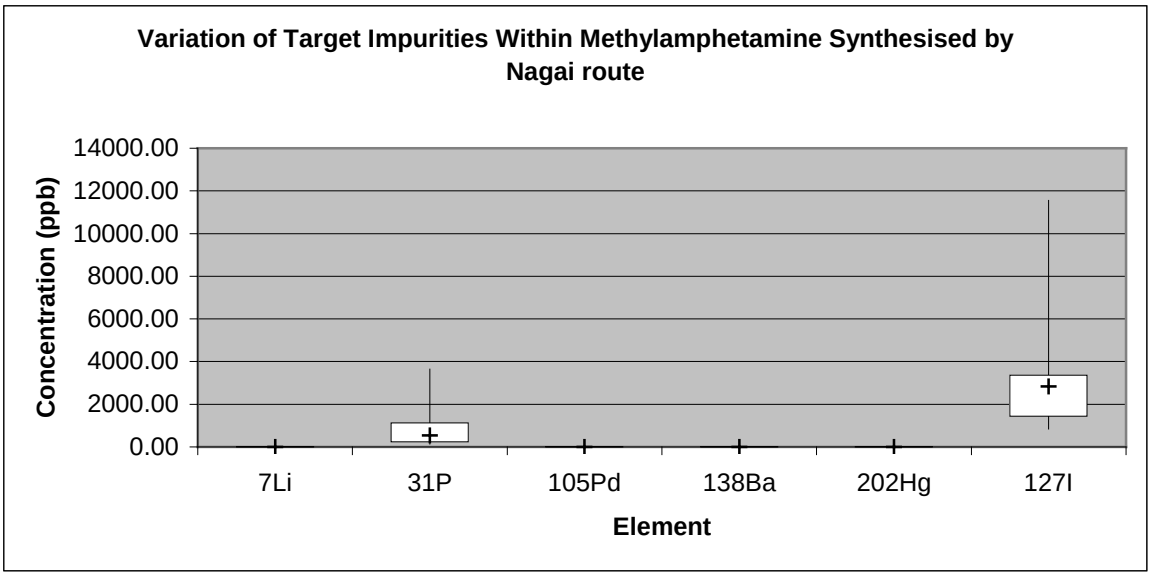

Figure 128: The variation of the selected target impurities across the 20 batches synthesised via the Nagai route.

Figure 128 shows that the variation of the concentrations of phosphorus and iodine are very high (P: 231.98-1123.75 ppb and I: 1495.50-3359.00 ppb) due to the utilisation of these elements in the synthesis.

7.2.4 Rosenmund route

Figure 129 reveals high concentrations for both palladium and barium across the 20 batches prepared via the Rosenmund route. $Pd/BaSO_4$ was introduced as a catalyst during the synthesis of methylamphetamine and acts as the source for both elements in the final products. Pd and Ba were found to be present in the range of 0.23-450.50 ppb and 7.82-851.70 ppb respectively.

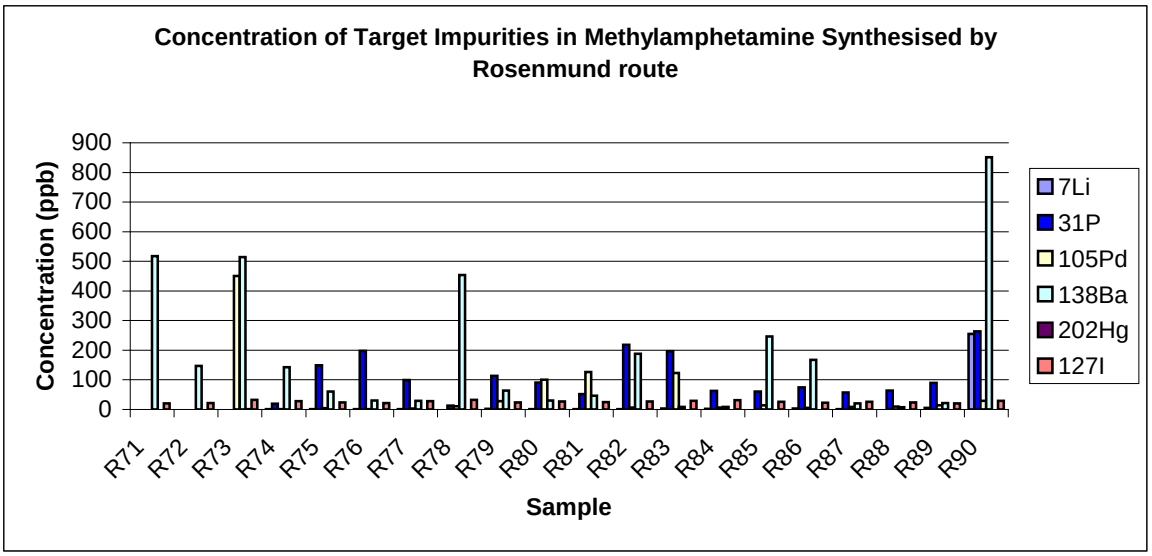

Figure 129: The concentration of the selected target impurities across the 20 batches synthesised via the Rosenmund route.

	7Li	31P	105Pd	138Ba	202Hg	127I
MIN	0.00	0.00	0.23	7.82	0.00	20.00
MAX	255.30	263.50	450.50	851.70	0.82	32.00
AVERAGE	13.94	90.99	47.25	177.84	0.11	26.00
STDEV	56.83	77.36	103.13	230.56	0.21	3.55
RSD	407.74%	85.02%	218.29%	129.65%	194.20%	13.67%
Q1	0.41	44.01	4.34	27.41	0.00	23.75
Q3	1.83	121.93	28.74	202.23	0.11	28.25
MEDIAN	0.79	68.70	9.37	62.21	0.01	26.00
BLANK	0.00	0.00	0.00	0.00	0.75	1.00

Table 60: Summary of the concentration (ppb) in samples within the Rosenmund route.

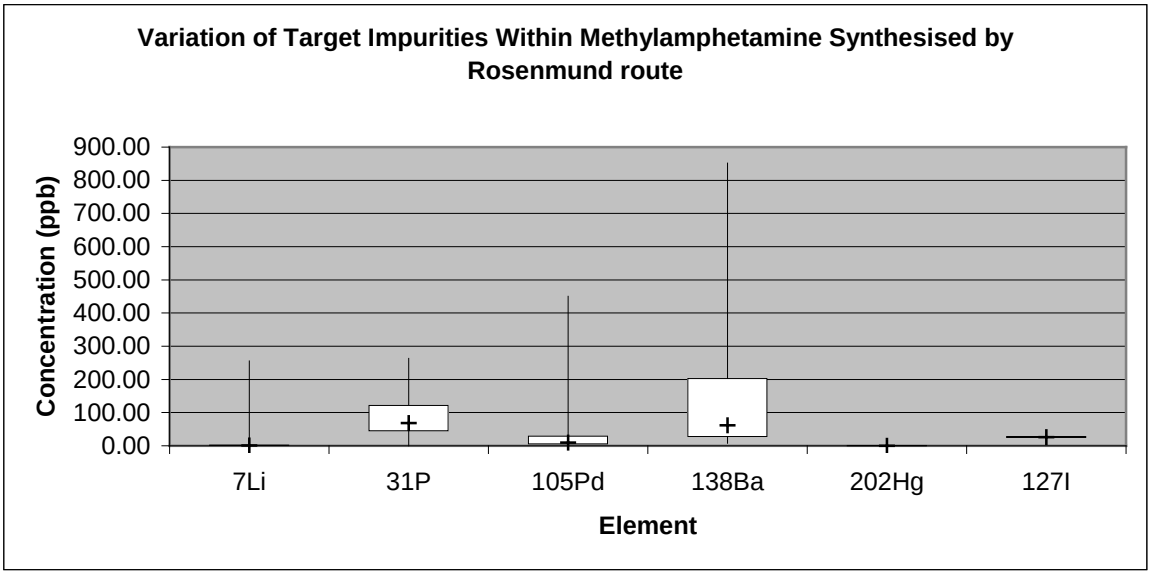

Figure 130: The variation of the selected target impurities across the 20 batches synthesised via the Rosenmund route.

Figure 130 shows that the variation of the concentrations of palladium and barium were both high (Pd: 4.34-28.74 ppb and Ba: 27.41-202.23 ppb) which is due to the utilisation of those elements in the synthesis. Methylamphetamine batches via the Rosenmund route were synthesised after the Nagai route samples. Surprisingly, phosphorus was also found to be present in the range of 0-263.50 ppb. This is most likely due to use of same glassware and sintered glass filter which was used in the production of samples via the Nagai route. There is a possibility of carry over of the phosphorus despite careful and through cleaning of the glassware between synthesis.

7.2.5 Birch route

Figure 131 revealed lithium present in high concentration throughout the 20 batches as expected because of the synthetic pathway. Li was introduced as a reducing agent during synthesis of methylamphetamine via the Birch route and the higher levels (20.66 - 2858.00 ppb : RSD 196.88%) reflect this.

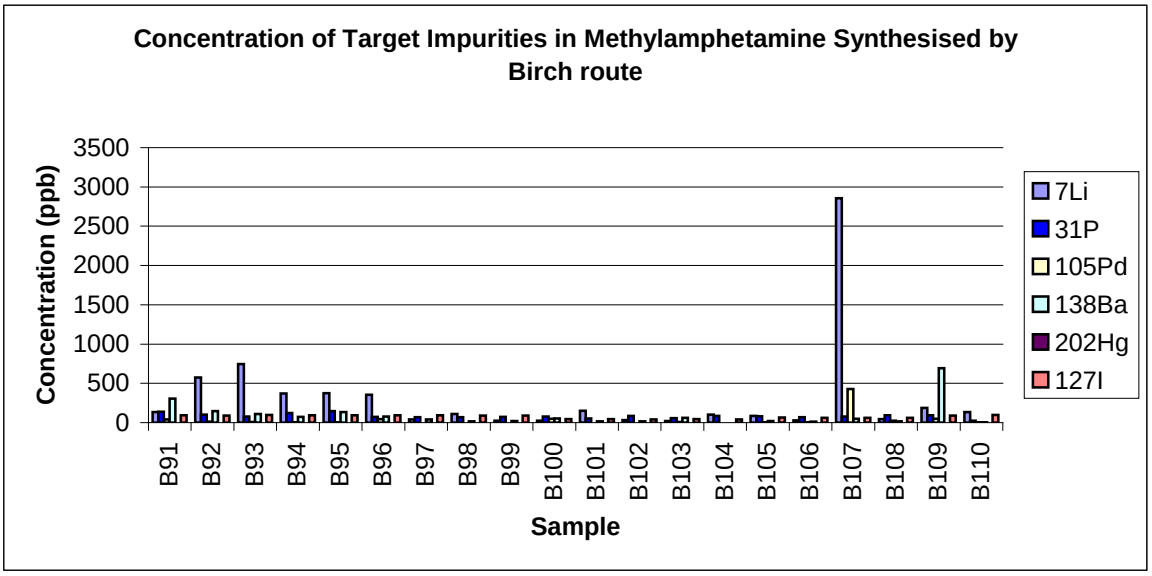

Figure 131: The concentration of the selected target impurities across the 20 batches synthesised via the Birch route.

	7Li	31P	105Pd	138Ba	202Hg	127I
MIN	20.66	26.00	0.08	1.67	0.00	40.00
MAX	2858.00	148.00	427.70	694.40	0.00	98.00
AVERAGE	320.01	83.40	34.38	93.30	0.00	74.55
STDEV	630.04	28.18	94.17	158.48	0.00	22.25
RSD	196.88%	33.79%	273.89%	169.87%	0.00%	29.84%
Q1	37.87	69.75	1.99	15.66	0.00	56.50
Q3	358.58	92.75	27.64	84.31	0.00	92.50
MEDIAN	121.45	77.00	4.73	45.13	0.00	90.00
BLANK	0.03	6	0.00	0.50	0.32	1.00

Table 61: Summary of the concentration (ppb) in samples within the Birch route.

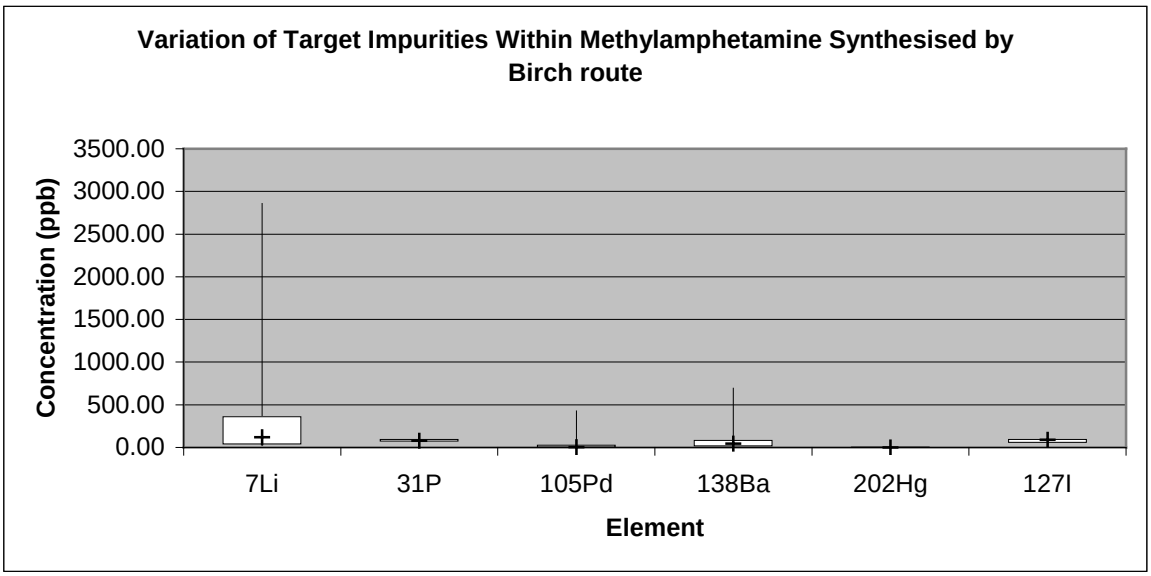

Figure 132: The variation of the selected target impurities across the 20 batches synthesised via the Birch route.

Figure 132 shows that the variation of the concentration of lithium is high (Li: 37.87-358.58 ppb) which is due to the utilisation of the element in the synthesis.

7.2.6 Emde route

Figure 133 revealed high concentrations of palladium and barium (26.60 - 3720.00 ppb RSD 166.00% and 49.17-772.40 ppb RSD 64.11% respectively) as expected reflecting the involvement of these elements as catalysts in the Emde synthesis. This is similar to the Rosenmund route as the same elements are used in the catalysis.

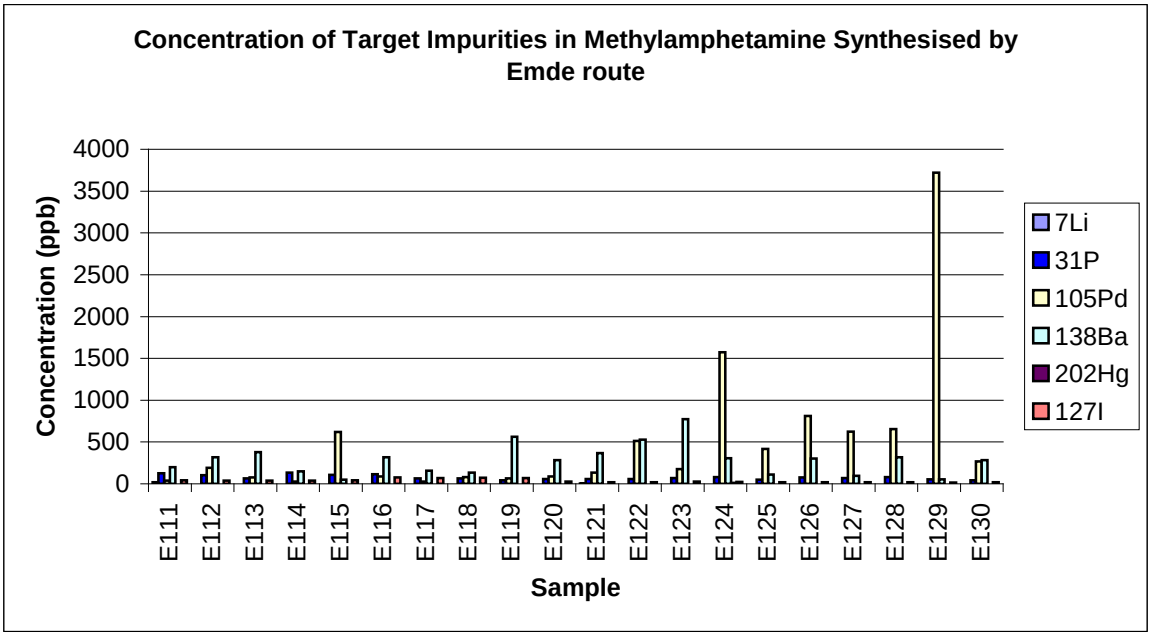

Figure 133: The concentration of the selected target impurities across the 20 batches synthesised via the Emde route.

	7Li	31P	105Pd	138Ba	202Hg	127I
MIN	0.25	42.94	26.60	49.17	0.00	16.00
MAX	18.08	134.60	3720.00	772.40	10.93	76.00
AVERAGE	1.75	76.00	509.75	284.62	0.70	35.70
STDEV	3.94	26.92	846.19	182.46	2.42	20.41
RSD	225.15%	35.42%	166.00%	64.11%	347.51%	57.18%
Q1	0.39	57.99	80.55	146.48	0.00	20.00
Q3	1.06	85.90	621.85	331.30	0.18	41.25
MEDIAN	0.62	67.07	184.90	293.50	0.04	25.50
BLANK	0.01	9.98	0.03	0.06	0.00	1.00

Table 62: Summary of the concentration (ppb) in samples within the Emde route.

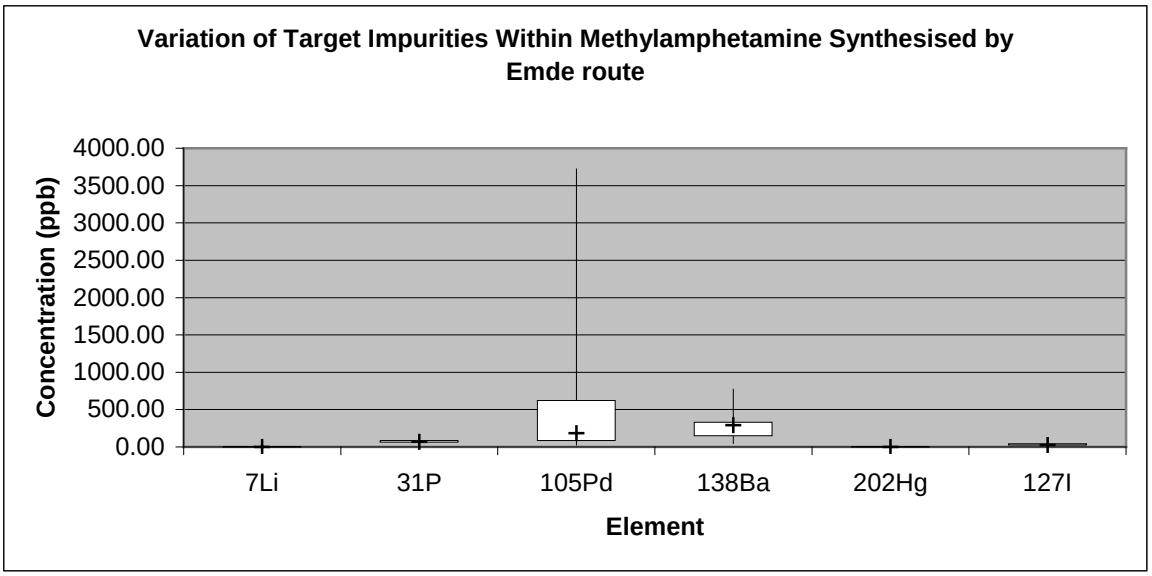

Figure 134: The variation of the selected target impurities across the 20 batches synthesised via the Emde route.

Figure 134 shows that the variation of the concentration of palladium and barium are high (Pd: 80.55-621.85 ppb and Ba: 146.48-331.30 ppb) which is due to the utilisation of those elements in the synthesis.

7.2.7 Moscow route

Figure 135 reveals phosphorous and iodine present at elevated concentrations. This is similar to the results revealed through analysis of the Nagai synthesised samples. Red phosphorus and iodine were introduced during synthesise of methylamphetamine via the Moscow route and were present in the range of 102.00-9817.00 ppb : RSD 231.92% and 220.00-77410.00 ppb : RSD 131.57% respectively. Both elements appeared at concentrations higher than those revealed in the Nagai synthesised samples most likely due to use of iodine crystals rather than hydriodic acid used during the synthesis.

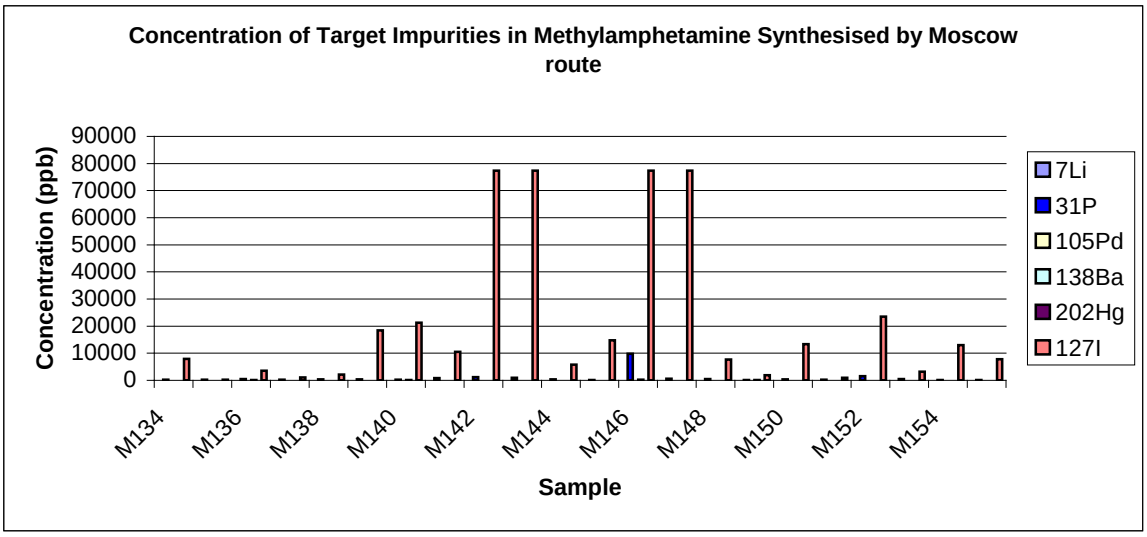

Figure 135: The concentration of the selected target impurities across the 22 batches synthesised via the Moscow route.

	7Li	31P	105Pd	138Ba	202Hg	127I
MIN	0.20	102.00	0.41	1.75	0.00	220.00
MAX	1.46	9817.00	5.26	236.30	4.69	77410.00
AVERAGE	0.50	875.58	1.61	39.22	1.06	21202.86
STDEV	0.32	2030.65	1.17	52.42	1.26	27895.91
RSD	63.60%	231.92%	72.77%	133.66%	118.33%	131.57%
Q1	0.29	235.38	0.69	7.79	0.19	3314.50
Q3	0.53	537.55	2.44	48.60	1.72	20520.00
MEDIAN	0.39	323.90	1.28	22.26	0.55	9194.50
BLANK	0.01	27.34	0.01	0.00	0.22	5.00

Table 63: Summary of the concentration (ppb) in samples within the Moscow route.

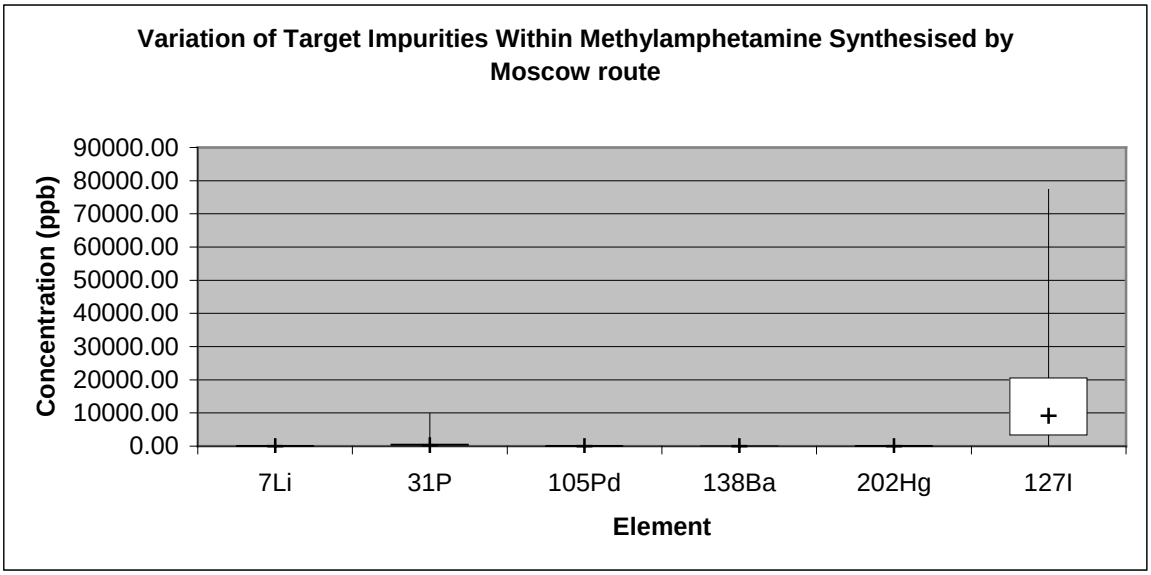

Figure 136: The variation of the selected target impurities across the 22 batches synthesised via the Moscow route.

Figure 136 show that the variations in the concentration of phosphorus and iodine are very high (P: 235.38-537.55 ppb and I: 3314.50-20520.00 ppb) which is due to the utilisation of those elements in the synthesis.

7.2.8 Comparison of between batch variations and variations between synthetic route

To assess the variation of the target elements between each batch and synthetic route, the mean of each element was calculated using the repeat methylamphetamine batches from each synthetic route. These values were then represented on a plot with the standard deviation as the upper and lower limit. The mean values for each of the elements present in each synthetic route are displayed in Figure 137 – Figure 142.

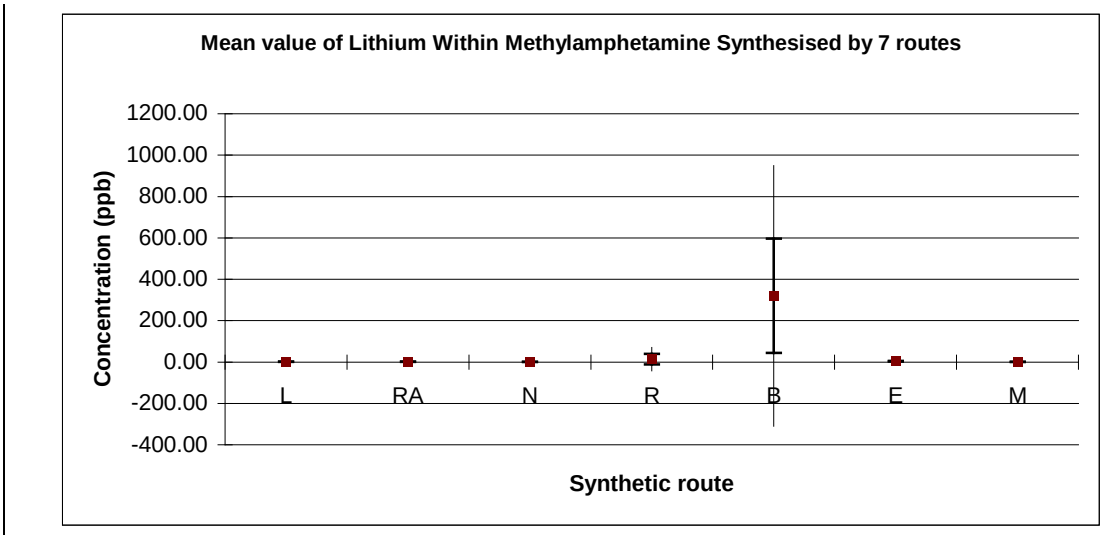

Figure 137: The mean value of Lithium across the seven synthetic routes. Error bars indicate 95% of the confidence interval of the mean for each route.

Figure 137 illustrates that lithium was present in significant amounts in the Birch synthesised samples in comparison to all other samples (mean value 320.01 ppb).

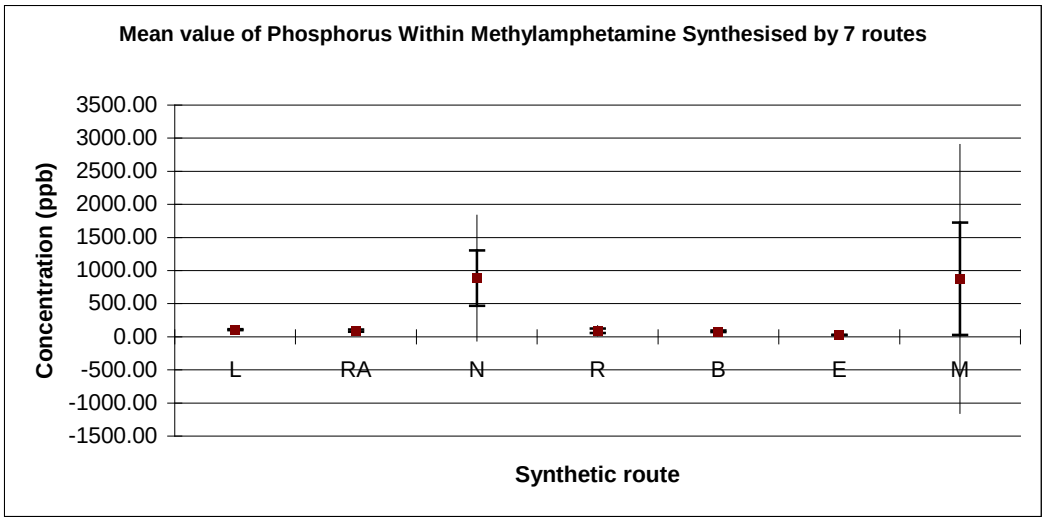

Figure 138: The mean value of Phosphorus across the seven synthetic routes. Error bars indicate 95% of the confidence interval of the mean for each route.

Figure 138 shows that phosphorus was present in significant quantities in both the Nagai (mean value of 886.59 ppm) and Moscow samples (mean value 875.58 ppb).

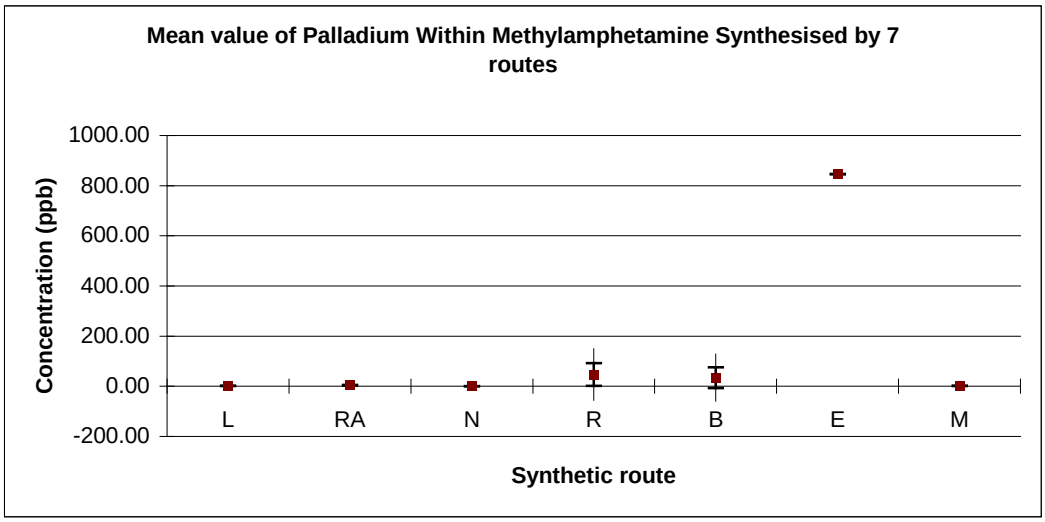

Figure 139: The mean value of Palladium across the seven synthetic routes. Error bars indicate 95% of the confidence interval of the mean for each route.

Figure 139 shows that palladium was present in significant amounts in the Emde samples (mean value 846.19 ppm). This element was also present at elevated levels in both the Rosenmund samples (mean value 47.25 ppb) as expected and in the Birch samples most likely due to contamination as previously discussed.

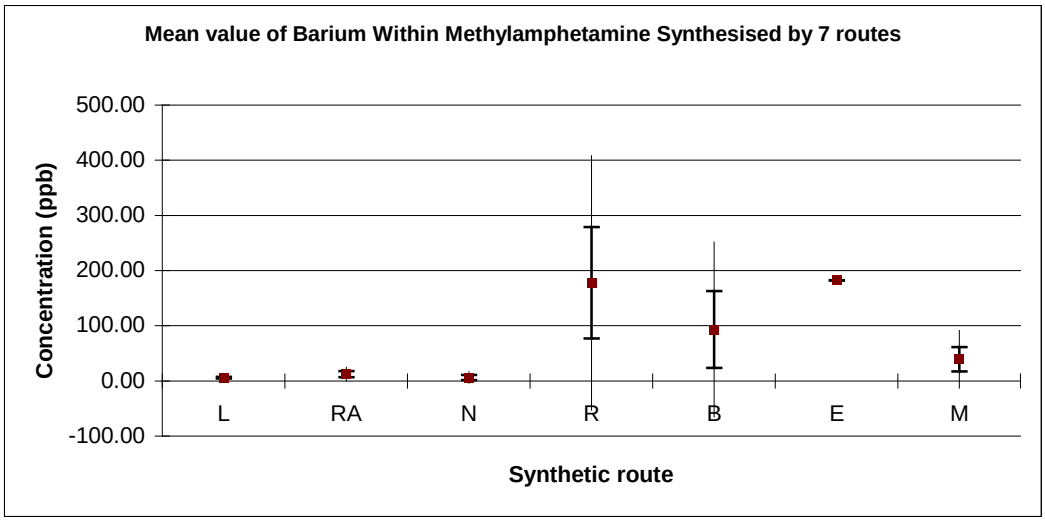

Figure 140: The mean value of Barium across the seven synthetic routes. Error bars indicate 95% of the confidence interval of the mean for each route.

Figure 140 shows that barium was present in significant amounts in the Rosenmund (mean value 177.84 ppb) and Emde route samples (mean value 182.46 ppb). Again the presence of this element in the Birch and Moscow samples may be due contamination of the glassware.

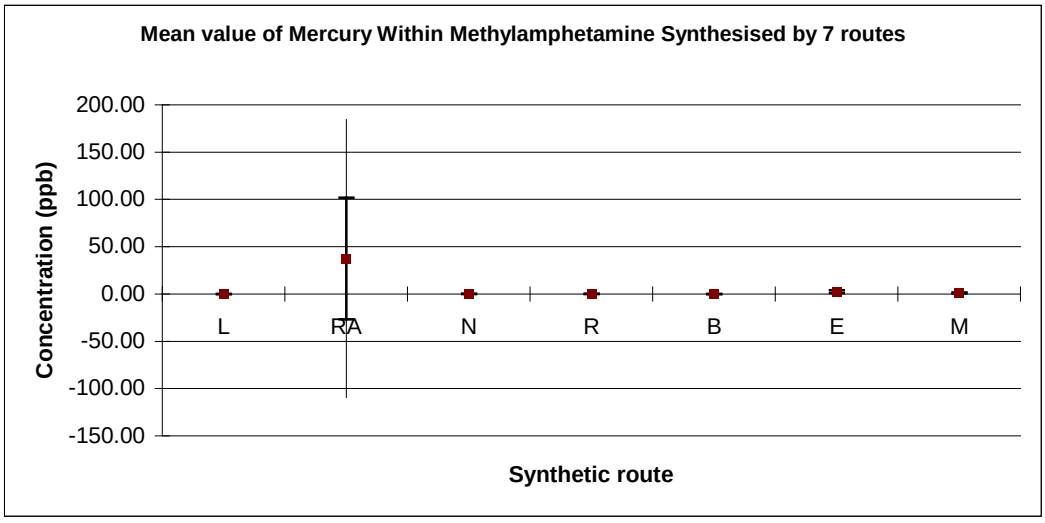

Figure 141: The mean value of Mercury across the seven synthetic routes. Error bars indicate 95% of the confidence interval of the mean for each route.

Figure 141 illustrates that mercury was present in significant amount in the Reductive Amination route samples (mean value 37.55 ppb) route as expected.

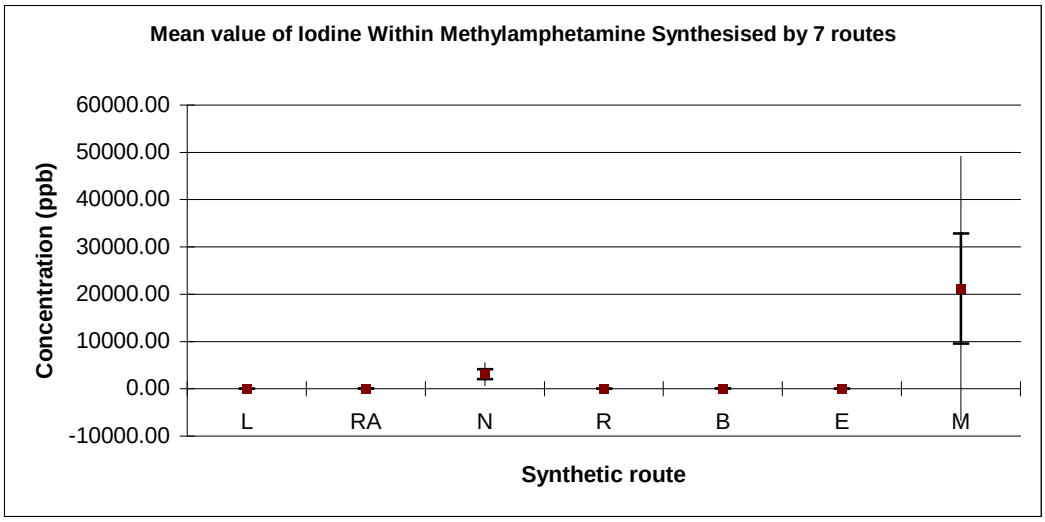

Figure 142: The mean value of Iodine across the seven synthetic routes. Error bars indicate 95% of the confidence interval of the mean for each route.

Figure 142 shows that iodine present in significant amount in (Nagai: 3095.30 ppb and Moscow: 21202.86 ppb) routes. Iodine present in high level in Moscow route compare to Nagai route

Some of the elements were present in the final product of methylamphetamine, even though these elements were not introduced in the synthesis. This is most likely due to contamination from the glassware used during synthesis or trace impurities present in the reactants and solvents. This was despite the cleaning of the glassware between synthesis.

To compare the elemental profiles, Pearson correlation coefficients were calculated for every pair of 146 samples. Impurities were normalised to the sum of the targets and pre-treated using the sixteenth root method, a threshold of 95.00 did not allow all of the samples from within each synthetic route to be deemed similar. This was due to the presence of all of the target impurities in each route.

7.3 Conclusions

ICPMS analysis were preformed in order to investigate whether or not the inorganic profile of the synthesised samples would provide any added information in relation to determining synthetic route specificity.

All of the target elements were present in each sample to some degree. However, as expected, elevated quantities of specific elements were revealed in samples from synthetic routes which used a reducing agent or catalyst containing the respective element. Hg and Li were the target impurities for samples synthesised via the Reduction Amination and Birch routes respectively. P and I were elements of interest in the Nagai and Moscow synthesised samples with both elements present in relatively higher amounts in the Moscow route samples. In the Rosenmund and Emde route samples, Pd and Ba were present in significantly higher amounts. Higher than expect quantities of some of these elements were also revealed in some of the samples presumably due to contamination from the glassware used, despite careful cleaning, or from the precursor synthesis itself. Due to the presence of each element in the samples produced via more than one route, the Pearson correlation coefficient was unable to relate the samples to their specific synthetic routes.

It should be noted that each synthetic route in this study was carefully controlled so that it could be 'exactly' repeated. Despite this, the variation of the target impurities was large when compared between batches within the synthetic routes. In reality, however, clandestine chemists are likely to work in a less controlled fashion during the manufacture of methylamphetamine and it is quite conceivable that this would introduce the presence of both unrelated elements and produce a wide variation in concentration. This would suggest that there are some limitations in the use of the elemental data derived from ICPMS analysis of methylamphetamine samples but it does have potential to provide useful information for certain routes (such as Reductive Amination, Birch, Nagai and Moscow.

7.4 References

1. Reid, H.J.; Bashammakh, A. A.; Goodall, P.S.; Landon, M.R.; Connor, C. O'.; Sharp, B.L., Determination of iodine and molybdenum in milk by quadrupole ICP-MS. *Talanta* 2008, 75, 189–197.

2. Synthesis of Phenyl-2-Propanone (P2P). Available at http://www.designer-drugs.com/pte/12.162.180.114/dcd/chemistry/phenylacetone.html#benzylcyanide. Last accessed on 25/03/10.

3. Synthesis of Methyl Iodide. Available at http://www.designer-drugs.com/pte/12.162.180.114/dcd/chemistry/methyliodide.html. Last accessed on 25/03/10.

CHAPTER 8: USING DATA ANALYSIS TECHNIQUES FOR SAMPLE DISCRIMINATION

8.0 Introduction

A variety of data analysis techniques were used to identify methods which could discriminate between methylamphetamine based on the analytical data derived from a set of samples of known provenance. Given the way in which the synthesised samples were produced, this discrimination could occur on a number of levels:

1. by starting material;
2. by synthetic route; or
3. by starting material and synthetic route, referred to as 'lab output,

The starting materials and samples synthesised were as follows:

Four batches of P-2-P (21 x Leuckart, 20 x Reductive Amination), three batches of ephedrine hydrochloride (10 x Nagai, 12 x Rosenmund, 11 x Emde, 21 x Moscow), three batches of *pseudo*ephedrine hydrochloride (10 x Nagai, 8 x Rosenmund, 9 x Emde, 1 x Moscow) and one batch of ephedrine base (20 x Birch) were used to synthesis the samples. Discrimination of the methylamphetamine samples into these four groupings would correspond to discrimination by starting material. For data analysis, the data of 143 out of 149 batches of synthesised samples were used.

Discrimination by synthetic route would correspond to the grouping of samples as follows: route 1: 21 x Leuckart; route 2: 20 x Reductive Amination; route 3: 20 x Nagai; route 4: 20 x Rosenmund; route 5: 20 x Birch; route 6: 20 x Emde; route 7: 22 x Moscow.

The final discriminating category was termed the 'lab output'. This was used to simulate the actual clandestine laboratory output where discrimination by starting material and synthetic route are required (lab output group 1: 21 x Leuckart; lab output group 2: 20 x Reductive Amination; lab output group 3: 10 x Nagai; lab output group 4: 12 x Rosenmund; lab output group 5: 11 x Emde; lab output group 6: 21 x

Moscow; lab output group 7: 10 x Nagai; lab output group 8: 8 x Rosenmund; lab output group 9: 9 x Emde; lab output group 10: 1 x Moscow; lab output group 11: 20 x Birch).

A summary of the samples for each level of discrimination are detailed in Table 64.

	By starting material	**By synthetic route**	**By 'lab output'**
Cluster 1	21 x Leuckart 20 x Reductive Amination	21 x Leuckart	21 x Leuckart
Cluster 2	10 x Nagai 12 x Rosenmund 11 x Emde 21 x Moscow	20 x Reductive Amination	20 x Reductive Amination
Cluster 3	10 x Nagai 8 x Rosenmund 9 x Emde 1 x Moscow	20 x Nagai	10 x Nagai
Cluster 4	20 x Birch	20 x Rosenmund	12 x Rosenmund
Cluster 5	n/a	20 x Birch	11 x Emde
Cluster 6	n/a	20 x Emde	21 x Moscow
Cluster 7	n/a	22 x Moscow	10 x Nagai
Cluster 8	n/a	n/a	8 x Rosenmund
Cluster 9	n/a	n/a	9 x Emde
Cluster 10	n/a	n/a	1 x Moscow
Cluster 11	n/a	n/a	20 x Birch

Table 64: Breakdown of the clusters which would be expected if discrimination were possible by starting material, by synthetic route, or by 'lab output'.

Data analysis techniques were undertaken on data sets consisting of the GCMS data alone, IRMS data alone, ICPMS data alone, a combination of two data; (GCMS and IRMS, GCMS and ICPMS, IRMS and ICPMS) and the combination of all three data sets. For the GCMS data, as before, the CHAMP impurities, target impurities identified within this work and the CHAMP impurities in combination with the target impurities from this study were investigated. In all cases the peak areas were

normalised to the sum of the peak area of the targets impurities. The sixteenth root data pre-treatment method was chosen since this delivered the most accurate discrimination by synthetic route for the samples using Pearson correlation coefficients. These different combination of the data resulted in 15 different data sets as follows:

1. GCMS (CHAMP impurities, norm to the sum, sixteen roots);
2. GCMS (Target impurities from this study, norm to the sum, sixteenth roots);
3. GCMS (CHAMP impurities plus target impurities from this study, norm to the sum, sixteenth root);
4. IRMS data;
5. ICPMS data;
6. GCMS (CHAMP impurities, norm to the sum, sixteenth root) + IRMS;
7. GCMS (Target impurities from this study, norm to the sum, sixteenth root) + IRMS;
8. GCMS (CHAMP impurities plus target impurities from this study, norm to the sum, sixteenth root) + IRMS;
9. GCMS (CHAMP impurities, norm to the sum, sixteenth root) + ICPMS;
10. GCMS (Target impurities from this study, norm to the sum, sixteenth roots) + ICPMS;
11. GCMS (CHAMP impurities plus target impurities from this study, norm to the sum, sixteenth root) + ICPMS;
12. IRMS + ICPMS
13. GCMS (CHAMP impurities, norm to the sum, sixteenth root) + IRMS + ICPMS;
14. GCMS (Target impurities from this study, norm to the sum, sixteenth root) + IRMS + ICPMS; and
15. GCMS (CHAMP impurities plus target impurities from this study, norm to the sum, sixteenth root) + IRMS + ICPMS.

To assess the level of the discrimination, if any, afforded by these data sets, hierarchical cluster analysis (HCA), principal component analysis (PCA), and

discriminant analysis (DA) were applied to all 15 data sets. The three data analysis techniques, the results and the conclusions drawn from each will be discussed in turn before the overall conclusions are detailed at the end of the chapter.

8.1 Hierarchical Cluster Analysis (HCA)

Hierarchical cluster analysis is an unsupervisied pattern recognition technique in which a set of data is clustered to produce a dendrogram, or a graphical representation of the similarities between the elements in the data set.[1] Dendrograms are similar to tree diagrams in that individual elements are linked to other elements and clusters until, finally, all elements are linked together.[1-3] Dendrograms can be generated in one of two ways: agglomerative (bottom to top) or divisive (top to bottom).[1-3] Agglomerative method is more commonly used and involves examination of the data objects together in a sequential way until the entire data set is linked together; the divisive method begins with all of the entities as one group and then breaks the set down until only clusters consisting of one element remain.[4-6] Divisive procedures have rarely, if ever, been applied to analytical data.[5]

A number of methods exist for determining how clusters should be combined, such as single, complete, group-average, centroid, median and Ward clustering.[6] Two of the most common of them are the nearest neighbour (single linkage) and the furthest neighbour (complete linkage) methods.[3] The nearest neighbour method is the simplest procedure and, in this case, the distance between two clusters is defined as the smallest distance between two elements, one from each cluster (see Figure 143).[3, 5, 6] This method can have the disadvantages of ‘space contracting’ (or ‘chaining’[6]), which is the result of the chaining together of poorly separated clusters into a long, linear cluster instead of the usual round or elliptical clusters.[1]

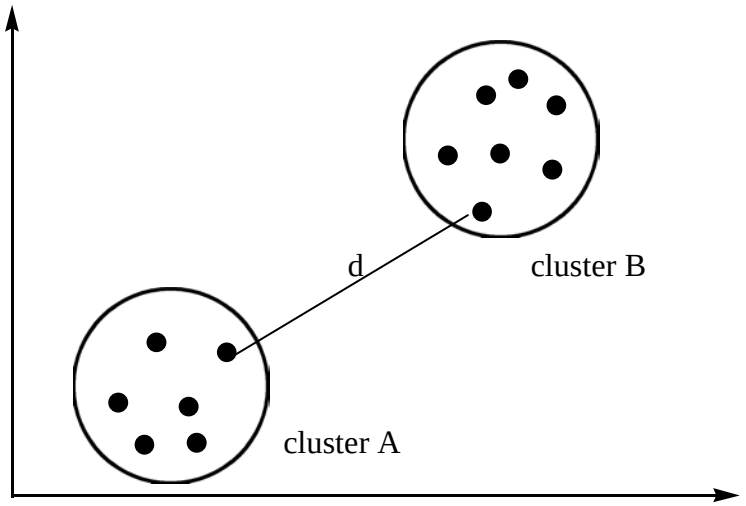

Figure 143: Distance, d, between clusters A and B as defined by the nearest neighbour method.[1]

As indicated by the name, the furthest neighbour clustering method is the opposite of nearest neighbour. With this method, the distance between two clusters is defined by the greatest distance between two objects, one from each cluster[5, 6]. Figure 144 illustrates this concept. The furthest neighbour method can have the disadvantages of 'space dilating', which results in many small clusters and is the opposite of the space contracting effect.[5]

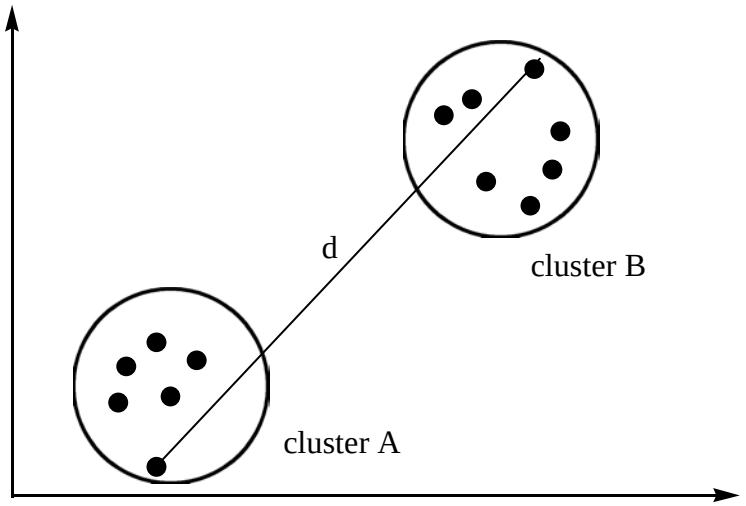

Figure 144: Distance, d, between clusters A and B as defined by the furthest neighbour method.[1]

A method of measuring the distance between clusters must also be selected for hierarchical cluster analysis. Two options to measure the interval are simple Euclidean distance, in which the straight line distance between the two points is calculated, and squared Euclidean distance, which is the same distance but squared.[7]

8.1.1 HCA Experimental

HCA was performed using SPSS software version 17.0 on the 15 data sets previously described. Two clustering methods, nearest and further neighbour, and two distance measures, Euclidean and squared Euclidean, were examined for each data set.[1] In total, four combinations of the clustering and distance methods were used for each identified data set as follows:

1. nearest neighbour, Euclidean distance;
2. nearest neighbour, squared Euclidean distance;
3. furthest neighbour, Euclidean distance; and
4. furthest neighbour, squared Euclidean distance.

The resulting dendrograms were examined for accurate clustering according to batch of starting material, synthetic route, and 'lab output' (see Table 64) and the best combination of clustering method and distance measure was assessed based on which, if, any, produced the most accurate clustering.

8.1.2 HCA Results and Discussion

(1) GCMS data

Using HCA, discrimination of all of the methylamphetamine batches was achieved for seven of the 15 data sets. Each of the four cluster-measure combinations achieved this discrimination. Discrimination by synthetic route, was achieved using GCMS data alone. It should be noted that CHAMP target impurities on their own were unable to distinguish between the Nagai and Moscow routes.

The dendrogram produced using furthest neighbour and Euclidean distance of GCMS data set is displayed in Figure 145 – Figure 147.

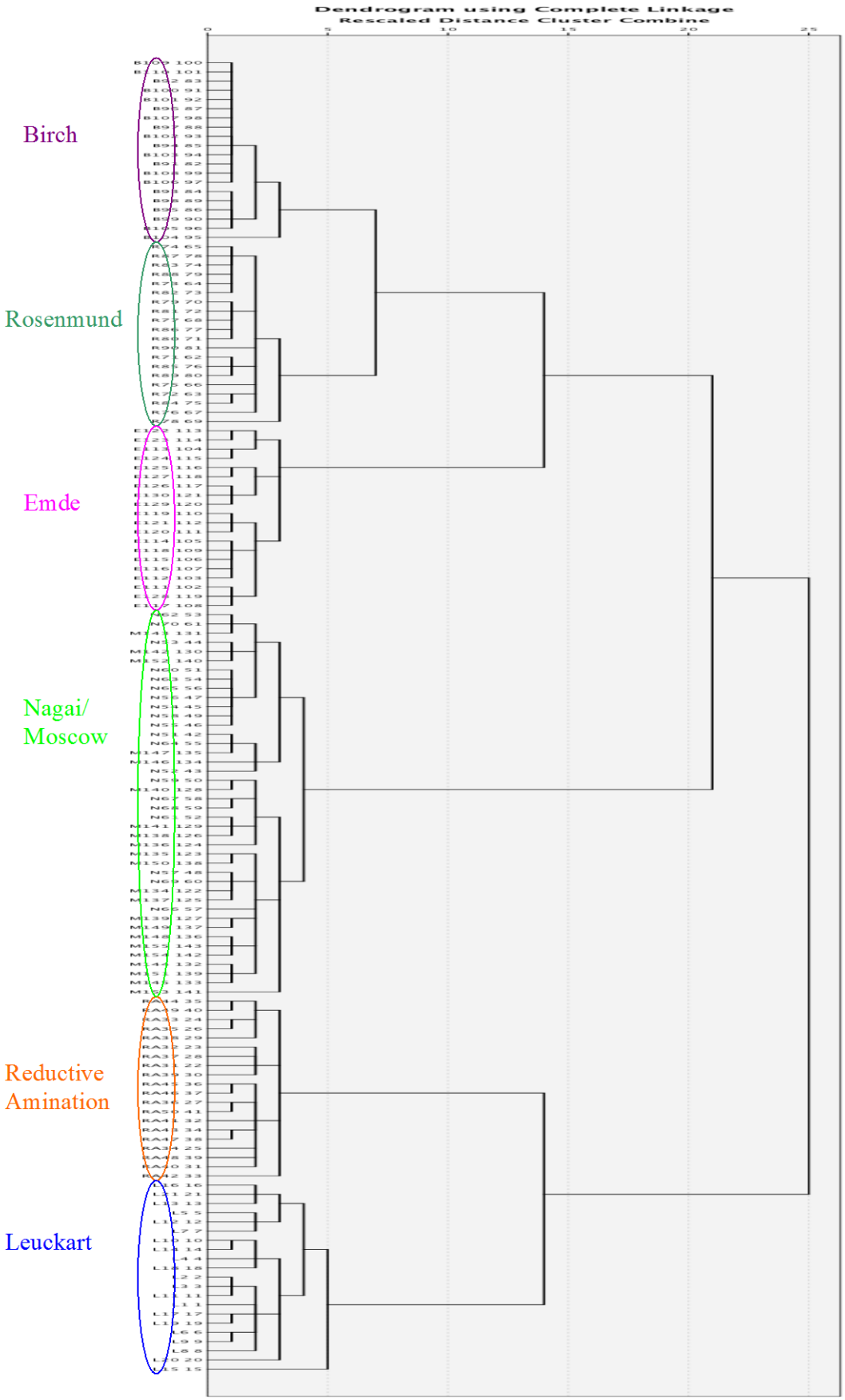

Figure 145: Dendrogram resulting from HCA (furthest neighbour, Euclidean distance) of the GCMS data (CHAMP impurities, norm to the sum, sixteenth root).

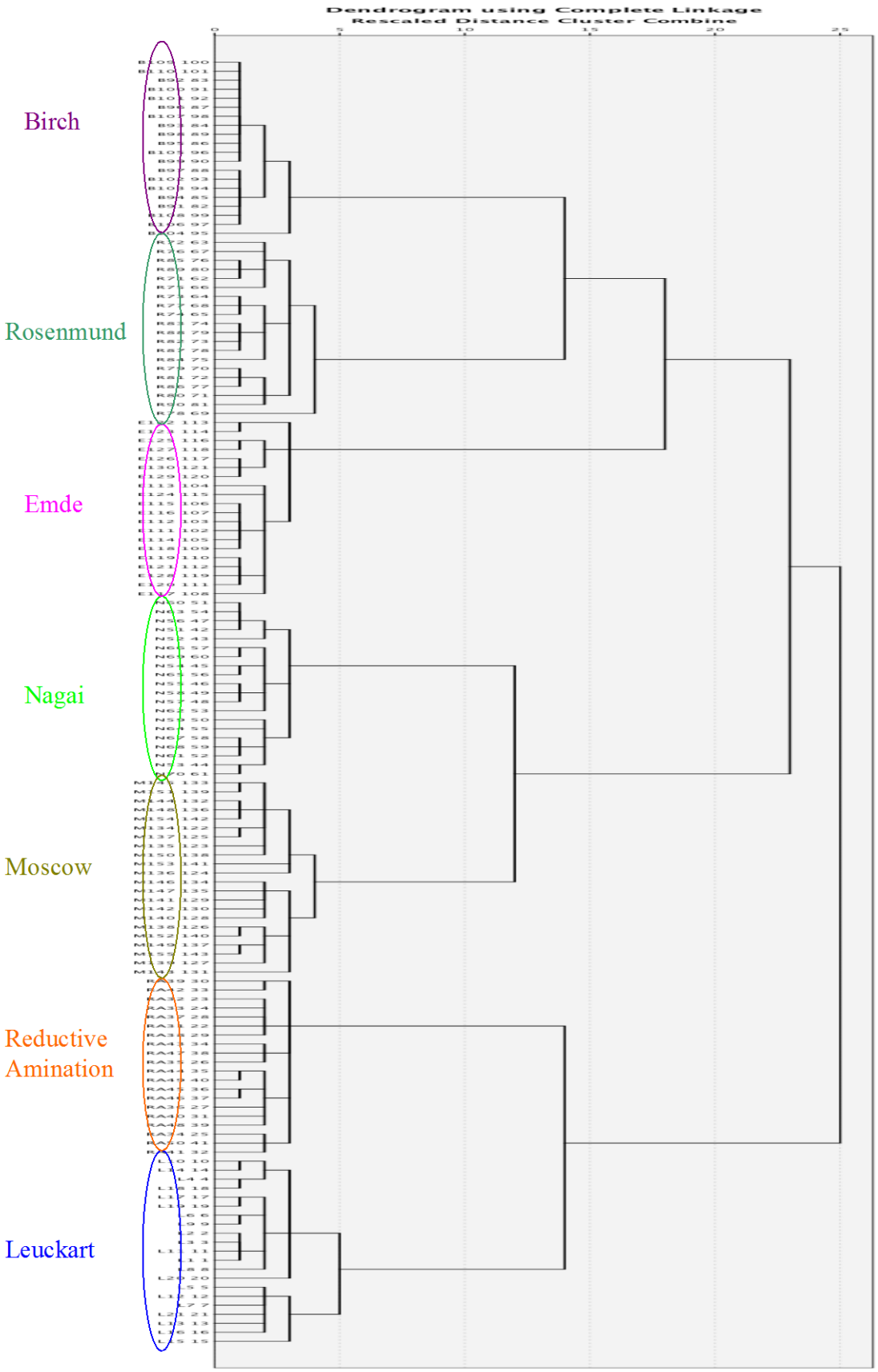

Figure 146: Dendrogram resulting from HCA (furthest neighbour, Euclidean distance) of the GCMS data (Target impurities from this study, norm to the sum, sixteenth root).

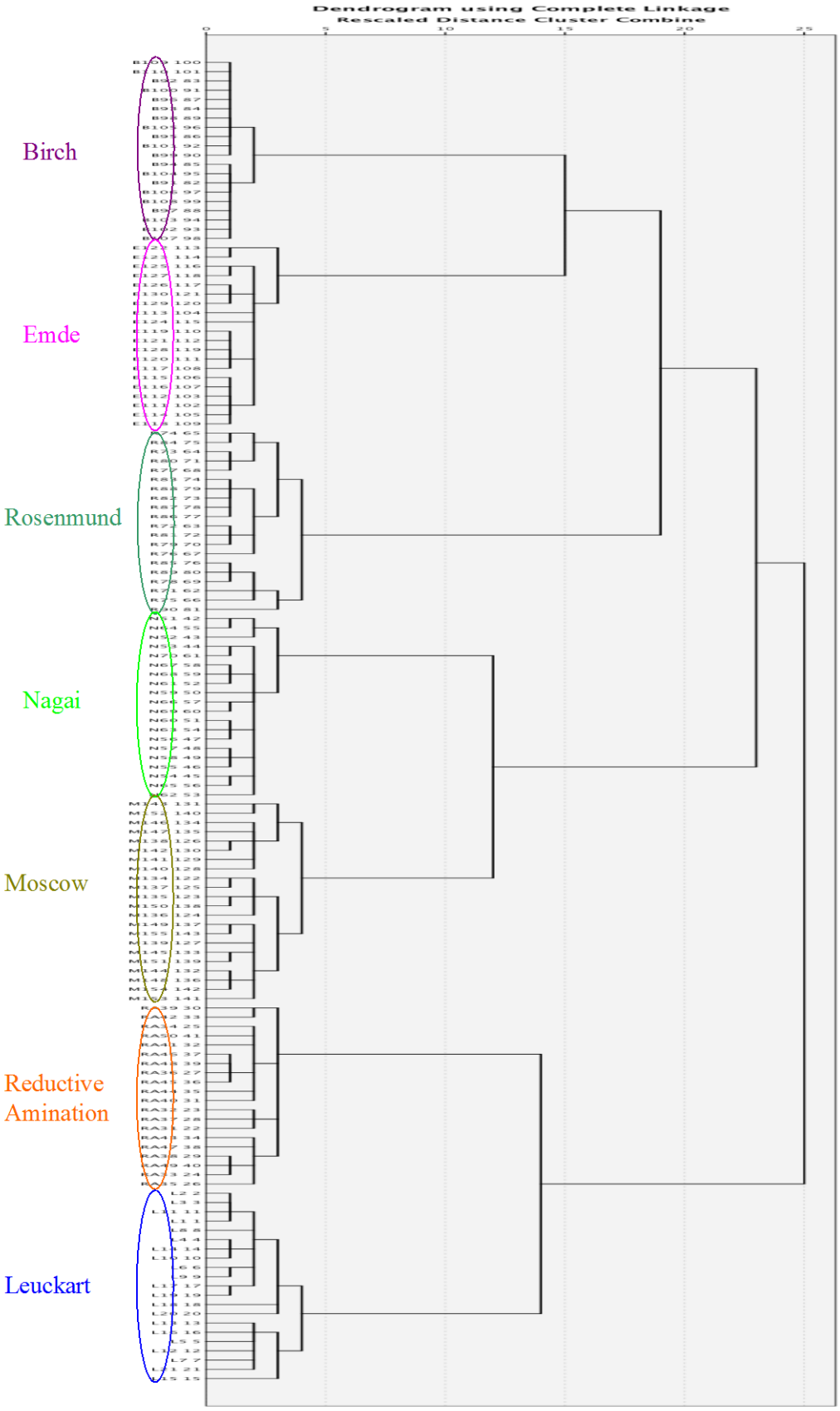

Figure 147: Dendrogram resulting from HCA (furthest neighbour, Euclidean distance) of the GCMS data (CHAMP impurities plus target impurities from this study, norm to the sum, sixteenth root).

(2) IRMS and GCMS data

Discrimination by starting material was achieved with IRMS data on its own or in combination with the GCMS data. Each of the four cluster-measure combinations facilitated this discrimination. The dendrogram produced using furthest neighbour and Euclidean distance of this data set is displayed in Figure 148 - Figure 149.

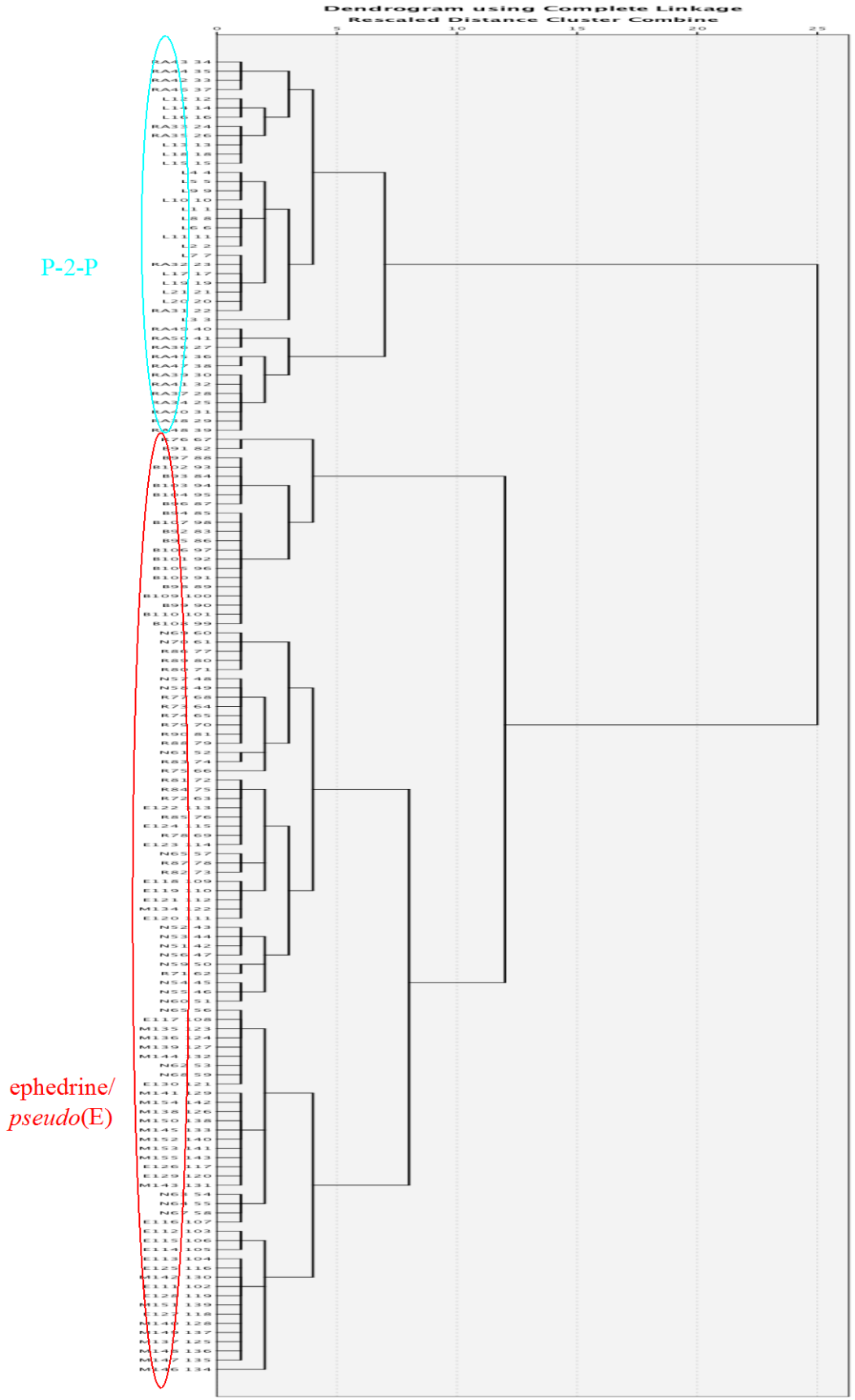

Figure 148: Dendrogram resulting from HCA (furthest neighbour, Euclidean distance) of the IRMS data.

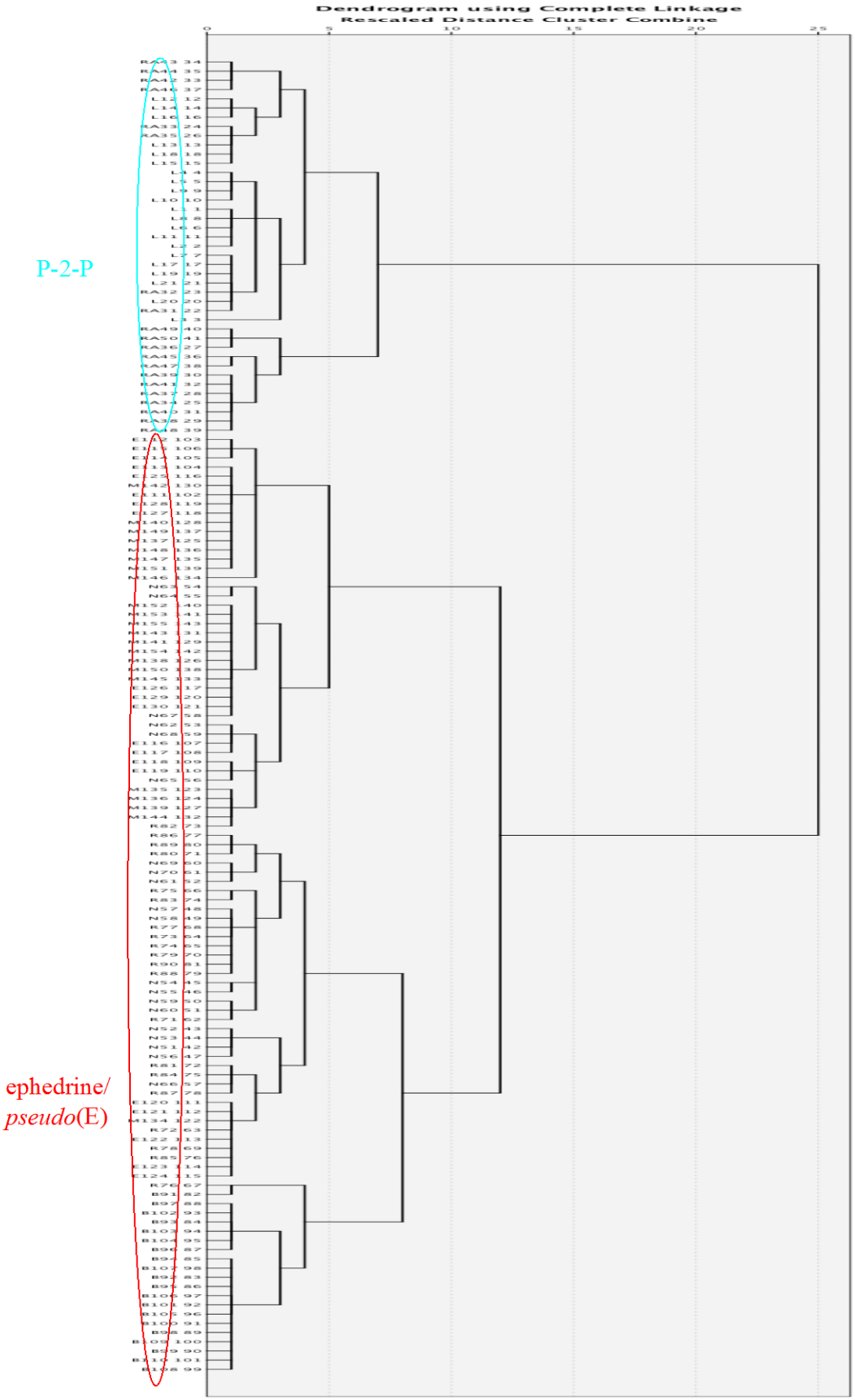

Figure 149: Dendrogram resulting from HCA (furthest neighbour, Euclidean distance) of the combination of IRMS and GCMS (CHAMP impurities plus target impurities from this study, norm to the sum, sixteenth root) data.

HCA applied to the IRMS data on its own or in combination with the GCMS data was not capable of demonstrating discrimination of the starting material as well as the synthetic route. Only discrimination between epehedrine/*pseudo*ephedrine and P-2-P starting material was achieved. Clustering by synthetic route was achieved in P-2-P. Accurate clustering by starting material (P-2-P or ephedrine/*pseudo*ephedrine) was produced by $\delta^{2}H$ data on its own or in $\delta^{15}N$ or $\delta^{13}C$ data. However, the $\delta^{13}C$ data on its own did discriminate between methylamphetamine synthesised from the ephedrine or *pseudo*ephedrine salt, ephedrine base and P-2-P. A dendrogram resulting from this further analysis is illustrated in Figure 150 – Figure 151.

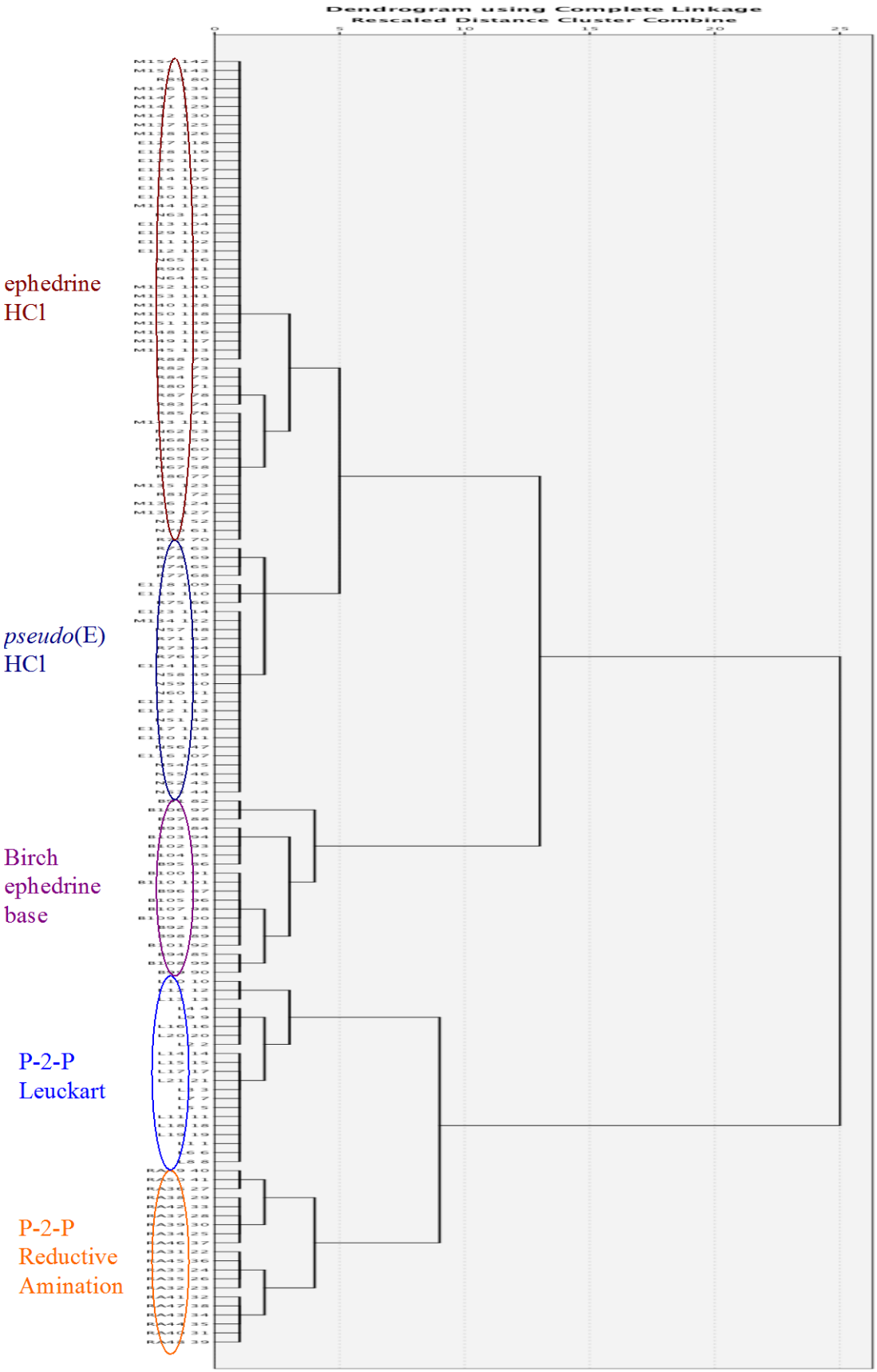

Figure 150: Dendrogram resulting from HCA (furthest neighbour, Euclidean distance) of the IRMS with $\delta^{13}C$ data alone.

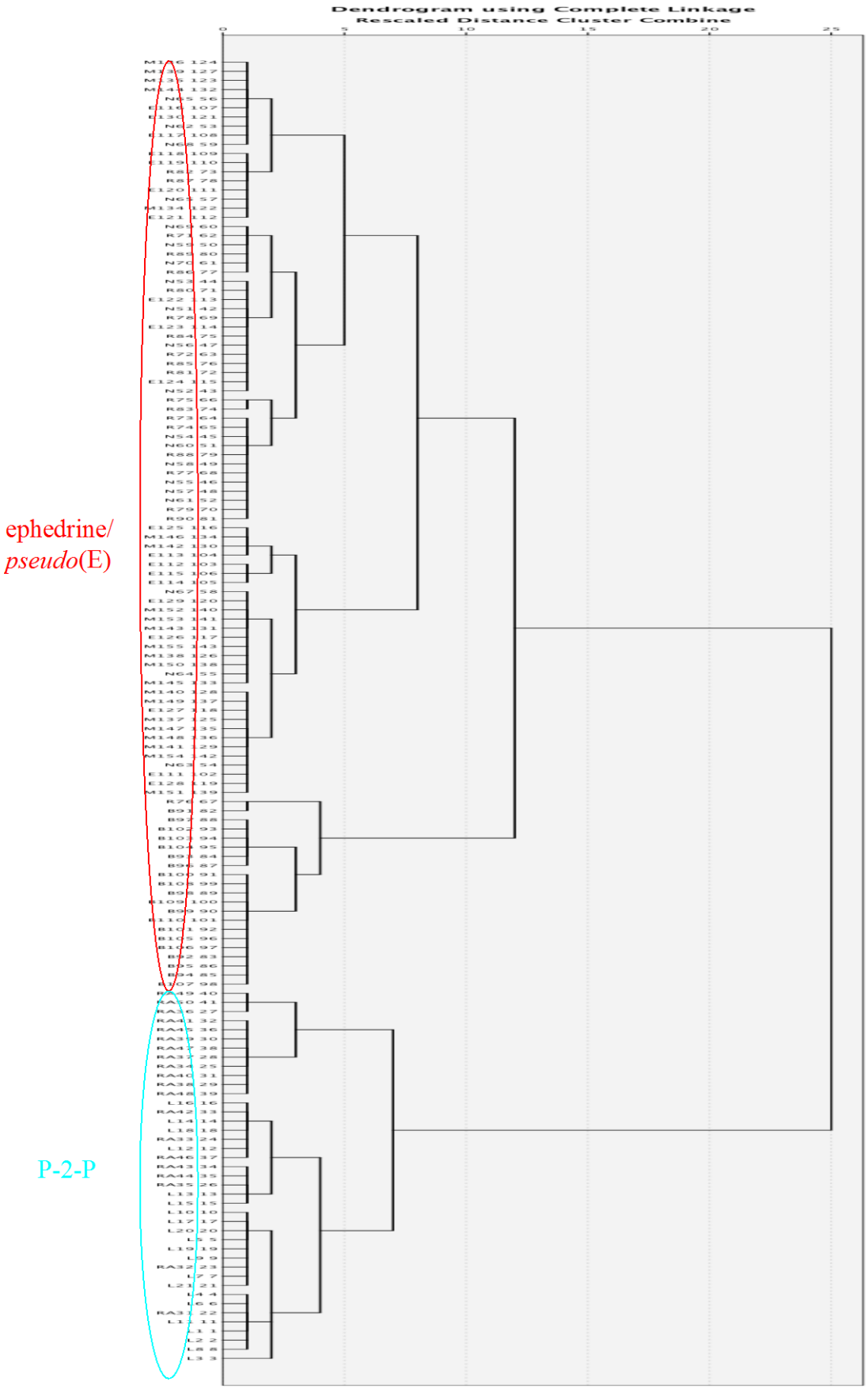

Figure 151: Dendrogram resulting from HCA (furthest neighbour, Euclidean distance) of the IRMS with δ^2H data alone.

(3) ICPMS data

Poor discrimination was demonstrated with HCA of the ICPMS data on its own or in combination with the GCMS and/or IRMS data. Figure 152 displays the dendrogram achieved using ICPMS data using the furthest neighbour and Euclidean distance combination.

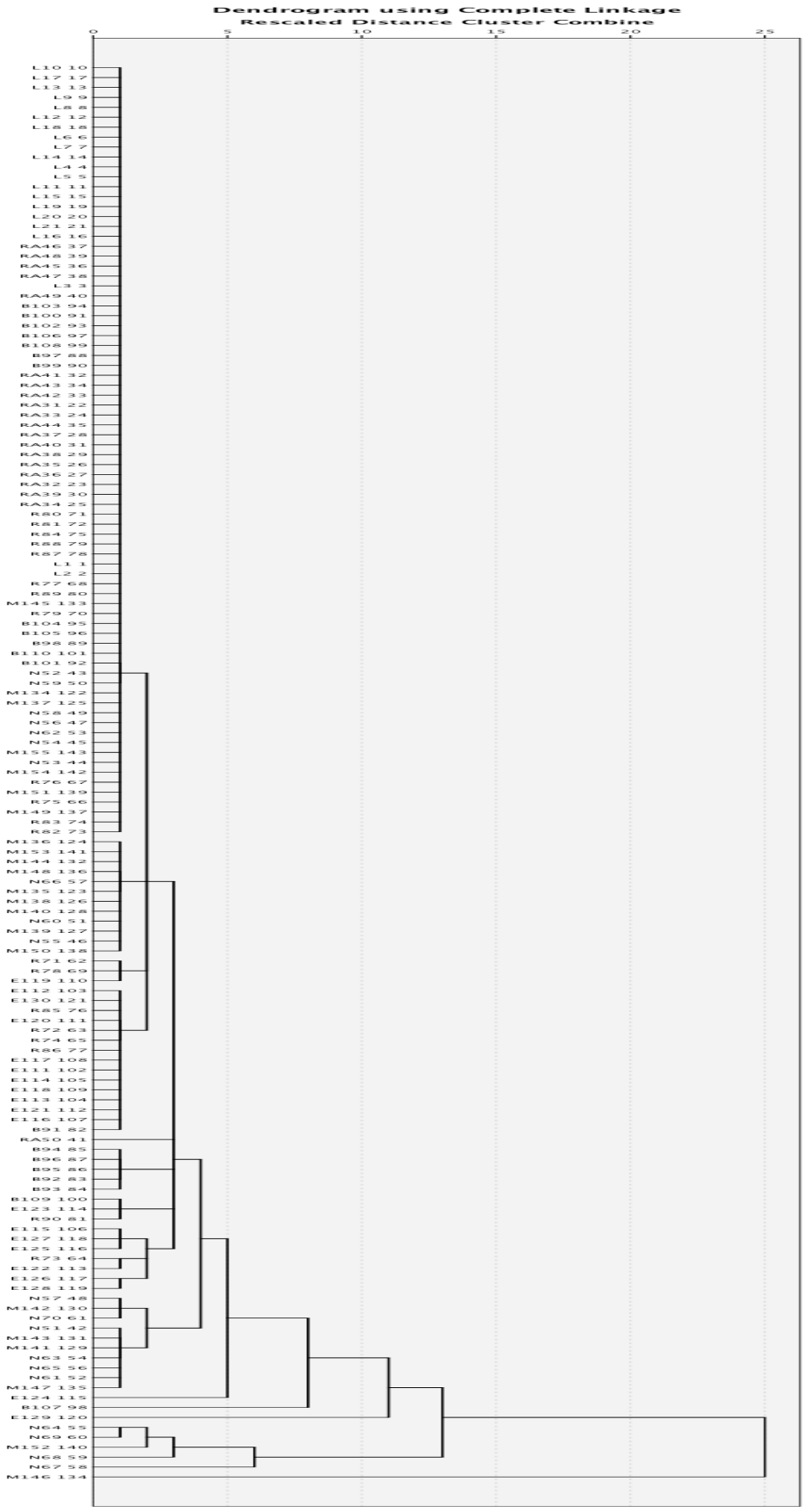

Figure 152: Dendrogram resulting from HCA (furthest neighbour, Euclidean distance) of the ICPMS data. Meaningful discrimination is not achieved.

8.1.3 HCA Conclusions

Application of HCA using any of the four distance-cluster methods with the GCMS data where the target impurities identified in this study (on their own or in combination with CHAMP impurities) to the 143 methylamphetamine batches revealed accurate discrimination of the samples by synthetic route only.

Discrimination by starting material could only be demonstrated for P-2-P and ephedrine/*pseudo*ephedrine groupings rather than any further refinement and was achieved with the IRMS data on its own or in combination with the GCMS data. When HCA was applied to the $\delta^{13}C$ data, discrimination into four different starting materials was achieved. In this case P-2-P groups could be distinguished from the samples prepared from ephedrine base and ephedrine or *pseudo*ephedrine hydrochloride. Further clustering by synthetic route was achieved in P-2-P. HCA of the ICPMS data on its own or in combination with the GCMS data and /or IRMS data was not able to produce any meaningful discrimination.

8.2 Principal Component Analysis (PCA)

In principal component analysis (PCA), the dimensionality of the data is often changed by the combination, or transformation, of the original variables into new variables, each of which accounts for more variance than the corresponding original variables. Reducing the dimensionality of the data is a common reason for performing PCA on multivariate data sets.[1, 8, 9]

PCA seeks to find linear combinations of the original variables, such that the greatest degree of variance is explained by the fewest number of new variables, or principal components (PCs).[1] A 'linear combination' of the original variables is a new set of variables created from the sum of the original variables, each weighted appropriately.[1] Once the first PC is found, a second linear combination is sought to explain the remaining variance. It is important to note that each principal component is constructed so that it is orthogonal (or uncorrelated) with the others. Mathematically, the variance explained by a PC is defined by its eigenvalue.[9, 10]

The interpretability of PC's can be improved through rotation. Rotation maximizes the loading of each variable on one of the extracted PC whilst minimizing the loading on all other PC's.[9] Rotation works through changing the absolute values of the variables whilst keeping their differential values constant.[9] There are methods of rotation. Varimax, quartimax and equamax are orthogonal rotations whereas direct oblimin and promax are oblique rotations.[9] The exact choice of rotation depends largely on whether the underlying PC should be related or not. Orthogonal rotations (Varimax) should choose for the PC to be independent.

PCs may be created until 100% of the variance in the data is explained (i.e. until the number of PCs equals the number of original variables); however, it is common to select a subset of the PCs such that the dimensionality of the original data set is reduced while very little information is lost overall.[9-11] According to one author on the subject,[12] normal practice dictates accepting those PCs which cumulatively account for 80-90% of the overall variance of the data.

The first PC is defined as:

$$PC1 = \alpha_{11}X_1 + \alpha_{12}X_2 + \ldots + \alpha_{1p}X_p \quad \text{Equation 8.1.}$$

where α_{1x} represents the weights or loadings for each of the original variables (X_1 to X_p) in PC1. Mathematically, these loadings are the elements of the eigenvectors, and they represent the slope of the new axis (PC1). Large absolute values of these loadings indicate a strong contribution of the corresponding original variable, and loadings near zero indicate a weak contribution.[1]

The PC 'scores' are the elements of the new variables (PC1, PC2, etc) which are derived from the loadings and the original variables. The PC scores represent the projection of the original data points onto the new axes.[1]

The power of PCA lies in the reduction of dimensionality of the data set. When, for instance, multivariate data sets contain more than two or three variables, graphical representation of the data becomes complicated, thus rendering the identification of similarities and differences between samples difficult. If two or three PCs can be identified which account for the majority of the variation in the data set, then graphical representation is simplified and it may be possible to visually identify clusters among the samples.[1]

8.2.1 PCA Experimental

PCA was performed using SPSS software version17.0. The correlation matrix option was selected since the variables were measured on different scales, and the varimax rotation method was utilised in order to minimise the number of variables with high loadings on each factor.[1]

PCA was applied to the 15 data sets described at the beginning of this chapter. The first two PCs of each analysis were then extracted and plotted to assess which data sets, if any, afforded any discrimination of the samples. A 3-D plot incorporating PC3 as the third axis was then constructed to investigate whether the addition of PC3 afforded better discrimination than PC1 vs PC2 alone.

The data sets which facilitated clustering of the samples using a plot of the first two PCs were then examined further to identify the variables which loaded most highly on PC1 and PC2.[1] The variable loadings are a measure of the correlation between the variable and the principal component, and the strength of this relationship is indicated by the magnitude of the loading (either positive or negative), where –1 indicates maximum negative correlation and +1 indicates maximum positive correlation. To assess which variables had the highest correlation with each principal component, the most highly loading variables were taken to the those which had magnitudes greater than 0.80.[1]

8.2.2 PCA Results and Discussion

PCA for each data set is discussed below.

(1) GCMS (CHAMP impurities, norm to the sum, sixteenth root) data

Four principal components had eigenvalues greater than one, and they accounted for 94.8% of the total variance in the data. PC1 and PC2 accounted for 63.6% of the total variance. However, a plot of PC1 and PC2 did not discriminate between the Nagai and Moscow batches (Figure 153).

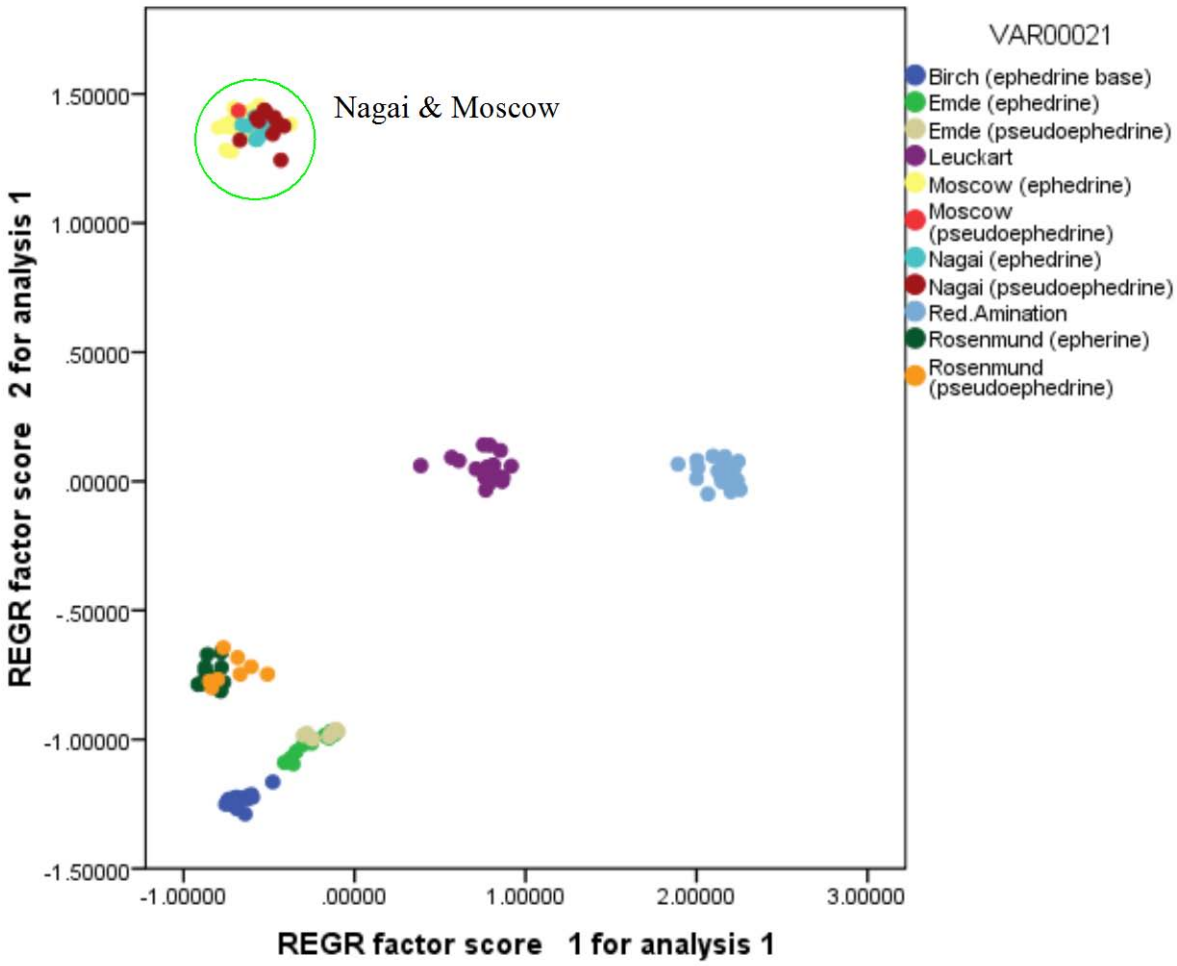

Figure 153: Scores plot for the first two PCs of the GCMS (CHAMP Impurities) data for all synthesised methylamphetamine samples.

(2) GCMS (Target impurities from this study, norm to the sum, sixteenth root) data

Six principal components had eigenvalues greater than one, and they accounted for 99.5% of the total variance in the data. PC1 and PC2 accounted for 53.3% of the total variance. A plot of PC1 and PC2 did not facilitate discrimination of Nagai, Moscow, Rosenmund and Emde batches (Figure 154). A 3D plot resulting from the addition of PC3 did not result in any further clarification.

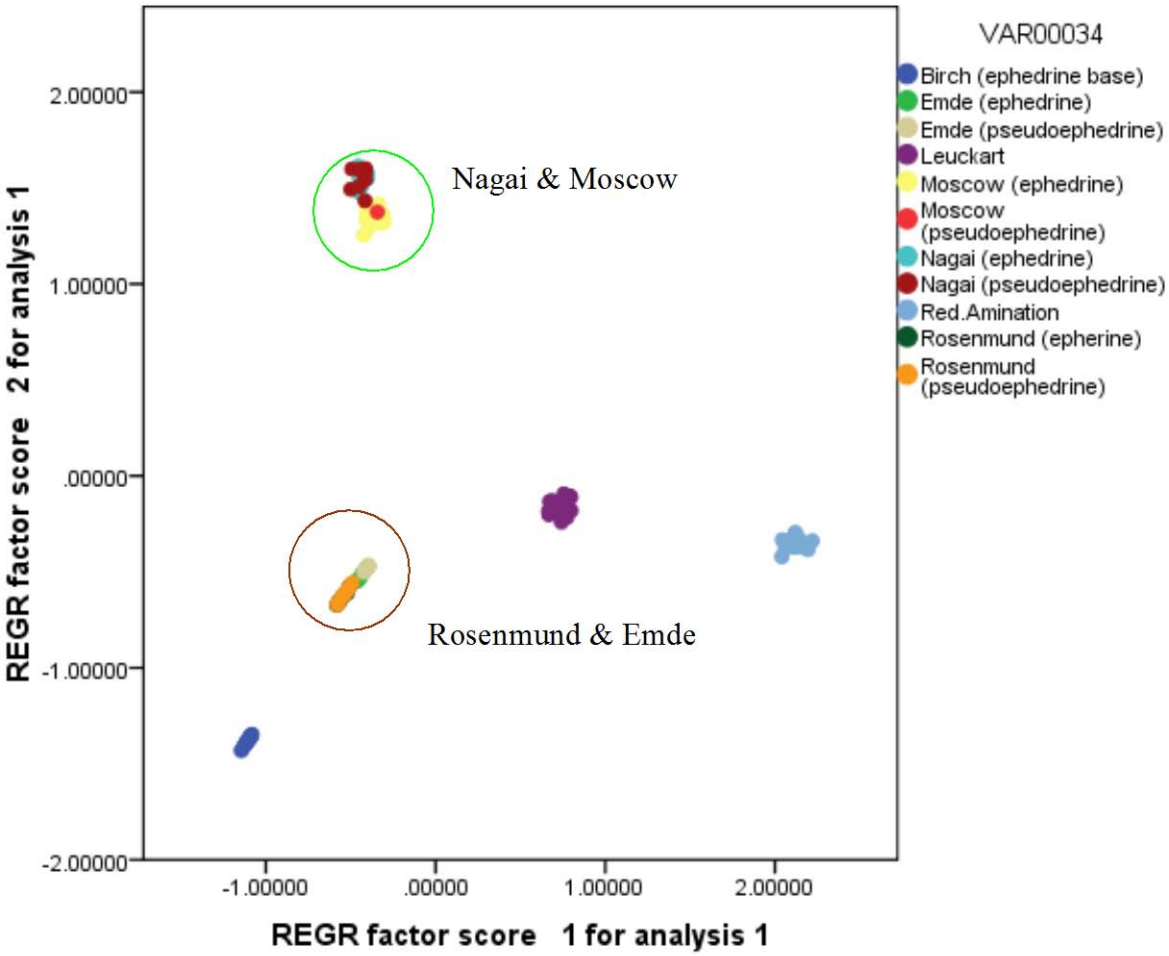

Figure 154: Scores plot for the first two PCs of the GCMS (Impurities from this study) data for all synthesised methylamphetamine samples.

(3) GCMS (CHAMP impurities plus target impurities from this study), normalised to the sum, sixteenth root data

Six principal components had eigenvalues greater than one, and they accounted for 98.5% of the total variance in the data. The 3-D (Figure 155) plot afforded better dicrimination than PC1 vs PC2 alone. PC1, PC2 and PC3 accounted for 66.4% of the total variance. However, a plot of PC1, PC2 and PC3 did not allow discrimination between Nagai and Moscow samples.

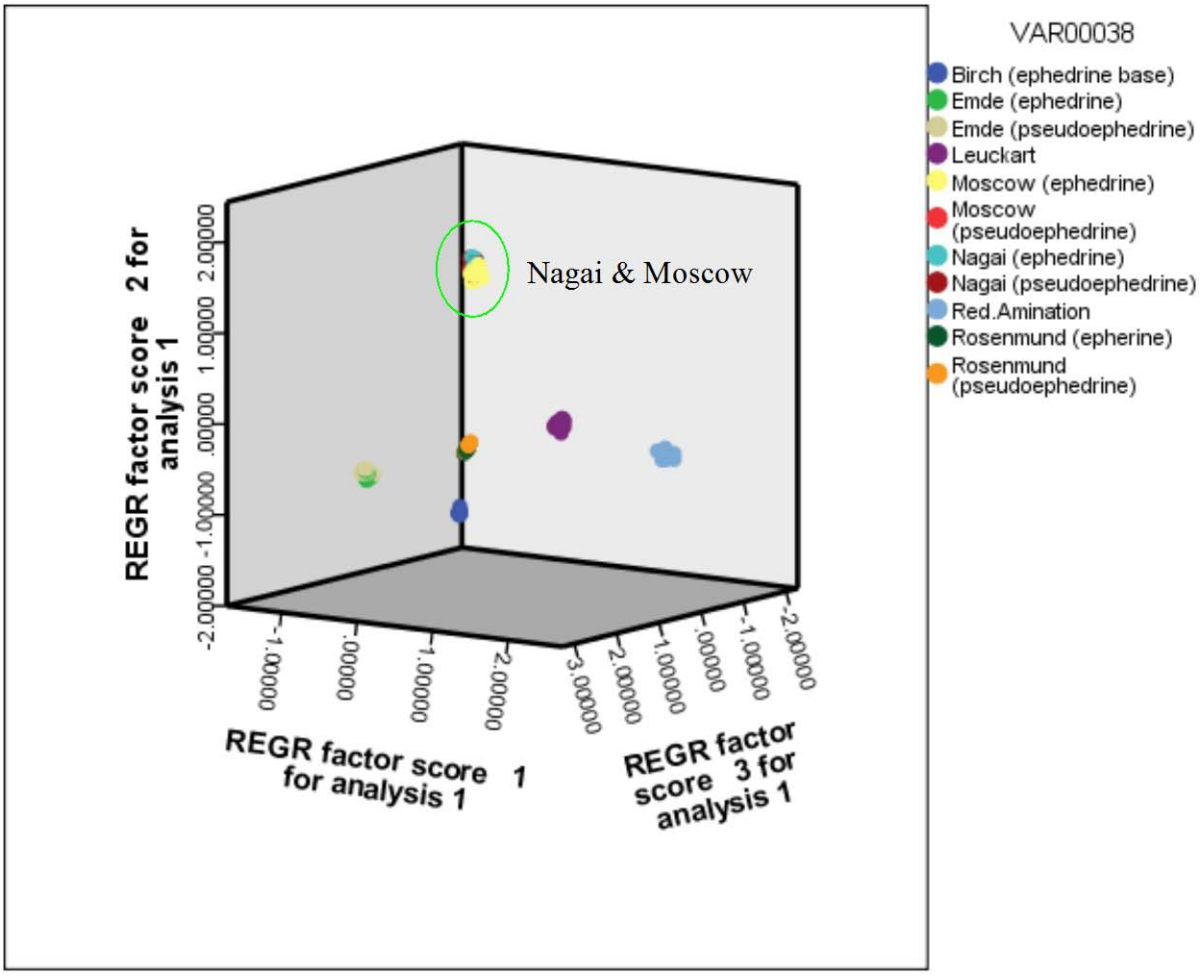

Figure 155: 3-D scores plot for the first three PCs of the GCMS (CHAMP impurities plus target impurities from this study) data for all synthesised methylamphetamine samples.

(4) IRMS data

Only two principal components had eigenvalues greater than one and they accounted for 90.9% of the total variance in the data. A plot of PC1 and PC2 allowed a clear discrimination between starting materials (P-2-P and ephedrine/*pseudo*ephderine) used during methylamphetamine synthesis (Figure 156).

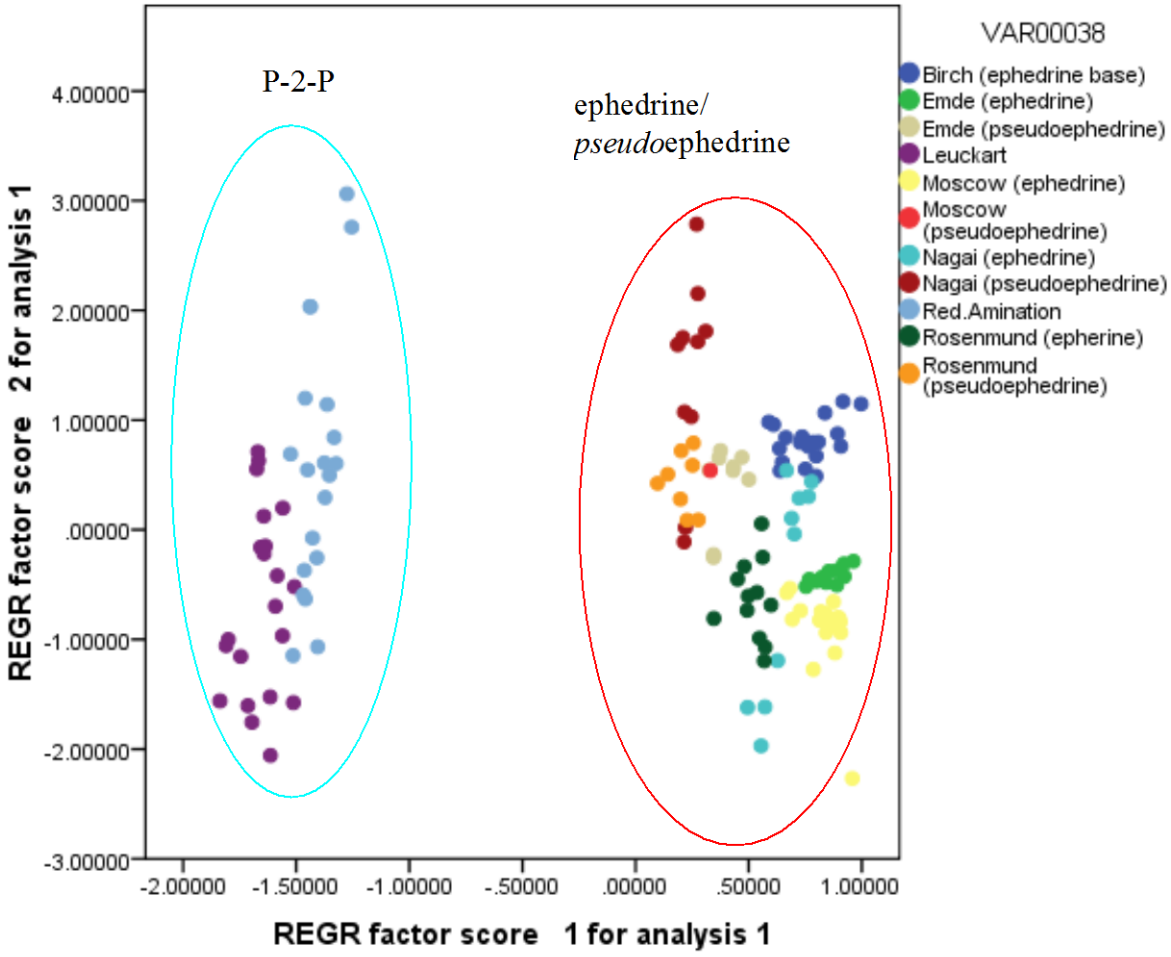

Figure 156: Scores plot for the two PCs of the IRMS data for all synthesised methylamphetamine samples.

(5) ICPMS data

Three principal components had eigenvalues greater than one, and accounted for 60.0% of the total variance in the data. PC1 and PC2 accounted for 43.0% of the total variance. A plot of PC1 and PC2 did not facilitate and useful discrimination (Figure 157).

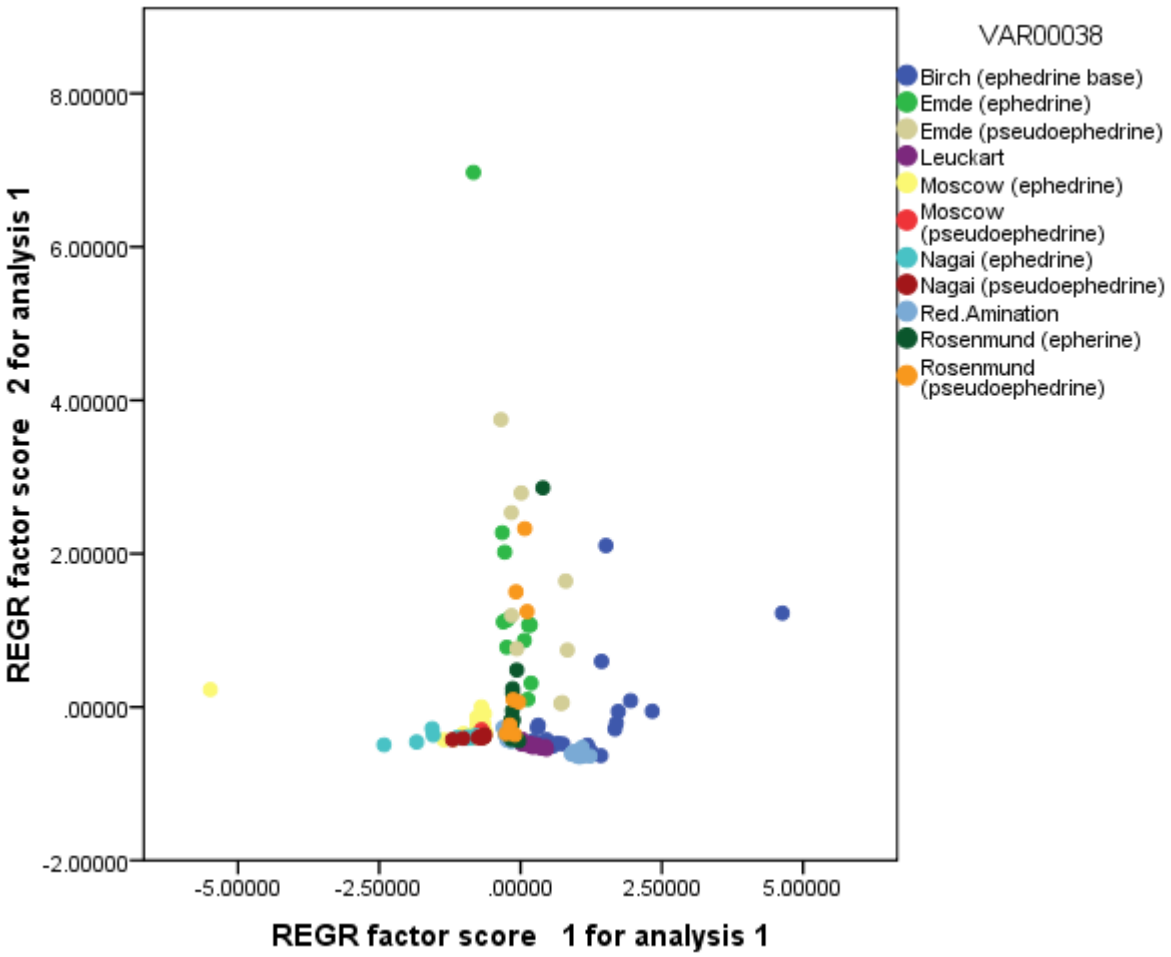

Figure 157: Scores plot for the first two PCs of the ICPMS data for all synthesised methylamphetamine samples.

(6) GCMS (CHAMP impurities, norm to the sum, sixteenth root) + IRMS data

Five principal components had eigenvalues greater than one, and accounted for 95.0% of the total variance in the data. PC1 and PC2 accounted for 60.3% of the total variance. A plot of PC1 and PC2 did not discriminate between the Nagai and Moscow samples. However discrimination by starting materials and synthetic routes were achieved for five of seven routes (Figure 158).

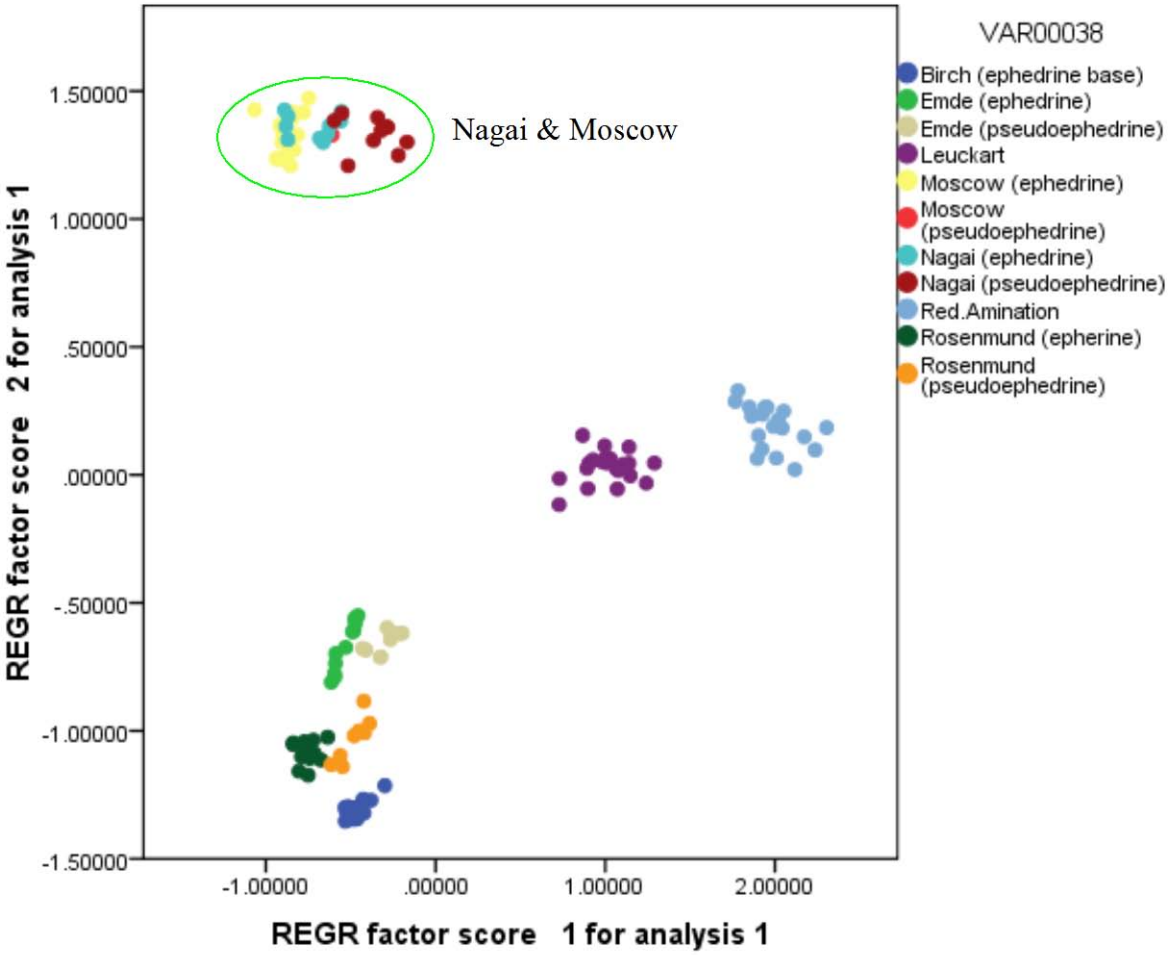

Figure 158: Scores plot for the first two PCs of the GCMS (CHAMP impurities) and IRMS data for all synthesised methylamphetamine samples.

(7) GCMS (Target impurities from this study, norm to the sum, sixteenth root) + IRMS data

Six principal components had eigenvalues greater than one, and accounted for 97.8% of the total variance in the data. PC1 and PC2 accounted for 54.3% of the total variance. A plot of PC1 and PC2 discriminated between the Nagai and Moscow batches but did not discriminate between the Rosenmund and Emde batches. However discrimination by synthetic routes are achieved by five of seven routes (Figure 159).

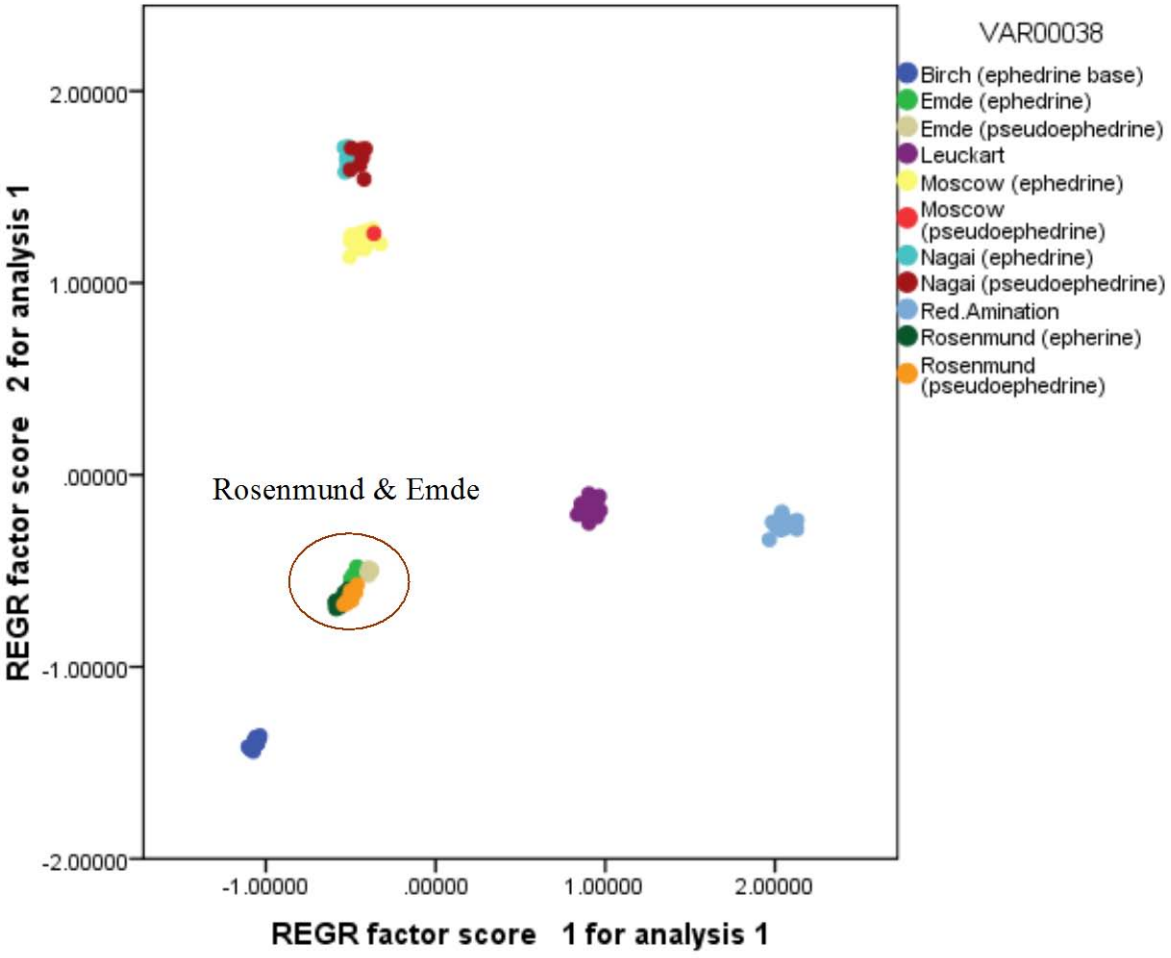

Figure 159: Scores plot for the first two PCs of the GCMS (Target impurities from this study) and IRMS data for all synthesised methylamphetamine samples.

However in this case the 3-D plot (Figure 160) with the addition of PC3 was able to show discrimination between Rosenmund and Emde batches as well. PC1, PC2 and PC3 accounted for 67.7% of the total variance. Discrimination by synthetic routes was therefore achieved for all the seven routes using this data set.

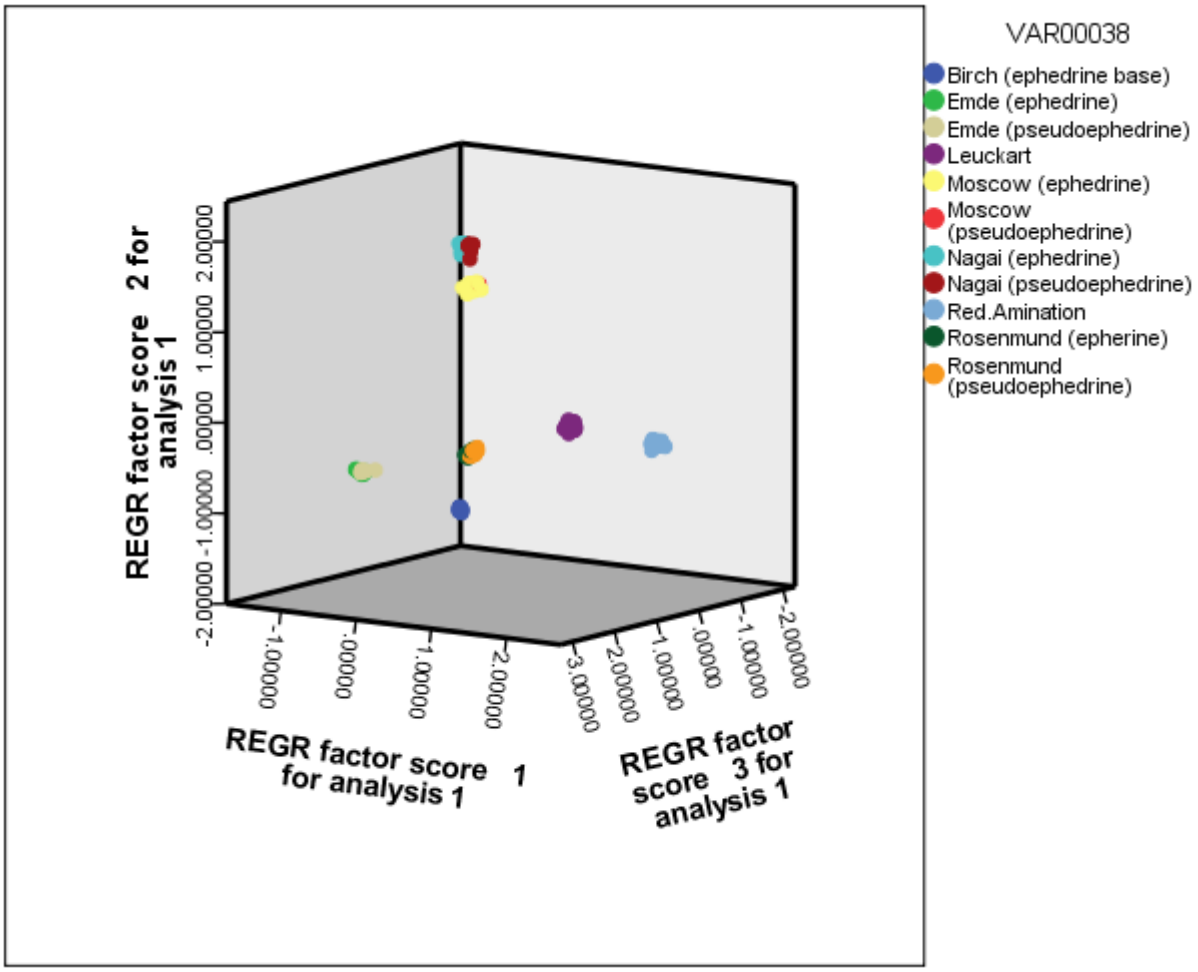

Figure 160: Scores plot for the first two PCs of the GCMS (Target impurities from this study) and IRMS data for all synthesised methylamphetamine samples.

(8) GCMS (CHAMP impurities plus target impurities from this study, norm to the sum, sixteenth root) + IRMS data

Six principal components had eigenvalues greater than one, and accounted for 96.9% of the total variance in the data. PC1 and PC2 accounted for 53.5% of the total variance. A plot of PC1 and PC2 (Figure 161) allowed discrimination of both the Nagai and Moscow samples but does not for Rosenmund and Emde samples.

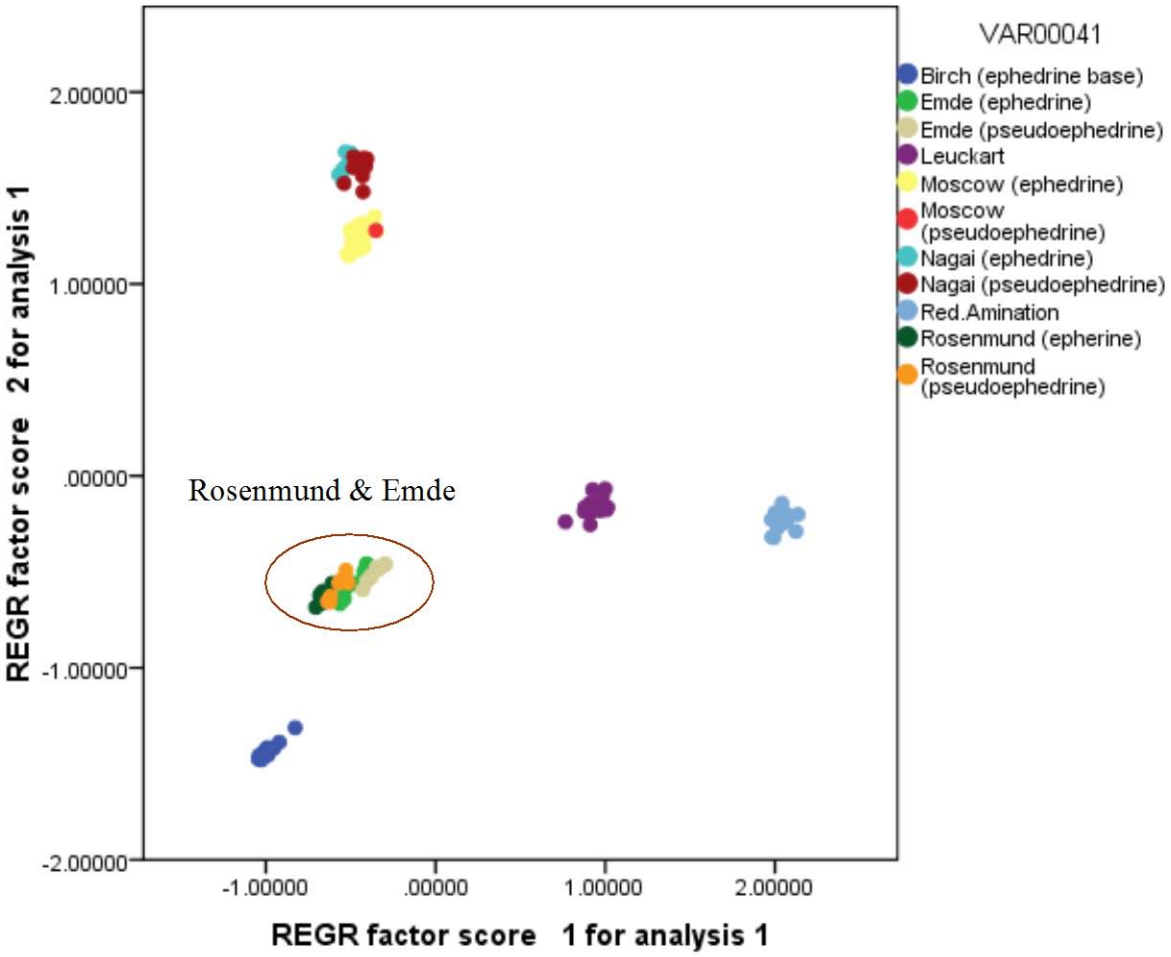

Figure 161: Scores plot for the first two PCs of the GCMS (CHAMP impurities plus target impurities from this study) and IRMS data for all synthesised methylamphetamine samples.

Again in this case the 3-D plot (Figure 162) with the addition of PC3 was able to show discrimination between Rosenmund and Emde batches but did not discriminate very clear between the Nagai and Moscow samples. PC1, PC2 and PC3 accounted for 66.7% of the total variance. Discrimination by synthetic routes was therefore achieved by five of seven routes using this data set.

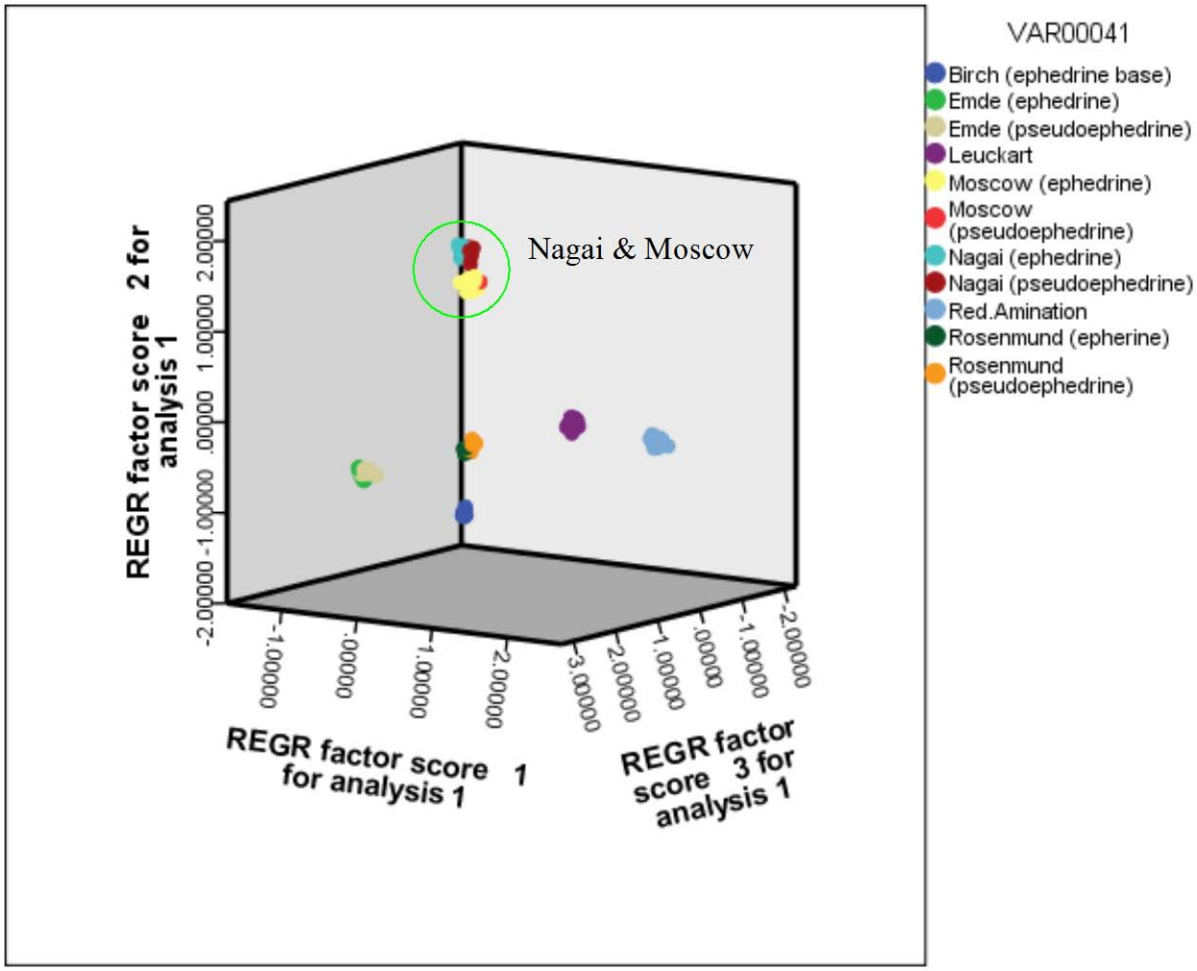

Figure 162: 3-D scores plot for the first three PCs of the GCMS (CHAMP impurities plus target impurities from this study) and IRMS data for all synthesised methylamphetamine samples.

(9) GCMS (CHAMP impurities, norm to the sum, sixteen roots) + ICPMS data

Five principal components had eigenvalues greater than one, and accounted for 83.9% of the total variance in the data. PC1 and PC2 accounted for 46.4% of the total variance. A plot of PC1 and PC2 (Figure 163) did not show discrimination for all seven routes. Only few routes were able to discriminate by synthetic routes.

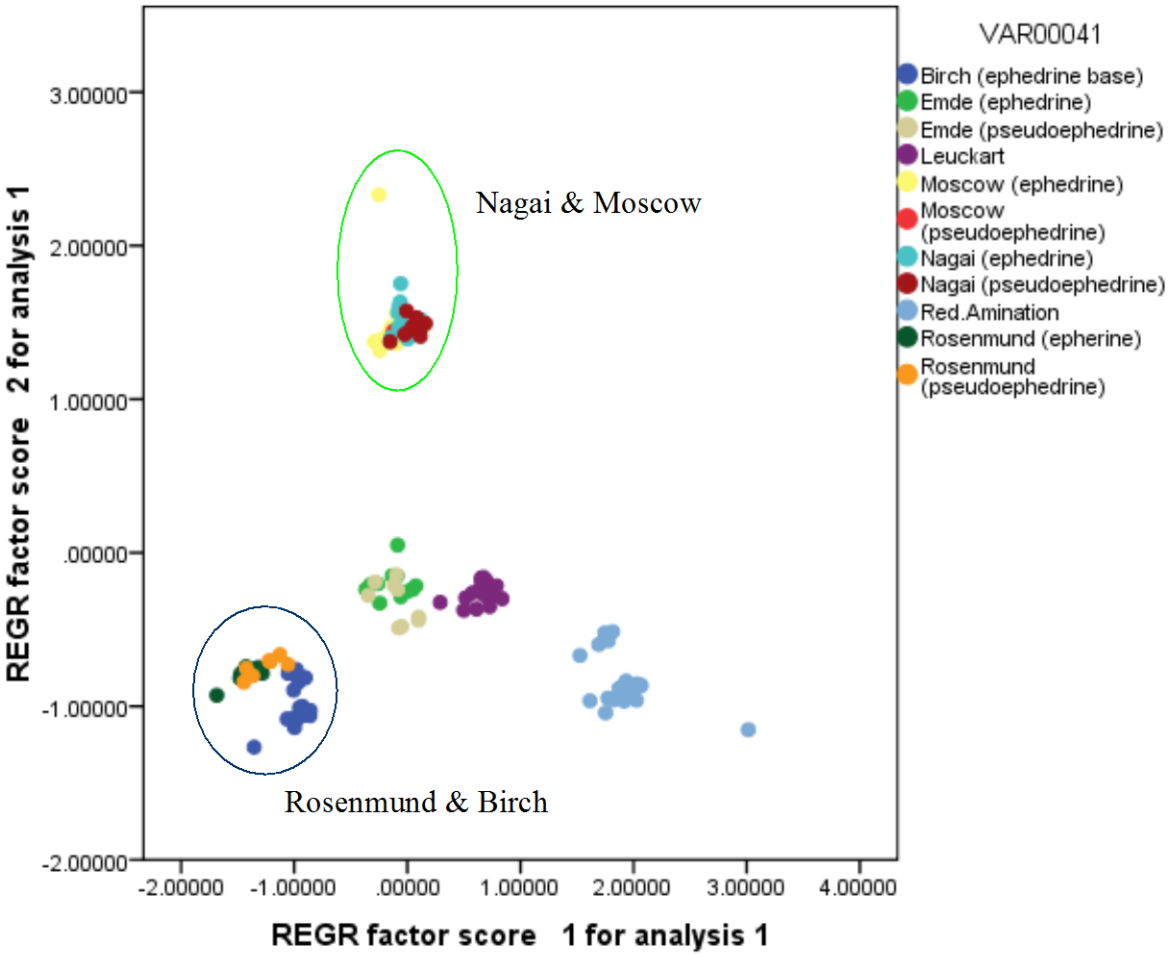

Figure 163: Scores plot for the first two PCs of the GCMS (CHAMP impurities, norm to the sum, sixteenth root) and ICPMS data for all synthesised methylamphetamine samples.

(10) GCMS (Target impurities from this study, norm to the sum, sixteenth root) + ICPMS data

Six principal components had eigenvalues greater than one and accounted for 89.4% of the total variance in the data. PC1 and PC2 accounted for 45.2% of the total variance. A plot of PC1 and PC2 did not show discrimination for Nagai and Moscow samples (Figure 164).

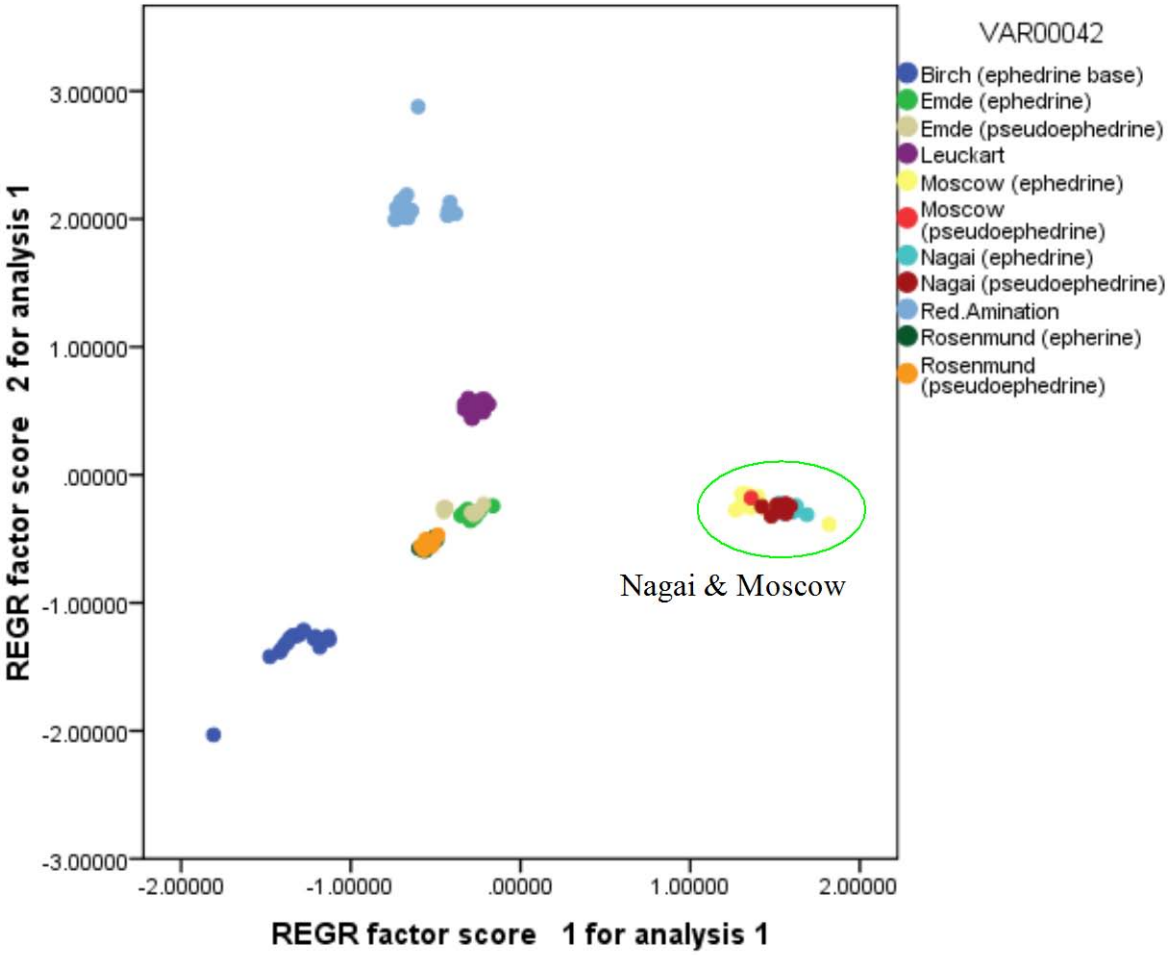

Figure 164: Scores plot for the first two PCs of the GCMS (Target impurities from this study, norm to the sum, sixteenth root) and ICPMS data for all synthesised methylamphetamine samples.

(11) GCMS (CHAMP impurities plus target impurities from this study, norm to the sum, sixteenth root) + ICPMS data

Six principal components had eigenvalues greater than one, and accounted for 91.3% of the total variance in the data. PC1 and PC2 accounted for 47.8% of the total variance. Again the Nagai and Moscow samples could not be distinguished from each other (Figure 165).

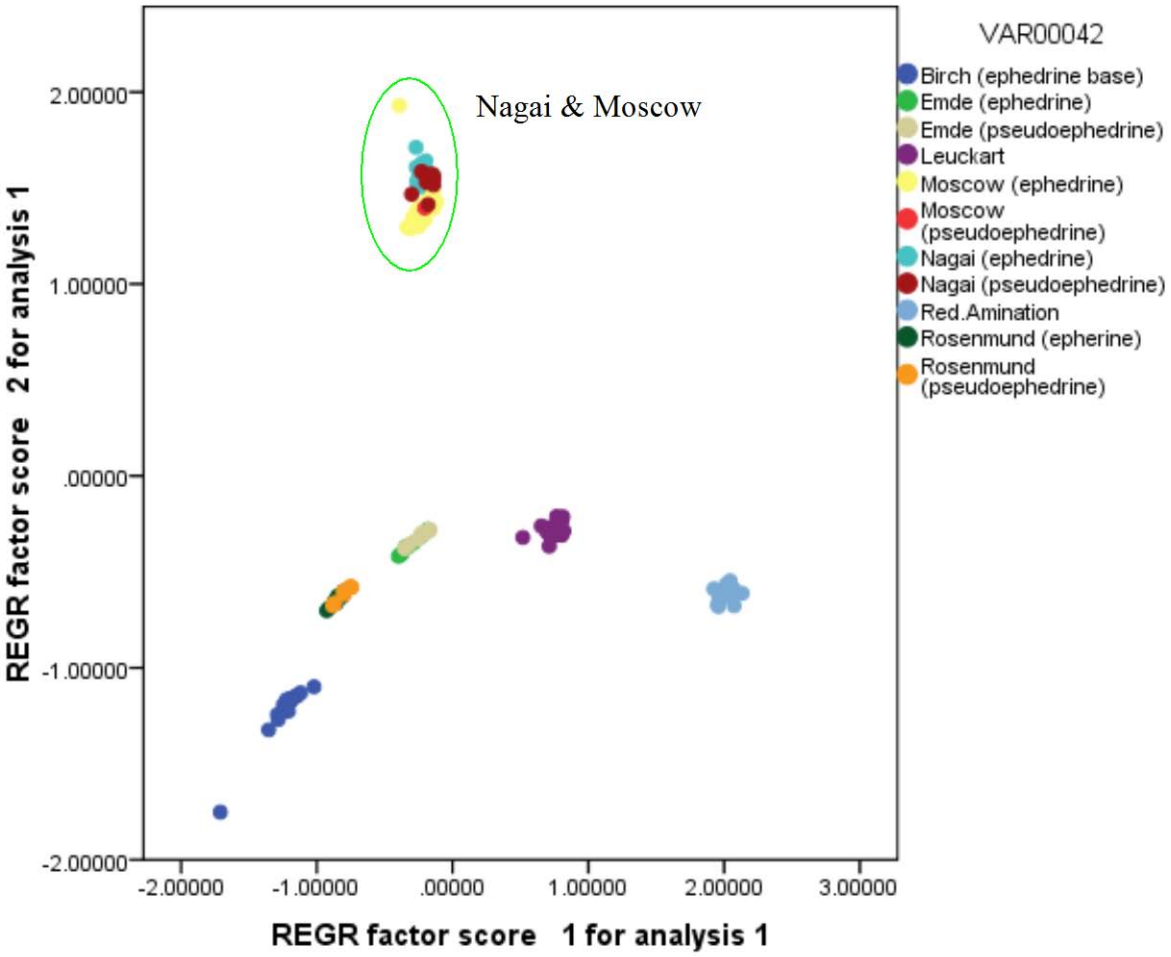

Figure 165: Scores plot for the first two PCs of the GCMS (CHAMP impurities plus target impurities from this study, norm to the sum, sixteenth root) and ICPMS data for all synthesised methylamphetamine samples.

(12) IRMS + ICPMS data

Three principal components had eigenvalues greater than one, and accounted for 62.7% of the total variance in the data. PC1 and PC2 accounted for 45.0% of the total variance. A plot of PC1 and PC2 discriminate the samples by starting material (P-2-P and ephedrine/*pseudo*ephderine) used during methylamphetamine synthesis (Figure 166).

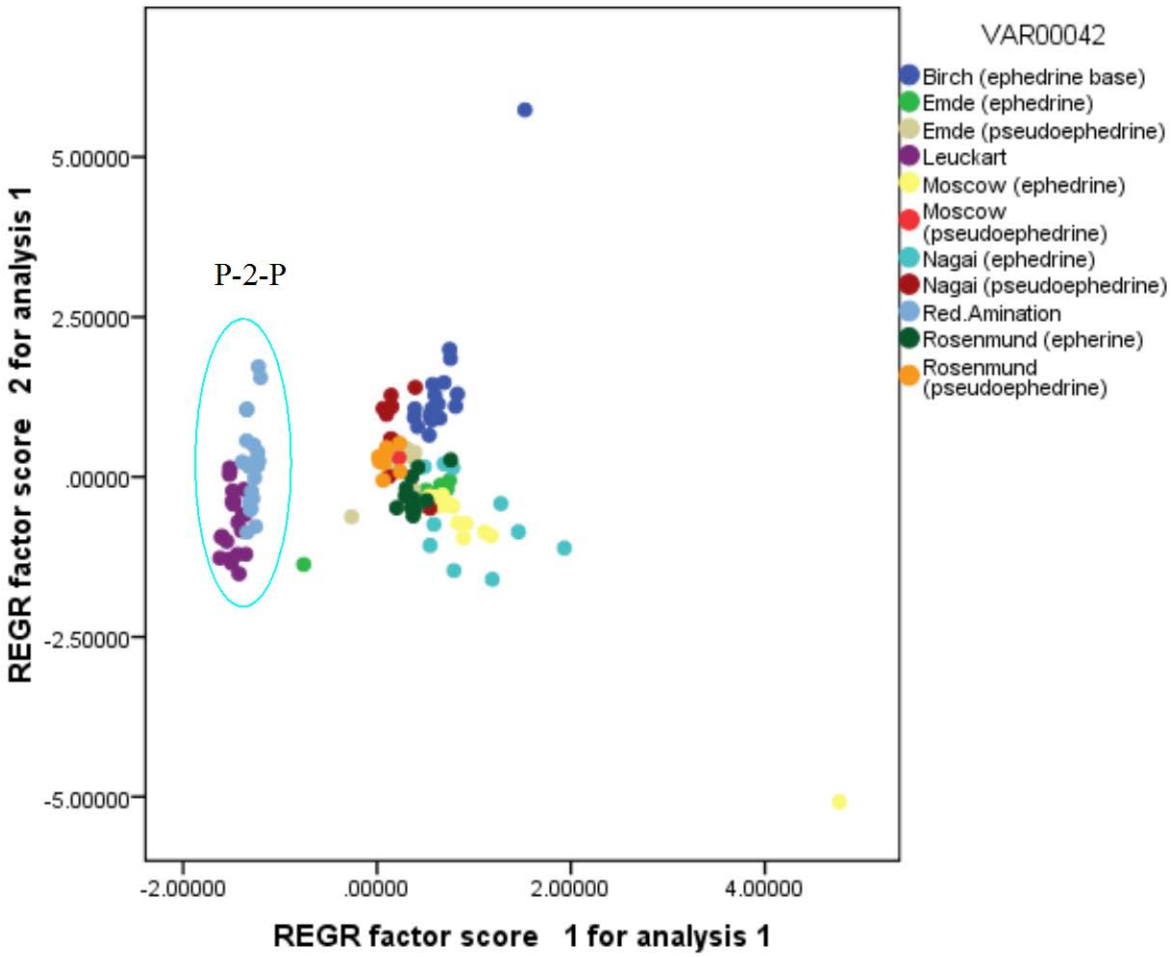

Figure 166: Scores plot for the first two PCs of the IRMS and ICPMS data for all synthesised methylamphetamine samples.

(13) GCMS (CHAMP impurities, norm to the sum, sixteenth root) + IRMS + ICPMS data

Five principal components had eigenvalues greater than one, and accounted for 85.7% of the total variance in the data. PC1 and PC2 accounted for 52.5% of the total variance. In this case no discrimination was possible for Nagai, Moscow, Rosenmund and Birch samples (Figure 167).

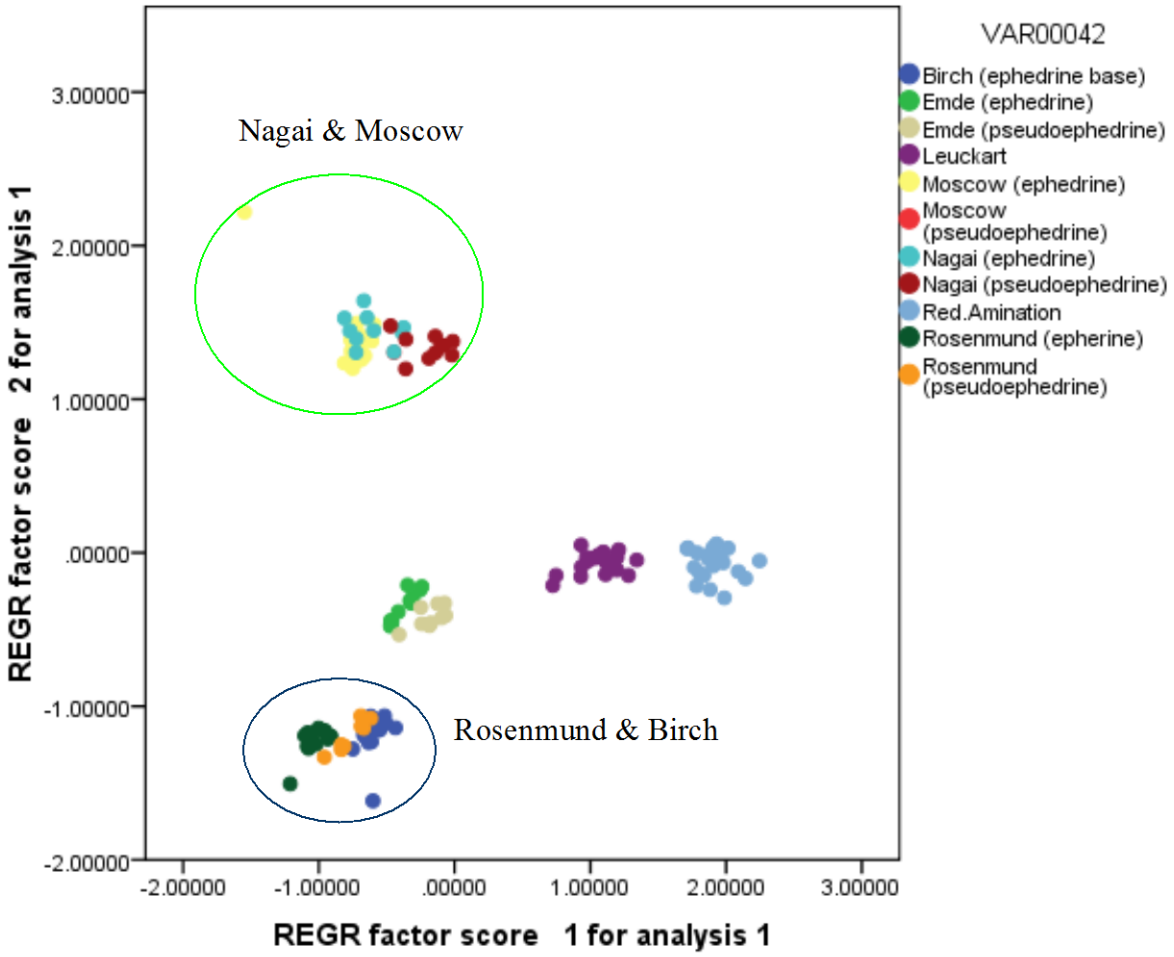

Figure 167: Scores plot for the first two PCs of the GCMS (CHAMP impurities norm to the sum, sixteen roots), IRMS and ICPMS data for all synthesised methylamphetamine samples.

(14) GCMS (Target impurities from this study, norm to the sum, sixteenth root) + IRMS + ICPMS data

Seven principal components have eigenvalues greater than one, and accounted for 91.0% of the total variance in the data. A 3-D (Figure 168) plot afforded better discrimination of the samples than PC1 vs PC2 alone. PC1, PC2 and PC3 accounted for 62.3% of the total variance. However, a plot of PC1, PC2 and PC3 again did not allow discrimination between Nagai and Moscow samples.

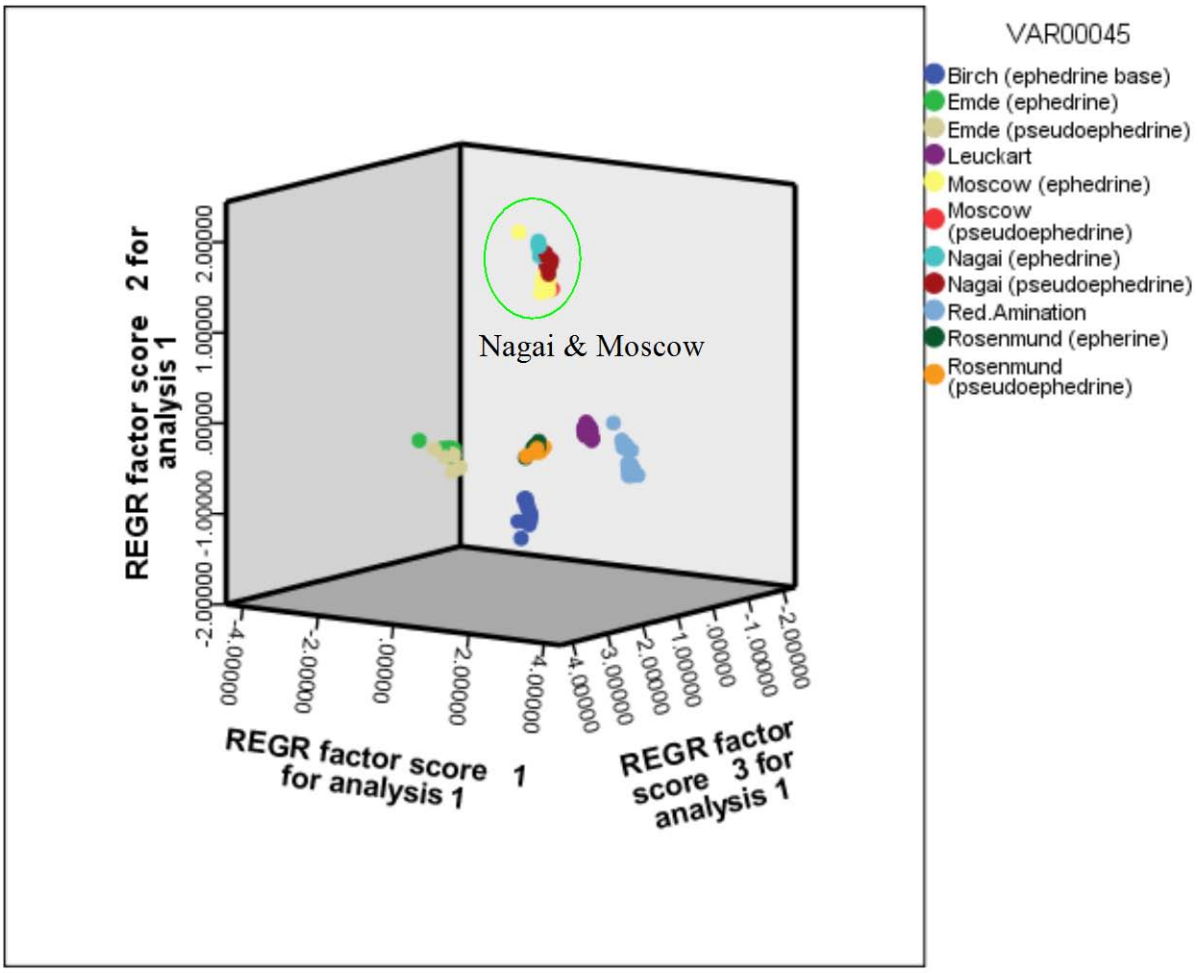

Figure 168: 3-D scores plot for the first three PCs of the GCMS (Target impurities from this study), IRMS and ICPMS data for all synthesised methylamphetamine samples.

(15) GCMS (CHAMP impurities plus target impurities from this study, norm to the sum, sixteenth root) + IRMS + ICPMS data

Six principal components had eigenvalues greater than one, and accounted for 90.4% of the total variance in the data. PC1 and PC2 accounted for 49.2% of the total variance however they could not discriminate between the Nagai and Moscow samples (Figure 169).

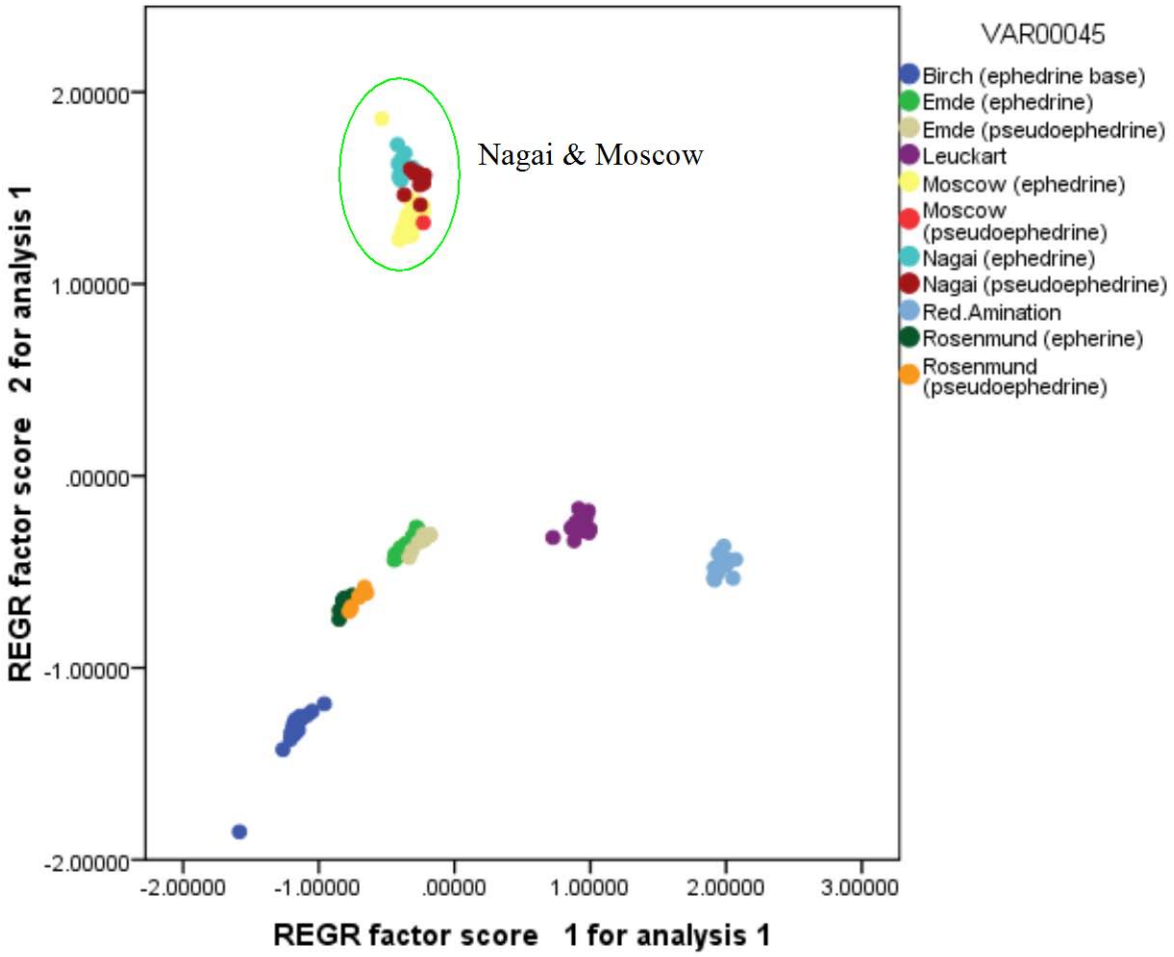

Figure 169: Scores plot for the first two PCs of the GCMS (CHAMP impurities plus target impurities from this study, norm to the sum, sixteen roots), IRMS and ICPMS data for all synthesised methylamphetamine samples.

Examination of the highest loading variables for the first two or three PCs of each data set reveals several GCMS impurities which seem to be important for discrimination of the data. These impurities are summarised in Table 65 – Table 67.

Data set	PC1	Loading
2	*N*-methyldiphenethylamine	0.908
	2,6-Dimethyl-3,5-diphenylpyridine	0.902
	Dibenzylketone	0.900
	N-methyl-*N*-(1-methyl-2-phenylethyl)-2-phenylacetamide	0.900
3	2,6-Dimethyl-3,5-diphenylpyridine	0.906
	Dibenzylketone	0.904
	N-methyl-*N*-(1-methyl-2-phenylethyl)-2-phenylacetamide	0.904
7	*N*-methyldiphenethylamine	0.937
	2,6-Dimethyl-3,5-diphenylpyridine	0.932
	Dibenzylketone	0.930
	Pyridine 7 and 14	0.930
	N-methyl-*N*-(1-methyl-2-phenylethyl)-2-phenylacetamide	0.930
8	2,6-Dimethyl-3,5-diphenylpyridine	0.938
	Pyridine 7 and 14	0.936
	N-methyl-*N*-(1-methyl-2-phenylethyl)-2-phenylacetamide	0.936
	Dibenzylketone	0.936
10	Benzylmethnaphthalene	0.944
	(Z)-N-methyl-N-(α-methylphenethyl) amino-1-phenyl-2-propanone	0.943
	Dimethylphenylnaphthalene	0.942
11	*N*-methyldiphenethylamine	0.876
	2,6-Dimethyl-3,5-diphenylpyridine	0.871
	Dibenzylketone	0.869
	N-methyl-*N*-(1-methyl-2-phenylethyl)-2-phenylacetamide	0.869
14	*N*-methyldiphenethylamine	0.901
	2,6-Dimethyl-3,5-diphenylpyridine	0.897
	Dibenzylketone	0.895
	Pyridine 7 and 14	0.895
	N-methyl-*N*-(1-methyl-2-phenylethyl)-2-phenylacetamide	0.895
15	*N*-methyldiphenethylamine	0.917
	2,6-Dimethyl-3,5-diphenylpyridine	0.912
	N-methyl-*N*-(1-methyl-2-phenylethyl)-2-phenylacetamide	0.911

Table 65: Details of the three highest variables (or > 0.80) on PC1 for each of the eight data sets that gave some degree of discrimination. Data set 8 discriminated between all seven synthetic routes.

Data set	PC2	Loading
2	Benzylmethnaphthalene	0.935
	(Z)-N-methyl-N-(α-methylphenethyl) amino-1-phenyl-2-propanone	0.934
	Dimethylphenylnaphthalene	0.933
3	Benzylmethnaphthalene	0.932
	(Z)-N-methyl-N-(α-methylphenethyl) amino-1-phenyl-2-propanone	0.932
	Dimethylphenylnaphthalene	0.931
7	Benzylmethnaphthalene	0.925
	Dimethylphenylnaphthalene	0.922
	(Z)-N-methyl-N-(α-methylphenethyl) amino-1-phenyl-2-propanone	0.922
8	Benzylmethnaphthalene	0.919
	(Z)-N-methyl-N-(α-methylphenethyl) amino-1-phenyl-2-propanone	0.917
	Dimethylphenylnaphthalene	0.916
10	1-phenyl-2-propanol	0.856
	2,6-Dimethyl-3,5-diphenylpyridine	0.83
	Dibenzylketone	0.829
11	Benzylmethnaphthalene	0.956
	(Z)-N-methyl-N-(α-methylphenethyl) amino-1-phenyl-2-propanone	0.955
	Dimethylphenylnaphthalene	0.954
14	Benzylmethnaphthalene	0.938
	(Z)-N-methyl-N-(α-methylphenethyl) amino-1-phenyl-2-propanone	0.936
	Dimethylphenylnaphthalene	0.935
15	Benzylmethnaphthalene	0.943
	(Z)-N-methyl-N-(α-methylphenethyl) amino-1-phenyl-2-propanone	0.942
	Dimethylphenylnaphthalene	0.94
	(E)-N-methyl-N-(α-methylphenethyl) amino-1-phenyl-2-propanone	0.94

Table 66: Details of the three highest variables (or > 0.80) on PC2 for each of the eight data sets that gave some degree of discrimination. Data set 8 discriminated between all seven synthetic routes.

The eight data sets which provided some discrimination by plots of PC1 and PC2, as discussed previously, all have 2,6-Dimethyl-3,5-diphenylpyridine, pyridine 7 and 14, dimethylphenylnaphthalene, benzylmethnaphthalene, *(Z)-N*-methyl-N-(α-methylphenethyl) amino-1-phenyl-2-propanone and *(E)-N*-methyl-N-(α-methylphenethyl) amino-1-phenyl-2-propanone as high loading variables on PC1 or PC2. Thus, it appears that these are particularly important for discriminating methylamphetamine samples by synthetic route using GCMS data.

Data set	PC3	Loading
2	*(E)*-α,α-dimethyldiphenethylamine	0.945
	(E)-*N*,α,α-trimethyldiphenethylamine	0.945
	(Z)-α,α-dimethyldiphenethylamine	0.944
	(Z)-*N*,α,α-trimethyldiphenethylamine	0.944
3	Unknown 4	0.958
	Chloroephedrine	0.958
	Methylamphetamine dimer	0.958
7	Unknown 4	0.952
	Chloroephedrine	0.952
	cis-aziridine	0.951
	Methylamphetamine dimer	0.951
8	Methylamphetamine dimer	0.955
	Unknown 4	0.954
	Chloroephedrine	0.954
10	Unknown 4	0.971
	cis-aziridine	0.971
	Chloroephedrine	0.97
11	*cis*-aziridine	0.976
	Unknown 4	0.975
	Chloroephedrine	0.975
14	*cis*-aziridine	0.967
	Unknown 4	0.967
	Chloroephedrine	0.967
15	*cis*-aziridine	0.973
	Unknown 4	0.973
	Chloroephedrine	0.973

Table 67: Details of the three highest variables (or > 0.80) on PC3 for each of the eight data sets that gave some degree of discrimination. Data set 8 discriminated between all seven synthetic routes.

Impurities which appear in seven of the eight data sets as high loading variables on PC3 are: unknown 4, chloroephedrine and methylamphetamine dimer. It appears that these impurities also play an important role in the discrimination of methylamphetamine by synthetic route using GCMS data.

8.2.3 PCA Conclusions

The 15 different data sets were subjected to PCA in order to reduce the dimensionality of the data so that a simple plot of the first two or three principal components could be examined in order to investigate clustering of the data. For seven of these data sets five synthetic groups could be discriminated relatively easily but separation of the Nagai and Moscow route samples was not possible. This is not surprising since their synthesis is very similar. Addition of PC3 was required for three of the data sets for better discrimination. In one case (GCMS with target impurities from this study, normalised to the sum, sixteenth root in combination with the IRMS data) facilitated discrimination into all synthetic routes. In all cases the target impurities identified by this study were required for any synthetic variation to be observed.

Secondly, six GCMS impurities were identified as having the highest loadings on PC1 and PC2 for the six data sets successfully clustered by synthetic route, indicating that these impurities are important for the discrimination of the batches by synthetic route. These impurities are: 2,6-Dimethyl-3,5-diphenylpyridine, pyridine 7 and 14, dimethylphenylnaphthalene, benzylmethnaphthalene, *(Z)*-*N*-methyl-N-(α-methylphenethyl) amino-1-phenyl-2-propanone and *(E)*-*N*-methyl-N-(α-methylphenethyl) amino-1-phenyl-2-propanone. In the two data sets which required the addition of PC3, three additional impurities were identified as having the highest loadings. These impurities are: unknown 4, chloroephedrine and methylamphetamine dimer, which facilitated the further discrimination of methylamphetamine between the Rosenmund and Emde route.

Thirdly, a plot of PC1 and PC2 for the IRMS data set alone allowed discrimination only between the starting materials P-2-P and ephedrine/*pseudo*ephderine used during methylamphetamine synthesis.

Lastly, when the ICPMS data was included, there is no indication of the contribution of the inorganic impurities in the discriminant functions by synthetic route and starting material.

8.3 Discriminant Analysis (DA)

Discriminant analysis is a method of supervised pattern recognition.[1, 4, 8, 12] This differs from unsupervised methods such as HCA in that the number of parent groups of the samples is known in advance, and representatives from these groups are available. Representatives of the samples act as a training set and are used to obtain one or more classification rules (or discriminant functions) which discriminate between the training set samples as accurately as possible. The discriminant functions can be generated by one of the two methods; enter independents together or use stepwise method. The discriminant function is then tested by one of several methods:[4, 8]

1. an independent set of samples not included in the training set:
2. the training set itself; and
3. the ‘leave one out’ method.

While the use of an independent set of samples is the obvious choice for validating the discriminant function, it is not always practical due to the size of the data set available. Splitting the data set into training and testing subsets is a possibility, but reducing the number of samples used for the development of the discriminant function(s) will likely lead to a less robust routine.[1, 8]

Using a training set for validation is a common option for overcoming this problem. With this option, the discriminant function is developed using the full training set, and then each item of the set is classified by the discriminant function as if it were an unknown sample. It is important to note that unless the number of samples is greater than about ten times the number of variables, the error rate of this method is biased low.[1, 4, 8]

Another option for validation of the discriminant function(s) is the ‘leave one out’ method. All samples apart from one are used to develop the discriminant function, and the excluded sample is used to test it. This process is reiterated until all samples have been excluded once and used for validation.[1] With this method, a discriminant function is derived for each scenario, so the analysis time can be relatively long.

Secondly, the error rate for this method is based on the average of all the discriminant function and may not be relevant for the particular rule that is applied to an unclassified sample.[8]

A method of assessing the overall significance of a discriminant analysis routine is the Wilks' λ test statistic.[1] The null hypothesis, H_0, states that the discrimination model is not viable; the alternative hypothesis, H_1, states that it is. Wilks' λ is defined as:

$$\lambda = \frac{SS_{(\text{within group})}}{SS_{\text{Total}}} \quad \text{.....Equation 8.2}$$

where SS stands for the sum of the squares.

In the stepwise selection method, Wilks' λ is used to determine whether adding a variable to the model will significantly improve classification. At each step, the variable that has the smallest Wilks' λ is entered into the system.[1]

As with the principal component analysis discussed in Section 8.2, DA seeks to identify linear combinations of the variables which explain the variance in the data. The derived discriminant functions take on the following form:[4]

$$Y = \alpha_1 X_1 + \alpha_2 X_2 + \ldots + \alpha_n X_n \quad \text{.....Equation 8.3}$$

where α_1 to α_n represent the coefficients for each of the original variables (X_1 to X_n).[1] The coefficients of the discriminant function are chosen such that Y best reflects the differences between the parent groups; thus, items assigned to group one will have similar Y values, and items assigned to group two will have similar Y values (but different from group one), and so forth.[4] Once the disrimination functions are derived, it is possible to identify the relative importance of the variables in predicting the parent groups by examining the magnitude of the discriminant function coefficients; that is, variables with largest coefficients contribute most to the prediction of group membership.[4, 8] The sign of the coefficient indicates the relationship.[13]

8.3.1 DA Experimental

For this project, disriminant analysis was performed with SPSS software version 17.0. Variables were selected using a stepwise method (i.e. they were entered or removed one at a time on the basis of a statistic). The Wilks' λ statistic was used to qualify a variable for entry or removal from the discriminant function. Validation of the discriminant functions was undertaken using the training set.

Discriminant analysis (DA) was undertaken on the same 15 data sets used for PCA (see the beginning of this chapter). Because DA requires the operator to specify a number of parent groups before the analysis can be undertaken, each data set was analysed three times using different parent groupings: four groups according to starting material, seven groups according to synthetic route, and 11 groups according to 'lab output', as defined in Table 64.

The coefficients in the discriminant functions of the data sets which allowed 100% accurate discrimination by DA were assessed in order to identify the relative importance of the variables in predicting the parent groups.

8.3.2 DA Results and Discussion

Because DA is a supervised pattern recognition technique, it was applied three times to each of the 15 data sets: once using four specified parent groupings (seeking discrimination by starting material), once using seven parent groupings (seeking discrimination by synthetic route), and once using 11 specified parent groupings (seeking discrimination by 'lab output'). The results will be discussed according to the level of discrimination sought.

8.3.2.1 Classification by Staring Material

For discrimination of samples according to starting material used, DA achieved 100% accuracy in five of the 15 data sets (Table 68). The successful data sets included: IRMS data in combination of GCMS data alone (CHAMP impurity list alone or with target impurity list from this study) or together with ICPMS data.

Data Set	**100% Accuracy**	**<100% Accuracy**
GCMS (CHAMP impurities, norm to the sum, sixteenth root)		X (81.8%)
GCMS (Target impurities from this study, norm to the sum, sixteenth root)		X (76.2%)
GCMS (CHAMP impurities plus target impurities from this study, norm to the sum, sixteenth root)		X (81.1%)
IRMS data		X (99.3%)
ICPMS data		X (61.5%)
GCMS (CHAMP impurities, norm to the sum, sixteenth root) + IRMS	X	
GCMS (Target impurities from this study, norm to the sum, sixteenth root) + IRMS		X (97.9%)
GCMS (CHAMP impurities plus target impurities from this study, norm to the sum, sixteenth root) + IRMS	X	
GCMS (CHAMP impurities, norm to the sum, sixteenth root) + ICPMS		X (80.4%)
GCMS (Target impurities from this study, norm to the sum, sixteenth root) + ICPMS		X (76.2%)
GCMS (CHAMP impurities plus target impurities from this study, norm to the sum, sixteenth root) + ICPMS		X (81.1%)
IRMS + ICPMS		X (99.3%)
GCMS (CHAMP impurities, norm to the sum, sixteenth root) + IRMS + ICPMS	X	
GCMS (Target impurities from this study, norm to the sum, sixteenth root) + IRMS + ICPMS	X	
GCMS (CHAMP impurities plus target impurities from this study, norm to the sum, sixteenth root) + IRMS + ICPMS	X	

Table 68: Summary of the accuracy of the DA classification for the 15 data sets. Grouping according to starting material (four cluster) was specified.

The 10 data sets in Table 68 which failed to achieve 100% classification through DA misclassified one or more of the methylamphetamine samples synthesised either by *pseudo*ephedrine and ephedrine. Since the two starting materials are diastereomers, they could potentially have been classified within same group; however discrimination was achieved when GCMS data was included with the IRMS data.

A summary of the variables with the highest discriminant function coefficients for the five successfully classified data sets are displayed in Table 69 – Table 71. (Since four parent groupings were specified for discrimination by starting material, three discrimination functions, df1-df3 were constructed.)

Data set	df1	Loading
6	Ephedrone	2.811
	Benzylmethnaphthalene	2.513
	(*Z*)-*N*-methyl-*N*-(α-methylphenethyl)-3-phenylpropenamide	1.164
8	1-phenyl-2-propanol	8.33
	(E)-α,α-dimethyldiphenethylamine	7.843
	$\delta^{13}C$	-0.88
13	Ephedrone	2.811
	Benzylmethnaphthalene	2.513
	(*Z*)-*N*-methyl-*N*-(α-methylphenethyl)-3-phenylpropenamide	1.164
14	1-phenyl-2-propanol	9.789
	(Z)-N,α,α-trimethyldiphenethylamine	6.426
	(Z)-α,α-dimethyldiphenethylamine	2.731
15	1-phenyl-2-propanol	8.33
	(E)-α,α-dimethyldiphenethylamine	7.843
	$\delta^{13}C$	-0.88

Table 69: A summary of the highest coefficients on the discriminant function (df1) for classification of methylamphetamine by starting material used. Only the data sets for which DA achieved 100% accuracy are included.

Data set	df2	Loading
6	*cis*-aziridine	2.757
	Benzylmethnaphthalene	2.642
	cis 3,4-Diphenyl-3-buten-2-one	2.182
8	*(E)*-α,α-dimethyldiphenethylamine	2.364
	1-phenyl-2-propanol	2.303
	Unknown 3	1.055
13	*cis*-aziridine	2.757
	Benzylmethnaphthalene	2.642
	cis 3,4-Diphenyl-3-buten-2-one	2.182
14	1-phenyl-2-propanol	2.645
	(Z)-N,α,α-trimethyldiphenethylamine	1.603
	(Z)-α,α-dimethyldiphenethylamine	1.243
15	*(E)*-α,α-dimethyldiphenethylamine	2.364
	1-phenyl-2-propanol	2.303
	Unknown 3	1.055

Table 70: A summary of the highest coefficients on the discriminant function (df2) for classification of methylamphetamine by starting material used. Only the data sets for which DA achieved 100% accuracy are included.

Data set	df3	Loading
6	Dimethylphenylnaphthalene	6.992
	Benzylmethnaphthalene	-6.574
	Ephedrone	3.068
8	*(E)*-α,α-dimethyldiphenethylamine	1.886
	$\delta^{13}C$	1.782
	1-phenyl-2-propanol	1.059
13	Dimethylphenylnaphthalene	6.992
	Benzylmethnaphthalene	6.574
	Ephedrone	3.068
14	*(Z)*-α,α-dimethyldiphenethylamine	2.938
	$\delta^{13}C$	2.095
	(Z)-N,α,α-trimethyldiphenethylamine	-0.933
15	*(E)*-α,α-dimethyldiphenethylamine	0.662
	$\delta^{13}C$	-0.631
	1-phenyl-2-propanol	-0.607

Table 71: A summary of the highest coefficients on the discriminant function (df3) for classification of methylamphetamine by starting material used. Only the data sets for which DA achieved 100% accuracy are included.

It is clear from Table 69 – Table 71 that, for the IRMS data, $\delta^{13}C$ drives the successful discrimination of the methylamphetamine samples by starting material. This is unsurprising since 10 of the 11 carbon atoms on the final methylamphetamine molecule via P-2-P route are contributed by the starting material and all 11 carbon atoms on the final methylamphetamine molecule via ephedrine/*pseudo*ephedrine route

are contributed by the starting material. It should however, be noted that 100% accurate classification by the starting material was not achievable with IRMS data on its own.

Assessment of the GCMS impurities demonstrated that the CHAMP impurity list was preferred. For the data sets involving the CHAMP list of impurities, the impurities which appeared frequently with high coefficients were: *cis*-aziridine, Ephedrone, Dimethylphenylnaphthalene, Benzylmethnaphthalene and (*Z*)-*N*-methyl-*N*-(α-methylphenethyl)-3-phenylpropenamide.

The five impurities discussed above which appear frequently in the discriminant functions with high coefficients, are not present in high coefficients in the target impurity list from this study. The discriminant functions built around the target impurities from this study included *(Z)*-α,α-dimethyldiphenethylamine , *(E)*-α,α-dimethyldiphenethylamine, *(Z)-N*,α,α-trimethyldiphenethylamine, 1-phenyl-2-propanol and Unknown 3. It is also notable that when the ICPMS data was included, no indication of the contribution of the inorganic impurities in the discriminant functions was evident.

8.3.2.2 Classification by Synthetic Route

For discrimination of samples according to synthetic route used, DA achieved 100% accuracy in 10 of the 15 data sets (Table 72). It appears that the target impurity list from this study was important to the ability of DA to successfully classify the methylamphetamine by synthetic route. DA was only able to classify by synthetic route using the GCMS (CHAMP list) data when in the presence of the IRMS data whereas the target impurities identified in this work always achieved 100% accurate discrimination either on their own or in combination with other data.

Data Set	**100% Accuracy**	**<100% Accuracy**
GCMS (CHAMP impurities, norm to the sum, sixteenth root)		X (97.2%)
GCMS (Target impurities from this study, norm to the sum, sixteenth root)	X	
GCMS (CHAMP impurities plus target impurities from this study, norm to the sum, sixteenth root)	X	
IRMS data		X (75.5%)
ICPMS data		X (61.5%)
GCMS (CHAMP impurities, norm to the sum, sixteenth root) + IRMS	X	
GCMS (Target impurities from this study, norm to the sum, sixteenth root) + IRMS	X	
GCMS (CHAMP impurities plus target impurities from this study, norm to the sum, sixteenth root) + IRMS	X	
GCMS (CHAMP impurities, norm to the sum, sixteenth root) + ICPMS		X (97.2%)
GCMS (Target impurities from this study, norm to the sum, sixteenth root) + ICPMS	X	
GCMS (CHAMP impurities plus target impurities from this study, norm to the sum, sixteenth root) + ICPMS	X	
IRMS + ICPMS		X (85.3%)
GCMS (CHAMP impurities, norm to the sum, sixteenth root) + IRMS + ICPMS	X	
GCMS (Target impurities from this study, norm to the sum, sixteenth root) + IRMS + ICPMS	X	
GCMS (CHAMP impurities plus target impurities from this study, norm to the sum, sixteenth root) + IRMS + ICPMS	X	

Table 72: Summary of the accuracy of the DA classification for the 15 data sets. Grouping according to synthetic route (seven cluster) was specified.

The discriminant function coefficients were examined for the 10 data sets which achieved 100% accurate classification. A summary of the variables with the three highest coefficients for the six discriminant functions generated are displayed in Tables 73 – Table 78. (Since seven parent groupings were specified for discrimination by synthetic route, six discriminant functions, df1- df6 were constructed.)

Data set	df1	Loading
2	*cis*-aziridine	1.298
	Ephedrine	1.286
	Ephedrone	0.532
3	*cis*-aziridine	1.028
	Chloroephedrine	0.697
	Ephedrine	0.68
6	Benzylmethnaphthalene	0.774
	(*Z*)-*N*-methyl-*N*-(α-methylphenethyl)-3-phenylpropenamide	0.742
	cis-aziridine	-0.488
7	*cis*-aziridine	1.298
	Ephedrine	1.286
	Ephedrone	0.532
8	*cis*-aziridine	1.028
	Chloroephedrine	0.697
	Ephedrine	0.68
10	*cis*-aziridine	1.298
	Ephedrine	1.286
	Ephedrone	0.532
11	*cis*-aziridine	1.028
	Chloroephedrine	0.697
	Ephedrine	0.68
13	Benzylmethnaphthalene	0.774
	(*Z*)-*N*-methyl-*N*-(α-methylphenethyl)-3-phenylpropenamide	0.742
	cis-aziridine	-0.488
14	*cis*-aziridine	1.298
	Ephedrine	1.286
	Ephedrone	0.532
15	*cis*-aziridine	1.028
	Chloroephedrine	0.697
	Ephedrine	0.68

Table 73: A summary of the highest coefficients on the discriminant function (df1) for classification of methylamphetamine by synthetic route used. Only the data sets for which DA achieved 100% accuracy are included.

Data set	df2	Loading
2	Benzylmethnaphthalene	0.678
	(*Z*)-*N*-methyl-*N*-(α-methylphenethyl)-3-phenylpropenamide	0.544
	Pyridine 7 and 14	-0.525
3	Benzylmethnaphthalene	0.616
	Pyridine 7 and 14	-0.571
	(*Z*)-*N*-methyl-*N*-(α-methylphenethyl)-3-phenylpropenamide	0.504
6	Pyridine 7 and 14	-0.647
	2,6-Dimethyl-3,5-diphenylpyridine	-0.564
	cis-aziridine	0.522
7	Benzylmethnaphthalene	0.678
	(*Z*)-*N*-methyl-*N*-(α-methylphenethyl)-3-phenylpropenamide	0.544
	Pyridine 7 and 14	-0.525
8	Benzylmethnaphthalene	0.616
	Pyridine 7 and 14	-0.571
	(*Z*)-*N*-methyl-*N*-(α-methylphenethyl)-3-phenylpropenamide	0.504
10	Benzylmethnaphthalene	0.678
	(*Z*)-*N*-methyl-*N*-(α-methylphenethyl)-3-phenylpropenamide	0.544
	Pyridine 7 and 14	-0.525
11	Benzylmethnaphthalene	0.616
	Pyridine 7 and 14	-0.571
	(*Z*)-*N*-methyl-*N*-(α-methylphenethyl)-3-phenylpropenamide	0.504
13	Pyridine 7 and 14	-0.647
	2,6-Dimethyl-3,5-diphenylpyridine	-0.564
	cis-aziridine	0.522
14	Benzylmethnaphthalene	0.678
	(*Z*)-*N*-methyl-*N*-(α-methylphenethyl)-3-phenylpropenamide	0.544
	Pyridine 7 and 14	-0.525
15	Benzylmethnaphthalene	0.616
	Pyridine 7 and 14	-0.571
	(*Z*)-*N*-methyl-*N*-(α-methylphenethyl)-3-phenylpropenamide	0.504

Table 74: A summary of the highest coefficients on the discriminant function (df2) for classification of methylamphetamine by synthetic route used. Only the data sets for which DA achieved 100% accuracy are included.

Data set	df3	Loading
2	Chloroephedrine	0.647
	cis-aziridine	0.584
	Unknown 3	-0.519
3	Unknown 3	-0.789
	cis-aziridine	0.472
	Chloroephedrine	0.438
6	*cis*-aziridine	0.884
	N-benzoylmethamphetamine	0.718
	Benzylmethnaphthalene	0.546
7	Chloroephedrine	0.647
	cis-aziridine	0.584
	Unknown 3	-0.519
8	Unknown 3	-0.789
	cis-aziridine	0.472
	Chloroephedrine	0.438
10	Chloroephedrine	0.647
	cis-aziridine	0.584
	Unknown 3	-0.519
11	Unknown 3	-0.789
	cis-aziridine	0.472
	Chloroephedrine	0.438
13	*cis*-aziridine	0.884
	N-benzoylmethamphetamine	0.718
	Benzylmethnaphthalene	0.546
14	Chloroephedrine	0.647
	cis-aziridine	0.584
	Unknown 3	-0.519
15	Unknown 3	-0.789
	cis-aziridine	0.472
	Chloroephedrine	0.438

Table 75: A summary of the highest coefficients on the discriminant function (df3) for classification of methylamphetamine by synthetic route used. Only the data sets for which DA achieved 100% accuracy are included.

Data set	df4	Loading
2	Unknown 3	0.807
	Unknown 1	-0.634
	Ephedrone	-0.432
3	Unknown 3	0.662
	N-acetylmethamphetamine	-0.631
	Unknown 2	-0.607
6	*(E)*-*N*,α,α-trimethyldiphenethylamine	0.749
	2,6-Dimethyl-3,5-diphenylpyridine	-0.57
	(Z)-α,α–dimethyldiphenethylamine	0.55
7	Unknown 3	0.807
	Unknown 1	-0.634
	Ephedrone	-0.432
8	Unknown 3	0.662
	N-acetylmethamphetamine	-0.631
	Unknown 2	-0.607
10	Unknown 3	0.807
	Unknown 1	-0.634
	Ephedrone	-0.432
11	Unknown 3	0.662
	N-acetylmethamphetamine	-0.631
	Unknown 2	-0.607
13	*(E)*-*N*,α,α-trimethyldiphenethylamine	0.749
	2,6-Dimethyl-3,5-diphenylpyridine	-0.57
	(Z)-α,α–dimethyldiphenethylamine	0.55
14	Unknown 3	0.807
	Unknown 1	-0.634
	Ephedrone	-0.432
15	Unknown 3	0.662
	N-acetylmethamphetamine	-0.631
	Unknown 2	-0.607

Table 76: A summary of the highest coefficients on the discriminant function (df4) for classification of methylamphetamine by synthetic route used. Only the data sets for which DA achieved 100% accuracy are included.

Data set	df5	Loading
2	(*E*)-*N*-methyl-*N*-(α-methylphenethyl)-3-phenylpropenamide	0.670
	Unknown 6	-0.642
	N-benzoylamphetamine	0.381
3	Unknown 6	0.703
	(*E*)-*N*-methyl-*N*-(α-methylphenethyl)-3-phenylpropenamide	-0.624
	(*Z*)-*N*-methyl-*N*-(α-methylphenethyl)-3-phenylpropenamide	0.331
6	δ^2H	0.852
	δ^{13}C	-0.728
	N-acetylmethamphetamine	0.631
7	(*E*)-*N*-methyl-*N*-(α-methylphenethyl)-3-phenylpropenamide	0.67
	Unknown 6	-0.642
	N-benzoylamphetamine	0.381
8	Unknown 6	0.703
	(*E*)-*N*-methyl-*N*-(α-methylphenethyl)-3-phenylpropenamide	-0.624
	N-benzoylamphetamine	-0.322
10	(*E*)-*N*-methyl-*N*-(α-methylphenethyl)-3-phenylpropenamide	0.67
	Unknown 6	-0.642
	N-benzoylamphetamine	0.381
11	Unknown 6	0.703
	(*E*)-*N*-methyl-*N*-(α-methylphenethyl)-3-phenylpropenamide	-0.624
	N-benzoylamphetamine	-0.322
13	δ^2H	0.852
	δ^{13}C	-0.728
	N-acetylmethamphetamine	0.631
14	(*E*)-*N*-methyl-*N*-(α-methylphenethyl)-3-phenylpropenamide	0.67
	Unknown 6	-0.642
	N-benzoylamphetamine	0.381
15	Unknown 6	0.703
	(*E*)-*N*-methyl-*N*-(α-methylphenethyl)-3-phenylpropenamide	-0.624
	N-benzoylamphetamine	-0.322

Table 77: A summary of the highest coefficients on the discriminant function (df5) for classification of methylamphetamine by synthetic route used. Only the data sets for which DA achieved 100% accuracy are included.

Data set	df6	Loading
2	*(E)*-*N*,α,α-trimethyldiphenethylamine	0.716
	(Z)-α,α–dimethyldiphenethylamine	0.600
	2,6-Dimethyl-3,5-diphenylpyridine	-0.502
3	*(E)*-*N*,α,α-trimethyldiphenethylamine	0.703
	(Z)-α,α–dimethyldiphenethylamine	0.591
	2,6-Dimethyl-3,5-diphenylpyridine	-0.508
6	Dimethylphenylnaphthalene	-1.547
	Benzylmethnaphthalene	1.467
	$\delta^{15}N$	0.554
7	*(E)*-*N*,α,α-trimethyldiphenethylamine	0.716
	(Z)-α,α–dimethyldiphenethylamine	0.6
	2,6-Dimethyl-3,5-diphenylpyridine	-0.502
8	*(E)*-*N*,α,α-trimethyldiphenethylamine	0.703
	(Z)-α,α–dimethyldiphenethylamine	0.591
	2,6-Dimethyl-3,5-diphenylpyridine	-0.508
10	*(E)*-*N*,α,α-trimethyldiphenethylamine	0.716
	(Z)-α,α–dimethyldiphenethylamine	0.6
	2,6-Dimethyl-3,5-diphenylpyridine	-0.502
11	*(E)*-*N*,α,α-trimethyldiphenethylamine	0.703
	(Z)-α,α–dimethyldiphenethylamine	0.591
	2,6-Dimethyl-3,5-diphenylpyridine	-0.508
13	Dimethylphenylnaphthalene	-1.547
	Benzylmethnaphthalene	1.467
	$\delta^{15}N$	0.554
14	*(E)*-*N*,α,α-trimethyldiphenethylamine	0.716
	(Z)-α,α–dimethyldiphenethylamine	0.6
	2,6-Dimethyl-3,5-diphenylpyridine	-0.502
15	*(E)*-*N*,α,α-trimethyldiphenethylamine	0.703
	(Z)-α,α–dimethyldiphenethylamine	0.591
	2,6-Dimethyl-3,5-diphenylpyridine	-0.508

Table 78: A summary of the highest coefficients on the discriminant function (df6) for classification of methylamphetamine by synthetic route used. Only the data sets for which DA achieved 100% accuracy are included.

The GCMS impurities driving the discrimination by synthetic route will be discussed first in relation to the list of target impurities suggested by this work. A range of target impurities always appear in the discriminant functions for each of the eight data sets. These are Unknown compounds 1, 2, 3 and 6, *(Z)*-α,α–dimethyldiphenethylamine, *(E)*-*N*,α,α-trimethyldiphenethylamine, (*Z*)-*N*-methyl-*N*-(α-methylphenethyl)-3-phenylpropenamide, (*E*)-*N*-methyl-*N*-(α-methylphenethyl)-3-phenylpropenamide, Benzylmethnaphthalene, 2,6-Dimethyl-3,5-diphenylpyridine, Pyridine 7 and 14, Chloroephedrine, Ephedrone, *cis*-aziridine and Ephedrine, indicating that these impurities drive the classification of methylamphetamine samples by synthetic route.

Of these compounds, 10 are present in the CHAMP list; *(Z)*-α,α–dimethyldiphenethylamine, *(E)*-*N*,α,α-trimethyldiphenethylamine, (*Z*)-*N*-methyl-*N*-(α-methylphenethyl)-3-phenylpropenamide, Benzylmethnaphthalene, 2,6-Dimethyl-3,5-diphenylpyridine, Pyridine 7 and 14, Chloroephedrine, Ephedrone, *cis*-aziridine and Ephedrine. It should be noted that discrimination by synthetic route was not achieved with the CHAMP impurity list alone.

In terms of the IRMS data set, $\delta^{13}C$, $\delta^{15}N$, and $\delta^{2}H$ stable isotopes drive discrimination according to the synthetic route. As discussed in the previous section, $\delta^{13}C$, is expected to hold information on the starting material used. It should be noted that this discrimination was achieved in the present of GCMS data. It is also evident from Table 76 that $\delta^{13}C$ and $\delta^{2}H$ appear with high coefficients in the discriminant functions for the data sets utilising a combination of the CHAMP GCMS and IRMS data. This indicates that, when CHAMP GCMS and IRMS data is available for derivation of the discriminant functions, $\delta^{13}C$ and $\delta^{2}H$ are often more useful than the majority of the CHAMP impurities.

Again, when the ICPMS data was included, there is no indication of the contribution of the inorganic impurities in the discriminant functions by synthetic route.

The frequent appearance of, and high coefficients for, 15 of the target impurities in the discriminant functions indicate that they drive the classification of methylamphetamine by synthetic route when the list of impurities suggested by this study is used with or without IRMS or ICPMS data. It should be reiterated, however, that DA of the GCMS data from this study on its own is sufficient for 100% accurate classification by synthetic route.

8.3.2.3 Classification according to 'Lab Output'

The discrimination of samples by 'lab output' is likely to be the most complicated task for DA since it has 11 parent groups in which to classify the samples and requires the classification based on both the starting material and the synthetic route.

For discrimination of samples according to 'lab output', DA failed to achieve 100% accuracy in the any of the 15 data sets (Table 79) and DA could not successfully classify the methylamphetamine by starting material in combination with synthetic route.

Data Set	100% Accuracy	<100% Accuracy
GCMS (CHAMP impurities, norm to the sum, sixteenth root)		X (80.4%)
GCMS (Target impurities from this study, norm to the sum, sixteenth root)		X (87.4%)
GCMS (CHAMP impurities plus target impurities from this study, norm to the sum, sixteenth root)		X (88.1%)
IRMS data		X (81.1%)
ICPMS data		X (42.7%)
GCMS (CHAMP impurities, norm to the sum, sixteenth root) + IRMS		X (98.6%)
GCMS (Target impurities from this study, norm to the sum, sixteenth root) + IRMS		X (95.1%)
GCMS (CHAMP impurities plus target impurities from this study, norm to the sum, sixteenth root) + IRMS		X (99.3%)
GCMS (CHAMP impurities, norm to the sum, sixteenth root) + ICPMS		X (81.8%)
GCMS (Target impurities from this study, norm to the sum, sixteenth roots) + ICPMS		X (87.4%)
GCMS (CHAMP impurities plus target impurities from this study, norm to the sum, sixteenth root) + ICPMS		X (88.1%)
IRMS + ICPMS		X (81.8%)
GCMS (CHAMP impurities, norm to the sum, sixteenth root) + IRMS + ICPMS		X (98.6%)
GCMS (Target impurities from this study, norm to the sum, sixteenth root) + IRMS + ICPMS		X (98.6%)
GCMS (CHAMP impurities plus target impurities from this study, norm to the sum, sixteenth root) + IRMS + ICPMS		X (99.3%)

Table 79: Summary of the accuracy of the DA classification for the 15 data sets. Grouping according to 'lab output' was specified.

Upon further inspection of the DA analysis, in 14 of the data sets methylamphetamine synthesised from Leuckart, Reductive Amination and Birch routes were successfully classified according to both the starting material and synthetic route as illustrated in Table 79. Only ICPMS data on its own failed to classify any of the samples based on the starting material and synthetic route together. From these results, it appears that the data sets which were most problematic were those involving ephedrine or *pseudo*ephedrine salt which included the Nagai, Rosenmund, Emde and Moscow routes. This is not surprising since ephedrine and pseudoephedrine are diastomers and difficult to differentiate between them.

It is also evident from Table 80 that for two data sets, the GCMS all impurities, norm to the sum, sixteenth root in combination with IRMS data alone or IRMS and ICPMS data correctly classified all samples by lab output apart from the Moscow synthesised samples.

Data sets	Leuckart	Reductive Amination	Nagai	Rosenmund	Birch	Emde	Moscow
1	X	X			X		
2	X	X			X		
3	X	X			X		
4	X	X			X		
5							
6	X	X		X	X	X	
7	X	X	X		X		
8	X	X	X	X	X	X	
9	X	X			X		
10	X	X			X		
11	X	X			X		
12	X	X			X		
13	X	X		X	X	X	
14	X	X	X		X	X	
15	X	X	X	X	X	X	

Table 80: Summary of the DA classification for the 15 data sets with further inspection for grouping according to 'lab output'.

Since there is no 100% accuracy in any of 15 data sets, the discrimination function coefficients were not examined.

8.3.3 DA Conclusions

Fifteen data sets were subjected to discriminate analysis using three different parent groupings which corresponded to discrimination by starting material, synthetic route, or ‘lab output’. DA achieved 100% accuracy in five data sets in discrimination according to the starting material. The successful data sets included: when IRMS data was used in combination of GCMS data alone (CHAMP impurity list alone or with the target impurity list from this study) or together with the ICPMS data.

DA was successful at discriminating the samples according to the synthetic route using 10 of the data sets suggested. This indicated that the GCMS (target impurity list from this study) data on its own, or a combination with the GCMS (CHAMP impurity list) or IRMS or ICPMS data could be used to accurately discriminate methylamphetamine according to synthetic route. The GCMS data was normalised to the sum of the target impurities and pre-treated using the sixteenth root method.

The purpose of discrimination by ‘lab output’ was to determine the capability of DA to accurately classify the samples by both starting material and synthetic route at the same time. Unfortunately DA failed to achieve 100% accuracy in the any of the 15 data sets. But in 14 cases DA was able to accurately classify three of the routes according to starting material and synthetic route and with two data sets successful discrimination of six out of the seven synthetic routes were discriminated.

DA, while excellent at illustrating the discriminating power of the GCMS, IRMS and ICPMS data, creates a somewhat false picture; the forensic practitioner will not usually know how many groups should be formed from a set of data. Thus, for instance, the practitioner might specify seven parent groups for one of the data sets discussed previously and obtain discrimination according to synthetic route, but he/she could easily have specified 11 groups and fail to achieved discrimination according to ‘lab output’.

It could be argued, however, that for intelligence purposes this drawback is only a minor one. After all, the cluster formed by DA of these data sets still provides meaningful discrimination, even if the practitioner does not know exactly which level of discrimination he/she is achieving. If a combination of GCMS and IRMS data is used, the practitioner will achieve clusters, so long as he/she specifies a reasonable number of parent groups. Of course, identifying what is a reasonable number of parent groups in an undoubtedly large data set will be difficult.

Nevertheless, DA has shown that the GCMS and/or IRMS data contain sufficient discriminating information about methylamphetamine synthesised by different routes and/or with different starting materials. Unfortunately the ICPMS data failed to give any additional information. Ideally, the next stage of research in methylamphetamine profiling will be to find a statistical system that can accurately and reliably compare samples to one another as well as within a larger database of samples.

DA of these data sets has also allowed insight into the impurities which hold the most discriminating power at each level of discrimination. Since the GCMS data on its own was more successful when the list of impurities suggested by this study was used, they should be used in preference to the CHAMP impurities. The 100% accurate discriminant functions for the classification by starting material were built around the impurities listed in Table 81.

Level of discrimination	Always present in df with high coefficient
starting material	1-phenyl-2-proponal Unknown 3 *(Z)*-α,α–dimethyldiphenethylamine *(E)*-α,α–dimethyldiphenethylamine *(Z)-N*,α,α-trimethyldiphenethylamine
synthetic route	Unknown 1 Unknown 2 Unknown 3 Unknown 6 *(Z)*-α,α–dimethyldiphenethylamine *(E)-N*,α,α-trimethyldiphenethylamine (*Z*)-*N*-methyl-*N*-(α-methylphenethyl)-3-phenylpropenamide (*E*)-*N*-methyl-*N*-(α-methylphenethyl)-3-phenylpropenamide Benzylmethnaphthalene 2,6-Dimethyl-3,5-diphenylpyridine Pyridine 7 and 14 Chloroephedrine Ephedrone *cis*-aziridine Ephedrine

Table 81: Summary of the list of impurities from this study with the highest discriminating power according to DA using two levels of discrimination.

8.4 Conclusions

All three data analysis methods utilised in this project were successful in classifying 143 methylamphetamine batches by starting material and synthetic route. However the third level of discrimination was not achieved using any of the data analysis mechanisms.

Successful discrimination at two of the three levels was achieved in HCA analysis. HCA analysis on the GCMS data (target impurities from this study on their own or in combination with the CHAMP impurities) allowed accurate discrimination of samples by all seven synthetic routes. Discrimination by the two different starting materials (P-2-P and ephedrine/*pseudo*ephedrine) was achieved with the IRMS data on its own or in combination with the GCMS data. When HCA was applied to the $\delta^{13}C$ data, discrimination of the 143 samples into five groups according to whether the samples had been synthesised using P-2-P and the Leuckart or Reductive Amination method, or synthesised from ephedrine base or ephedrine/*pseudo* ephedrine salt.

Principal component analysis successfully discriminated all of the samples by synthetic route and partial discrimination by starting material was achieved. Discrimination by synthetic route required the GCMS data using the list of target impurities from this study and IRMS data where three PCs were utilised. A plot of PC1 and PC2 of the IRMS data set allowed discrimination between starting material (P-2-P and ephedrine/*pseudo*ephderine) used during the synthesis.

Discriminant analysis of the GCMS (target impurities from this study) data on its own or in combination with any other analytical data provided 100% discrimination by starting material.

ICPMS data did not provide any added value to the data analysis. However the ICPMS data does provide additional information in discrimination of the various batches of methylamphetamine by synthetic route as some of the inorganic elements present in elevated amounts could be used to indicate the synthetic route without any data analysis.

PCA, in this project, has been used a method for extracting two or three principal components so that they can be plotted in a two or 3-D dimensional plot and examined for accurate clustering of the data. PCs should be extracted until about 80% of the variance in the data is accounted for. To account for more variance, a third PC was extracted and plotted in the third dimension, but these plots offer better discrimination than PC1 vs PC2 plots only in certain data set. Discriminant analysis has a major disadvantage for the profiling scenario, and that is the need for the practitioner to input the number of parent groups before the analysis is undertaken. Obviously this information is not usually known, so the practitioner would have to input a 'best guess' of the number of groupings, and perhaps this estimation could be derived from other intelligence information.

The results from all the three data analysis methods have shown that sufficient information was contained within the GCMS and IRMS data sets to allow discrimination of methylamphetamine samples at various levels. Furthermore, the PCA and DA techniques have revealed that certain GCMS impurities hold more discriminating power than others. The target impurities identified in this work as high loading variables for PCA and variables with high coefficients for DA were 2,6-Dimethyl-3,5-diphenylpyridine, pyridine 7 and 14, dimethylphenylnaphthalene, benzylmethnaphthalene, *(Z)-N*-methyl-N-(α-methylphenethyl) amino-1-phenyl-2-propanone and *(E)-N*-methyl-N-(α-methylphenethyl) amino-1-phenyl-2-propanone. Unknown 1, Unknown 2, Unknown 3, Unknown 6, *(Z)*-α,α–dimethyldiphenethylamine, *(E)-N*,α,α-trimethyldiphenethylamine, Chloroephedrine, Ephedrone, *cis*-aziridine and Ephedrine. In total, 34 compounds were identified as target impurities in this project. These included the CHAMP compounds as well as the route specific impurities identified as part of this work. Of these compounds only the 16 listed above were the main driving forces behind the successful PCA and/or DA discrimination.

8.5 References

1. Buchanan, H.A.S., *An evaluation of isotope ratio mass spectrometry for the profiling of 3,4-methylenedioxymethamphetamine*, PhD Thesis in Department of Pure and Applied Chemistry, University of Strathclyde: Glasgow, 2009, 116-119.

2. Gordon, A.D., *Classification*. Chapman & Hall/CRC: 1999, USA

3. Hierarchical clustering. Available at http://www.resample.com/xlminer/help/HClst/HClst_intro.htm. Last accessed on 07/04/10.

4. Miller, J.N.; Miller, J.C., *Stastistic and Chemometrics for Analytical Chemistry*. 4th ed.; Pearson Education Limited: U.K., 2000.

5. Massart, D.L.; Kaufman, L. *The Interpretation of Analytical Chemical Data by the Use of Cluster Analysis*. John Wiley & Sons: New York, 1983.

6. Everitt, B.S., *Cluster Analysis*, 3rd ed.; Arnold (a member of the Hodder Headline Group): London, 1993

7. Software, I.O. Euclidean and Euclidean Squared. Available at http://www.improvedoutcomes.com/docs/WebSiteDocs/Clustering/Clustering Parameters/Euclidean_and_Euclidean_Squared_Distance_Metrics.htm. Last accessed on 07/04/10.

8. Adams, M.J., *Chemometrics in Analytical Spectroscopy*, 2nd ed.; The Royal Society of Chemistry: Melbourne, Australia, 2004.

9. Kline, P., *An Easy Guide to Factor Analysis*. Routledge: London, 1994.

10. Bell, S.E.J., *Forensic Chemistry*. Pearson Education Inc: Upper Saddle River, New Jersey, 2006.

11. Gorsuch, R.L., *Factor Analysis*. W.B.Saunders Company: Philadelphia, 1974.

12. Gardiner, W.P., *Statistical Analysis Methods for Chemists: A Software-based Apporach*. The Royal Society of Chemistry: Glasgow, Scotland, 1997.

13. Garson, D., Discriminant Analysis: Statnotes from North Carolina State University. Available at http://faculty.chass.ncsu.edu/garson/PA765/discrim.htm. Last accessed on 07/03/10.

CHAPTER 9: CONCLUSIONS AND FUTURE WORK

9.0 Summary of Conclusions

Methylamphetamine production sites have traditionally been located in North America and Asia, but the most recent (2009) UNODC *World Drug Report* [1] indicates that production sites are spreading around the world. Research into methylamphetamine profiling has been investigated by researchers around the world and recently been advanced with the modification of a 'harmonised' amphetamine GCMS [2] method in an effort to facilitate methylamphetamine profiling at an international level. The CHAMP method, involving a collaboration of seven labs in seven countries, is based on utilising a GCMS amphetamine impurity profiling method for impurity analysis of methylamphetamine samples followed by statistical comparison of the organic impurities using correlation coefficients.

Potential problems have been suggested with profiling based on the chromatography of impurities alone, such as the difficulty in obtaining reproducible chromatograms, the often highly pure drugs in circulation, and an appropriate 'target' list of the impurities with which sample comparisons are made can be difficult to find. A further problem with the CHAMP profiling method is that it was developed using seized samples of which the provenance was unknown and the original GCMS method was developed with amphetamine in mind rather than methylamphetamine.

This research involved repetitive synthesis of methylamphetamine using seven methods most accessible to clandestine chemists and various analytical or profiling techniques were employed to evaluate their potential to supply sufficient data to enable the known samples to be unequivocally linked. In total 149 samples were prepared reflecting a wide variety of clandestine preparative methods. Out of 149 samples, 143 samples were analysed using three different techniques, namely GCMS, IRMS and ICPMS and the resultant data sets subjected to four different mathematical data processing methods.

In the first technique, organic impurities were extracted and analysed by GCMS. Prior to this, the analytical method for the organic impurity profiling was modified from published literature methods. As a result a method for the extraction of samples using both basic and acidic buffers was used for the recovery of identified route specific impurities. Comparison of the resulting impurity profiles was made by calculating the Pearson correlation coefficient for each pair of samples. To draw out the best performance of the method, a list of target impurities from this study was used. The target impurities from this study normalised to the sum of the targets and pre-treated with the sixteenth root gave the most accurate discrimination allocating all samples to their appropriate synthetic route. With this data set, the 95.00 threshold value facilitated correct linkage of samples from the 143 batches within and between synthetic routes.

IRMS technique has shown potential for dug profiling in terms of identifying geographic origin and determining synthetic pathway. Again most previous studies have concentrated on the analysis of seizures samples for which the original geographical origin is unclear. Some recent research has investigated precursor origin but involved limited synthetic variety. In this study, the stable isotope ratios of carbon ($\delta^{13}C$), nitrogen ($\delta^{15}N$) and hydrogen ($\delta^{2}H$) were measured by EA/TC-IRMS. The synthesised methylamphetamine batches could be discriminated using plots of δ values by precursor. The $\delta^{13}C$ values offered the best discrimination which was to be expected as all of the carbon atoms on the final methylamphetamine molecule are contributed by the starting material. $\delta^{2}H$ values could discriminate whether the methylamphetamine was prepared from either a P-2-P or ephedrine/*pseudo*ephedrine pathway and the $\delta^{15}N$ data appeared to be the most sensitive to inadvertent differences in preparative method. Two dimensional plots of carbon and hydrogen or carbon and nitrogen data discriminated all samples by the nature of the starting material, that is to say whether the starting material was P-2-P, ephedrine salt, ephedrine base or *pseudo*ephedrine salt. If these methylamphetamine HCl samples had been seized and subjected to IRMS analysis, $\delta^{13}C$ and $\delta^{2}H$ or $\delta^{13}C$ and $\delta^{15}N$ data would have allowed tentative visual discrimination into groups corresponding to the precursors used for manufacture

Previous research into the applicability of ICPMS for methylamphetamine profiling has suggested that the results of inorganic analysis compliment organic impurity analysis. To date ICPMS studies have focused on samples of unknown origin and methylamphetamine synthesised by the ephedrine/*pseudo*ephedrine synthetic routes. The results obtained in this work suggest that ICPMS provides limited drug profiling information. The trace metal impurities recovered by ICPMS did facilitate discrimination to some extent by synthetic pathway. Hg and Li are target impurities were present in large amounts in both the Reduction Amination and Birch route samples respectively. P and I were present in the Nagai and Moscow route samples. In the Rosenmund and Emde route samples, Pd and Ba were present in high quantity. Due to the present of each element in more than one route, the Pearson correlation coefficient matrix was unable resolve the samples into their specific synthetic routes. However some specific inorganic impurities present in high concentration level in certain synthetic routes and this at least can contribute to some additional information.

A variety of data analysis techniques were investigated to identify methods which could discriminate between methylamphetamine based on the analytical data derived from of the sample sets prepared in this project. Pattern recognition techniques were applied to the GCMS data on its own, IRMS data on its own, ICPMS data on its own, a combination of two data and all three data sets to investigate their abilities to link samples by (1) starting material, (2) synthetic route, or (3) 'lab output' (i.e. discrimination by both starting material and synthetic route). All the three data analysis (HCA, PCA and DA) methods utilised in this project were successful in classifying a set of 143 methylamphetamine batches by starting material and synthetic route. However the third level discrimination was not achieved by any of the data analysis methods investigated

HCA analysis of the GCMS data allowed accurate discrimination of samples by seven synthetic routes. Discrimination (by two different starting materials (P-2-P or ephedrine/*pseudo*ephedrine)) was achieved with the IRMS data on its own or in combination with the GCMS data. When HCA was applied to the $\delta^{13}C$ data, discrimination to four different starting materials was achieved. With PCA, successful discrimination by synthetic route and partially by starting material was achieved.

GCMS data (the target impurities identified in this study) was required for discrimination by synthetic route. A plot of PC1 and PC2 in IRMS data set allowed meaningful discrimination between starting material (P-2-P and ephedrine/*pseudo*ephderine) used during methylamphetamine synthesis.

DA of the GCMS data on its own or in combination with any other data set was able to discriminate all samples by synthetic route. DA of the IRMS data in combination with the GCMS data was 100% accurate for the discrimination by starting material but DA of IRMS data on its own was less successful.

Based on the number of data sets affording accurate discrimination by HCA, PCA and DA, the list of target impurities provided by this study proved more successful than the suggested CHAMP impurities, and the sixteenth root data preprocessing method gave the best discrimination in all cases.

This study has shown that GCMS and IRMS are clear and reliable methods for methylamphetamine profiling. However, utilising the impurities suggested by the CHAMP study alone is not sufficient and the inclusion of the route specific impurities investigated in this study was essential for correct assignation to the appropriate synthetic route. Furthermore, analysis using a DB-5 column as opposed to the DB-1 column suggested in some of the existing literature provided the opportunity of analysing the samples using one extraction only to recover all target impurities.

This project has demonstrated conclusively that the data derived from both techniques holds information which can allow discrimination of methylamphetamine samples at various levels (i.e. by starting material and by synthetic route), as evidenced by the application of HCA, PCA and DA to the data sets. To fully understand and utilise this discriminatory power, further work and more sophisticated data analysis techniques must be explored on methylamphetamine samples which are both of known provenance and relevant to current drug circulation. In this way, it is likely that methylamphetamine profiling will have value for both intelligence and evidential purposes.

9.1 Recommendations for Future Work

Future methylamphetamine profiling could proceed in a number of different ways. Firstly, repetitive synthesis of methylamphetamine via the hypophosphorous acid 'Hypo' route should be carried out. The 'Hypo' route is an upcoming method in clandestine laboratory manufacture and is another variation of the Nagai and Moscow synthesis utilising iodine and red phosphorous. GCMS, IRMS, ICPMS analysis should be undertaken so that the derived data can be incorporated into the existing data for this study and the full range of pattern recognition analysis applied.

The effect of the catalyst obtained from different suppliers used in the Rosemnund method should be further explored.

The identity of individual compounds (impurities) in this work was confirmed by NIST library matching and reference to the published literature. This should further confirmed using QTOF (Mass Quadrupole Time-of-Flight) technique.

GCMS impurity profiling works well on samples rich in impurities. However high purity samples may result in a reduction in the concentration of impurities present and provide difficulties with impurity extraction. The samples prepared in this work should be recrystalised and re analysed using the developed GCMS methods to determine the effect of purification of the impurity profile. Similarly a comparison between the impurity and other profiling data related to methylamphetamine and corresponding crystal methylamphetamine samples to elucidate any differences would also be of interest.

The samples prepared in this work have been synthesised from laboratory grade reagents. Synthesis of samples from illicit precursor sources (such as cold medication for example) to investigate further the ability of the analytical techniques to link samples to precursors would be of considerable interest.

This work analysed bespoke synthetic samples and successfully characterised these samples by starting material (for IRMS) and synthetic route (GCMS). An extension of this work would be to apply the analytical methodology and data analysis

mechanisms to street seized samples to establish a drug profiling system for case work. It would be recommended that such samples are analysed using the DB-5 column using the single extraction technique. Compound specific IRMS should be used on authentic methylamphetamine should also be explored.

Other supervised pattern recognition techniques such as artificial neural networks could be applied to the data. Statisticians interested in statistical problems in the forensic science context have recently suggested a solution to the problem of comparison of two sets of continuous multivariate measurements to determine if the two items share a common origin by following a Bayesian network approach and this may also provide an interesting route to potentially link case samples and one which could be explored further.

9.2 References

1. United Nations Office on Drugs and Crime, *World Drug Report*; 2009.

2. Andersson, K.; Lock, E.; Jalava, K.; Huizer, H.; Jonson, S.; Kaa, E.; Lopes, A.; Poortman, A.; Sippola, E.; Dujourdy, L.; Dahle´n, J., Development of a harmonised method for the profiling of amphetamines VI Evaluation of methods for comparison of amphetamine. *Forensic Science International* 2007, 169**,** 86–99.

Appendix A: Spectral Data for Identification of Synthesised Compounds

The ^{1}H NMR, ^{13}C NMR, and FTIR spectra for methylamphetamine base and methylamphetamine hydrochloride and ^{1}H NMR spectra for chloroephedrine hydrochloride are displayed in Figure 170 – Figure 177.

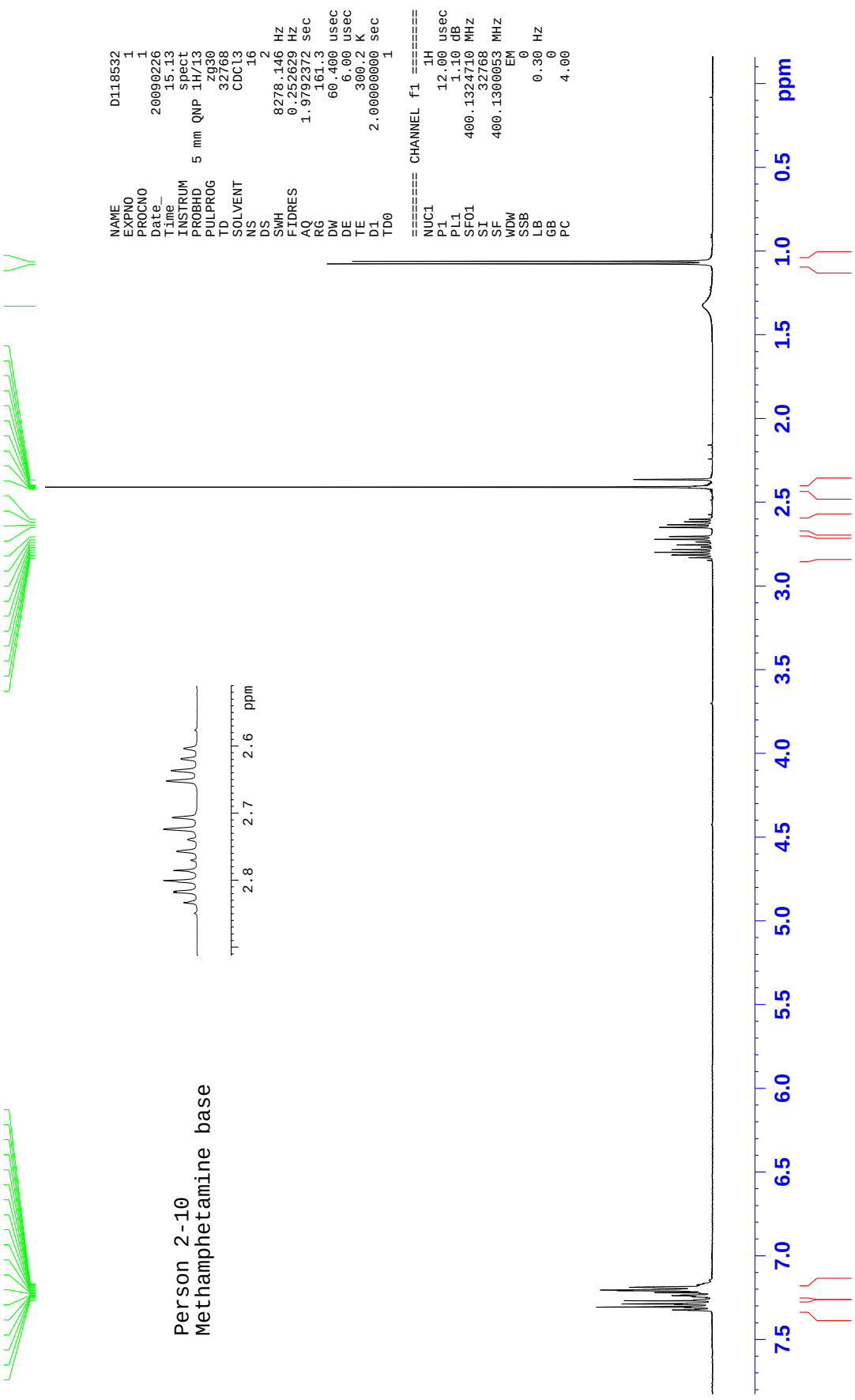

Figure 170: ^{1}H NMR of methylamphetamine free base.

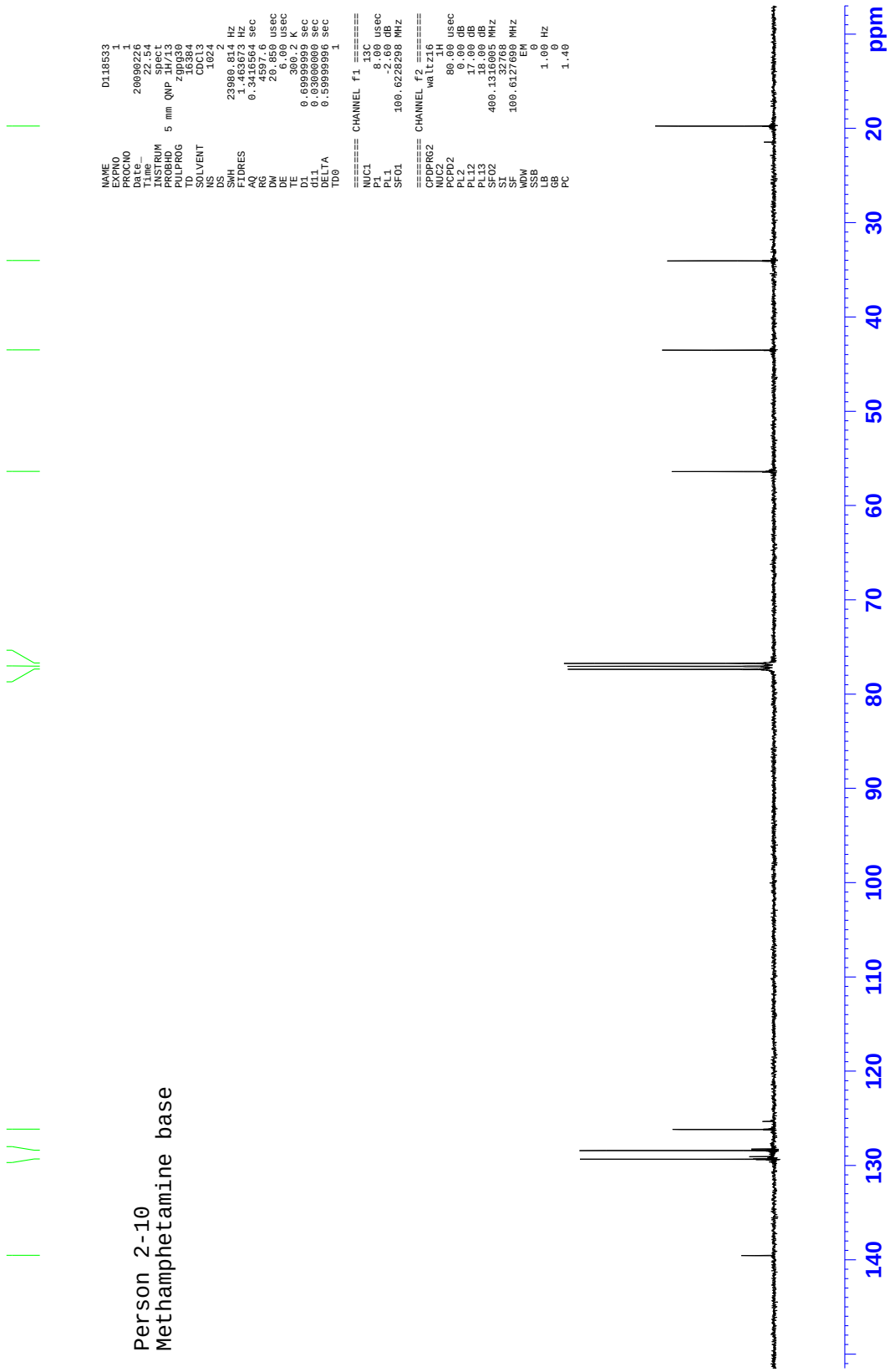

Figure 171: ^{13}C NMR spectrum of methylamphetamine free base.

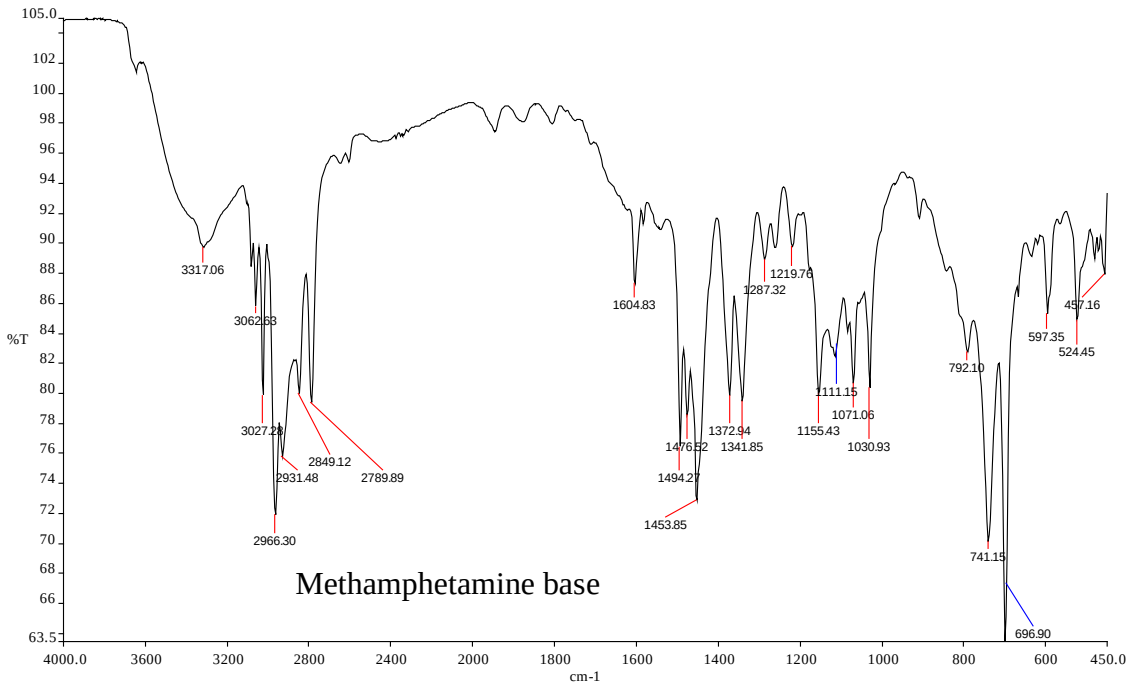

Figure 172: IR spectrum of methylamphetamine free base.

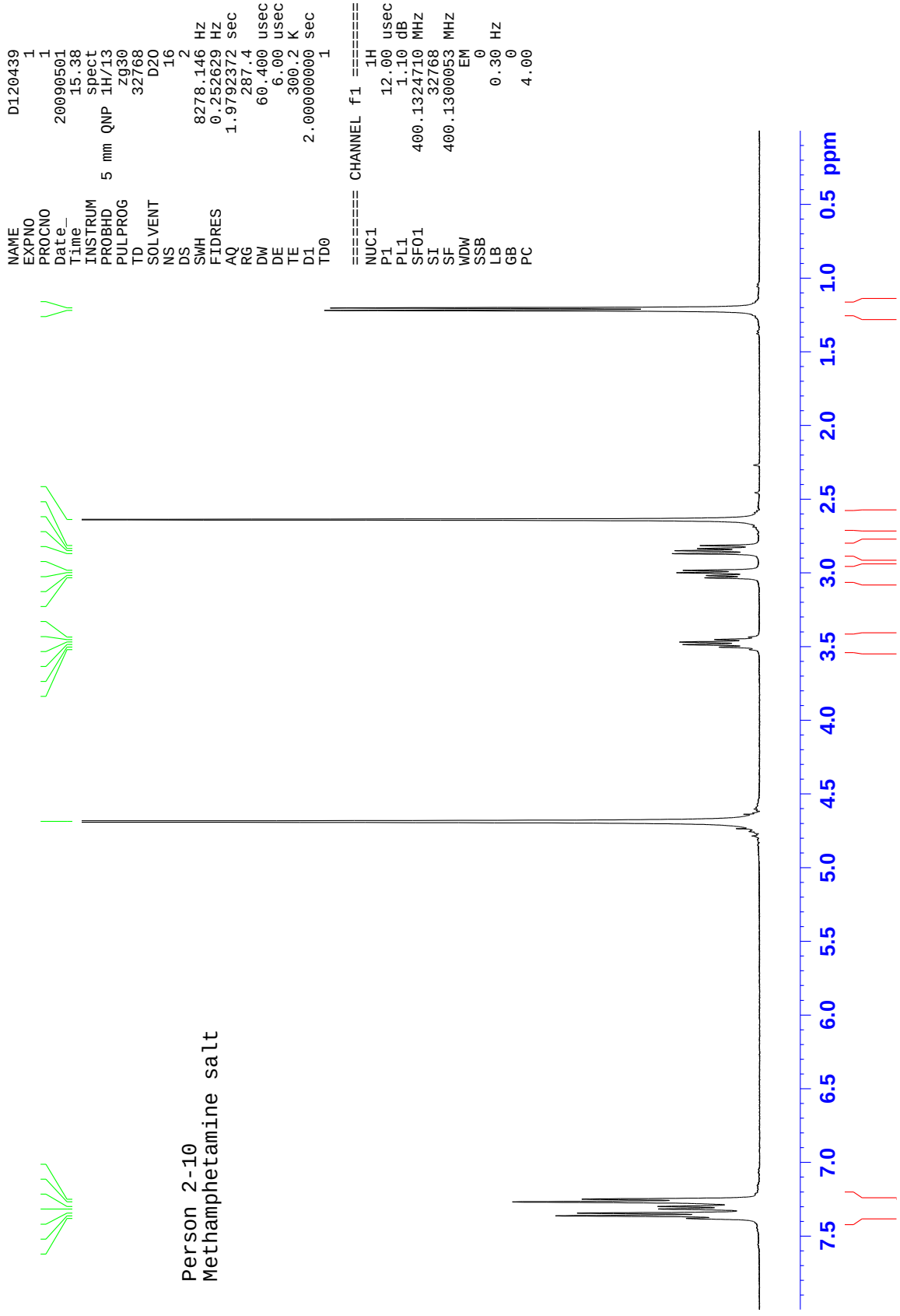

Figure 173: ^{1}H NMR spectrum of methylamphetamine salt.

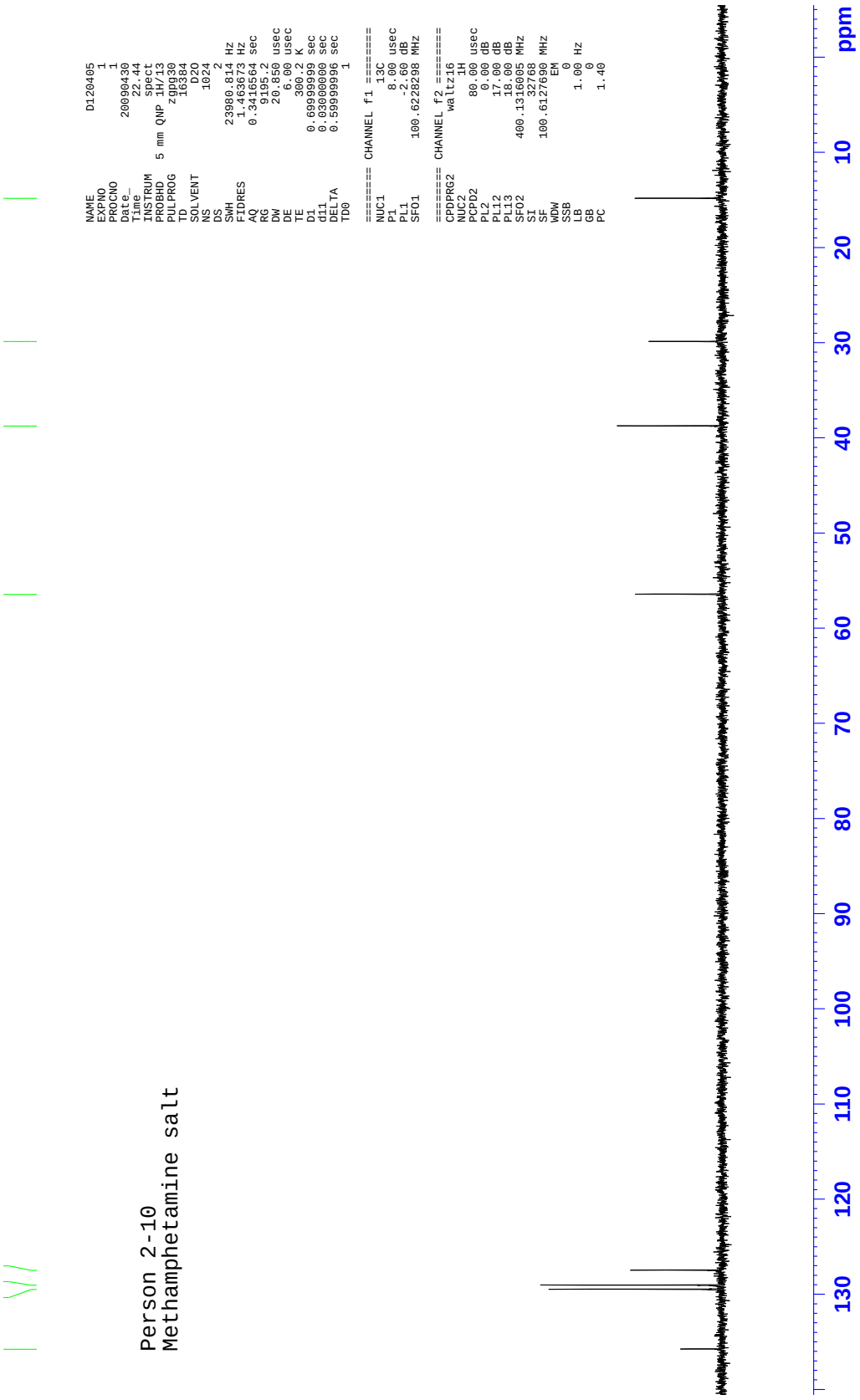

Figure 174: ^{13}C NMR spectrum of methylamphetamine salt.

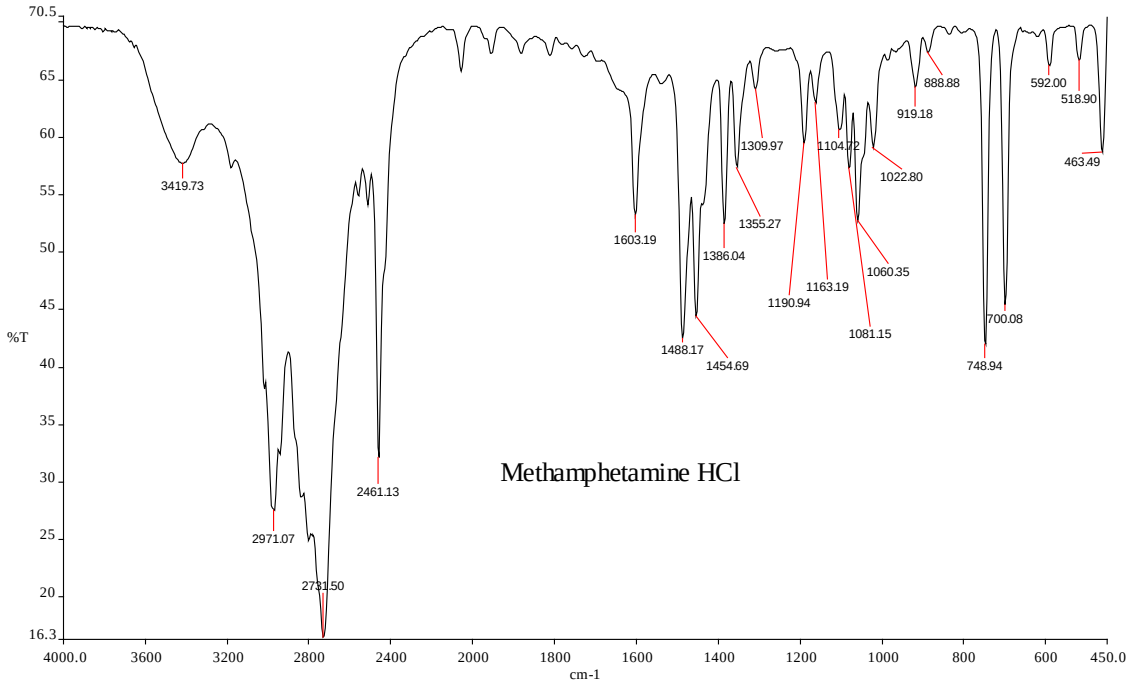

Figure 175: IR spectrum of methylamphetamine hydrochloride.

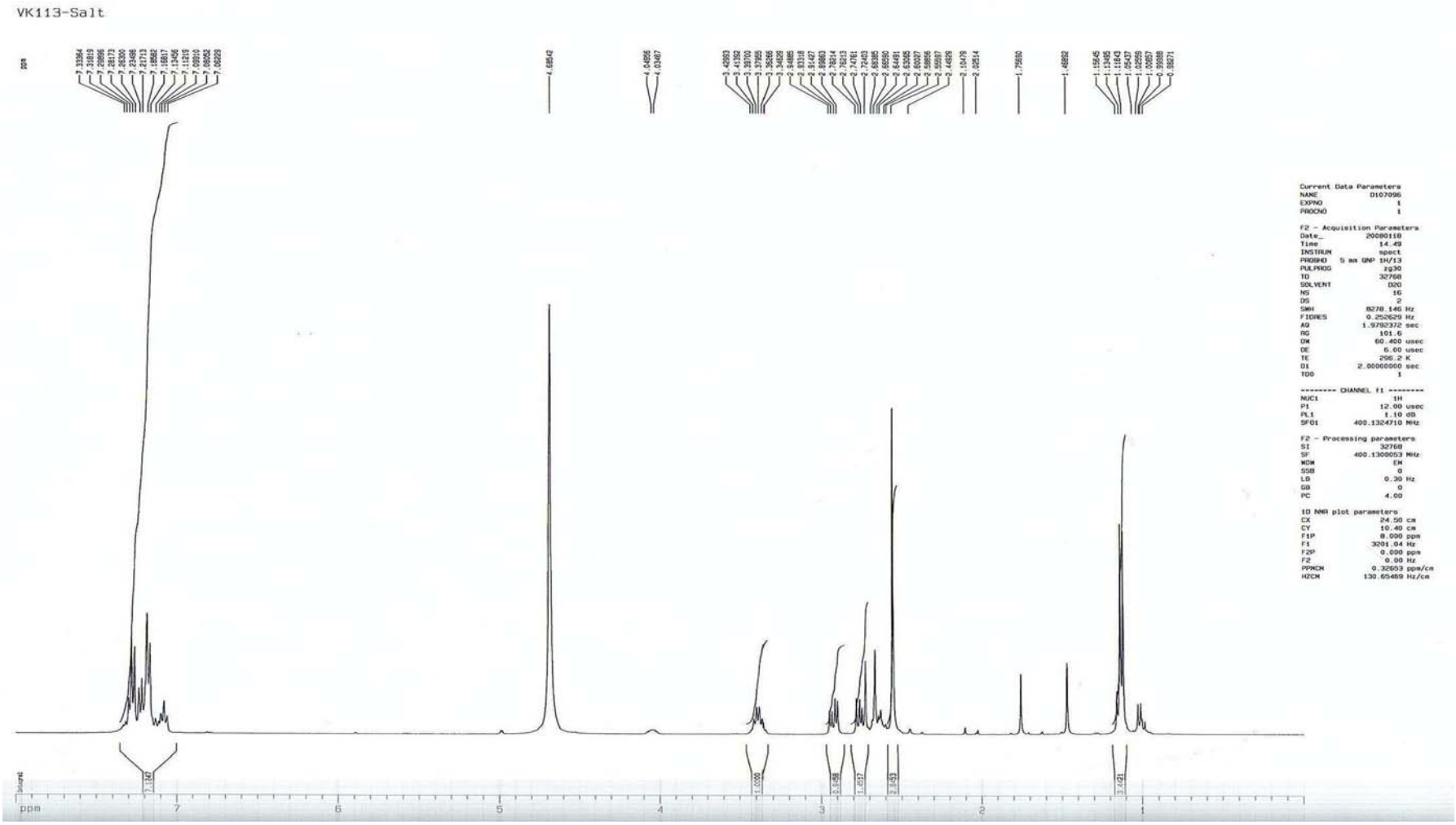

Figure 176: ^{1}H NMR spectrum of methylamphetamine salt (Rosenmund method).

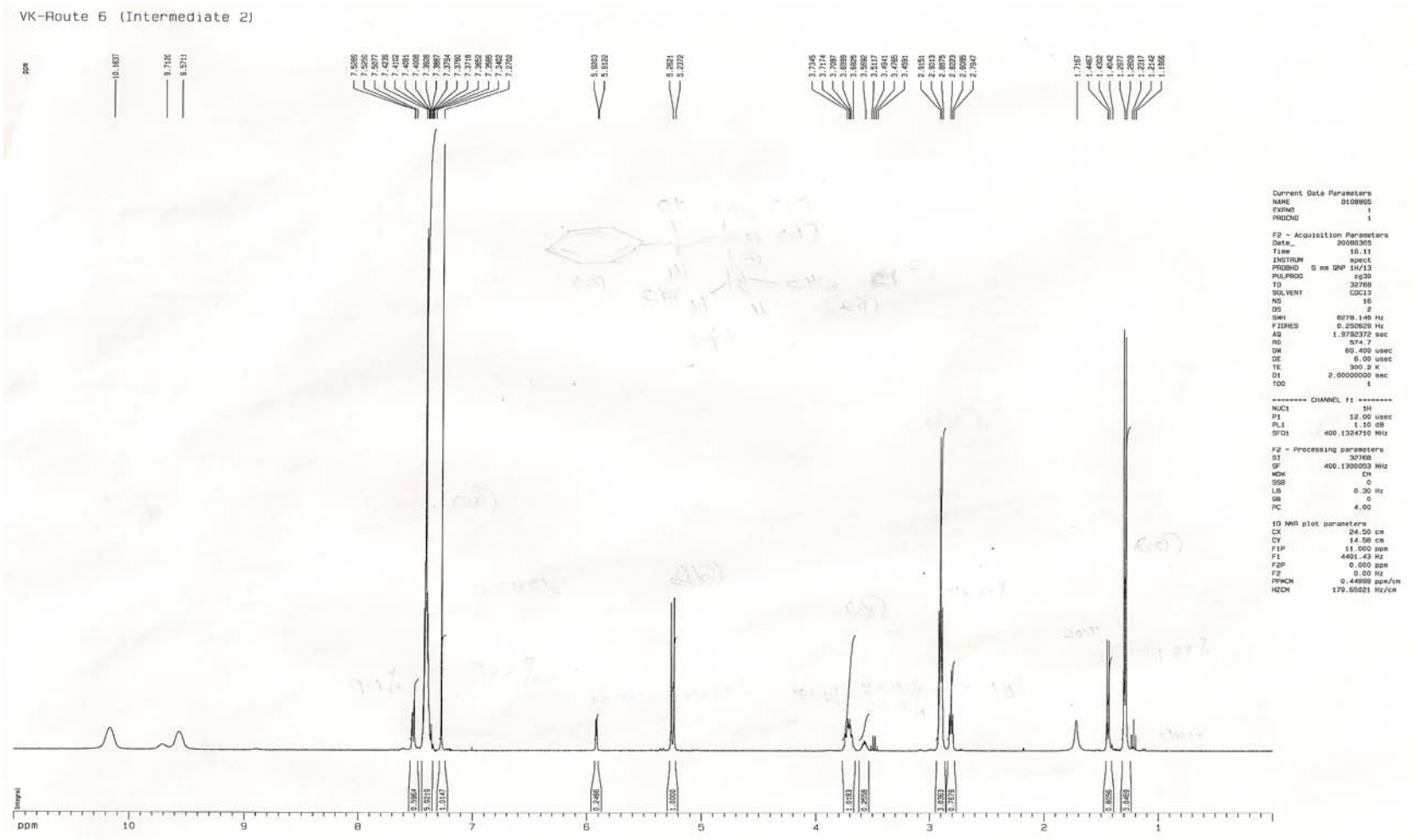

Figure 177: ^{1}H NMR spectrum of chloroephedrine HCl (Emde route).

Appendix B: Molecular Weight for Compounds

No	Compound	Molecular Weight
1	Methylamphetamine	149
2	Acetic acid	60
3	Amphetamine	135
4	Dimethylamphetamine (DMA)	163
5	*N*-formylamphetamine	163
6	Bibenzyl	182
7	*N*-formylmethylamphetamine	177
8	*N*-acetylmethylamphetamine	191
9	Dibenzylketone	210
10	*cis* and *trans* 3,4-Diphenyl-3-buten-2-one	222
11	α-benzyl-N-methylphenethylamine	225
12	Benzylmethylamphetamine	239
13	*N*-β-(phenylisopropyl) benzyl methyl ketimine	251
14	α,α-dimethyldiphenethylamine	253
15	*N*-methyldiphenethylamine	239
16	*N*,α,α-trimethyldiphenethylamine	267
17	*N*-benzoylamphetamine	239
18	*N*-benzoylmethylamphetamine	253
19	2,6-Dimethyl-3,5-diphenylpyridine	259
20	Pyridine 7 and 14	259
21	*N*,*N*-di-(β-phenylisopropyl) formamide	280
22	*N*-methyl-*N*-(1-methyl-2-phenylethyl)-2-phenylacetamide	267
23	1-phenyl-2-propanone	134
24	1-phenyl-1,2-propanedione	148
25	1-phenyl-2-propanol	136
26	*N*-*N*-Dimethylbenzylamine	135
27	*(Z)* and *(E)* 1-phenylpropan-2-one oxime	149
28	3,4-Dimethyl-5-phenyloxazolidine	191
29	Dimethylphenylnaphthalene	232
30	Benzylmethnaphthalene	218
31	*N*-methyl-N-(α-methylphenethyl) amino-1-phenyl-2-propanone	281
32	(*Z*) and (*E*)-*N*-methyl-*N*-(α-methylphenethyl)-3-phenylpropenamide	279
33	Benzaldehyde	106
34	Ephedrone	163
35	Ephedrine	165
36	Ethylamphetamine	163
37	*N*-acetylamphetamine	177
38	*cis* and *trans*-1,2-dimethyl-3-phenylaziridine	147
39	Chloroephedrine	183
40	Methylamphetamine dimer	296
41	1-(1,4-cyclohexadienyl)-2-methylaminopropane (CMP)	151

Table 82: Molecular weight for compounds identify in this study.

Appendix C: Overlay of Intrabatch Chromatograms

1.1 Reductive Amination

Intrabatch

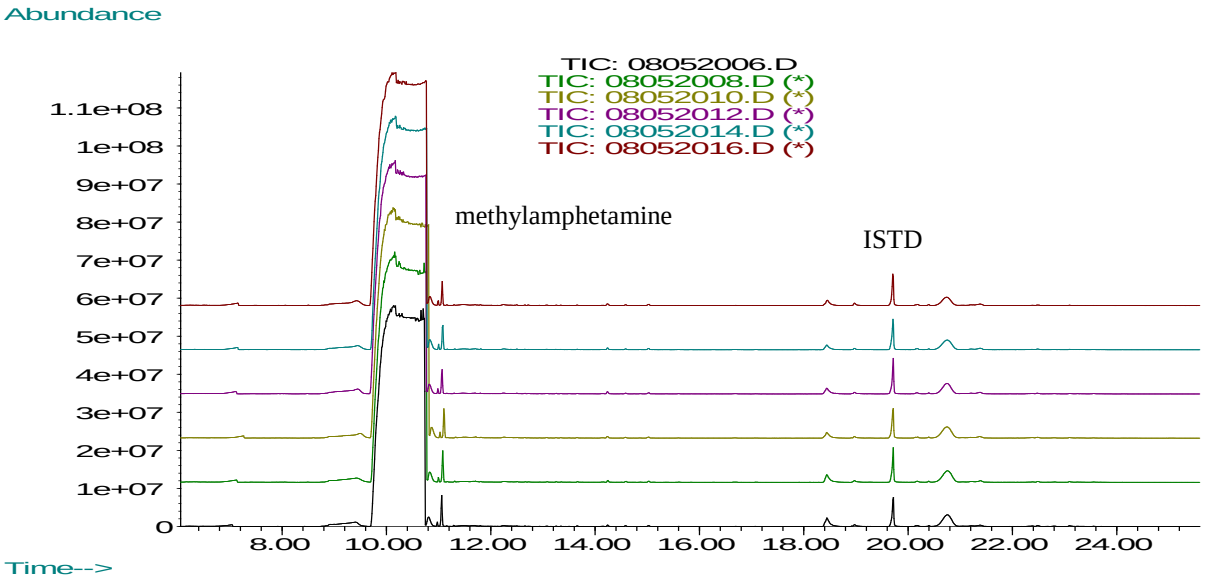

Figure 178: Overlay of the impurity profiles from the six extracts at pH 10.5.

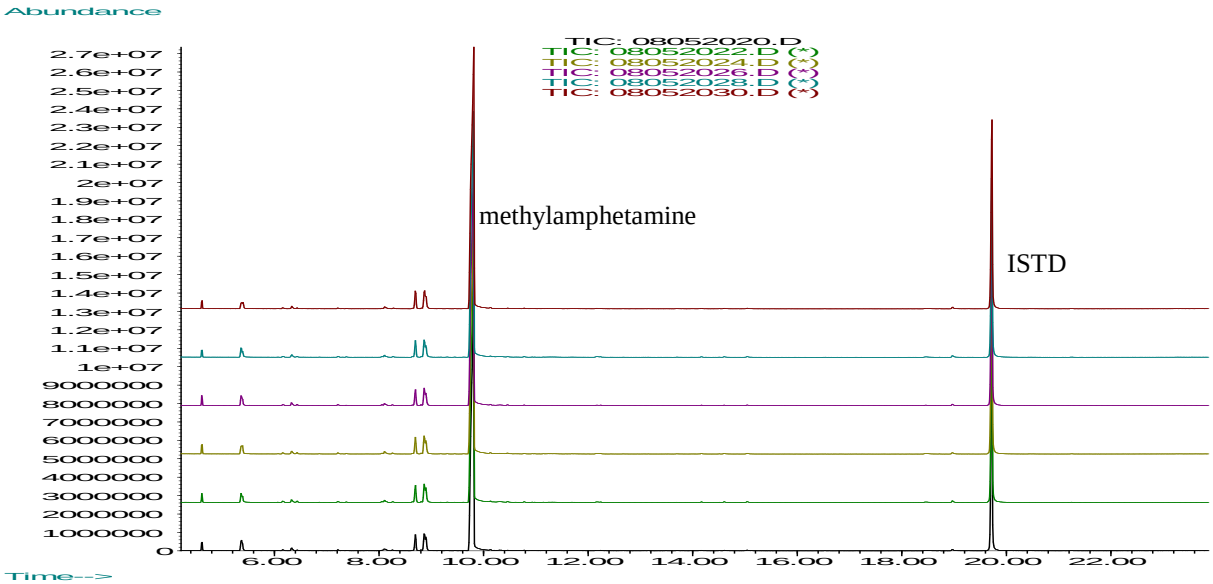

Figure 179: Overlay of the impurity profiles from the six extracts at pH 6.

1.2 Nagai Method

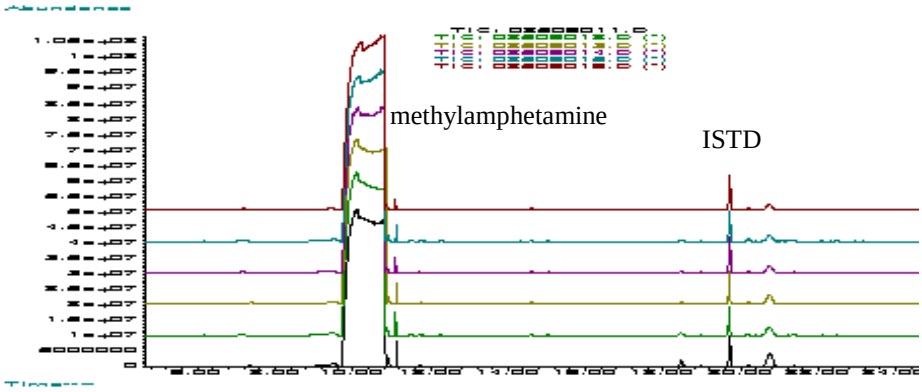

Figure 180: Overlay of the impurity profiles from the six extracts at pH 10.5.

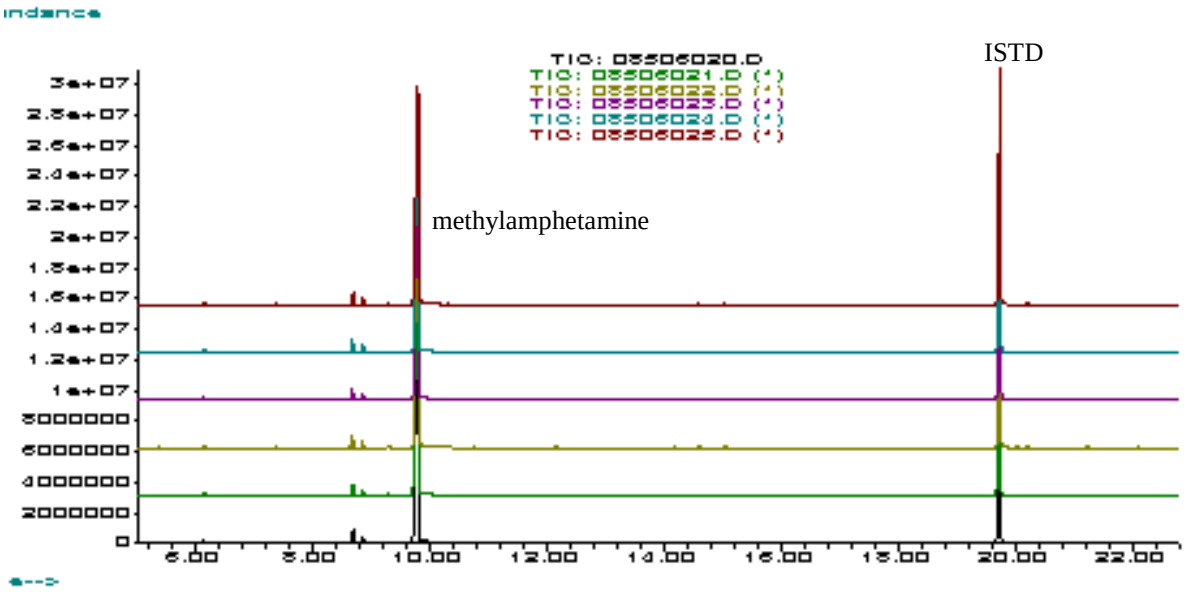

Figure 181: Overlay of the impurity profiles from the six extracts at pH 6.

1.3 Rosenmund Method

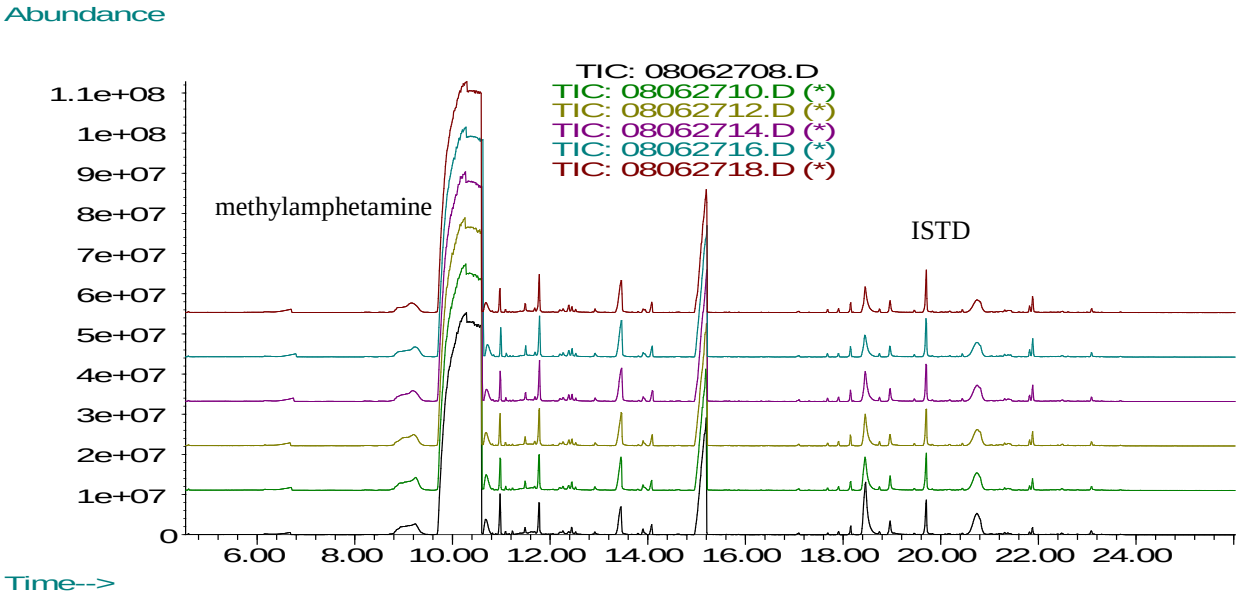

Figure 182: Overlay of the impurity profiles from the six extracts at pH 10.5.

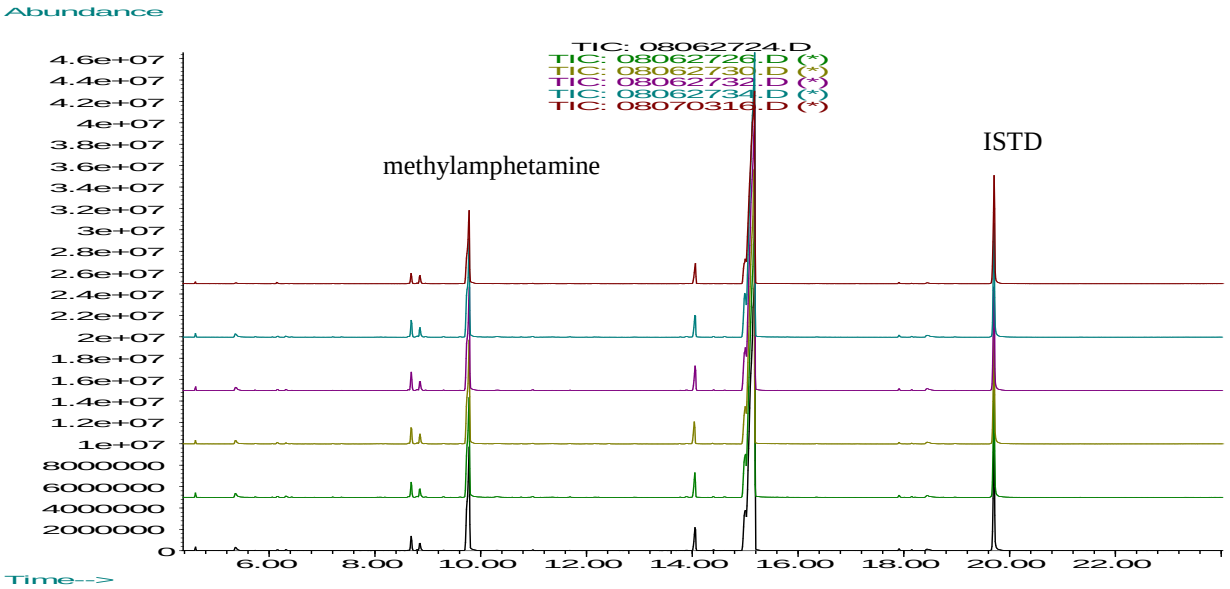

Figure 183: Overlay of the impurity profiles from the six batches extract at pH 6.

1.4 Birch Method

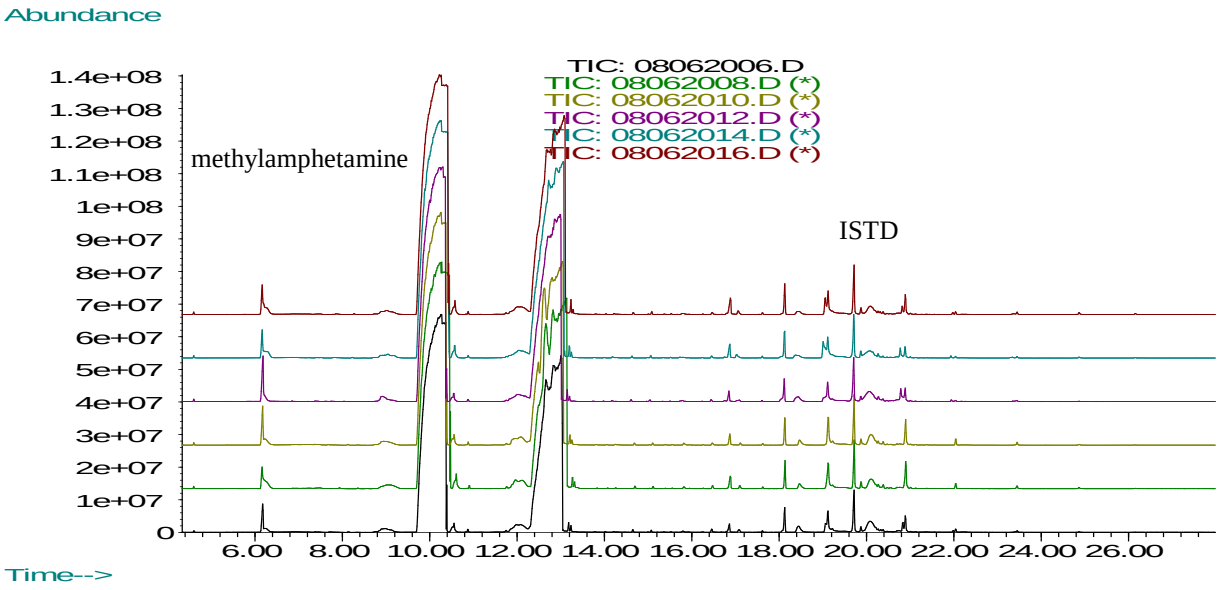

Figure 184: Overlay of the impurity profiles from the six extracts at pH 10.5.

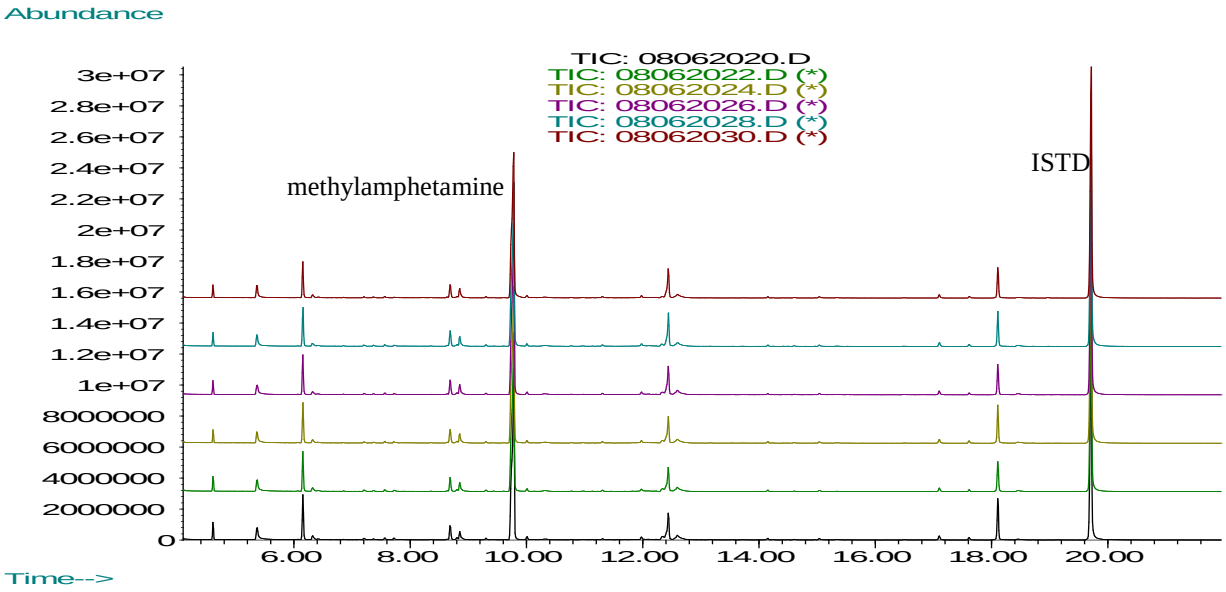

Figure 185: Overlay of the impurity profiles from the six batches extract at pH 6.

1.5 Emde Method

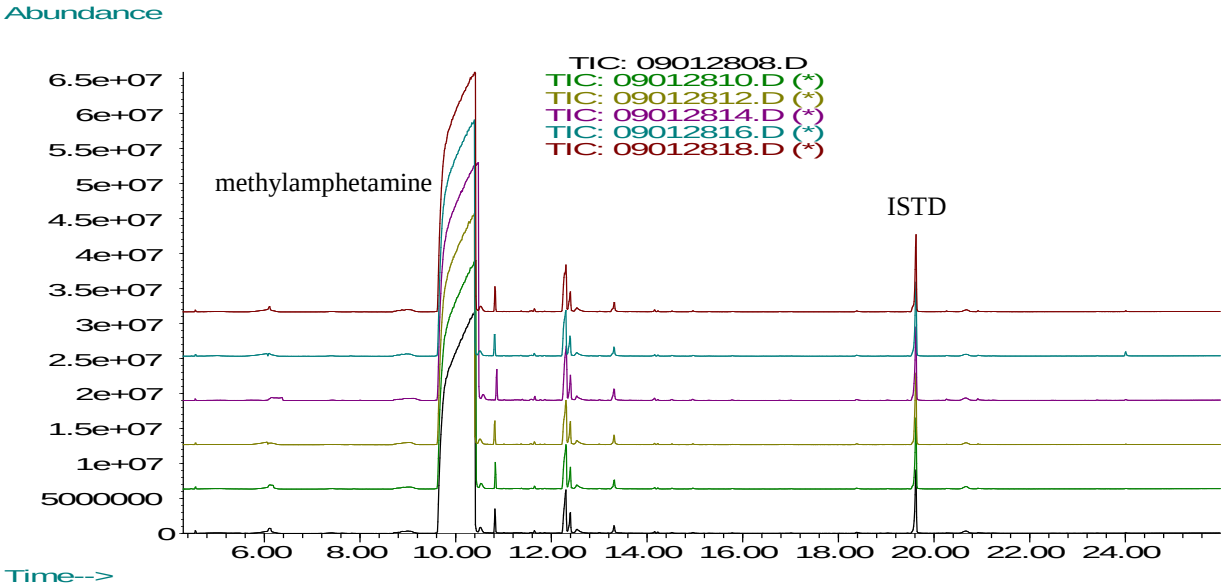

Figure 186: Overlay of the impurity profiles from the six extracts at pH 10.5.

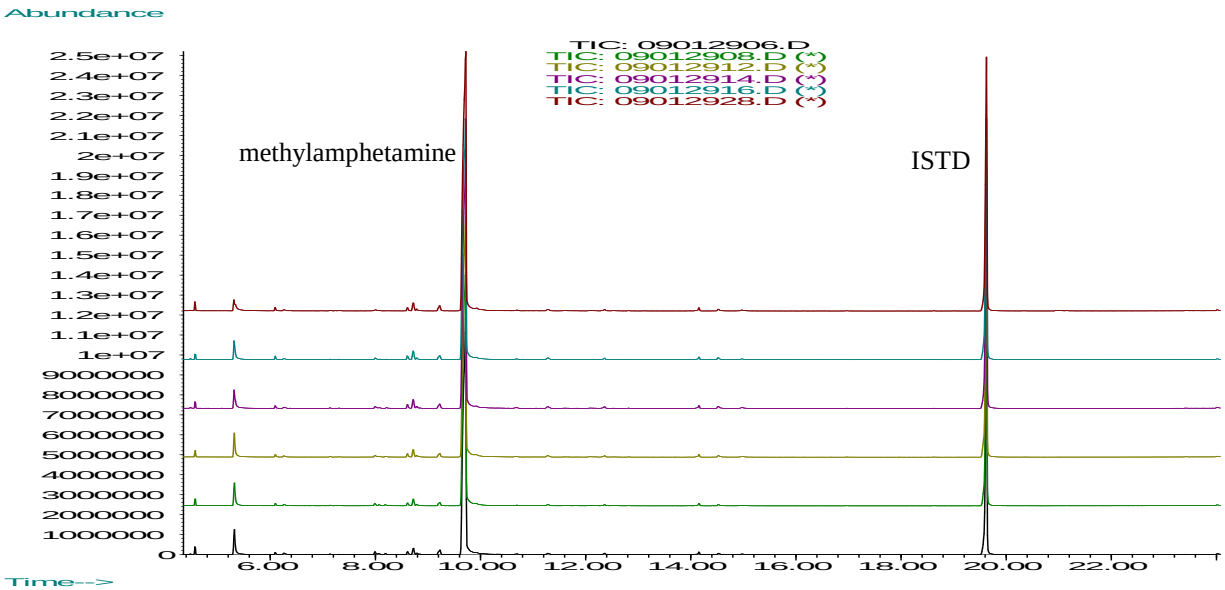

Figure 187: Overlay of the impurity profiles from the six batches extract at pH 6.

1.6 Moscow Method

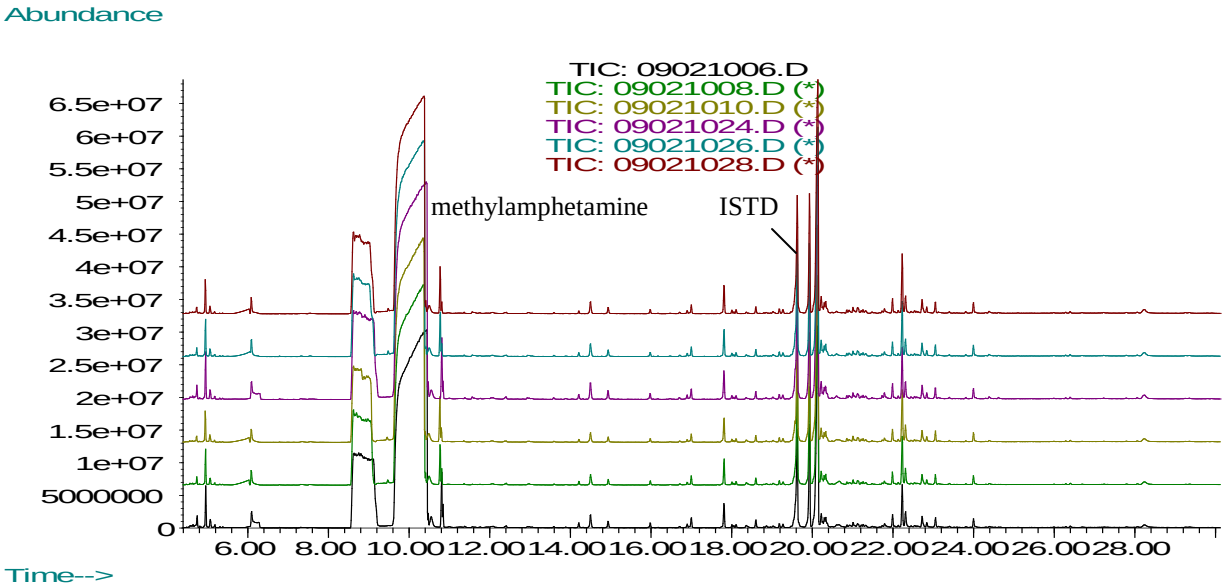

Figure 188: Overlay of the impurity profiles from the six extracts at pH 10.5.

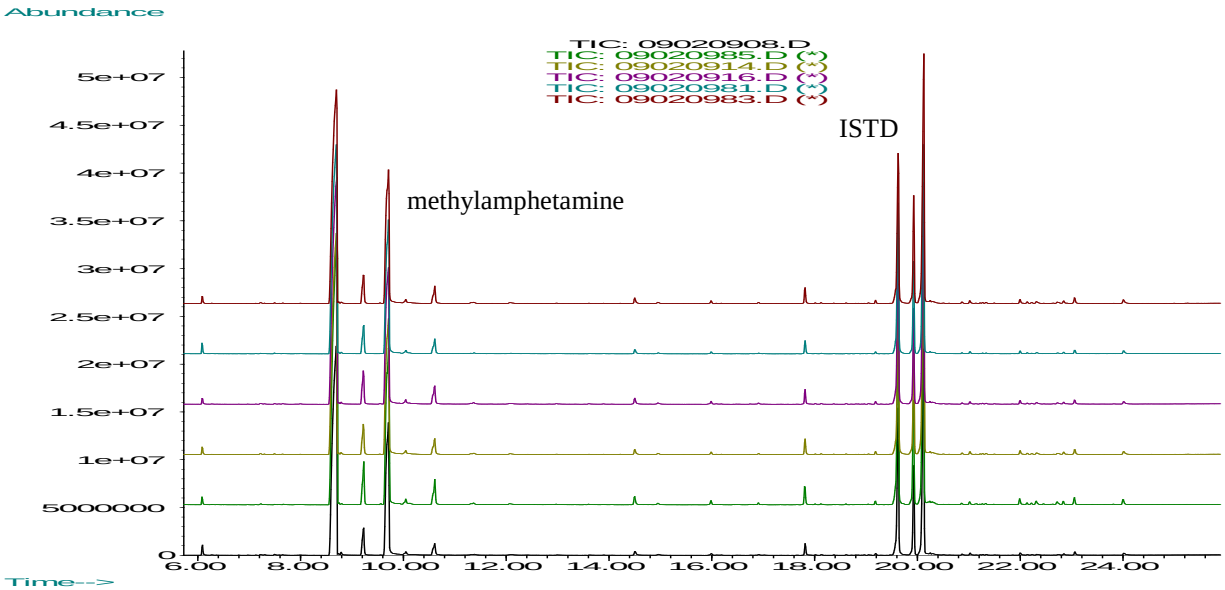

Figure 189: Overlay of the impurity profiles from the six batches extract at pH 6.

Appendix D: Impurity Lists for CHAMP and this study

Impurities (CHAMP)	Impurities (This study)
N-formylmethamphetamine	Dibenzylketone
N-acetylmethamphetamine	*cis* 3,4-Diphenyl-3-buten-2-one
cis 3,4-Diphenyl-3-buten-2-one	α-benzyl-*N*-methylphenethylamine
α-benzyl-*N*-methylphenethylamine	*trans* 3,4-Diphenyl-3-buten-2-one
α,α-dimethyldiphenethylamine	α,α-dimethyldiphenethylamine
α,α-dimethyldiphenethylamine	α,α-dimethyldiphenethylamine
N-methyldiphenethylamine	N-methyldiphenethylamine
N,α,α–trimethyldiphenethylamine	N,α,α–trimethyldiphenethylamine
N,α,α–trimethyldiphenethylamine	N,α,α–trimethyldiphenethylamine
N-benzoylmethamphetamine	N-benzoylamphetamine
2,6-Dimethyl-3,5-diphenylpyridine	N-benzoylmethamphetamine
Pyridine 7 and 14	2,6-Dimethyl-3,5-diphenylpyridine
N,N-di-(β-phenylisopropyl) formamide	Pyridine 7 and 14
N-methyl-N-(1-methyl-2-phenylethyl)-2-phenylacetamide	N,N-di-(β-phenylisopropyl) formamide
Dimethylphenylnaphthalene	N-methyl-N-(1-methyl-2-phenylethyl)-2-phenylacetamide
Benzylmethnaphthalene	Dimethylphenylnaphthalene
(Z)-N-methyl-N-(α-methylphenethyl)-3-phenylpropenamide	Benzylmethnaphthalene
Ephedrone	N-methyl-N-(α-methylphenethyl) amino-1-phenyl-2-propanone
Ephedrine	N-methyl-N-(α-methylphenethyl) amino-1-phenyl-2-propanone
cis-1,2-dimethyl-3-phenylaziridine	(Z)-N-methyl-N-(α-methylphenethyl)-3-phenylpropenamide
methamphetamine dimer	(E)-N-methyl-N-(α-methylphenethyl)-3-phenylpropenamide
	Ephedrone
	Ephedrine
	Ethylamphetamine
	Unknown 1
	Unknown 2
	Unknown 3
	cis-1,2-dimethyl-3-phenylaziridine
	Unknown 4
	Chloroephedrine
	methamphetamine dimer
	Unknown 5
	Unknown 6
	1-phenyl-2-propanol

Table 83: Target impurities by DB-1MS column.

Impurities (CHAMP)	Impurities (This study)
N-formylmethamphetamine	Dibenzylketone
N-acetylmethamphetamine	α-benzyl-N-methylphenethylamine
α-benzyl-*N*-methylphenethylamine	*cis* 3,4-Diphenyl-3-buten-2-one
cis 3,4-Diphenyl-3-buten-2-one	*trans* 3,4-Diphenyl-3-buten-2-one
α,α-dimethyldiphenethylamine	α,α-dimethyldiphenethylamine
α,α-dimethyldiphenethylamine	α,α-dimethyldiphenethylamine
N–methyldiphenethylamine	*N*–methyldiphenethylaminε
N,α,α–trimethyldiphenethylamine	*N*,α,α–trimethyldiphenethylamine
N,α,α–trimethyldiphenethylamine	*N*,α,α-trimethyldiphenethylamine
N-benzoylmethamphetamine	*N*-benzoylamphetamine
2,6-Dimethyl-3,5-diphenylpyridine	*N*-benzoylmethamphetamine
Pyridine 7 and 14	2,6-Dimethyl-3,5-diphenylpyridine
N,N-di-(β-phenylisopropyl) formamide	Pyridine 7 and 14
N-methyl-N-(1-methyl-2-phenylethyl)-2-phenylacetamide	*N,N*-di-(β-phenylisopropyl) formamide
Dimethylphenylnaphthalene	*N*-methyl-N-(1-methyl-2-phenylethyl)-2-phenylacetamide
Benzylmethnaphthalene	1-phenyl-2-propanol
(Z)-N-methyl-N-(α-methylphenethyl)-3-phenylpropenamide	Dimethylphenylnaphthalene
cis-1,2-dimethyl-3-phenylaziridine	N-methyl-N-(α-methylphenethyl) amino-1-phenyl-2-propanone
Ephedrone	Benzylmethnaphthalene
Ephedrine	N-methyl-N-(α-methylphenethyl) amino-1-phenyl-2-propanone
methamphetamine dimer	(Z)-N-methyl-N-(α-methylphenethyl)-3-phenylpropenamide
	(E)-N-methyl-N-(α-methylphenethyl)-3-phenylpropenamide
	cis-1,2-dimethyl-3-phenylaziridine
	trans-1,2-dimethyl-3-phenylaziridine
	Ephedrone
	Ephedrine
	Ethylamphetamine
	Unknown 1
	Unknown 2
	CMP
	Unknown 3
	Unknown 4
	Chloroephedrine
	methamphetamine dimer
	Unknown 5
	Unknown 6

Table 84: Target impurities by DB-5 column.

Structures of CHAMP impurities (DB-1MS)

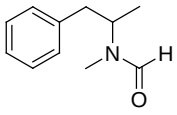

N-formylmethamphetamine

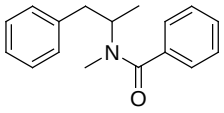

N-Benzoylmethamphetamine

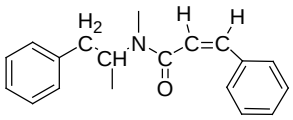

N-methyl-*N*-(α-methylphenethyl)-3-phenylpropenamide

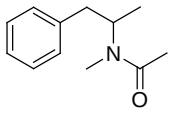

N-acetylmethamphetamine

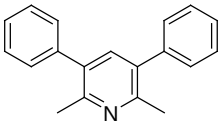

2,6-Dimethyl-3,5-diphenylpyridine

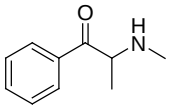

Ephedrone

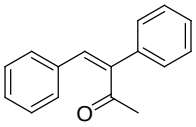

3,4-Diphenyl-3-buten-2-one

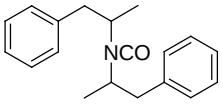

N,*N*-di(*β*-phenylisopropyl)formamide

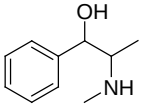

Ephedrine

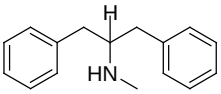

α-Benzyl-*N*-methylphenethylamine

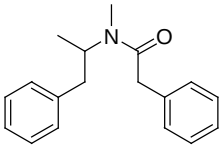

N-methyl-*N*-(1-methyl-2-phenyl-ethyl)-2-phenyl-acetamide

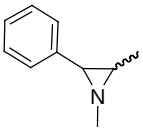

1,2-dimethyl-3-phenylaziridine

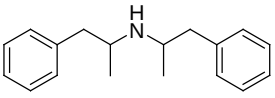

α,α-dimethyldiphenethylamine

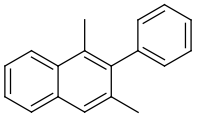

1,3-dimethyl-2-phenylnaphthalene

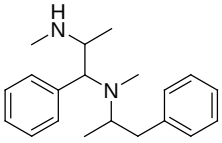

methylamphetamine dimer

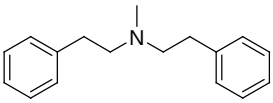

N-methyldiphenethylamine

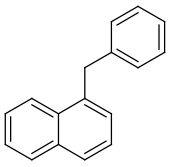

1-benzyl-3-methyl-naphthalene

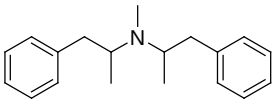

N–α,α-trimethyldiphenethylamine

Structures of this study impurities (DB-1MS)

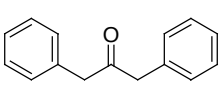

Dibenzylketone

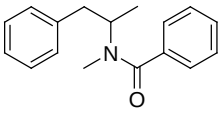

N-Benzoylmethamphetamine

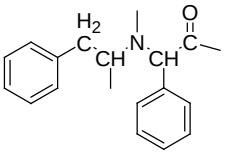

N-methyl-*N*-(α-methylphenethyl) amino-1-phenyl-2-propane

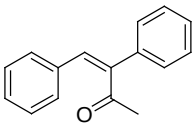

3,4-Diphenyl-3-buten-2-one

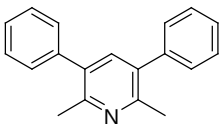

2,6-Dimethyl-3,5-diphenylpyridine

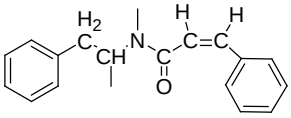

N-methyl-*N*-(α-methylphenethyl)-3-phenylpropenamide

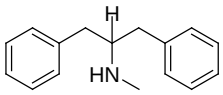

α-Benzyl-*N*-methylphenethylamine

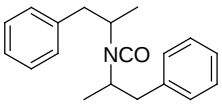

N,*N*-di(β-phenylisopropyl)formamide

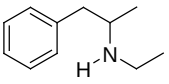

Ethylamphetamine

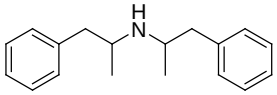

α,α-dimethyldiphenethylamine

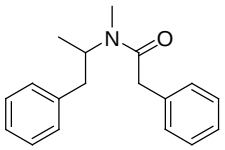

N-methyl-*N*-(1-methyl-2-phenyl-ethyl)-2-phenyl-acetamide

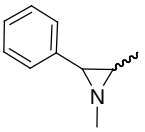

1,2-dimethyl-3-phenylaziridine

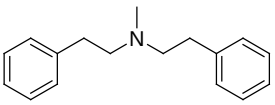

N-methyldiphenethylamine

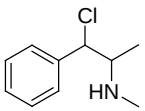

Chloroephedrine

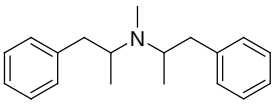

N–α,α-trimethyldiphenethylamine

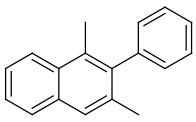

1,3-dimethyl-2-phenylnaphthalene

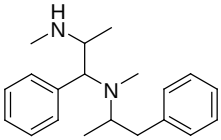

methylamphetamine dimer

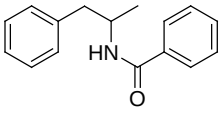

N-Benzoylamphetamine

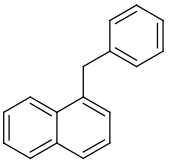

1-benzyl-3-methyl-naphthalene

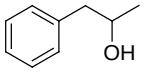

1-Phenyl-2-propanol

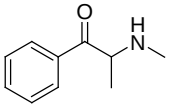

Ephedrone

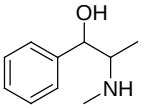

Ephedrine

Structures of CHAMP impurities (DB-5)

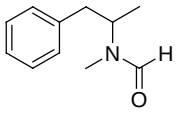

N-formylmethamphetamine

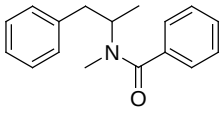

N-Benzoylmethamphetamine

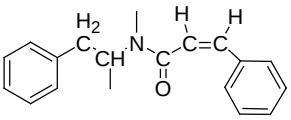

N-methyl-*N*-(α-methylphenethyl)-3-phenylpropenamide

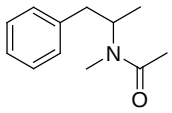

N-acetylmethamphetamine

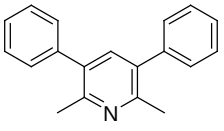

2,6-Dimethyl-3,5-diphenylpyridine

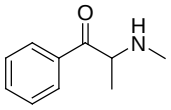

Ephedrone

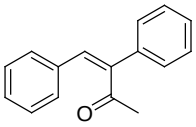

3,4-Diphenyl-3-buten-2-one

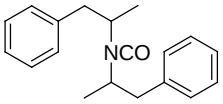

N,*N*-di(β-phenylisopropyl)formamide

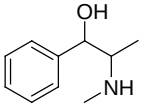

Ephedrine

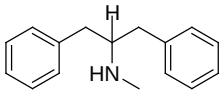

α-Benzyl-*N*-methylphenethylamine

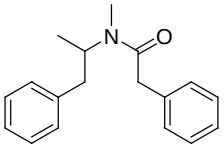

N-methyl-*N*-(1-methyl-2-phenyl-ethyl)-2-phenyl-acetamide

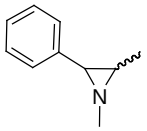

1,2-dimethyl-3-phenylaziridine

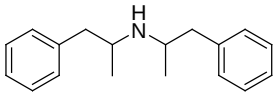

α,α-dimethyldiphenethylamine

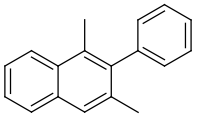

1,3-dimethyl-2-phenylnaphthalene

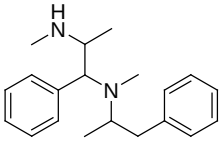

methylamphetamine dimer

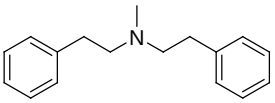

N-methyldiphenethylamine

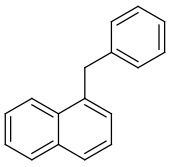

1-benzyl-3-methyl-naphthalene

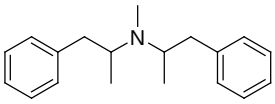

N–α,α-trimethyldiphenethylamine

Structures of this study impurities (DB-5)

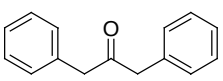

Dibenzylketone

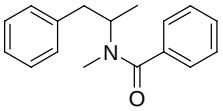

N-Benzoylmethamphetamine

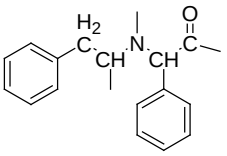

N-methyl-*N*-(α-methylphenethyl) amino-1-phenyl-2-propane

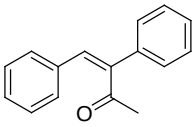

3,4-Diphenyl-3-buten-2-one

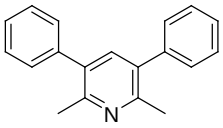

2,6-Dimethyl-3,5-diphenylpyridine

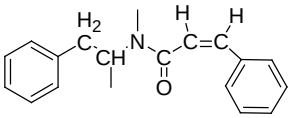

N-methyl-*N*-(α-methylphenethyl)-3-phenylpropenamide

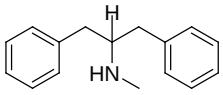

α-Benzyl-*N*-methylphenethylamine

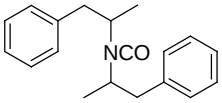

N,*N*-di(β-phenylisopropyl)formamide

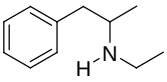

Ethylamphetamine

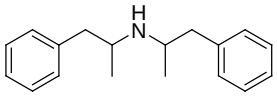

α,α-dimethyldiphenethylamine

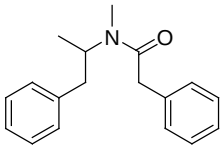

N-methyl-*N*-(1-methyl-2-phenyl-ethyl)-2-phenyl-acetamide

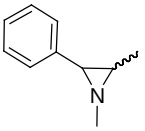

1,2-dimethyl-3-phenylaziridine

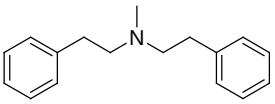

N-methyldiphenethylamine

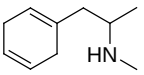

CMP

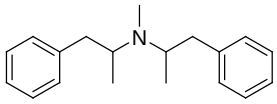

N–α,α-trimethyldiphenethylamine

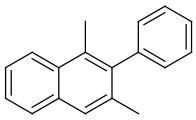

1,3-dimethyl-2-phenylnaphthalene

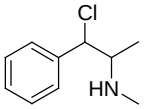

Chloroephedrine

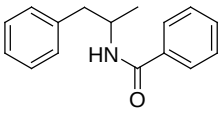

N-Benzoylamphetamine

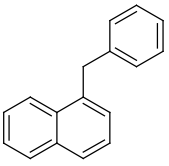

1-benzyl-3-methyl-naphthalene

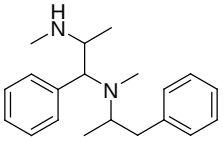

methylamphetamine dimer

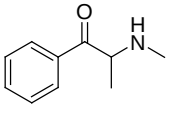

Ephedrone

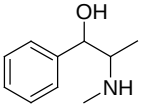

Ephedrine

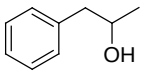

1-Phenyl-2-propanol

Appendix E: Partial Method Validation for DB-5

1.1 Instrumental Precision and Repeatability of Chromatography

Instrumental precision was assessed based on the internal standard ($C_{20}H_{42}$) peak of six injections of one extract. The relative standard deviation of the peak across these six injections was calculated. The RSDs value was calculated and found to be 1.86%, a level of instrumental precision acceptable for the intended purpose of the analysis.

Similar to the assessment of instrumental precision, the repeatability of the chromatography was assessed by six replicate injections of one extract of Grob mix. Results are displayed in Table 85.

No	Components	RSD(peak area)
1	1-octanol	1.80%
2	2,6-dimethylphenol	1.91%
3	2,6-dimethylaniline	2.00%
4	dodecane, C12	1.78%
5	tridecane, C13	1.60%
6	methyl decanoate ester	1.39%
7	methyl undecanoate ester	1.65%
8	dicyclohexylamine	1.64%
9	eicosane, C20	1.08%
10	tetracosane, C24	0.90%

Table 85: Relative standard deviation of Grob mixture.

1.2 Linearity of the Detection Response (by serial dilution)

Table 84 illustrates illustrates the correlation coefficient for the calibration curve of each of the 10 compounds within the Grob mixture ranging in concentration from 0.002mg/mL to 0.0010 mg/mL.

Serial dilutions of the Grob mixture (0.002 mg/mL, 0.004mg/mL, 0.006mg/mL, 0.008mg/mL, 0.010mg/mL) were prepared from a 0.040 mg/mL stock solution. Each standard was injected 6 times. Graphs of concentration versus average of peak area were plotted for each compound.

Table 86 shows the value of correlation coefficients of each of the10 compounds.

	1	2	3	4	5	6	7	8	9	10
R^2	0.9907	0.9990	0.9973	0.9981	0.9991	0.9992	0.9985	0.9992	0.9992	0.9995

Table 86: Correlation coefficient of 10 components in Grob mixture from serial dilution.

1.3 Instrumental Parameters

A GCMS method reported in the literature for quality test of column was selected.[1, 2] Analysis was performed using a Hewlett Packard 6890 gas chromatograph (GC) coupled to a 5973 mass selective detector. The column was a DB-5 J & W column (30 m length × 0.32 mm inner diameter, 1.0 μm film thickness). The oven temperature was programmed as follows: 60°C for 1 min, 10°C/min to 300°C, and then a hold at 300°C for 1 min. The injector and detector temperatures were set at 260 and 250°C, respectively. Helium was used as the carrier gas at a constant column flow-rate of 0.5 ml/min. Injection of 1 μL of the extract was made in the splitless mode (purge on time; 1.0 min). Hewlett-Packard HP3365 Chemstation software was used for controlling the GCMS system, data acquisition and integration of the gas chromatograms. Data were acquired at a rate of 20 Hz and a peak width of 0.05 min.

1.4 References

1. Grob Jr, K.; Grob, K., Evalluation of Capillary Columns by Separation Number of Plate Number. *Journal of Chromatography A* 1981, 207, 291-297.

2. Grob Jr, K.; Grob, G.; Grob, K., Comprehensive, Standardized Quality Test for Glass Capillary Columns. *Journal of Chromatography A* 1978, 156, 1-20.

Appendix F: Published Work

Anal. Chem. **2009**, *81*, 7342–7348

Characterization of Route Specific Impurities Found in Methamphetamine Synthesized by the Leuckart and Reductive Amination Methods

Vanitha Kunalan,[†] Niamh Nic Daéid,[*,†] William J. Kerr,[‡] Hilary A. S. Buchanan,[†] and Allan R. McPherson[‡]

Centre for Forensic Science and Department of Pure and Applied Chemistry, WestCHEM, University of Strathclyde, 204 George Street, Glasgow G1 1XW, Scotland, U.K.

Impurity profiling of seized methamphetamine can provide very useful information in criminal investigations and, specifically, on drug trafficking routes, sources of supply, and relationships between seizures. Particularly important is the identification of "route specific" impurities or those which indicate the synthetic method used for manufacture in illicit laboratories. Previous researchers have suggested impurities which are characteristic of the Leuckart and reductive amination (Al/Hg) methods of preparation. However, to date and importantly, these two synthetic methods have not been compared in a single study utilizing methamphetamine hydrochloride synthesized in-house and, therefore, of known synthetic origin. Using the same starting material, 1-phenyl-2-propanone (P2P), 40 batches of methamphetamine hydrochloride were synthesized by the Leuckart and reductive amination methods (20 batches per method). Both basic and acidic impurities were extracted separately and analyzed by GC/MS. From this controlled study, two route specific impurities for the Leuckart method and one route specific impurity for the reductive amination method are reported. The intra- and inter-batch variation of these route specific impurities was assessed. Also, the variation of the "target impurities" recently recommended for methamphetamine profiling is discussed in relation to their variation within and between production batches synthesized using the Leuckart and reductive amination routes.

Globally, methamphetamine is one of the most frequently abused drugs worldwide. It is mainly produced in North America (34%) and East and South-East Asia (62%). According to the 2008 World Drug Report,[3] methamphetamine production in Europe continues to be limited to only a few countries, notably the Czech Republic, the Republic of Moldova, and Slovakia. The National Association of Counties in America found that methamphetamine is the primary illegal drug in 47% of the states in the United States, a higher percentage than that of any other drug.[4]

Methamphetamine can be synthesized by one of several routes using either of two precursors. Each route results in an organic and inorganic impurity profile that is influenced by the precursors, reagents, and synthetic method used for production.[5] An important goal of impurity profiling is the identification of "route specific" impurities for each of the common methods, in this case, of methamphetamine manufacture. Route specific impurities are those which, when present in an illicit substance, indicate the use of a particular synthetic pathway. Impurity profiling therefore has the potential to be a useful tool for both evidential and intelligence purposes.

Synthesis methods for methamphetamine can be categorized according to the starting material used. Routes most commonly used in Asia and the U.S.A.,[6–8] such as the Nagai, Rosenmund, Birch, Emde, and Moscow methods, all require ephedrine or pseudoephedrine as a starting material. Two routes commonly used in Europe and the U.S.A., the Leuckart and reductive amination with aluminum/mercury (Al/Hg) amalgam techniques, both require 1-phenyl-2-propanone (P2P) as the starting material (see Figure 1). The route specific impurities for the two methods utilizing P2P within a single controlled study will be discussed in this paper.

Previous studies have focused on the identification of route specific impurities present in methamphetamine synthesized by the Nagai,[9] Emde,[10] and Leuckart[1] methods, and several analytical techniques have been utilized for the identification of both organic and inorganic impurities.[6,11] Previous work has been dominated by GC/MS analysis with one study investigating IRMS with gas

* To whom correspondence should be addressed. E-mail: n.nicdaeid@strath.ac.uk. Phone: +44-141-548-4700. Fax: +44-141-548-2532.
[†] Centre for Forensic Science.
[‡] Department of Pure and Applied Chemistry.

(1) Kram, T. C.; Kruegel, A. V. *J. Forensic Sci.* **1977**, *22* (1), 40–52.
(2) Verweij, A. M. A. *J. Forensic Sci.* **1989**, *1* (1), 1–11.
(3) United Nations Office on Drugs and Crime. *2008 World Drug Report*, Volume 1: Analysis; 2008.
(4) Facts and figures about the methamphetamine epidemic in America. Available at http://methlabhomes.com/2008/11/facts-and-figures-about-meth-in-america/ (accessed on 04/12/08).
(5) Dujourdy, L.; Dufey, V.; Besacier, F.; Miano, F.; Marquis, R.; Lock, E.; Aalberg, L.; Dieckmann, S.; Zrcek, F.; Bozenko Jr., J. S. *J. Forensic Sci.* **2008**, *177*, 153–161.
(6) Lee, J. S; Chung, H. S.; Kuwayama, K.; Inoue, H.; Lee, M. E.; Park, J. H. *Forensic Sci. Int.* **2006**, *161* (2–3), 209–215.
(7) Ko, B. J.; Suh, S.; Suh, Y. J.; In, M. K.; Kim, S. H. *Forensic Sci. Int.* **2007**, *170* (1), 142–147.
(8) Ely, R. A.; McGrath, D. C. *J. Forensic Sci.* **1990**, *35* (3), 720–723.
(9) Windahl, K. L.; McTigue, M. J.; Pearson, J. R.; Pratt, S. J.; Rowe, J. E.; Sear, E. M. *J. Forensic Sci. Int.* **1995**, *76*, 97–114.
(10) Allen, A. C. *J. Forensic Sci.* **1987**, *32*, 953–962.
(11) Suh, S.; Ko, B. J.; Suh, Y. J.; In, M. K.; Kim, S. H. *The International Association of Forensic Toxicologists (TIAFT) 2006 Poster*, 2006.

10.1021/ac9005588 CCC: $40.75
Published on Web 07/28/2009

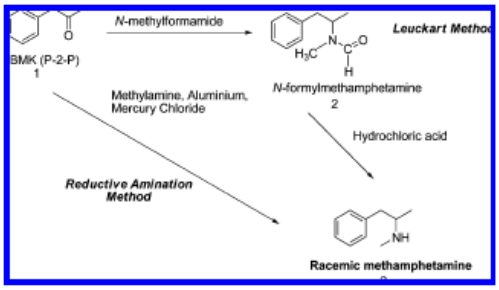

Figure 1. Methamphetamine synthesized from 1-phenyl-2-propanone (P2P).

chromatographic analysis for impurity profiling. Studies, however, are normally conducted on methamphetamine samples which have been seized by police authorities and of which the history is unknown; therefore, the unequivocal identification of route specific impurities is difficult. Furthermore, previous research[1,2] characterizing impurities present in methamphetamine synthesized by the Leuckart or reductive amination methods has *only* looked at one route or the other, rather than both pathways in conjunction with each other, by the same scientist and laboratory. The research presented here which involves in-house synthesized samples allows assessment of the variability of impurities *within* and *between* production batches where the provenance of the sample is definitively known.

Currently, the recommended methods for identifying links between methamphetamine samples relies on the relative concentrations of selected impurities present in samples. Thus, information on the variability of relative quantities of impurities from the same and different batches is crucial, as this will dictate the level at which links can be made (i.e., between samples from a single production batch or, more broadly, between samples from different production batches from the same chemist or laboratory).

In this study, 20 batches of methamphetamine were synthesized by the Leuckart method and 20 batches were synthesized by the reductive amination (Al/Hg) route. The preparative methods were taken from published materials which are accessible to and used by the clandestine chemist.[12] It should be noted that while every effort was used to exactly mimic the reaction conditions used for clandestine synthesis, safety considerations also influenced the synthesis and these may not be as stringently used in clandestine laboratories.

To obtain a broad spectrum of basic *and* acidic impurities in each batch, two impurity extracts (pH 6.0 and pH 10.5) were taken from the synthesized methamphetamine hydrochloride using an extraction method developed in-house from those published in the literature.[13,14] The acidic and basic extracts for each production batch were then analyzed by GC/MS using conditions based on those published by Inoue et al.[14] The combination of both acidic and basic impurity profiles has not previously been reported.

In this study, the intra- and inter-batch variation of 24 target impurities suggested by the CHAMP (Collaborative Harmonisation of Methods for Profiling of Amphetamine type Stimulants) method identified[5] in the in-house synthesized methamphetamine is discussed.

EXPERIMENTAL SECTION

Reagents and Materials. 1-Phenyl-2-propanone, *N*-methylformamide, and methylamine hydrochloride were purchased from Sigma-Aldrich, and all other chemicals and solvents were purchased from Fisher Scientific. Twenty batches of methamphetamine hydrochloride were synthesized by the Leuckart route, and 20 batches were synthesized by the reductive amination method, as outlined below.

Synthesis of Methamphetamine by the Leuckart Method.[12] To 1-phenyl-2-propanone (5.4 mL, 40.2 mmol) was added *N*-methylformamide (13.4 mL, 229 mmol, 5.7 equiv) with stirring. The temperature was gradually increased to 165−170 °C and held for 24−36 h. After cooling to room temperature, a 10 M NaOH solution (24 mL, 0.24 mmol) was added, and the reaction mixture refluxed for 2 h. After cooling to room temperature, the aqueous layer was discarded, and 37% HCl (10.7 mL, 0.004 mmol) added to the red organic layer. The mixture was refluxed for 2 h. After cooling to room temperature, an 8.3 M NaOH solution (16.0 mL, 0.13 mmol) was slowly added, and the crude methamphetamine base extracted with toluene (3 × 20 mL). The combined organic layers were dried over $MgSO_4$ and the volatiles removed in vacuo to reveal the crude methamphetamine base as a brown oil. The crude methamphetamine base was distilled under vacuum (2 mbar, 60−100 °C) using Kugelrohr distillation to yield methamphetamine as a clear to pale yellow oil (2.5 g, 42%). Analysis was in agreement with published data for IR,[15] ^{1}H NMR and ^{13}C NMR.[16]

IR ν_{max} (film)/cm^{-1}: 1605 (N−C), 1454, 1373, 1155, 741, 697. ^{1}H NMR (400 MHz, $CDCl_3$): δH 1.08 (d, 3H, J = 8.0 Hz, CH_3), 2.42 (s, 3H, CH_3), 2.62 (dd, 1H, J = 20.0, 8.0 Hz, CH), 2.65 (dd, 1H, J = 20.0, 4.0 Hz, CH), 2.71−2.83 (m, 1H, CH), 7.17−7.37 ppm (m, 5H, C_6H_5). ^{13}C NMR (100 MHz, $CDCl_3$): δ 19.8, 34.0, 43.5, 56.4, 126.2, 128.4, 129.3, 139.5 ppm.

Conversion of the methamphetamine base to the hydrochloride salt was achieved by dissolving the base in toluene (50 mL) and bubbling through anhydrous hydrogen chloride gas until formation of a white precipitate. The resulting white precipitate was filtered, washed with toluene, and dried under high vacuum to produce methamphetamine hydrochloride as a white salt (2.0 g, 27%). Analysis was in agreement with published data for IR,[17] ^{1}H NMR,[1] and ^{13}C NMR.[18]

IR ν_{max} (KBr)/cm^{-1}: 3419 (N−H), 2971, 2731, 2461 (C−C), 1603 (N−C). ^{1}H NMR (400 MHz, D_2O): δH 1.22 (d, 3H, J = 8.0 Hz, CH_3), 2.64 (s, 3H, CH_3), 2.87 (dd, 1H, J = 24.0, 8.0 Hz,

(12) Uncle Fester. *Secrets of Methamphetamine Manufacture: Including Recipes for MDA, Ecstasy, & Other Psychedelic Amphetamines*, 5th ed.; Loompanics Unlimited: Port Townsend, WA, 1999.
(13) Tanaka, K.; Ohmori, T.; Inonue, T.; Seta, S. *J. Forensic Sci.* **1994**, *39* (2), 500–511.
(14) Inoue, H.; Kanamori, T.; Iwata, Y. T.; Ohmae, Y.; Tsujikawa, K.; Saitoh, S.; Kishi, T. *Forensic Sci. Int.* **2003**, *135* (1), 42–47.
(15) United Nations. *Recommended Methods for Testing Amphetamine and Methamphetamine*, Manual for Use by National Narcotics Laboratories, 2004, 27–29.
(16) Almena, J.; Foubelo, F.; Yus, M. *J. Org. Chem.* **1994**, *59*, 3210–3215.
(17) Chappell, J. S. *Analyst* **1997**, *122*, 755–760.
(18) Lee, G. S. H.; Taylor, R. C.; Dawson, M.; Kannangara, G. S. K.; Lee, G. S. H.; Wilson, M. A. *Solid State Nucl. Magn. Reson.* **2000**, *16*, 225–237.

CH), 3.03 (dd, 1H, J = 20.0, 8.0 Hz, CH), 3.44−3.50 (m, 1H, CH), 7.25−7.38 (m, 5H, C_6H_5). ^{13}C NMR (100 MHz, D_2O): δ 14.8, 29.9, 38.8, 56.4, 127.5, 129.1, 129.5, 135.8 ppm.

Synthesis of Methamphetamine by the Reductive Amination Method.[12] To aluminum foil (2.9 g) cut into 2 cm squares was added distilled water (100 mL) containing mercuric chloride (0.067 g, 0.247 mmol). The amalgamation was allowed to proceed for 15 min. The water was then decanted, and the aluminum foil rinsed with distilled water (2 × 300 mL).

In a separate flask, NaOH (4.4 g, 109 mmol, 2.7 equiv) was dissolved in methanol (20 mL). Methylamine hydrochloride (7.2 g, 107 mmol, 2.7 equiv) was added, and the mixture cooled to −10 °C. 1-Phenyl-2-propanone (5.4 mL, 40.2 mmol) was then added to the solution.

The 1-phenyl-2-propanone solution was poured onto the activated aluminum with swirling. During this addition process, the flask was immersed in an ice bath as necessary to keep the temperature around 0 °C. After the addition process, the reaction mixture was heated to around 50−60 °C. After 90 min the reaction was complete (as determined by NMR of preliminary reaction runs). Celite was added to the alcohol solution containing the product. The resultant mixture was then filtered and rinsed with methanol. The combined organic layers were dried over $MgSO_4$ and the volatiles removed in vacuo to reveal the crude methamphetamine base as a pale yellow oil. The crude product was distilled according to the procedure detailed above to reveal a clear to pale yellow colored oil (4.09 g, 69%). The methamphetamine base was then converted to the hydrochloride salt, again, according to the procedure detailed above. Analyses were as described previously.

Extraction of Impurities from Methamphetamine Hydrochloride. *Basic Extract.* A 0.1 M phosphate buffer (pH 7.0) was brought to pH 10.5 by the addition of 10% Na_2CO_3. Synthesized methamphetamine hydrochloride (100 mg) was homogenized with a mortar and pestle and dissolved in the pH 10.5 phosphate buffer (2 mL). The mixture was sonicated (5 min) within a sonication bath, and vortexed (2 min) using a vortex mixer. Ethyl acetate (0.4 mL) containing eicosane (as an internal standard at 0.05 mg/mL concentration) was added. After centrifugation (5 min), the organic layer was transferred into a microvial insert for GC/MS analysis.

Acidic Extract. A 0.1 M acetate buffer (pH 8.16) was brought to pH 6.0 by addition of acetic acid. The pH 6.0 acetate buffer was used to extract acidic impurities from the synthesized methamphetamine in an identical fashion to that described above for the basic extraction.

GC/MS Analysis. GC/MS analysis was performed using an Agilent 6890 GC and a 5973 mass selective detector (MSD). The mass spectrometer was operated in the electron ionization mode at 70 eV. Separation was achieved with a non-polar capillary column (DB-1MS, 25 m × 0.2 mm i.d., 0.33 μm, J & W Scientific) with helium as the carrier gas at a constant flow rate of 1.0 mL/min. The oven temperature program adapted from Inoue et al.[14] started at 50 °C for 1 min, was increased to 300 °C at a rate of 10 °C/min, and then held at 300 °C for 15 min. A 1 μL aliquot of the impurity extract was injected in the splitless mode with a purge time of 1 min. The injector and the GC interface temperatures were maintained at 250 and 300 °C, respectively. Mass spectra were obtained in the full scan mode (30−550 amu).

RESULTS AND DISCUSSION

We wished to examine the potential for drug profiling to identify route specific impurities and the expected variation of these route specific variations due to the chemical synthetic process only. As a consequence the inter- and intra-batch variations reflected in the data are those derived from the synthesis only, with all other variables (chemist, reagents, glassware, analytical process, etc.) being held as constant as possible.

Impurities Common to Both the Leuckart and Reductive Amination Methods. To date, only one route specific impurity for Leuckart-synthesized methamphetamine has been suggested: *N*-formylmethamphetamine.[19,20] However, a study by Qi et al.[21] cast doubt on the "route specific" status of this impurity; the authors reported *N*-formylmethamphetamine in seized methamphetamine samples which were believed to have been synthesized from ephedrine (i.e., not from the Leuckart or reductive amination routes, which have P2P as the starting material). In the present work, *N*-formylmethamphetamine was found in *all* batches of methamphetamine, regardless of whether the Leuckart or reductive amination routes were used, thus confirming that *N*-formylmethamphetamine is not route specific for the Leuckart method of methamphetamine synthesis.

Previous work by Kram and Kreugal[1] identified several impurities present in methamphetamine hydrochloride known to have been synthesized by the Leuckart method: dibenzylketone, α-benzyl-*N*-methylphenethylamine, and *N*-methyldiphenethylamine. The authors recognized that, while these impurities were associated with the Leuckart synthesis, it was not possible to determine if they were route specific. Again all batches of methamphetamine synthesized in this study were found to contain all three of these impurities and, therefore, they cannot be deemed route specific for the Leuckart method.

Route Specific Impurities for the Leuckart Method. From comparison of the impurities present in methamphetamine synthesized by the Leuckart and reductive amination methods, it is possible to identify two impurities which are route specific for the Leuckart method. These are α,α′-dimethyldiphenethylamine and *N*,α,α′-trimethyldiphenethylamine. These two impurities were originally associated with the Leuckart method in the 1970's (by Barron et al.,[18] and Kram and Kreugal[1]), but it was not possible at that time to preclude them from being formed by other synthetic methods. In the present study, these two impurities were only identified in the samples synthesized by the Leuckart method. α,α′-Dimethyldiphenethylamine was detectable in both the basic and acidic extracts. Having stated this, the extraction of this specific impurity was more efficient under basic conditions (see Figure 2). Some of the impurities identified in the acidic and basic extracts of Leuckart-synthesized methamphetamine are displayed in Tables 1−2.

It is worthy of note that pyridines 7 and 14, which were identified in the CHAMP amphetamine and methamphetamine

(19) Barron, R. P.; Kruegel, A. V.; Moore, J. M.; Kram, T. C. *J. Assoc. Off. Anal. Chem.* **1974**, *57* (5), 1147–1158.
(20) Bailey, K.; Boulanger, J. G.; Legault, D.; Taillefer, S. L. *J. Pharm. Sci.* **1974**, *63* (10), 1575–1578.
(21) Qi, Y.; Evans, I.; McCluskey, A. *Forensic Sci. Int.* **2007**, *169*, 173–180.

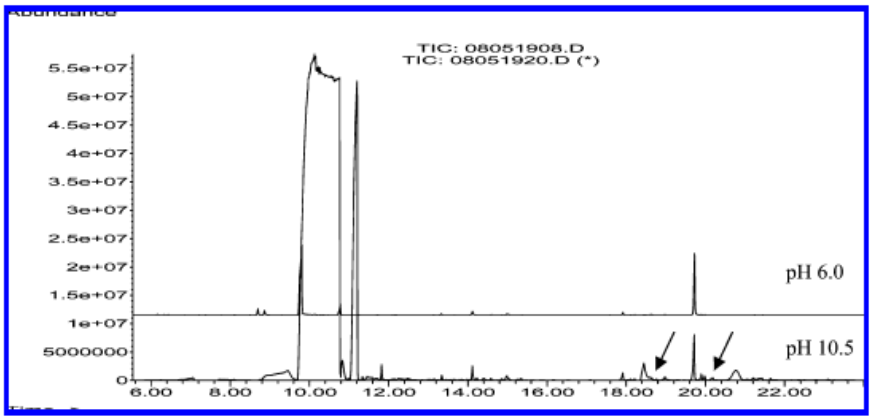

Figure 2. Impurity profile under basic and acidic conditions.

Table 1. List of Some of the Impurities Identified in the pH 6.0 Extract of Methamphetamine Synthesized by the Leuckart Route[a]

no.	RT	impurity extracted at pH 6.0	semiquantitative concentration mg/mL	intra-batch (n = 6) RSD	inter-batch (n = 20) RSD
1	8.705	1-Phenyl-2-propanone	5×10^{-3}	6%	37%
2	8.872	Amphetamine	5×10^{-3}	6%	39%
3	9.322	1-Phenyl-1,2-propanedione	2×10^{-4}	12%	80%
4	10.201	*N*-*N*-Dimethylbenzylamine	2×10^{-4}	34%	92%
5	10.786	Dimethylamphetamine (DMA)	1×10^{-2}	3%	121%
6	13.704	*N*-Formylamphetamine	2×10^{-4}	12%	72%
7	14.613	*N*-Formylmethamphetamine*	5×10^{-4}	16%	147%
8	15.052	*N*-Acetylmethamphetamine*	6×10^{-4}	12%	61%
9	18.461	Unidentified	7×10^{-4}	17%	69%
10	18.619	**α,α-Dimethyldiphenethylamine***	4×10^{-4}	**15%**	**59%**
11	18.661	**α,α-Dimethyldiphenethylamine***	5×10^{-4}	**15%**	**75%**
12	21.253	Pyridine 7 and 14*	2×10^{-5}	38%	73%
13	23.261	*N*-Methyl-*N*-(1-methyl-2-phenylethyl)-2-phenylacetamide*	5×10^{-3}	19%	63%

[a] RSDs were calculated using peak areas normalized to the sum of the CHAMP target impurities present in the relevant chromatogram. Route specific impurities for the Leuckart route are emboldened, and CHAMP target impurities are marked with an asterisk.

projects, are potentially route specific for the Leuckart route since they were found in all of the Leuckart batches only. However, these impurities can also be present in amphetamine samples; therefore, it is possible that detection of these impurities in methamphetamine samples could be the result of methamphetamine mixed with amphetamine, despite this combination being unlikely in our experience.

It is highly probable that the formation of *N*,α,α′-trimethyldiphenethylamine is as a result of the presence of methylamine within the reaction mixture. Two consecutive reductive amination processes, involving methylamine and the starting ketone, P2P, would ultimately lead to the production of *N*,α,α′-trimethyldiphenethylamine. To explain the origin of the aforementioned methylamine, careful consideration must be given to the proposed synthetic mechanism which leads to the production of methamphetamine via the Leuckart method. In this respect, during the initial iminium ion formation between P2P and *N*-methylformamide, hydroxide will be generated. Consequently, hydroxide-mediated hydrolysis of *N*-methylformamide leads to the production of residual methylamine (as well as the hydride required for the reduction of the intermediate iminium ion to deliver *N*-formylamphetamine). A second possible source of methylamine is as a contaminant in the commercially sourced *N*-methylformamide, as methylamine is a key component used within the industrial manufacture of *N*-methylformamide.

In relation to α,α′-dimethyldiphenethylamine, we propose that the formation of this species arises as a result of further specific impurities contained within the supplied *N*-methylformamide; these impurities are ammonia and formamide, and these species allow two possible routes into the second byproduct to be envisaged. First, ammonia could undergo two consecutive reductive amination processes with the starting ketone (vide supra), resulting in the direct formation of α,α′-dimethyldiphenethylamine. It is conceivable that ammonia may be present within the *N*-methylformamide as it is used in the large scale manufacture of methylamine, which, as discussed previously, is a key component in the production of *N*-methylformamide. In relation to the second impurity, formamide, it is plausible that *N*-formyl-α,α′-dimethyldiphenethylamine could be formed via two consecutive reductive amination processes involving formamide and the starting ketone. The subsequent acid-mediated hydrolysis (the second step of the Leuckart synthesis) would result in the production of the same α,α′-dimethyldiphenethylamine byproduct. Formamide is a likely impurity within the manufacture of *N*-methylformamide

Table 2. List of Some of the Impurities Identified in the pH 10.5 Extract of Methamphetamine Synthesized by the Leuckart Route[a]

no.	RT	impurity extracted at pH 10.5	semiquantitative concentration mg/mL	intra-batch ($n = 6$) RSD	inter-batch ($n = 20$) RSD
1	7.126	Acetic acid	1×10^{-2}	34%	74%
2	9.156	Amphetamine	3×10^{-2}	80%	67%
3	10.828	*N*-(1-Methyl-2-phenylethylidene)methenamine	3×10^{-3}	17%	104%
4	11.048	Dimethylamphetamine (DMA)	7×10^{-4}	30%	103%
5	13.672	*N*-Formylamphetamine	2×10^{-3}	28%	76%
6	14.331	Bibenzyl	1×10^{-3}	71%	114%
7	14.592	*N*-Formylmethamphetamine*	5×10^{-3}	62%	98%
8	15.031	*N*-Acetylmethamphetamine*	3×10^{-4}	42%	48%
9	16.286	Dibenzylketone*	3×10^{-4}	102%	115%
10	**17.917**	3,4-Diphenyl-3-buten-2-one*	2×10^{-4}	30%	237%
11	**18.043**	α-Benzyl-*N*-methylphenethylamine*	7×10^{-4}	39%	164%
12	18.116	Benzylmethamphetamine	7×10^{-5}	34%	229%
13	18.221	3,4-Diphenyl-3-buten-2-one*	9×10^{-3}	28%	180%
14	18.461	*N*-β-(Phenylisopropyl)benzyl methyl ketimine*	4×10^{-4}	22%	106%
15	**18.608**	**α,α-Dimethyldiphenethylamine***	$\mathbf{3 \times 10^{-4}}$	**30%**	**131%**
16	**18.649**	**α,α-Dimethyldiphenethylamine***	$\mathbf{2 \times 10^{-3}}$	**32%**	**136%**
17	18.858	*N*-Methyldiphenethylamine*	5×10^{-3}	33%	94%
18	**19.904**	**N-α,α-Trimethyldiphenethylamine***	$\mathbf{3 \times 10^{-3}}$	**28%**	**87%**
19	**19.988**	**N-α,α-Trimethyldiphenethylamine***	$\mathbf{2 \times 10^{-2}}$	**28%**	**82%**
20	**20.186**	*N*-Benzoylamphetamine	$\mathbf{9 \times 10^{-3}}$	**29%**	**66%**
21	20.406	*N*-Benzoylmethamphetamine	1×10^{-3}	35%	75%
22	21.065	2,6-Dimethyl-3,5-diphenylpyridine*	2×10^{-5}	48%	58%
23	21.211	Pyridine 7 and 14*	2×10^{-5}	32%	78%
24	22.34	*N,N*-Di-(β-phenylisopropyl)formamide	2×10^{-5}	30%	142%
25	23.25	*N*-Methyl-*N*-(1-methyl-2-phenylethyl)-2-phenylacetamide*	1×10^{-5}	40%	262%

[a] RSDs were calculated using peak areas normalized to the sum of the CHAMP target impurities present in the relevant chromatogram. Route specific impurities for the Leuckart route are emboldened, and CHAMP target impurities are marked with an asterisk (*).

due to residual ammonia present in the methylamine used in the production of this *N*-methylamide.

At this point it is worth considering how the quantities of these (route specific) impurities could be lessened. In relation to this, if the impurities were indeed being produced via the proposed pathways, we believe that their formation could be suppressed by careful manipulation of the reaction conditions employed. In this regard, if the route specific byproduct were the result of ammonia or methylamine contaminants within the sourced *N*-methylformamide, processes involving these volatile species could be suppressed by performing the reaction under (slightly) reduced reaction pressures. Alternatively, impurities arising from these same two amine species, as well as from formamide, within the commercially supplied *N*-methylformamide could be lessened by accessing a superior grade of this starting reagent. It should also be noted that *N*,α,α′-trimethyldiphenethylamine could form as a result of methylamine generated within the reaction manifold (vide supra). If this source of methylamine was, indeed, the route by which this trimethyl impurity was forming, this could be suppressed by increasing the equivalents of *N*-methylformamide with respect to the starting ketone. This amendment to the reaction protocol would increase the rate of formation of the desired and initially formed iminium ion, which would, in turn, reduce any undesired reductive amination processes and, ultimately, *N*,α,α′-trimethyldiphenethylamine byproduct formation.

Route Specific Impurities for the Reductive Amination (Al/Hg) Method. Comparison of the impurity profiles of methamphetamine synthesized by both methods reveals only one impurity which is route specific for reductive amination: 1-phenyl-2-propanol. This observation confirms that purported in 1989 in Verweij's review of the literature relating to impurities found in methamphetamine.[2] It is worth noting that this same impurity, 1-phenyl-2-propanol, was not detected in the basic impurity extract; the acidic extract was required for its detection (see Figure 3). Impurities identified in both extracts of reductive amination synthesized methamphetamine are given in Tables 3, 4.

With specific regard to 1-phenyl-2-propanol, it would appear that this impurity is formed by direct reduction of the starting ketone, P2P. Consequently, formation of this byproduct could be suppressed by prolonging the duration of the initial imine formation step of the overall process. This would serve to lower any quantities of unreacted starting ketone present in the reaction mixture at the stage when the subsequent reducing medium is introduced. In a further practical amendment, more complete removal of water from the generated amalgam would drive the ketone-to-imine equilibrium toward imine formation and, ultimately, lead to reduced levels of the alcohol byproduct, which results from reduction of the starting ketone.

Assessment of Intra- and Inter-batch Variation of Route Specific Impurities. The samples used in this study were synthesized by the same chemist using the same method, chemicals, and apparatus. Intra-batch variation, that is, variation of the quantities of impurities in separate extractions from one homogenized batch of methamphetamine, was assessed by performing impurity extractions of six sub-samples of a single batch of methamphetamine. Intra-batch variation is important because it affects how accurately samples from the same production batch can be linked together.

Inter-batch variation of selected impurities was also assessed. Inter-batch variation in this study is defined as the variation of the presence and quantities of impurities in extractions from different batches of methamphetamine synthesized by the same

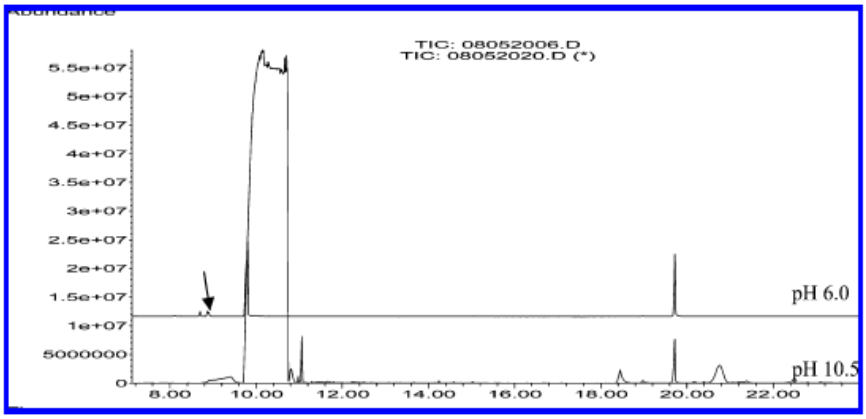

Figure 3. Impurity profile under basic and acidic condition.

Table 3. List of Some of the Impurities Identified in the pH 6.0 Extract of Methamphetamine Synthesized by the Reductive Amination Route[a]

no.	RT	impurity extracted at pH 6.0	semiquantitative concentration mg/mL	intra-batch (n = 6) RSD	inter-batch (n = 20) RSD
1	8.695	1-Phenyl-2-propanone	4×10^{-3}	3%	29%
2	8.873	Amphetamine	3×10^{-3}	7%	16%
3	**8.89**	**1-Phenyl-2-propanol**	$\mathbf{3 \times 10^{-3}}$	**6%**	**27%**
4	10.786	Dimethylamphetamine (DMA)	3×10^{-4}	6%	5%
5	14.603	*N*-Formylmethamphetamine*	2×10^{-4}	14%	16%
6	15.042	*N*-Acetylmethamphetamine*	4×10^{-4}	22%	20%

[a] RSDs were calculated using peak areas normalized to the sum of the CHAMP target impurities present in the relevant chromatogram. Route specific impurities for the reductive amination route are emboldened, and CHAMP target impurities are marked with an asterisk (*).

Table 4. List of Some of the Impurities Identified in the pH 10.5 Extract of Methamphetamine Synthesized by the Reductive Amination Route[a]

no.	RT	impurity extracted at pH 10.5	semiquantitative concentration mg/mL	intra-batch (n = 6) RSD	inter-batch (n = 20) RSD
1	7.034	Acetic acid	6×10^{-3}	55%	179%
2	9.408	Amphetamine	5×10^{-2}	49%	119%
3	10.715	*N*-(1-Methyl-2-phenylethylidene)methenamine	5×10^{-1}	15%	52%
4	11.06	Dimethylamphetamine (DMA)	3×10^{-2}	53%	98%
5	13.664	*N*-Formylamphetamine	3×10^{-3}	106%	109%
6	14.445	Bibenzyl	6×10^{-3}	144%	112%
7	14.584	*N*-Formylmethamphetamine*	2×10^{-2}	103%	77%
8	15.034	*N*-Acetylmethamphetamine*	2×10^{-2}	93%	142%
9	16.289	Dibenzylketone*	1×10^{-3}	100%	196%
10	17.92	3,4-Diphenyl-3-buten-2-one*	7×10^{-3}	166%	154%
11	18.014	α-Benzyl-*N*-methylphenethylamine*	8×10^{-4}	129%	164%
12	18.119	Benzylmethamphetamine	2×10^{-3}	138%	162%
13	18.192	3,4-Diphenyl-3-buten-2-one*	4×10^{-3}	131%	129%
14	18.453	*N*-β-(Phenylisopropyl)benzyl methyl ketimine*	6×10^{-2}	64%	77%
15	18.83	*N*-Methyldiphenethylamine*	2×10^{-3}	120%	153%
16	20.189	*N*-Benzoylamphetamine	4×10^{-3}	51%	82%
17	20.409	*N*-Benzoylmethamphetamine	1×10^{-2}	92%	118%
18	21.046	2,6-Dimethyl-3,5-diphenylpyridine*	3×10^{-2}	82%	173%
19	21.214	Pyridine 7 and 14*	2×10^{-2}	76%	65%
20	22.385	*N,N*-Di-(β-phenylisopropyl)formamide	5×10^{-3}	113%	89%
21	23.253	*N*-Methyl-*N*-(1-methyl-2-phenylethyl)-2-phenylacetamide*	4×10^{-3}	87%	108%

[a] RSDs were calculated using peak areas normalized to the sum of the CHAMP target impurities present in the relevant chromatogram. Route specific impurities for the reductive amination route are not present in the basic extract. CHAMP target impurities are marked with an asterisk (*).

chemist using the same preparative method. This translates to the ability of law enforcement to link together batches produced by the same clandestine laboratory or chemist.

The intra- and inter-batch variation were assessed in extraction using both pH 6.0 and pH 10.5 buffers, and for methamphetamine synthesized by both the Leuckart and reductive amination

methods. In each case the relative standard deviations (RSD) of the peak area of an identified impurity peak, normalized to the sum of the area of the "target impurities" suggested in the CHAMP profiling method,[5] was assessed.

Both isomers of the Leuckart route specific impurity α,α-dimethyldiphenethylamine had relatively high intra-batch variation indicated by RSDs of 30% and 32%. These RSDs increased significantly to 131% and 136%, respectively, when assessing inter-batch variation (see Table 2). Similar variability is observed for both isomers of the other Leuckart route specific impurity, *N*-α,α-trimethyldiphenethylamine: intra-batch RSDs for both isomers were 28%, which increased to 87% and 82% when calculating inter-batch RSDs (see Table 2).

Given the high intra-batch variability of the two Leuckart route specific impurities, it is not surprising that the inter-batch RSDs are also high. However, since the inter-batch RSDs are considerably greater than those from the intra-batch analyses, it is likely that variation in the quantities of the impurities occurs from batch to batch. This indicates that batches of methamphetamine produced by the same chemist using the same equipment, chemicals, and synthetic method would not be expected to contain consistent amounts of (at least) these key impurities from batch to batch.

The route specific impurity for the reductive amination route, 1-phenyl-2-propanol, has much lower variability. Intra-batch variation of this impurity (Table 3) is 6%, indicating that the quantity of this impurity is extracted and chromatographed consistently using six sub-samples from a single homogenized batch of methamphetamine. The inter-batch variation increases to 27%, indicating that there is some variation in the quantity of this impurity across 20 batches of methamphetamine synthesized by the same chemist using the same equipment, method, and reagents. Accordingly, the variability of the quantity of 1-phenyl-2-propanol in batches made by the same chemist may be too great to allow batch to batch linkage of the final products.

CONCLUSIONS

This is the first report where the impurities found in methamphetamine synthesized in-house from the same starting material (P2P) by both the Leuckart and reductive amination (Al/Hg amalgam) methods have been compared. Using both basic and acidic extracts with buffers at pH 10.5 and pH 6.0, respectively, it has been possible to identify two Leuckart route specific impurities present in the pH 10.5 extract: α,α-dimethyldiphenethylamine and *N*-α,α-trimethyldiphenethylamine (both isomers of each were present). Only one route specific impurity for the reductive amination method was identified, and this was found only in the acidic extract: 1-phenyl-2-propanol.

There are, of course, other methods used for methamphetamine manufacture, some of which are more common than those discussed here. The identification of route specific impurities for the Nagai, Rosenmund, Birch, Emde, and Moscow methods is currently underway in our laboratory and will be submitted for publication at a later date.

SUPPORTING INFORMATION AVAILABLE

The FT-IR and NMR spectra of the preparative compounds, the structures of impurities from both routes at each extracting pH, and the mass spectra of the route specific impurities for each route are presented together with additional chromatograms. This material is available free of charge via the Internet at http://pubs.acs.org.

ACKNOWLEDGMENT

N.N.D. and W.J.K. gratefully acknowledge financial support of this work through the Malaysian Government which provided a studentship for V.K.

Received for review March 18, 2009. Accepted July 6, 2009.

AC9005588